

Department of Civil Engineering

**Development of a Long Life Design Procedure for Australian
Asphalt Pavements**

Bevan William Sullivan

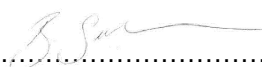
This thesis is presented for the Degree of
Doctor of Philosophy
of
Curtin University

September 2015

Declaration

To the best of my knowledge and belief this thesis contains no material previously published by any other person except where due acknowledgement has been made.

This thesis contains no material which has been accepted for the award of any other degree or diploma.

Signature: 

Date: 18 February 2016

List of Publications

- Sullivan, B, Gabrawy, T, Youseidoost, S, 2013, *“Advanced Material Characterisation of Australian Mixes for Pavement Design”*, AAPA International Flexible Pavement Conference, Brisbane
- Sullivan, B, Rickards, I, Youseidoost, S, 2013, *Interconversion of Laboratory Measured Modulus Results to Field Modulus and Strain*, AAPA International Flexible Pavement Conference, Brisbane
- Sullivan, B, 2014, *“Towards a Long Life Pavement Design for Australian Asphalt Pavement Design”*, IPWEA Conference, Fremantle
- Sullivan, B, Nikraz, H, 2014 *“Development of a Validated Long Life Pavement Threshold Criterion for Australian Asphalt Pavement Design”*, 26th ARRB Conference, Sydney, NSW
- Sullivan, B, Youdale. G, Rickards, I, 2014 *“Development of a Validated Design Procedure for Australian Long Life Pavements”*, International Conference on Perpetual Pavements, Ohio
- Sullivan, B, Prasad, A, Gabrawy, T, 2015, *“Establishment of the Fatigue Endurance Limit of EME and A5E Mixes for Incorporation into the AAPA Long Life Design Procedure”*, AAPA International Flexible Pavement Conference, Gold Coast
- Sullivan, B, Denneman, E, 2015, *“Inter-Conversion of Australian Modulus Test Methods ”*, AAPA international Flexible Pavement Conference, Gold Coast

Abstract

In 2011 the Australian Asphalt Pavement Association (AAPA) commenced the Asphalt Pavement Solutions for Life (APS-fL) project. This project was initiated to address the concerns of clients, consultants and industry that current pavement design procedures were producing overly conservative asphalt thickness requirements.

It was believed that these overly conservative design outcomes were due to a number of issues, such as;

- limited data on material characterisation of Australian mixes which is resulting the use of overly conservative material properties,
- the lack of a calibrated and validated shift factor between laboratory observations and field performance,
- the lack of incorporation of the healing mechanism in asphalt mixes, and
- the lack of recognition of a “threshold” strain or Fatigue Endurance Limit (FEL) below which no damage occurs.

Most importantly, it was felt that if a FEL concept could be incorporated into a pavement design procedure, Long Life Asphalt Pavements (LLAPs) could be introduced to Australia. The result of which would be that the maximum thickness of asphalt could be determined, beyond which any increase in design thickness will result in little to no increase in the structural capacity of the pavement. This aspect was conducted as part of the APS-fL project, with the intent of developing a framework for the incorporation of the LLAP design into the Austroads, Mechanistic Empirical Design procedures.

In addition to the lack of a FEL one of the primary issues identified by industry was the limited data on material characteristics of typical Australian production mixes. Because of this limited dataset it was believed the values being adopted for the purpose of pavement design were overly conservative. Additionally they were not validated to field measurements. To obtain actual information and fill this gap, the APS-fL project set out to characterise typical Australian production mixes using the dynamic modulus test.

By reviewing the strategies for designing and maintaining long-life pavements in Australia, the UK, France, Netherlands and several states in the US, it was found LLAP could be achieved with a maximum thickness of 300-350mm and a minimum of 200mm was required for LLAP performance.

The results of the material characterisation study of 28 Australian mixes were used to develop a full set of dynamic modulus master curves. This will enable, for the first time, the calculation of modulus of Australian production mixes at any load frequency and temperature applicable to Australian field conditions.

There is still significant debate about the exact conversion between frequency in the dynamic modulus tests and loading time in a pavement structure. Hence this study used the results of field measured modulus from the FWD testing on the NCAT, Westrack and MnRoads test tracks sites to develop and validate a direct inter-conversion between the dynamic modulus test and field stiffness. The conversion was then used to validate strain results obtained at the NCAT test track against strains predicted by the use of layered elastic analysis and the converted stiffness.

The results of the modulus inter-conversion study found that 3 of the 4 common Australian test methods time has a different physical meaning and a frequency conversion is needed to shift between the time and frequency domain. It was found that shift factors could be established from single time/temperature testing and that the time shift factors found from the single time and temperature testing and are valid across the whole time frequency domain.

This study then investigated a number of procedures for the incorporation and modelling of the FEL using both Australian and overseas laboratory data. The procedures were then compared against the performance of LLAP, by examining the effects of temperature, modulus and strain levels at the NCAT test track and a recommended and calibrated modelling approach was developed. The recommended NCAT model was then validated against Australian LLAP sites and was adjusted to match the field performance of Australian and UK pavements incorporating a confidence based FEL modelling approach.

The study then made recommendations on the model form, number of seasons and vehicle classification required to model performance based on calibration and validation against actual performance. This provides an effective and efficient methodology to design LLAP.

Acknowledgements

I would like sincerely acknowledge the Australian Asphalt Pavement Association (AAPA) and members of the working APS-fL committee of the APS-fL project (Warren Carter, Erik Denneman, Geoff Jameson, Ryan Jansz, Mike Pickering, Nigel Preston, Ian Rickards, Greg Stephenson and Geoff Youdale who have contributed to the development of the APS-fL project.

I wish to specifically acknowledge the contribution of Geoff Youdale and Dougall Broadfoot for their input and encouragement in development of the LLAP design procedure. Ian Rickards who conceptualised and gained support for the APS-fL project. Tom Gabwray, Fulton Hogans Product Development Manager(Asphalt), who not only managed the testing undertaken as part of the APS-fL project, but the the historical testing ustalised in this study. Saeed Yousefdoost who undertook the majority of the material characterisation testing. David Paine, who was the project manager for the RMS STEP study who gratefully made the extensive database developed as part of that study available to the AAPA study.

I would also like to thank my employer, Fulton Hogan, for supporting me though the process.

Finally, I would like to sincerely extend my appreciation to my supervisor, Prof Hamid Nikraz, for his help, guidance and encouragement during this research work.

Table of Content

	Page
1 Introduction and Objectives	1
1.1 Background	1
1.2 Need for the Development of a Long Life Asphalt Pavement Design Procedure....	4
1.3 Research Objectives	4
1.4 Report Organisation	7
2 Literature Review and Theoretical Background.....	8
2.1 Introduction to Long Life Asphalt Pavements	9
2.2 Conventional Fatigue Characterisation	10
2.2.1 Fatigue Cracking of Asphalt Pavements.....	10
2.2.2 Conventional Fatigue Mechanistic Analysis.....	11
2.3 Viscoelastic Theory	13
2.3.1 Dissipated Energy Due to Load	13
2.3.2 Dissipated Energy and Fatigue	15
2.3.3 Relaxation and Creep	16
2.3.4 Dynamic Modulus Testing.....	17
2.4 Fatigue Endurance Limits in Asphalt	18
2.4.1 Existence of Endurance Limits.....	18
2.4.2 Healing a Source of Endurance Limits.....	21
2.4.3 Effect of Rest Periods on Healing	22
2.5 Laboratory Estimation of Fatigue Endurance Limits	23
2.5.1 Stiffness Ratio Methods	23
2.5.2 Ratio of Dissipated Energy Change	26
2.5.3 Healing Index	28
2.6 Long Life Asphalt Pavements	31
2.7 LLAP Material Selection.....	34
2.8 Field Observation of LLAP	35
2.8.1 US Studies	35
2.8.2 Designed LLAP Sections	37

2.8.3	UK TRL Studies.....	37
2.8.4	Australian Field Investigations on LLAP	39
2.8.5	The Asphalt Pavement Alliance (APA) Perpetual Pavement Awards.....	40
2.8.6	LLAP Terminal Thickness Requirements.....	42
2.9	Design Procedures for LLAP.....	44
2.9.1	Pavement Structural Distresses.....	44
2.9.2	Structural Rutting.....	44
2.9.3	Fatigue Cracking	45
2.9.4	Empirical Approaches	46
2.9.5	Terminal Thickness or Traffic.....	47
2.9.6	Mechanistic Empirical	48
2.9.7	NCAT Test Track.....	49
3	Experimental Plan.....	52
3.1	Overall Design.....	52
3.2	Material Classification Experimental Design.....	52
3.2.1	Mix Selection	53
3.2.2	Supply of Asphalt Mixes	53
3.2.3	Supplied Asphalt Mix Materials	54
3.3	Asphalt Mix Properties	55
3.3.1	Gradation.....	55
3.3.2	Volumetric Properties	57
3.4	Sample Preparation	58
3.4.1	Reheating of Mixes.....	59
3.4.2	Compaction of Mixes.....	59
3.4.3	Shear-Box Compactor.....	60
3.4.4	Coring and Trimming.....	62
3.5	The Dynamic Modulus Test	63
3.5.1	Testing System Set Up	63
3.6	Linking AAPA database with Overseas Research.....	64
3.7	Calibration Using NCAT Test Track Sites.....	65
3.7.1	Selected Test sites	65

3.7.2	Accelerated Loading at NCAT.....	66
3.7.3	Monitoring Field Performance (NCAT).....	67
3.7.4	Instrumentation.....	67
3.8	Other Calibration Sites	67
3.9	Validation with Field Data.....	68
3.10	RMS STEP Database	68
3.10.1	Database Development.....	69
3.11	UK VALMON Site Data	70
4	Dynamic Modulus Testing and Results	71
4.1	Reasons for Adopting the Dynamic Modulus Test.....	71
4.2	Master Curve Development and Time Temperature Superposition	72
4.2.1	Numerical Optimisation for Determination of Master Curves.....	74
4.3	Master Curves and Dynamic Modulus Test Results	76
4.3.1	Master Curve Fitting Parameters	76
4.4	Grouping of Australian Mixes	80
4.5	Typical Master Curves and Development of Confidence Intervals	83
4.5.1	Distribution of Errors around Master Curve	84
4.6	Development of Confidence Based Master Curves	85
4.7	Correlation with NCAT	87
4.8	Conclusions and Recommendations	Error! Bookmark not defined.
5	Conversion between Laboratory and Field Response.....	93
5.1	Introduction.....	93
5.1.1	Data for Comparison	93
5.2	Factors Effecting Conversion	94
5.2.1	Time Frequency Conversion	94
5.2.2	Vehicle Speed and Load Frequency.....	95
5.2.3	Empirical Relationships to Frequency.....	96
5.2.4	Dynamic Modulus and Field Strain	97
5.3	Calibration Plan	98
5.4	Optimisation Approach.....	98
5.4.1	Field Modulus Measurements	99

5.4.2	Effective Layer Modulus	100
5.4.3	Strain Calibration Validation	101
5.5	Conversion between FWD and Dynamic Modulus	104
5.5.1	Combined NCAT Sections	105
5.5.2	Validation against MnRoads and WesTrack	108
5.6	Calibration of Strain	110
5.6.1	Validation of Stress Based Approaches	110
5.6.2	Numerically Optimised Approach	112
5.7	Use of Australian Dynamic Modulus Master Curves to Predict Strain	115
5.7.1	Calculation of Modulus	115
5.7.2	Speed Incorporated Design Modulus Charts	117
5.8	Laboratory to Field Conversions Conclusions and Recommendations	Error!
	Bookmark not defined.	
6	Inter-Conversion of Current Australian Modulus Test Methods	123
6.1	Background	123
6.2	Introduction	123
6.2.1	Scope of Study	124
6.3	Theoretical Background	124
6.3.1	Observations	124
6.4	Differences in Test Results	125
6.4.1	Stress Susceptibility	125
6.4.2	Time Conversion	126
6.4.3	Stiffness in the Austroads Pavement Design Guide	127
6.4.4	Current Modulus Classification Methods in use in Australia	128
6.4.5	Previous Research	129
6.5	Materials and Test methods	129
6.5.1	Modulus Test Methods	129
6.5.2	Strain in Beam Fatigue	130
6.6	Comparison of Modulus Tests	131
6.6.1	Stress Dependency	131
6.6.2	Resilient to Dynamic Modulus	132

6.6.3	Dynamic Modulus to Flexural Beam Modulus.....	135
6.6.4	Summary.....	137
6.7	Master Curve Analysis	137
6.7.1	Un-Shifted Data.....	138
6.7.2	Shifted Master Curves.....	139
6.8	Summary Conclusions	Error! Bookmark not defined.
7	Development of a Field Calibrated FEL model for Pavement Design	142
7.1	Background	142
7.1.1	Scope	143
7.2	Laboratory Studies on FEL	143
7.2.1	Other FEL Recommendations.....	145
7.3	Single FEL Design Approach.....	146
7.4	Design Endurance Limit as a Distribution of Strain at Failure	146
7.4.1	Issues with Cumulative Distribution of Strain.....	148
7.5	Stiffness Based FEL Relationships.....	148
7.5.1	Incorporating Australian Mixes.....	148
7.6	Calibration of FEL for Pavement Design.....	151
7.6.1	Shifting of Cumulative Distribution of Strain.....	151
7.6.2	Development of a Stiffness Based FEL	153
7.6.3	FEL Relationship and Laboratory Shift from NCAT	155
7.7	Conclusions.....	Error! Bookmark not defined.
8	Validation with Australian Long Life Asphalt Pavement Sites	159
8.1	Introduction.....	159
8.2	Australian Long Life Pavement Sites	159
8.2.1	Current Condition of LLAP	162
8.2.2	Indeterminate Structures.....	169
8.2.3	Condition Assessment (FWD).....	171
8.2.4	Mid Layer Depth	172
8.3	Insitu Material Assessment	173
8.3.1	Layer Elastic Analysis	174
8.3.2	Bedrock	174

8.3.3	Assessing the Answers from Back-Calculation.....	175
8.3.4	Implications on Forward Calculations	176
8.3.5	Pavement Model for Back-calculation.....	176
8.4	Validation of Stiffness-FEL Relationship with Australian Data.....	179
8.5	Establishing Confidence Levels	182
8.6	Laboratory to Field Shift	185
8.7	Endurance limits for lower level traffic	185
8.8	Conclusions of the Validation of Modulus Based FEL.....	Error! Bookmark not defined.
9	Austrroads Supplement Recommendations	188
9.1	Introduction.....	188
9.2	(3) Construction and Maintenance Considerations.....	188
9.2.1	(3.2.5) Working Platforms	188
9.2.2	(3.7) Pavement Layering Considerations.....	188
9.2.3	(3.12) Maintenance Strategy.....	189
9.3	(4) Environment.....	189
9.3.1	(4.3) Temperature	189
9.3.2	(4.3.1) Calculation of Effective Layer Temperature	189
9.3.3	(4.3.1.1.) Surface Temperature (Summer).....	190
9.3.4	(4.3.1.1.) Lower Surface Temperature (Winter).....	191
9.3.5	(4.3.1.1.) Effective Pavement Temperature	191
9.4	(5) Subgrade Evaluation	191
9.4.1	(5.1) Measures of Subgrade Support.....	191
9.4.2	(5.9) Subgrade Failure Criteria.....	192
9.5	(6.4) Asphalt.....	192
9.5.1	(6.4.1.3) Characteristics for Design.....	192
9.5.2	(6.4.2) Factors Affecting Modulus and Poisson's Ratio	193
9.5.3	(6.4.2.1) Binder Class and Content.....	193
9.5.4	(6.2.2.2) Air Voids.....	193
9.5.5	(6.2.2.3) Aggregates	193
9.5.6	(6.2.2.4) Temperature	194

9.5.7	(6.4.2.2) Rate of Loading (Time)	194
9.5.8	(6.4.3.2) Laboratory Measurement.....	195
9.5.9	(6.4.3.3) Typical Charts	196
9.5.10	(6.4.5) Suggested Fatigue Endurance Limit	197
9.6	(7) Design Traffic.....	197
9.7	(8) Design of LLAP	198
9.7.1	(8.1) Mechanistic Procedure	198
9.7.2	(8.2.3) Combined Asphalt Layer Modulus.....	198
9.8	Example	201
10	Conclusions and Recommendations	203

Appendices

Appendix A Mix Details and Dynamic Modulus Results

Appendix B STEP Sites

Appendix C Confidence Interval Calculations

Appendix D Laboratory to Field Conversions

1 FWD

2 Strain

Appendix E Backcalculation results

Appendix F FEL Validation

1 LLAP Sites

2 Non LLAP Sites

List of Figures

Figure 2-1 Typical Fatigue (Crocodile) Cracking	10
Figure 2-2 Relationship between fatigue Equation Constants.....	12
Figure 2-3 Typical Stress Strain Curve for Visco-elastic Solid	14
Figure 2-4 Strain Load Relationship Illustrating the FEL (after Thompson et al. (2006))	19
Figure 2-5 Weibull Fitting Function (Sullivan 2015)	25
Figure 2-6 Accuracy of Weibull Fitting Functions after, Sullivan (2015)	25
Figure 2-7 Dissipated Energy Plot and Plateau Value.....	27
Figure 2-8 Plateau Value-Nf Relationships (after Carpenter et al. (2006)).....	28
Figure 2-9 Stiffness vs. Number of load cycles with and without rest period.	29
Figure 2-10 Endurance limit determination at each temperature based on HI	30
Figure 2-11 Typical Survivor Curve, After NCHRP Report 646	36
Figure 2-12 TRL Design Chart, after Nunn (2001)	48
Figure 3-1 Gradation plots "Nominal" 14mm mixes	56
Figure 3-2 Gradation plots "Nominal" 20mm mixes	56
Figure 3-3 Volumetric Plots (a) 14mm Mixes.....	57
Figure 3-4 Volumetric Plots 20mm Mixes	58
Figure 3-5 Shear box Compaction Concept.....	60
Figure 3-6 Shear Box Compactor	62
Figure 3-7 Dynamic Modulus Test Setup.....	64
Figure 3-8 Phase II NCAT Structural Sections, after Timm et al (2006).....	66
Figure 4-1 Construction of Dynamic Modulus Master curve and Temperature Shift Factor Function.....	75
Figure 4-2 Temperature Shift Factor Function.....	75
Figure 4-3 Master curves 14mm	78
Figure 4-4 Master curves (a) 20mm.....	79
Figure 4-5 Typical Modulus Grouping Results AC20 AR450.....	81
Figure 4-6 Accuracy of Grouping Approach.....	82
Figure 4-7 Typical Modulus Grouping Results and distribution of errors around the master curve	84
Figure 4-8 Confidence Interval Master Curve	86
Figure 4-9 Comparison of NCAT and AAPA modulus results	89
Figure 4-10 NCAT and AAPA Modulus Results mix 14-10.....	90
Figure 4-11 NCAT and AAPA Modulus Results mix 14-13.....	90
Figure 5-1 Model used to Calculate Load Duration	96
Figure 5-2 S9 Control Mix Frequency Conversion.....	105
Figure 5-3 Accuracy NCAT Converted Dynamic Modulus vs. FWD Stiffness.....	107
Figure 5-4 NCAT Converted Dynamic Modulus vs. FWD Stiffness.....	107
Figure 5-5 MnRoads Modulus Comparison	108

Figure 5-6 Westrack Modulus Comparison.....	109
Figure 5-7 Validation of Pulse with Depth Approaches Brown	111
Figure 5-8 Validation of Pulse with Depth Approaches CalMe	112
Figure 5-9 Unconstrained Optimisation Equivalent Layer	113
Figure 5-10 Unconstrained Optimisation Multilayer	114
Figure 5-11 Design Modulus Chart DG14 A15E.....	118
Figure 5-12 Design Modulus Chart DG14 C320	118
Figure 5-13 Design Modulus Chart DG14 AR450.....	119
Figure 5-14 Design Modulus Chart DG20 C320	119
Figure 5-15 Design Modulus Chart DG20 AR450.....	120
Figure 5-16 Design Modulus Chart DG20 C600	120
Figure 6-1 Modulus Comparisons.....	125
Figure 6-2 Flexural Fatigue Test (after NCHRP 9-44(2013)).....	130
Figure 6-3 Stress Susceptibility	131
Figure 6-4 Resilient vs. Dynamic Modulus.....	134
Figure 6-5 Flexural Dynamic Modulus Frequency Shift.....	136
Figure 6-6 Comparison of Modulus Results (Un Shifted)	138
Figure 6-7 Shifted Master Curves	140
Figure 7-1 Stiffness FEL Relationships.....	144
Figure 7-2 Cumulative Distribution of Strain NCAT, after Willis et al. (2009)	147
Figure 7-3 FEL Stiffness Curve Australian Mixes	150
Figure 7-4 Modulus Strain Relationship NCAT Phase II.....	153
Figure 7-5 Modulus Strain Relationships NCAT	154
Figure 7-6 NCAT Calibrated FEL Relationship	156
Figure 8-1 H-S22 New England Freeway	162
Figure 8-2 Pacific Motorway (N.B), Bar Point	163
Figure 8-3 Pacific Motorway (N.B), Mooney Mooney	163
Figure 8-4 Pacific Motorway Ourimbah, (SB)	164
Figure 8-5 Pacific Highway, (Maitland Road) (NB)	164
Figure 8-6 Pacific Highway Cumbalum (NB)	165
Figure 8-7 Picton Road, Avon (EB).....	165
Figure 8-8 Botany Road, Port Botany, (NB).....	166
Figure 8-9 Milpera Road, (WB), Condell Park	166
Figure 8-10 Bruce Highway (Q5), Kallangur (SB).....	167
Figure 8-11 Bruce Highway (Q6), Kallangur (SB).....	167
Figure 8-12 Camden By-Pass (SB)	168
Figure 8-13 Alpha Street Blacktown (EB)	168
Figure 8-14 Atherton Road, Oakleigh, (EB).....	169
Figure 8-15 Deflection Bowls LLAP	171

Figure 8-16 Deflection Bowls Non LLAP.....	172
Figure 8-17 Estimating the Depth to Bedrock.....	175
Figure 8-18 Modulus Strain Endurance Curve Australian Sites	180
Figure 8-19 Validated Stiffness-Strain Endurance Curve Australian Sites.....	181
Figure 8-20 Normal Score (FEL).....	183
Figure 8-21 Confidence Limits and LLAP Sections	185

1 Introduction and Objectives

1.1 Background

Fatigue cracking of an asphalt pavement, along with roughness and rutting, is one of the most common forms of pavement distress. Fatigue cracking in asphalt pavements manifests itself as a series of interconnected cracks resembling the skin of a crocodile and as such, is often referred to as crocodile cracking. This cracking is caused by a fatigue failure of the asphalt mix from repeated bending of the asphalt under traffic loading. The repeated bending of the asphalt layer(s) in the pavement results in elongation (tensile strains) at the base of the asphalt layer and the established theory states that each cycle of this bending results in un-recoverable damage to the asphalt mix. The sum of this repeated damage eventually results in the loss of structural integrity of the asphalt, and at a critical point in the damage process, the formation of a crack. Once the crack is formed the continual action of traffic propagates it through the asphalt resulting in fatigue cracking of the asphalt mix. However, recent studies show that not all loading to asphalt pavements may induce damage and if strains are kept low enough this cracking may not occur. Even after decades of research the modelling of fatigue performance of asphalt mixes is far from an exact science and a better understanding would enable significant advances in pavement design and construction.

To accurately predict the response of a pavement to loading and therefore the subsequent performance, the fundamental material characterisation property, modulus or stiffness, must be representative and able to characterise an asphalt mix across the full range of temperatures and loading speeds experienced by the pavement. Internationally, the Dynamic Modulus (DC-CY) test has gained widespread acceptance for the characterisation of asphalt mixes across the full temperature frequency range. One of the principal advantages of the dynamic modulus test is the broad database which has been and is continually being developed to link laboratory results to actual field performance (modulus and strain), particularly at the NCAT test track. As with all modulus tests there are a number of issues with the conversion of laboratory results to field response, namely; time inter-conversion, stress susceptibility, effective temperature, and loading pulse width, none of which had been fully validated.

The current Austroads pavement design procedure (AGPT02 (2012)) (and most mechanistic procedures throughout the world) uses conventional theory that assumes every cycle of loading to a pavement does damage to the asphalt layer(s) and therefore uses a proportion of the asphalt's life. However, as previously mentioned, recent studies have shown that asphalts have a Fatigue Endurance Limit (FEL) and that if strains remain below this limit, the healing potential of the asphalt will, at some time, become greater than the damage sustained within the loading cycle. If the strains within the asphalt layers are kept below this

FEL the asphalt can withstand an extremely large number of loading cycles, often referred to as infinite, without experiencing fatigue failure.

The concept of a FEL was introduced in metals by Wohler in the 1870's. Wohler defined the FEL as the stress level below which fatigue failure did not occur. In pavement design the concept is not new with the design of concrete pavements incorporating a FEL, expressed as a minimum strength to stress ratio. In asphalt pavements the concept was introduced by Monismith and McLean (1972) who found that there appeared to be a strain level below which damage to an asphalt mix does not appear to occur.

Field verification of the FEL and the resulting Long Life Asphalt Pavement (LLAP) was found to exist in the United Kingdom by Nunn (2001) who observed the performance of a number of sites across UK between 1984 to 1997, and found that pavements which should have been weakening with traffic loading (as per the conventional theory), showed no signs of structural deterioration. Contrary to the conventional theory, Nunn found that *"the great majority of the thick pavements examined have maintained their strength or become stronger over time."* Subsequent studies by US researchers such as, Mahoney (2001) and Powell (2010) also found LLAP indeed existed most likely due to the presence of the FEL.

Over the past decades a number of test protocols have been developed to determine the fatigue behaviour of asphalt mixes. The accuracy of these test procedures in being able to predict the fatigue performance of an asphalt mix in the field depends on how accurate the test procedure replicates the field conditions of support, stress state, environment, loading conditions and frequency. In Australia the most common fatigue test is the 4 Point Bending (4PB-PR) beam fatigue test. Even though this test has been in existence for 20 years there are still significant difficulties in simulating actual field conditions with this test, some of which were identified by Denneman (2013). For this reason a shift is required between laboratory results and field performance. However, as found by Harvey (1997) the shift factor varies according to a number of conditions and Harvey reported shift factors ranging between 10 and 100. Research by Thompson et al. (2006) found that the wide variety of shift factors was due to the constrained model form used in the conventional fatigue analysis and concluded that a global shift could not exist. While a shift factor is known to exist, the current AGPT02 (2012) offers no recommendations on calculating or applying the shift factor for the purpose of pavement design, most likely due to the complexity of recommending one. Clearly, the prediction and modelling of the fatigue performance of an asphalt mix is difficult and a simpler design approach would be to simply design fatigue out of asphalt pavements by using the FEL concept.

The realisation that LLAP exist and there may indeed be an FEL for asphalt mixes, has led researchers to examine and develop mechanistically based models and test methods for the prediction and incorporation of the FEL into pavement design. Thompson and Carpenter

(2006) showed that the performance of a number of asphalt mixes at low strains was distinctly different from that at larger strain levels and that at small strain levels, any small decrease in the strain level resulted in a very large increase in fatigue life. Based on this testing Thompson and Carpenter developed a method for the prediction of the fatigue performance and the FEL of an asphalt mix based on laboratory testing using the Ratio of Dissipated Energy Change.

Further research undertaken as part of the NCHRP 9-44 study (2013) by Witczak et al. confirmed the existence of the FEL and showed that the FEL of all mixes varied with both temperature and length of the rest period, with the FEL increasing with increasing rest periods. It was hypothesized that this increase in the FEL was directly related to the healing potential of the asphalt mix. The 9-44 study recommended an alternative approach for the determination of the FEL based on the work done by Schapery's (1978) elastic-viscoelastic correspondence principle and the pseudo stiffness and Healing Index (HI) approach.

In addition to simplifying the design approach, if the FEL could be incorporated into pavement design it will become an important parameter to determine the limiting thickness of the asphalt layer, beyond which any increase in the thickness of the asphalt layers results in no increase in the structural capacity of the pavement. To incorporate the FEL into LLAP design, most researchers have recommended design approaches based on the use of a single FEL, as originally recommended by Monismith (1972). However, the use of a single FEL is contrary to the most recent research undertaken as part of the NCHRP 9-38 (2012) and 9-44 (2013) projects, both of which found the FEL is not fixed and changes with changes in both mix properties and temperature. These researchers found that stiffness could be used as a surrogate for the effect of temperature and mix properties on the FEL and that the FEL was directly related to the stiffness of the mix, with the 9-44 study recommending the use of stiffness-FEL relationships for LLAP design.

Understanding the significant limitations in applying a single FEL for the purpose of design, the NCAT researchers developed an alternative LLAP design approach, the Cumulative Distribution of Strain (CDS) concept. The CDS approach was unique in that it allowed for variability in FEL in practice, with the approach in reality controlling the strains so only a limited number of loads exceed the FEL of the mix.

Clearly, significant sustainability advantages can be achieved in Australia by designing LLAP. Realising this, AAPA undertook the Asphalt Pavements Solution for Life (APS-fL) project and developed a detailed plan to explain and validate a mechanistic design procedure for the incorporation of the FEL into pavement design. In particular, the procedure needed to consider the Australian environmental conditions and incorporate the effects of the increased healing potential of Australian mixes due to the higher pavement temperatures experienced in Australia relative to much of the rest of the developed world.

1.2 Need for the Development of a Long Life Asphalt Pavement Design Procedure

The value of an asphalt pavement is not the total thickness of the asphalt layers, nor the lowest strain or deflection in the pavement. It is the serviceability the customer realises from the pavement throughout its life, relative to what they pay for the pavement. A pavement is not quality because it is thick, contains polymers or costs a lot of money. If the current Australian design procedure produces asphalt pavements which contain asphalt which offers little value to the customer, there is a loss of value, sustainability and waste of resources in the solution.

This potential loss of value was recognised by clients, industry and consultants with the 2011 AAPA Master Class raising concerns that the current Australian design procedure produces overly conservative asphalt pavement designs, particularly at high temperatures and high loadings, leading to suboptimal value in the pavement solution.

At that 2011 Master Class, a number of issues were raised which were believed to possibly contribute to the overly conservative designs being produced in Australia. The issues identified were;

1. limited data on material characterisation of Australian mixes resulting the use of overly conservative material properties,
2. lack of recognition of the effect of confining stress when charactering mixes at low speeds and high temperatures,
3. the lack of a calibrated and validated shift factor between laboratory observations and field performance,
4. the lack of incorporation of the healing mechanism in asphalt mixes
5. discrepancies in the modelling of the fatigue potential of asphalt mixes at higher temperatures, and,
6. the lack of recognition of a “threshold” strain or FEL below which no damage occurs.

If some or all of these concepts could be incorporated into the current pavement design procedure, more efficient design could be developed. In particular, it was felt that if the FEL could be incorporated into a pavement design procedure, Australia could design LLAP, meaning the limiting thickness of asphalt could be determined, beyond which any increase in design thickness will result in no increase in the structural capacity of the pavement.

1.3 Research Objectives

This research was undertaken as part of the APS-fL project and the main objective of this phase of the APS-fL project was the development of a LLAP design procedure for Australia. To achieve this goal, an extensive experimental plan was developed. This phase of the study consisted of 4 main tasks and a number of subtasks for each as shown following.

- **Task 1 Development of Dynamic Modulus Database.** Task 1 consisted of a material characterisation study, undertaken to provide real data on the performance characteristics of actual standard Australian production mixes. To be consistent with the direction being taken internationally, the experimental design of the project was developed with an ultimate goal of developing a set of dynamic modulus master curves for real Australian production mixes. The primary advantage of the development of master curves is that the curves can be used for the determination of modulus and visco-elastic properties of Australian asphalt mixes across the full spectrum of temperature and load speeds relevant to Australian field conditions. To accomplish this the following subtasks were undertaken:
 - A comprehensive laboratory testing program to characterise typical Australian Asphalt mixes using the Dynamic Modulus test of a full range of Australian production asphalt mixes.
 - Development of a computerised database summary of these test responses and mix characteristics.
 - A comparison of the material properties of Australian mixes against US and European mixes to confirm similar performance and therefore the transferability of the results from the US and Europe to Australian conditions.
 - Recommendation of a modeling method for the prediction of dynamic modulus based on primary material properties (binder type, aggregate size) for the purpose of pavement design.

- **Task 2 Laboratory to Field Modulus Inter Conversion.** At the time of undertaking the study, there was no recommended method found in the literature for the conversion of laboratory determined dynamic modulus to strains under a moving vehicle which had been validated against actual field measurements. Without an accurate prediction of strain, the calibration of any FEL model would be difficult, if not impossible. Fortunately, the NCAT track has a significant amount of data which was used to determine if an inter-conversion was possible between laboratory dynamic modulus and field stiffness and subsequent strain. To establish this inter-conversion the following sub-tasks were undertaken:
 - Establish if any valid and accurate correlation/relationship exists between laboratory modulus and field stiffness using laboratory results and field measurements from FWD testing at full scale test tracks. (NCAT, MnRoads and Westrack)
 - Determine the effect of stress susceptibility on the measurement of modulus and recommendation of how to consider stress susceptibility in the modeling of field response.
 - Development of a quantitative method that can be used to inter-convert between laboratory modulus and field stiffness for the prediction of strain

under a moving vehicle, using the relationship developed between laboratory modulus and field stiffness and strain/stress pulse relationship.

- **Task 3, Relationship between Dynamic Modulus and Current Australian Test Methods.** Australia has a number of characterisation tests for the determination of asphalt modulus which are different from the dynamic modulus test used in this study and produce different modulus results. These differences have the potential to create confusion and errors in design. In order to not to lose existing experience and to add to the robustness of the project, an additional task was added to the study, to inter-convert the dynamic modulus test with the current Austroads test methods, namely:
 - Development of an inter-conversion between the dynamic modulus test and the resilient modulus test conducted at 25°C and with a rise time of 0.04sec.
 - Development of an inter-conversion between the dynamic modulus test and the flexural modulus test undertaken at 20°C and 10Hz.
 - And as a consequence the interconversion between the resilient and flexural modulus test.
- **Task 4 Recommendation of Method for Incorporation of FEL into Pavement Design.** Once an accurate prediction of pavement response had been established, it was then possible to calibrate mechanistic models for the prediction of structural damage, (or lack of in the APS-fL project), through calibration and validation of a FEL model against field performance. In the case of the APS-fL project, the procedure developed ensures the pavement response remains below FEL to ensure little to no damage occurs to the pavement. The objective of the research was to develop a procedure based off laboratory investigations and calibrated using full scale test track data and finally, validated using real in-service asphalt pavements. The resulting procedure developed is then able to model the effects of changes in asphalt mix properties (stiffness) and most importantly for Australian conditions, the increase in the FEL which is known empirically and has been subsequently confirmed in laboratory testing to increase with increasing pavement temperature. To accomplish this a number of sub sub-tasks were developed and undertaken, namely:
 - Development of a modeling procedure for the incorporation of a FEL in pavement design based off the examination of both laboratory analysis and field performance of LLAP at the NCAT test track.
 - Calibration of the modeling procedure developed by the examination of the NCAT test track data based on the performance of real LLAP sections on the NCAT test track.
 - Validation of the modeling procedures based on in service Australian LLAP and time series data obtained from real United Kingdom LLAP pavement sections.

1.4 Report Organisation

The content of this report is divided into 9 chapters. The description of these chapters is as follows.

- 1) Chapter 1, Introduction and Research Objectives. As already observed Chapter 1 is intended to outline the research background, objective and scope of the research.
- 2) Chapter 2, provides a literature review and the theoretical background of:
 - Conventional fatigue analysis
 - Visco Elastic Theory
 - Endurance Limits and healing characterisation
 - Laboratory estimation of FEL
 - LLAP asphalt pavements
 - LLAP material selection
 - Field observation of LLAP
 - Design of LLAP
- 3) Chapter 3, documents the major scope of the comprehensive laboratory experimental testing program undertaken on production mixes from actual projects across Australia. The summary of the master computerised database of the dynamic modulus testing is shown in Appendix A.
- 4) Chapter 4, provides analysis of the dynamic modulus results, the production of master curves and recommendations on the use of the dynamic modulus results for pavement design.
- 5) Chapter 5, develops an inter-conversion between laboratory modulus results and field stiffness based off FWD testing at the NCAT, MnRoads and Westrack test tracks. These results are then used to develop a method for modeling the effect of vehicle speed on frequency to predict strain under a moving vehicle.
- 6) Chapter 6, recommends a method for the conversion of dynamic modulus results to the current Australian test methods, flexural and resilient modulus.
- 7) Chapter 7, documents the development of FEL design approach based on laboratory data and full scale test track data. This chapter examines the use of the single FEL, cumulative distribution of strain and the use of modulus based FEL for the purpose of pavement design.
- 8) Chapter 8 uses the recommendation of Chapter 7 and reviews and validates the recommendations based upon the results of actual field performance of pavements in both Australian and UK.
- 9) Chapter 9, brings the previous research findings together and documents a proposed supplement to the Austroads Pavement Design Guide.
- 10) The concluding chapter, Chapter 10, provides a summary of the major findings of the research study and provides recommendations for use of the research findings as well as recommendations for future research.

2 Literature Review and Theoretical Background

This chapter is divided into nine major sections, the structure of which is shown following:

- Introduction to LLAP
- Conventional fatigue analysis
 - Fatigue cracking of asphalt pavements
 - Conventional mechanistic analysis
- Visco elastic theory
 - Dissipated energy due to load
 - Dissipated energy and fatigue
 - Relaxation and creep
 - Dynamic modulus testing
- Fatigue endurance limits in asphalts
 - Existence of Endurance Limits
 - Healing a source of endurance limits
 - Effect of rest periods on healing
- Laboratory estimation of fatigue endurance limits
 - Stiffness ratio methods
 - Ratio of dissipated energy change
 - Healing index
- Long Life Asphalt Pavements
- LLAP material selection
- Field Observation of LLAP sections
 - US Studies
 - Designed LLAP sections
 - UK TRL studies
 - Australian field investigations
 - APA perpetual pavement awards
 - LLAP terminal thickness requirements
- Design procedures for LLAP
 - Pavement structural distress
 - Structural rutting
 - Fatigue cracking
 - Empirical approaches
 - Terminal thickness or traffic
 - Mechanistic Empirical
 - NCAT test track

2.1 Introduction to Long Life Asphalt Pavements

The concept of Long-Life Asphalt Pavements (LLAP) (long lasting, extended life, or perpetual) was developed in both the United Kingdom and the United States in the early 90's and now is well recognised internationally. In Australia, this concept is recognised by owners, industry and consultants alike, with the 2011 AAPA Master Class agreeing that there was a FEL and the FEL was an important parameter needed for future pavement design in Australia. Throughout the world there are two primary definitions for LLAP pavements, principally originating from the UK and US definitions respectively;

- a pavement which gets stronger with time (i.e. deflections reduce)
- or, a pavement which does not structurally crack.

Whether designs are produced by either definition is a pure theoretical debate as both definitions produce the same effect, which is a long-life pavement.

Sharp (2001) postulated the existence of LLAP in Australia, the presence of which was subsequently confirmed by Rickards et al. (2010) by the examination of the LTPP sites across Australia, Rickards concluded, *"The empirical evidence from Australia, the US and UK, suggest that the continual application of our current design models for thick asphalt pavements, results in overly conservative and wasteful designs and some designs appear long-life."*

The performance of LLAP pavements can be explained by the presence of either, or both, a Fatigue Endurance Limit (FEL) and thermal healing and in most cases both are combined to a single FEL (with fixed healing for a rest period). Regardless, of the explanation of the mechanism, the design objective is the same, to design an asphalt pavement structures where at some point in the life of the pavement, the rate of healing becomes greater than the rate of damage and therefore macro cracking will never occur and as a consequence no structural maintenance will be required and maintenance will be limited to periodic resurfacing. The mechanism for both thermal healing and FEL are described following:

- Thermal healing is the ability of a material to self-recover its mechanical properties (stiffness or strength) to some extent upon resting due to the closure of micro cracks.
- Threshold strain or FEL is the strain level below which result in no damage occurring to the asphalt and the asphalt mix tends to have an extraordinary long fatigue life.

2.2 Conventional Fatigue Characterisation

2.2.1 Fatigue Cracking of Asphalt Pavements

Fatigue cracking of an asphalt pavement is one of the most common forms of pavement distress along with roughness and rutting. The appearance of fatigue cracking is a series of interconnected cracks resembling the skin of a crocodile and as such, is often referred to as crocodile cracking. This cracking is caused by the fatigue failure of the asphalt mix from repeated bending of the asphalt under traffic loading.

The repeated bending of the asphalt layer(s) in the pavement results in elongation or tensile strain at the base of the asphalt layer. Conventional theory states that with each bending cycle some of the elongation is continually un-recoverable and damage occurs to the asphalt mix. The sum of this un-recoverable damage eventually results in the loss of structural integrity of the asphalt and at a critical point, the formation of a macro-crack. Once this crack is formed the continual action of traffic propagates the crack through the asphalt material resulting in fatigue cracking of the asphalt mix, as shown in Figure 2-1 following.



Figure 2-1 Typical Fatigue (Crocodile) Cracking

Even after decades of research the modelling of fatigue performance of asphalt mixes is far from an exact science and any better understanding will enable significant advances in both pavement design and construction. Over the past decades a number of test protocols have been developed for determining the fatigue behaviour of asphalt mixes. The accuracy of these test procedures in being able to predict the resistance of an asphalt mix in the field to fatigue depends on how accurate the test procedure replicates the field conditions of, support, stress state, environment, loading conditions and frequency. In Australia the most popular fatigue test is the beam fatigue test. Even though this test has been in existence for over 20 years, as described by Molenaar (2013) and others, significant gaps between the

laboratory test method and actual field conditions and performance have been identified. To account for these gaps a “shift” factor is often recommended between laboratory testing and field performance. However, as identified by Harvey (1997) the shift factor varies according to a number of conditions and shift factors of between 10 and 100 have been reported. The same finding has been reported by numerous other researchers such as Roque (2006). Roque also found trend reversals between laboratory performance and field performance (i.e. good performance in the laboratory and worse performance in the field), and aged materials giving better performance than un-aged. While the shift factor is recognised in AGPT002 (2012), there are no recommendations on calculating or applying the shift factor for the purpose of pavement design.

2.2.2 Conventional Fatigue Mechanistic Analysis

In conventional Mechanistic-Empirical pavement design, the fatigue of asphalt mixes is based on the principle that the repeated cyclic strain (at the underside of the asphalt layers as a result of bending) ultimately results in cracking and fatigue failure of the pavement. To predict the life of the pavement before this cracking occurs, most mechanistic design methods make use of a theoretical damage relationship to ensure the magnitude of the strains are controlled below a critical level.

For the structural design of asphalt pavements the conventional model for the prediction of the fatigue life of an asphalt layer(s), is a straight line (log scale) relationship between the tensile strain and the number of allowable number of load repetitions to failure (N_f) (strain- N_f). In Australia (as in the majority of the world), failure is commonly taken as a 50% reduction in initial modulus and is shown in Equation 2-1, following:

$$N_f = \left(\frac{k}{\mu\varepsilon} \right)^n \quad \text{Equation 2-1}$$

Where;

- N_f is the number of load cycles to failure,
- $\mu\varepsilon$ is the tensile strain, in micro-strain at the outer fibre of the asphalt mix,
- k and n are regression constants from the laboratory testing.

Because of the phenomenological nature of this relationship (relationship built on observations), most researchers propose that an adjustment factor be applied to obtain a “better fit” with observed results. The most notable adjustment addition is the addition of a modulus term, as shown in Equation 2-2 following, which is usually applied when multiple mixes or temperatures are being included, as in the AGPT002 (2012).

$$N_f = k \left(\frac{1}{E_0} \right)^c \left(\frac{1}{\mu\varepsilon} \right)^n \quad \text{Equation 2-2}$$

Where;

- E_0 is the initial modulus of the mix,
- C is a regression constant from the laboratory testing.

Thompson et al. (2006) found that the fundamental nature of the strain relationship accounted for 90% of the prediction in the data and the addition of the modulus term accounted for the remainder, and for the inadequacies of a non-fundamental relationship. Thompson et al. identified the main failing of the current model form was the inclusion of mix variables primarily in the “k” term and the use of a constant “n” value, regardless of the asphalt materials or test temperature. Thompson stated that the use of this model form ignores the vast majority of test data which has shown that k and n are integrally related in a consistent manner. This consistent relationship was found by Thompson et al. (2006) and is supported by observed Australian data, as shown in Figure 2-2 following. This figure illustrates the relationship between n and k based off the results of over 100 different mixes from Fulton Hogan database undertaken over the past 20 years.

In the data set air voids varied from 4 to 7 percent. Nominal maximum aggregate size has varied from 10mm to 28mm. Asphalt binders varied from C170 to C600, with both neat and polymer modified (SBS, SBR, EVA) materials being used.

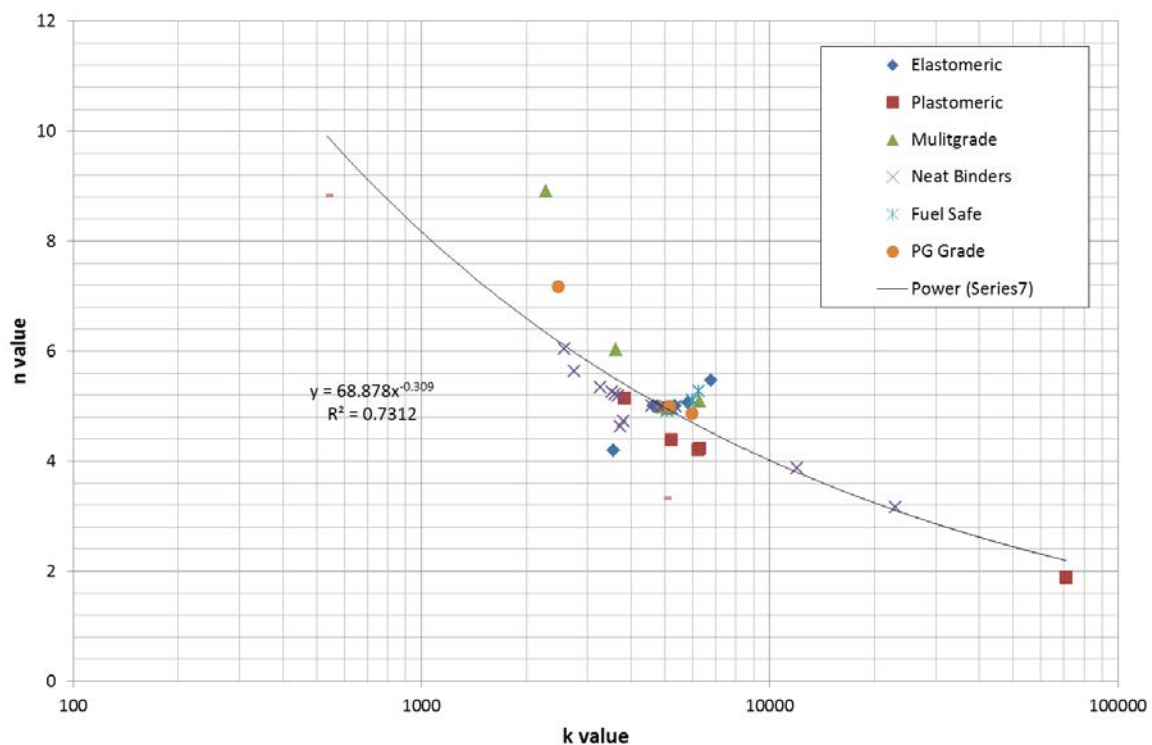


Figure 2-2 Relationship between fatigue Equation Constants

As found by Thompson et al. (2006) on US mixes, there is a distinct relationship between k and n for Australian mixes, given this relationship, any model that fixes “ n ” will be incorrect. Thus the outcome of the use of the k and n relationship (Equation 1) will be overshadowed by the use of a constant n relationship, so any attempt at national calibration would not be expected to be indicative of the performance found in varying regions of Australia. It is not surprising therefore, that the variable shift factors are consistently obtained in laboratory to field calibrations (Harvey (1997)).

The other main failing of the classical model is the assumption that every cycle does damage. This assumption ignores the presence of relaxation, healing and the FEL concept. If these parameters are included in the classical model, bottom-up fatigue cracking, which the classical models predict, can be avoided, not just designed for.

2.3 Viscoelastic Theory

Any study on the characterisation of asphalt mixes including stiffness, healing and the FEL, needs to be undertaken with a background understanding of viscoelasticity. Whereas, pavement structures are commonly assumed to be linear elastic materials in design, the effect of time and temperature, the amount of damage, relaxation and healing of the asphalt mixes are all related to its viscoelastic nature.

Fundamentally, viscoelastic materials are those where the relationship between stress and strain depends on time. Due to this time dependent behavior, some of the properties of viscoelastic material are:

- If the stress is held constant, the strain increases with time, (creep).
- If the strain is held constant, the stress decreases with time, (relaxation).
- The effective stiffness or modulus depends on the rate of application of the load.
- If cyclic loading is applied, a phase lag (hysteresis) occurs, leading to a dissipation of mechanical energy.

Unlike purely elastic materials, a viscoelastic material has both an elastic component (spring) and a viscous component (dampener). It is the viscous component of a viscoelastic material that results in the strain response being dependent on time and is why they are commonly referred to as time dependent materials. The time dependent behaviour of viscoelastic materials is commonly explained by constitutive equations, which include time as a variable in addition to stress and strain.

2.3.1 Dissipated Energy Due to Load

When a load or stress is applied to a material, the material will deflect under that load (strain), the resulting area under the stress-strain curve is the energy applied to the sample. For a purely elastic material (such as most metals in the elastic region) when the load is

removed from the material, the deformation is fully recovered. If the loading and unloading curves overlap, all of the energy put into the material is recovered and the sample returns to its original state, as is the case for elastic materials.

However, for viscoelastic materials the two curves do not coincide, as shown conceptually in Figure 2-3 following, and energy is lost in the material. This energy can be lost through mechanical work, heat generation, or damage. Because energy is lost, the material will not fully return to its original shape and some permanent deformation is observed. This energy difference between the loading and unloading curve is the dissipated energy of each loading cycle, Ghuzlan (2001).

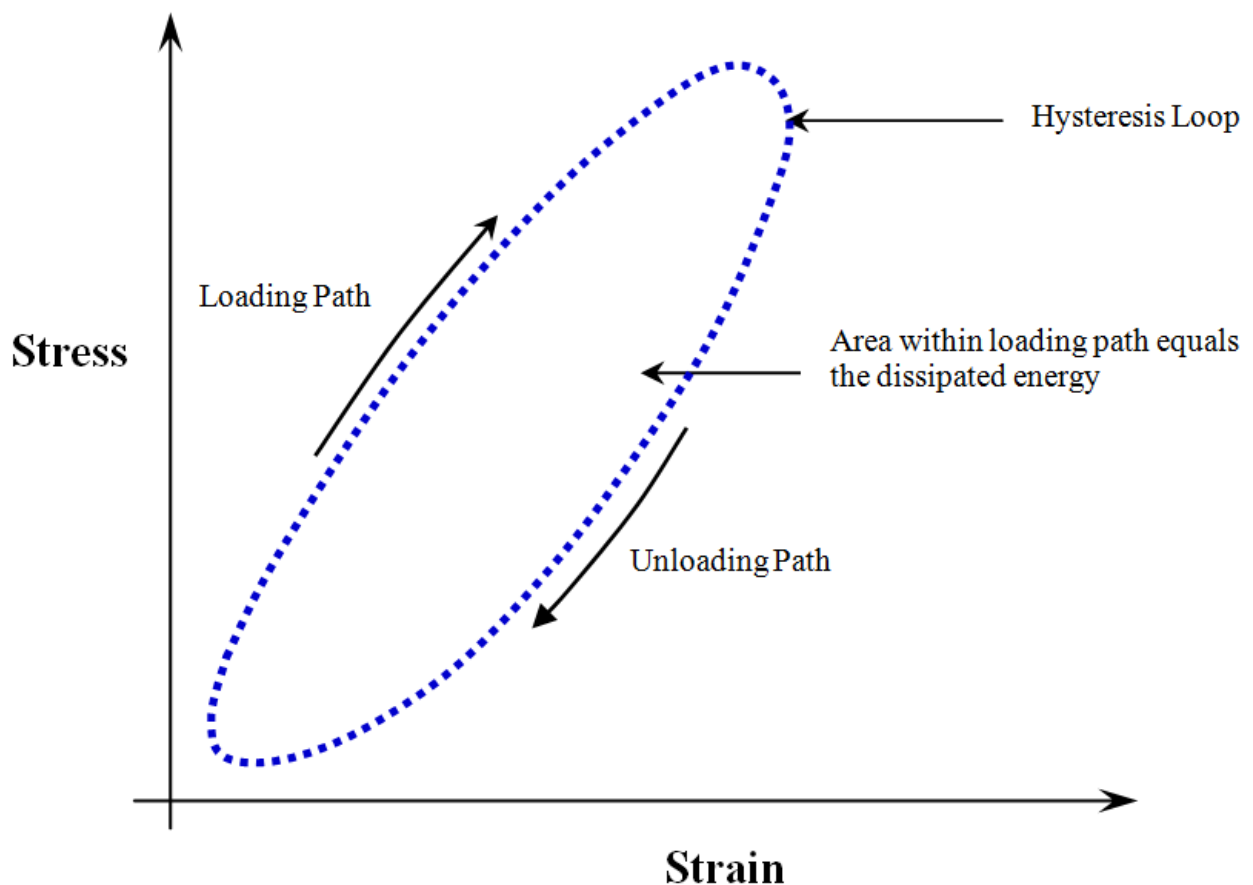


Figure 2-3 Typical Stress Strain Curve for Visco-elastic Solid

In damage analysis of asphalt mixes it is a common assumption that all of the dissipated energy went into damaging the material. However, due to the viscoelastic nature of the asphalt materials, a hysteresis loop will always be created, even when there is no damage to the asphalt, and in the loading and unloading cycle only part of the total dissipated energy

will go into damaging the material, with the remainder due to viscoelasticity, heating and other factors.

Manfredi (2001) demonstrated that not all dissipated energy goes into damaging the sample. Manfredi showed experimentally that energy dissipated during plastic cycles did not contribute to damage and should be excluded from the total energy. Hilton et al. (1992) found that part of the dissipated energy was converted to thermal energy through viscoelastic damping. Additionally, any source of release energy (which is still part of the overall dissipated energy) which does not go into crack formation and propagation should be eliminated from the total dissipated energy calculation for predicting damage.

For all linear viscoelastic material, such as asphalt, the equation for calculating dissipated energy per cycle in cyclic flexural fatigue test is given by Equation 2-3 following, (Tayebali et al., 1994):

$$\omega_i = \pi \sigma_i \varepsilon_i \sin \varphi_i \quad \text{Equation 2-3}$$

Where;

- ω_i is the dissipated Energy at load cycle i
- σ_i is the stress at the load cycle i,
- ε_i is the strain at the load cycle i, and
- φ_i is the phase angle between stress and strain at load cycle i.

2.3.2 Dissipated Energy and Fatigue

Various representations and applications have been proposed to relate fatigue life of asphalt mixes to energy. The initial work on energy used the total dissipated energy as either initial dissipated energy or used a cumulative dissipated energy approach. While these methods provide sound mechanistic relationships between stress, strain, energy, and fatigue life, and can be applied under a wide variety of environmental factors, reliable prediction of fatigue life cannot be predicted without extensive fatigue testing.

To determine the fatigue life from dissipated energy, fatigue tests need to be conducted where the phase angle, mixture modulus, and dissipated energy are measured throughout the test. Several mechanistic parameters are then calculated and used to relate fatigue life to dissipated energy by the Equation 2-4 following:

$$N_f = \left(\frac{W}{A} \right)^{-z} \quad \text{Equation 2-4}$$

Where;

W is the Total dissipated energy (sum of dissipated energy found from Equation 3)

A, Z are Mixture characterisation constants

The cumulative dissipated energy approach was researched by Van Dijk and Visser (1977) who found that the fatigue behaviour of asphalt mixes from different tests, loading frequencies and temperature conditions could be described by a single mix specific relationship. Van Dijk and Visser found that a single relationship existed between the number of cycles to fatigue failure (N_f) and the cumulative amount of energy dissipated during the fatigue test. It was found that all the variables, including rest period, mode of loading, temperature, and frequency, did not significantly influence this dissipated energy relationship. The researchers found that the slopes of the fatigue lines for different mixes were nearly all the same and similar to the 0.67 slope suggested by Chomton and Valayer (1972). However contrary to this finding, other researchers have found that the relationship was mix dependent (Van Dijk et al. (1972) and SHRP A-404, (1994), with the University of California (Berkeley) study under SHRP-A-404, (1994) finding that all energy- N_f fatigue lines were not parallel and have different slopes, similar to the conventional model form.

In an attempt to account for the reality that not all dissipated energy goes into damaging the asphalt, various alternatives to the initial dissipated energy and cumulative dissipated energy approach have been developed such as; work ratio approach, dissipated energy approach and ratio of dissipated energy change. Of these, the dissipated energy change approach has been found to provide promising results in the prediction of both the fatigue and FEL of an asphalt mix and will be discussed in depth in section 2.5.2.

2.3.3 *Relaxation and Creep*

Relaxation modulus is generally considered the fundamental material property that determines the strain (or stress) development in flexible pavements and is needed not only for the characterisation of the viscoelastic behaviour of asphalt mixes but also the characterisation of material damage where it exhibits non-linear behaviour. However, the measurement of relaxation modulus is difficult and other tests are commonly used such as, creep, stress relaxation and dynamic modulus testing.

Jaeseung et al. (2008) found that creep compliance or complex modulus tests alone were not capable of providing complete information over the typical time or frequency range used in single-temperature tests. It was found that in general, the dynamic modulus test provides accurate creep compliance at short loading time, while the creep compliance test provides accurate creep compliance at longer loading time.

Relaxation modulus can be determined from either a creep compliance test using static loading or a complex modulus test using cyclic loading. Since the nature of each test is different, creep compliance determined from the complex modulus test can be different from that determined from the creep compliance test.

The relaxation modulus, $E(t)$, is defined as the stress response of a viscoelastic material due to a unit step of strain input. The relaxation modulus can be calculated as the time-dependent stress divided by the applied strain level. For a linear material, as with the creep compliance, relaxation curves obtained at different strain levels can be superimposed by defining the relaxation modulus as shown in Equation 2-5 following:

$$E(t) = \frac{\sigma(t)}{\varepsilon_0} \quad \text{Equation 2-5}$$

Where;

- $E(t)$ is the relaxation modulus
- $\sigma(t)$ is the time-dependent stress, and
- ε_0 is the constant applied strain.

At short loading times, the modulus is at a high plateau level (glassy or elastic modulus) and falls to the equilibrium (rubbery) modulus at longer times

2.3.4 Dynamic Modulus Testing

While creep and relaxation tests are suitable to characterise material responses over long times, they are however less accurate for shorter times. It has been found by numerous researchers such as Katicha (2007), that the dynamic tests are more suitable to describe the short-term response. When a viscoelastic material is subjected to a cyclic stress, a steady state is reached in which the resulting strain is also cyclic, with the same frequency but lagging behind the stress, this is the phase lag (δ).

Dynamic modulus is such a test which is applicable to characterise short-term response of an asphalt mix due to its inherent viscoelastic nature. The dynamic modulus test is undertaken by applying a vibratory load (stress) and measuring the resulting displacement (strain). Unlike purely elastic materials, where the stress and strain occur in phase to each other, due to the viscous component in asphalt there is a lag between stress and strain or a phase lag (δ). Under a continuous, sinusoidal loading (vibratory) the response of the asphalt can be defined by a complex number, called "complex modulus" (E^*). The absolute value of this complex modulus is defined as the Dynamic Modulus ($|E^*|$).

Mathematically, the response of the asphalt to the vibratory stress can be represented using the following equations:

$$\text{Strain} : \varepsilon = \varepsilon_0 \sin(\omega t) \quad \text{Equation 2-6}$$

$$\text{Stress} : \sigma = \sigma_0 \sin(\omega t + \delta) \quad \text{Equation 2-7}$$

Where,

$\omega = 2\pi f$ and f is frequency of stress oscillation,

t is time,

δ is phase lag between stress and strain.

There are two components to Dynamic Modulus: The storage and loss modulus, the stored energy, representing the elastic portion, and the energy dissipated as heat, representing the viscous portion. The storage and loss moduli are defined as follows:

$$\text{Storage modulus: } E' = \frac{\sigma_0}{\varepsilon_0} \cos\delta \quad \text{Equation 2-8}$$

$$\text{Loss modulus: } E'' = \frac{\sigma_0}{\varepsilon_0} \sin\delta \quad \text{Equation 2-9}$$

Complex variables can then be used to express the Complex Modulus E^* as follows:

$$E^* = E' + iE'' \quad \text{Equation 2-10}$$

Where;

i is the imaginary unit

And Dynamic Modulus as, the absolute value of stress and strain:

$$|E^*| = \frac{\sigma_0}{\varepsilon_0} \quad \text{Equation 2-11}$$

2.4 Fatigue Endurance Limits in Asphalt

2.4.1 Existence of Endurance Limits

The concept of the asphalt FEL was first postulated in the early 1970's by Prof. Carl Monismith and published by Monismith and McLean (1972). These researchers found that there appeared to be a strain level below which damage to an asphalt mix does not appear to occur. Since that time considerable research has continued and while there is widespread acceptance of the laboratory FEL concept its relationship to mix variables and temperature is still not fully understood and its incorporation into pavement design is not common place.

The FEL concept was further investigated by Carpenter at the University of Illinois from the early 2000's, Carpenter et al. (2000), and more recently by researchers at NCAT and under the NCHRP 9-38 (2012) and 9-44 (2013) projects. In the early studies by Carpenter (2000), and Thompson (2006), the FEL was determined using a combination of standard fatigue tests at high strain levels and by conducting extremely lengthy fatigue tests at low strain levels. The resulting strain-Nf relationships obtained by Carpenter et al (2006) are shown in Figure 2-4 following. The researchers found a consistent relationship for all mixes, being the

traditional straight line strain-Nf relationship followed by a near horizontal slope and for all the mixes tested in the study, none deviate from this typical result.

These FEL studies found that there was a definite point for each mix, where the response deviated from the conventional straight line (log scale) strain-Nf relationship. After this point the slope of the line for all practical purposes becomes flat. The flat slope indicated that at lower strains asphalt mixes can produce extremely long fatigue lives, often referred to as "infinite." It was defined by Thompson that this transition point was the FEL of the mix. At a strain level below the FEL the mix will begin to show an extraordinarily long fatigue life, significantly higher than those predicted by the traditional straight line fatigue model.

Examination of the results from both Thompson et al. (2006) and the testing undertaken as part of NCHRP 9-38 (2012) found that none of the mixes tested had strains lower than $70\mu\epsilon$ to achieve the transition to the virtual flat slope. Both Thompson et al. and the 9-38 study found that depending on the binder type, this extended transition point was achieved at significantly different strain levels.

As can be seen on Figure 2-4 following, Thompson found that there was not a single FEL for asphalt mixes and there was a range of FEL, which varied according to the mix tested. Thompson found the difficulty in differentiating the mix variables and their impact on the FEL derives from the use of the phenomenological relationship for strain and loads to failure. Because this relationship is not fundamental it cannot adequately describe mix performance under varying inputs.

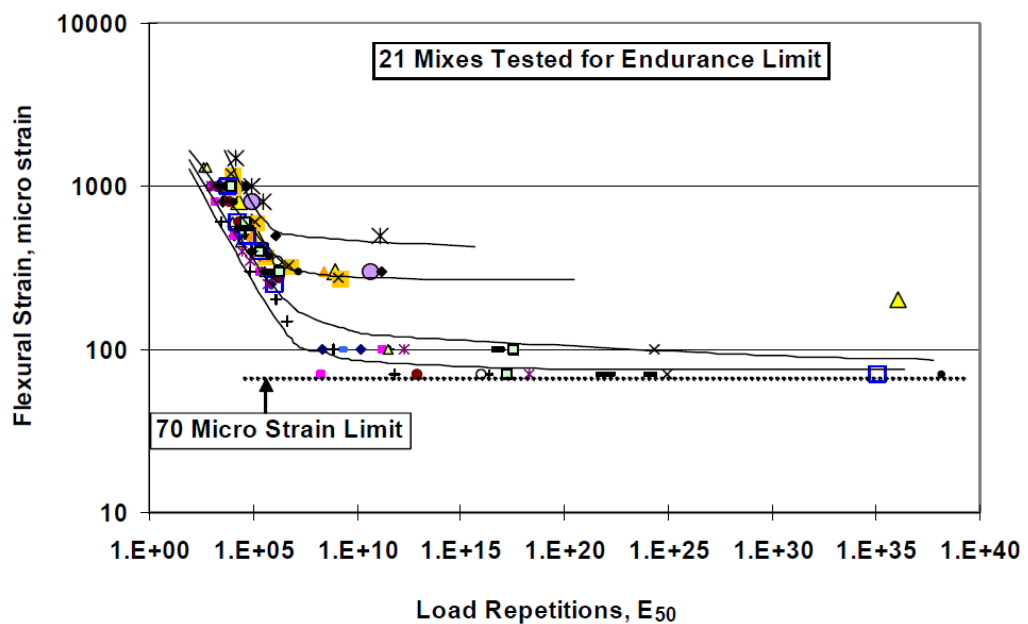


Figure 2-4 Strain Load Relationship Illustrating the FEL (after Thompson et al. (2006))

Following on from the work of Thompson an extensive research study was carried out under the NCHRP project 9-38 in 2010 to investigate, the existence of FEL in asphalt mixes, the effect of asphalt mix characteristics on the FEL, and the potential for the FEL to be incorporated into structural design of flexible pavements. The results of the study were published as the NCHRP report 646(2012) and the main findings of this study are summarized following:

- The endurance limit for a long-life pavement was defined as a pavement being able to withstand 50 million design load repetitions in a 40-year design period.
- The data supported the existence of an FEL for all the studied mixes. The estimated endurance limit for each of the six studied mixes in this research varied from 75 to 200 $\mu\epsilon$ and was the one-sided, 95% confidence lower prediction limit that produces a fatigue life of 50 million cycles.
- Both beam fatigue and uniaxial tension testing were conducted to determine fatigue life of the mixes. It was indicated that the uniaxial tension testing method provided a promising technique and could be used to more rapidly determine the endurance limit of a mix as it would not require the production of an asphalt beam and instead would use a sample more closely related to those being contemplated for Simple Performance Tests (SPT) for dynamic modulus. However, there were reported discrepancies in the predicted fatigue life trends defined by beam fatigue and uniaxial tension testing which necessitated further evaluation of the uniaxial tension testing results.
- The role of the quality of construction along with pavement thickness design and materials selection to achieve a durable LLAP structure was emphasised.
- Shift factors ranging from 4.2 to 75.8 based on fatigue transfer functions were introduced to correlate the laboratory and field fatigue performance.
- Using the FEL determined from laboratory beam fatigue tests conducted as part of the study and a typical principal arterial traffic stream, the LLAP thickness determined with PerRoad was approximately the same as the 20 and 40 year conventional (no endurance limit) MEPDG or 1993 AASHTO Pavement Design Guide pavement thicknesses. However, the MEPDG perpetual thickness was approximately 50% thicker and the overall conclusions at the end of a 20 or 40 year period were significantly different. With the conventional designs, the pavements would have failed in bottom-up fatigue with cracking over 20% of the lane area at 90% reliability while no cracking would be expected if the endurance limit was considered.

2.4.2 *Healing a Source of Endurance Limits*

The effect of rest periods and healing potential of asphalt mixes has been investigated by researchers for many years starting with researchers at Shell in the 1960's (Roque 2006). Healing is commonly considered the capability of a material to self-recover its mechanical properties (stiffness or strength) to some extent upon resting due to the closure of cracks. Healing is not confined to asphalt mixes and in fact, a number of materials have been found to possess the ability to undergo healing, including metals, plastics and rubbers.

Current asphalt thickness design procedures ignore healing potential. As a consequence, the conventional analysis suggests the traffic applied at high pavement temperature (in theory) does a disproportionately greater amount of fatigue damage because of the high strain levels, resulting from the low asphalt stiffness. The NCHRP 9-44 (2013) proposed the use of a method for the incorporation of healing into pavement design based on the use of stiffness-FEL relationships for different rest periods. The application of this model found that traffic at the high end of the temperature spectrum causes relatively less damage than mid-range due to healing effects. It was also apparent that at low temperature the high asphalt stiffness reduced strain more than offsets the reduced healing.

While a significant amount of research has been undertaken on the effect of rest periods on the fatigue life of asphalt mixes, little research has been focused on the actual mechanism of healing. Phillips (1998) proposed that the healing of asphalt mixes is a three-step process consisting of:

- 1) The closure of micro-cracks due to wetting (adhesion of two crack surfaces together driven by surface energy);
- 2) The closure of macro-cracks due to consolidating stresses and binder flow; and
- 3) The complete recovery of mechanical properties due to diffusion of asphaltene structures.

The first process was believed to be the fastest, resulting only in the recovery of stiffness, while the second and third processes are believed to occur at a much slower rate and improve not only stiffness, but also the strength of asphalt mix with properties returned to levels similar to that of the original material.

Jacobs (1995) also found that the introduction of rest periods has a beneficial effect on the fatigue resistance of the mixes. He proposed that this "healing" in the rest periods occurred by diffusion of the low molecular weight component of bitumen, maltenes, through the micro-cracks and re-establishing the bonds in the cracked area. Jacobs believed that the maltenes were involved because they are the most mobile components of the bitumen, although higher molecular weight molecules (asphaltenes) could also diffuse during longer rest

periods, and as found by Phillips (1998) could result in completely restored material properties.

Lytton (2005) used the “dissipated pseudo strain energy concept” to explain the fracture and healing process in asphalt mixes. Lytton concluded that the fracture or healing of an asphalt mix was related to two mechanisms:

- The surface energy storage or the surface energy release, which was related to polar or non-polar characteristic of the binder.
- The energy stored on or near the newly created crack faces which governs the energy available to make the crack grow. It was found that this surface energy depended mainly on the chemical composition of the binder.

Lytton (2005) concluded that the micro-fracture and healing of the asphalt aggregate mix was controlled by the energy balance per unit of crack area between the “dissipated pseudo-strain energy” released and the energy that is stored on the surface of the crack.

Even when considering healing, debate exists as to when healing occurs; during rest periods, during all the loading and unloading periods, or just under certain conditions such as certain temperature and material damage levels. It appears that these different conclusions are mainly based on the laboratory test setup used and the research approach adopted. Most researchers now believe that healing occurs in all conditions, just at varying rates (NCHRP 9-44 (2013)) at stiffnesses below the glass transition point.

While the healing concept is only in its infancy in pavement engineering, it is well understood in polymer engineering and a considerable amount of work has been completed on the study of the healing phenomenon of polymeric materials. Prager and Tirrell (1981) described the healing phenomenon:

"When two pieces of the same amorphous polymeric material are brought into contact at a temperature above the glass transition, the junction surface gradually develops increasing mechanical strength until, at long enough contact times; the full fracture strength of the virgin material is reached. At this point the junction surface has in all respects become indistinguishable from any other surface that might be located within the bulk material: we say the junction has healed."

2.4.3 Effect of Rest Periods on Healing

Some of the early work to develop a mechanical approach to quantify the healing potential of an asphalt mix was developed by Kim and Little (1990). In developing this approach they performed cyclic loading tests with varying rest periods on notched beam specimens of sand asphalt and found that the rest period has a significant effect on the enhancement of the fatigue life through healing and relaxation mechanisms.

To explain healing they proposed to use a concept called the Healing Index (HI), which was found to be highly sensitive to binder properties. The researchers then applied Schapery's elastic-viscoelastic correspondence principle (1978) to separate out the viscoelastic relaxation from chemical healing. After separating the relaxation from the healing, the magnitudes of pseudo energy density before and after rest periods were used to calculate the HI. The NCHRP 9-44 (2013) project expanded on the work undertaken by Kim and Little (1990) and used the pseudo energy and HI approach to determine the FEL for a range of mixes. The testing conducted under the 9-44 project consisted of both uniaxial fatigue testing and 4 point bending. The NCHRP project found that the effect of rest periods was a significant factor and could increase the FEL by a factor of 3 at reset periods of greater than 10 seconds relative to a 1 second rest periods. The NCHRP project also found that rest periods of greater than 10 seconds resulted in little increase in healing potential.

2.5 Laboratory Estimation of Fatigue Endurance Limits

For routine determination of the FEL of an asphalt mix, it is impractical to undertake extended laboratory fatigue testing as originally undertaken by Monismith (1972). Consequently, for practical implementation of testing for FEL a method needed to be established where limited cycle fatigue testing could be undertaken and the data extrapolated to establish the fatigue life of the mix. Ideally, any method of extrapolation should be able to be used to extrapolate the results of any fatigue test whether the test is conducted below, at, or above the FEL of the mix.

2.5.1 Stiffness Ratio Methods

The NCHRP study 9-38 (2010) examined a number of different model forms for the extrapolation of fatigue curves (stiffness vs. N), namely;

- exponential (AASHTO T321),
- logarithmic,
- power, and
- Weibull function.

By comparing the models prediction to the actual data the study found that the exponential model consistently underestimates the stiffness at 50 million cycles and was slow to converge to the measured stiffness. This means that testing would need to be conducted to a high number of cycles to even approach the measured stiffness.

Again by comparing the models prediction to the actual data, it was found that both the logarithmic and power models would converge to a reasonable predicted stiffness within 10 million cycles. However, the use of both the logarithmic and power function required a high degree of user input in establishing where to start the curve fitting. The reason for this is that when all of the loading cycles are used (including the primary stage with initial heating

phase), the resulting fit would overestimate the stiffness at 50 million cycles and, consequently, would overestimate the fatigue life. To obtain a reasonable fit the primary stage would have to be ignored.

The study found that the single-stage Weibull function converges quickly and provided the most accurate results for one of the samples tested. It was however, found to do a relatively poor job at estimating stiffness for all other samples examined. For long-life fatigue tests conducted at strain levels slightly above the FEL, it was found that, the single-stage Weibull function provided the most accurate extrapolation of fatigue life. However, the three-stage Weibull function was found to provide the best fit to the stiffness versus loading cycle data and was most probably the best method for estimating the fatigue life at strain levels below that of the FEL. The conclusion of the study was that the Weibull functions were “*the best methods for extrapolating fatigue tests that did not fail within 50 million cycles*”.

The Weibull function first recommended by Tsai (2002) is shown in Equation 2-12 following.

$$\ln(-\ln(SR_n)) = \ln(\delta) + \gamma \ln(n) \quad \text{Equation 2-12}$$

Where;

- SR_n = Stiffness ratio or stiffness at cycle n divided by the initial stiffness
- n = Number of cycles
- δ = scale parameter (intercept), and
- γ = shape parameter (slope)

To improve the accuracy of the single stage Weibull function Tsai et al. (2002) developed a methodology for fitting a three stage Weibull curve (as used in the NCHRP9-38 study). It was theorised that three stage model fitted the three stages of the loading cycles vs. stiffness stages; initial heating and temperature equilibrium, crack initiation and crack propagation. In the case of testing below the FEL the third stage does not occur and represents a stage of decreasing damage with time.

Sullivan (2015) examined the use of the of the Weibull function for the prediction of both the stiffness curve and N_f of Australian mixes. The results are shown Figure 2-5 and Figure 2-6 following, and shows the model fit of both the one stage and three stage Weibull function for an EME mix close to that of the FEL, while Figure 2-6 shows the accuracy of the prediction of the number of cycles to failure of a number of mixes using both the one stage and three stage Weibull function over a range of fatigue lives.

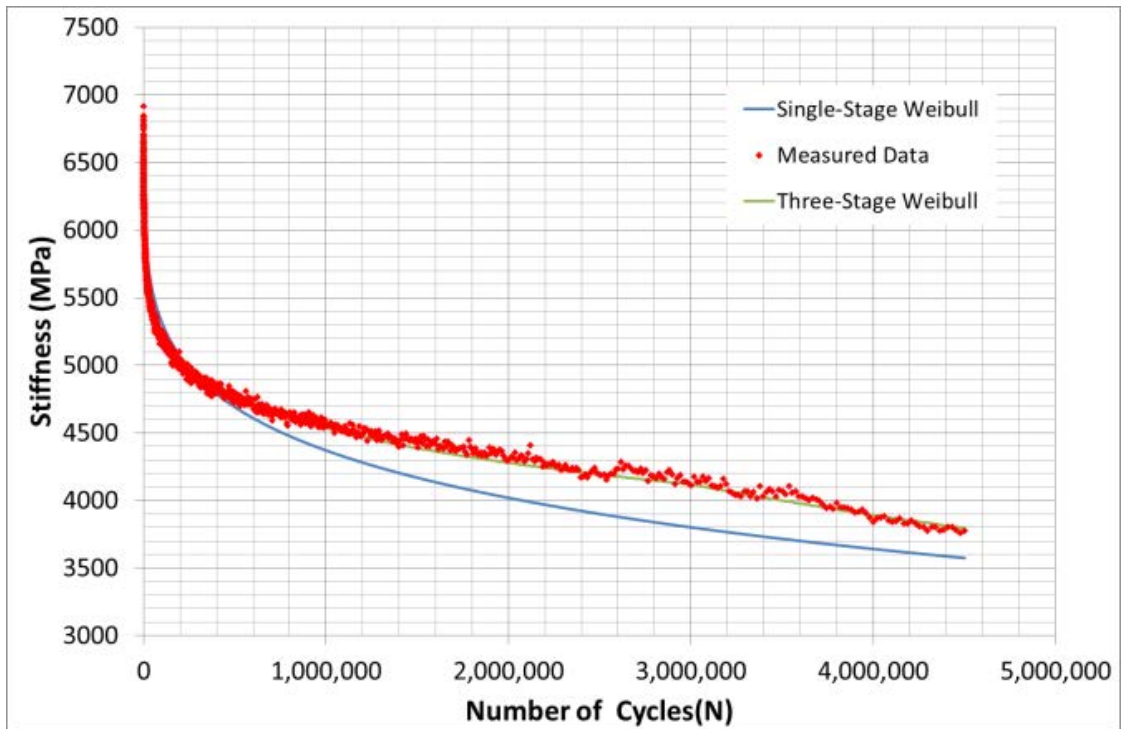


Figure 2-5 Weibull Fitting Function (Sullivan 2015)

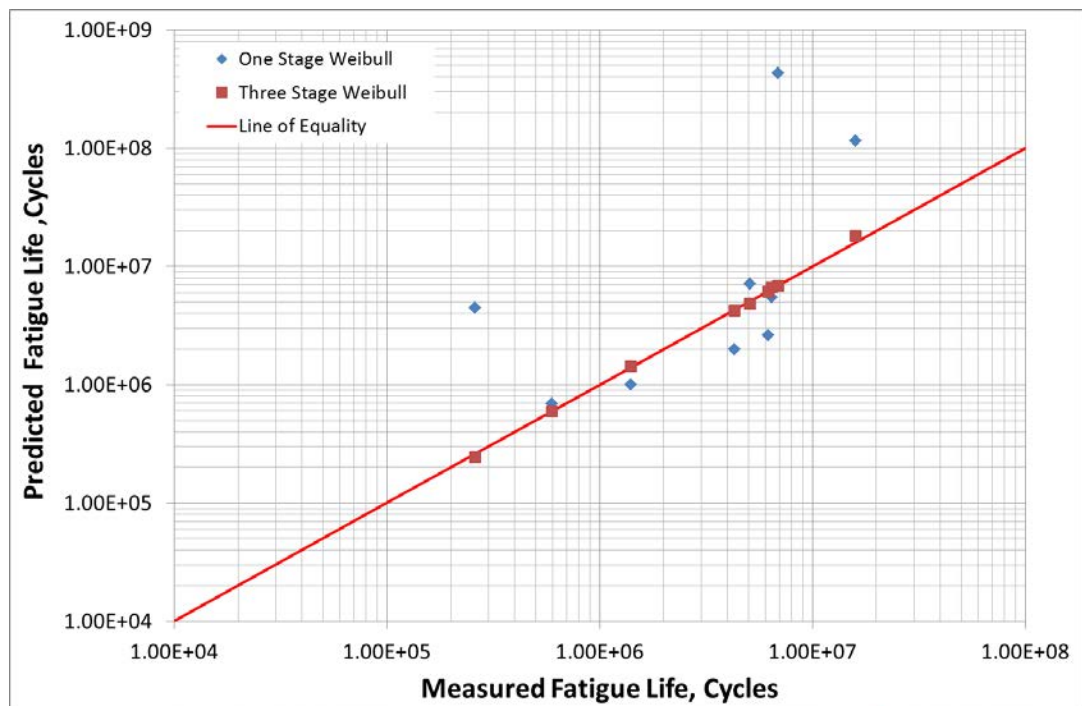


Figure 2-6 Accuracy of Weibull Fitting Functions after, Sullivan (2015)

It was found that for all results close to and below the FEL the three-stage Weibull function captures the shape of the stiffness curve to a high degree of accuracy and can be used to accurately predict the extended fatigue life of mixes. Instead of using the approach recommended by Tsai et al. (2002) for the calculation of the three stages, Sullivan used the

Solver function in MS Excel® to solve for the best fit of the three stage model. The results showed that while the one-stage model gives an accurate prediction of the number of cycles to failure for standard test conditions, at the lower temperatures (mixes tested at 10°C) the model consistently over predicted the number of cycles to failure, as the model did not capture the third stage brittle failure. For the three stage model it was found that the model accurately predicts the number of cycles to failure over all strain levels.

Based on the testing and analysis Sullivan et al. recommended the use of three stage Weibull model to estimate the failure points.

2.5.2 Ratio of Dissipated Energy Change

Ghuzlan and Carpenter (2004) used the dissipated energy change approach to predict both fatigue failure and the FEL of an asphalt mix. Dissipated energy is the measure of the energy that is lost through mechanical work, heat generated or damage to the sample in a testing cycle. Some researchers have used the total cumulative dissipated energy to define the damage within a sample by assuming that all dissipated energy is responsible for damage. As dissipated energy may be a function of heat generation or work done within the sample Ghuzlan and Carpenter (2004) postulate that only a proportion of dissipated energy is responsible for actual damage.

The Dissipated Energy Change is different from pure dissipated energy approaches, as it uses the ratio of the amount of dissipated energy change between different loading cycles to represent the damage propagation. The basic premise of this approach is that the change in dissipated energy per cycle of loading is related to the growth of damage that occurs in an asphalt mix.

Shen (2005) improved the dissipated energy approach initially developed by Tayebali et al. (1992) and renamed it, based on the changes made to the approach to the Ratio of Dissipated Energy Change (RDEC). In the recommended approach the RDEC is defined as the average change in dissipated energy between two cycles divided by the dissipated energy from the first of the two cycles. This ratio illustrates the percentage of input dissipated energy which goes into damage for a cycle. The representation of damage produces a U shaped curve as shown following in Figure 2-7, following.

The RDEC was defined as the average change in the dissipated energy between two cycles relative to the initial two cycles. Shown mathematically by Equation 2-13 following:

$$RDEC_a = \frac{(DE_a - DE_b)}{(b - a) \times DE_a} \quad \text{Equation 2-13}$$

Where:

RDEC_a = Ratio of dissipated energy change for cycle a

DE_a = Dissipated energy for cycle a and

DE_b = Dissipated energy for cycle b.

The basic assumption of the approach is that the change in dissipated energy is directly related to the growth of damage in that cycle.

It was hypothesised by Thompson et al. (2006) that the RDEC approach provides a unique relationship between damage and load cycles to failure (Figure 2-8) and that there was one unique Plateau Value (6.79×10^{-9}) of the RDEC where the behaviour of an asphalt changes from traditional accumulation of damage to a point where damage does not occur or healing potential is greater than damage. This is the balancing point (FEL) between healing and damage in the asphalt mix. It should be noted, that the balancing point in the RDEC approach is for the case of the test conditions undertaken in the testing, which was, 10Hz haversine loading (i.e. no rest periods). Different balancing points should be expected with different rest periods and loading frequencies. It was proposed by Shen (2005) that this point (Plateau Value) be defined as the FEL for all mixes and is denoted as Plateau Value, PV_L on the following figures.

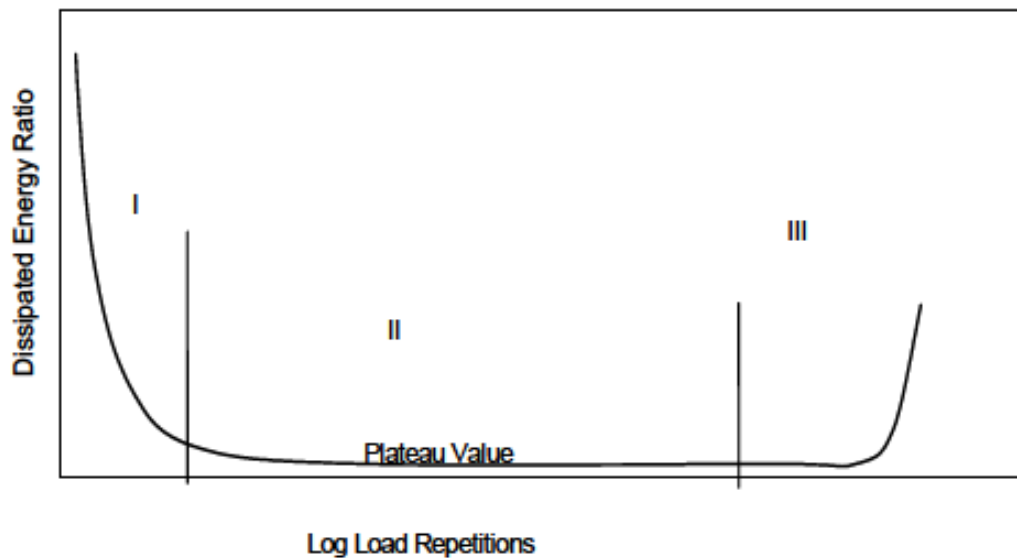


Figure 2-7 Dissipated Energy Plot and Plateau Value

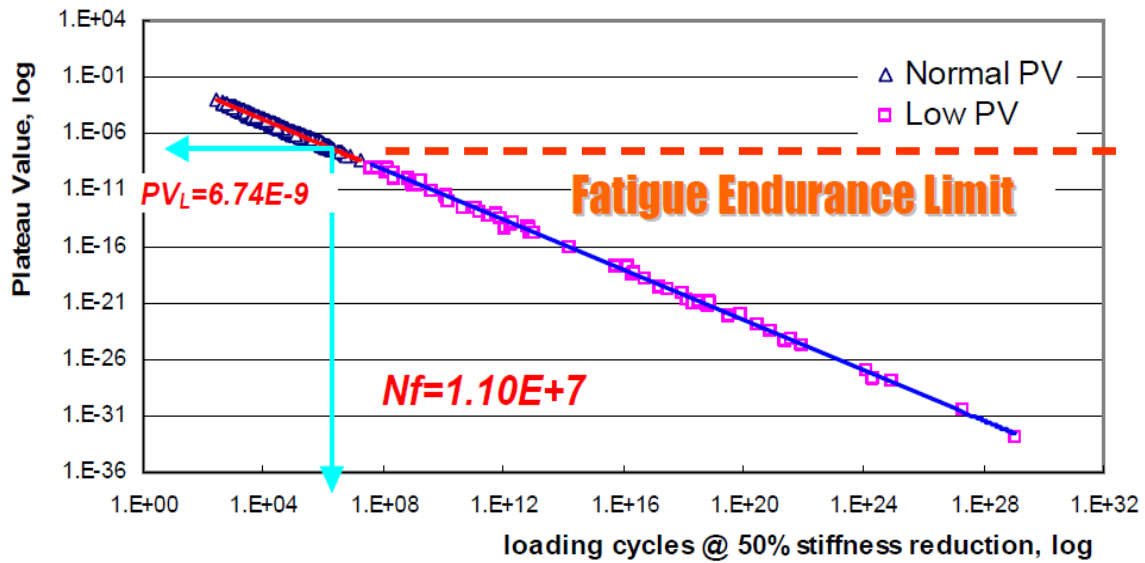


Figure 2-8 Plateau Value-Nf Relationships (after Carpenter et al. (2006))

As can be seen in the figures along with a unique PV_L there is a unique relationship between the PV and the cycles to failure. Given the proposed constant PV_L and the unique relationship indicates a constant number of cycles (1.1×10^7) to the transition point in the straight line strain-Nf curve and that the FEL can be estimated from the traditional straight line strain-Nf plot at a constant number of cycles (1.1×10^7), Sullivan et al. (2015) showed that the unique PV_L found for US mixes was applicable and could be used to estimate the FEL of Australian mixes.

2.5.3 Healing Index

Under the NCHRP 9-44 study (2013) fatigue and healing potential (and subsequent FEL) was analysed by using two fatigue tests (either uniaxial tension-compression or flexural bending tests). The first test was conducted under continuous loading condition with no rest periods, the second introduced rest periods between loading cycles. The inclusion of the rest periods decreases the stiffness deterioration through partial healing of fatigue damage. The result is that the stiffness deteriorates at a slower rate compared to the test without rest period, as can be seen in Figure 2-9 following.

The difference between the tests conducted with a rest period and the test without was defined as the Healing Index (HI), with the concept shown graphically in Figure 2-9 following, and numerically in Equation 2-14 following.

$$HI = [SR_{w/RP} - SR_{w/o RP}]_{at Nf_{w/o RP}} \quad \text{Equation 2-14}$$

Where:

$SR_{w/RP}$ = Stiffness ratio with rest period

SR w/o RP = Stiffness ratio without rest period

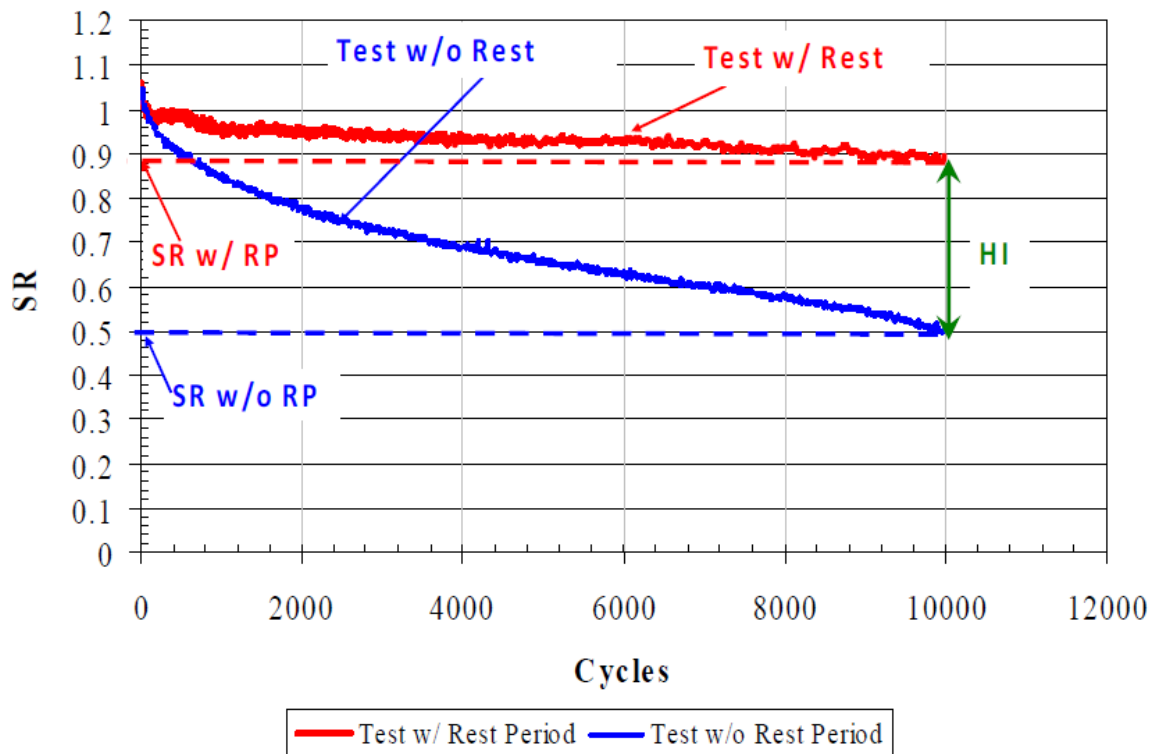


Figure 2-9 Stiffness vs. Number of load cycles with and without rest period.

It was hypothesised that FEL occurred when no damage (no modulus reduction) occurred in a test with rest period. Given that failure in a beam fatigue test is defined as a 50% reduction in modulus, the definition implies that the FEL could be estimated at a HI of 0.5; which means $SR_{w/o\ RP} = 0.5$ (i.e. failed sample) and $SR_{w/ RP} = 1.0$ (no damage or loss of modulus).

To estimate the FEL, the 9-44 project used both the number of repetitions to failure (Nf) without a rest period and the Nf on a fatigue test with a rest period to develop a Stiffness Ratio model based on fitting regression fitting of the experimental data for both tests, as shown conceptually in Equation 2-15 following. The SR was determined for both tests with and without rest period and all data points were used to establish the general SR model. With Equation 2-15 following showing the general form of the SR model based on the six factors, used in Phase 1 of the NCHRP 9-44 project:

$$SR = a_1 + a_2 AC + a_3 Va + a_4 (BT) + a_5 (RP) + a_6 (T) + a_7 Nf_{w/o\ RP} + 2\text{-factor interactions} + 3\text{-factor interactions} \quad \text{Equation 2-15}$$

Where;

SR = Stiffness Ratio

$a_1, a_2 \dots a_n$ = Regression coefficients

AC = Percent asphalt content

V_a = Percent air voids

BT = Binder type

RP = Rest period (sec)

T = Temperature (F)

$N_{f \text{ w/o RP}}$ = Number of cycles to failure (test without rest period)

Once the SR model was developed, the HI for any test combination could be computed as shown previously in Equation 2-15. The next step is to correlate the computed healing index to the FEL. To do this all HI data points were plotted versus the strain levels that were used for each test at each temperature separately, since it was expected that different temperatures would have different FEL. This concept is shown conceptually in Figure 2-10 following, which illustrates a schematic relationship between healing index and strain at each temperature estimated from the SR model, this approach was used to extend the results to any rest period to get at SR and subsequent HI. Then, the FEL limit could then be estimated for any temperature and binder content by assuming a HI of 0.5, again shown conceptually in Figure 2-10 following.

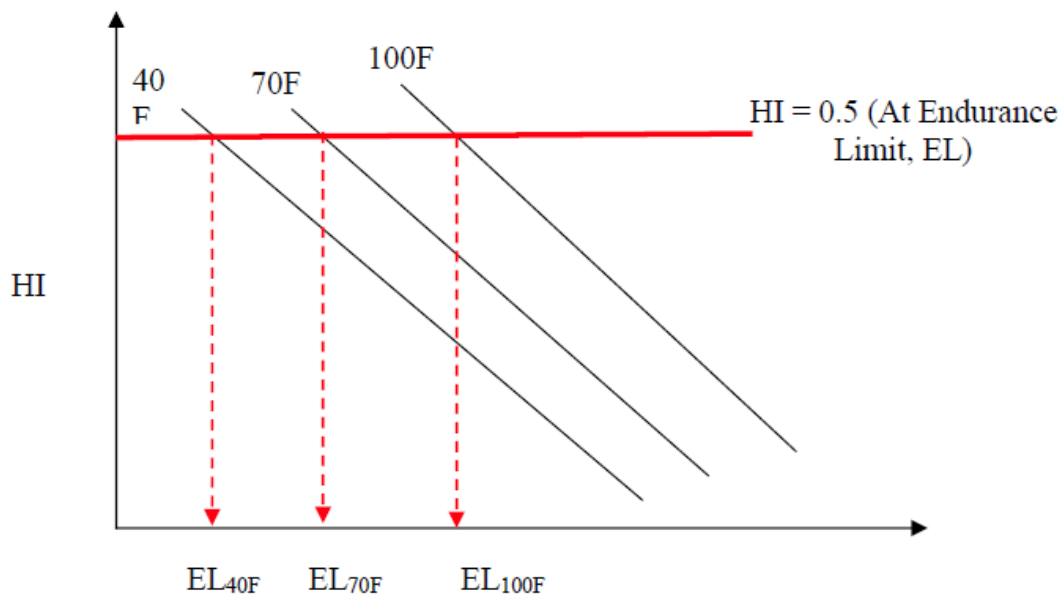


Figure 2-10 Endurance limit determination at each temperature based on HI

Further research under the 9-44 project found that the binder terms (BT, AC) and the temperature (T) in Equation 2-15 could be directly replaced by using the initial stiffness of the mix, with no loss in model accuracy. The use of the stiffness enabled estimation of the FEL for any stiffness and any rest period and the production of stiffness-FEL relationships, which were recommended for pavement design.

2.6 Long Life Asphalt Pavements

In the US, the Asphalt Pavement Alliance (APA), under Newcomb et al. (2010) introduced the concept of LLAP as *“an asphalt pavement designed and built to last longer than 50 years without requiring major structural rehabilitation or reconstruction, and needing only periodic surface renewal in response to distresses confined to the top of the pavement”*. As with the studies of Nunn, the APA found that contrary to conventional theory, many of the full-depth or deep-strength pavements which had been in service for decades were only requiring surface renewals (mills and re-sheets) of the upper surface (Asphalt Pavement Alliance ,2002) and had no signs of structural failure.

Based on these findings the Newcomb et al. (2010) found that the use of LLAP could offer significant benefits to the US economy and with the current budget shortage for expansion and rehabilitation of the network and the increasing demand on the road network, the LLAP concept could play an important role in providing a life-time solution to maintain and construct asphalt pavements.

In the US two main schemes have been utilised for LLAP design, full-depth and deep strength pavements, each of which can lead to design of thinner overall pavement structures in comparison to thick granular base pavements. Full-depth pavements consist of asphalt layers placed directly on subgrade material (modified or unmodified) while deep-strength pavements are where the asphalt layers are placed on top of a thin granular base. It was found by APA that these pavements can exceed their design life with minimal rehabilitation if their cracking potential (surface initiated) could be confined to the upper removable wearing layers Asphalt Pavement Alliance (2002).

In traditional pavements, fatigue cracking and rutting are the two major failure mechanisms of pavements which can occur at or before the end of design life Mahoney (2001). Both deep-strength and full-depth pavements can be designed to be structurally resistant to these distresses. The concept of LLAP evolved from recent attempts of pavement engineers to design pavements which are resistant against bottom-up fatigue cracking and rutting, Newcomb, Willis & Timm (2010). However, according to both the current and previous, mechanistic-empirical and empirical design approaches, the thickness of the pavement increases with the increase in traffic level to resist these modes of failure. Whereas according to the LLAP concept, any thickness of the pavement beyond a certain level may lead to unnecessary added expenses Newcomb, Willis & Timm (2010) and new design

approaches are required. As with thickness, there is also no point and a lack of sustainability, in the excessive usage of non-renewable natural resources as a result of over-designing pavements according to the current pavement design procedures. For example, Huber et al. (2009) reported on an over-designed pavement in India by 40-115 mm, which was designed in accordance with the 1993 AASHTO pavement design led to waste of 900-3000 tons of material per lane kilometre.

The recent research which has shown that there is a level of stress or strain below which no structural damage will occur to the asphalt pavement, has resulted in suggestions that a pavement can be designed to last indefinitely without any major structural damage, if the pavement is designed and constructed so that no damage occurs under the cyclic traffic load. While no structural damage will occur, surface maintenance and overlays will still be required to keep the pavement in a serviceable condition Newcomb, Buncher & Huddleston (2001), Powell et al. (2010). Ferne (2006) suggested a broader definition for long-lasting pavements: *“long-life pavement is a well-designed and constructed pavement that could last indefinitely without deterioration in the structural elements provided it is not overlooked and the appropriate maintenance is carried out”*. Various other definitions of perpetual pavement can be found in the literature all of which indicate almost the same concept; a summary of perpetual pavement definitions are listed following:

- Transportation Research Laboratory (TRL):

Well-constructed fully-flexible pavements designed for 40 years and for traffic in excess of 80×10^6 LLAP pavements Nunn, Brown & Weston (1997).

- Asphalt Pavement Alliance (APA):

A Perpetual Pavement is defined as an asphalt pavement designed and built to last longer than 50 years without requiring major structural rehabilitation or reconstruction, and needing only periodic surface renewal in response to distresses confined to the top of the pavement, Asphalt Pavement Alliance (2002).

- The European Long-Life Pavement Group (ELLPG):

A long-life pavement is a type of pavement where no significant deterioration will develop in the foundations or the road base layers provided that correct surface maintenance is carried out, FEHRL (2004).

This concise definition can be elaborated with the following clarification.

Deterioration: This includes whatever the network manager considers important e.g. significant cracking or (progressive) deformation in the structural layers of a fully flexible pavement; for other types of pavement ‘deterioration’ could be quite different.

Later in 2009 the definition was revised as: A long-life pavement is a well-designed and well-constructed pavement where the structural elements last indefinitely provided that the designed maximum individual load and environmental conditions are not exceeded and that appropriate and timely surface maintenance is carried out, FEHRL (2009).

- The World Road Association (PIARC):

A pavement is considered as a “success story” when it has proved to behave better than expected when it was designed. Such a pavement must be clear of structural maintenance and still be in good shape, despite the fact that it has sustained a cumulated traffic higher than the one contemplated at its design, PIARC Technical Committee 4.3 Road Pavements (2009).

- National Cooperative Highway Research Program (NCHRP)

A long-life or perpetual pavement is one able to withstand 50 million axle repetitions in a 40-year period without failing or a mix that provided 50 million cycles or more of fatigue life in the laboratory, Prowell et al. (2010).

Rickards and Armstrong (2010) believed that the TRL findings provided a rational measure of the achievement of the perpetual pavement status in which, over time, the deflections in a full depth perpetual pavement remained constant or indeed reduced despite heavy traffic loading (according to the UK network study); this was later confirmed in extensive German research.

As stated by Newcomb et al. (2010) LLAP performance is more than a function of design traffic, climate, subgrade and pavement parameters (such as modulus), pavement materials, construction, and maintenance levels, all contribute to how a pavement will perform over the course of its life. Most researchers and pavement engineers (Merrill, Van Dommelen & Gáspár (2006) and Walubita et al. (2008)) now believe that alongside the construction issues LLAP should be designed in a way that their structures remain intact during their life time and distresses such as fatigue cracking and permanent deformation won't occur, the should also be durable enough to withstand damage from traffic and environment.

Although the initial construction costs of perpetual pavements may be higher than conventional pavements designed to a lower life (< 30 years), Timm & Newcomb (2006) have shown that perpetual pavements have the following benefits over conventional designs:

- They eliminate reconstruction costs at the end of a pavement's structural capacity.
- They lower rehabilitation-induced user delay costs.
- They reduce use of non-renewable resources like aggregates and asphalt.
- They diminish energy costs while the pavement is in service.

All of these result in a lower life-cycle cost of the pavement network.

The concept of LLAP's has now been adopted by many countries (USA, UK, Germany, Canada, and China) and is being implemented on some of their most heavily-trafficked highways Asphalt Pavement Alliance (2002). In US, states such as California, Washington and Ohio have designed and developed LLAP (Hornyak et al. 2007; Monismith 1992; Ursich 2005). In Texas, Scullion (2006) reported on eight completed LLAP completed in 2005. In addition, Texas published design guidelines (Texas Transportation Institute), based on the findings of a study done by Walubita et al. (2009). The design guide contained recommendations for structural thickness design, design software, response criteria, mix design, and layer moduli values for Texas LLAP structures were presented (Walubita & Scullion (2010)). National Centre for Asphalt Technology (NCAT) also conducted studies on and developed methods for LLAP design in 2000, 2003 and 2006, the details of which are discussed in detail in Chapter 7 (Willis & Timm 2007).

Mahoney (2001), in a study for Washington Department of Transportation (WSDOT) specified goals which would define a pavement as perpetual pavement (LLAP). These goals, along with basic LLAP concepts, give engineers, the design qualifications for perpetual pavements.

1. Perpetual pavements should have a wearing course life of 20 years
2. Perpetual pavements should have a structural design life of 40 to 50 years
3. Perpetual pavements use a mill and fill (re-sheet) as their primary surface rehabilitation
4. Perpetual pavements contain their distresses to the top few centimetres of the surface

2.7 LLAP Material Selection

As found by Newcomb, Willis & Timm (2010) achieving a LLP is not just a matter of pavement thickness. The composition and the structure of a perpetual pavement also play an important role in achieving a LLAP. In a Washington State's study by Mahoney (2001) of long-lasting pavements, it was found that many pavements with shorter life-cycles were actually thicker than pavements with superior life-cycles. Additional research has shown that while increasing the pavement thickness can help with decreasing the tensile strain at the bottom of the asphalt layer, the magnitude of strain reduction is highly mix dependent Romanoschi et al. (2008).

According to Newcomb et al. (2010) material properties and mix designs are the two other important factors along with pavements thickness to achieve extended-life distress resistant LLAP. Newcomb et al. (2001) recommended that the LLAP structure should include a rut and wear resistant impermeable upper asphalt layer. In many cases, a stone matrix asphalt

(SMA), an open grade friction course (OGFC), or a dense graded asphalt (DGA) design can be used in this location. Below the wearing course there is a rut resistant and durable intermediate layer and below that there is a fatigue resistant and durable base layer, which can be achieved by the use of a low air void mix (usually achieved by higher bitumen content). This theme is consistently found in the literature with, (Gierhart (2007), Harm (2001), Newcomb, Buncher & Huddleston (2001)) all recommending a common structure, consisting of four parts to reduce the initiation and propagation of fatigue cracking and rutting in LLAP:

- 1) A solid foundation and/or working platform
- 2) A flexible, fatigue-resistant base asphalt layer
- 3) A durable, rut-resistant intermediate asphalt layer
- 4) A rut-resistant, renewable surface layer.

Bushmeyer (2002) reported on the first purposely designed LLAP in the US, the I-710 in California, which used a similar structure to the recommended LLAP concept. It consisted of 25mm open graded friction course (OGFC), 75mm of high temperature rutting resistant polymer modified asphalt as the surface layer, 150mm of standard asphalt as the intermediate layer, 75mm rich-bottom fatigue resistant (with bitumen content above the optimum) as the base layer.

(Newcomb, Willis & Timm 2010 reported on the LLAP concept recommended by Texas which proposed a very similar full depth asphalt pavement structure, which from top to bottom comprises of 25-40mm optional porous friction course (PFC), 50-75mm Stone Mastic Asphalt (SMA) course, 50-75mm transitional asphalt layer, 200mm plus rut resistant asphalt layer, 50-100mm fatigue resistant asphalt layer, all placed on a 150mm lime stabilised granular base layer. All pavement layers are supported by a natural well compacted subgrade). It is believed that this composition would undergo 30million equivalent single axle loads (ESALs) during the pavements life cycle (Walubita et al. (2008), Walubita, Scullion & Scullion (2007)). More technical details of the four of the required layers in the perpetual pavement structure can be found summarised in Yousefdoost (2015).

2.8 Field Observation of LLAP

2.8.1 US Studies

The first US study which identified the possible occurrence of LLAP in the field was undertaken by Schmorak and Van Dommelen (1996) who investigated 176 pavement sections contained in the SHRP-NL database for evidence of traditional bottom up fatigue cracking. Their observations found that for pavement sections with asphalt thicknesses greater than 160mm traditional bottom up fatigue cracking did not occur and cracking was confined to the surface and had a maximum depth of 100mm. From this, they concluded that

that traditional bottom up fatigue cracking was unlikely to occur in thick asphalt pavements. These observations did not however confirm the existence of LLAP. The observations only confirmed that surface initiated cracking would occur first.

Von Quintus (2006) conducted a review and analysis of field investigation data from Long Term Pavement Performance (LTPP) asphalt test sections across North America in 1995 and again in 2006, the purpose of which was to confirm the presence of LLAP and the FEL. While not formally documented, the 1995 study utilised randomly selected LTPP sites and field observations of cracking, to conduct survivability and probability of failure analysis for full depth asphalt pavements more than 10 years old. The survivability analysis was completed to estimate a field based FEL value based on fatigue cracking observations, rather than just use values estimated from limited laboratory test programs available at the time.

The definition of failure used by Von Quintus for confirming the FEL was nominally no fatigue cracking, which in practice was taken as 2% fatigue cracking to account for recording errors. For each site the EVERSTRESS linear elastic model was used to calculate the maximum tensile strain at the bottom of the asphalt layer. A typical survival curve, based on amount of fatigue cracking and probability of occurrence, is shown in Figure 2-11, following.

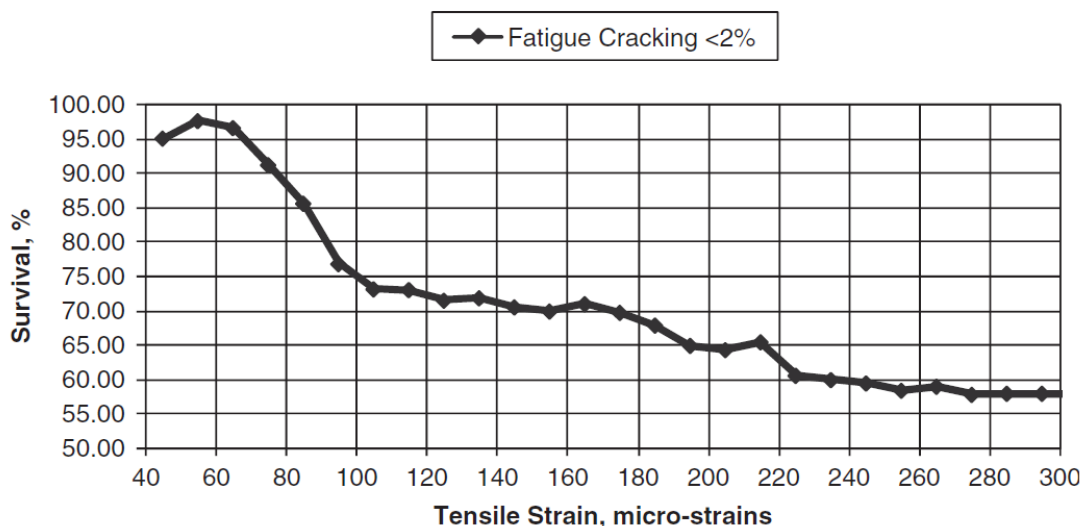


Figure 2-11 Typical Survivor Curve, after NCHRP Report 646 (2012)

Based on the 1995 LTPP analysis, Von Quintus suggested the existence of an endurance limit of $65\mu\epsilon$ at a 95 percent confidence level for an 80kN single axle load at the equivalent annual temperature for the specific site. Conversely, the survival analysis completed with the updated LTPP performance data in 2006, did not support the concept of FEL. Von Quintus noted that the volume of heavy vehicles used in the sections in the updated study was lower

than would be considered heavy truck traffic and that much higher level of heavy vehicle traffic were needed to validate the endurance limit design premise with field observations and data. Additionally the analysis did not examine the source of the cracking, which may have been either surface or base initiated cracking.

Although Von Quints (2006) believed that the endurance limit is a valid design premise and an asphalt mix property, he noted that no definite conclusion could be reached from the field performance data collected without a forensic investigation, to identify the source of the fatigue cracking.

2.8.2 Designed LLAP Sections

In the US and Canada there are a number of non-instrumented test sites where the performance of LLAP designs are being observed. Rosenberger et al. (2006) documented a LLAP design undertaken using Per-Road on a by-pass around Bradford, Pennsylvania that consisted of 330mm of asphalt over 315mm of granular base. Lane et al. (2006) documented three pavements in Canada which were constructed in Ontario on Highway 402, near Sarnia. These sections included a high binder asphalt layer, asphalt with a Superpave mix as the base, and a conventionally designed pavement section. These LLAP sections, again designed by PerRoad, were 325mm of asphalt over 500mm of granular base, and the conventional section, designed according to the empirical 1993 AASHTO design guide, had 240mm of asphalt over 550mm of granular material.

2.8.3 UK TRL Studies

In the United Kingdom (UK) Nunn (1997) performed experimental studies on field pavements and proposed concepts for LLAP for which classical bottom-up fatigue cracking would not occur. Nunn defined LLAP as those that last at least 40 years without structural strengthening. He drew together information from full-scale experimental pavements, studies of deterioration mechanisms on the road network, long-term deflection monitoring of motorways and condition assessments with the aim of producing a design method for LLAP. The UK's pavement design system was based on experimental roads that had carried up to 20 million standard axles. When the study by Nunn et al. was conducted, these relationships were being extrapolated to more than 200million standard axles. Nunn evaluated the most heavily travelled pavements in the UK, most of which had carried in excess of 100million standard axles to evaluate the current design system. Nunn concluded the following:

- Pavements with less than about 180mm of asphalt deformed at a high rate but thicker pavements deform at a rate about two orders of magnitude less; the sudden transition suggesting a threshold effect.
- No correlation existed between the rate of rutting and pavement thickness for thick (180+ mm) asphalt pavements.

- The level of traffic loading was not the major factor affecting the residual fatigue life of the thick asphalt pavements.
- Deterioration of thick, well-constructed, fully-flexible pavements was not structural, and that deterioration generally occurred at the surface in the form of cracking and rutting
- Any evidence of fatigue cracking or damage in the main structural layers of the thicker, more heavily trafficked pavements was unable to be detected.
- Deterioration, either cracking or deformation, was far more likely to be found in the surfacing than deep in the pavement structure.
- The great majority of the thick pavements studied became stronger over time, rather than gradually weakening with trafficking as assumed.

In addition to the visual assessment, Nunn et al. undertook laboratory investigation of a number of sections of four motorways representing a range of ages (11 to 23 years) and traffic loadings (22 to 71 million standard axles). All the pavements examined, had carried more traffic than they were originally designed to carry. Cores were cut to enable the structural properties of materials that had been subjected to heavy commercial traffic in the wheel path of Lane 1 to be compared to the lightly trafficked material of the same age and nominal composition from between the wheel-paths in Lane 3. The laboratory measured residual fatigue life was then calculated. Analysis of the data showed no consistent difference between the measured residual fatigue lives with most of the difference being accounted for by variations in binder hardness and binder content between the samples extracted from the two lanes. Nunn & Ferne (2001) found that when these factors were taken into account, none of the differences were statistically significant.

The testing undertaken by Nunn et al. (2001) found that all the material tested in their experiment had a residual fatigue life lower than that of new material and traffic loading could not account for that reduction. The authors attributed this lower laboratory residual fatigue life to aging of the material. However, the relationships developed as part of the study showed that the increase in elastic stiffness with age resulted in a reduction in the traffic-induced, tensile strains, responsible for bottom up fatigue, which more than compensated for any reduction in the laboratory fatigue life. The net effect was that the predicted fatigue life increased with age.

Nunn and Ferne also examined the deflection histories of 10 heavily trafficked sections of motorway to investigate whether the stiffness of thick, fully flexible pavements reduced with time and traffic. As expected, the deflections of these sites showed considerable fluctuations which was attributed partly to the difficulty of applying accurate temperature corrections, seasonal variations in the subgrade stiffness, and variation in alignment of successive surveys. Further confirmation of these deflection trends were also provided by Falling Weight Deflectometer (FWD) measurements on the same sites. The results from

FWD surveys showed that all sections had a trend of steady or decreasing deflection with age and traffic, with one exception that showed no decisive trend either way. The authors concluded that the traffic-induced stresses and strains in the road base and the subgrade, which were considered to be responsible for structural deterioration, contrary to conventional theory were decreasing due to stiffening of the pavement over time.

As a result of the work by Nunn et al. the UK procedure for design of asphalt pavements was revised in 1997 to include a maximum asphalt thickness corresponding to minimum threshold pavement strength for the most common asphalt mixes, beyond which the pavement should have a very long but indeterminate structural life.

2.8.4 Australian Field Investigations on LLAP

Ross reviewed the design and construction of deep strength asphalt pavements, including 14 sites in Victoria which were constructed between 1971 and 1995. For this investigation, the current traffic volume data was collected, deflections were measured using the FWD and actual pavement layer thicknesses and asphalt resilient modulus for the top, middle and bottom sections of the pavement structure were determined by taking cores. Ross concluded that the majority of the investigated sites would exceed or had already exceeded the design life predicted by mechanistic analysis without further structural improvement. He also noted that the performance of the majority of the deep strength asphalt pavements studied was much better than predicted.

Based on the results, of the laboratory testing of core samples, Ross reported that the top layers of asphalt had higher modulus than the bottom layers for 11 out of total 14 investigated sites. This difference was quite significant on some of the older pavements, albeit the lower layers were 20mm mixes compared with 14 mm or 10 mm in the top layers. Ross suggested the age hardening of the top layer could be the most probable reason for the stiffness discrepancies.

Tsoumbanos (2006) examined the performance of four pavement sections aged from 20 to nearly 30 years, against roughness, rutting, cracking, strength (deflection) and stiffness (curvature). The thickness and resilient modulus of the top, middle and lower asphalt layers were determined through coring. It was found that:

- Roughness at all locations was increasing; however, it was below VicRoads intervention criteria.
- Rutting was generally between 3 and 10 mm, with two sites exhibiting constant average rutting depth and two sites exhibiting an increase in average rutting depth of approximately 1 mm per year.
- There was an increasing proportion of cracked pavement for all sites, though the rate of increase varied.

- Very low average deflections and curvature were obtained utilising VicRoads deflectograph, in all lanes and both wheel-paths.
- Higher modulus values, from resilient modulus testing of core samples, were obtained for the bottom layers compared with the top for two sites, consistent with observations by Ross but inconclusive overall.

Tsoumbanos concluded that for three of the four sites investigated, typically higher thicknesses than 210 mm, and the sites generally showed expected performance of LLAP in that;

- cracking was mostly confined to the top 40 to 60 mm of the surface layer,
- and, collected deflection data suggested a very strong pavement structure and no structural maintenance was required to date.

Carteret & Jameson (2009) identified that Tsoumbanos did not undertake coring between wheel-paths and therefore definitive conclusions on whether micro-cracking due to fatigue occurred below the surface could not be determined. However, this may not be significant as identified by Thompson et al. (2006) LLAP can be achieved with some damage to the asphalt layer, as long as the balancing point is achieved, and the lack of macro cracking is what is important.

The mechanistic analysis undertaken by Tsoumbanos of the four studied pavement sections, found that the tensile strain threshold of $70\mu\epsilon$, proposed by Monismith (1972), was exceeded for all four sites and yet no visual sign of fatigue cracking of the pavement sections which had been in-service for 20 to 30 years, was observed.

2.8.5 *The Asphalt Pavement Alliance (APA) Perpetual Pavement Awards*

The APA developed the Perpetual Pavement award for owners of LLAP pavements that:

- Are at least 35 years old
- Never have had a structural failure,
- Had average intervals between resurfacing of no less than 13 years
- And, the road must demonstrate the qualities expected from long-life asphalt pavements: excellence in design, quality in construction, and value to the traveling public.

Nominations, for the Perpetual Pavement Award are assessed by a panel of industry experts at the National Centre for Asphalt Technology (NCAT).

Table 2-1 following summarises a number of the perpetual pavement award winners, which can aid in expansion of the knowledge of LLAP. While the awards also include numerous awards for lower traffic pavement sections with less than 150mm of total asphalt thickness

and while these sections show that the LLAP concept can be allied to lower volume roads, it is outside the scope of this study and has not been included in the Table 2-1.

Table 2-1 APA Perpetual Pavement Awards

Asphalt Thickness (mm)	Year of Const.	Location	Base Conditions	Traffic (AADT)	Heavy Vehicles (%)
250	1952	I-287 New Jersey Turnpike	Clay/Marsh	175,000	40
230-355	1964	I-90, Washington State		4x10 ⁵ -1x10 ⁶ ESA/year	
306	1967	I-65, Marshall County Tennessee	200mm crushed rock	21,000	
305	1962	I-40, Oklahoma City	Sandy loam	45,000	16
300	1966	I-35 Pine County, Minnesota	300mm granular base, upper 75 Bitumen treated	14,000	
500	1962	I-80 Johnson County, Iowa			
300	1963	I-17 Don Valley Parkway City of Toronto		100,000	1x10 ⁶ ESA/year
210	1963	Missouri DOT US 63, Texas County	170 stone base		
190	1955	Garden State Parkway, New Jersey Turnpike	200mm gravel base		
320	1969	I-181 Johnson City Tennessee	200mm Crushed limestone	39,000	30mill
250	1969	I-26 Spartanburg County South Carolina	90mm sub base 180mm base		20 mill
260	1937		overlays	11,000	4
180		Minnesota Department of Transportation Trunk Highway 10, Mileposts 224 to 227	18'		13.5
406	1969	Kentucky Transportation Cabinet Julian Carroll-Jackson Purchase Parkway	Unstable Marsh		

320	1966	Mississippi Department of Transportation Interstate 59, Lauderdale County	150mm lime on sand clay base	15,000	26
270	1966	Tennessee DOT, I-24, Coffee County	200 crushed rock	25 mill	
240	1965	Virginia DOT, I-81, Mile Posts 318.4 to 324.9	150mm base, 300mm sub base	25,000	26
180	1966	California CDOT San Diego Freeway, I-405,	165mm sub base 100mm base, 190 base		
305	1972	US-41, Wisconsin Abram	305mm sub-base	12 million	
250	1969-72	Interstate 5, WSDOT Snohomish County	Embankment fill 15 feet 150mm 250granular base	23 mill	

These awards show that LLAP can be achieved in pavements ranging from 180mm to over 300mm depending on the level of support given to the asphalt layers by the subgrade and sub-base. The results also show that the limiting thickness is close to that as found by Nunn (2001) that “270mm of asphalt would be sufficient for any traffic loading” and 340mm will give high confidence level.

2.8.6 LLAP Terminal Thickness Requirements

Since the concept of designing long-life pavements began in 2000, the required thickness for LLAP has been much studied and investigated. Nunn et al. (2001) first proposed the idea of thickness limit for LLAP and proposed both an upper and lower limit for pavement thicknesses. The researchers found that any asphalt in excess of 390mm (*N.B. this thickness included safety factors of 100mm for top down cracking and 20mm for increased load limits*) determined from the existing UK design procedure, would be of no benefit in prolonging the fatigue life of the pavement, as such pavements would perform perpetually. On the other hand, they stated that pavements with thicknesses less than 180mm would not last 40 years and were considered substandard for heavily traffic roads. Nunn et al. (2001) found that structural deformation, rapidly increasing surface cracking and eventually premature pavement failure were found to occur in thinner pavement sections.

The APA (2002) believed that there would be no additional life-cycle benefit to the pavement structure when its thickness is more than a certain limit. Gierhart (2007) found that in the US, a thickness of 500mm is proposed by some states while others have experienced surface confined distresses in pavements as thin as 160mm. Walubita, Scullion & Scullion (2007) found that the thickness of a typical pavement in Texas designed by Asphalt Institute (AI) Mechanistic-Empirical (M-E) method was greater than 500mm, however, by using perpetual pavement design concepts, the pavement thickness could be reduced by 180mm to 340mm.

In Europe, Merrill et al. (2006) continued research on pavement thickness and its effects on propagation of cracks in pavement structure in Netherlands and found evidence of full-depth cracking in thin pavements with thicknesses less than 80mm while only 28% of the studied pavements with thicknesses of more than 290mm showed signs of cracking. Moreover, all cracking in these thick asphalt sections was found to be confined to the top layers, suggesting LLAP. They found that there was a distinct change in the predominant form of cracking that occurred at a thickness in the region between 170 and 200mm. Merrill found that at this point, the formation of cracks changed from full-depth cracking to top down surface cracking).

In a study on pavement thickness and its effect on pavement structure, Rolt (2001) found results which validated the findings of Merrill et al. Rolt reported that well-designed and constructed asphalt pavements with 270mm of thickness could provide a fatigue resistant pavement structure while little deformation would accumulate in 180mm thick pavements over time. Rolt suggested a very conservative thickness of 370mm assuming the propagation of surface cracks up to 100mm into the pavement structure and excluding the cracked section of the pavement from contributing to load spreading. However, Rolt believed that a well-built pavement of 300mm thickness was likely to be structurally resistant with some minor surface deterioration.

Al-Qadi et al. (2008) found that the tensile strain at the bottom of asphalt and the maximum shear strain in the pavement are strongly influenced by the asphalt thickness. They reported a significant strain reduction when the thickness of the pavement was increased beyond 250mm. Also, the results from their study showed that the strains in pavements 350mm thick were smaller than the recommended endurance limit to prevent bottom-up fatigue cracking by Carpenter et al (2006).

Wu & Hossain (2002) found that some in service roads in the US, despite having pavement structures thinner than 330mm and being in service for over 40 years, such as the Kansas Turnpike, have had little or no sign of fatigue cracking. While Mahoney (2001) found in studies on long-lasting asphalt pavements in Washington State that pavements with thicknesses greater than 160mm, cracks (if any) were initiated at the surface and generally didn't propagate through the full depth of the pavement structure.

Fee (2001), by reviewing the strategies for designing and maintaining long-life pavements in the UK, France, Netherland and several states in the US, concluded that to achieve an extended life asphalt pavement, typically a thickness of 300-350mm was required and a minimum of 200 mm was required.

2.9 Design Procedures for LLAP

Notwithstanding the wide acceptance of the fatigue endurance limit concept its introduction into LLAP thickness design is problematic. Its introduction into pavement design has been subject to two major US studies under NCHRP project 9-38 and 9-44. One of the key issues under research is the healing of micro-cracks and restriction of fatigue crack propagation from the bottom of the asphalt base.

In order to successfully design a pavement section, the designer needs to consider the appropriate thickness for the pavement layers taking into account the heaviest anticipated traffic loads while avoiding overdesigning the thickness. Newcomb, Willis & Timm (2010) showed that by limiting the mechanistically defined stresses, strains and displacements of the pavements layers, the initiation of deep cracking or rutting in the pavement structure can be avoided. These thresholds are often referred to as limiting pavement responses.

2.9.1 Pavement Structural Distresses

For the design of LLAP defining critical pavement responses (stress, strain or displacement) below which no accumulation of structural damage to the pavement occurs is required. In the LLAP design concept it is assumed that if the load-induced pavement responses remain below such a level, then the design can be considered as a LLAP or perpetual pavement. Currently, as identified by, Newcomb, Willis & Timm (2010) most LLAP design approaches deal with pavement responses associated with structural rutting and bottom-up fatigue cracking.

2.9.2 Structural Rutting

When the overall strength of the pavement structure is incapable of resist the traffic loading structural rutting may occur from induced deformations either in the granular base or subgrade. As identified by Nunn (2001) and by Newcomb, Willis & Timm (2010), although structural rutting is rarely seen in modern thick asphalt structures, it necessitates major rehabilitations and reconstructions. Rolt (2001) and Brown et al. (2002) based on the findings from the National Centre for Asphalt Technology (NCAT), found that no structural rutting (that is rutting of the subgrade) takes place in thick asphalt pavements and rutting is was confined to the upper few centimetres of these pavements, which can be easily repaired by mill and resheet treatments. To limit structural rutting Harvey et al. (2004) and Walubita et al. (2008) recommended the use of a vertical compressive strain of $200\mu\epsilon$ at the top of

subgrade layer as the limiting design parameter. They found that rutting (plastic deformation) in the lower layers would not take place if the compressive strain at the top of the subgrade was kept below $200\mu\epsilon$. Newcomb, Willis & Timm (2010) identified that this limiting response can be achieved by either increasing the overall pavement structural thickness or increasing the stiffness of one or more of the pavement layers.

The researchers at the University of Illinois used a different approach, being the ratio of subgrade stress to the unconfined compressive strength of the soil, Subgrade Strength Ratio (SSR), as the limiting response characteristic. Bejarano & Thompson (2001) and Bejarano, Thompson & Garg (1999) recommended for the clay soils studied in their research, that the critical value for SSR was found to be in the range of 0.5 to 0.6. They suggested an SSR of 0.42 for design purposes.

2.9.3 *Fatigue Cracking*

The other major mode of distress in flexible pavements is bottom-up fatigue cracking. After formation, this cracking propagates to the surface through the layers of the asphalt. This causes the infiltration of water into the pavement layers and subsequently changes of unbound material properties and can result in accelerated surface deterioration, pumping and rutting. Huang (1993) identified that conventional theory states that high repeated load induced strains at the bottom of the asphalt layer is the cause of this mode of distress. Conventional design procedures control this fatigue cracking by controlling the horizontal strains at the bottom of the asphalt layer. The main approach used to decrease the probability of bottom-up fatigue cracking is to increase the thickness of the pavement structure.

Willis (2008) reported on a 2006 survey of Accelerated Pavement Testing (APT) facilities in the US that to predict and study fatigue potential a large majority of the responding facilities measured horizontal strain at the base of the asphalt layer. LLAP projects such as the I-5 in Oregon (Estes (2005), Scholz et al. (2006)) have incorporated measuring strain, Hornyak et al. (2007) identified that the Marquette Interchange in Wisconsin have incorporated measuring strain at the base of the asphalt layer into their research.

While the predominate research is to measure strain at the underside of the asphalt layers to study fatigue, it has been shown by numerous researchers that cracking in thick pavements is generally confined to the pavement surface due to reduction in intensity of strains at the bottom of asphalt pavement (Al-Qadi et al. (2008), Asphalt Pavement Alliance (2002), Martin et al. (2001), Merrill, Van Dommelen & Gáspár (2006), Newcomb, Buncher & Huddleston (2001)).

As identified by Mahoney (2001) and Rolt (2001), for thick asphalt pavements the critical location of the strains in pavements may change from the bottom of the asphalt layer to the

surface of the structure as the strains at the bottom of the asphalt layer are reduced. Ferne (2006) showed that by controlling the strains at the bottom of the asphalt layer and hence confining the distresses to the surface layer, deep structural rehabilitations and reconstructions can be avoided and maintenance would be limited to functional maintenance such as skid resistance and ride quality. Mahoney (2001) identified that surface cracking in these pavements can be maintained by, a “mill and fill” (mill and resheet) maintenance plan for extending the pavement’s life.

Beside the advantages of thick asphalt pavements to control fatigue cracking, studies on thick pavements at the National Centre for Asphalt Technology (NCAT) Pavement Test Track Brown et al. (2002) and research done by Rolt (2001) have shown that rutting is also limited to the surface layer in thick pavement structures.

Al-Qadi et al. (2008) has shown that the longitudinal strain at the bottom of asphalt layer has proven to be critical in thinner pavements and in a fully-bonded pavement, it is always the location of highest tensile strain. Walubita et al. (2008) recommended that a typical threshold limit for strain (FEL) at the bottom of asphalt layer to prevent bottom-up fatigue cracking should be $70\mu\epsilon$. However, some other research has shown different threshold values.

Based on laboratory testing, Romanoschi et al.(2008) proposed that the strain threshold of 60 to $100\mu\epsilon$ be applied everywhere in the pavement structure, while according to an experimental pavement project in China, Yang et al.(2005) reported a value of $125\mu\epsilon$.

However, as identified by Willis & Timm (2009b), it should be noted that pavement responses and FEL of flexible pavements rely on the type of mixes and the conditions of the testing undertaken in each reviewed study and that results based on tests on different mixes with different material and testing conditions may not be globally representative.

2.9.4 Empirical Approaches

Von Quintus (2001b) developed one of the earlier approaches to LLAP design for the State of Michigan. Von Quintus chose to use a mechanistic approach employing the ELSYM5 computer program to calculate stresses and strains in the pavement structure. This approach applied the concept of cumulative damage to determine the appropriate section for a design period of up to 40 years. Von Quintus used this methodology, in the absence of other approaches, as a way of determining a reasonable range of pavement thicknesses for LLAP.

In the definition of LLAP Von Quintus used low levels of predicted distresses for the design criteria rather than limiting strains. As part of the procedure Von Quintus recommended rehabilitation strategies to enable the pavement to last for a period of 40 years. In line with the current approach to LLAP the rehabilitation strategies were mill and resheet operations

at years 15 and 30, except for the lowest level of traffic where they were scheduled for years 32 and 40. The result of this analysis was that Von Quintus developed a catalogue of LLAP design for Michigan.

2.9.5 *Terminal Thickness or Traffic*

As a result of the work done by Nunn et al. the UK procedure for the design of asphalt pavements was revised in 1997 to include a limiting thickness for the most common asphalt thicknesses. Beyond this thickness the pavement would have an indeterminate structural life.

The structural section for the LLAP in the United Kingdom includes the use of granular base and sub-base layers below a thick asphalt pavement. The thickness of the asphalt is such that traditional bottom-up fatigue cracking and structural rutting are avoided. Nunn and his associates found that pavements having a total asphalt thickness of less than 180mm are prone to structural rutting, while the rutting in thicker pavements is confined to the top of the structure. Rutting occurs mainly in the top 100mm of thick asphalt roads in the United Kingdom. The TRL approach allows for an adjustment in asphalt thickness according to the type of mix and stiffness of the binder. The standard dense bitumen macadam base uses a 100-penetration asphalt binder and has a limiting thickness of 390mm. For the DBM50 which is similar to Australian C320 and 450, mixes a limiting thickness of 340mm is recommended.

Using increasingly stiff binders allows for the design of thinner sections according to the British approach. However, the British researchers placed an upper limit on asphalt thickness based upon observed distresses. Studies of the performance of British roads show that additional pavement thickness, beyond that required for 80 million ESAL, would not provide additional benefit as shown in Figure 2-12. Nunn and his associates state that the fourth power law, traditionally used for describing the relationship between pavement damage and axle loads, is not appropriate for thick asphalt pavements.

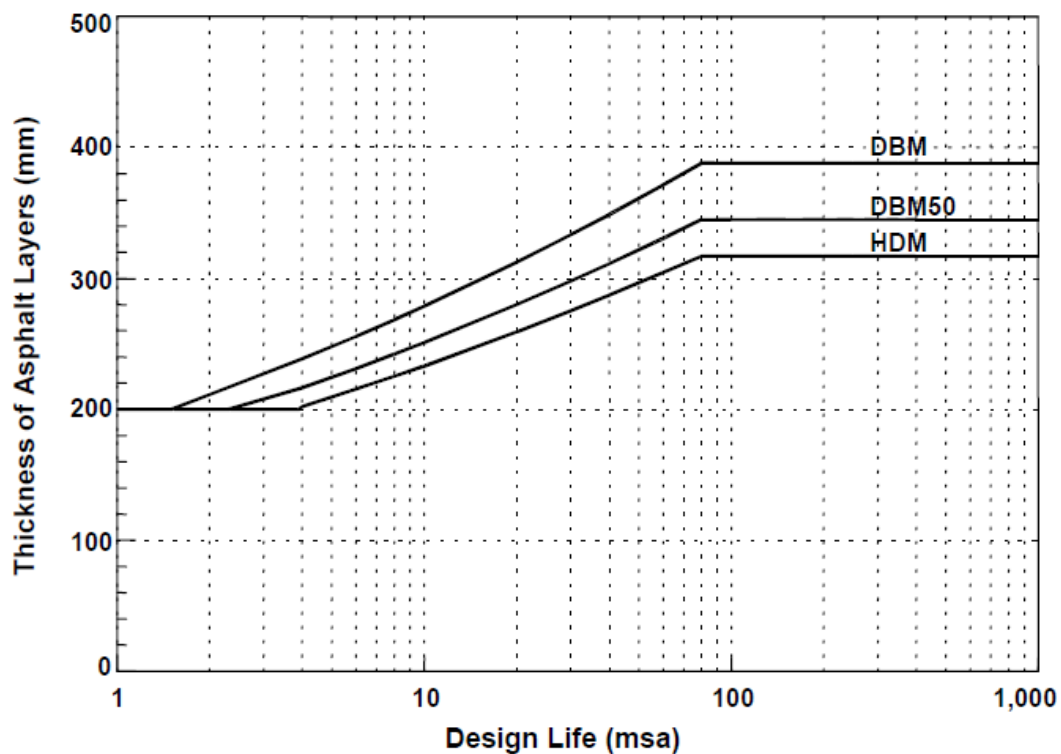


Figure 2-12 TRL Design Chart, after Nunn (2001)

2.9.6 Mechanistic Empirical

The Asphalt Pavement Alliance worked with Auburn University Timm (2008), to develop PerRoad, a computer analysis program to design LLAP using Mechanistic Empirical principles. The program couples layered elastic analysis with a statistical analysis procedure (Monte Carlo simulation) to estimate stresses and strains within a pavement Timm and Newcomb, (2006). In order to predict the strains which would prove detrimental for fatigue cracking or structural rutting, PerRoad requires the following inputs:

- Seasonal pavement moduli and annual coefficient of variation (COV)
- Seasonal resilient moduli of unbound materials and annual COV
- Thickness of bound materials and COV
- Thickness of unbound materials
- Load spectrum for traffic
- Location for pavement response analysis
- Magnitude of limiting pavement responses
- Transfer functions for pavement responses exceeding the user-specified level

For accumulating damage PerRoad follows a linear sum of damage approach. The Monte Carlo simulation is simply a way of incorporating variability into the analysis to more

realistically characterise the pavement performance. The output for PerRoad consists of an evaluation of the percentage of load repetitions lower than the limiting pavement responses specified in the input, an estimate of the amount of damage incurred per single axle load, and a projected time to when the accumulated damage is equal to 0.1. On high volume pavements, the critical parameter for LLAP design is the percentage of load repetitions below the limiting strains. It is generally recommended that the designer ensure that 90 percent or more loads are less than the critical threshold value.

Thompson and Carpenter (2004) presented LLAP design concepts in the context of laboratory work undertaken at the University of Illinois. In this case the model employed to represent the pavement was a finite element program called ILLI-PAVE in which 8kN and 8.5kN axle loads served as the loading condition. These researchers reasoned that this would be the extreme case in hot weather as these loads would represent the worst condition with very few loads being greater than this. Their work showed that up to 30 percent of the fatigue life of the pavement could be consumed, yet if the remaining strains were below the FEL, there would be no fatigue cracking. They went on to verify these results with field deflection measurements. From these, they were able to conclude that many existing pavements could be classified as LLAP.

The US AASHTO Mechanistic-Empirical Pavement Design Guide AASHTO, (2008) can be used for LLAP design by incorporating a Fatigue Endurance Limit (FEL). The design procedure is currently being calibrated and adopted by a number of states across the U.S. It predicts the accumulation of a variety of pavement distresses over a user-prescribed analysis period. Based on information from NCHRP Project 9-38 Prowell et al. (2006), Witczak et al. (2006) incorporated an optional FEL ranging between 75 and 250 $\mu\epsilon$.

Researchers have begun to investigate the use of the MEPDG in conjunction with the FEL to optimize pavement designs (Behbahais et al., 2009; Tarefoller et al., 2009). In fact, Willis and Timm (2009) found good agreement between PerRoad and the MEPDG in terms of thickness requirements when the FEL was employed.

2.9.7 *NCAT Test Track*

Willis et al. (2009) and researchers at NCAT examined the performance of three cycles of the test track (2000, 2003 and 2006) to develop strain criteria for prevention of fatigue cracking in LLAP. They estimated the strain distributions for the 2000 test track experiment using the mechanistic pavement modelling program PerRoad and for the 2003 and 2006 cycles, direct strain measurements from the base of the asphalt layers were used to develop strain profiles. In 2000 test track, six test sections that had experienced at least 20 million ESA's (Equivalent Single Axle load) without showing signs of fatigue cracking, were selected and studied for theoretical strain analysis. The stiffness of the asphalt and the resilient modulus of the soil were characterised using FWD (AASHTO two-layer back-calculation

methodology). Relationships were developed between the asphalt modulus and the midpoint temperature in the asphalt for each test section during the time of testing.

Using the developed relationships, cumulative distributions of the stiffness were developed by calculating stiffness based on the average hourly temperature under trafficking.

In the 2003 test track, embedded asphalt strain gauges were used to measure the strain at the base of the asphalt layer(s) of the pavement structure in eight sections. Detailed trucking databases allowed precise loading configurations to be analysed and weekly measured pavement responses were used to develop continuous strain distributions for the structural sections. These two design components were linked to the observed pavement performance of the section to make correlations between pavement response and performance in test sections. Previously developed relationships between pavement response and temperature were used to develop cumulative distribution of strain for the life of the pavement. Similar to 2003 cycle, in the 2006 test track the actual strains were measured at the base of the asphalt and the same procedure was used to create the cumulative strain distributions. In the 2006 test track, relationships between longitudinal strain and temperature by axle for each section instead of by truck were also developed.

Willis et al. derived distinction between the cumulative strain distributions of the sections that failed in fatigue to those that did not. The comparison of the field performance and cumulative strain distribution of each test section suggested the existence of a limiting cumulative distribution of strain to avoid asphalt fatigue cracking. Three criteria were considered to help develop a new strain-criterion for flexible perpetual pavement design:

- 1) The section could not be overdesigned;
- 2) The section could not have exhibited any fatigue cracking;
- 3) The section had to have experienced at least 20 million ESALs. Analyses for N3 and N4 test sections by axle and by truck met the criteria.

Allowing $\pm 15\mu\epsilon$ confidence boundary, Willis et al. 2009 determined that the average of the strain distributions for these test sections were an appropriate field-based strain threshold for designing LLAP. Rickards & Armstrong (2010) believed that the concept of LLAP thickness design based on compliance with limiting cumulative distribution of asphalt strain has considerable merit. It has the potential to avoid the acknowledged uncertainty in theoretical fatigue modelling and constrain management of asphalt fatigue and durability to satisfying compliance hurdles.

2.10 Summary and Recommendations

International research has shown that due to issues with the form and use of the conventional fatigue model global shift factors cannot be developed and a global model would not be indicative of the performance found in varying regions of Australia. It is not

surprising therefore, that the variable shift factors are consistently obtained in laboratory to field calibrations. The literature review found that the other main limitation of the classic fatigue model was the lack of the incorporation of a FEL. It has been found that the modelling of the fatigue performance of asphalt mixes is a complex process and a simpler approach would be to design fatigue out of the pavement by use of a FEL, with research showing that the FEL is due to two factors, healing and the presence of an endurance limit, both of which can be incorporated into a single FEL.

The visco elastic nature of asphalt materials was shown to be responsible for the time dependant nature of asphalt of the stiffness of asphalt mixes, with the relaxation modulus being shown to be the fundamental property which determines the stress and strain in flexible pavements. As well as the time dependant nature of the material the visco elastic nature of asphalt was found to be responsible for the disputed energy damage within a loading cycle. It was found that this dissipated energy was directly related to the in fatigue life of the asphalt mix, although not all dissipated energy results in damage and there was an energy level where healing become greater than damage.

The international research has shown that the FEL clearly exist for all asphalt mixes and is a function of binder type, test temperature and healing potential of the mix. It was shown that methods exist for the determination of the FEL from short time scale testing.

The presence of FEL was confirmed in field studies with many researches, particularly in the UK and US finding that converse to conventional theory, many pavements were getting stiffer with time and not exhibiting any signs of structural failure.

By reviewing the strategies for designing and maintaining long-life pavements in Australia, the UK, France, Netherlands and several states in the US, it was found LLAP could be achieved with a maximum thickness of 300-350mm and a minimum of 200mm was required for LLAP performance.

3 Experimental Plan

3.1 Overall Design

The overall design of the study was divided into five (5) main tasks, as shown following and described in depth in the following chapter.

1. Material classification experiment
2. Laboratory field modulus interconversion study
3. Modulus inter-conversion study
4. Development and calibration of a LLAP design procedure
5. Validation of the LLAP design procedure using Australian and UK LLAP data.

3.2 Material Classification Experimental Design

The objective of the material characterisation component of the APS-fL project was to provide real data on the performance characteristics of actual standard Australian production mixes. Given the combination of binders, aggregate sources, producers across Australia, obviously not all production mixes could be included in the study. Therefore in order to keep the size of the characterisation study to a manageable level, the design of the experiment was rationalised to 30 mixes by the Project Steering Committee as selected by the Project Steering Committee. The 30 mixes were selected to cover the majority of the combinations of aggregate sources and binder types used across Australia, without duplication of relatively similar mixes.

The performance characteristics of asphalt mixes are primarily influenced by the following key factors;

- mix size and gradation,
- bitumen type and content,
- aggregate type and proportions,
- and, air void content.

In order to capture the effects of these parameters on the standard asphalt materials, the study primarily focused on the asphalt mixes produced by Australia's major asphalt producers, for State Road Authorities. It was believed that these mixes would most likely be used in major projects where the LLAP concept is most likely to be implemented.

The design of the experiment was limited to 30 asphalt mixes, nominally 15 each of 14mm and 20mm mixes. As the overall objective of the project is the development of LLAP design procedure, the emphasis was placed on the harder binder grades, which are believed to offer greater structural benefit. Likewise, as the main structural layers in the pavement will be the larger stone mixes, focus was placed on 20mm mixes.

As the goal of the project is to model actual field performance as close as possible, the experiment was designed using plant produced asphalt mixes, as it was believed that these materials more closely matched the reality of asphalt produced and placed in the field than that produced in the laboratory. One item noted in using plant produced mixes is that the current Austroads mix design and pavement design characterisation is based on laboratory mixes. However, this is not always the case in practice with State Road Agencies such as the NSW Roads and Maritime Services, Queensland Department of Main Roads and DPTI, moving to plant validation of asphalt mixes over laboratory values. Additionally, nearly all designs in Australia to date are based on indicative values with little validation of the actual modulus values used across the spectrum.

3.2.1 Mix Selection

Currently, there are three major suppliers who operate in all states of Australia. If all suppliers, in all states, were to contribute to the program, the size of the experiment would become be very large and result in the duplication of essentially identical mixes. It was therefore considered necessary to firstly go through a rationalisation process to constrain the experiment to a manageable size without lessening the value of the output. This was achieved by limiting the duplication of mixes, comprising the same bitumen and aggregate components, as it is accepted that these components have the greatest influence on the characterisation of the asphalt mix. An asphalt mix with the same components from different suppliers should have similar performance. (There are obviously other factors that will impact on the performance results e.g. mix gradation and in particular fine fractions and fillers).

To accomplish this as a first step, suppliers were requested to fill out, for each mix submitted, the 'Asphalt Material Component and Gradation Details', results of which are shown in Appendix A. The anonymous summary was then reviewed by the Project Steering Committee and materials for the subsequent testing program selected and the supplier advised accordingly and samples requested.

3.2.2 Supply of Asphalt Mixes

In order to ensure an adequate supply and reserve of the selected materials, producers were requested to supply a minimum 300kg of a current production plant manufactured mix.

Prior to packaging each of the samples was subjected to standard compliance testing (maximum density, bulk density binder content and gradation) and identified only by the AAPA mix identification code. This code was provided to the Fulton Hogan's National Laboratory to enable the compaction of cylinders and beams at the Australian standard 5% target air void level. Additionally, for all samples, the supplier was to supply the: aggregate

composition, the gradation, their design method, volumetric, quantity of Recycled Asphalt Product (RAP) and binder type, the results of which are shown in Appendix A.

3.2.3 Supplied Asphalt Mix Materials

The results of the initial rationalisation identified 30 mixes for use in the study. These mixes were identified to cover the spectrum of aggregate types, design methods and non-modified Australian bitumen (Classes 320; 450; 600 and Multigrade) used in Australia. In states where multiple suppliers use common aggregate types, only a single supplier provided the mix.

Given the objective to model actual field performance as close as possible, the experiment was designed using plant produced asphalt mixes. It was believed that these materials more closely matched the reality of asphalt produced and placed in the field than that produced in the laboratory.

Of the 30 mixes identified for inclusion in the study, 28 were in production over the experimental period and therefore included in the study. Table 3-1 following summarises the resultant 28 mixes used with their volumetric properties and mix design method.

Table 3-1 Supplied Materials

Nominal Size (mm)	Binder Type	Mix Design Method	Design Voids (%)	Design VMA (%)	Design VFB (%)
14	A15E	Marshall 50 blow	4	14.7	73
		Gyratory 120 cycles	5.4	15.5	65
	AR450	Gyratory 120 cycles	4.2	15.5	73
		Gyratory 120 cycles	5	15	72
		Gyratory 120 cycles	4.3	15.5	73
		Gyratory 120 cycles	5.4	15.5	65
	C320	Gyratory 120 cycles	4	15	73
		Marshall 75 blow	5.01	15.17	67
		Marshall	4.9	16	70
		Marshall 75 blow	5.5	16.4	66
		Marshall 50 blow	5.2	15.6	66
		Gyratory 80 cycles	4.5	14.5	69
		Gyratory 80 cycles	4.5	14.6	69
		Marshall 75 blow	3.8	14.2	73
	Multi Grade	Marshall	5.7	15.7	64

20	AR450	Gyratory 120 cycles	4.8	15.5	69
		Gyratory 120 cycles	4.9	14	70
		Gyratory 120 cycles	5.2	15.6	67
	C320	Marshall	5	15.2	67
		Marshall 75 blow	3.8	14.2	73
		Marshall 50 blow	5.3	15.2	69
		Gyratory 80 cycles	4.5	13.5	66
		Marshall 75 blow	3.8	14.2	73
		Gyratory 120 cycles	3.9	14	72
	C600	Marshall 50 blow	5	15.2	68
		Marshall 50 blow	4.8	14.8	68
		Marshall 50 blow	4.6	13.9	67
	Multi Grade	Marshall	4.5	14.6	69

3.3 Asphalt Mix Properties

For each of the 28 supplied production mixes, the volumetric properties and aggregate gradations were supplied by the producer. A comparison of the supplied information was undertaken for each nominal aggregate size in order to obtain an indication of the variability of standard production mixes across Australia, the results of which are discussed in the following section.

3.3.1 Gradation

The gradation of the supplied nominal 14mm and nominal 20mm mixes can be seen graphically in Figure 3-1 following, on a 0.45 power gradation curve.

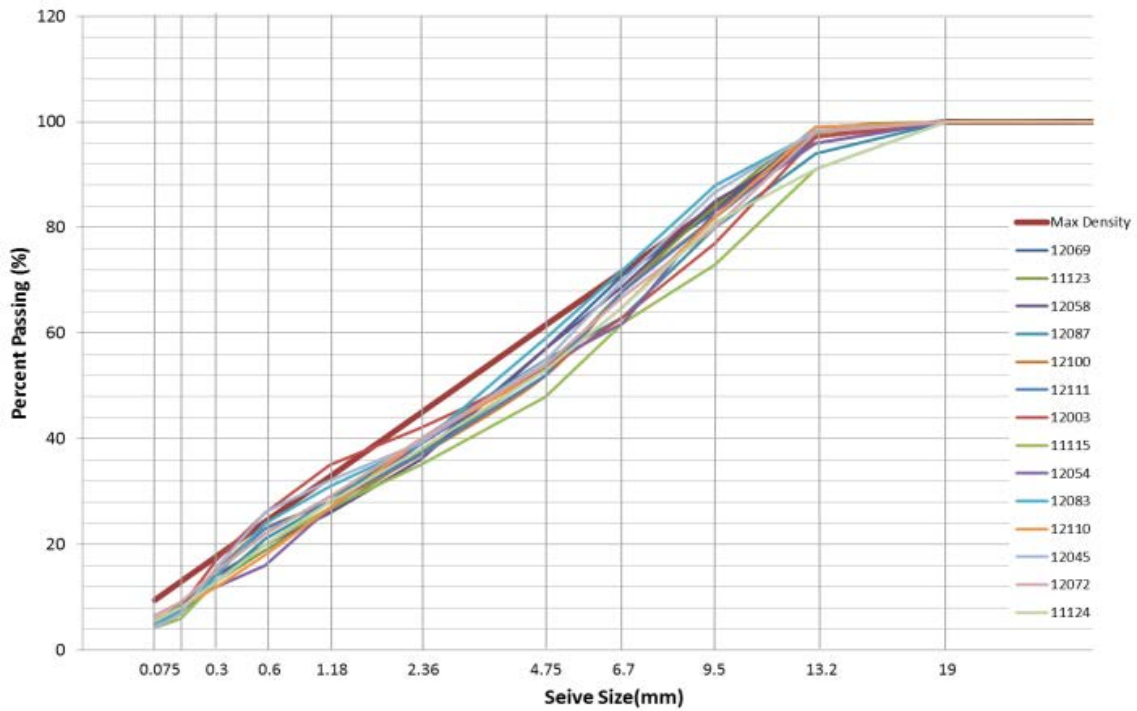


Figure 3-1 Gradation plots "Nominal" 14mm mixes

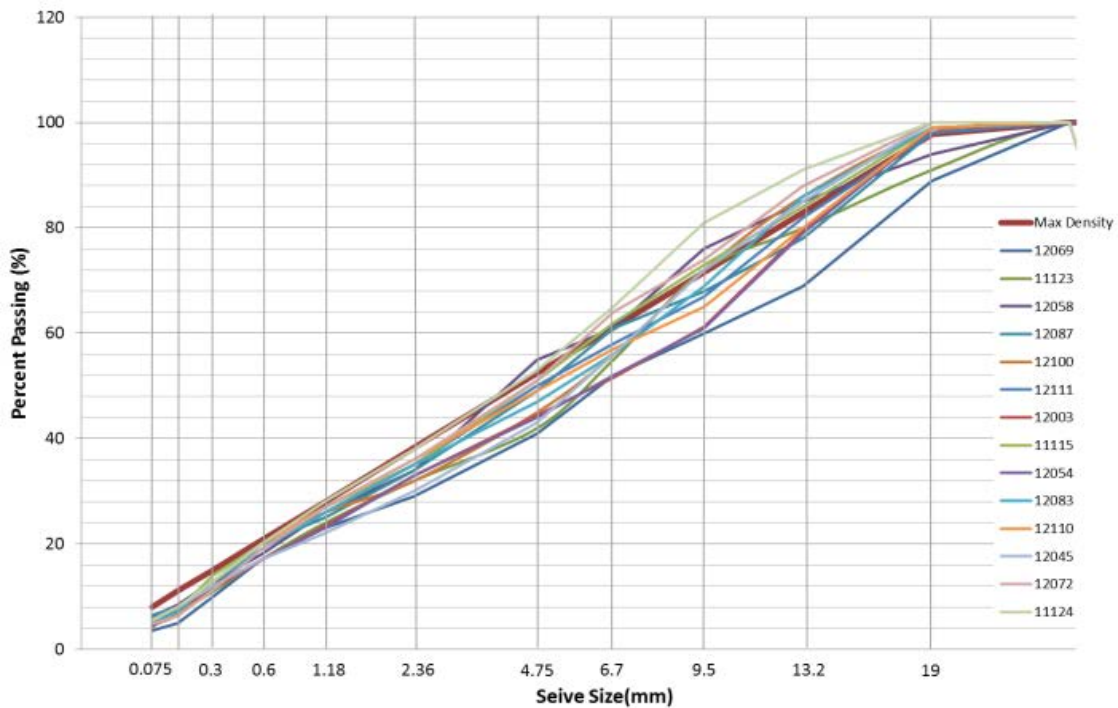


Figure 3-2 Gradation plots "Nominal" 20mm mixes

The plots show that for both the 14mm and 20mm nominal mixes, nearly all gradations closely follow the maximum density line, with, nearly all slightly coarse graded. The results show that fine and gap graded mixes do not appear to be commonly used in production

mixes for major projects throughout Australia. What is evident in the gradations, particularly in the 20mm mixes, is that the definition of “nominal” does vary across Australia and some mixes defined as 20mm nominal mixes would be classified differently in other states.

These results may indicate it may be difficult to distinguish between Australian asphalt based on aggregate gradation, due to the limited variation.

3.3.2 Volumetric Properties

The volumetric properties of the supplied mixes are shown graphically on a four axis volumetric plots, for the 14mm nominal mixes and the 20mm nominal mixes, in Figure 3-3 and Figure 3-4 following.

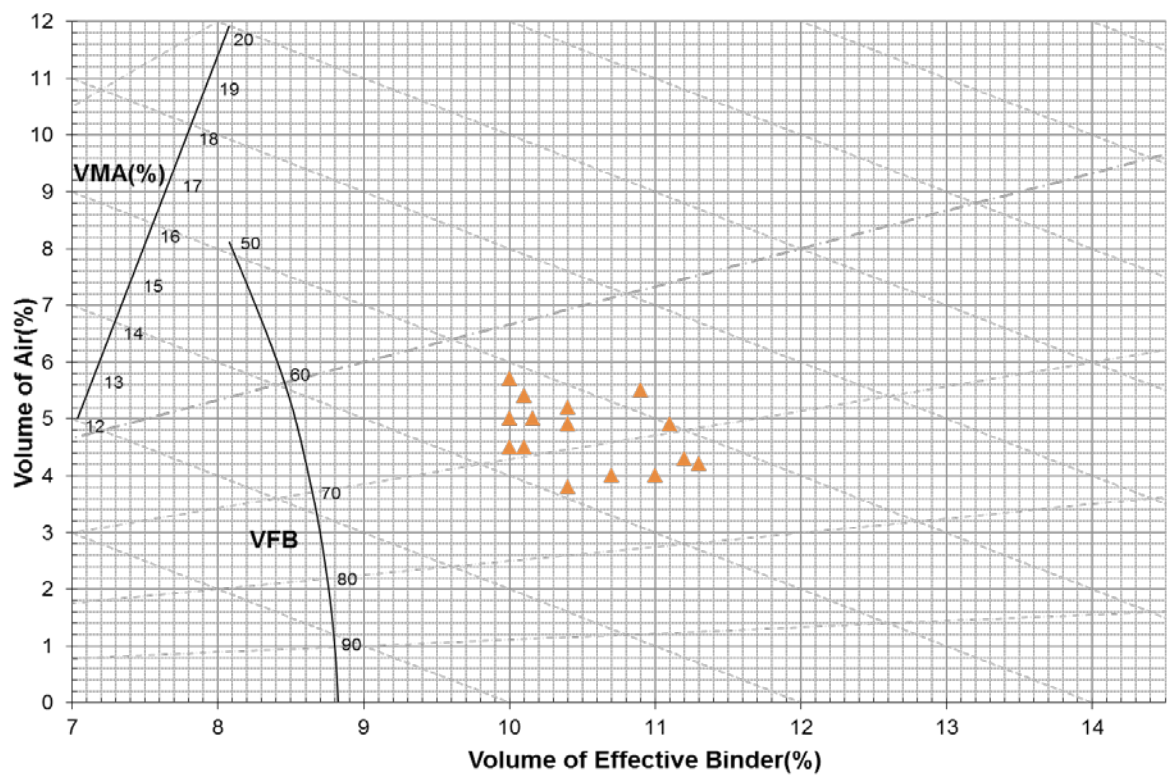


Figure 3-3 Volumetric Plots (a) 14mm Mixes

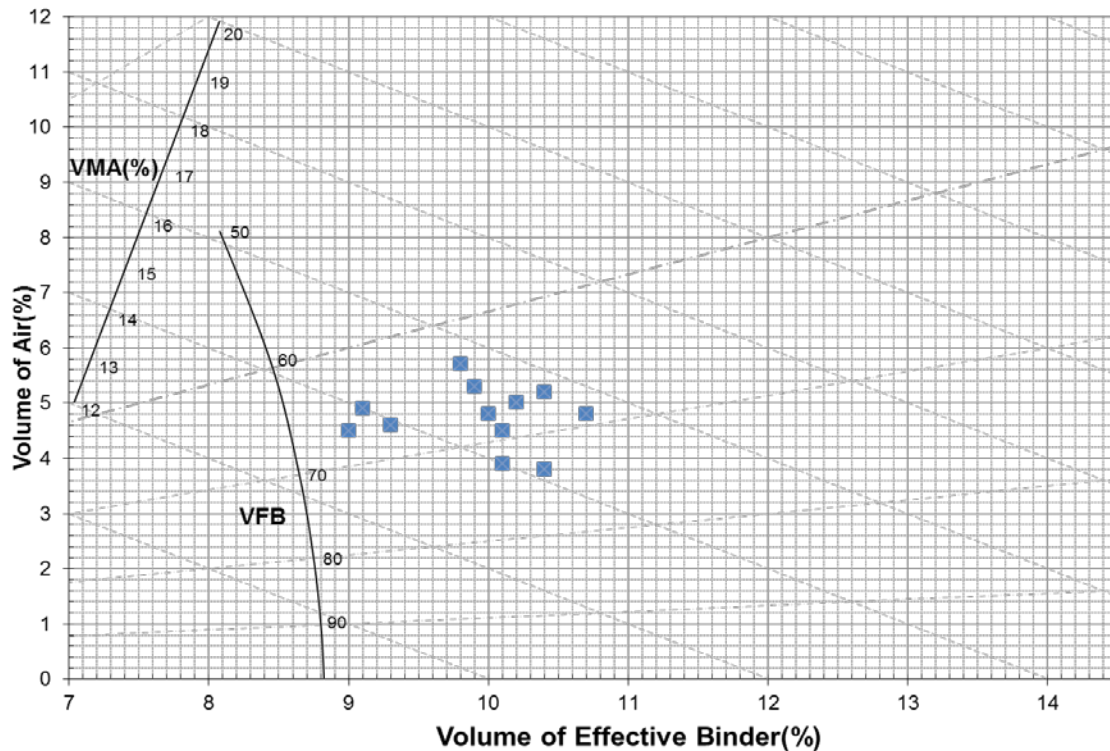


Figure 3-4 Volumetric Plots 20mm Mixes

What is noteworthy, given the variability in the design methods (Marshall, gyratory and Superpave) and the differing compaction efforts, is that all mixes fit into a very small volumetric window.

- For the 14mm nominal mixes all mixes had VMA between 14 and 16%, VFB between 65 and 75% and volume of effective binder between 10 and typically 11%.
- For the 20mm mixes there was a slightly higher but still surprisingly small variation, with all mixes having VMA between 13.5 and 15.5%, VFB between typically 60 and 70% and volume of effective binder typically between 9 and 10.5%.
- All mixes had design voids between 4 and 6%.

As with the results of the gradation analysis these results indicate it may be difficult to distinguish between Australian asphalt based on volumetric properties due to the limited variation in mixes across Australia.

3.4 Sample Preparation

For the 28 production mixes 300kg of representative asphalt samples were taken from plant production mixes from actual projects, cooled and delivered to Fulton Hogan's National Technical Laboratory in sealed nominal 20kg containers.

3.4.1 Reheating of Mixes

Reheating was standardised across all mixes to minimise any effect aging may have on the measured material characterisation. To accomplish this, the following reheating process was undertaken.

1. Material was warmed to 70°C and broken down by hand on a quartering tray and quartered to give representative 28-30kg for each shear-box block.
2. The mix was placed into two separate shear-box feeding trays.
3. Thermo couples were inserted into the centre of the loose mix for each tray.
4. The shear-box trays were covered and placed in preheated ovens at 150°C for conventional binder and 165°C for the polymer modified binder.
5. Temperature was monitored via the thermal couples inserted in the sample until a constant temperature of the mix was achieved.

3.4.2 Compaction of Mixes

The compaction method chosen for the production of laboratory samples was the shear box compactor. It was recognised the Shear-box compactor is not used in AASHTO and Europe standards for material characterisation (although there is a current draft ASTM method) and the method has not been adopted by Austroads. However, the shear-box compactor was selected as:

1. The current Austroads practice (gyratory compactor) would not produce specimens of the correct size and air void distribution for use in dynamic modulus test.
2. The US the standard compaction method, the Superpave Gyratory Compactor, was not readily available in Australia, produces samples with a higher degree of variability between samples than the shear box, and requires more laboratory time and material than the shear box.
3. The rolling wheel compactor was impractical and as stated by Harman (2002) *“rolling wheel compaction proved to be somewhat impractical as a sole means of laboratory compaction, the equipment proposed was large and required very large batches of mix.”*
4. The shear box is highly repeatable, as confirmed by Qiu et al. (2009) who found *“The asphalt mix specimens obtained from the same asphalt mix block has a variation in voids content of less than 1%”* and that *“the shear box compactor provides a reliable means of sample preparation, making it very suitable for producing specimens with constant volumetric properties”*.

While the Shear-box was selected as the preferred method for compaction, most work undertaken in the US uses a different compaction method, the Superpave Gyratory Compactor. Therefore it was noted parallel testing needed to be undertaken to ensure the

result of shear box compacted mixes are directly comparable to Superpave Gyrotory Compactor compacted mixes.

3.4.3 Shear-Box Compactor

The concept of the Shear-box compactor is shown in Figure 3-5, following. The concept of the shear-box is that a sample, at a controlled temperature and of prescribed size and prismatic shape is subjected simultaneously to constant static vertical pressure and to a lateral (shearing) stress that alternates in direction. The vertical pressure, shearing rate (no. of cycles/minute) and shear angle are controlled during compaction and compaction is continued until a predetermined height is achieved.

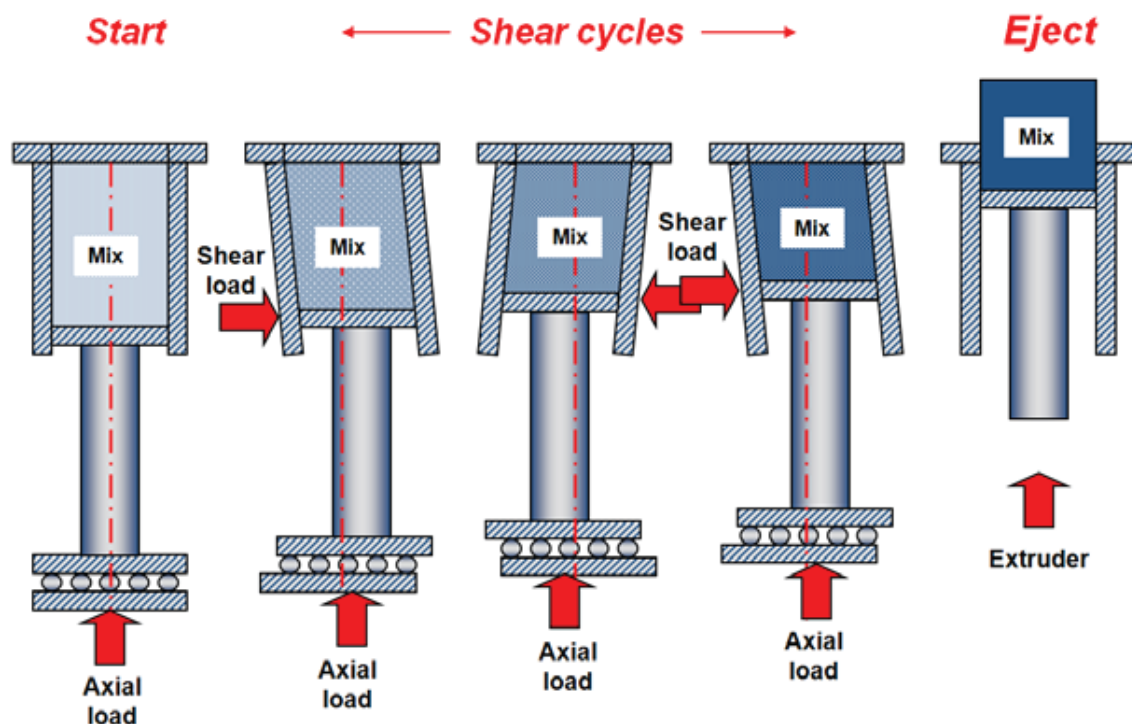


Figure 3-5 Shear box Compaction Concept

Because the shear box compactor produces large rectangular prismatic blocks, multiple specimens can be obtained from the same block, therefore reducing the variability between samples.

For the AAPA study the dimension of each shear box compactor prism was 450 x 150 x 180 to 200mm (L x W x D). From this block 3 AMPT samples (i.e. 3 by 100 x 150mm cylinders); were obtained by coring of manufactured block.

1. The process followed to compact the shear-box prisms is as follows.
2. The top and bottom platen of the shear box is preheated to the mix temperature

3. A mix feeder is placed on top of mould, the feeder is designed to minimise segregation and provide particle orientation in the direction of compaction and achieve uniform density
4. The sample was fed into the mould using two feeder trays designed one from each side of the mould
5. The surface of the sample is manually levelled using minimum mixing to avoid surface segregation
6. The top platen is placed on surface of the sample
7. A 750kPa constant vertical pressure is applied to the sample
8. Shearing is applied to the sample at a rate of 3 cycles per minute, at an shear angle of 2°
9. Shearing is continued until the required density of the specimen is achieved.
10. The number of cycles and shear force required to compact each prism to the target void were recorded
11. Bulk density of each block was recorded by water displacement method AS 2008
12. Any remnant of each of the un-compacted materials was retained in their original drums for possible future examination.

Repeats were sometimes necessary to quantify the effect of boundary conditions on sample density.



Figure 3-6 Shear Box Compactor

3.4.4 *Coring and Trimming*

Each asphalt sample prism from the shear box was cored to produce 3 cylinders using a 100mm diameter diamond tipped coring apparatus. Each sample was then trimmed to 150mm height, with approximately 15mm being taken from each end of the sample, using a diamond tipped automated saw, to produce test specimens with a diameter of 100mm and height of 150mm.

The density of the trimmed samples was calculated and tested for consistency and conformity with the target voids (5%) voids and two of the three cylindrical samples tested in the AMPT. The third sample was kept as a reference and stored for any future/replicate testing.

3.5 The Dynamic Modulus Test

To obtain real information on the characterisation of standard production mixes used throughout Australia, the APS-fL project undertook dynamic modulus test on all of the supplied 28 actual production mixes. As at the time of testing it was unknown what state of stress would be required to accurately model the response of the pavement to cover all possible stress states, the AAPA study conducted dynamic modulus testing in both unconfined and confined state. For the confined state three levels of confinement were used: 50, 100 and 200kPa.

For each of the 28 supplied mixes the dynamic modulus test was performed according to AASHTO TP62-07 using an IPC AMPT. To minimise potential damage to the specimen, testing was undertaken in the following order, before the next sequential test; the reason for this approach is asphalts are stronger at lower temperatures and higher frequencies.

- For each test temperature, E^* tests were conducted on each specimen at a full sweep of loading frequencies (25, 10, 5, 1, 0.5 and 0.1Hz).
- Testing was conducted at 200, 100, 50 and 0kPa confining pressures.
- Test temperatures were used from coolest to highest 5, 20, 35 & 50°C.
- Two replicates samples were tested for each factor combination for both confined and unconfined testing.

3.5.1 Testing System Set Up

An Industrial Process Controls (IPC) AMPT (Asphalt Materials Property Tester), formally SPT, was used to conduct the dynamic modulus test. The AMPT is a closed-loop servo-hydraulic testing system manufactured by IPC in Australia. The machine is capable of applying load over a wide range of frequencies (from 0.1 to 25 Hz). The servo hydraulic system is controlled by an IPC controller. The temperature control system of the AMPT is refrigeration-based and is able to control temperatures in the range of 5 to 55°C, for extended periods.

The measurement system is computer controlled and capable of measuring and recording a minimum of 8 channels, simultaneously. For the dynamic modulus test 7 channels are used; three channels for on-sample vertical deformation measurements, two channels for the load cell and the actuator Linear Variable Differential Transducer (LVDT), one channel for temperature, and one channel for the confinement pressure measurement.

Loads are measured using electronic load cells capable of measuring loads with an accuracy of ± 0.1 %. Vertical deformations are measured using three LVDTs. Figure 3-7 following, shows the AMPT testing system.

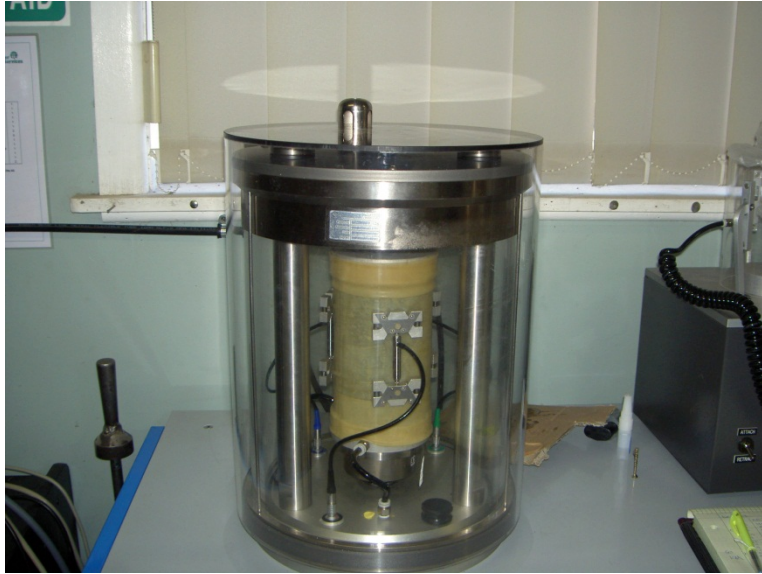


Figure 3-7 Dynamic Modulus Test Setup

3.6 Linking AAPA database with Overseas Research

In the United States the Superpave Gyrotory Compactor (SGC) is generally used for sample compaction and preparation for dynamic modulus testing. This compaction method is different from the shear-box compaction used in the AAPA study. It was unknown whether the AMPT results on samples manufactured using SGC compaction will vary relative to the shear-box compacted samples. Hence, to investigate whether this different method of compaction has any influence on the material characterisation results, a small subset of the production mixes was sent to NCAT and compacted using the Superpave Gyrotory Compactor.

These mixes were tested at the NCAT laboratories for Dynamic Modulus using the same equipment, an IPC Global Asphalt Mix Performance Tester (AMPT). NCAT uses a both a different test procedure, AASHTO TP 79-12 “Determining the Dynamic Modulus and Flow Number for Hot Mix Asphalt (HMA) Using the Asphalt Mix Performance Tester (AMPT)” and used different testing frequencies and temperatures as shown in Table 3-2 following. The NCAT testing used one confining pressure only, 200kPa.

Table 3-2 NCAT testing Frequencies and Temperatures

Test Temperature (°C)	Loading Frequencies (Hz)
4.0	25,10,5,1,0.5,0.1
20.0	25,10,5,1,0.5,0.1
35.0	25,10,5,1,0.5,0.1, 0.01
50.0	25,10,5,1,0.5,0.1

In order to allow direct comparison of results obtained by NCAT and results obtained in the AAPA study, four shear-box compacted samples were sent to NCAT for Dynamic Modulus testing. The mixes sent to NCAT were chosen to cover the range of typical mixes used in the study and range of modulus results, namely: A15E, C320, AR450 and C600. In addition to the four samples compacted using shear box compactor, two loose samples were sent to NCAT for sample preparation using the SGC to determine if the compaction method has any effect on the material characterisation results.

3.7 Calibration Using NCAT Test Track Sites

Currently there are no long term instrumented pavement research studies in operation in Australia, with accompanying dynamic modulus characterisation. While instrumented studies are being developed by both Curtin University and University of the Sunshine Coast; data will not be available from these studies for a number of years. Therefore, the study had to rely on test track results from US research to determine:

1. The conversion between laboratory and field modulus.
2. The relationship between ambient and pavement temperature regimes.
3. The effects of a moving load on asphalt modulus and calculated strain using linear elastic analysis.
4. The determination/calibration of the threshold modelling method for LLAP pavement design, whether that is, the cumulative distribution of strain, threshold strain criteria or a threshold traffic loading.

It was found that the NCAT instrumentation test sections would provide all the data which can be used to meet these objectives. Additionally, it is noted the climate in Alabama is not dissimilar to the lower east coast of Australia, although it is recognised that validation against Australian data and sites of the proposed models developed from the NCAT test track will be required.

3.7.1 Selected Test sites

The APS-fL project examined the NCAT test track and concluded that the 2003 test cycle would provide the most valuable information for the calibration of a LLAP design procedure. The 2003 NCAT Test Track cycle included eight structural sections. The eight structural sections were selected to evaluate pavement sections designed for varying levels of traffic, polymer modified and standard binders, stone mastic asphalt (SMA), and high binder layer. For the experiment, all eight sections were placed on 150mm (6 in.) granular base, the test section layout is shown in Figure 3-8 following.

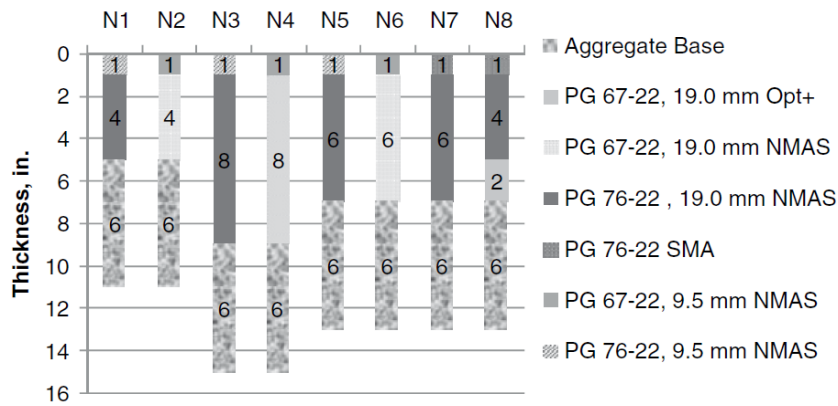


Figure 3-8 Phase II NCAT Structural Sections, after Timm et al (2006).

The pavement sections were constructed using both a standard PG 67-22 binder (similar to an Australian C450 binder) and a styrene-butadiene-styrene (SBS) modified PG 76-22 (similar to an Australian A10E binder). Loading on the 2003 track, was provided by tri-trailer trucks and one five-axle single trailer. For the tri-trailer, the typical weight of each set of dual wheels was just over 9 tonnes. For the five-axle single trailer, the typical dual wheel load was just less than 8 tonnes. Tyre inflation pressures were typically 700kPa (105 psi).

During the test cycle six of the eight structural sections developed some degree of fatigue cracking, the exception being sections N3 and N4 which were the 230mm thick asphalt sections. (These two sections have not failed in subsequent studies and have now had in excess of 6×10^7 cycles). Of those sections which cracked, three of the sections failed, (N1, N2, and N8) with failure defined as fatigue cracking exceeding 20%. The remaining sections N5, N6 and N7 failed in subsequent studies. Detailed data on the performance of each section is reported by Timm and Priest (2009). During the test cycle, the performance of the rich bottom section N8 was unexpected, particularly when compared with the performance of Section N7. The performance of this section was investigated by Willis et al. (2007) who conducted a forensic evaluation of the N8 section and found that slippage between the rich bottom layer and the overlying base layer had occurred and that cracking began in the overlying base layer. Due to potential bias that this may introduce it was decided to exclude section N8 from the analysis in this study.

3.7.2 Accelerated Loading at NCAT

The research being undertaken at NCAT is what is commonly referred to as accelerated pavement testing (APT). Accelerated pavement testing compresses a full design life of truck damage (up to 20 years) into 2 years. At NCAT, loading of the facility generally begins in the US autumn after the completion of construction, and the collection of baseline data. The loading of the pavement operates on two shifts, an am shift which runs from 5am until 2pm, and a pm shift, which runs from 2pm until 11pm. Under this operation each truck in the 5

truck fleet runs approximately 1000km (680 miles/day) to load the experimental pavements. Because all sections are subjected to identical and precisely monitored levels of traffic, it is possible to complete meaningful field performance comparisons between asphalt material types and designs. The NCAT test track has been through a number of full test cycles.

3.7.3 Monitoring Field Performance (NCAT)

The performance of each of the pavement sections on the NCAT test track is monitored on a weekly basis. The following performance monitoring is undertaken:

1. Rutting, roughness and surface are measured on the full track using an inertial profiler equipped with a full lane width dual scanning laser "rutbar".
2. Random locations selected from within each section are used to measure wheel path densities using non-destructive testing. The transverse profiles are measured along these same locations so that rutting may be verified using a contact method.
3. Falling Weight Deflectometer (FWD) testing is typically run weekly, which is also the case with high speed structural response data collection and surface crack mapping.

3.7.4 Instrumentation

From Phase II of the NCAT test track (2003 study), the researchers began to equip the test track with full instrumentation for the measurement of temperature profiles and high speed instrument arrays for measurement of pressure and strain in the pavement. The temperature probes for the measurement of temperature profiles were also paired with data from an onsite automated weather station, which can be used to characterize the performance environment. For the structural experimental sections, (the sections of most use to the APAA study), high speed instrumentation arrays consisting of strain gauges and pressure plates are installed at critical depths within the pavement. Measurement data generated by these devices can be used to quantify the response to passing loads at a given temperature in the pavement. It is this data which will be extremely useful in calibrating the proposed mechanistically based APS-fL LLAP pavement design methodology.

3.8 Other Calibration Sites

Apart from the NCAT test track a number of additional sources of information were available in the literature, which could be used to compare laboratory dynamic modulus to field stiffness. Additional data was available from MnRoads, Clyne et al. (2004), and the WesTrack test tracks, Ullditz et al. (2006) and Pellinen (2001). Both sites have documented results for field measured stiffness determined from FWD testing and laboratory characterisation of asphalt mixes undertaken using the dynamic modulus test.

3.9 Validation with Field Data

Because the NCAT data may not extend to true LLAP pavements (>50million cycles) the theoretical examination of pavement performance of both Australian and UK data (over a much longer period of time) may prove beneficial to validate the results of the calibration undertaken from the NCAT results.

In the UK numerous sites have been identified that clearly achieve the LLAP status i.e. the pavement deflection is reducing with time. With the assistance of TRL and the members of the European LLAP Pavement Assessment Group (ELLPAG) details of some of the pavements were made available to the AAPA study.

Additionally, as part of the development of the development of the Structural Testing and Evaluation of Pavement (STEP) procedure for the assessment of pavement Remaining Life, the New South Wales Roads and Maritime Services developed an extensive database of sites throughout the state which can be interrogated to find LLAP.

With knowledge of the appropriate climatic data, the combination of these data sets can be used to validate the mechanistic models developed from the laboratory experiments, theoretical models and the calibrated NCAT data.

3.10 RMS STEP Database

The Roads and Maritime Services (RMS) of NSW developed an extensive database of pavement profiles, materials and condition of pavement across NSW as part of the development of the STEP modelling system. This database was made available to the AAPA APS-fL life project by RMS, to validate the presence of LLAP in Australia and aid in the development of criteria for the design of LLAP.

The RMS STEP database was developed with a number of surfaced flexible pavement types, namely:

- Sprayed seals over unbound granular base and sub-base layers
- Sprayed seals over granular layers including cemented layers
- Asphalt layers of variable thickness over unbound granular layers
- Asphalt layers over granular layers including stabilised layers

Of interest to the APS-fL project were the asphalt pavements over unbound granular base and sub-base layers and particularly those pavements with greater than 150mm of asphalt thickness.

3.10.1 Database Development

The development of the STEP database was a significant project for RMS and represents the most significant database of pavement structures, condition and materials in Australia. Although the STEP database only represent a single point in time, the distribution of pavement types, age and condition represent a significant tool for validating the presence and performance requirements of LLAP in Australia.

As part of the development of the database RMS determined the type, extent and severity of cracking on site by a visual assessment, the remaining life of the pavement by an experienced practitioner and the condition of the asphalt by an inspection of the asphalt obtained from the bore-hole investigation at each location.

- a) Deflection Data: For each location FWD testing was undertaken. The FWD testing was undertaken at a target pressure of 700kPa, and measure the full deflection bowl and surface layer temperature.
- b) Visual Assessment: The field information collected in the database included the surface cracking, if present, drainage type and estimates of the drainage effectiveness. The assessment of surface condition was undertaken by a visual inspection and noted the type of cracking (crocodile, longitudinal, block), if any, and the severity of the cracking (low, medium or high). Additionally an assessment was made of the remaining life of each location in terms of years by an experienced engineer.
- c) Geotechnical Information: For each location a borehole investigation was undertaken, the borehole investigation documented the material type, thickness and gave an assessment of the condition of each layer. i.e. for asphalt layers the investigation noted if the asphalt was sound, cracked, stripped etc.
- d) Construction and Maintenance History: In preparation of the database RMS cross matched the chosen locations to the corporate RAMM asset database to obtain the construction year and maintenance history for each location. It was recognised by RMS that some of the maintenance history was lacking and not all maintenance activities would have been included.
- e) Traffic Data: The traffic data in the database was in terms of AADT, traffic mix, ESA per commercial vehicle and growth rates. The traffic data was actual design traffic loading as opposed to "design" traffic loading, i.e. without design safety factors.

For the RMS STEP database a location represents a single point on the road and not an area. In this way deflection data, materials, thickness can be exactly matched, eliminating risk associated with variability in the pavement.

For the validation study a subset of the STEP database was selected which included, only:

- Structural Asphalt pavements, with greater than 140mm of asphalt.
- Pavements which had not been overlaid or strengthened in their life.

The database of the subset of structural asphalts, with the assessed condition, deflection result, traffic loading, materials and maintenance history can be found in Appendix B of this report.

3.11 UK VALMON Site Data

The Highways Agency (HA) of the UK maintains a network of approximately 45 VALMON sites distributed across their trunk road network in England. The sites have been annually surveyed and monitored for the past 10 years in order to build a database of pavement structural and functional data, which can be used to VALidate and MONitor the Highways Agency pavement designs and assessment methods. The AAPA project made use of the deflection history data (FWD) for ten of these VALMON test sites on the most heavily-trafficked UK motorways. These sections were used as they were the same sections were examined as part of the TRL report 250 undertaken by Nunn et al. (1997) to establish the UK LLAP design procedure.

The data provided to AAPA, via ARRB, consisted of a total of 33 sites monitored during the VALMON project which included 25 fully flexible and 8 flexible composite sites, for each site the location, construction and maintenance details, performance surveys (FWD and deflectograph), asphalt thicknesses, traffic data and construction specifications were provided by TRL. Details of the sections and deflection histories can be found in Yousefdoost (2015).

4 Dynamic Modulus Testing and Results

4.1 Reasons for Adopting the Dynamic Modulus Test

Given the ultimate goal of the material characterisation study was the development of modulus master curves to enable calculation of asphalt modulus at any temperature or vehicle speed, the dynamic modulus test was selected over other modulus tests such as the resilient modulus. This ability to calculate the modulus at any temperature or vehicle speed will offer a substantial improvement on the current Australian method which is based on a single standard laboratory test temperature and time of loading. In addition, the dynamic modulus test was selected as the primary material characterisation test for a number of reasons:

- Researchers such Loulizi et al. (2006) have established that “the dynamic modulus test provided a better characterisation of asphalt mixes than the resilient modulus test because of its full characterization of the mix over a range of temperatures and load frequencies”.
- The dynamic modulus test and the resulting master curves are internationally accepted as being able to discriminate key asphalt performance properties. The NCHRP 9-19 project Witzcak (2002), concluded the dynamic modulus, and creep properties (flow number or flow time) had the best correlation with field performance, observed on major US field trials (WesTrack, MnRoad and the FHWA ALF).
- The dynamic modulus test has been used as a key material characterisation test at a number of international accelerated pavement test tracks, (FHWA ALF, NCAT, MnRoads and WesTrack). This enables the development of a quantitative process for the calibration of the performance of asphalt materials in the laboratory, against the performance of real pavements in the field.
- Because of the ability to model the asphalt mixes at any temperature and frequency, the results of the dynamic modulus test and subsequent master curves will enable the rational and quantitative assessment of asphalt materials used in the historical LLAP sections constructed in the Australia, the US and Europe at the specific temperatures and vehicle speeds encountered at those sites.

Given these benefits, the dynamic modulus test and the resulting master curves will facilitate the ultimate goal of the APS-fL project, which is, the structural analysis of the performing LLAP sections and the determination of the threshold design method. The finding of this threshold design method can then be transposed to different environmental conditions found in Australia, using the dynamic modulus master curves to form the basis of the development of LLAP design procedure.

4.2 Master Curve Development and Time Temperature Superposition

Because of the viscous component of asphalt mix, the material response is a function of both time of loading and temperature; the time-temperature dependency. For asphalt mixes it is common to represent this time temperature dependency by the construction of dynamic modulus master curves. Master curves enable comparison of viscoelastic materials when tested using different loading times or frequencies and test temperatures. The construction of master curves is achieved by using the principle of time-temperature superposition and reducing all testing data to a common curve. The application of this principle typically involves the following steps:

- Experimentally determine the frequency dependent modulus curves at a number of temperatures.
- Calculation of a “shift” factor to correlate the modulus over the temperature and frequency range, relative to a reference temperature
- Development of a master curve showing the effect of frequency for a wide range of frequencies.
- Use of the “shift” factor to determine the temperature dependant moduli over the whole range of the master curve frequencies.
- The amount of shifting at each temperature described the temperature dependency of the mix; this is determined by the Time-Temperature superposition principal.
- Time-temperature superposition, is a well-established procedure which can be applied to asphalt mixes to either;
- determine the temperature dependency of the asphalt
- or, to expand frequency at a given temperature at which the material behaviour is being determined.

The time–temperature superposition principle can only be applied to “Thermorheologically Simple” materials, that is, to materials in which the shift factor is identical for all relaxation times. Fundamentally, the use of the time temperature superposition principle allows the prediction of long-term behaviour of asphalt from relatively short-term tests, as in the dynamic modulus test.

For Australia, it was agreed by the APS-fL Project Steering Committee, to use a reference temperature of 25°C, as opposed to the standard of 20°C used in the US. The 25°C temperature was selected to be consistent with current Australian characterisation methods. It was also agreed that dynamic modulus master curve should be modelled using a sigmoidal (S shaped) function, as recommended by Witczak (2002). However, due to the current debate over the definition of time in the dynamic modulus test, the sigmoidal function would be determined as a function of frequency, not time, as described by the following function:

$$\log(|E^*|) = \alpha + \frac{\beta}{1 + e^{(\gamma + \delta)(f_r)}} \quad \text{Equation 4-1}$$

Where:

f_r = reduced frequency at the reference temperature

α = the minimum value of E^*

$\alpha + \beta$ = the maximum value of E^*

γ, δ = shape fitting parameters, determined through numerical optimisation of experimental data.

In this process a shift factor, a_T is used to calculate the reduced frequency, f_r , required to shift the dynamic modulus test results on the frequency scale to form a continuous curve at the 25°C reference temperature. The shift factor can be mathematically shown in Equation 4-2 following:

$$a_T = \frac{f_r}{f} \quad \text{Equation 4-2}$$

Where;

a_T = shift factor

f = frequency of loading at desired temperature

f_r = reduced frequency of loading

T = temperature

While classical viscoelastic theory suggests a linear relationship between $\log(a_T)$ and T , Anderson et al. (1994) and research Pellinen (2001), has shown that a higher precision is achieved by the use of a second order polynomial relationship between the logarithm of the shift factor ($\log(a_T)$) and the temperature (T). The use of 2nd order polynomial relationship can be further simplified by directly incorporating the reference temperature in the polynomial form. This polynomial shift factor approach was adopted by the Steering Committee as the method to be used for the AAPA study, as shown in Equation 4-3 following:

$$a_T = 10^{a(T - T_{ref})^2 + b(T - T_{ref})} \quad \text{Equation 4-3}$$

Where:

T = temperature of interest

T_{ref} = 25°C

a, b = coefficients of the polynomial

This process of master curve development is shown graphically in Figure 4-1, which shows the measured dynamic modulus results of a typical mix as a function of frequency for four test temperatures.

Firstly, the results at the four individual test temperatures are shifted to the reference temperature (25°C) on the frequency scale to form a continuous curve as shown in Figure 4-2. Once the continuous curve is formed, the sigmoidal function is fitted to the measured data to construct a master curve. The curve is usually fitted by using a numerical optimisation procedure, such as the Solver function in Excel®, by minimising the sum of the squared errors between the measured and predicted values.

The amount of shifting required on the frequency axis to make the continuous curve is the shift factor. The amount of shifting for each temperature is then plotted against the temperature, as can be seen in Figure 4-2, to develop the temperature shift factor equation. The figure illustrates the higher precision of the polynomial shape of the shift factor relationship recommended by the Steering Committee. (All master curves in the AAPA study had R² values of greater than 0.98 and typically greater than 0.99)

4.2.1 Numerical Optimisation for Determination of Master Curves

When manually undertaken the process for accomplishing the horizontal shifting and sigmoidal function fitting for dynamic modulus, is a two phase process. However, in practice the two steps can be undertaken in one using a numerical optimisation process. In this process, initial trial values for the coefficients of the polynomial shift factor (a, b) and the sigmoidal function (α , β , γ and δ) are assumed to calculate the dynamic modulus. This calculated modulus is then compared to the measured modulus and the squared error is obtained between calculated modulus and measured modulus as shown in Equation 4-4 following.

$$OF = \sum_{j=1}^M [\log(E_{calc}^*) - \log(E_{meas}^*)]^2 \quad \text{Equation 4-4}$$

The sum of squared errors is then set as the Objective Function, (OF) in the non-linear optimisation, with an objective of minimising OF by changing the coefficients of the polynomial shift factor (a, b) and the sigmoidal function (α , β , γ and δ). In this study the fitting parameters were established using a coded procedure, using a polynomial error minimisation technique, due to the number of mixes. However, normally the objective function is minimised using the Solver Function in Excel®.

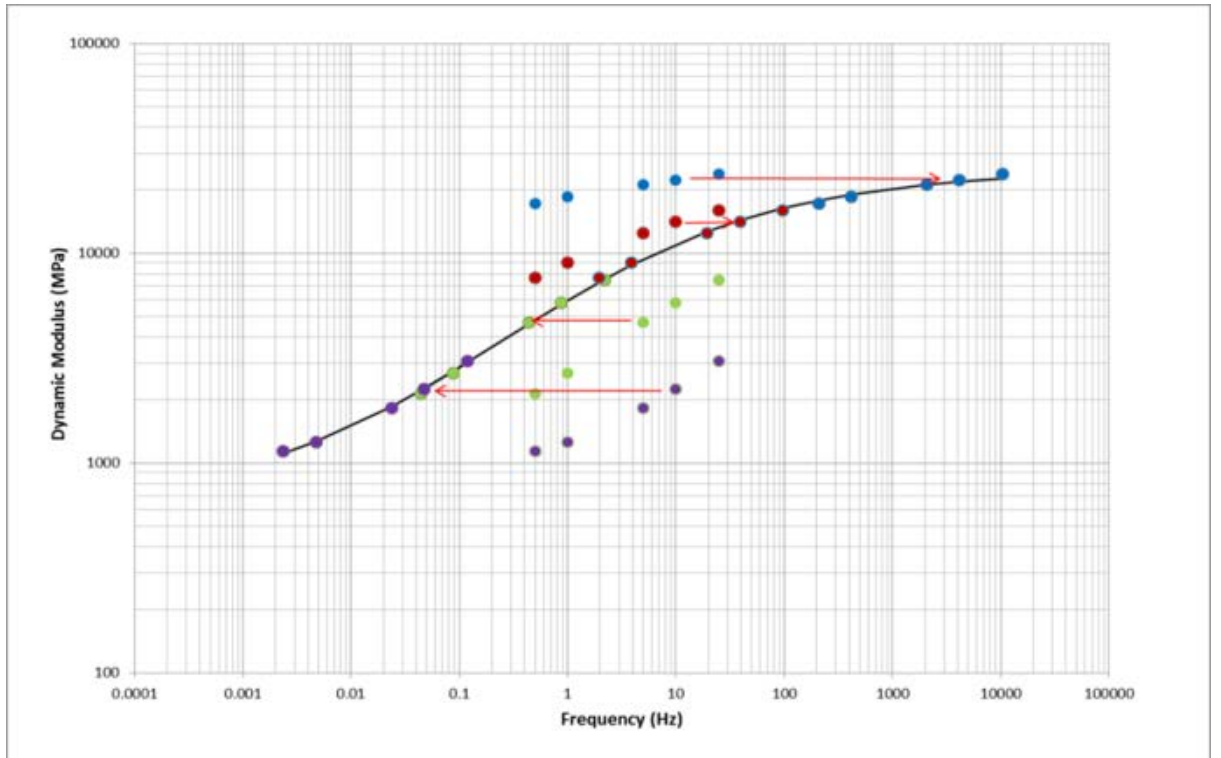


Figure 4-1 Construction of Dynamic Modulus Master curve and Temperature Shift Factor Function

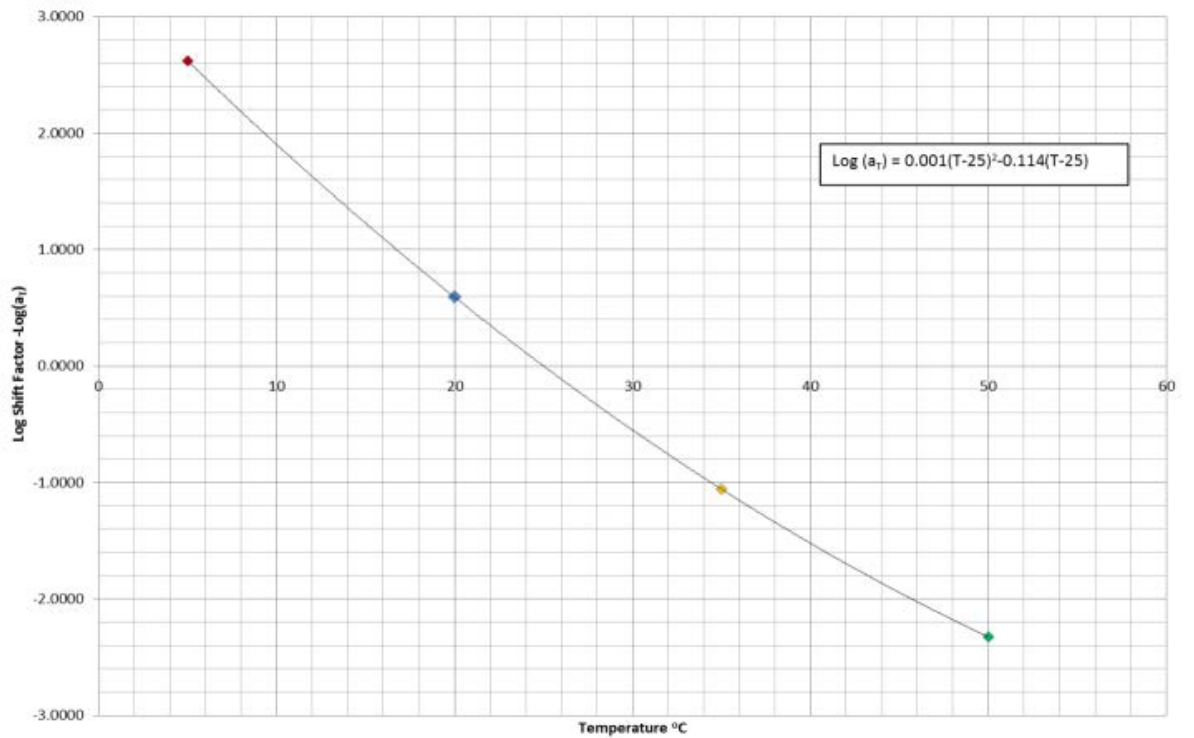


Figure 4-2 Temperature Shift Factor Function

4.3 Master Curves and Dynamic Modulus Test Results

4.3.1 Master Curve Fitting Parameters

The dynamic modulus results for the 28 mixes tested were used to generate master curves for each individual mix, which would cover the spectrum of the pavement temperature and vehicle speeds encountered under Australian conditions. The master curves were all created at a reference temperature (25°C) which allows the stiffness of the Australian mixes to be viewed without temperature as a variable. This method of analysis allows for relative comparisons to be made between multiple mixes.

In solving the master curves, all fitting parameters were free to be solved to obtain the best fit between the measured and predicted data (i.e. not constrained).

The fitted parameters for the sigmoidal and the polynomial shifting parameters for the 28 different mixes examined in the study are shown in Table 4-1 and Table 4-2 following.

The fitted parameters for the sigmoidal function and the temperature shifting factor for the 28 different mixes examined in the study can be seen in Table 4-1 and 4-2 following. The fitting parameter R^2 for all mixes greater than 0.99. While the master curves can be seen graphically in Figure 4-3 and Figure 4-4 following for the 14 and 20mm mixes respectively. In the figures the red curves are for C320 mixes, green are AR450, yellow are C600, blue are A15E and purple are Multigrade mixes.

Table 4-1 Master Curve Fitting Parameters

Nominal Size (mm)	Binder Type	SN	Binder (%) eff	RAP (%)	α	β	γ	δ
14	A15E	12105	4.7	0	1.550	2.919	-0.566	-0.590
		12039	4.4	0	1.360	2.897	-0.758	-0.583
	AR450	11124	4.3	15	1.275	3.040	-1.595	-0.755
		12040	4.4	0	1.310	2.983	-1.180	-0.637
		12061	4.8	0	1.276	3.079	-1.311	-0.743
		12062	4.9	15	1.359	3.022	-1.525	-0.677
	C320	12048	4.8	20	1.187	3.167	-1.245	-0.710
		12106	4.4	20	1.297	3.105	-1.241	-0.712
		12051	4.3	0	1.344	3.034	-1.435	-0.709
		12072	4.3	15	1.240	3.194	-1.318	-0.750
		12082	4.8	20	1.202	3.139	-1.341	-0.766
		12002	4.7	0	1.303	3.061	-1.426	-0.732
		12098	4.3	7	1.255	3.086	-1.116	-0.606

		11119	4.4	0	1.238	3.142	-1.469	-0.764
	Multi	12013	4.3	0	1.724	2.759	-1.038	-0.443
20	AR450	12100	4.6	15	1.359	3.033	-1.466	-0.719
		11123	3.9	20	1.445	2.882	-1.480	-0.779
		12058	4.5	0	1.274	3.160	-1.338	-0.631
	C320	12045	4.3	30	1.342	3.065	-1.371	-0.716
		12054	4.4	0	1.407	2.979	-1.169	-0.615
		11115	4.1	0	1.276	3.141	-1.441	-0.744
		12069	3.8	15	1.310	3.113	-1.338	-0.754
		12003	4.4	0	1.177	3.216	-1.291	-0.752
		12083	4.3	20	1.275	3.091	-1.315	-0.753
	C600	12110	4.1	15	1.444	2.940	-1.563	-0.676
		12087	4.4	0	1.452	3.043	-1.210	-0.621
		12111	4.3	0	1.373	3.069	-1.368	-0.686
	Multi	12017	4.3	15	1.771	2.702	-1.206	-0.405

Table 4-2 Polynomial Shift Factors

Nominal Size (mm)	Binder Type	SN	Binder (%) eff	RAP (%)	A	b
14	A15E	12105	4.7	0	0.0006	-0.109
		12039	4.4	0	0.0006	-0.107
	AR450	11124	4.3	15	0.0005	-0.111
		12040	4.4	0	0.0006	-0.108
		12061	4.8	0	0.0007	-0.112
		12062	4.9	15	0.0002	-0.104
	C320	12048	4.8	20	0.0005	-0.110
		12106	4.4	20	0.0005	-0.112
		12051	4.3	0	0.0004	-0.103
		12072	4.3	15	0.0005	-0.104
		12082	4.8	20	0.0006	-0.114
		12002	4.7	0	0.0004	-0.107
		12098	4.3	7	0.0003	-0.107
		11119	4.4	0	0.0006	-0.107
Multi	12013	4.3	0	0.0005	-0.112	
20	AR450	12100	4.6	15	0.0004	-0.107
		11123	3.9	20	0.0005	-0.109
		12058	4.5	0	0.0004	-0.107

	C320	12045	4.3	30	0.0003	-0.107
		12054	4.4	0	0.0004	-0.106
		11115	4.1		0.0007	-0.115
		12069	3.8	15	0.0008	-0.111
		12003	4.4	0	0.0006	-0.111
		12083	4.3	20	0.0006	-0.116
	C600	12110	4.1	15	0.0003	-0.104
		12087	4.4	0	0.0004	-0.107
		12111	4.3	0	0.0004	-0.108
	Multi	12017	4.3	15	0.0004	-0.111

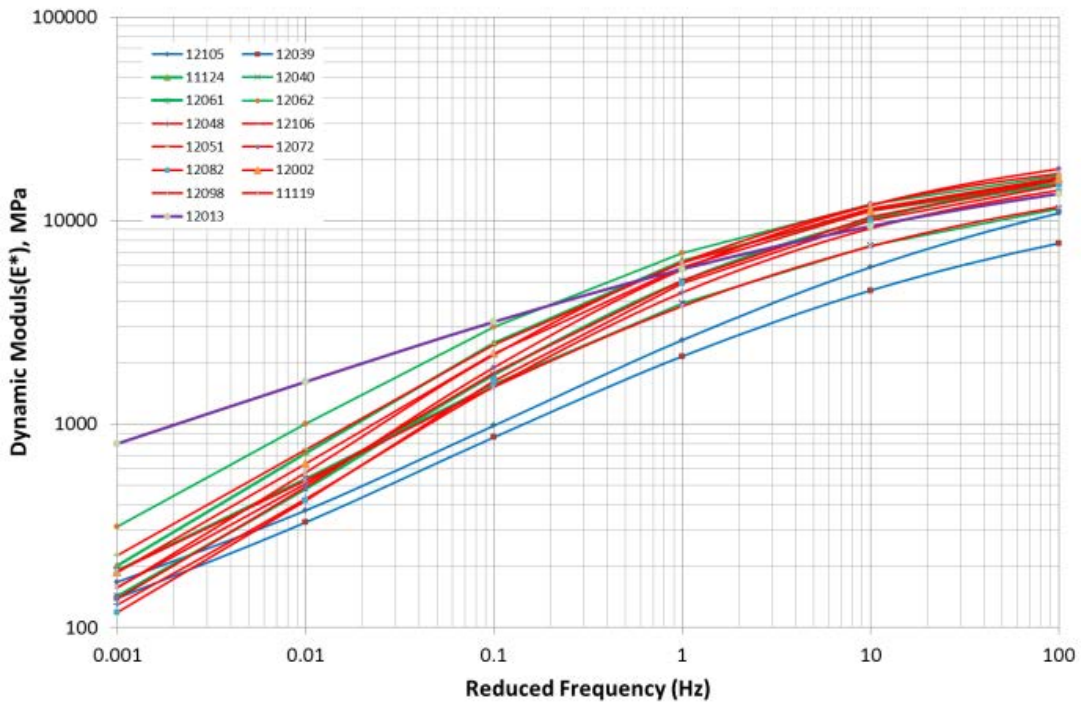


Figure 4-3 Master curves 14mm

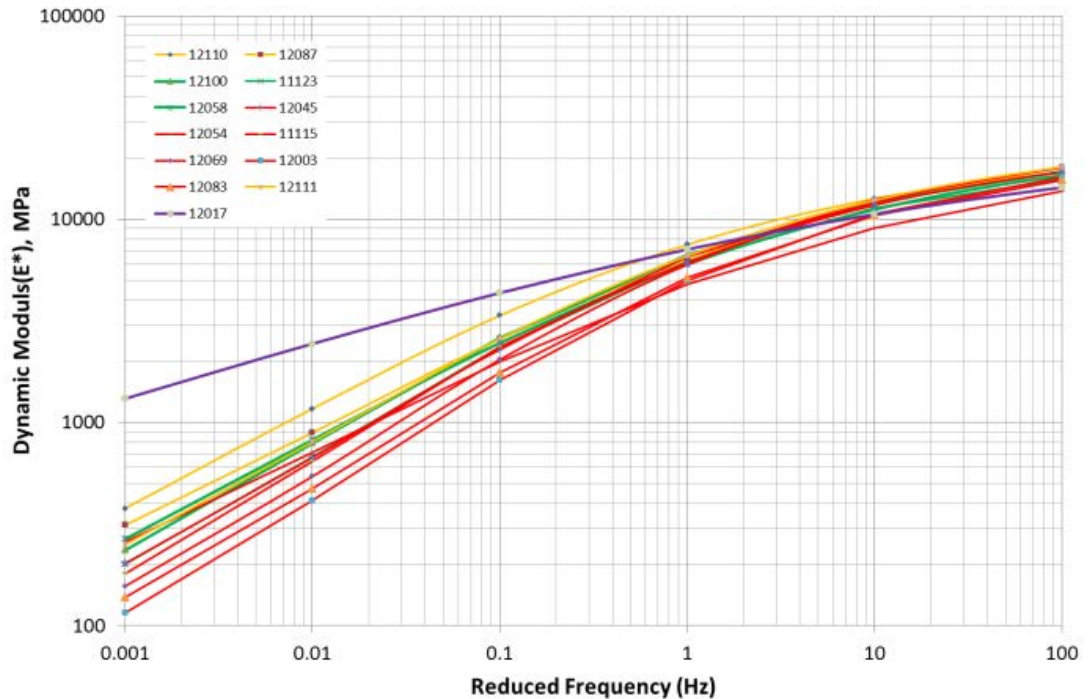


Figure 4-4 Master curves (a) 20mm

The initial examination of the results shows that the minimum modulus values as expected increase with an increase in binder grade, with C320 mixes being lower than AR450, which are lower than C600 and Multigrade binders. As expected nominal 20mm mixes are also typically higher than the 14mm mixes. This is consistent with the latest version of the Witczak model, with Bari (2006) finding the minimum modulus value, α , was affected by aggregate gradation, volume of air, volume of binder and binder stiffness. This finding suggests the minimum modulus value appears best at distinguishing between different binder grades. As there was little to no change in air void level of typical Australian mixes (typically 5%), the effect of air void level on the minimum modulus value could not be assessed.

Unexpectedly, no correlation was found between the minimum modulus and RAP content indicating that at current RAP contents, RAP content has little effect on the minimum modulus value and therefore overall modulus values (plant characteristics appear to be more important). While the minimum modulus value appears to be influenced by effective binder content, and the amount of filler, due to the relatively small change in the effective binder volume, the effects to changes in the volume of binder are small and cannot be easily assessed.

The β parameter or the maximum modulus value parameter appears not to be sensitive to changes in binder grades for conventional (neat) binders or maximum aggregate size, which

is the same finding as Bari who found that the β value was a function of volumetric properties of the mix and finer fraction of the gradation.

The examination of the relative shape of the master curves tends to indicate that for the current Australian mixes, the design method, aggregate source and the relatively small variance in volumetric properties appears to have little effect on the shape of the master curve, with results of the γ and δ factors showing little change within binder types.

For conventional binders, the shape factors (γ and δ) appear to be relatively consistent regardless of the grade of binder. However, this is not the case for multi-grade and A15E, which have a different shape from the conventional binders indicating lower time-temperature susceptibility. This is somewhat consistent with the findings of Bari (2006), who found γ the shape factor was a function of binder properties only. However, for Australian binders, this change of shape is only evident when comparing conventional and modified binders. It is clear that the shape factor, γ , should not be constant across different binder classes.

On first examination, due to the consistency of these parameters within a binder grade and nominal aggregate size, it may be practical for design purposes to define the whole master curve using one point only and use this point to shift the master curve either up or down based on a limited number of test points. While this will not be as accurate as the measurement of the whole master curve and risk may be associated with its use, it may be a practical solution for level 2 analysis, with level 1 being typical modulus values and level 3 being the measurement of the whole master curve.

4.4 Grouping of Australian Mixes

The initial intent of the APS-fL project was to validate and calibrate one of the two well-known prediction models for dynamic modulus. However this may not be necessary. Unlike the US, Australia has limited grades of binder and these grades are controlled under an Australian Standard. Also, as show in Section 3, the volumetric properties and gradations for typical Australian mixes do not vary to a great extent between suppliers and even between states, regardless of the design method used or specification. Given the consistency of; gradation, volumetric properties, and the consistency of the shape of the master curve for a given binder type and nominal mix size, it may not be necessary in Australia for practical implementation to develop complex master curve equations such as the Witczak or the Hirsch model for routine pavement designs. It may be more relevant to group or sub group mixes to have typical modulus values.

To investigate the applicability of this approach the dynamic modulus results were grouped by nominal aggregate size (14 and 20mm) and binder grade (C320, AR450 and C600) to

produce six subgroups within the study. The data from each of these subgroups was then used to create a typical master curve for all results with that subgroup.

For each of these subgroups master curves were generated by minimising the squared error between the measured and predicted data in the log space i.e. $(\log E^*_{\text{meas}} - \log E^*_{\text{pred}})^2$ using the previously described sigmoidal function and the polynomial temperature shift factor. For all master curves all parameters were free to be solved to obtain the best fit between the measured and predicted data.

Figure 4-5 following, shows a typical result of the subgroup of mixes, in this case mixes with a nominal aggregate size of 20mm and an AR450 binder. RAP contents in these mixes varied between 0 and 20%.

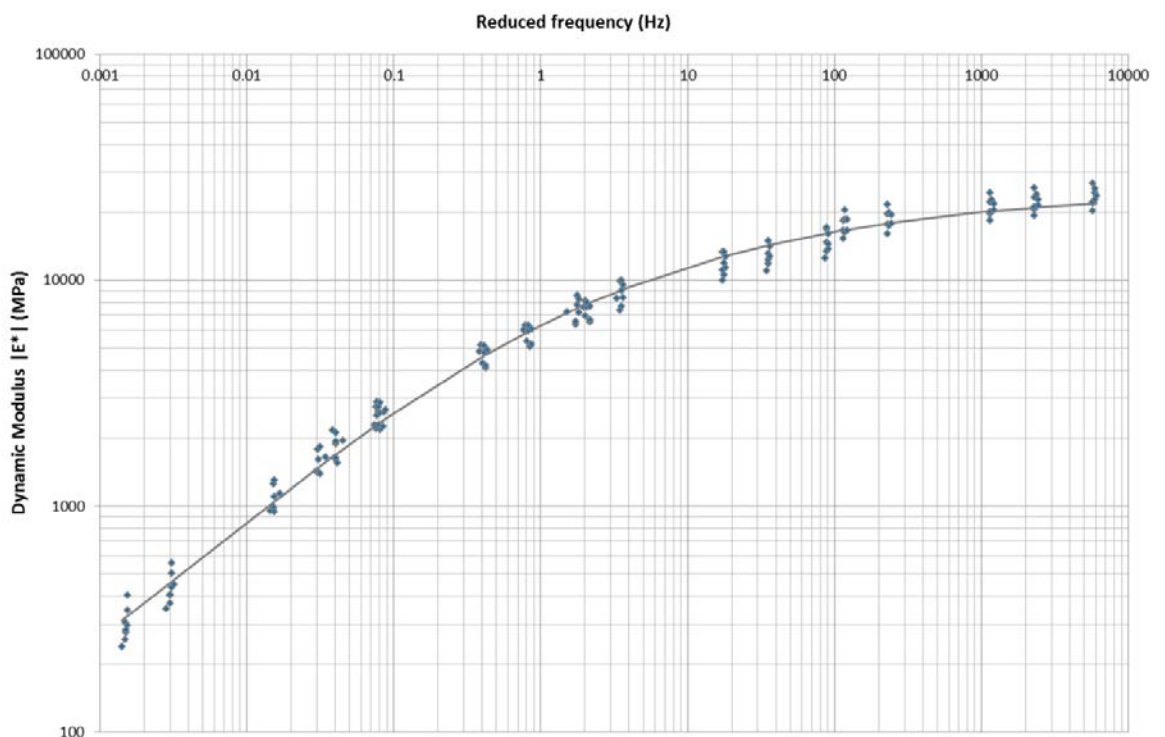


Figure 4-5 Typical Modulus Grouping Results AC20 AR450

The validity of using these typical master curves for design will understandably depend on the accuracy of the typical master curves in the prediction of modulus and the degree in which confidence can be obtained around those results.

To investigate this validity, the relative accuracy of the proposed approach was compared against the accuracy of the two well-known models for the prediction of dynamic modulus, the Witczak and Hirsch models. The accuracy obtained from the prediction of modulus using the grouped results was compared against the published accuracy of both the Witczak and Hirsch models in terms of the coefficient of determination and the standard error (R^2 , S_e).

As shown by Bari (2006), the current versions of the Witczak and Hirsch models have a R^2 of 0.9 and 0.92 respectively in the log space and 0.8 in the arithmetic space for the Witczak model. Given the range of data used in the two published data sets (Witczak/Hirsch) and the AAPA database are very similar (500 to 25000MPa), comparison of the coefficient of determination alone will provide a good comparison of the relative accuracy of the two approaches.

The accuracy of the grouping approach can be seen in Figure 4-6 following, which shows the measured modulus against the typical modulus master curve for the six grouped mixes, grouped by nominal aggregate size, 14 and 20mm mixes and the three primary binder classes used in Australia, C320, AR450 and C600. The variability of the measured modulus data for the grouped mixes can be seen in Table 4-3 following.

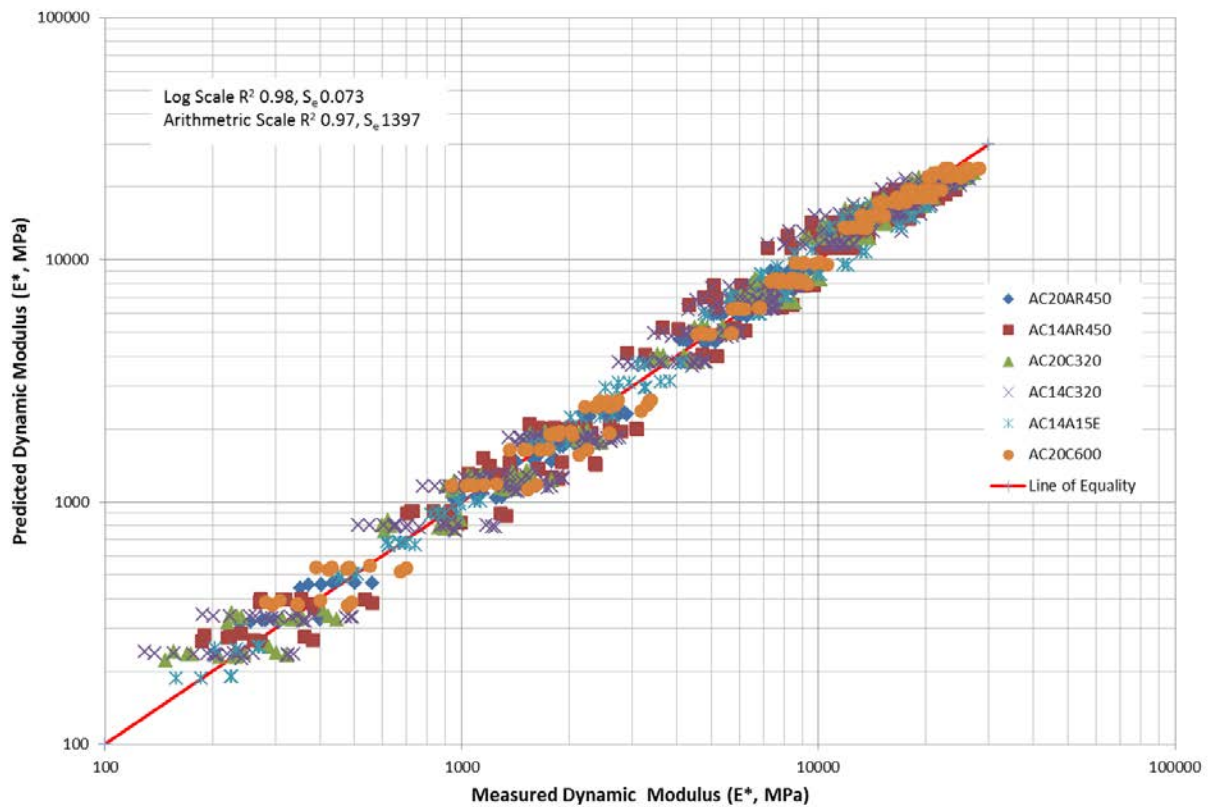


Figure 4-6 Accuracy of Grouping Approach

Table 4-3 Grouping Accuracy

Nominal Size(mm)	Binder Type	Arithmetic Space		Log Space	
		Coefficient of Determination (R^2)	Standard Error (Se)	Coefficient of Determination (R^2)	Standard Error (Se)
14	C320	0.97	1457	0.98	0.085
	AR450	0.95	1551	0.98	0.073
	A15E	0.93	1468	0.99	0.063
	Multigrade	N/A			
20	C320	0.97	1393	0.99	0.068
	AR450	0.97	1315	0.99	0.052
	C600	0.98	1139	0.99	0.054
	Multigrade	N/A			

As can be seen in both the figure and table the grouping of results provided an “excellent” fit with the coefficient of determination being 0.98. This accuracy is significantly better than both the Witczak and Hirsch models (0.9 and 0.92) in both the log and arithmetic space.

These findings are significantly beneficial to Australia, indicating that Australia can achieve a higher degree of confidence in the predicted modulus values by grouping common mixes together, than from the use of complex model forms, such as the Hirsch and Witczak models which require volumetric properties, binder shear modulus and aggregate gradation, all of which will not be typically available to the consultant at the time of design.

4.5 Typical Master Curves and Development of Confidence Intervals

As already established the modulus of the grouped mixes will vary throughout Australia in production due to use of RAP, binder source, and effective binder content amongst others factors. At least initially this variation will not be known to the pavement designer who will not know the binder source, aggregate gradation and percentage of RAP. The designer will generally only specify a grade of binder and a nominal aggregate size. While the results of the grouping approach showed that the variation prediction was small compared to published prediction models, it does present some risk in the design process. Therefore the designer should consider the risk, or the level of confidence required from the modulus, when assigning a design modulus for the purposes of pavement design.

One of the main benefits of the grouping approach is that this risk can be rationally assessed as confidence limits can be developed around the prediction of modulus. These rational confidence levels can be established because, like most engineering parameters the prediction of modulus should follow a normal distribution and by using this distribution and

the variation or standard error in the prediction, it is possible to assign confidence to the prediction of modulus values. This is a significant benefit over the typical median values developed by standard predictive models.

4.5.1 Distribution of Errors around Master Curve

Like most engineering parameters the prediction of dynamic modulus is assumed to follow a normal distribution. This assumption can be easily checked by plotting a histogram of the residuals or errors (difference between measured and predicted values). If the results are normally distributed a plot looking like a normal distribution centred on zero should be obtained.

For the prediction of dynamic modulus from the grouped data, it was found that the residuals followed a normal distribution where the residual was in the log space i.e. $\log(E^*_{\text{measured}}) - \log(E^*_{\text{predicted}})$. A typical plot of the residuals, in the log space, is shown in Figure 4-7 in this case for the AC14 C320 mixes.

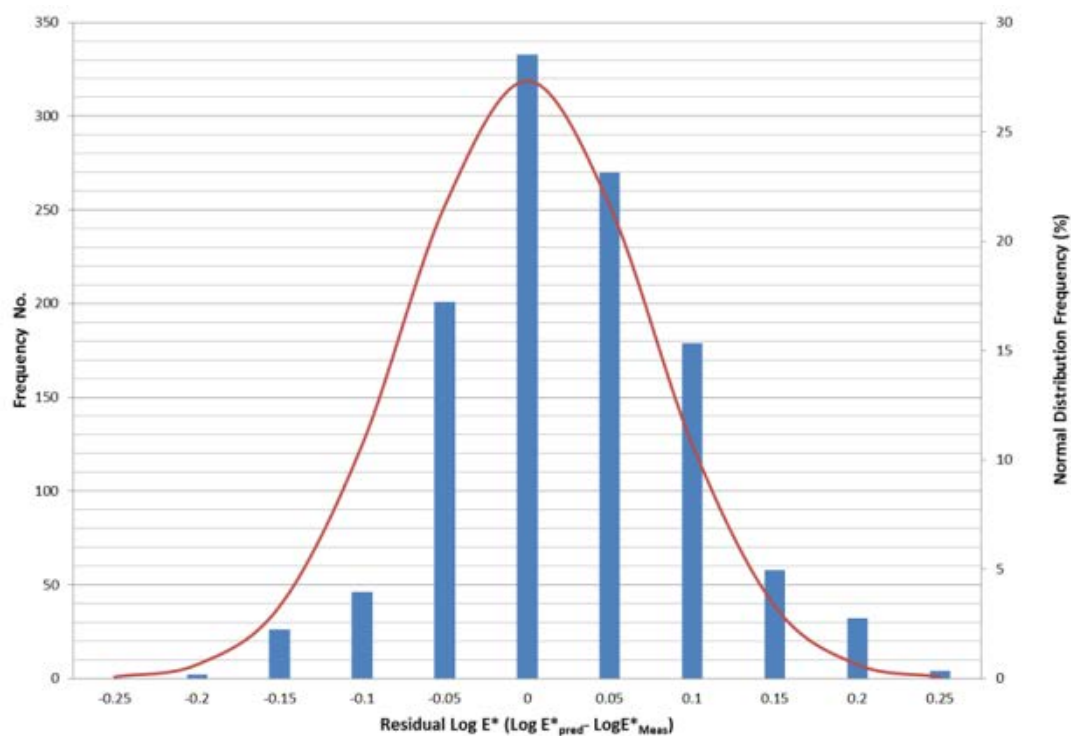


Figure 4-7 Typical Modulus Grouping Results and distribution of errors around the master curve

As can be seen in the figure, the shape of the distribution reasonably follows that of a normal distribution with the standard deviation equal to that of the standard error. Therefore, for practical purposes the residuals can be assumed to follow a normal distribution in the log space. This finding is important in developing confidence in the prediction of results, as it

shows that a normal distribution can be placed directly around the sigmoidal function in the log space

4.6 Development of Confidence Based Master Curves

Given the residual errors around the master curve can be assumed to follow a normal distribution with the standard error equal to the standard deviation, it is possible to establish confidence limits, for each of the proposed sub-groups of Australian production mixes. The practical result of this will be to enable the designer to say they are x% confident that the adopted modulus value used in design will not exceed the design value.

As the residuals are normally distributed around the master curve, for practical purposes the master curve can be simply shifted up and down on the modulus axis to obtain any degree of confidence. This means that for design purposes confidence limits can be simply established by varying the α parameter to shift the curve up or down to cover a greater or lesser number of results or simply assigning the normal distribution to the minimum modulus value. Because of the limited sample size used in the grouping of mixes, it was decided that a student's t distribution would give a better measure of confidence than that of the normal distribution. The student's t distribution was used in preference to the normal distribution to account for the limited observations obtained from the normal distribution for estimating the confidence value of the α parameter.

The student's t distribution and standard error were then used to determine the minimum modulus value, α , which would give 50, 75 and 95% confidence in prediction of modulus for all sub groups of Australian mixes. The full listing of confidence values and master curves for each subgroup can be found in Table 4-4 following while Figure 4-8 following shows one of the typical confidence interval plots, in this case AC14 AR450 mix, with the results for each subgroup being found in Appendix C.

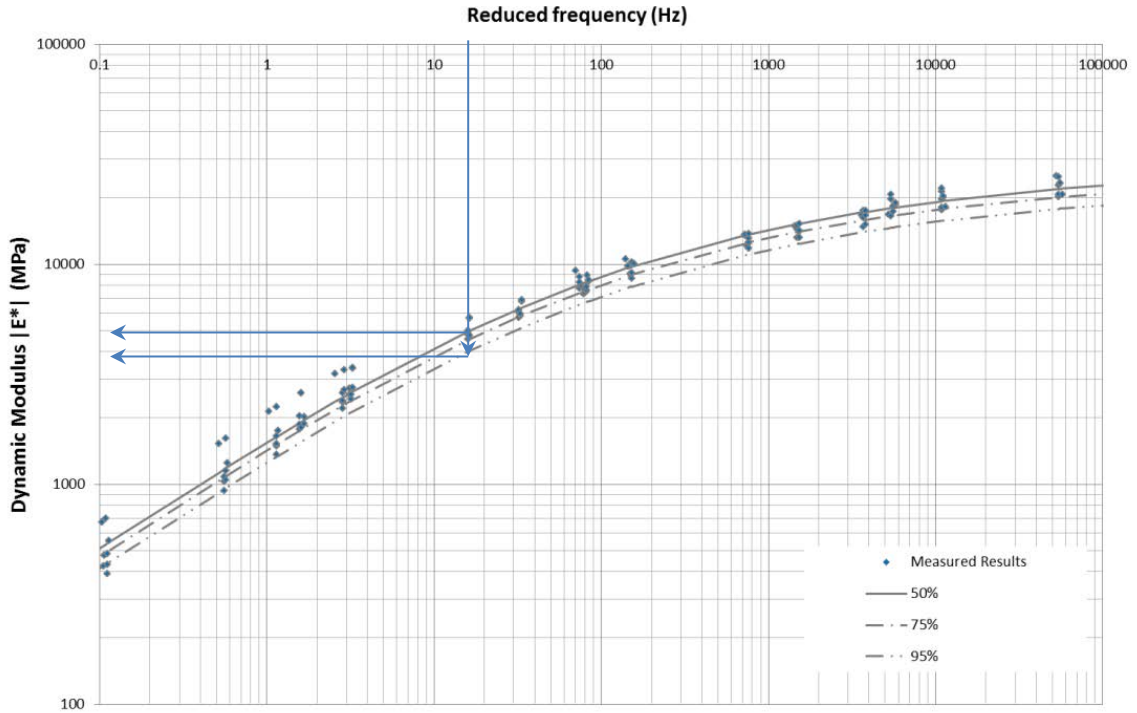


Figure 4-8 Confidence Interval Master Curve

Table 4-4 Master Curve Fitting Parameter

Nominal Size(mm)	Binder Type	Master Curve Sigmoidal Fitting Parameters					
		β	γ	δ	Confidence Level		
					α		
					50%	75%	90%
14	C320	3.184	-1.287	-0.676	1.218	1.160	1.076
	AR450	3.080	-1.384	-0.670	1.269	1.208	1.118
	A15E	3.446	-0.827	-0.502	0.978	0.935	0.873
	Multi	2.760	-1.040	-0.440	1.720	N/A	N/A
20	C320	3.132	-1.276	-0.694	1.289	1.243	1.176
	AR450	3.075	-1.417	-0.668	1.324	1.289	1.238
	C600	3.068	-1.377	-0.631	1.377	1.340	1.287
	Multi	2.702	-1.206	-0.405	1.771	N/A	N/A

Using this figure the designer can easily establish the modulus of a standard Australian mix at any temperature, frequency of loading and confidence level.

For example, and shown on Figure 4-8, consider if the designer wants to establish the modulus of the mix at a frequency of 12Hz and 25°C. The first step would usually be to

calculate the reduced frequency. However because the temperature required is the reference temperature, no shift is required on the frequency axis and the reduced frequency is the frequency required. The designer then simply selects 12Hz on the horizontal scale and follows the value down till it meets the desired confidence master curve. The value is then read off the vertical axis, in this case 3800MPa at 95% confidence or 4500MPa at 50% confidence.

4.7 Correlation with NCAT

To establish if there was any bias or variability between the Shear-box compacted samples and samples compacted using the US Superpave Gyrotory Compactor (SGC) and most importantly, whether Australia can use the results of NCAT testing to develop and calibrate performance models. Four Shear-box compacted samples were sent to NCAT, by Fulton Hogan's National Laboratory for comparison testing. In addition, two loose mixes were sent to NCAT for compaction in the SGC. This was undertaken to enable a direct comparison to be made between the Shear-box compacted samples and the SGC samples. It needs to be noted, that because of the time between compaction and testing the Shear-box compacted samples sent to the NCAT could have been up to 3 month old.

Table 4-5 following summarises the results of testing under taken by NCAT on the prefabricated cylinders and the NCAT fabricated cylinders.

Table 4-5 NCAT Modulus Results Australian Mixes

Temp, °C	Freq, Hz	Dynamic Modulus (MPa)					
		Pre-Fabricated Cylinders				NCAT Fabricated Cylinders	
		BKR	BLB	BKC	BKB	14_10 (BKB)	14_13 (BKR)
4	25	21858	14343	22319	25990	23702	20960
4	10	20413	13148	21331	24621	22449	19325
4	5	19293	12231	20483	23448	21467	18053
4	1	16727	10051	18332	20514	18871	15316
4	0.5	15582	9131	17339	19167	17685	14127
4	0.1	13152	7038	14902	15887	14681	11571
20	25	13387	7445	14267	16412	15192	11974
20	10	11819	6182	12754	14483	13198	10397
20	5	10712	5315	11585	13012	11740	9292
20	1	8378	3580	8908	9636	8473	7037
20	0.5	7459	2975	7802	8262	7185	6182
20	0.1	5607	1918	5447	5414	4490	4480

35	25	7833	3829	8416	8788	7239	6762
35	10	6602	2956	6918	6988	5551	5588
35	5	5785	2424	5872	5736	4421	4807
35	1	4177	1542	3784	3410	2507	3351
35	0.5	3625	1303	3065	2701	2000	2868
35	0.1	2571	948	1845	1696	1292	2010
35	0.01	1589	767	987	1123	919	1319
50	25	3924	1699	3342	3391	2666	3294
50	10	3217	1401	2482	2518	1962	2637
50	5	2767	1238	1984	2044	1594	2232
50	1	1993	987	1260	1405	1112	1582
50	0.5	1768	937	1080	1255	1001	1395
50	0.1	1373	863	829	1043	847	1085

For the two mixes where a direct comparison of the NCAT testing could be undertaken (Shear-box and SGC), similar behaviours were observed in the dynamic modulus results at different frequencies and temperatures. However, for both mixes, the shear-box compacted specimens were slightly stiffer than the SGC fabricated specimens across the full range of temperatures and frequencies. For both mixes, there was an increase in stiffness of typically 10% between the Shear-box compacted samples in comparison to the SGC prepared samples. For each mix, the master curves behaved in identical fashion over the full range of temperatures and frequencies but were separated by an offset. This separation in the curves could be caused by several variables. Initially, it was concluded that the most likely difference was due to the way the specimens were handled and compacted in the laboratory during the specimen fabrication process. However, the direct comparison between samples tested in Australia just after fabrication and by NCAT after fabrication in the SGC, shows this is not the case.

The direct comparison between the two test methods can be seen in Figure 4-9 following, which shows the dynamic modulus results obtained at NCAT against that of the dynamic modulus results obtained in the AAPA study of the shear-box compacted samples.

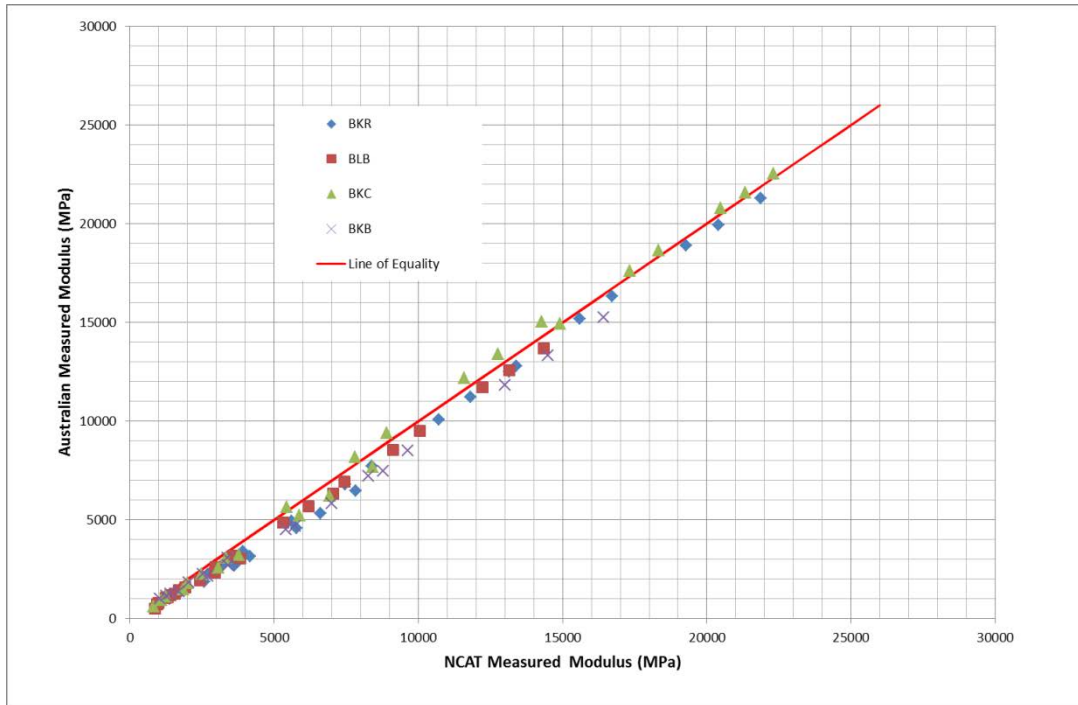


Figure 4-9 Comparison of NCAT and AAPA modulus results

The direct comparison between the two approaches was undertaken by comparing the dynamic modulus results obtained at NCAT against that of the dynamic modulus results obtained in the AAPA study using the shear-box compacted samples. What was quickly noticed is that the trend was the same as the trend found in the direct comparison undertaken by NCAT, that the older samples (results obtained by NCAT) were about 10% higher than that recorded in the AAPA study. Given the trend was the same as found by NCAT, the results would indicate a slight ageing of the samples and that the stiffness has increased in the period between fabrication and testing.

This ageing was confirmed when the results of the NCAT prepared SGC prepared samples were compared directly to the initial results obtained in the AAPA study, as shown in and Figure 4-10 and Figure 4-11 following. In this case the figure shows that the results for all practical purposes, for the two master curves, are identical.

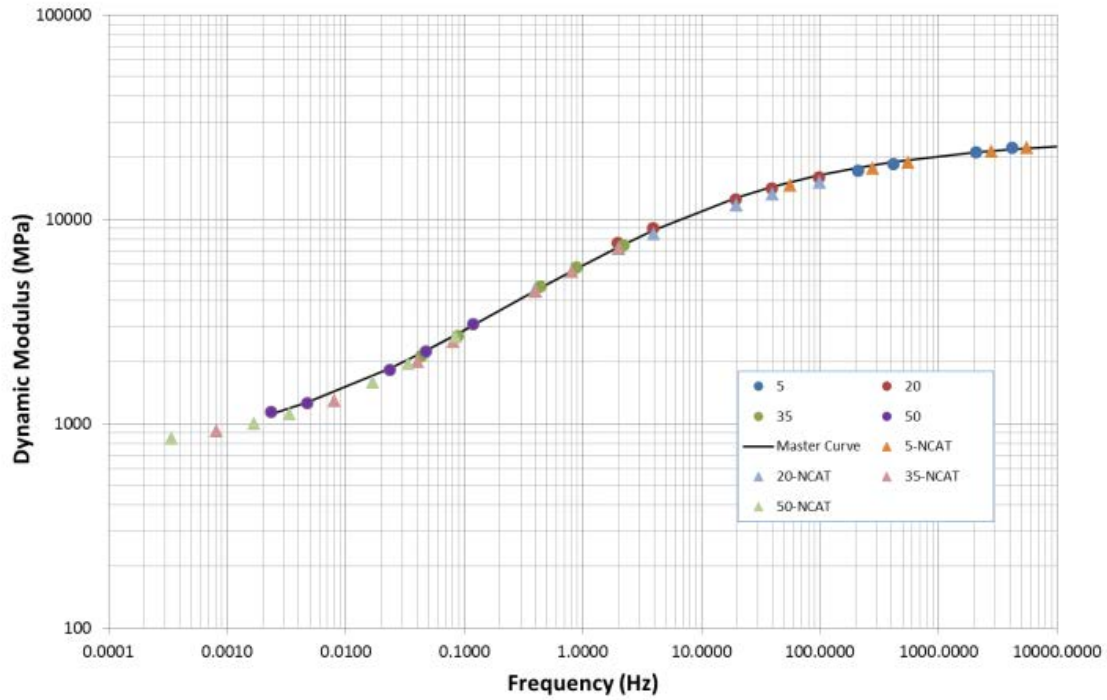


Figure 4-10 NCAT and AAPA Modulus Results mix 14-10

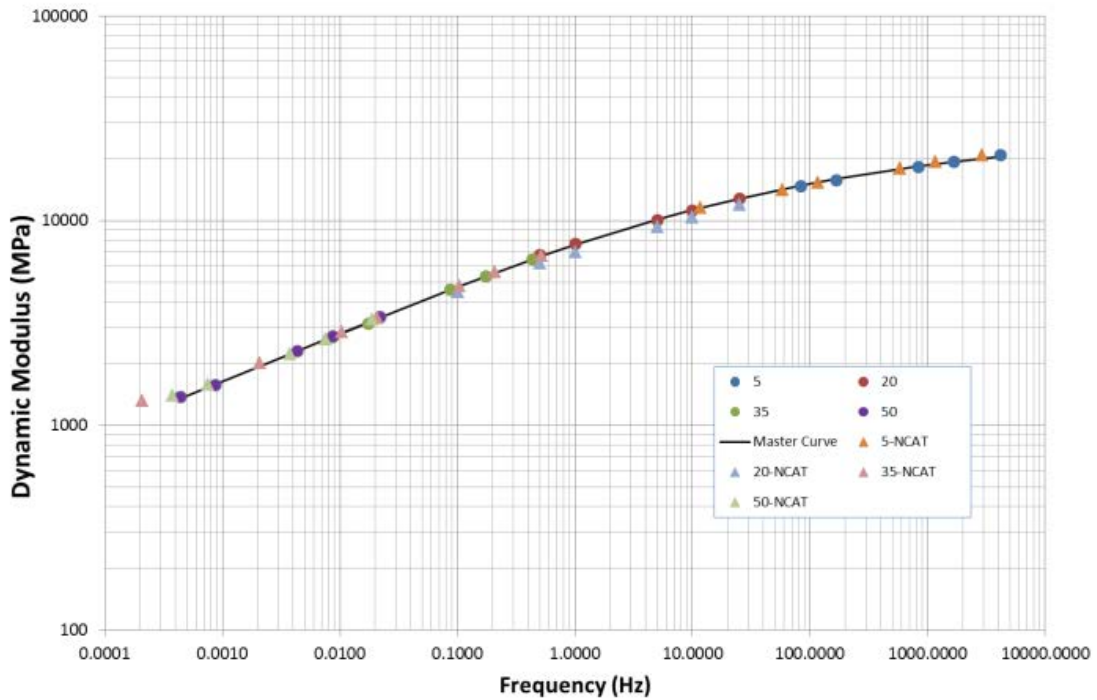


Figure 4-11 NCAT and AAPA Modulus Results mix 14-13

This would indicate that the differences seen in the comparison of the results obtained by NCAT between the SGC samples and Shear-box compacted samples, as well as the

difference seen between the NCAT tested Shear-box samples and the AAPA results are primarily due to a slight ageing of the samples.

The comparison of the results on the two un-aged samples show that the difference in the compaction method and test method have no practical influence on the dynamic modulus results, with identical results obtained. Therefore, it can be concluded that the APS-fL project can utilise NCAT modulus results and performance data with confidence for those sites where dynamic modulus testing has been undertaken to:

- Correlate dynamic modulus estimates from back analysis of deflection data
- Validate measured strain and predicted strain using Linear Elastic Analysis
- And, develop threshold strain levels based on calibrated strain and field performance.

4.8 Summary and Recommendations

International research has established that the dynamic modulus test provides a better characterisation of an asphalt mix over the resilient and other modulus tests because of its ability to fully characterise a mix over a range of temperatures and load frequencies. Additionally, the dynamic modulus test is internationally accepted as being able to discriminate key asphalt performance properties. For these reasons and most importantly, the ability to link dynamic modulus to a number field studies, AAPA selected the dynamic modulus test to undertake a full characterisation of standard Australian production mixes for the APS-fL project.

Examination of the gradation and volumetric properties of Australian SRA production mixes shows that despite the variability in the design methods (Marshall, gyratory and Superpave) and the differing compaction efforts, all mixes fit into a very small volumetric window. Additionally it was found the design gradation of all standard Australian production mixes closely follow the maximum density line, with nearly all mixes being slightly coarse graded, indicating that distinguishing between Australian mixes based on gradation and volumetric properties may be difficult.

The comparison of the results obtained by AAPA and NCAT on two un-aged samples showed that the difference in the compaction method and test method had no influence on the measured dynamic modulus results, with identical results obtained. Therefore, it can be concluded that the APS-fL project can utilise the results of NCAT testing for modulus and the performance data with confidence to:

- Correlate dynamic modulus estimates from back analysis of deflection data
- Validate measured strain and predicted strain using linear elastic analysis
- And, develop fatigue endurance limits.

Examination of the master curves of standard Australian production mixes suggests the minimum modulus value appears to be the best at distinguishing between binders and nominal aggregate size. As there is little difference in the volumetrics of Australian mixes, no significance could be found in air void levels or binder contents within sub mix types. Unexpectedly, no correlation was found between the minimum modulus and RAP content, indicating that at current RAP levels, RAP has little effect on the minimum modulus value and therefore overall modulus values. The results showed that most likely because of the small variance in aggregate gradation and volumetric properties there was no change in the shape of the master curve within grouped binder types and nominal aggregate size.

Because of the consistency of the master curve for a given binder type and nominal mix size, for practical implementation it was found that it was not necessary to develop complex master curve equations for routine pavement designs. The results of grouping of Australian mixes showed that Australia can achieve a higher degree of accuracy by grouping common mixes than from the use of complex models such as the Witczak or the Hirsch models.

It was found that because the residuals in the prediction of modulus approximated a normal distribution with the standard deviation equal to that of the standard error, confidence could be established from the grouped data by simply varying the minimum modulus data to move the dynamic modulus curve down the modulus scale. By doing this it was shown that confidence level master curves could be established for the nominal 14 and 20mm mixes and the three primary binder classes used in Australia, C320, AR450 and C600.

5 Conversion between Laboratory and Field Response

5.1 Introduction

This study proposed the use of the frequency-temperature dependent dynamic master curves as the method for determining the modulus of the asphalt under field loading conditions. Dynamic modulus helps to define the viscoelastic nature of asphalt mixes by quantifying the effects of temperature and frequency on stiffness under dynamic loading. This effect of frequency and temperature is necessary to accurately predict the pavement responses to varying load speeds and temperatures throughout the pavement's cross-section.

Currently, limited research has been undertaken to compare the behaviour of asphalt mixes in the laboratory using the dynamic modulus test and the behaviour of asphalt mixes in the field using measured response. Presently, no information exists in Australia to enable the comparison of modulus determined in the field from FWD testing with that of dynamic modulus test results, which can be used for development of a design procedure. While this information does not exist in Australia, Phase II and Phase IV of testing at the NCAT test track provides a valuable source of information for the comparison. As part this project, as shown in Chapter 4, a direct link has been established between NCAT dynamic modulus testing and the AAPA dynamic modulus database, showing there to be no significant difference between dynamic modulus results determined in the AAPA study and modulus determined by NCAT. Therefore the results obtained from a comparison of dynamic modulus and field modulus and ultimately field strain at NCAT should be directly transportable to Australia and can be directly used for accurate validate of a FEL design approach.

A main objective of the phase of the project was the determination of the stiffness of the asphalt mixes which can be used in multi-layer elastic model to accurately predict the pavement response under traffic load. There are two ways of accomplishing this objective.

- First, pavement responses can be predicted by multi-layer elastic model using different stiffness and then compared with measured responses.
- The second method is to back-calculate the layer moduli from measured pavement responses and compare the back-calculated moduli to laboratory determined moduli.

5.1.1 Data for Comparison

As part of the experimental plan of the Phase II and Phase IV test cycles at the NCAT test track, structural testing using FWD was undertaken on known pavement structures. This measured response was used to determine the effective modulus of the combined asphalt layers throughout each phase of the test cycles. Furthermore, for the structural sections of

the test track of both Phase II and Phase IV a series of laboratory dynamic modulus tests were performed on each of the individual mixes used in the structural experiment sections.

In addition to the NCAT, there are a number of sources of valuable information in the literature which can be used to compare laboratory dynamic modulus to field modulus, with data also being available from both MnRoads and the WesTrack test tracks. Both of these have documented results for field stiffness determined from FWD testing and laboratory characterisation of asphalt mixes undertaken using the dynamic modulus test.

5.2 Factors Effecting Conversion

5.2.1 Time Frequency Conversion

There is currently significant debate amongst researchers on how frequency is related to time in the dynamic modulus test. The two primary schools of thought are the angular frequency approach vs. the pulse frequency approach. Researchers such as Dongre et al. (2006) recommend the angular frequency approach, $t = 1/\omega$, while researchers such as Katicha et al. (2008) recommend the pulse frequency, $t = 1/f$, approach. The theory on frequency conversion will be covered in depth in the discussion of conversion of laboratory test methods in Chapter 6.

It appears that the earliest use of the angular frequency approach, $t = 1/\omega$, for asphalt mixes was from the work undertaken by Papazianin at the First International Conference on the Structural Design of Asphalt Pavements (1962). This approach was then adopted by Shell for their development of a ME pavement design procedure, subsequently adopted as the basis of the AGPT002 (2012) asphalt characterisation method. However, the angular frequency approach has not been universally adopted by all design procedures, with the US MEPDG following the $t = 1/f$, approach.

The reason the $t = 1/\omega$ approach is recommended by some researchers is based on the solution of the Inverse Fourier Transformation (IFT) which is required to convert from the frequency to time domain, to determine the relaxation modulus, $E(t)$, from angular frequency testing, from the storage modulus E' , as follows, Ferry (1980).

$$F^{-1} \left[E'(\omega) = \frac{1}{2\pi} \int_0^{\infty} H(\tau) \frac{\omega^2 \tau^2}{1 + \omega^2 \tau^2} d\tau \right] \quad \text{Equation 5-1}$$

Where,

ω is angular frequency in rad/s

f is the cyclic frequency in Hz

τ is loading time in seconds

$H(\tau)$ is the continuous spectrum of the relaxation time

F^{-1} is the Inverse Fourier Transformation

Dongre (2006) found that the exact solution of the IFT to calculate relaxation modulus from the dynamic modulus test was $t = 1/\omega$. This is somewhat contrary to the early recommendations of Van der Poel (1954) who suggested the conversion was only approximate. Notwithstanding this, Dongre did not establish that the testing in dynamic modulus test was an angular frequency, which would require the above conversion. The issue is still not resolved amongst researchers.

5.2.2 Vehicle Speed and Load Frequency

The case of the FWD loading is relatively simple, being a relatively fixed load time with depth. This however is not the case for a moving load which varies with depth and vehicle speed. Therefore in order to compare dynamic modulus test data with the response of a pavement in the field, the equivalent loading pulse time of the design vehicle needs to be determined. Early research in mechanistic pavement design identified two approaches to model the pulse time within an asphalt layer; time as a function of the strain pulse or time as a function of stress pulse.

The approach to modelling time as a function of strain pulse was first hypothesised by Coffman (1967) who believed that to translate laboratory tests to field modulus the cycle length and the phase shift needed to be known. Coffman based his recommendation on the correlation of field testing and analytical work and determined that cycle length was a function of the measurement of field strains under a moving load. Coffman found that it was possible to fit a sine wave to the measured deflection and therefore determine the cycle length. Coffman found that 6 feet was a good choice for average cycle length and also that the use of higher frequencies for upper most pavement layer layers and lower frequencies for the lower pavement layers was not justified.

The approach of using the stress distribution appears to have been first postulated Brown (1973) based on work done by Barksdale (1971). Brown's approach was to use the use the average loading time for both vertical and horizontal stress pulses throughout the asphalt layer. The equation developed by Brown using the average stress loading time is shown in Equation 5-2 following:

$$\log t = 0.5h - 0.2 - 0.94\log V \quad \text{Equation 5-2}$$

Where;

t= loading time (sec)

h = thickness (mm)

V = vehicle velocity (km/hr.)

Brown's method has subsequently gained widespread acceptance and forms the basis of various different design processes throughout the world, including the current Austroads design procedure.

Ullditz (2006) proposed an alternative approach to using stress distributions to determine loading pulse, using a simplified model incorporating tyre contact area with the load being distributed at 45° from the tyre radius. The model proposed by Ullditz is shown conceptually in Figure 5-1 and numerically in Equation 5-3 following:

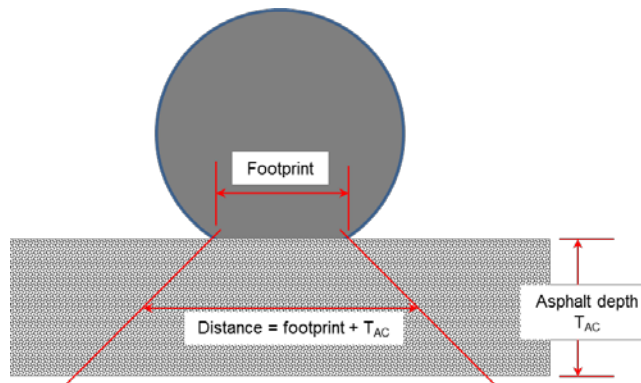


Figure 5-1 Model used to Calculate Load Duration

$$t = \frac{200 + 2h}{S} \quad \text{Equation 5-3}$$

Where;

S = the vehicle speed in (mm/s)

h is the desired thickness

200 = is assumed to be the length of the tyre contact

The US Mechanistic Empirical Design Guide (MEPDG) uses a similar approach to that proposed by Ullditz; however, it does not use a fixed stress path. The approach makes use of Odemarks approach, to transform asphalt layers into an equivalent thickness of subgrade material over the actual subgrade layer. These results in an increase in the asphalt layer thicknesses and in theory should result in significantly longer loading times than the approach adopted by Ullditz and Brown.

5.2.3 Empirical Relationships to Frequency

Yager (1974) used the early work by Coffman to relate vehicle speed to test frequency. Using the 6 foot load pulse, Yager determined frequencies of 1, 6 and 12Hz related to speeds of 10, 40 and 80km/hr. respectively. Jacobs et al. (1996) recommended a loading frequency of 8Hz to correspond to a vehicle speed of 60km/hr. In NCHRP report 465

Witczak et al. (2002) recommended 10Hz be used as the frequency for highway speed and 0.1Hz for creep – intersection traffic. The Asphalt Institute assumes a value of 10Hz regardless of the conditions Asphalt Institute (1999). These empirical recommendations would indicate that frequencies in the range of 0.1 to 12Hz are representative of vehicle speeds for the purpose of pavement design. However, none appear to be validated to field performance.

As previously mentioned, the US MEPDG uses the relationship of frequency as the reciprocal of pulse time ($1/t$) to convert between frequency and load pulse time in the field. Using this method, frequencies in the range of 1 to 100Hz, would be expected if a stress pulse was used. Clearly this is a long way from the empirical recommended values.

The use of the angular frequency approach would give frequency ranges of 0.1 to 14Hz, which are in line with empirical recommendations. The belief that the frequencies used in the MEPDG are too high, is supported by a review of the accuracy of the MEPDG by NCHRP 2006, which found that the use of the cyclic frequency approach lead to unrealistically high modulus values.

5.2.4 *Dynamic Modulus and Field Strain*

It is not surprising, given the debate about;

- the conversion between time and frequency in the dynamic modulus test,
- the effect of depth on load pulses times and
- the effect of stress distributions within the pavement structure,

that currently little published work has been found to determine a direct correlation between laboratory modulus, field modulus and strain.

Some work relating strain to dynamic modulus has been undertaken by Bayat et al. (2005). In a series of field-controlled wheel load tests, Bayat found that longitudinal strain in asphalt followed an exponential relationship to pavement mid-depth temperature, when speed was constant. This finding is similar to the findings of Timm et al. (2006). However, Timm found the relationship was a power relationship at the NCAT test track. Bayat found that dynamic modulus was directly related to measured strain and found that dynamic modulus was inversely proportional to the field measured asphalt longitudinal strains and found “*dynamic modulus test replicates pavement field response*”. However neither Bayat nor Timm’s research recommended a final method for the conversion of laboratory measured modulus to field modulus.

5.3 Calibration Plan

There appears to be no easy solution to the debate about the exact conversion between frequency in the dynamic modulus test and time of loading in pavement structures, with the solution requiring complex mathematics which currently can only be numerically approximated, does not appear to be easily solved and are even then still open for debate. The mathematical solution of this problem was determined to be outside of the scope of this project. It was accordingly decided to disregard the solution of the mathematics and to develop a direct conversion between dynamic modulus and field measured modulus using FWD testing, and the results of dynamic modulus testing undertaken at NCAT, WesTrack and MnRoads. The relationship between dynamic modulus and field modulus would be used to develop and validate a direct conversion between dynamic modulus frequency and field pulse loading, skipping the solution of the mathematics.

In this way, conversion factors can be established which enable the conversion between laboratory and field modulus and pavement temperature, without resorting to solving the complex differential equations (where no exact solutions exist).

This conversion can then be used to validate strain results obtained at the NCAT test track to strains predicted by the use of layered elastic analysis and the converted modulus and determine calibration coefficients, if any.

To determine the conversion between dynamic modulus, back-calculated FWD results and strains under wheel loading, a series of stepwise numerical optimisation procedures was undertaken. Based on the results of this analysis, a series of conclusions and recommendations can then be drawn to determine strains under a moving vehicle load using the results of dynamic modulus testing.

5.4 Optimisation Approach

Due to;

- the complexity of the problem being solved
- the number of possible combinations of each variable, and
- most importantly, the requirement for the nonlinear optimisation to have seed values which need to be relatively correct to ensure the solver function converges on the correct optimal solution,

a three stage sequential optimisation approach was used in the analysis. The three stage sequential optimisation is as outlined in Table 5-1 following. The Solver function of Excel® was used for the nonlinear optimisation, to assess the combination and contributions of each variable and therefore, optimising the calibration of modulus and the prediction of strain under a moving vehicle from dynamic modulus.

Table 5-1 Optimisation Approach

	Process	Data Source
Stage 1- Calibrate laboratory field modulus interconversion	Calibrate Frequency Interconversion	FWD Data NCAT
	Calibrate Temperature Profile	
	Validate findings with WesTrac and MnRoads	FWD WesTrack and MnRoads
↓		
Stage 2- Calibrate frequency under moving load	Calibrate load pulse width	NCAT E* and strain
	Calibrate effect of frequency with depth	
↓		
Stage 3- Validate multi-layer asphalt	Validate Multi-layer findings	NCAT E* and strain

The first stage was to use the results of the field modulus from the FWD to determine the frequency conversion between the laboratory modulus and field modulus and determine the temperature correction required to account for any difference between mid-depth measured on site and the effective temperature within the asphalt layers.

The second stage was to calibrate for any static/dynamic effects, temperature effects, determine the load pulse width and the corresponding stress path within the pavement using an equivalent single layer of asphalt.

The final stage was to optimise the model for use with multi-layer asphalt pavements.

5.4.1 Field Modulus Measurements

The first stage of the proposed optimisation process requires the use of field measured modulus values from FWD testing combined with the results of dynamic modulus testing. Three sources of information were identified in the literature to accomplish this; NCAT, MnRoads and WesTrack.

At the NCAT test track, in-service modulus was determined from the results of FWD testing undertaken using a Dynatest FWD. The field testing process undertaken at NCAT is described in depth by Timm et al. (2003). The back-calculation of modulus from the results of the FWD testing was accomplished using Evercalc. Timm (2005) described the several simulated cross sections that were attempted to determine the best grouping of the pavement layers for back-calculation to determine the optimal cross section. The optimal

cross section was determined to have the aggregate base and fill material combined into a single layer.

The second source of field modulus was taken from the MnRoad test track. Since construction in August 1999 (Cells 33, and 34), FWD testing has been performed several times on the cells at MnRoad, Clyne (2004). Several locations have been tested in each cell, and load, deflection, and temperature data has been collected with each test. For MnRoads these results were then used to back-calculate the modulus of the asphalt pavement. The back-calculation method again utilised Evercalc.

The Westrack test track also utilised FWD testing for field validation of modulus. However WesTrack utilised Elmod 5 for the purpose of back-calculation of layer moduli. Back-calculation of the asphalt layer moduli was done for all of the FWD test series, and for the test positions between the wheel paths as well as in the right wheel path.

5.4.2 Effective Layer Modulus

As mentioned back-calculation nearly always considers the entire depth of the asphalt layers, while the dynamic modulus test considers each mix separately. This was the case for the NCAT test track where different asphalt layers were used within the pavement structure.

As the initial optimisation process proposes the use of a single layer for the conversion of laboratory measured dynamic modulus to field measured modulus from FWD testing, the individual asphalt layers will need to be combined into a single equivalent asphalt layer. The individual asphalt layers were combined into an equivalent single asphalt layer using the concept of conservation of the moment of inertia (method of equivalent thickness) via Equation 5-4 following.

$$\left(\sum_{i=1}^n h_i \right) E_{eff}^{\frac{1}{3}} = \sum_{i=1}^n h_i E_i^{\frac{1}{3}} \quad \text{Equation 5-4}$$

Where;

E_{eff} is the effective modulus of the combined layers

h_i is the thickness of layer i

E_i is the modulus of layer i

n is the number of asphalt layers

In this process each moduli result from the dynamic modulus test, (from Timm (2003) and Vargas-Nordbeck (2013)), at each frequency and test temperature were combined using the as constructed layer thickness to determine the effective modulus at each test frequency

and test temperature. These effective modulus values were then used to construct an effective dynamic modulus master curve, using the sigmoidal function and polynomial shift factor as described in Section 4.3.

The master curve fitting parameters for the resulting master curve for the combined layers are shown in Table 5-2 following. The sites chosen for the analysis were 6 NCAT test cells where little damage had occurred. Additionally, shown in Table 5-2 are the master curve parameters for the two MnRoad test sites (cell 33 and 34) and the 6 Westrack test sites, with dynamic modulus results being obtained from Clyne (2004) and Pellian (2001).

Table 5-2 Modulus Calibration Master curve Fitting Parameters

Test Cell	Temperature Shift Factors ($T_{ref} = 20^{\circ}\text{C}$)		Sigmoidal Fitting Parameters			
	a	B	α	β	γ	δ
N3-Phase III	0.0003	-0.116	1.810	2.774	-0.711	-0.363
N5 Modified-Phase II	0.0004	-0.119	1.688	2.896	-0.770	-0.347
N7-SMA	0.0004	-0.122	1.787	2.897	-0.649	-0.359
S9-Control	0.0004	-0.115	1.868	2.708	-0.709	-0.372
S10 WMA-F	0.0004	-0.115	1.704	2.638	-0.998	-0.457
S11 WMA-A	0.0004	-0.115	2.014	2.316	-0.769	-0.5060
MnRoad C34	0.0007	-0.118	1.564	2.883	-0.500	-0.5231
MnRoad C33	0.0003	-0.109	1.891	2.397	-0.592	-0.6270
WesTrac C2	0.0005	-0.135	1.900	2.281	-0.721	-0.4830
WesTrac C5	0.0001	-0.148	2.138	1.912	-0.640	-0.4840
WesTrac C6	0.0016	-0.155	2.171	1.915	-0.551	-0.6850
WesTrac C7	0.0008	-0.136	2.055	2.151	-0.550	-0.5929
WesTrac C23	0.0017	-0.156	2.172	1.915	-0.550	-0.6850
WesTrac C24	0.0008	-0.135	2.029	2.044	-0.651	-0.4937

5.4.3 Strain Calibration Validation

To better understand mechanistic design principles Phase II of NCAT test track included the installation of strain gauges at the underside of the asphalt layer, enabling direct measurement of the pavement response in terms of strain. Based on the findings of Phase II the use of strain gauges was extended into Phase III and IV. However, both Phase III and IV used a different definition for the recording of strain, producing strain values typically larger than the Phase II definition. The inclusion of two definitions in the calibration would

add a degree of complexity to the analysis and could force the solution in the wrong direction. Furthermore the AAPA APS-fL project includes a sub-task for calibration of strain against performance, so any difference in definition can be handled in the performance calibration phase. It was therefore decided that only the standard definition used in Phase II of Test track would be used in the calibration.

For each test section twelve strain gauges were installed; therefore, one truck pass produced at most, six readings in both the longitudinal and transverse orientation. The maximum reading of each orientation (transverse and longitudinal) was considered the “best hit” of a tire over a gauge strain, and was therefore, the value for that tyre pass. The strain gauges were installed at three lateral orientations to help ensure that one of the three offsets would very closely register a direct hit of the tire over the gauge, thus producing if not the maximum, close to the maximum strain value.

For the initial calibration of strain determined from linear elastic analysis against measured strain, individual raw data, in terms of temperature at strain recordings was not available. However, Timm et al. (2006) determined the effect of temperature on strain in the Phase II NCAT structural test cells for both the triple trailer and a box trailer. As the box trailers have a fairly uniform load per tyre of 21,000lbs and lower potential for dynamic effects the box trailers only would be used in this analysis. Timm et al. found the effect of temperature on strain for a given site followed a power relationship as shown in Equation 5-5 following, with the fitting relationships for each cell shown in Table 5-3 following.

$$\varepsilon_t = \beta T^{\beta_T} \tag{Equation 5-5}$$

Where;

T is temperature in °F

β and β_T are fitting parameters

Table 5-3 Box trailer regression results (after Timm (2006))

Section	β_1	β_T	R^2
N2	3.922×10^{-5}	3.579	0.871
N3	5.501×10^{-3}	2.332	0.773
N4	1.304×10^{-3}	2.632	0.733
N6	1.852×10^{-2}	2.155	0.881
N7	8.310×10^{-4}	2.796	0.821

It should be noted that there was not enough collected strain data to develop a relationship for the box trailer in section N1 and section N8 was found to have a slippage between the high binder layer base and the layer above and was excluded from the calibration.

In order to calculate strain values using a linear elastic code the support to the subgrade needs to be known. To undertake this analysis the average support values for the combined base/fill and effective subgrade as published by Timm et al. (2006) was used in the calculations, with the values shown in Table 5-4 following.

Table 5-4 Subgrade Fill Modulus

Section	Base/Fill Layers		Subgrade	
	Thickness(mm)	Modulus(MPa)	Thickness(mm)	Modulus(MPa)
N2	635	69	N/A	110
N3	533	90	N/A	214
N4	533	83	N/A	221
N5	584	48	N/A	193
N6	584	76	N/A	221
N7	584	79	N/A	221

N.B the reasons for the differences in published modulus values between fill and subgrade can be found in Timm et al. (2006).

5.5 Conversion between FWD and Dynamic Modulus

To initially determine which of the two approaches debated in the literature most closely matches field performance, the results obtained from test section S9 from the Phase IV study of the NCAT test track was examined. This section was selected due to the low scatter of the results from the back calculation, limiting the chance of drawing the wrong conclusion due to variability in the results.

Because of the current debate on the accuracies of both approaches, it was decided for initial analysis to compare the findings from both approaches and from this initial assessment determine the approach which most accurately predicts field performance to use as the “seed” value for the full calibration exercise.

To accomplish this, the frequency determined by both the angular frequency, $t = 1/2\pi f$, and pulse frequency, $t = 1/f$ approach was used to determine the modulus in the equivalent master curves at the mid-layer temperature. The time used for the FWD load pulse was a haversine load pulse with duration of 30ms for both comparisons between dynamic modulus and FWD modulus.

Therefore to establish dynamic modulus at 0.030 seconds from the master curves the two comparison frequencies were utilised:

- $1/0.03$ or 33Hz
- or $1/\omega$ 33 rad s⁻¹ or 5.3hz

Utilising the equivalent master curves for NCAT test section 9 and the two frequencies currently being debated by researchers, the measured modulus was compared against the predicted modulus from the equivalent master curves. The results of the comparison are shown in Figure 5-2, for both the angular frequency approach and the cyclic pulse frequency approach.

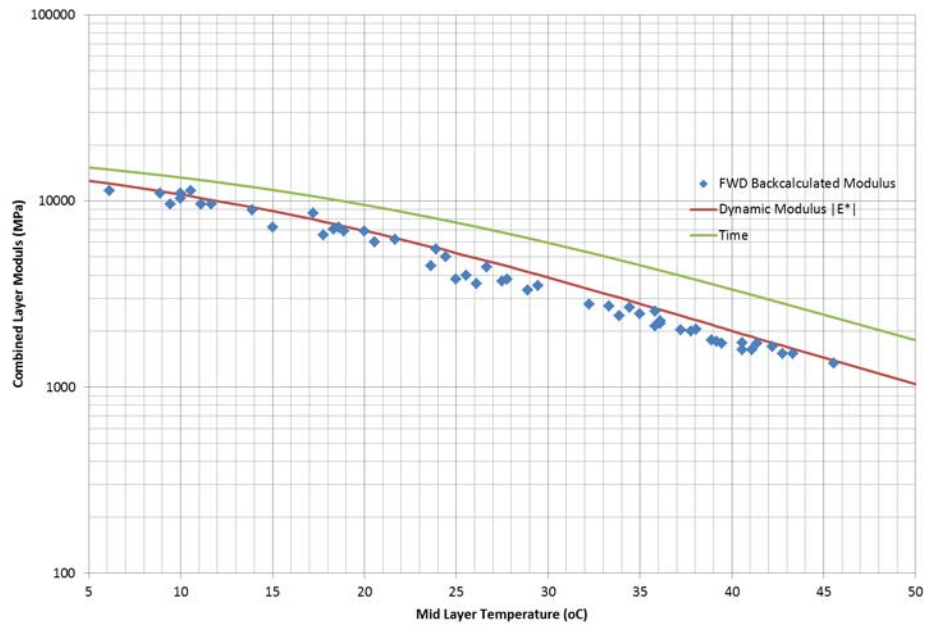


Figure 5-2 S9 Control Mix Frequency Conversion

The results of the comparison of the Phase IV control section S9, suggest that the angular frequency approach appears to significantly correlate better. The results show that the cyclic frequency approach is out of phase with the test results and predicts higher modulus than determined under the pulse load of the FWD. The results show, a phase correction of 2π applied to the dynamic modulus results to convert from angular frequency to cyclic frequency closely matches the measured data. When this correction is applied the dynamic modulus test can be accurately used to predict the response of an asphalt layer under FWD pulse loading.

While highly correlated, the results do show that dynamic modulus test has determined slightly higher modulus than measured in the field. This is most likely due to temperature variations within the asphalt layers, as in the day the average temperature of the asphalt layer will be marginally higher than temperature recorded at mid-depth in the pavement.

5.5.1 Combined NCAT Sections

Based on the initial findings obtained from the control section S9 at the NCAT test track, the study was extended to a number of sites used at both the 2003 and 2009 test track, where dynamic modulus test results were available and field testing of modulus testing against temperature was undertaken.

In order to undertake the first part of the proposed multistep optimisation, the optimisation was set up to determine the optimal conversion factor, k , between the dynamic modulus test

and field measured modulus, and the effect, if any, of the temperature gradient within the pavement structure on the conversion.

$$f_{dm} = \frac{1}{kt_p} \quad \text{Equation 5-6}$$

$$T_{ave} = at_{mid} + b \quad \text{Equation 5-7}$$

Where f_{dm} is the frequency in the dynamic modulus test, a, b and k are optimisation constant. The seed values used in the analysis were taken from the results of the analysis of section S9, being 1, 1, and 2π for a, b and k respectively.

The seed and trail calibration coefficients were then used with the effective dynamic modulus master curves to predict the laboratory modulus at the equivalent reduced frequency applicable and effective temperature. The optimisation was then run fully unconstrained with k, a and b being free to minimise the sum of the difference between predicted and measured modulus.

The results of the optimisation can be found in Appendix D of this report and found that the frequency time conversion constant, k, for all practical purposes was equal to the value recommended by Dongre (2006) of 2π . Given the recommendation by Dongre and the results of the optimisation it was decided that all future calculations, the frequency-time conversion factor, k, should be assumed to be 2π .

It was found through the optimisation that the temperature equivalency multiplication factor, a, approached that of 1 and the addition factor, b, approached 2. For simplicity, the value of a and b was set at 1 and 2 respectively. The following figures shows the results of the comparison with the constants of 2π , 1 and 2 applied with Figure 5-3 showing the FWD modulus results against that of the Dynamic modulus results, and with Figure 5-4 showing the same results only this time plotted against average layer temperature.

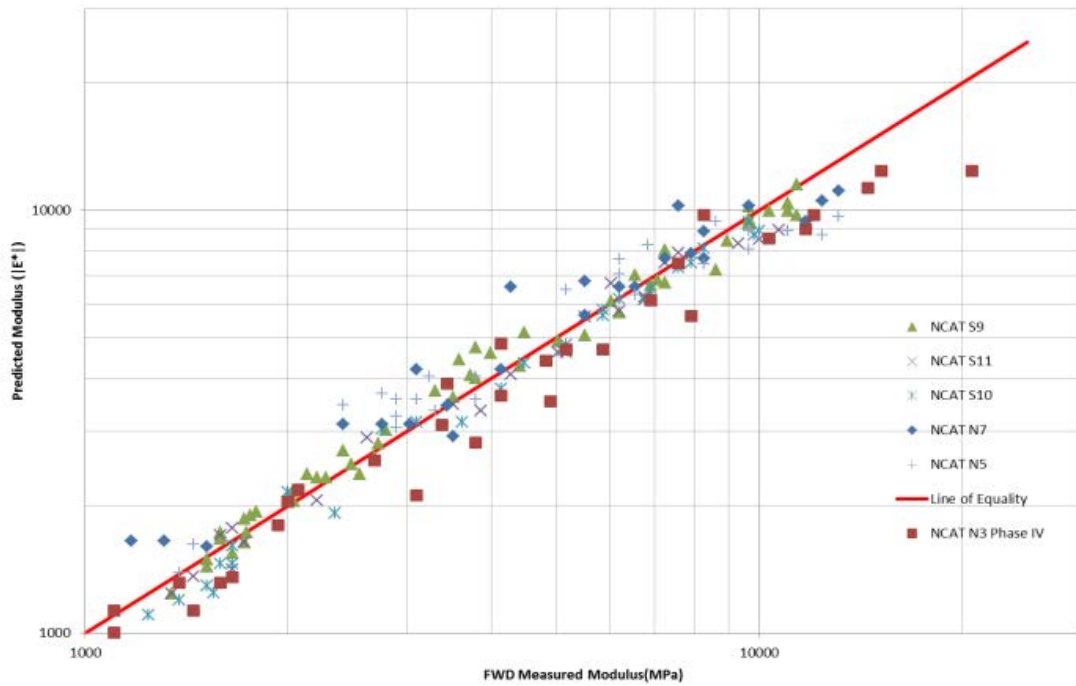


Figure 5-3 Accuracy NCAT Converted Dynamic Modulus vs. FWD Stiffness

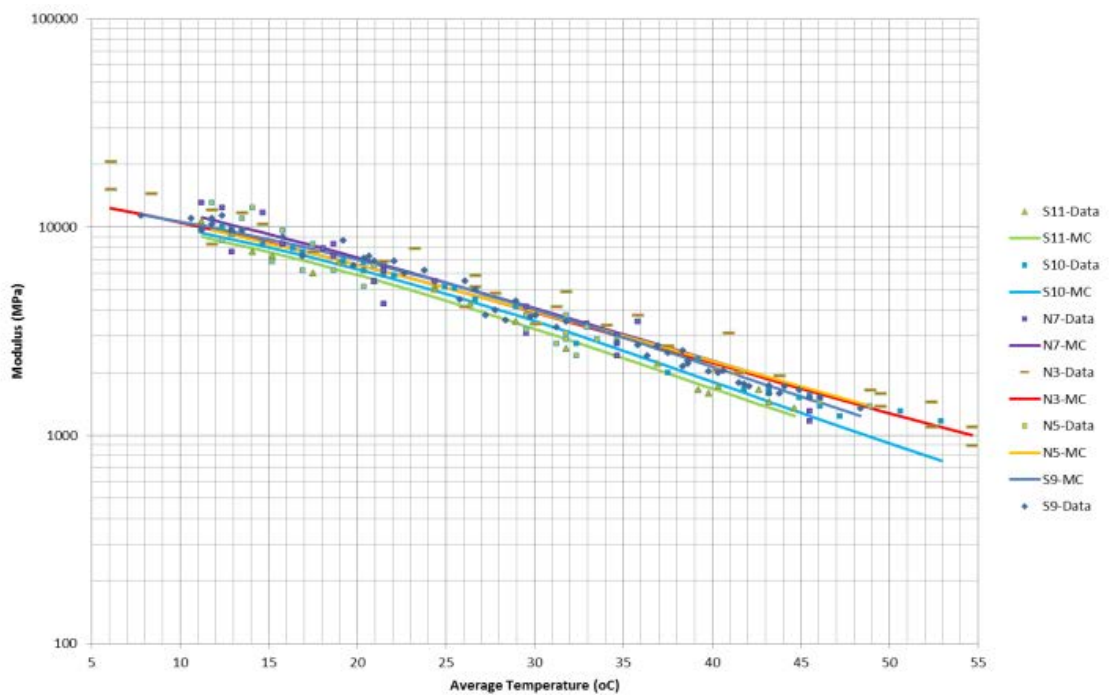


Figure 5-4 NCAT Converted Dynamic Modulus vs. FWD Stiffness

From both figures it is clear that there is a very strong correlation between dynamic modulus and effective modulus determined from FWD testing. The nonlinear optimisation of frequency and average temperature support the recommendation of Dongre (2006) in comparing dynamic modulus results against resilient modulus, that dynamic modulus

frequency should be considered as an angular frequency and a frequency conversion is required to convert from radians/sec to time. The optimisation found to convert between laboratory dynamic modulus and modulus measured in the field under a 0.03 seconds FWD load pulse a frequency of 5.3Hz should be used in the dynamic modulus test.

The multi-variable optimisation also found that if mid-depth temperature is used to determine the pavement response, a correction of + 2°C degrees should be used for daytime analysis to compensate for the average temperature results being slightly higher than the mid-layer temperature.

5.5.2 Validation against MnRoads and WesTrack

To validate the findings obtained from the NCAT test sites and determine whether the results were transferable to other mixes and climate, the dynamic modulus results and field modulus reported for MnRoads and WesTrack test tracks were analysed using the same calibration factors.

Figure 5-5 following shows the results of the comparison undertaken on MnRoads and Figure 5-6 for WesTrack test tracks. For MnRoads field modulus data was available across a range of temperatures for Cell 33 and 34. For WesTrack, Figure 5-6, only results were published for Phase 1 testing at a single temperature for a number of sites.

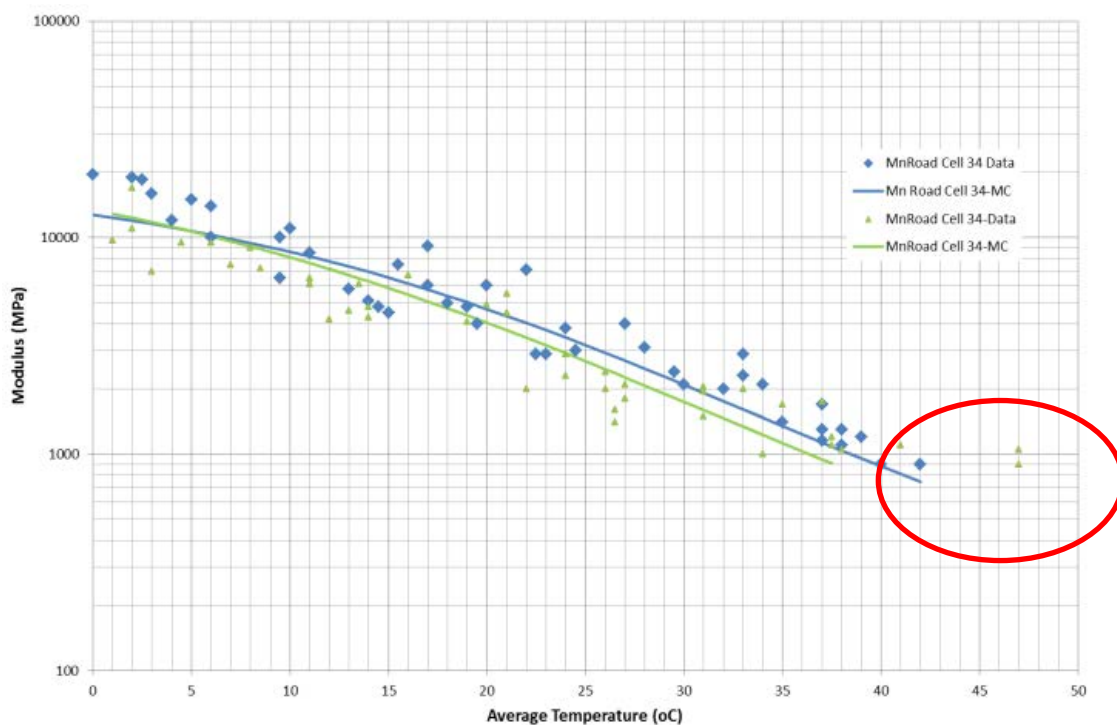


Figure 5-5 MnRoads Modulus Comparison

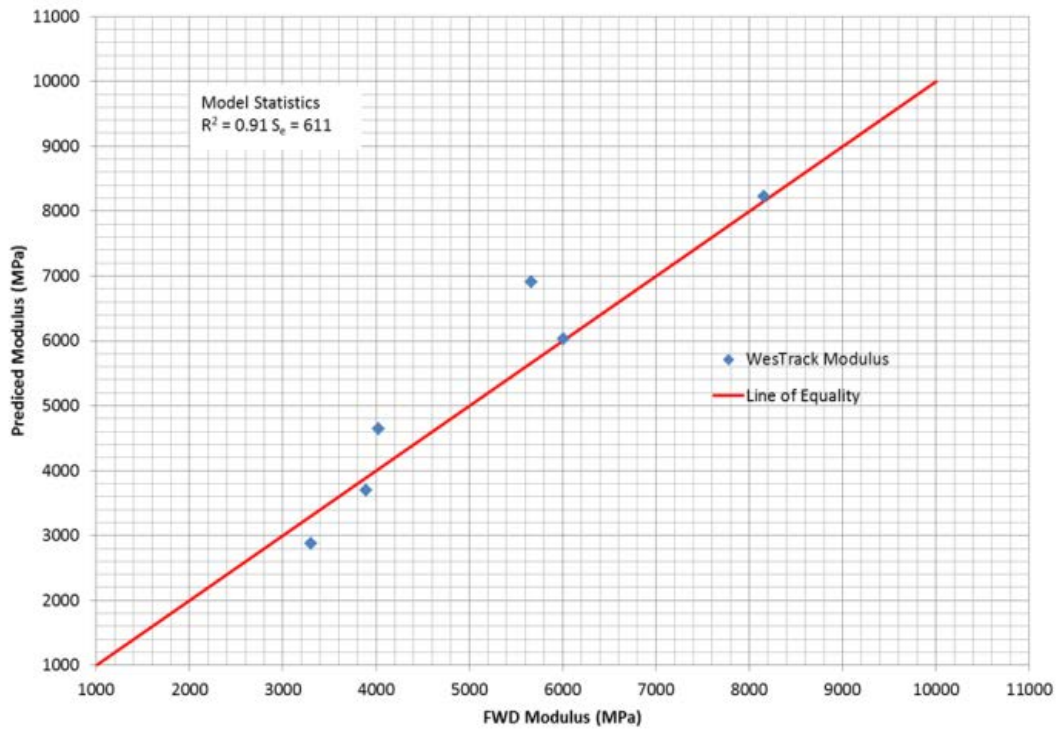


Figure 5-6 Westrack Modulus Comparison

While the scatter of results is higher than found at NCAT, from both Figures 5-3 and 5-4, it is clear that at these two additional locations with a number of different mixes, there is again a very strong correlation shown between dynamic modulus and modulus determined from FWD testing and no bias is observed in the comparison.

Additionally, it is worth noting that at the higher temperatures on cell 34 the predicted modulus from the unconfined modulus test began to deviate from that of the measured modulus, with the results beginning to asymptote around a value of 1000MPa. This is consistent with the findings of the effect of stress susceptibility (as discussed in Section 5.10), that at higher temperature and low frequencies modulus is stress susceptible. The results show that the effect of stress susceptibility in the pavement has a positive effect on modulus and is best represented by applying confinement to the sample in the laboratory. While more work will need to be undertaken to quantify this effect the results tend to indicate that a confinement of approximately 200kPa is required to model asphalt pavements where unconfined modulus falls below a value of approximately 1000MPa. This is not surprising considering the confining stress in an asphalt pavement for 150 to 200mm asphalt layers averages between 200 and 70kPa. The results also indicate that laboratory tests which apply tensile strains to the specimen may be ineffective in characterising mixes at higher temperatures and lower rates of loading.

Based on these findings, it is clear that Dynamic modulus in the laboratory can be directly related to modulus determined under a pulse loading in the field, by equating time and frequency as follows:

$$f_{dm} = \frac{1}{2\pi t_p} \quad \text{Equation 5-8}$$

Where;

- f_{dm} is the frequency in the Dynamic modulus test (Hz)
- t_p is the time of the pulse loading (sec)

This equation should be used to determine the equivalent dynamic modulus frequency to any pulse loading in the field.

The results have shown that dynamic modulus is highly correlated to modulus measured by the FWD when a frequency conversion is applied to the dynamic modulus results, based upon studying the results of the NCAT test track, MnRoads and WesTrack. It was found that for a median depth temperature a temperature correction was required for day time testing to compensate for the temperature gradient within the pavement. Therefore if calculations of modulus are going to be undertaken at times of day other than typically mid-day (11am-3pm), more work will be required on modelling the full temperature with depth profile in the pavement structure to determine the effective temperature of the asphalt layers.

5.6 Calibration of Strain

5.6.1 Validation of Stress Based Approaches

Using the developed relationship between dynamic modulus and pulse loading established from the NCAT testing and validated against the results of both MnRoads and WesTrack, the validity of the two existing frequency with depth models used in literature, the Brown model and the CalMe model was assessed.

Both these models calculate an equivalent loading time with depth. This loading time was then used with the relationship found between field loading time and frequency in the dynamic modulus test to validate the accuracy of both approaches. For this analysis, the calculation the pulse width with depth as proposed by Brown (1977) was for the whole pavement layer (i.e. effectively the mid depth of the layer) while for the CalMe (2008) the depth was taken as both the mid layer depth and the depth at the bottom of the asphalt layer.

To undertake this analysis and to calculate strain, the dynamic modulus was used with the subgrade and fill support layers modulus values for each of the selected Phase II test cells, as shown by Table 5-4 and taken from Timm et al. (2003), to calculate the strain at the underside of the asphalt layer using Linear Elastic Analysis. These strains were then

compared against the typical strain, from Timm (2005), for mid-depth temperatures ranging from 5°C to 45°C for five Phase II test sites. The test sites used in the analysis consisted of those sites from the Phase II study where asphalt thicknesses were greater than 150mm (Constant stress), as the LLAP pavement solution method will only be concerned with the thicker asphalt pavement sections.

The results of the analysis can be found in Appendix D of the report and are summarised in Figure 5-7 following for case (a) using the Brown model and case (b) the CalMe approach, this case with load time taken at the bottom of the asphalt layer.

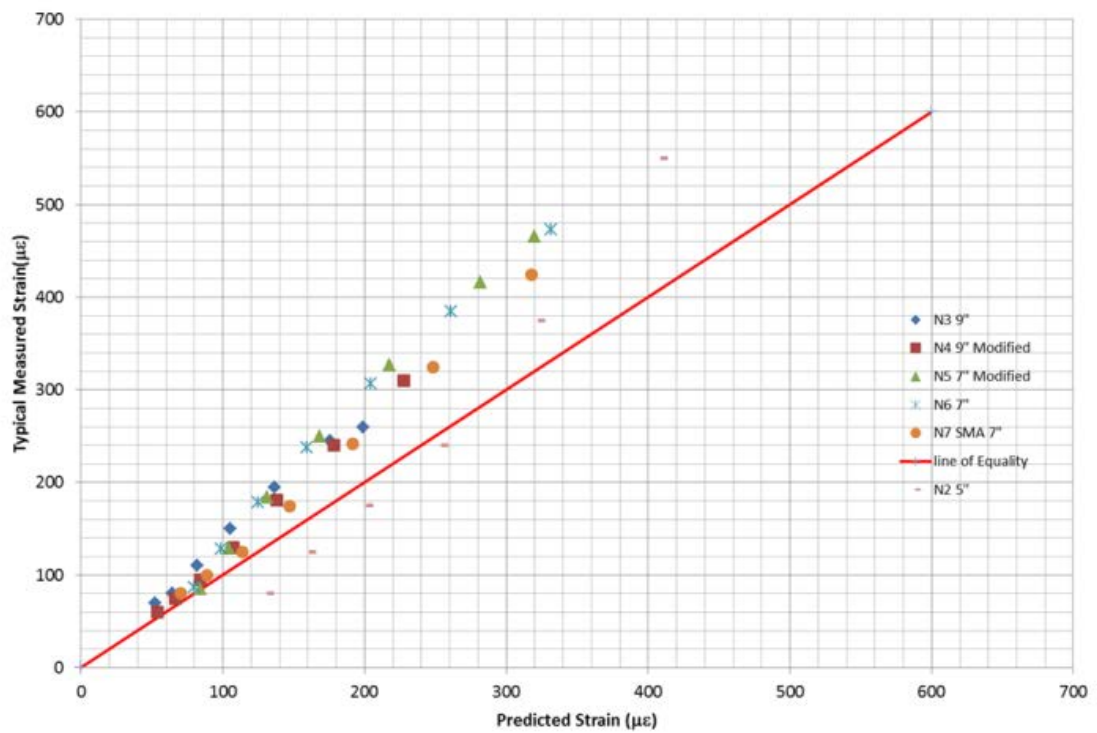


Figure 5-7 Validation of Pulse with Depth Approaches Brown

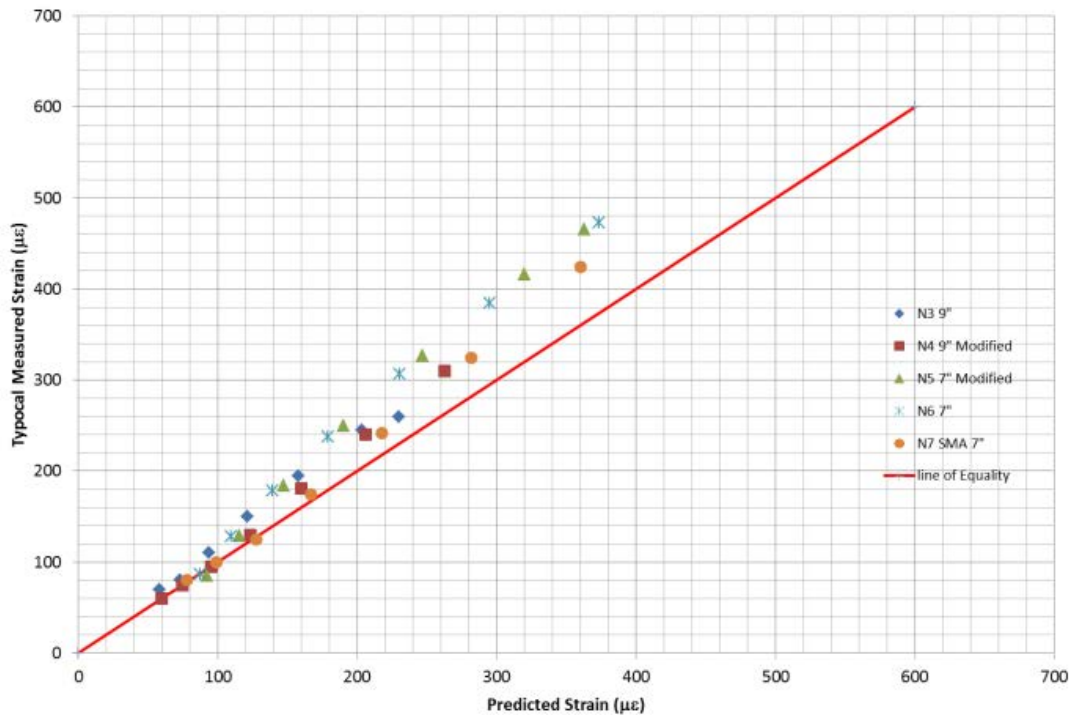


Figure 5-8 Validation of Pulse with Depth Approaches CalMe

As can be seen both of the proposed pulse time approaches, (using a stress pulse), result in an under prediction of strain values. This is due to an underestimate of the time of loading which in turn results in an overestimate of modulus under the moving vehicle. While initially there appears to be a lower bias in the CalMe model than the Brown model, this is solely due to the depth in the CalMe model being taken at the bottom of the asphalt layer in the figure, while the Brown model uses the average time within the asphalt layer.

The results also show for both models that the two thicknesses are grouped together, with the 9" pavements being closer to the line of equality than the 7" layers. As in the models the time of load increases with decreasing depth, the results imply that the thickness of the asphalt layer may not be as important in determining the response of the pavement under a moving load as both the Brown and CalMe model imply. Based on this finding it was concluded that a pure calibration of either the CalMe model or the Brown Model was not warranted, as there appears to be an incorrect assumption in how both models determine the effect of depth on loading time.

5.6.2 Numerically Optimised Approach

Given both the Brown and CalMe models did not appear to effectively model both the time of load and the effect of frequency with depth, a fully unconstrained optimisation approach was run to determine whether better agreement could be achieved between the measured and predicted strain. In the unconstrained optimisation the slope of the load pulse, the

dynamic/static ratio and the surface contact length were all allowed to be unconstrained to determine the optimal solution.

That is, the time of loading was allowed to be optimised as a function of depth, by the following relationship:

$$t_p = \frac{a + bh}{v} \quad \text{Equation 5-9}$$

Where a is the calibration coefficient for the effective length of the load pulse and b is the effect of depth on the load pulse, t_p and v are as before the time of loading and the velocity of the design vehicle.

The results of the fully unconstrained optimisation can be seen in Figure 5-9 following for the equivalent layer approach and Figure 5-10 for the multi-layer pavement.

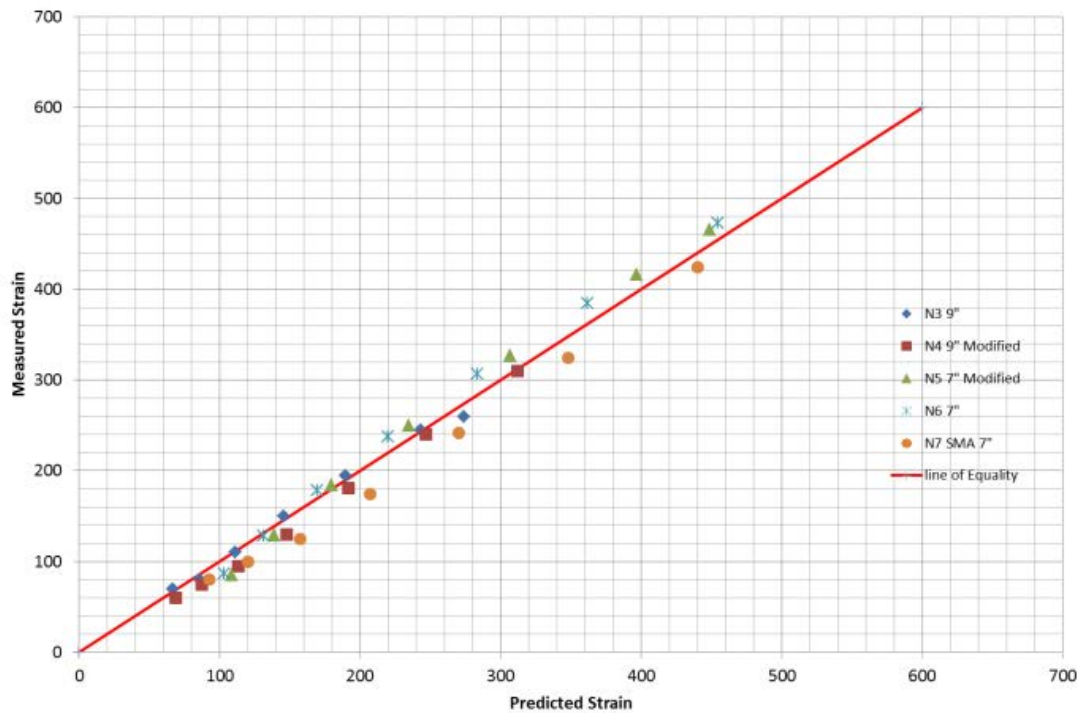


Figure 5-9 Unconstrained Optimisation Equivalent Layer

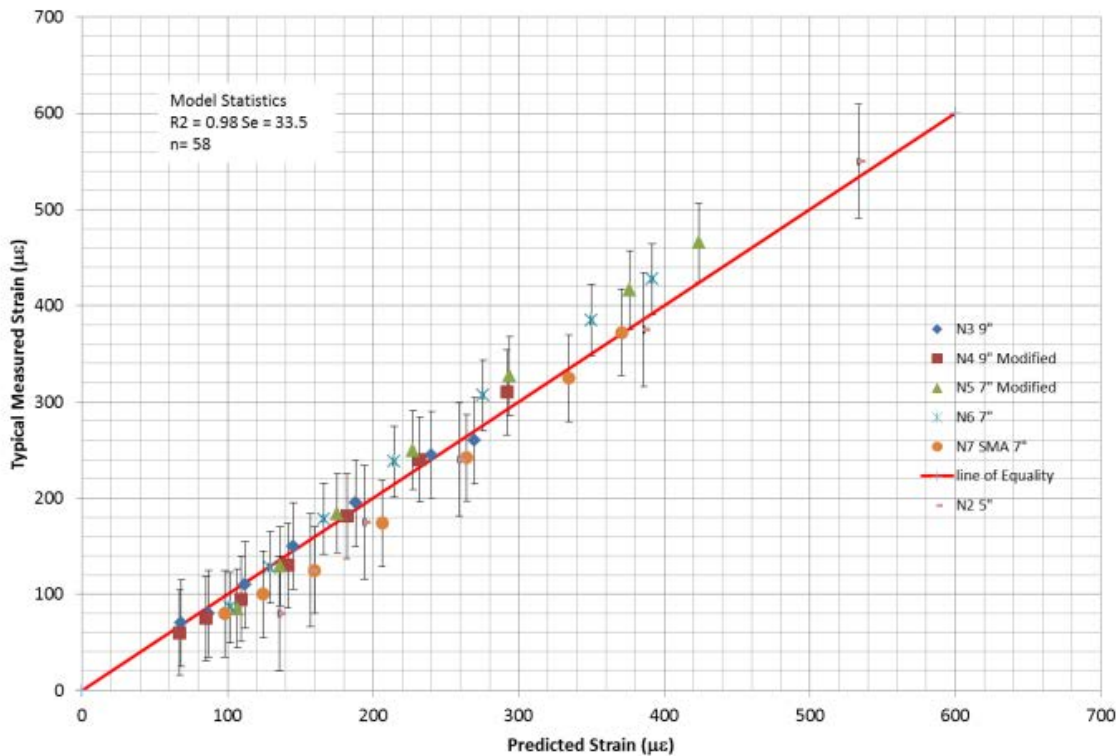


Figure 5-10 Unconstrained Optimisation Multilayer

The results of the equivalent layer analysis show that an extremely high correlation was achieved with the unconstrained model, with no bias observed between the measured and predicted values.

Surprisingly, the optimisation found that thickness of the asphalt layer played little to no part in determining the effective frequency, with the slope value (b) approaching 0. The results also found that the wave length of the pulse on the surface of the pavement was significantly larger than would be predicted by any stress pulse model, at 1.79m. Vehicle dynamic effects were determined to have little to no effect on measured response, with the optimisation determining a constant of 1.

At first, these results were surprising as they are contrary to current design procedures. However, if the results are compared against the findings and recommendation of Coffman back in 1967, remarkably similar results have been obtained. Remember that Coffman found that a vehicle acts as a cyclic load with a wave length of 6 feet and that using higher frequencies in the upper most layer and lower frequencies for the lower layers does not appear justified. His findings are identical to the findings of the optimisation of 1.79m and depth has no effect on determining the effective frequency.

The primary difference in the approach of researchers such as Brown against that of Coffman was that Coffman used deflection (strain) to determine the load pulse, while the

approach of Brown and others used stress. The results show that when using loading time in a pavement to evaluate the results against laboratory determined modulus, the time of loading should be considered as the time of loading of the strain pulse, not the commonly used stress pulse.

From this it is recommended that a cyclic load of 1.8m should be used to determine the loading time in a full or partial depth asphalt pavement (>125mm) and a constant frequency be used for all thicknesses.

$$t_p = \frac{1.8}{v_m} \quad \text{Equation 5-10}$$

Where;

v_m is the vehicle speed in ms^{-1}

The result of this analysis was then extended to that of a multi-layer asphalt pavement, Figure 5-10. The results confirm the single layer findings that time of loading within an asphalt pavement should be a constant for a given vehicle speed. The results show that the use of a multilayer asphalt pavement results in a small change in the goodness of fit of the model and little change in the bias of the results by using a constant loading time in a multilayer asphalt pavement. While the results show that multilayer asphalt pavements can be accurately modeled in a linear elastic code to calculate strain under a moving load, the model is sensitive to the chosen layer thicknesses and more work is required on determining both the appropriate sub-layering of multilayer asphalts and the effect of temperature profiles within the sub layering.

Based on this analysis it is recommended that a constant frequency be used for all layers of asphalt in a multi-layer asphalt pavement and until the question of sub layering and temperature with depth profile is answered, the effective modulus of the combined asphalt layers be used for the purpose of design.

5.7 Use of Australian Dynamic Modulus Master Curves to Predict Strain

5.7.1 Calculation of Modulus

It has been identified that for Australian mixes at higher temperatures and low rates of loading there can be a difference between the modulus of asphalt in tension and compression due to the stress susceptibility of asphalt. For normal operating conditions this difference is negligible. However, at higher operating temperature stress susceptibility begins to have an influence on modulus. In typical, full or partial depth asphalt pavement the effect of confinement under loading is compressive. This phenomenon is shown in the results of FWD testing at NCAT, Westrack and MnRoads where the FWD stiffness has a limiting value of approximately 1000MPa. Examination of the Australian mixes shows that

the same limiting value appears when the asphalt is tested at confining pressures of approximately 200kPa.

Therefore it is not recommended for modelling at higher temperatures (>30°C), that modulus values determined from tensile, flexural or test without confinement tests be used for the purpose of pavement design. It is recommended that modulus be determined based on the results of compressive tests with approximately 200kPa confinement.

As the dynamic modulus master presented in Chapter 4 were all developed using the results of unconfined testing, which as demonstrated, will not match reality at higher temperatures and to match reality at higher temperatures and slower rates of loading confining pressure of approximately 200kPa must be used. To accomplish this, the confidence based master curves of Chapter 4 were recalculated using the results of the confined testing conducted at 200kPa confinement pressure, the results of which are shown in Table 5-5. It is recommended that these values be used for the purpose of design.

Table 5-5 Master Curve Fitting Parameter

Nominal max. Size(mm)	Binder Type	Master Curve Sigmoidal Fitting Parameters					
		β	γ	δ	Confidence Level		
					α		
					50%	75%	95%
14	C320	1.878	0.043	0.706	2.528	2.467	2.379
	AR450	1.860	-0.023	0.735	2.489	2.435	2.357
	A15E	1.820	0.104	-0.678	2.529	2.487	2.426
	Multi	N/A					
20	C320	1.715	0.157	0.818	2.659	2.622	2.569
	AR450	2.328	-0.454	0.647	2.083	2.051	2.005
	C600	2.363	-0.465	0.658	2.079	2.041	1.985
	Multi	N/A					

Combining the angular frequency conversion with the stress pulse relationship obtained from the NCAT test results gives the following relationship (Equation 5-11) between vehicle speed (in km/hr.) and dynamic modulus test frequency.

$$f_{dm} = 0.0246v \quad \text{Equation 5-11}$$

Where;

v = vehicle speed in kmhr^{-1}

f_{dm} = frequency in dynamic modulus test

5.7.2 *Speed Incorporated Design Modulus Charts*

The effect of the strain pulse and frequency conversion can now be easily incorporated into a series of curves for each mix group.

Figure 5-11 to Figure 5-16 following show the Nomographs for the 95th percentile confidence interval for the six subgroups of Australian mixes.

It needs to be noted that these charts represent an equivalent stiffness to obtain strain under a moving vehicle. As such, the modulus is a converted modulus which more closely represents the relaxation modulus of the mix. It would therefore be technically incorrect to refer to these charts as dynamic modulus charts.

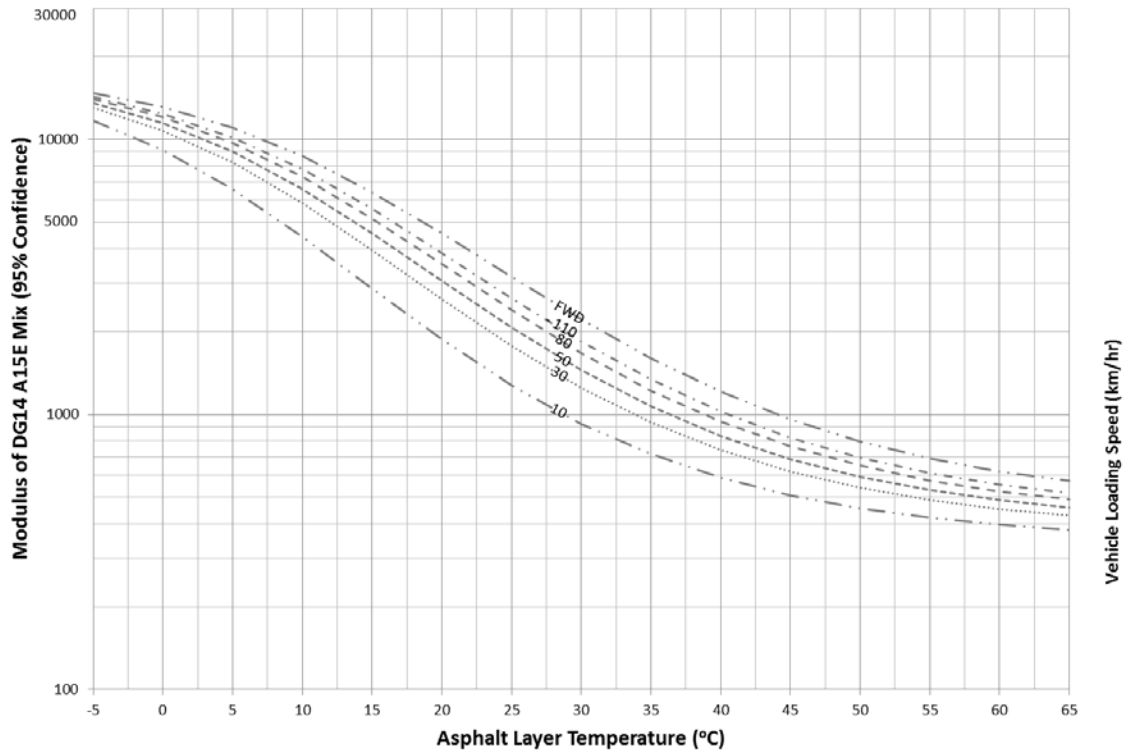


Figure 5-11 Design Modulus Chart DG14 A15E

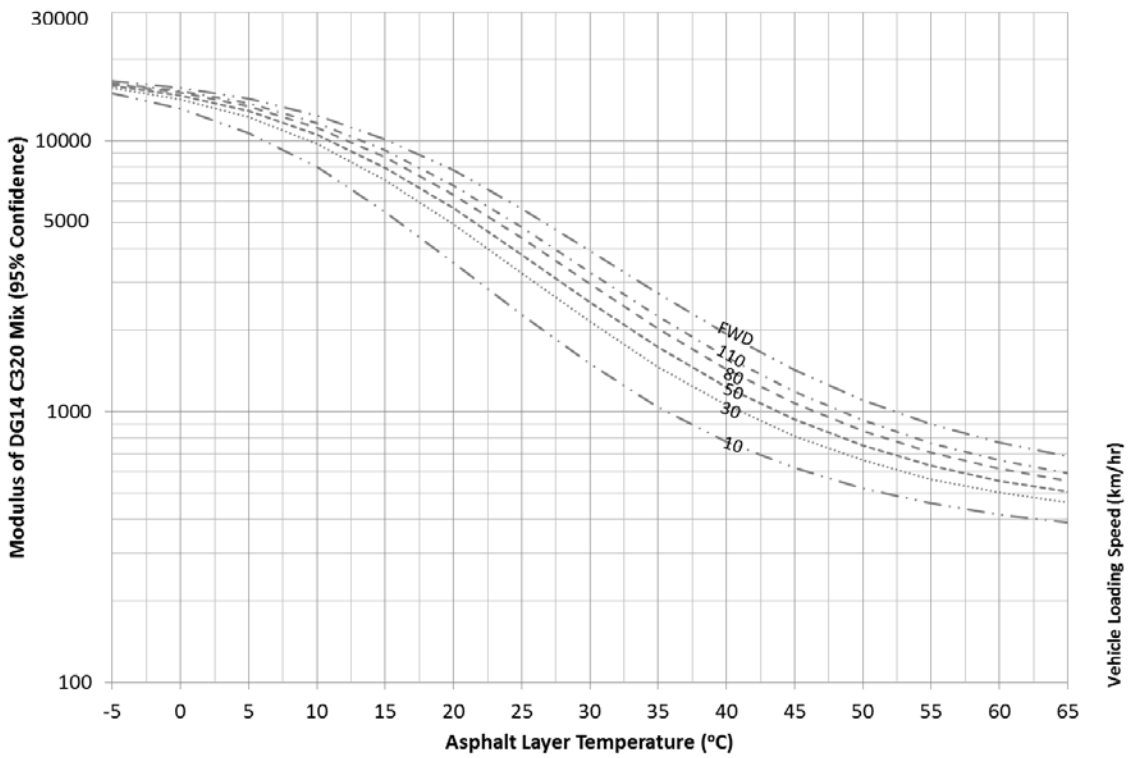


Figure 5-12 Design Modulus Chart DG14 C320

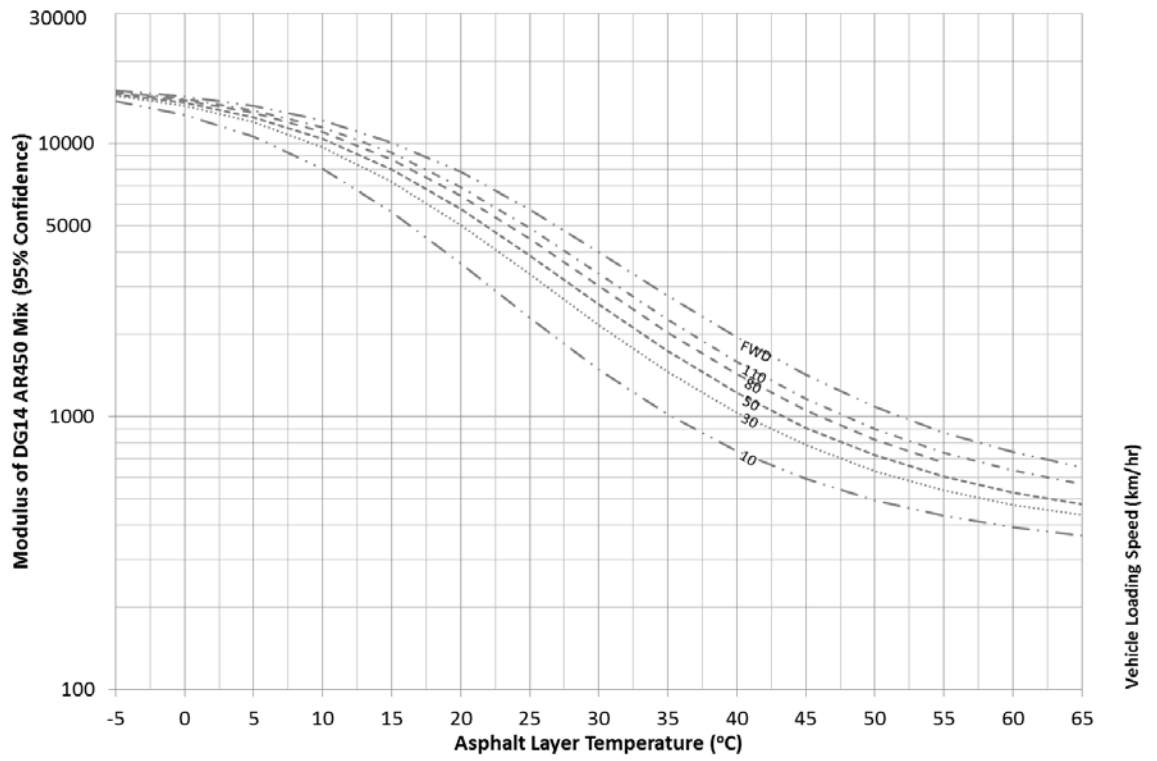


Figure 5-13 Design Modulus Chart DG14 AR450

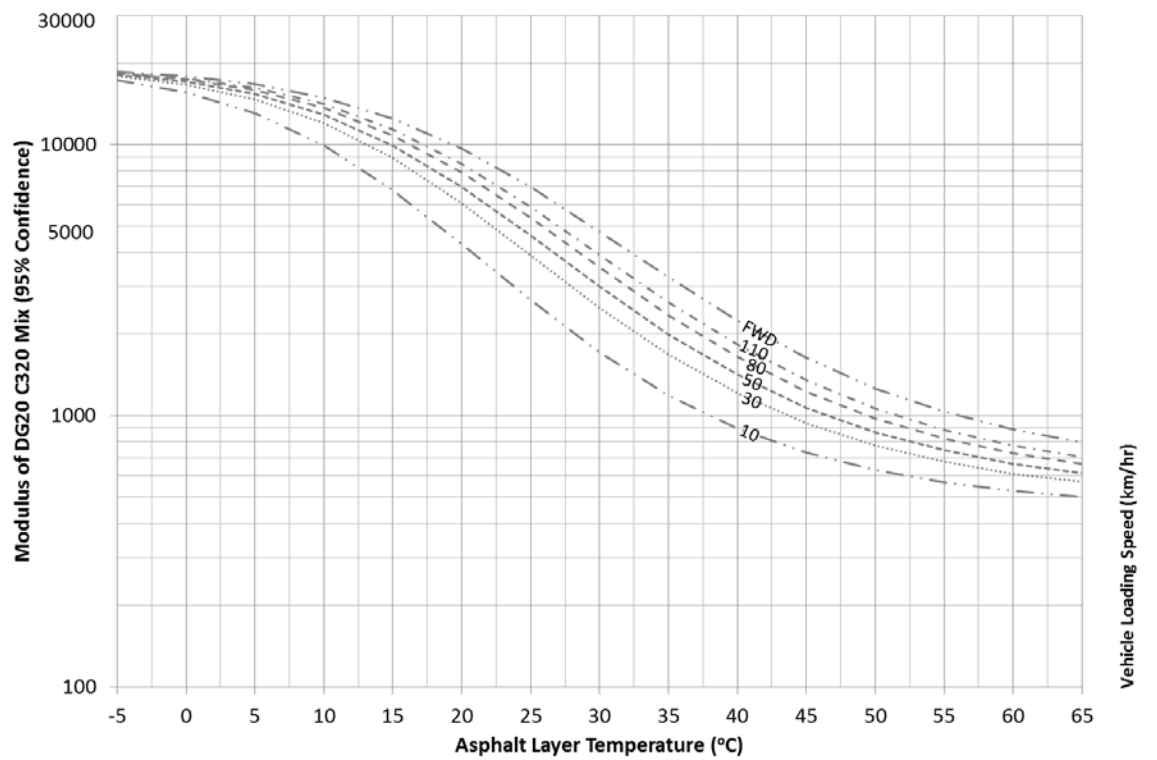


Figure 5-14 Design Modulus Chart DG20 C320

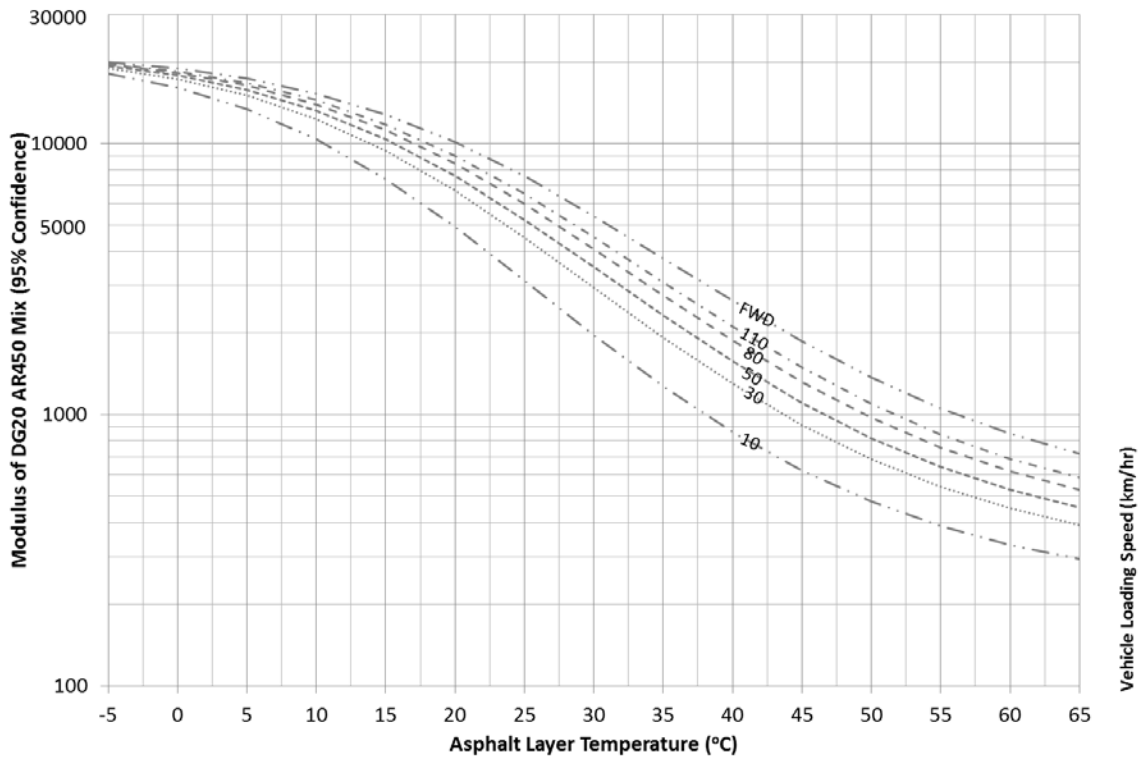


Figure 5-15 Design Modulus Chart DG20 AR450

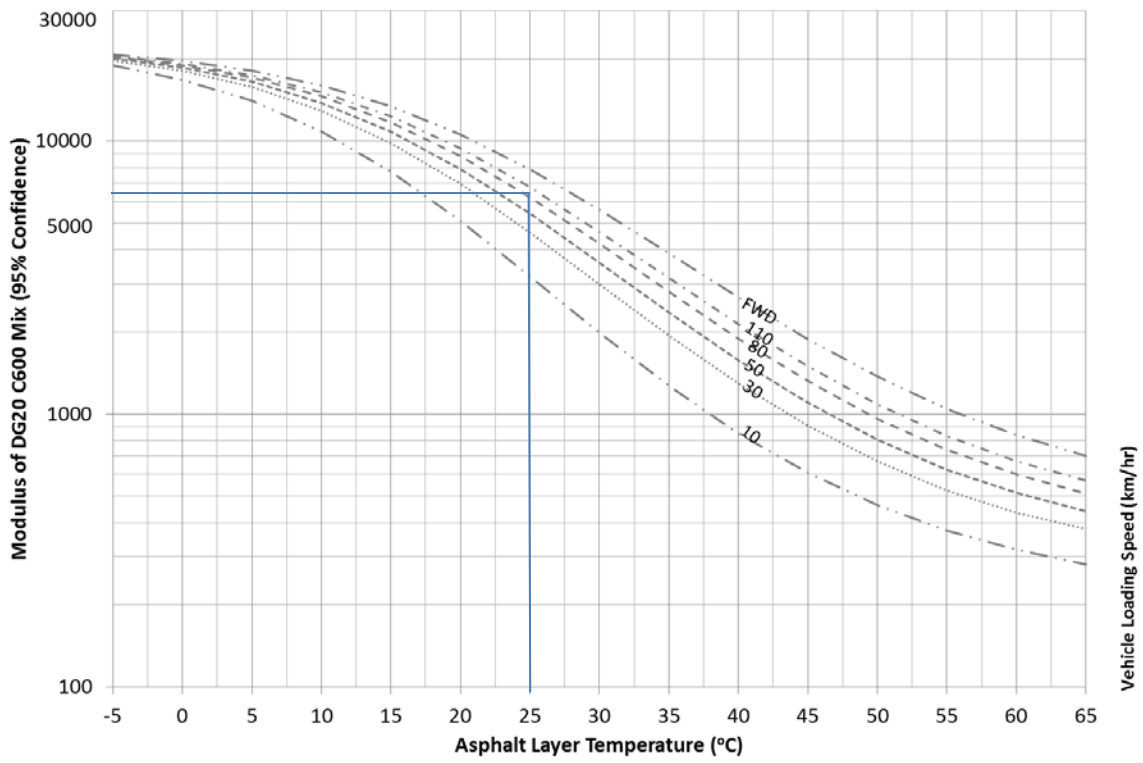


Figure 5-16 Design Modulus Chart DG20 C600

5.8 Summary and Recommendations

The analysis of dynamic modulus test results from NCAT, MnRoads and WesTrack, against field modulus determined from FWD testing, found that frequency in the dynamic modulus test should be considered as an angular frequency and that a shift of $1/2\pi$ on the frequency axis will allow the use of dynamic modulus values to determine the modulus resulting from a pulse loading in the field. Using this conversion it was found that dynamic modulus results at 5.3Hz ($1/(2\pi \cdot 0.03)$) could be used to accurately predict the modulus determined from FWD loading with a pulse width of approximately 0.03seconds over a wide range of temperatures. The results of the optimisation found that the use of the mid-layer depth resulted in a slight underestimation of the effective asphalt layer modulus for day time testing and that if mid-layer depth is used a correction of +2°C is required to correct for the average temperature within the asphalt layers. Therefore, if modulus calculations are going to be undertaken at times of day other than typically mid-day, more work on modelling the full temperature with depth profile in the pavement structure would be needed to determine the effective temperature of the asphalt layers.

Using the pulse frequency conversion and temperature correction obtained from comparison with FWD testing, the multi-variable optimisation found that dynamic modulus could be used to accurately predict strain under a moving load using layer elastic analysis when time of load is corrected for the effective load length. It was found that when computing strain under a moving load, contrary to some published recommendations, the thickness of the asphalt layer was insignificant in determining strains. It was also found that the time of loading is more related to the length of the deflection response than the current approach of the use of a stress pulse.

The results of the optimisation on the thick asphalt sections of Phase II NCAT support the recommendation of Coffman that a vehicle acts as a cyclic load with a wave length of six feet, with the optimisation determining the wave length of 1.79m. Based on these findings the following frequencies in the dynamic modulus test are recommended for use in pavement design with an equivalent combined asphalt layer.

Table 5-6 Recommended Frequencies

Speed (km/hr.)	50	60	70	80	90	100	110
Recommended Frequency Dynamic Modulus [E*] Test (Hz)	1.2	1.5	1.7	2.0	2.2	2.5	2.7

The analysis showed that multi layers were sensitive to the chosen sub layer thicknesses and more work would be required on determining both the appropriate sub layering of multilayer asphalts and the effect of temperature profiles in the sub layering, before a

multilayer approach should be recommended over the use of the equivalent asphalt layer approach.

The analysis has shown that there is a direct link between laboratory modulus and strain under a moving vehicle and dynamic modulus can be used in the structural design of LLAP's. The use of the master curves will enable the determination of either threshold strains or cumulative distribution of asphalt strain in LLAP structures as a function of the climatic conditions and the traffic distribution spectrum. This calculated strain will provide the means to rationally evaluate the compliance of candidate LLAP structures with the limiting threshold strain or cumulative strain distribution empirically derived from the evaluation of international LLAP's.

6 Inter-Conversion of Current Australian Modulus Test Methods

6.1 Background

A fundamental parameter required for the characterisation of an asphalt mix in any mechanistic design procedure is the modulus or stiffness of the material. While this study has used the dynamic modulus test and master curves, traditionally, in Australia two methods have existed for the measurement of the modulus of an asphalt mix, the resilient modulus test and the 4 point flexural modulus test. Additionally, the Austroads Pavement Design Guide is based on the 2 point bending flexural modulus testing.

While all these tests measure modulus (or stiffness) of the mix, none have the same definition of frequency (or time) or use the same loading shape. The different load shapes and definitions of frequency result in different modulus values being obtained for the same “frequency” and temperature for each test method. The different results obtained by the different test methods has led to confusion on how to report and convert modulus results obtained from one test method to another or convert to a field modulus and if commonality is not obtained could lead to confusion in the use of the APS-fL procedure.

The mathematics behind the conversion between the different modulus tests is complex and open to interpretation. Therefore instead of trying to solve the complex mathematics, this chapter looked at the direct inter-conversion of the modulus tests and recommends a standard approach to converting and reporting modulus results

6.2 Introduction

Asphalt is a viscoelastic material whose response under load depends on the rate of loading and the temperature. Stiffness, being one of those responses is one of the most important properties of asphalt for pavement design. The concept of stiffness for asphalt mixes was introduced by Van der Poel (1954) who distinguished stiffness from the modulus (E) of elasticity. Various properties of asphalt mixes can be used to characterise the stiffness of asphalt mixes, including; creep compliance, relaxation modulus, complex modulus and resilient modulus.

Since various ways exist to measure stiffness and the stiffness measured in the laboratory is often used as an input into pavement design to predict response under load, an accurate way is needed to convert between different laboratory tests to convert to field stiffness and to accurately predict the response in a multi-layer pavement.

Australia uses two common tests for the characterisation of asphalt mixes and Austroads has placed high priority on the retention of these methods. While Australia has two test methods and the AGPT002 (2012) is based on a third, a standard reporting method has not been established. Adding to this, this project has for reasons stated in chapter 2, introduced

a fourth test, the dynamic modulus test. To avoid confusion the inter-conversion between dynamic modulus, resilient and 4 point flexural and 2 point flexural modulus need to be understood.

As shown in Section 5, the APS-fL project developed an inter-conversion between dynamic modulus and field response under a pulse load. However, as stated previously the dynamic modulus test is not the standard test procedure used in Australia. If a conversion can be achieved between the dynamic modulus test, resilient modulus test, and the 2 and 4 point flexural beam tests direct conversion to field response can be undertaken using either the dynamic modulus test and standard Australian tests and the significant benefits offered by the dynamic modulus test can be employed with understanding of the relationships.

6.2.1 Scope of Study

Two principal hypotheses exist as to why there are differences between different modulus test methods; (i) stress susceptibility, where tensile loads result in lower stiffness than compressive loads and (ii) different definitions of frequency, where some tests are undertaken in the frequency domain and some are undertaken in the time domain.

This study will examine the validity of the two hypotheses, with regards to Australian mixes and test methods and determine the conversion, if any, between the common Australian test methods.

The initial portion of this chapter presents a summary of the background and methods for the determination of stiffness or modulus of asphalt mixes. The next portion examines the results of individual resilient and flexural modulus tests against those of the dynamic modulus test. The final section uses the conversions found from the individual tests to validate the single temperature/frequency corrections across the full temperature frequency space using master curves for, flexural modulus (2 point bending and 4 point bending), resilient modulus and dynamic modulus.

6.3 Theoretical Background

6.3.1 Observations

It is commonly observed that dynamic modulus results are higher than both resilient and 4 point bending modulus results, as shown in Figure 6-1 following for a typical Australian mix.

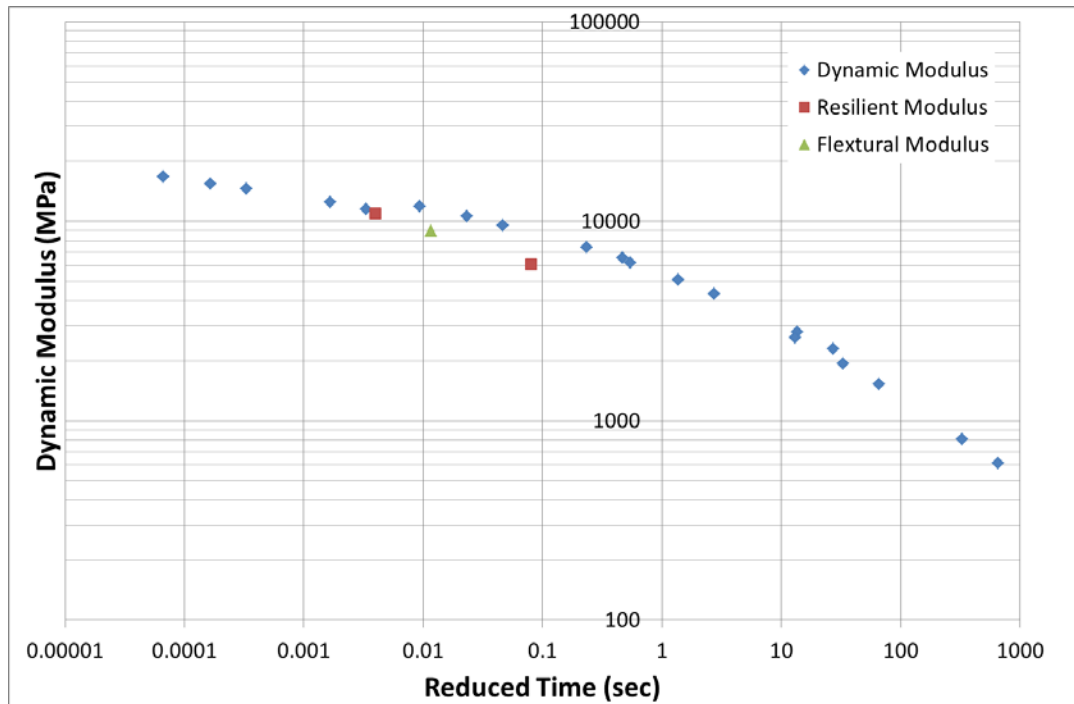


Figure 6-1 Modulus Comparisons

To explain the differences between resilient, flexural and dynamic modulus two explanations are generally used:

- Dynamic modulus, as a compressive modulus results in higher values than the resilient modulus test as a tensile modulus, due to stress susceptibility of the asphalt mix. That is the bulk stress in the dynamic modulus test is higher.
- Time of loading is not directly comparable as time of loading in the resilient modulus test needs to be shifted to the frequency domain. (I.e. appropriate frequencies need to be selected to convert loading time in the resilient modulus test to angular frequency in the dynamic modulus test.)

6.4 Differences in Test Results

6.4.1 Stress Susceptibility

Many researchers have concluded that the difference between the bending tests, indirect tests and direct compression tests are the results of different modes of loading; flexure, tension and compression respectively, Kim (1992).

Generally asphalt materials are assumed to be linear elastic or linear visco-elastic. While this assumption is true at lower temperature and higher frequency range (Antes et al. (2003)), at higher temperature ranges and low frequencies the assumption may not be valid. This effect was observed by Molenaar (1983) who observed that at temperatures of 35°C and 1 second loading the modulus in compression was double that of the tensile modulus. Additionally,

Pellinen (2001) found that beyond certain strain levels non-linearity (stress dependency) is exhibited by asphalt mixes regardless of test temperature. These two findings would suggest that it would be reasonable to assume that a difference in the modulus determined from tensile and the compressive tests could be due to a difference in the stress (bulk stress) applied to the sample. However, Pellinen also found that at small strain levels (like those used in modulus testing), stress susceptibility was only evident at high temperatures and low frequencies. Additionally, in strength tests the compressive strength of asphalt is significantly higher than the tensile strength.

The assumption that modulus measured in the direct compression tests is higher than that of the tensile tests (flexural fatigue and resilient modulus) due to stress susceptibility, appears to be only justified from the results of large strain tests and strength tests. In large strain test, the modulus of asphalt can be a magnitude higher as a result of changes in the bulk stress applied to the material. The assumption, however, of stress susceptibility being significant at the small strain and mid-range temperatures used in the modulus test appears to be questionable.

6.4.2 Time Conversion

In Physics text books, such as Tipler (1992), the period of loading, T , not t , is simply the period of a harmonic cycle in seconds and may be expressed as:

$$T = \frac{1}{f} = \frac{2\pi}{\omega} \quad \text{Equation 6-1}$$

Where;

- T is the period of the cycle
- f is the frequency of the loading, Hz
- and ω is the angular frequency, rad.s^{-1}

For each of the loading shapes used in the Australian test methods, the period of loading, T , (the period of the cycle) is related to the pulse time, t , however it is not necessarily the same;

- For cyclic loading the period T is the pulse time, t .
- For the case of a harmonic frequency load the period, T , is in fact angular period and, is $2\pi t$

It is hypothesized by some researchers that because of these different periods that comparison of results obtained from one test to another is difficult and in some cases results do not appear to be directly related. More specifically, it is not always evident whether a test sets up a cyclic response or a harmonic response.

There is currently significant debate amongst researchers on how frequency is related to time in the dynamic modulus tests. The two primary schools of thought are the angular frequency approach vs. the pulse frequency approach. Researchers such as Dongre et al. (2006) recommend the angular frequency approach, $t = 1/\omega$, while researchers such as Katicha et al. (2007) recommend the pulse frequency, $t = 1/f$, approach.

It appears that the earliest use of the angular frequency approach, $t = 1/\omega$, in asphalt mixes was the work undertaken by Papazianin (1962) at the First International Conference on the Structural Design of Asphalt Pavements. This approach was then adopted by Shell for their development of a ME pavement design procedure, which was subsequently adopted as the basis of the AGPT002 (2012) characterisation method. However, the angular frequency approach has not been universally adopted with the US MEPDG following the $t = 1/f$, approach.

Dongre (2006) found that the exact solution of the IFT to calculate relaxation modulus from the dynamic modulus test was $t = 1/\omega$, this is somewhat contrary to the early recommendations of Van der Poel (1954) who suggested the conversion was only approximate.

Notwithstanding this, Dongre (2006) did not establish that the testing in dynamic modulus test was an angular frequency, which would require the above conversion. The issue is still not resolved amongst some researchers.

What is important in the Australian case is to establish how to compare the modulus results determined from the various test methods used in practice and relate them to a standard measure and field stiffness.

6.4.3 Stiffness in the Austroads Pavement Design Guide

The modulus values used in the AGPT002 (2012) have their origin in the set of Nomographs published by Shell (1978). These Nomographs are a combination of two Nomographs developed by Vander der Poel (1954), for determining the stiffness of binder and Bonnaure et al. (1977) for determining the stiffness of a bitumen mix.

In developing the binder stiffness nomograph Van der Poel (1954) stated that the stiffness of the binder could be treated as either; the inverse of the creep compliance at a loading time, t , or the dynamic modulus at an angular frequency, $\omega = 1/t$. What is important here is understanding that the conversion is a conversion between dynamic modulus and stiffness modulus (inverse of creep compliance), the conversion is a conversion to time domain and that the conversion is only an approximate conversion (Van der Poel). However, other researchers such as Dongre et al. (2006) have stated that the conversion is an exact conversion.

In developing the mix stiffness nomographs, Bonnaure et al. (1977) used the modulus determined from extensive 2 Point Bending on Trapezoidal Beams (2PB-TR) with a sinusoidal load. To connect the bitumen stiffness to the asphalt mix modulus Bonnaure et al. (1977) used the stiffness modulus of the bitumen from the Van der Poel Nomograph. The result is that the frequency used in the nomographs is an angular frequency, $\omega=1/t$.

In recent developments of the AGPT002 (2012) there is a general assumption that the 4 Point Bending test on Prismatic Beams (4PB-PR) measures the same modulus as the 2PB-TR,(Jameson (2001)). This assumption was supported by comparison testing conducted in Europe by Francken et al. (1994) which showed that 4PB-PR and 2PB-TR modulus values achieve results which are in good agreement provided that: tests are performed at small strain and the sample geometry and mass are taken into account in the calculation of modulus, Francken. An Austroads test method to perform this type of small strain complex modulus measurement in line with European specifications has recently been introduced (AGPT/T274). Whether the flexural modulus calculated as part of fatigue experiments in the past using the AGPT/T233 (typically at high strain levels) provides modulus values equivalent to these small strain experiments is not known.

6.4.4 Current Modulus Classification Methods in use in Australia

For the past two decades in Australia, the predominant method used for determining the modulus of asphalt materials for both pavement thickness design and for material characterisation has resilient modulus test (AS 2891.13.1-1995) using Indirect Tensile load on a CYlindrical sample (IT-CY). Under this test method the modulus is defined as the ratio of the applied stress to the recoverable strain. More recently the 4 Point Bending on a PRismatic beam (4PB-PR) (AG:PT/T233 2006), has gained favour in some specifications (Vic Roads) for characterisation of Australian mixes and by researchers such as Denneman et al. (2013) who have begun to report modulus master curves developed from the 4PB-PR test. However Denneman (2013) has used sinusoidal loading over the common haversine load used in Australia. In addition the AAPA APS-fL project introduced the Direct Compression test on CYlindrical samples (DC-CY) (AASHTO TP79) for the determination of modulus and the recent introduction of EME2 mixes has brought the 2 Point Bending TRapezoidal 2PB-TR (EN12697-24) test to Australia.

To successfully implement different classification methods in practice, the differences in characterisation of modulus obtained from the IT-CY, 4PB-PR, 2PB-TR and DC-CY modulus tests need to be fully understood. Without a thorough understanding of the differences between the modulus tests the implementation of four systems modulus classification into the one material classification and design system of would be confusing for designers and specifies and could diminish the technical credibility of the specifications, design system and testing standards.

6.4.5 Previous Research

Internationally, research such as the studies by Dongre et al. (2006), Kim et al. (1995) and Adhikari et al. (2008) have reported differences between the results of resilient and dynamic modulus of between 30 and 100%. Dongre (2006) concluded that the difference in the resilient modulus test and the dynamic modulus test was a result of a different definition of time in both tests. However, while Kim et al. also found that overall resilient modulus values were generally lower than the dynamic modulus results, the researchers concluded that the difference between the dynamic modulus and resilient modulus was a result of the dynamic modulus being conducted in the compressive mode while the resilient modulus was undertaken in the tensile mode.

In chapter 5 it was found that the differences between field loading and dynamic modulus testing (DC-CY) was due to differences in the definition of time and that the dynamic modulus test should be considered an angular frequency with $t = 1/2\pi f$ when compared to the time of loading imparted by a vehicle's single pulse load.

6.5 Materials and Test methods

6.5.1 Modulus Test Methods

Throughout the world, the characterisation of asphalt mixes has been undertaken using a variety of different loading forms, such as; sinusoidal, haversine, pulse, square and triangular wave forms with and without, rest periods, all used in an attempt to simulate the response of a pavement to vehicular loads. Internationally, the most commonly used wave forms to characterise asphalt materials are, the sinusoidal and haversine waves (Huang (2004)), while in Australia it is the quasi haversine step load of the IT-CY resilient modulus test.

For the four test methods being examined in this study the following describes the wave forms used in the test method.

- Resilient Modulus (IT-CY), AS 2891.13.1 (1995), test uses a standard reference test condition temperature (25°C) and a single pulse load of 0.04seconds rise time, with a controlled load.
- Flexural Modulus (4PB-PB), uses a standard load frequency of 10Hz, with a continuous load (AG:PT/T233 (haversine) AG:PT/T234(sinusoidal)) and controlled displacement
- Direct Compression on Cylindrical (DC-CY) samples (ASHTO TP62 or AASHTO TP79) uses a continuous haversine load with a target strain within the sample
- Flexural 2 Point Bending on Trapezoidal (2PB-TR) samples (EN12697-24) uses a continuous sinusoidal load and controlled strain within specimen.

Clearly the loading shapes used in the test methods are different and all cannot be the same as per the assumption of Bonnaure et al. (1977).

6.5.2 Strain in Beam Fatigue

Another complication occurs in the 4PB-PR (AG:PT/T233) used in Australia, which is a controlled displacement test with a haversine load. In the controlled deflection test, the deflection input is haversine, which bends the beam with the same peak-to-peak magnitude, at least initially, as the sinusoidal test except in one direction only. However, due to the viscoelastic nature of asphalt the beam creeps under load. This creep results in permanent deformation in the initial loading cycles. As a result of this deformation in the test the neutral axis position of the beam also shifts down. After a few loading cycles, typically less than 50, the neutral axis in the centre of the beam shifts down and as a result the haversine load has changed to a sinusoidal load, with the beam being push and pulled in the test. This is shown conceptually Figure 49 following.

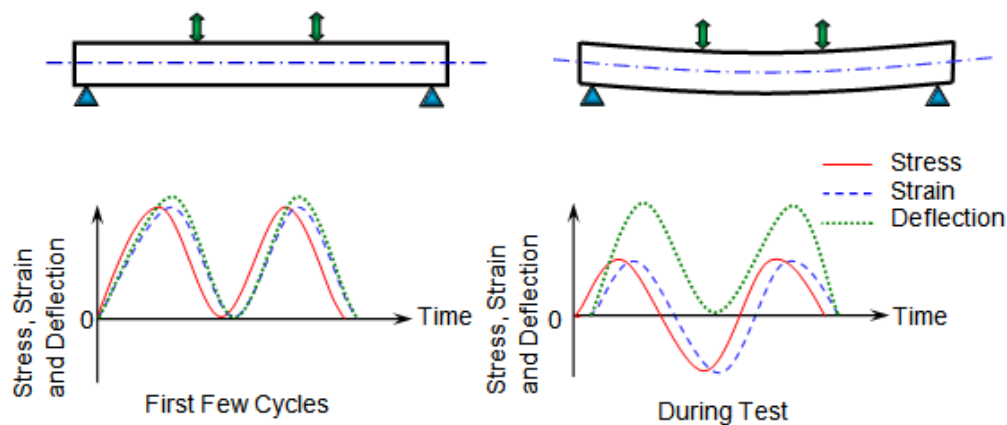


Figure 6-2 Flexural Fatigue Test (after NCHRP 9-44(2013))

The figure shows conceptually what happens in the beam fatigue, that due to the shifted position of the beam, the developed stress/strain immediately changes from haversine, tension only, to sinusoidal, alternating tension and compression. Due to the change from tension only to alternating tension and compression the magnitude of the strain developed is only half that of the initial strain applied, at the beginning of the test, as shown in Figure 6-2. At the end of the test, when the load is removed, the beam remains in the bent position showing permanent deformation.

6.6 Comparison of Modulus Tests

6.6.1 Stress Dependency

If the difference between dynamic modulus and resilient modulus is explained by the difference in the mode of loading (tensile, flexure or compressive), then at the test temperature and the strain levels applied in the modulus test the mix response should be nonlinear and the asphalt mix should exhibit stress susceptibility behaviour.

So the question is “Does stress dependency exists in asphalt mixes under the loading conditions used in the resilient modulus test used in Australia”? To answer this, the results of the dynamic modulus test performed at different confining pressures (different bulk stresses) were examined to see when the typical Australian asphalt mixes exhibit stress dependency. Figure 6-3 following; shows the dynamic modulus plot of a typical Australian mix tested at 4 confining levels (0, 50, 100 and 200kPa) in this case an AC14 AR450 mix.

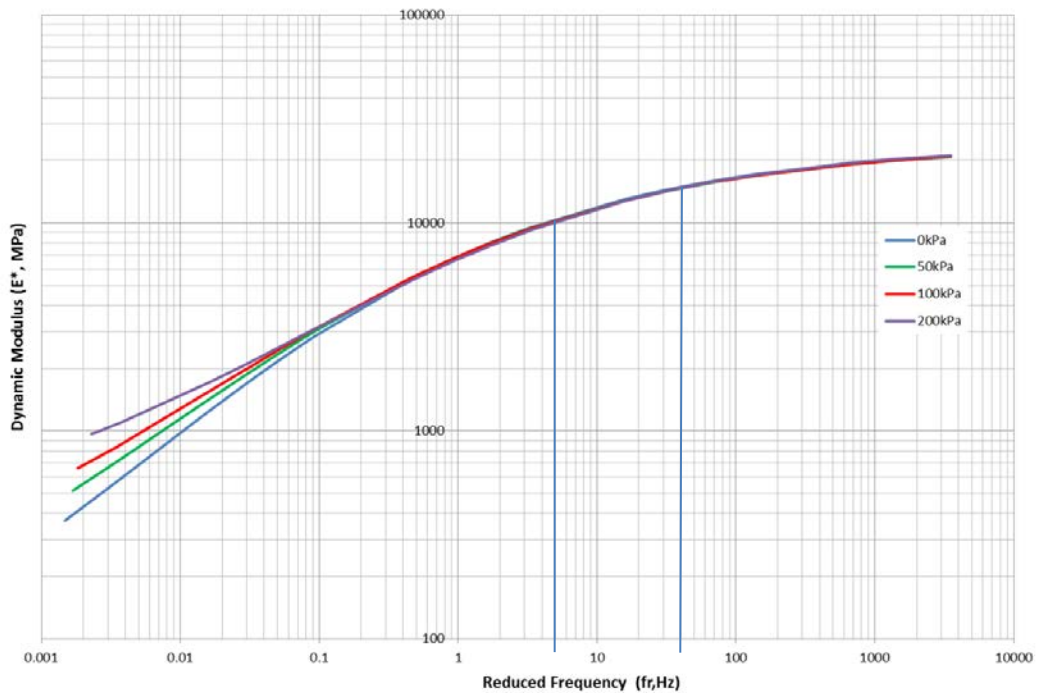


Figure 6-3 Stress Susceptibility

The examination of the results show that at the standard Australian reference temperature of 25°C the AR450 mix only begin to exhibit stress susceptibility when the reduced frequency of loading falls below approximately 0.1Hz, or a haversine pulse width of 10 seconds in the dynamic modulus test. By comparison, the conditions used in the resilient modulus in Australia (25°C and rise time of 40msec), which equate to a frequencies of 12Hz, ($1/t$) or 2Hz ($1/2\pi t$) respectively, using the two frequency assumptions which are currently being debated. It can be seen in Figure 6-3 that at these set frequencies (and the 25°C test temperature),

there is little no difference in the measured modulus in the dynamic modulus test. This result indicates that under the standard Australian test condition used in the resilient modulus test, stress susceptibility may have little to no effect on the modulus of typical Australian mixes.

The implication of this is that under the standard test conditions Australian asphalts are not stress susceptible and the mode of loading (tension, compression or bending) will have little to no effect on the measured modulus. That is, the mode of loading cannot explain the differences obtained between the test methods.

This finding is supported by those of Kallas (1970) and Khanal et al. (1995) both of whom found little differences, if any, between the modulus of asphalt under harmonic compressive and tensile loading except at low frequencies and high temperatures. This supports the view of Dehlen (1968) who concluded that non-linearity was not significant for practical design of pavements.

6.6.2 Resilient to Dynamic Modulus

In order to compare between the dynamic and resilient modulus a cross referencing of Fulton Hogan’s database of resilient and dynamic modulus testing undertaken since 2006, was carried out and resulted in 46 mixes with corresponding resilient (IT-CY) and dynamic modulus tests(DC-CY). This database has an extensive range of aggregate types from throughout Australia and covers the full range of conventional and polymer modified binders used in Australia.

To cover the two proposed loading definitions debated by researchers of:

$$t = \frac{1}{f} \text{ or } t = \frac{1}{\omega} = \frac{1}{2\pi f} \quad \text{Equation 6-2}$$

Two frequencies in the DC-CY dynamic modulus were considered, 12.5 and 2Hz for the 0.08sec loading time of the Australian IT-CY test.

Table 6-1 following, shows the mix descriptions, measured resilient modulus and the dynamic modulus (DC-CY) at 2 and 12.5Hz of the 46 mixes in the Fulton Hogan database where a comparison could be undertaken. Figure 6-4 following, shows a plot of the dynamic modulus results at 12.5Hz and 2Hz versus the average resilient modulus for each asphalt mix

Table 6-1 Resilient and Dynamic Modulus Results

Mix Description	Resilient Modulus (MPa)	Dynamic Modulus E* MPa	
		2Hz	12.5Hz
AC10 5.7% Mex AP	3674	3653	6392

AC10, 5.7% C450	5174	4586	7653
AC10, 5.7% Mex AP + Sasobit (New)	3705	3558	6017
AC10, 5.7% Mex AP + Sasobit	3812	3675	6441
AC10, 5.7% C320	4673	4579	7959
AC10, 5.7% A10E	2016	1684	3852
AC10, 5.7% A15E	1988	2595	4333
AC10, 5.7% Multi 1000	5024	4982	7299
AC10, 5.7% Multi 600	4625	3856	4692
AC10, 5.7% A20E	2521	2104	4136
AC10, , 5.7% A35P (EVA)	4406	4877	7565
AC10, 5.7% Mexphalte Fuelsafe	3217	4336	7181
AC10, 5.7% Mexphalte Airport	3783	3653	6392
AC10 LCC Qld.	5739	4978	7854
AC14 R116 C320 Rutherford	5803	4863	8528
AC14 Wallgrove C320	6864	7193	10490
AC20 +AS2150 4.2% C320 (30% Coarse RAP)	8337	7344	10994
DG14 4.72% A15E ex-Crestmead	6192	5308	7645
14H 4.9% C600, Vic	8055	7900	11375
DG20 4.65% C320 25% RAP Qld	7178		8372
SMA14 + FGLS & HL 6.5% C450	4675	4665	7309
AC14 + Hydrated Lime 5.2% C450	5801	6655	10356
AC14 + Hydrated Lime 5.2% C450	6780	6655	10356
SMA10, S50R	2828	2931	5131
SMA10, C320	4117	4304	7462
SMA10, C320	4158	4304	7462
14TCI Base S2, Vic	3412	2919	5654
14TCI Base S1, Vic	4071	4511	7908
14TCI Intermediate S1, Vic	6401	5848	9668
14TCI Intermediate S2, Vic	7052	5973	9649
AC10, 5.7% Mexphalte C	997	694	1005
AC20 WA Base 5.2% 320 with Hydrated Lime " Conforming Mix"	2824	3600	6880
AC20 Base 5.3% BP C320 + Redicote N422 M2B3 "Job Mix"	2936	3163	6002
AC10 5.7% C450	4537	5164	8404
AC14 "C" 6.55% C320	3982	4311	7371
A14 "MD" 6.28% C320	5329	4847	8152
AC14 "VC" 6.62% C320	3996	4510	7325

AC "MD" 6.28% C320	5246	4847	8152
AC14 "VF" 7.4% C320	4446	4847	7819
AC14 "F" 5.9% C320	6879	6997	10226
AC14 5.4% C600	4426	5289	8310
AC14 5.4% AR450	4073	5060	8260
AC14 5.4% C320	4118	4491	7463
AC14 Multi100	5386	5460	8080
AC14 5.4% C1000	7583	6422	9007

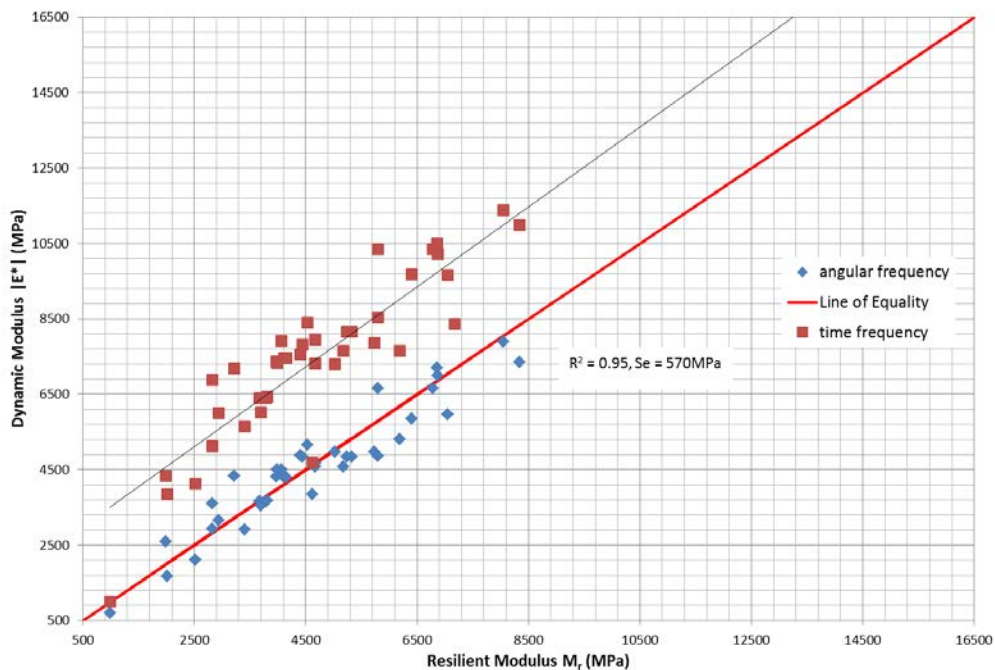


Figure 6-4 Resilient vs. Dynamic Modulus

The results and figure show that a clear and strong correlation exists between the dynamic modulus and the resilient modulus and that the correlation is not mix dependent. The results show that at the cyclic frequency of 12.5Hz the dynamic modulus results, while highly correlated to the resilient modulus are offset by a factor of approximately 2,500MPa, i.e. the results of the dynamic modulus test will be approximately 2,500MPa higher than that of the resilient modulus test. At the angular frequency of 2Hz, the results are again highly correlated but this time centred on the line of equality. The centring on the line of equality indicate that equivalent results are obtained between the dynamic modulus test and the Australian resilient modulus test at a frequency of 2Hz, the angular frequency in the dynamic modulus test.

The results of the comparison of the dynamic modulus frequency against that of the pulse load in the resilient modulus IT-CY test confirm the results found in the comparison to field study that the dynamic frequency should be considered a cyclic frequency. Given that the conversion between IT-CY test and the DC-CY tests is equivalent to that found from the DC-CY test to field study in Chapter 5, it can be concluded that time is equivalent and that:

$$t_{hp} = 2R_t \quad \text{Equation 6-3}$$

Where;

t_{hp} = load duration sections

R_t is the rise time (typically 0.04sec)

and

$$t_{hp} = \frac{1}{2\pi f_{dm}} \quad \text{Equation 6-4}$$

where;

f_{dm} is the equivalent dynamic modulus frequency

6.6.3 *Dynamic Modulus to Flexural Beam Modulus*

Historically, it is known that the Austroads beam fatigue test produces results which are less than those of the dynamic modulus results. The standard test conditions in the Austroads AGPT/T233 method use deflection controlled haversine load with a 10Hz load frequency. The test is also typically run at a displacement resulting in a relatively high strain condition of $400\mu\epsilon$ in the beam specimen. This introduces an additional complexity in comparing the results of the test to those of other modulus tests, which are run in small strain configuration. For this reason, the new Austroads AGPT/T274 method modulus testing is performed at $50\mu\epsilon$ (sinusoidal).

As was established in Section 6.6.1 the reason for the difference in the modulus results cannot be attributed to stress dependency, under the standard loading conditions. Given the 4PB-PR test constantly measures modulus values which are less than that of the DC-CY test a direct conversion between frequencies was not undertaken (i.e. $f_{4PB-PR} = f_{DC-CY}$) and only a frequency conversion was undertaken.

As previously described, the test which the results are based, initially applies a haversine load and after a few cycles the test applies a continuous sinusoidal load. Clearly a continuous sinusoidal load is a different wave shape to the quasi haversine pulse found in field loading or as used the Australian resilient modulus test.

As previously shown the dynamic modulus (DC-CY) test should be considered angular frequency test, when compared to single pulse loads such as in the IT-CY or field loading. What is not known is the conversion which should be applied between the 4 point bending test and frequency in the dynamic modulus test. To undertake this analysis, three conversions were assessed, as shown following:

$$f_{4PB-PR} = f_{DC-CY} \quad \text{Equation 6-5}$$

$$f_{4PB-PR} = 2\pi f_{DC-CY} \quad \text{Equation 6-6}$$

$$f_{4PB-PR} = \pi f_{DC-CY} \quad \text{Equation 6-7}$$

Where;

f_{4PB-PR} is the frequency of the 4PB-PR, flexural test, and
 f_{DC-CY} is the frequency of the DC-CY, dynamic modulus test.

For the 10Hz frequency used in AGPT/T233, the equivalent harmonic frequency in the dynamic modulus test would be 10, 1.6Hz or 3.2Hz for the three options respectively.

Figure 6-5 following shows the modulus obtained from the DC-CY dynamic modulus test at the angular equivalent frequency of 3.2Hz and the initial modulus measured from the 4PB-PR flexural test for 35 mixes tested in the Fulton Hogan Laboratory, since 2004

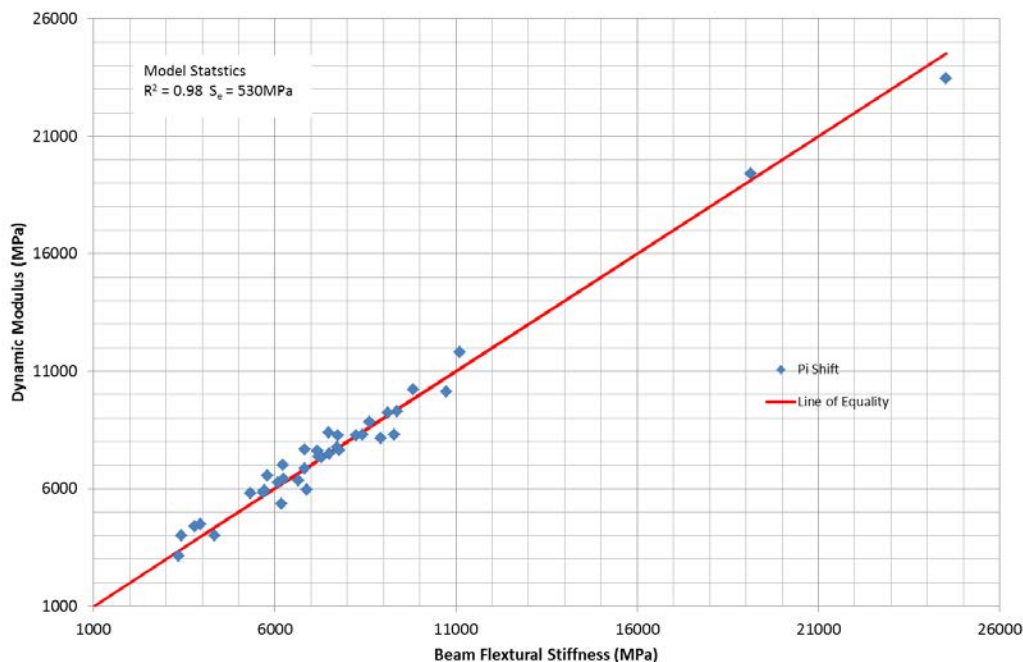


Figure 6-5 Flexural Dynamic Modulus Frequency Shift

As can be seen in the figure, at a frequency of 3.2Hz results in the DC-CY dynamic modulus test are highly correlated with the 4PB-PR flexural test and centred on the line of equality. The results show that the 4PB-PR, when tested at high strain for fatigue, should not be

considered a dynamic modulus test and that the results appear to exist in the time domain, with a time of loading given by:

$$t_{hp} = \frac{1}{2f_{4PB-PR}} \quad \text{Equation 6-8}$$

and

$$f_{4PB-PR} = \pi f_{DC-CY} \quad \text{Equation 6-9}$$

This finding compares very favourably to the results found by Ulditz et al. (2006) at the Westrak test track that the equivalent frequency of the flexural beam fatigue test to convert to field pulse loading (FWD loading) was 15Hz or 35ms which is nearly exactly the time of loading of an FWD.

6.6.4 Summary

The results shown that Dynamic modulus is only different to both resilient modulus and flexural modulus (haversine), if and only if, an inconsistent period (T) of the cycle is used. Stress dependency was found to play no part in the conversion of modulus between the Australian resilient and flexural modulus test and the dynamic modulus test for Australian mixes.

6.7 Master Curve Analysis

To further expand on the results found in the previous section for a single time and temperature the study was extended to examine the effects over the full range of temperatures and frequencies. This was done by developing a full set of master curves for 4 mixes and the 4 test methods used in Australia. For this study two sets of testing were undertaken:

- Set 1, which comprised of two mixes-a French EME2 mix and a high RAP C320 mix. Testing in this set was undertaken by ARRB for IT-CY resilient modulus and 4PB-PR. *(It should be noted that in undertaking this study the research was undertaken in accordance with the new Austroads AGPT/T274 test protocol.)* The DC-CY dynamic modulus testing was undertaken by both the University of the Sunshine Coast (USC) and by Fulton Hogan and two sets of results are shown.
- Set 2, contains the results of the development of two Australian EME2 mixes by Fulton Hogan. In this set of results all testing was undertaken by Fulton Hogan at the national laboratory, with one supplemental 4PB-PR beam undertaken by the Shell laboratories in France (EN12697-24). Along with the IT-CY, DC-CY and 4PB-PR test Fulton Hogan undertook a full temperature frequency sweep test using the

2PB-TR (EN12697-24) test (the reference test of AGPT-Part2 (2012)). For all test air voids were targeted at 5%[±]. 1%.

6.7.1 Un-Shifted Data

The differences between the IT-CY, DC-CY and the 2PB-TR and 4PB-PR results can be seen in the following, Figure 6-6 a),b),c) and d), which shows the resulting master curves of the French EME2, the C320 high RAP mix, the NSW EME2 and the QLD EME 2 mix respectively.

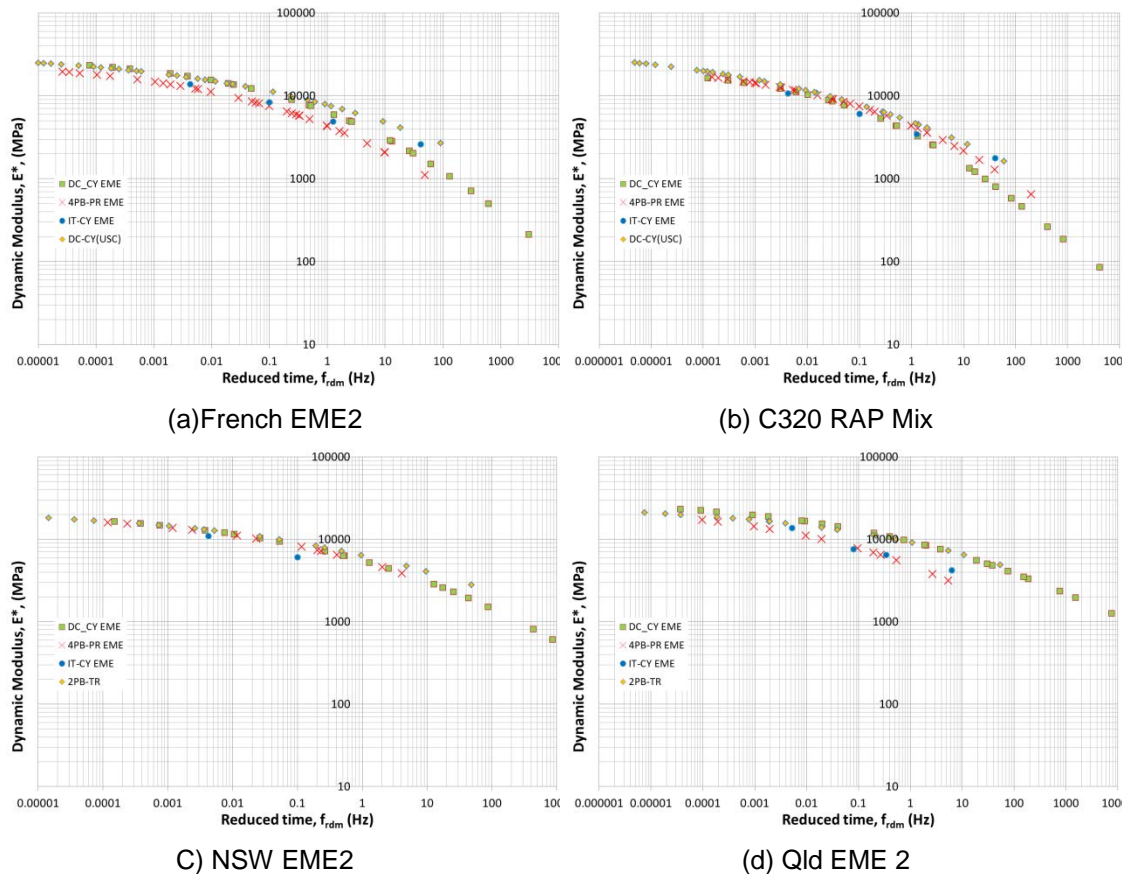


Figure 6-6 Comparison of Modulus Results (Un Shifted)

As can be seen from Figure 6-6(a), (b), (c) and (d) across the full temperature frequency spectrum the DC-CY results are higher than the 4PB-PR results. For one mix, the NSW EME, the results did tend to converge with the DC-CY but were still always lower. These results would tend to confirm the finding of the single point high strain study that the tests exist in a different time domain.

The results show that the IT-CY results do tend to converge to the 4PB-PR results at low temperatures, they are however higher at high temperatures. The results show that as with the single point data the IT-CY samples modulus is always lower than that of the DC-CY dynamic modulus results.

The observation can be made that the 2PB-TR results appear to be equivalent to the DC-CY results and the same frequency should be used. This same observation was found with the single test undertaken by Shell Laboratories in France. This is somewhat contrary to the findings of Francken et al. (1994) who found that DC-CY modulus was out by a factor of two compared to the bending tests; this however was based on only 1 observation. This shows that more work is required on this conversion.

The result show that the testing of the C320 high by FH appears to be an outlier, with significantly different results to USC and the DC-CY dynamic modulus results obtained more in-line with that of a C320 without RAP. While the results are included in the subsequent analysis, results should be view with caution.

6.7.2 *Shifted Master Curves*

The previous section (Section 4) established that frequency shift factors were valid for a single temperature and time of loading to equate modulus measured by one test to another. To determine whether the time shift factors found from the single time and temperature testing are valid across the whole time frequency domain, the results of the DC-CY, 4PB-PR and 2PB-TR were shifted with the correction factors obtained in section 4 for the 4 mixes tested. The results of the shifting is found in Figure 6-7 a,b,c and d for the French EME2, the C320 high RAP mix, the NSW EME2 and the QLD EME 2 mix respectively. The DC-CY and 2PB-PR tests were shifted to, t_{hp} using Equation 6-8 and the 4PB-PR test was shifted using Equation 6-9.

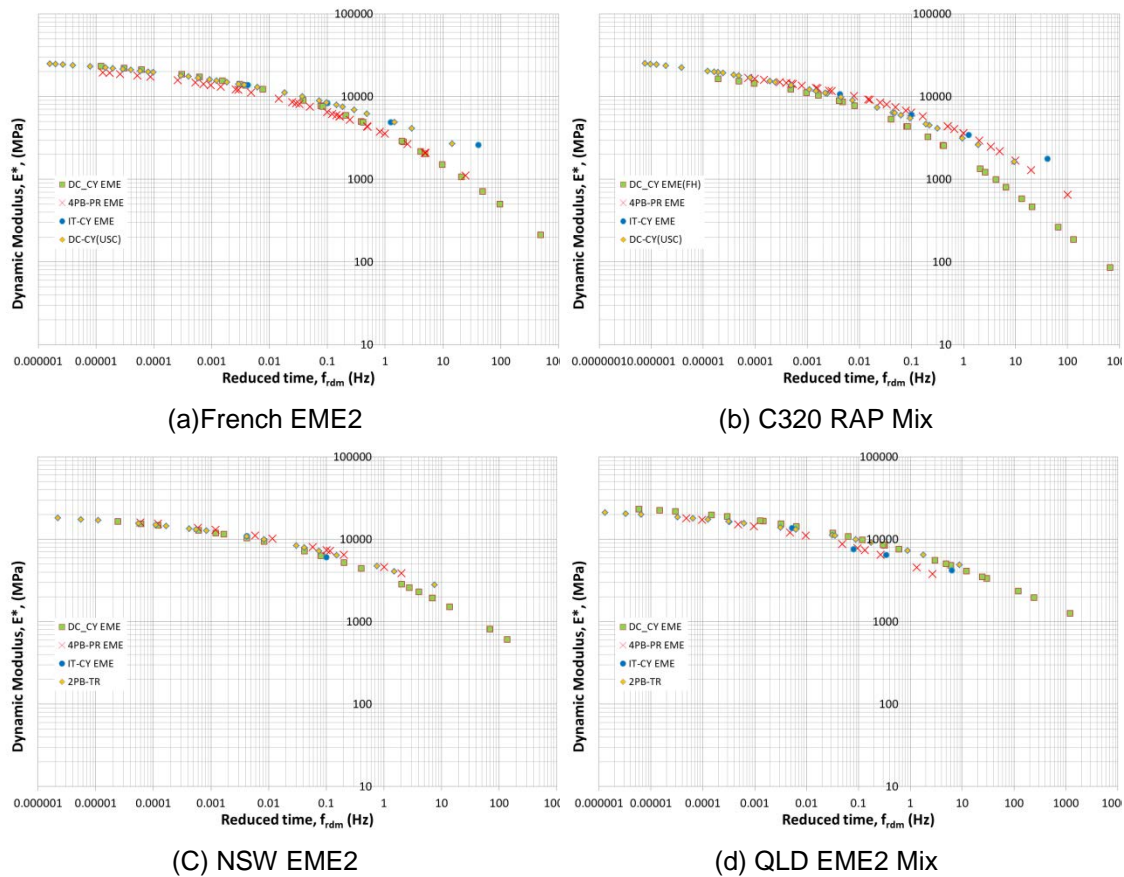


Figure 6-7 Shifted Master Curves

It can be seen from the figures that when corrected the 4PB-PR results for both the sinusoidal and the haversine loading fall closely around and both above and below the DC-CY master curve, the same is true for the IT-CY test and the 2PB-TR tests.

Given that the variability of the corrected results are well within the variability in modulus obtained in testing due to sample preparation (voids and binder differences) and the results fall above and below each other, it can be concluded that the time shift factors found from the single time and temperature testing are valid across the whole time frequency domain. The results show that the shift factors can be used to shift data obtained from one test to a reference test at any temperature or loading time.

6.8 Summary and Recommendations

The results of the study found that 3 of the 4 test methods have a different definition of time and need frequency shift factors to shift between the time and frequency domain. It was found the shift factors could be established from single time/temperature testing and that the time shift factors found from the single time and temperature testing are valid across the whole time frequency domain

For the purposes of standardisation, the modulus results need to be converted to a reference stiffness value. Comparable stiffness is obtained, with reference to the Australian

IT-CY test from the three test methods by using a constant definition of time (inter-conversion) as shown in Table 6-2, following.

Table 6-2 Modulus Inter Conversion Factors

Conversion From	Conversion To		
	IT-CY _(time)	4PB-PR _(frequency)	DC-CY _(frequency)
IT-CY _(time)		$\frac{1}{2t_{IT-CY}}$	$\frac{1}{2\pi t_{IT-CY}}$
4PB-PR _(frequency)	$\frac{1}{2f_{4PB-PR}}$		$\frac{f_{4PB-PR}}{\pi}$
DC-CY _(frequency)	$\frac{1}{2\pi f_{DC-CY}}$	πf_{DC-CY}	

It is evident from this study the frequency in the common test can have different physical meaning and the reporting of modulus at a frequency, without reference to the loading type is confusing. To remove this confusion, it is recommended that standard practice be established for the reporting of modulus values from different test methods and is referenced back to an equivalent design modulus. The study underlines the considerable challenges in comparing the modulus results from various test methods. It would be highly recommendable to harmonise testing across Australia and implement a standard reporting method. The interconversions have a direct practical application in the recommended design approach of Chapter 9.

For both the low strain 4PB-PR results and the 2PB-TR only limited data has been used and the results should be confirmed over a wider range of mixes.

7 Development of a Field Calibrated FEL model for Pavement Design

The purpose of this chapter is to develop a mathematical procedure for the incorporation of the FEL concept into the design of LLAP. As opposed to previous research projects that studied these concepts separately, the proposed procedure will incorporate the asphalt healing phenomenon directly into the FEL. To enable the design of LLAP in Australia the proposed procedure will need to incorporate the four major factors affecting the fatigue response of asphalt mixes; (i) binder type, (ii) binder content, (ii) temperature and (iv) the magnitude of the rest period applied after each loading cycle.

7.1 Background

Current conventional mechanistic design procedures, design pavements to fatigue, or put simply crack after a particular amount of traffic. This study proposes a different design concept. Instead of designing when the pavement will experience structural cracking, the concept is to design a pavement where structural cracking will never form. To design structural cracking out of the pavement, the concept will be to design the pavement structure in such a way that critical stress and/or strains remain below a “threshold” or FEL level. By remaining below the FEL, at some point in the life of the pavement a balancing point will be achieved and no net damage will occur in subsequent loading cycles. As no subsequent damage occurs, micro cracking will never form into macro cracking, which then ensures no structural cracking and subsequent long-life performance.

The concept of endurance limits is not new, structural and aeronautical engineers have been using the principle for years in fatigue analysis of metals. However, asphalt behaviour is not as simple as metals. Asphalt material properties change with temperature and loading speed, along with this asphalt material can undergo healing (repair of damage). All these factors may affect the FEL and for these reasons no single FEL has not been established for asphalt mixes. Because a single FEL may not exist, the development of an effective and practical approach for the incorporation of the FEL across different environments, mixes and traffic speeds has proven difficult and to date has not been developed.

While the incorporation of a FEL into pavement design has proven difficult, if a threshold criteria could be incorporated into a practical pavement design process, a limiting thickness of asphalt could be determined, beyond which any increase in design thickness will result in no increase in the structural capacity of the pavement. This, if developed, will have a significant potential in lowering cost of construction and increasing sustainability.

As part of the APS-fL project, a validated procedure has been developed (refer Chapter 5) for the direct conversion of laboratory determined dynamic modulus to field stiffness and the subsequent prediction of strain under a moving load. The accurate prediction of strain was the first step in development of a LLAP design procedure, this prediction will then allow

strain to be combined with the results of laboratory FEL analysis from sources such as the NCHRP 9-44 study, Thompson et al. (2006), Australian mixes and actual performance from the NCAT accelerated test track data, to develop and calibrate a practical design method for LLAP design.

While current approaches for LLAP design make use of the single FEL, the latest research undertaken, such as Thompson et al.(2006) and the NCHRP 9-44 project (2013) have established that there is no single FEL for asphalt mixes, with the endurance limit changing as a function of temperature and mix type. This has resulted in significant debate over what is the single critical threshold value which should be used for LLAP design for different environments and different asphalt types. As a result, none of these threshold limits have been widely accepted or is transportable to different regions. As no validated LLAP modelling approach exists for a wide variety of mixes and operating conditions, this study examined the applicability of using three different threshold modelling methods;

- the single FEL criteria,
- the cumulative distribution of strain concept, and
- varying a FEL criterion which is a function of mix properties and operating conditions.

These three approaches were then assessed and calibrated against the performance of actual pavements at the NCAT test track. The assessment also assessed the transportability of the criteria to different loading conditions and environments and, most importantly, the practicality for use in pavement design. Based on this a recommended modelling approach is developed for validation against Australian long-life flexible pavements.

7.1.1 Scope

The scope of work covered in this chapter as part of the overall project comprised of:

- Examination of laboratory and other field based FEL and the factors which affect the FEL of asphalt mixes.
- Comparison of overseas laboratory studies to Australian data.
- Development and calibration of a modelling approach for the design of LLAP asphalt pavements incorporating FEL limits based on the results of the full scale NCAT test track findings.

7.2 Laboratory Studies on FEL

The early work on endurance limits by Monismith et al. (1972) recommended a single FEL (70 $\mu\epsilon$) for LLAP design. However, subsequent research by Thompson et al. (2006) showed that the use of the single 70 $\mu\epsilon$ level was conservative and that the FEL was reached at significantly different strain levels depending on the binder type and or content. This finding

was reinforced by the findings of the NCHRP 9-44 (2013) study which found the FEL was not only a function of binder type and content but, additionally, the test temperature and length of the rest period. These studies found that the original assumption of a single FEL is not valid for a range of asphalt mixes and temperatures.

Thompson et al. (2006) attributed the differences in FEL to be a result differences in binder. However, because of the lack of data on the binders used in the study, Thompson could only undertake an assessment against the stiffness. Nevertheless, Thompson found a high correlation existed between FEL and stiffness. This finding was confirmed and expanded by the NCHRP 9-44 (2013) study, which found that the use of mix stiffness alone was as accurate as the use of binder content, binder type and temperature to relate to the FEL. The conclusion of both of these studies was that the basic material property, stiffness, is an extremely good surrogate for mix variables and stiffness alone may be a practical approach and directly related to the FEL. The stiffness-FEL relationship is shown conceptually on Figure 7-1 following, which shows the recommended stiffness-FEL relationships from the NCHRP 9-44 (2014) study for both a 1 second and 10 second rest period and the data and the fitted relationship to the Thompson et al. (2006) findings. (*N.B. In the figure the measured strain from the Thompson et al (2006) data has been halved to account for the different test methods (haversine vs. sinusoidal).*)

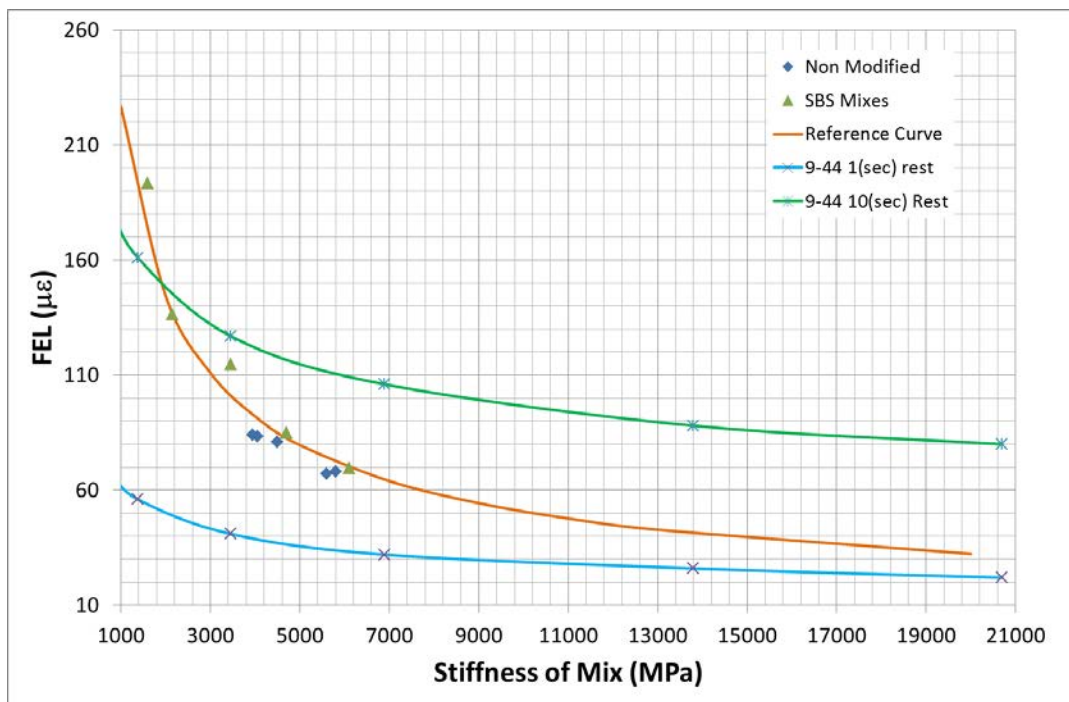


Figure 7-1 Stiffness FEL Relationships

While both approaches show a strong relationship between stiffness and FEL, there is a distinct difference in the predicted FEL, with different values and shapes of the stiffness-FEL curves. Notwithstanding the different values, it is evident is that both approaches show a

strong relationship between stiffness and FEL. These differences are most likely due to different definitions of the FEL being used in the testing, with the FEL recommended by Thompson et al. representing the point where cracking will not occur, but some damage may still occur to the mix, while the HI approach recommended by the NCHRP 9-44 study represents the case where no damage will occur (including internal heating).

While there is a difference in the value and shape of the curves, in all cases as stiffness increases the FEL decreases asymptotically and will most likely reach a limiting value, with the limiting value most likely being a function of the rest period. What is important is not the definition of the FEL, it is the adoption of the approach which most closely represents field performance. Of the two approaches, it is believed that the FEL recommended by Thompson et al. (2006) will more closely match the definition of the FEL used in this project of *“the maximum tensile strain at which, whilst damage might occur, the asphalt will never develop macro-cracking requiring deep structural treatment”*.

The findings of both these two extensive studies undertaken by the University of Illinois and Arizona State University have shown that the use of the basic material property, stiffness, can be directly related to the FEL of a mix and can allow for healing. If this concept was to hold true in actual pavements this simplified approach could provide a practical tool which could be used for the purpose of LLAP design incorporating binder changes, healing and temperature effects.

7.2.1 Other FEL Recommendations

Thompson et al. (2006) and the 9-44 (2013) study showed that the FEL of an asphalt mix varies due to binder grade, binder content, air voids and temperature and as found by Lytton (2005) and Zeiada (2012) with the length of rest periods. It is therefore not surprising that different researchers have recommended different FEL for LLAP design, based on the mixes they assessed, the operating (or testing) temperature and the environment, such as:

- In Japan Nishizawa (1996) analysed in-service pavements in Japan and recommended an endurance limit of 200 $\mu\epsilon$.
- In Kansas, Wu et al. (2004) using back-calculated Falling Weight Deflectometer (FWD) data, reported strains at the bottom of the asphalt layer between 96 and 158 $\mu\epsilon$ for a long-life pavement.
- Bhattacharjee et al. (2009) obtained endurance limit values through uniaxial testing which ranged from 115-250 $\mu\epsilon$.
- Thompson and Carpenter suggested fatigue endurance limits under certain circumstances may indeed be above 350 $\mu\epsilon$.

7.3 Single FEL Design Approach

Notwithstanding the acceptance of the FEL concept, the wide-ranging recommended FEL found in the literature has resulted in confusion on the actual value of the FEL which should be used and when the FEL can be used in pavement design. As a result the use of FEL for routine pavement design has not gained general acceptance. In addition to the inconsistency of the published FEL, there is complexity in the translation of the limited laboratory conditions (single temperature and rest period) to the multitude of conditions experienced in the field with complex vehicle loadings, rest period and a range of operating temperatures and conditions, which all result in changing FEL.

It is clear from the examination of both the results of the laboratory testing and field based recommendations that the use of a "single" FEL is not practical for a range of mixes and is not transportable to different environments. Any LLAP design procedure must include a variable FEL which can cover changes in temperature and mix type. The fact that different FEL's are obtained for different mixes and binder types and that the FEL changes with changes in temperature make the use of a single FEL impractical for general pavement design. As such, the use of single FEL was excluded for development of the APS-fL project, as it would not be transportable between the different mixes used across Australia and to the different environments of Australia.

Previous research has found that any practical design approach needs to incorporate a variable FEL, which is able to accommodate changes in temperature, rest periods and changes in mixes.

7.4 Design Endurance Limit as a Distribution of Strain at Failure

Realising the significant limitations in applying a single endurance limit for the purpose of design, the NCAT researchers developed the concept of using the Cumulative Distribution of Strain (CDS) as a method for the design of LLAP. In reality, the CDS approach determines a pavement which limits the number of load applications which can exceed the FEL of the asphalt, for a given environment, resulting in a LLAP.

The CDS allows incorporated changes in the FEL, as a result of changes in temperature, by the use of the distribution of strains and may be a practical approach for pavement design. The concept of the CDS approach is that if the distribution of strains (at the underside of the asphalt layer) is kept below a tolerable distribution of strains (the threshold distribution), a LLAP will be achieved. The concept of the cumulative distribution of strain is illustrated in the Figure 7-2 following.

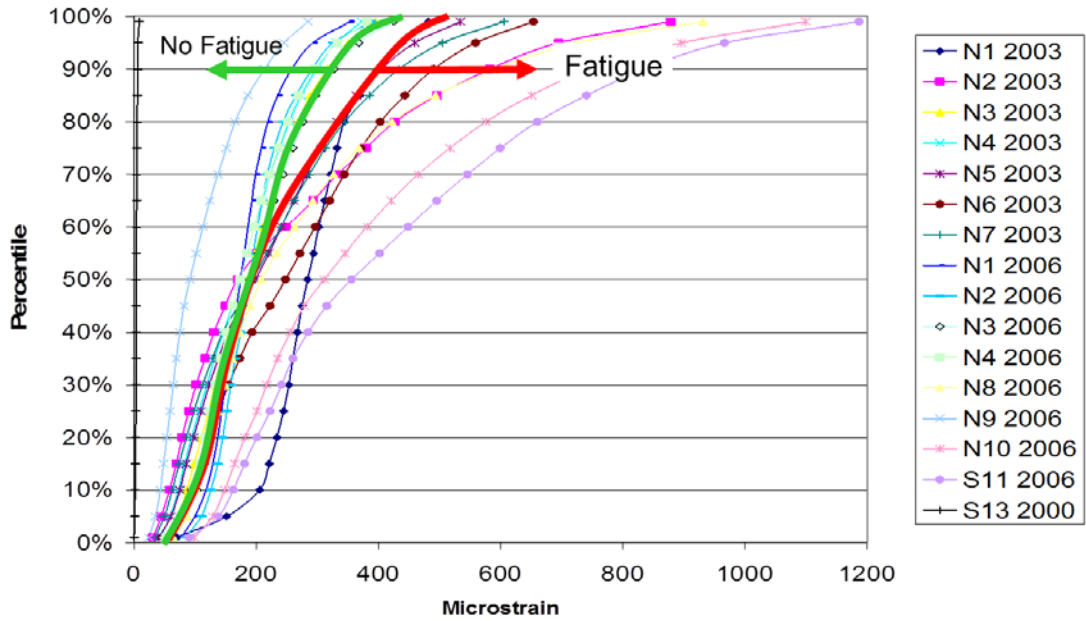


Figure 7-2 Cumulative Distribution of Strain NCAT, after Willis et al. (2009)

The CDS concept was developed by the NCAT researchers by plotting the cumulative measured strain for each of the structural sections (test cell) of the NCAT test track. In examination of the distribution of strains of the structural sections the researchers found, that as logically expected, strains increased with increased temperature as a result of the decrease in the stiffness of the asphalt. Surprisingly though, the researchers found that as the stiffness of the asphalt decreased with increasing temperature, strains in excess of $400\mu\epsilon$ were recorded on sections with no cracking. These field observations are well above the $70\mu\epsilon$ adopted by early researchers, again showing the difficulty in using a single FEL for LLAP design.

The threshold distribution proposed for design was developed by comparing the calculated cumulative distribution of strain for each test section against the field performance. When comparing the results the researchers found that a distinct difference was observed in the distributions between those sections which cracked (failed) and those sections which did not.

The examination of the results suggested to the researchers that there was a limiting value to the CDS or a threshold strain distribution, which if the strains in the pavement remained below, the pavement would avoid cracking and therefore be a LLAP. NCAT subsequently published this distribution as an interim threshold distribution for LLAP design.

7.4.1 *Issues with Cumulative Distribution of Strain*

While the cumulative distribution of strain is considered to be a practical, simple and rational design approach and able to include the changes in the FEL with changes in temperature or mix properties, the use of the published CDS across the range of temperatures experienced in Australia and loading conditions does have some limitations, namely:

- The maximum loading on the NCAT test track to date, is approximately 6×10^7 ESA. While this a LLAP, this load level has not been agreed to define LLAP and the CDS may not equate to a true LLAP
- The assumption that there is one distribution of strain which can be used as a threshold level for pavement design has limitations in:
 - The threshold level is the same regardless of mix type, ignoring mix composition. This is contrary to evidence that stiffer asphalt mixes have lower threshold limits than more flexible mixes.
 - The threshold level is the same regardless of the environment, meaning that the thickness in requirements in Brisbane (hotter climate and therefor higher strains) will be greater than Melbourne (cooler climate and lower strains). This is contrary to testing which shows increasing FEL with temperature and the empirical evidence that longer lives are experienced at higher temperatures.
 - There is no fundamental test developed that could be used to predict the required CDS for alternative mixes or which could be used for design and quality control purposes.

7.5 Stiffness Based FEL Relationships

The NCHRP 9-44 study (2013) recommended that the basic material property, stiffness, be used to develop a practical stiffness-FEL relationship for LLAP design. The advantage of the use of stiffness is that it can be used as a surrogate for changes in mix properties and temperature, eliminating many of the issues associated with the CDS approach, namely transportability with temperature and changes in asphalt mixes.

7.5.1 *Incorporating Australian Mixes*

Before the use of a single stiffness-FEL relationship could be recommended for routine pavement design in Australia, it needed to be established whether the single stiffness-FEL relationship found for a range of US mixes held for Australian mixes. To examine this, a range of multi strain 4PB-PR fatigue tests undertaken on Australian mixes in the Fulton Hogan historical database were assessed to determine the FEL of each mix. The FEL of each mix was determined using the constant PV of the RDEC approach and the constant

strain-Nf to failure level (1.1×10^7) recommended by both Thompson et al. (2006) and the NCHRP 9-38 (2011) project.

The results of this analysis is summarised in Table 7-1 following, which documents the mixes used in the analysis, the slope and intercept of the straight line strain-Nf to failure curve and the estimated FEL. These results are also shown graphically on Figure 7-3 following.

Table 7-1 FEL Australian Mixes

Mix Description	Binder %	Binder Type	Fatigue Equation Constants		Initial Stiffness (MPa)	FEL ($\mu\epsilon$)
			k	n		
AC14 5.4% A5E	5.4	A5E	2127	6.9	9722	150
EME NSW Bass Point Mix	5.6	EME2	3295	6.1	9021	168
Fulton Hogan PortPhalt	5.4	APH	1243	9.1	8580	169
AC20 C320 Wallgrove (AS2150)	4.2	C320	2740	5.6	9178	109
14mm Granite C320 Perth	4.5	C320	3676	5.2	7996	110
AC20 AR450 High RAP	4.7	AR450	3801	4.7	8519	81
C320 Geelong High RAP	4.9	C320	3413	4.8	7947	77
14TCI Base (sample 1)	4.9	C320	3587	5.2	8848	110
14TCI Intermediate sample 1	4.9	C320	2880	5.6	9111	111
MSTR Bunbury	5.2	C320	3521	6.0	4790	170
AC14 Hun 5.3% (NZ)	5.3	PG64	5163	5.0	5681	134
AC14 5.4% C320	5.4	C320	3441	5.3	6828	107
AC14 C600	5.4	C600	2816	5.8	7256	122
DG10 C170 W.A. Granite	5.6	C170	4853	5.0	6125	126
AC10 5.7% C450	5.7	AR450	3599	5.2	8947	109
AC10 5.7% C320	5.7	C320	3266	5.3	7730	109
DG10 Granite Perth 5.1%	5.1	C320	4578	5.0	5738	120
10mm DG Granite (21) Perth	5.1	C320	4955	5.0	7214	128
10mm DG Granite (22) Perth 2	5.1	C320	5012	5.0	7218	131
AC14 Hun 4.65% Bitumen PGT64 15% RAP10	4.65	PG64	2467	7.2	5807	195
DG10 Granite	5.1	A15E	5765	4.8	6021	133
DG14 4.72% A15E ex-Crestmead	4.7	A15E	5570	5.0	7510	149
AC14 5.4% Toner Binder (MK II) 2 M2 B2	5.4	A10E + Tonner	2268	8.5	3594	265
AC14 5.4% A10E	5.4	A10E	4012	6.7	3504	262

AC10 5.7% A10E	5.7	A10E	6768	5.5	3342	243
AC10 5.7% A15E	5.7	A15E	7014	5.7	3423	284
AC10 5.7% A20E	5.7	A20E	6653	5.1	4347	188
WA Testing PMB AC14 Ex Port Hedland	5.1	A10E	5350	5.0	6966	142
10mm Granite /75 blows C320 + PMB	5.0	A15E	6412	5.3	5002	200
DG10 Granite	4.8	A15E	5765	4.8	6021	133
14mm MSR Basalt A20E ex-Bunbury	5.0	A20E	5490	5.0	4826	145
AC14 5.0% A35P Racetrack	5	A35P	6286	4.2	6891	86
AC14 5.4% A35P	5.4	A35P	3578	5.6	7789	140
AC10 5.7% A35P (EVA)	5.7	A35P	5115	5.0	7120	131
14mm Granite PMB	4.8	A35P	4648	5.0	7010	122
20mm Granite EVA ex-Hazelmere	4.3	A35P	5206	4.4	10273	83
14mm Granite EVA ex-Hazelmere	4.8	A35P	3824	5.1	6865	111
10mm Granite /75 blows C320 + EVA	5.1	A35P	9785	3.6	8920	63
DG10 EVA ex-WA	5.1	A35P	5834	5.1	5507	161

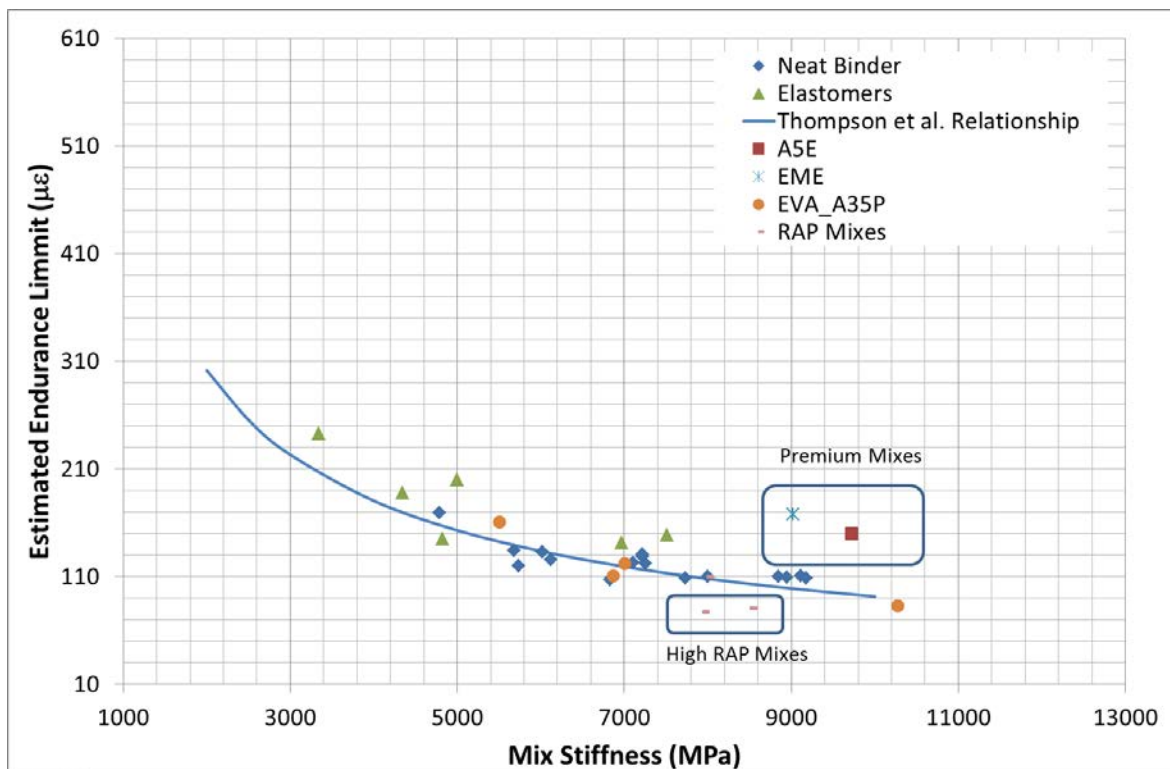


Figure 7-3 FEL Stiffness Curve Australian Mixes

What can be seen in the figure is that the results of the conventional, elastomeric (A10 and A15E) and plastomeric (A30 and A35P) mixes, follow the same shape as the results found in the Thompson et al. (2006) study. This finding is not overly surprising as both datasets contained both conventional and SBS modified mixes and under the same loading

conditions (haversine). As with the results of Thompson et al. (2006) the SBS modified mixes in general fall slightly above that of the conventional mixes, suggesting a different FEL-stiffness relationship may be required for modified mixes, but for practical purposes may not be warranted.

Given the similarities in the results both the Thompson et al.(2006) data and the Australian, the data was combined to develop a standard stiffness-FEL relationship which can be used to estimate the FEL for conventional, EVA and SBS modified mixes and is described in Equation 7-1 following:

$$FEL = k_1 20200 S_{mix}^{-0.65} \quad \text{Equation 7-1}$$

Where;

FEL is the Fatigue Endurance Limit

S_{mix} is the stiffness of the mix, and

k_1 is an adjustment factor for differences in rest periods and/or confidence levels.

While it was initially believed and recommended in the 9-44 study (2013) that a single FEL could be established that related stiffness to the FEL for any mix, this only appears to hold true for a range of conventional and modified asphalts, with binder contents in the range of typical asphalt mixes (4.2-5.5% binder) and it does not appear to be true for highly modified mixes. This can be seen in Figure 7-3 which shows that for mixes produced with high modification or high binder contents significantly higher FEL's can be achieved and a shift factor may be needed for those mixes.

It is also noted that the two mixes examined produced with high RAP contents (>30%) exhibited significantly lower FEL. While this dataset is only small and may not hold with the use of rejuvenators, until additional studies are undertaken it is not recommended that high RAP mixes (>30%) be used in the fatigue susceptible layers of a LLAP.

7.6 Calibration of FEL for Pavement Design

7.6.1 Shifting of Cumulative Distribution of Strain

To overcome the limitations of the single environment used in the development of the CDS and to modify the CDS to incorporate a measure of the mix property, the results of the Phase II NCAT test sections were re-examined in an attempt to incorporate either the standard stiffness-FEL relationship shown in Equation 7-1 and the NCHRP 9-44(2013) recommendations into the CDS approach.

It was hypothesised that if the single stiffness-FEL relationship holds true under field loadings and temperatures conditions, the relationship between stiffness and FEL may

provide a practical tool for the shifting of the threshold distribution curve as a function of changes in mix type and/or environments.

To test this hypothesis, the following approach was undertaken:

- The effective modulus master curve of the combined asphalt layers for each section of the Phase II structural sections (N2-N8) was determined in accordance with the previously developed and calibrated method (Chapter 5), with the resulting master curve fitting parameters shown in Table 7-2 following.

Table 7-2 Master Curve Fitting Parameters

Test Cell	Temperature Shift Factors ($T_{ref} = 20^{\circ}\text{C}$)		Sigmoidal Fitting Parameters			
	A	b	α	β	γ	δ
N2	0.0003	-0.1173	1.763	2.828		
N3	0.0003	-0.1163	1.810	2.774	-0.711	-0.363
N4	0.0005	-0.1291	1.688	2.896	-0.770	-0.347
N5	0.0004	-0.1193	1.688	2.896	-0.770	-0.347
N6	0.0003	-0.1184	1.715	2.882	-0.709	-0.372
N7	0.0004	-0.1221	1.787	2.897	-0.998	-0.457
N8	0.0004	-0.1221	1.787	2.897	-0.769	-0.5060

- The stiffness was determined for the effective asphalt layer, over the full range of mid-point layer temperatures experienced at the NCAT test section (0, 5, 10, 15, 20, 30 and 40°C) at the equivalent loading frequency in the DC-CY dynamic modulus test (2Hz), equating to the design speed of 80km/hr.
- The design axle loading used in the forward calculation was the 90kN (axle weight on the NCAT test track)
- For each mid-point temperature, the horizontal strain at the base of the combined asphalt layer, the critical location for fatigue cracking, was calculated using the elastic material properties of the base and subgrade support values from Timm (2009) and Layered elastic theory.
- For each temperature the calculated strains at the asphalt stiffness were plotted against each other for each Phase 2 structural test section as shown in Figure 7-4 following.

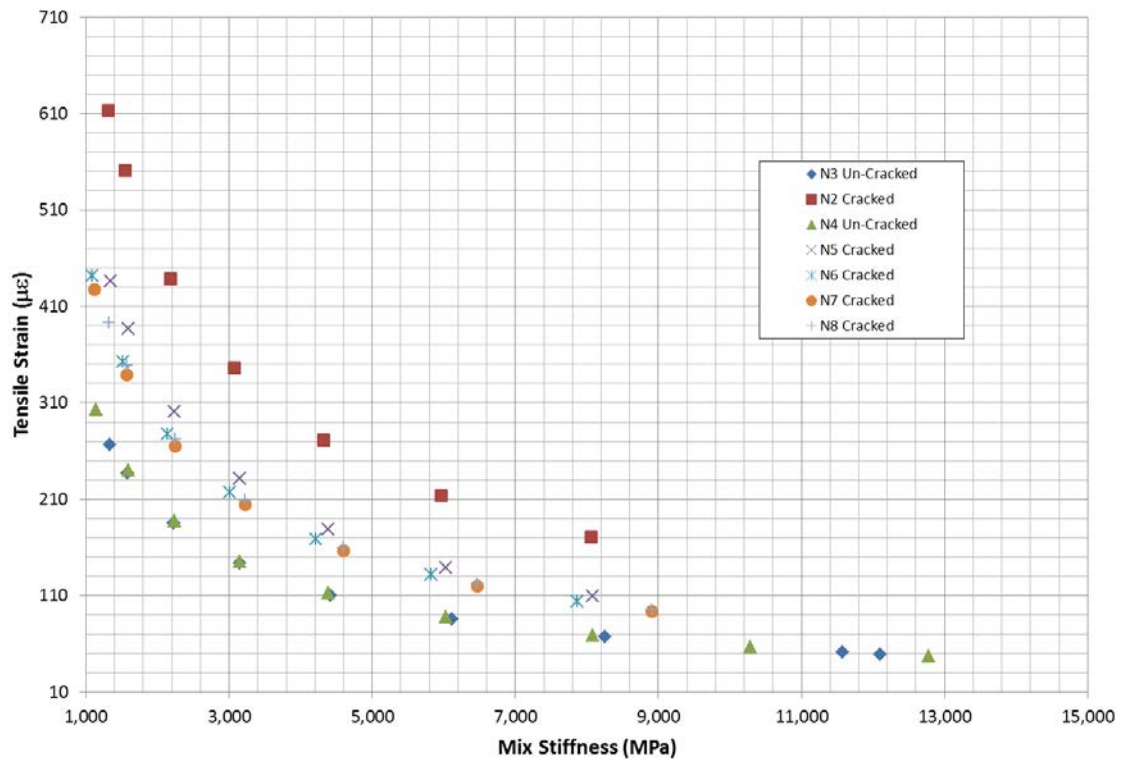


Figure 7-4 Modulus Strain Relationship NCAT Phase II

It is not surprising and expected to see, that a clear relationships exists for each mix between stiffness and strain and that that stiffness alone may be able to be used to “shift” the threshold CDS. The results show, as logically expected, that as stiffness decreases with increasing temperature the strain also increases and additionally, as can be seen from section N3 and N4, softer mixes produce higher strains. This not surprisingly shows the effect of both the changes in temperature and mix type is captured in the stiffness-strain relationship for a pavement.

7.6.2 Development of a Stiffness Based FEL

When the stiffness-strain relationships are more closely examined as shown in Figure 7-5 following, it can be seen that two sections N4 and N3, which did not crack in the Phase II and the subsequent studies, had strain levels across the whole stiffness range which are lower than the sections which cracked. As with the CDS approach the figure suggest that a deviation exists between sections which did not exhibit structural failure (lack of cracking) (N3 and N4) and those which did exhibited failures (cracking) (N2, N5, N6, N7 and N8). As can be seen in the figure, the sections which failed had strain levels across the whole stiffness (temperature) range, which were higher than the sections which exhibited no signs of failure. These field observations support the results of the laboratory findings in that;

- stiffness as found by Thompson et al.(2006) in the 9-44 study(2013) and for Australian mixes is a good surrogate for binder and temperature effects,
- FEL is not a constant and varies as a function of stiffness,
- and, structural failure or lack of, is a function of induced strains.

These observations also show that strain alone is an effective tool for assessing the support provided to the asphalt layer(s) from all underlying layers. This observation of the structural sections on the NCAT test track would support that a single stiffness-FEL may alone be a practical tool for the design of LLAP and the design procedure may not need to include the CDS approach.

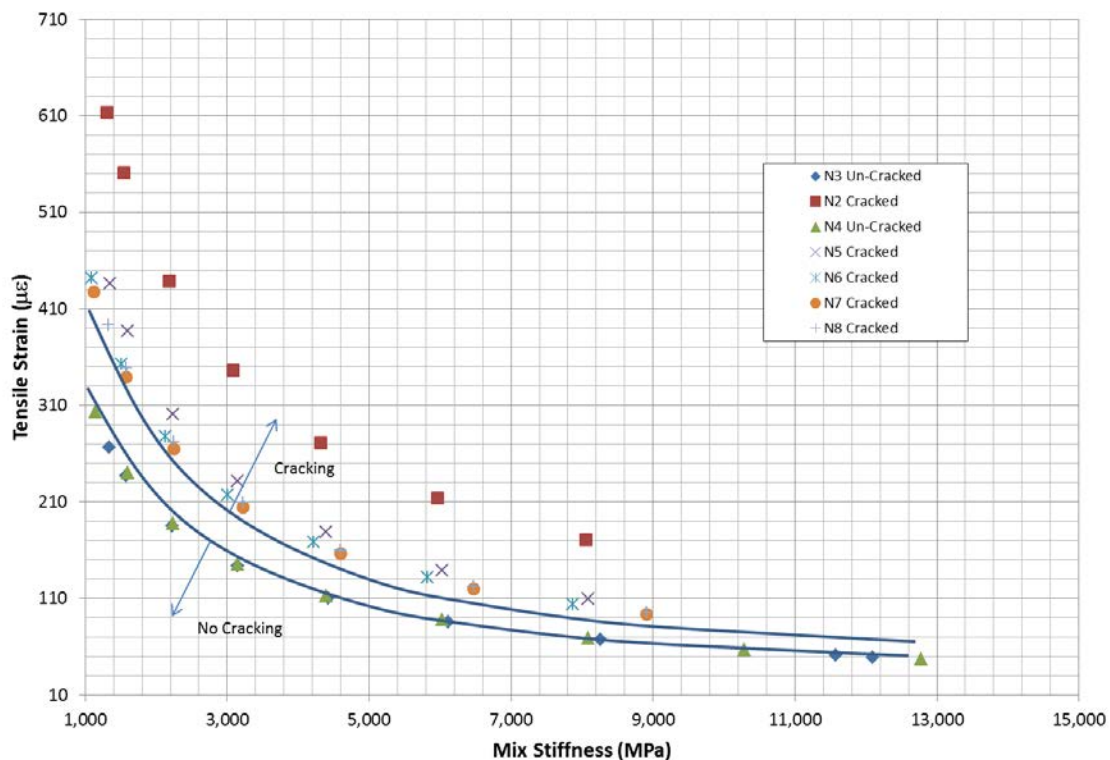


Figure 7-5 Modulus Strain Relationships NCAT

While it might be argued that sections N3 and N4 have not been fully established as LLAP, as described by Timm et al. (2009) “sections N3 and N4 strain profiles can be used to represent the least conservative strain profiles which are able to withstand trafficking without fatigue cracking”. Therefore, at least initially, these two sections can be used to determine the deviation or upper limit for a field-based FEL and will provide an excellent starting point for development of a field based FEL design model. However, due to this limitation it is not recommended that the FEL relationship developed from the analysis of the NCAT test sections be used for design and that any recommendation needs to be further validated from investigation of actual LLAP’s.

Comparing the relationship between strain and stiffness for the two LLAP sections to the often used laboratory FEL of 70 to 100 $\mu\epsilon$, it can be seen that for both sections strain values are constantly higher than these values. The results from NCAT clearly show that measured strains in the field can easily exceed the previously accepted laboratory FEL and in fact, strains in excess of 400 $\mu\epsilon$ can be experienced without any fatigue damage occurring. The infield performance shows that the 70 to 100 $\mu\epsilon$, level is clearly conservative and confirms that the use of a single FEL will not provide a useable design approach.

While different binders (conventional and SBS modified) were used in the N3 and N4 sections, it can be seen that the relationship between stiffness and strain for these two sections, for all practical purposes is identical. The relationship was the same even though section N4 was placed with lower stiffness mix which resulted in higher strains at a given temperature. This clearly shows that any FEL design procedure must incorporate a mix property in the process and the basic material property, stiffness, can be used to do this. As if non-stiffness based FEL was developed, the approach may predict failure of section N4 before N3 which was not observed.

The findings from the NCAT test track confirm the findings of the laboratory test studies, (NCHRP 9-44 (2013) study, Thompson et al. (2006) and validated with Australian mixes), that the use of a variable FEL limit directly related to stiffness, is able to capture the effects of changes in temperature and mixes in the field and the tolerable strain and may be able to provide a simple practical approach for design which can be calibrated to field performance.

This simple approach offers significant advantages over the previous CDS approach, in that:

- It is transportable to different stiffness (low modified) mixes, through binder properties being a direct input to stiffness
- It is transportable to different environmental conditions through temperature being a direct input to stiffness.

7.6.3 FEL Relationship and Laboratory Shift from NCAT

As previously stated, Timm et al. (2009) recommended that the strain profiles of sections N3 and N4 be used to represent the least conservative strain profiles that were able to withstand trafficking without fatigue cracking. Due to the LLAP performance of these two sections the sections were extended into the two latter studies and have subsequently received triple the traffic of any other section in the 2003 study, and have shown no signs of structural failure. It is therefore rational that these two sections be used, at least initially, to determine and calibrate the upper limit for a field-based fatigue threshold. While it needs to be understood that the cells N4 and N3 at the current time have only experienced a traffic level (6×10^7) which is not generally considered to be a true LLAP, they are close to if not at

the accepted endurance level and will provide a good starting point for development of the threshold. Given this potential limitation, any LLAP design procedure calibrated from the NCAT test track data will need to be further validated against actual LLAP asphalt pavements, it is anticipated that there will still be some shift from the NCAT calibration to account for potential aging and higher traffic levels of actual LLAP.

Further to developing and calibrating the stiffness-FEL relationship, the analysis will need to establish whether any laboratory to field conversion exists. This is relatively simple to accomplish and can be undertaken by comparing the recommendations of the NCHRP 9-44 (2013) study and the standard relationship (Equation 7-1) developed from the Australian mixes and the Thompson et al.(2006) data, against the threshold established from the structural sections of the NCAT test track. This can be seen in Figure 7-6 following which shows the stiffness strain relationship of sections N3 and N4, the standard relationship and the two of the NCHRP9-44 recommended relationships. When comparing the results it needs to be understood that in the standard relationship, there is no rest period, for the 9-44 study the recommended FEL were made for rest periods of between 1 to 20 seconds. Plotted on the chart is the case of a 20 second rest period, which has the highest recommended permissible strains.

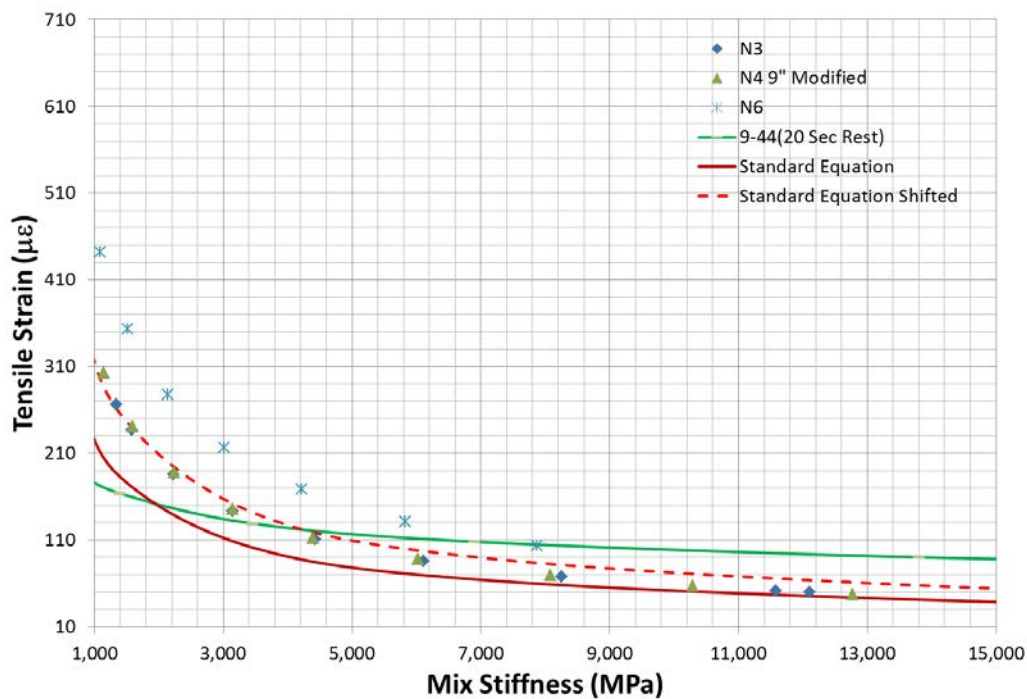


Figure 7-6 NCAT Calibrated FEL Relationship

The figure shows that at high temperatures the FEL from the standard relationship is a factor lower than the values which have been shown to not produce fatigue in the field, but they converge at the lower temperatures. The comparison with field performance does however suggest the shape of the FEL relationship of the standard equation closely matches the

shape of that of the observed field performance and might be out by a “shift factor”. The requirement for a shift is not surprising as the relationship was developed from testing undertaken without any rest periods, as found by numerous researchers, such as Zeiada (2012), rest periods have a significant effect on the endurance limit, with recorded FEL being up to double in samples with rest periods and compared to samples without rest periods.

The figure also shows that the Healing Index (HI) approach as proposed in NCHRP 9-44 (2013) does not appear to match field performance across the range of modulus values encountered at NCAT. It is clear that at higher temperatures, even at high rest periods (20sec), the approach underestimates the strain values which have been shown to not cause damage. For the N3 and N4 sections strains of well in excess of 300µε were experienced on the test track, while the recommendations only allows a maximum of approximately 180µε at high temperatures and the relationship crosses the field observation curve at a stiffness level of 4000MPa. The results would tend to indicate that it will be difficult to apply a simple correction factor to the recommended approach. A simple calibration factor will result in either underestimating the fatigue endurance limit at higher temperatures or over estimating the endurance limit at lower temperatures.

While it is clear and expected that there will need to be a shift factor between laboratory and field FEL, for the standard relationship, this may be a simple constant applied to the calculated strain and this shift factor may be all that is required to shift the results from the laboratory to field.

Using both the results of the NCAT sections N3 and N4 and the standard relationship a preliminary relationship and laboratory to field correction can be obtained, as shown in the Equation 7-2 following and as shown in Figure 7-6, previously.

$$FEL = 1.4 \times 20200S_{mix}^{-0.65} \quad \text{Equation 7-2}$$

Where;

FEL = is the NCAT Fatigue Endurance Limit; and

S_{mix} = asphalt mix stiffness (modulus) (MPa)

k₁ = 1.4 and is the laboratory to field adjustment factor.

7.7 Summary and Recommendations

The examination of extensive overseas research showed that there is a clear and strong relationship between mix stiffness and the FEL of asphalt mix. The international research has found that as stiffness of the mix increases the FEL decreases asymptotically and most likely reaches a limiting value. The research work showed that the use of the basic material property, stiffness, is directly related to the FEL of a mix and can be used to allow for changes in binder, temperature and healing.

The examination of the LLAP sites from the NCAT Phase II study confirmed, in field, the variable nature of the FEL relationship and that LLAP can withstand strains significantly higher than previously recommended when the asphalt has low stiffness without undergoing damage. The examination of the two LLAP on the NCAT test track showed a direct relationship exists between infield stiffness-strain curve of the two undamaged sections and the stiffness-FEL developed from Australian and US mixes.

8 Validation with Australian Long Life Asphalt Pavement Sites

8.1 Introduction

The calibration of the stiffness-FEL relationship developed from the NCAT test track found that a single stiffness-FEL relationship could be used as a practical design tool for LLAP design and this relationship was directly related to laboratory testing. The results found that the difference in binder content and grades as well as temperature could be adequately covered using this single stiffness-FEL relationship. However, it still needs to be remembered that this relationship is only a convenient observational relationship and must be only applied within the limits of the data used to develop the relationship. Given the relationship is not a fundamental; the application of the single relationship to the Australian environment and mixes is not recommended.

Given there is expected to be differences in traffic loading, environments, binder sources and most especially aging, it would be expected that further validation may be required from the NCAT relationship to Australian field performance. However, when investigating this, it needs to be recalled (see Chapter 5) that typical Australian asphalt mixes fall into a relatively small volumetric window. Also, Australian mixes, in terms of stiffness, binder content and gradation are no different from US mixes, as confirmed in the comparison of Australian and US FEL. Therefore, it may be the case that the practical single relationship found between stiffness-FEL for US data on the NCAT test track may require only a small, if any, shift to be transportable to Australian mixes and conditions.

8.2 Australian Long Life Pavement Sites

In 2009 the then RTA of NSW (now Roads and Maritime Services, (RMS)) undertook a study on the performance, composition and condition of the different pavement structures at a number of locations throughout the state in order to develop the STEP remaining life procedure. One of the outcomes of this study was an extensive database of pavement condition, structural capacity, layer thicknesses, materials and visual condition of the pavements. This database was made available to AAPA for use in the APS-fL life project for development and validation of a LLAP design procedure for Australia

In order to validate the stiffness-FEL model developed from the NCAT test track, the RMS step database was examined to find both partial and full depth asphalt pavements which may be either a non LLAP or a LLAP. This subset of the RMS step database was then re-examined to separate out potential LLAP in the database. This subset was obtained by filtering for pavements which;

- had greater than 140mm of combined asphalt thickness
- were greater than 20 years old,
- had cumulative traffic greater than 30million ESA,

The subsequent subset of the data can be found in Appendix B of this report.

Additional sites were added to the analysis, which could be used to establish the break point between LLAP and fatigue susceptible pavements. These were sites which had greater than 240mm of asphalt and have fatigue cracking, regardless of the traffic loading and or age.

The potential LLAP sections were then individually assessed and categorised into three categories

- LLAP,
- Possible LLAP
- or Non LLAP

The categorisation was undertaken by examining the results of the visual survey undertaken at the time of testing, the current visual condition of the pavement and any comments on asphalt condition and by examining the assessment of the remaining life of the pavement determined as part of the visual assessment.

In addition to the RMS sites the data collected by Sharp (2001) for the AAPA pilot study was inspected to find any additional sites which could be used to establish the FEL for Australian LLAP design. The data collected by Sharp(2001) and subsequently by Foley (2008) was examined to find Australian LLAP sites which would provide valuable information in the establishment of the design level FEL for asphalt pavements. In his study Sharp (2001) identified a number of LLAP and undertook site investigation of asphalt material properties and layer thickness, Foley (2008) undertook subsequent FWD testing and analysis on these sites.

Table 8-1, following, summarises the sections of pavement identified as LLAP, while Table 8-2 summarises the sections identified as Non-LLAP. The sites obtained from Sharp (2001) and Foley (2008) are marked with an asterisk (*) in Table 8-1 following. The full details of the geotechnical investigation and material properties for the LLAP sections and the non LLAP sections can be found in Appendix B. Under the pavement heading the asphalt layer thickness is shown and each subsequent layer of granular pavement above the natural subgrade is shown.

Table 8-1 Australian LLAP Validation Sites

Site ID	Road/Location	Cumulative Traffic		Const. Year	Pavement
		2009	2015		
H-S22	New England Highway Beresfield	8x10 ⁷	1x10 ⁸	1970	190-210mm Asphalt Fine to Course Gravel Poorly Graded Sand SG
H-S27	Pacific Motorway,	5x10 ⁷	6x10 ⁷	1990 ¹	180-205mm Asphalt

	Cheero Point				300mm Fine to Coarse Gravel Fine to Coarse Gravel
H-S28	Pacific Motorway, Mooney Mooney	5x10 ⁷	6x10 ⁷	1990 ¹	265-285 Asphalt 300mm Fine to Coarse Gravel Fine to Coarse Gravel
H-S29	Pacific Motorway 1.5km south of Ourimbah exit	5x10 ⁷	6x10 ⁷	1989	140-160mm Asphalt 300mm Fine to Coarse Gravel Fine to Coarse Gravel
H-S48	Maitland Road Westgate	6x10 ⁷	6x10 ⁷	1970	130-140mm Asphalt 260-370mm Gravel 400-200mm Clayey Gravel Clay
N-S56	Pacific Highway, Cumbalum	1x10 ⁷	2x10 ⁷	1988	200mm Asphalt 300mm Argillite Silty Sand
SOU-S035	Picton Road	4x10 ⁷	5x10 ⁷	1966	215-280 Asphalt 1000mm Sandy Iron Stone Gravel Bedrock
Syd-S11	Botany Road, Banksmedow	4x10 ⁷	4x10 ⁷	1977	205mm Asphalt Fine to Coarse Gravel Poorly Graded Sand
Syd-S13	Hume Motorway, St Andrews	1x10 ⁸		1973	260-270mm Asphalt Gravel Clayey gravel SG
Syd-S14	Milperra Rd, Condell Park	4x10 ⁷	4x10 ⁷	1966	150mm Asphalt 650mm Fine to Coarse Gravel Clayey Sand
Syd-S15	Hume Motorway, St Andrews	1x10 ⁸		1973	300mm Asphalt 175mm Gravel Clay
Q5*	Bruce Highway, Kallangur, 1.3-1.5km South of Boundary Road (SB)		3x10 ⁷	1979	320mm Asphalt Working Platform Subgrade
Q6*	Bruce Highway 2.2-2.4km South of Boundary Road (SB)		3x10 ⁷	1979	300mm Asphalt Working Platform Subgrade
N4*	Camden By-Pass Narellan Rd to Macarthur Bridge (SB)		9x10 ⁶	1976	180mm Asphalt 220mm DGB20 330mm SGS
N7*	Alpha Street, Patrick to Flushcombe Rd, EB		3x10 ⁶	1974	225mm Asphalt Subgrade
V6*	Atherton Road, Oakleigh, Drummond St to Atkinson St (EB)		4x10 ⁶	1971	190mm Asphalt 75mm FCR Sandy Clay

1 age ??

For most of the RMS sites, 3 individual test pits, FWD tests and borehole logs were undertaken within the section. While for each section similar profiles were found, there were differences in the thickness of each individual layer and material types. The combination of

the result of the 3 locations per RMS site, and the use of the lower 90th percentile deflection for the Sharp (2001) sites, resulted in 28 individual Australian LLAP sites being used in the analysis. To further expand on this data set and add an extra degree of confidence, these 28 sites were then with combined with the data obtained for the three lowest stiffness Valmon test sites and the structural sections of the NCAT test track data. The resulting LLAP database comprising of 33 pavements, which was selected to establish the FEL for LLAP design is statistically significant for the establishment of the FEL criteria.

In addition to the LLAP identified for use in this study a significant number of additional sites are available in the literature from other studies such as, Foley(2008), Sharp(2001) and Rickards et al.(2012). If these sites were included in the analysis, it would have been possible to have over 50 LLAP sites. However, as with the stiffer analysis sections in the TRL UK Valmon data, these sites are principally deep strength asphalt pavements over modified, stabilised or cemented base. As the strain levels in these pavements are well below that of the FEL the additional information obtained from the analysis of these sites would offer little to no benefit to the validation of the FEL, as what is important is to distinguish the shift from indeterminate pavement to a true LLAP.

8.2.1 Current Condition of LLAP

Figure 8-1 to Figure 8-11 following show the current condition of the Australian LLAP sites, with the exception of the Hume Motorway (St Andrews) which is not included as it was recently widened (2010) with an extra lane in each direction.



Figure 8-1 H-S22 New England Freeway



Figure 8-2 Pacific Motorway (N.B), Bar Point



Figure 8-3 Pacific Motorway (N.B), Mooney Mooney



Figure 8-4 Pacific Motorway Ourimbah, (SB)



Figure 8-5 Pacific Highway, (Maitland Road) (NB)



Figure 8-6 Pacific Highway Cumbalum (NB)



Figure 8-7 Picton Road, Avon (EB)



Figure 8-8 Botany Road, Port Botany, (NB)



Figure 8-9 Milpera Road, (WB), Condell Park



Figure 8-10 Bruce Highway (Q5), Kallangur (SB)



Figure 8-11 Bruce Highway (Q6), Kallangur (SB)



Figure 8-12 Camden By-Pass (SB)



Figure 8-13 Alpha Street Blacktown (EB)



Figure 8-14 Atherton Road, Oakleigh, (EB)

If the current condition of the pavements is compared against the definition of a LLAP used in this study of “a pavement which, while damage might occur, the asphalt will never develop macro-cracking requiring deep structural treatment”, it can be seen from the figures all pavement sections, with the exception of the Pacific Highway (Maitland Road), have no evidence of structural cracking or macro cracking which would require structural treatment. While some pavement sections have an older oxidise surface and sections of the Sydney Newcastle freeway have a ravelling open grade no damage extends beyond the surface of the pavement. The Pacific Highway (Maitland Road) is now showing the early signs of cracking as can be seen in Figure 8-5, previously. While this site may have a long and indeterminate life it is not deemed a LLAP site and subsequently was not included in the LLAP analysis.

8.2.2 Indeterminate Structures

As mentioned, to validate the threshold limit between an indeterminate structures and LLAP pavements, a number of non LLAP sections are considered in this study. In reality more information is obtained from the determinate and indeterminate pavement structures than that of the LLAP, as in concept, the thickest pavement to experience any degree of fatigue failure can be used to establish the limit between the indeterminate structures and LLAPs.

The sections which are included in the analysis as being indeterminate were all sections of asphalt pavement greater than 30 years old and greater than 150mm of asphalt which had experienced any signs of fatigue cracking. In addition and any pavement which had greater than 200mm of combined asphalt thickness which had experienced fatigue cracking has been included with the indeterminate structures. These non-LLAP sections are found in

Table 8-2 following. As with Table 8-1 under the pavement heading the asphalt layer thickness is shown and each subsequent layer of granular pavement above the natural subgrade is shown.

Table 8-2 Australian Non LLAP Pavement Validation Sites

Site ID	Road/Location	Cumulative Traffic	Const. Year	Pavement
H-S23	New England Highway	8x10 ⁷	1970	220mm Asphalt 230mm Fine to course gravel 810mm Poorly graded sand SG
Sou-SO86	Princess Highway, South of Gerringong	9x10 ⁶	1969	200mm Asphalt 200mm Unbound gravel 300mm Gravelly clay SG
Syd-S26	Bunnerong Rd. Matraville	1.4x10 ⁷	1960	160mm Asphalt 200mm Poorly graded gravel 300mm Poorly graded sand SG
Syd-S23	The Grand Parade, Monterey	4.5x10 ⁶	2000	200mm Asphalt 150mm Poorly graded gravel 550mm Poorly graded sand SG
Syd-S46	Rocky Point Road, Beverly Park	1.6x10 ⁷	1966	160mm Asphalt 240mm Poorly graded gravel 550mm Poorly graded sand SG
H-S39 ²	Sydney Newcastle Freeway,	8.9x10 ⁷	1970	155-165mm Asphalt 440mm Fine to course gravel Clay
H-S24	Sydney Newcastle Freeway	8.9x10 ⁷	1970	240-260mm Asphalt 220-330mm fine to course gravel gravel
Syd-S24	Woodville Road, Merrylands	3.7x10 ⁷	1970	190-180mm Asphalt 300mm Fine to course gravel (some poorly graded) Clay
Syd-S25	Woodville Road, Guilford	3.7x10 ⁷	1970	150mm Asphalt 200-450mm poorly graded gravel
Syd-S33	Bunnerong Road, Matraville	1.2x10 ⁷	1960	150mm Asphalt 320mm Fine to course gravel Poorly graded sand
Sou-S089	Princess Highway, Conjola	1.2x10 ⁶	1985	240mm Asphalt 120mm Quartz gravel Sandy Gravel

² It is known that stripping of asphalt has occurred with the mixes placed at in these locations. However, as no stripping was observed in the cores, for conservatism this site has been included in the fatigue susceptible pavements.

The analysis of the database of non-LLAP again supports the finding obtained from LLAP studies undertaken internationally that a limiting thickness of around 280mm exists for asphalt pavements, regardless of support to the asphalt layer, with the thickest section of asphalt pavement to experience fatigue cracking being 260mm.

8.2.3 Condition Assessment (FWD)

For each of the sites in the RMS STEP database full Falling Weight Deflectometer (FWD) survey results were available, in terms of the:

- Full load deflation bowls,
- Surface temperature
- Air Temperature Data

All FWD testing undertaken as part of the STEP database development was conducted using a standard approach and in all cases the pressure on the load plate was targeted at 700kPa. The use of a standard 700kPa load pressure is convenient as it equates to a load of 49kN. The advantage of the 49kN is that the loading is close to that of the recommended ½ axle loading of 45kN, meaning that the effect on non-linearity on granular materials will be little to nothing.

The results of the FWD survey can be seen in Figure 8-15 and Figure 8-16 following which show the full deflection bowls for the LLAP sites and the non LLAP sites respectively.

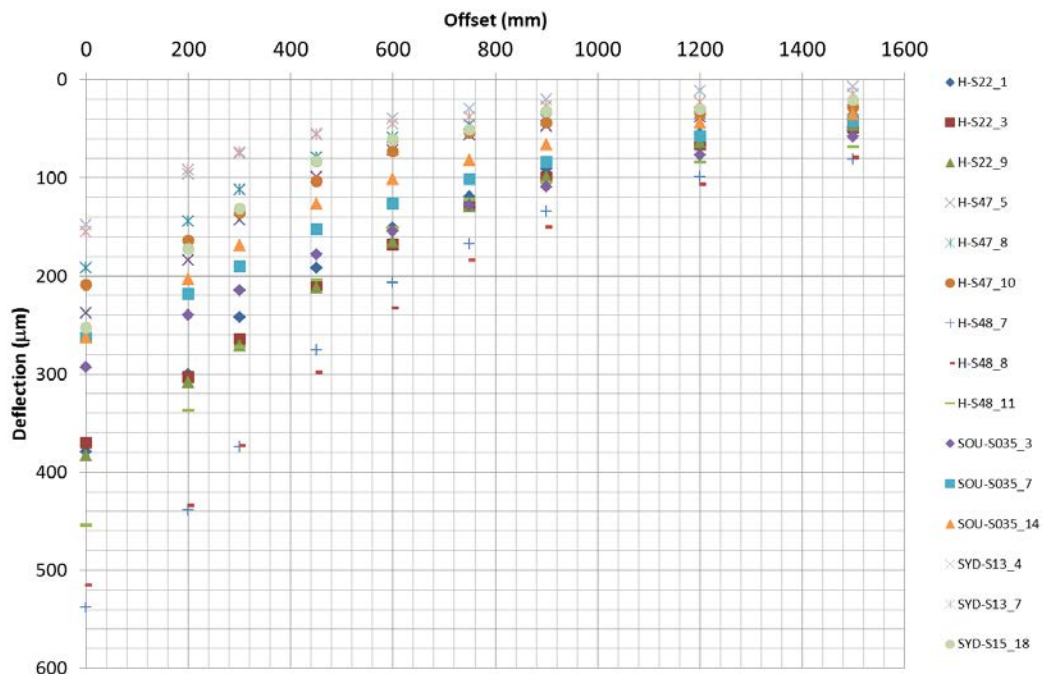


Figure 8-15 Deflection Bowls LLAP

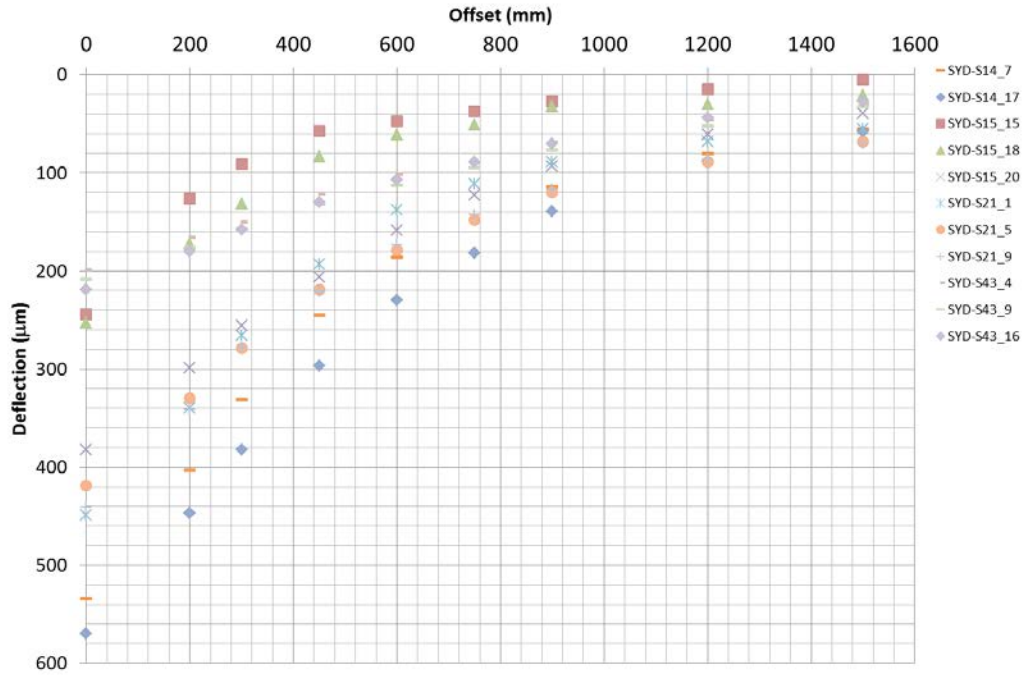


Figure 8-16 Deflection Bowls Non LLAP

What the figures show is that the overall deflection ranges of the two sets of data are close to identical. The implication of this, as expected, is that low or high deflection alone cannot be used to define a LLAP and as found with the calibration undertaken on the NCAT test track, strain appears to be much more significant in predicting the occurrence of LLAP.

8.2.4 Mid Layer Depth

Additionally, the database included the mid layer asphalt temperature of the combined asphalt layers. The mid layer temperature was calculated using the surface temperature measured in the FWD testing and the modified Bells equation developed by Roberts et al. (2010) and as shown in Equation 8-1 following.

$$T_2 = AAF \times \left[8.77 + 0.649 \times T_0 + (2.2 + 0.044 \times T_0) \times \sin \left(2\pi \times \frac{hr - 14}{24} \right) + \log_{10} \left(\frac{h_i}{100} \right) \times \left(-0.503 \times T_0 + 0.786 \times MMAT + 4.79 \right) \times \sin \left(2\pi \frac{hr - 18}{24} \right) \right] \quad \text{Equation 8-1}$$

Where;

MMAT = Mean Month Air Temperature, for the month of testing

- T_o = surface temperature at time of day
- hr = time of test on 24 hour (decimal) clock. (eg: 14.33 = 2.20 pm)
- h_i = Combined asphalt layer thicknesses (mm)
- T_2 = temperature at mid-point in pavement layer
- AAF = *Adjustment Factor*, = $0.0175 \times MMAT + 0.6773$.

While it is understood that ARRB are currently undertaking further studies on the improvement of the prediction of pavement temperature with depth equations for Australian condition, at this point there appeared to be no advantage in using an alternative approach to the method developed by Roberts and as such the ARRB modified Bells equation was used in the analysis.

If an alternative approach emanating from the ARRB studies is developed and recommended in the future, it would be recommended that the calibration exercise be re-undertaken to ensure the linkage with actual field performance.

8.3 Insitu Material Assessment

While some may question the accuracy of back-calculation methods, back-calculation remains the most accepted and practical method to assess the insitu stiffness of pavement layers. Most significantly, for the sites used in this analysis the FWD testing was undertaken at the location of each test-pit, meaning exact layer thicknesses and material type were known. This significantly reduces potential inaccuracies in the back-calculation.

At present there are three main back-calculation methods that are widely used. The three methods are primarily based on the forward calculation procedure. In a study for the Texas DOT Uzan (1994) analysed several existing back-calculation procedures and concluded that the main differences among all procedures are related to the forward calculation model used to predict the pavement response as well as the error minimization scheme utilised. The forward calculation schemes investigated included, numerical integration (Linear Elastic (LE) methods, matrix based Finite Element (FE) methods and approximation methods (Method of Equivalent Thicknesses (MET)). He found that although the approximation methods are faster, in some cases they may lead to unacceptable errors in the forward calculation that in turn would lead to errors being reflected in the computed modulus values.

However, by far the most important parameters to ensuring correct results from the back-calculation process found by numerous researchers, is to incorporate the right set of rules to define the pavement system (layer ratios, maximum and minimum modulus value etc.). These “rules” have been found to be rather more important than the method used in the forward calculation and the method used to determine the minimum error. This was reinforced by Appea et al. (2002) who found that the “*considerations such as the allowable*

ranges and seed values appeared to have more impact on the back-calculated moduli than the software package used.”

8.3.1 Layer Elastic Analysis

The best overall solution at the present time is to use the numerical integration methods based on linear elastic solutions. It was Burmister who provided the first theoretical solutions for a system of two or more elastic pavement layers, using a series of Bessel functions. In 1962 Schiffman expanded this knowledge and provided solutions for an n-layered pavement system. The solution found by Schiffman, led to a series of computer programs. All of these programs developed based on Schiffmans solution compute stresses and strains based on the following assumptions.

- Surface load is uniformly distributed over a circular area
- All layers are homogeneous, isotropic (except CIRCLY) and linear elastic
- Upper layers extended horizontally to infinity
- The bottom layer is a semi-infinite half space

An iterative procedure is then used to determine those modulus values that result in the same deflections as measured.

8.3.2 Bedrock

If the subgrade is assumed to be a semi-infinite half space, as in the proposed LE methods, the effect of a stiff layer, or bedrock layer, at a shallow depth can be quite significant. The failure to consider the stiff layer can cause erroneous results in the upper layers. If a stiff layer is to be considered in back-calculation the question must be asked how deep is infinity? Or to put it another way, when should a stiff layer be considered? Irwin (1994) found that the stiff layer has little to no effect on the back-calculated modulus values when the layer is deeper than 12m, other researchers, such as Ullditz (1987) have found that a level of 5m may be appropriate. Whichever is the case, it is clear that many pavement structures may be affected by the presence of a bedrock layer and the bed rock layers should be considered not only in back calculation but forward calculations as well.

There are two main methods recommended to calculate the depth to the stiff layer in a back-calculation procedure. By far the most widely accepted is the method used in WDOT design manual. In this method the measured deflection is plotted against the reciprocal of the distance from the load ($1/r$). In this analysis if $1/r$ has an intercept that is not equal to zero, it indicates the presence of a stiff layer at shallow depth. This is based on Boussinesq's equations as shown in §4.3. If the pavement is, in fact, a $1/2$ space the deflection will only be zero when the distance from the load is infinite i.e. $1/r = 0$. Using this approach an assumption is then made, which has been found to be fairly accurate that the radial distance

to the point where the deflection is zero is equal to the depth of the stiff layer i.e. the surface deflection is equal to the horizontal deflection at depth. This approach is shown in Figure 8-17, following.

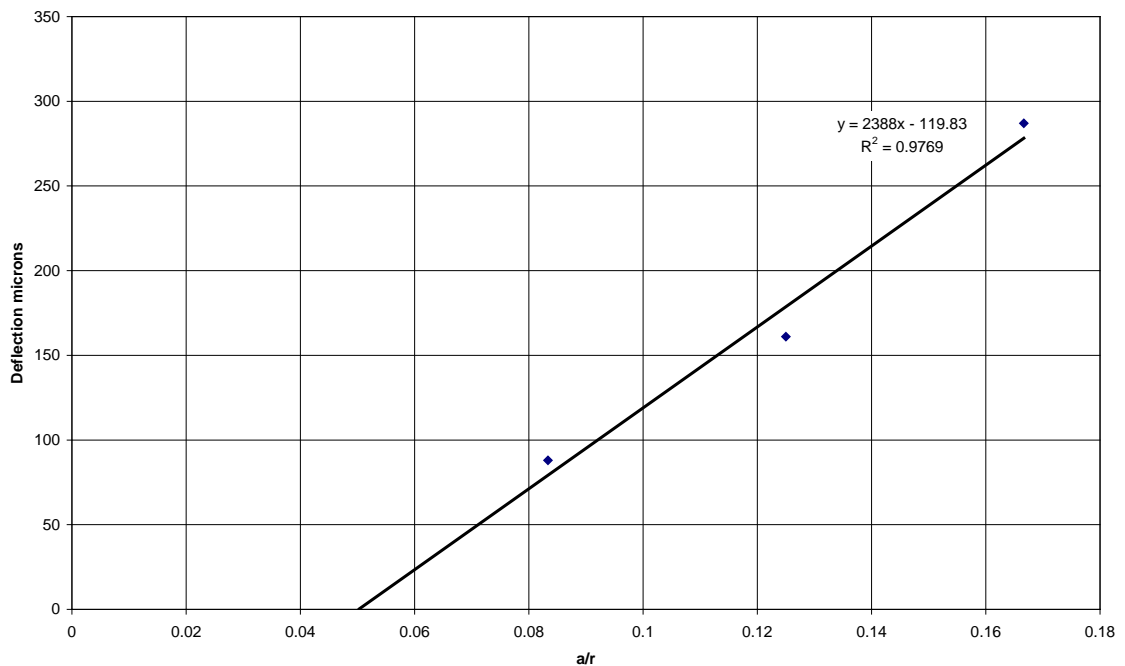


Figure 8-17 Estimating the Depth to Bedrock

In the figure, the plot of the last three deflection measurements (>900mm) are plotted against the reciprocal of the distance from load divided by the plate radius (to normalize the results). If the pavement was truly a linear elastic half space at a distance of infinity the deflection should be zero. If the deflection reaches zero at some other distance less than infinity it implies there is a stiff layer. In the preceding figure, the intercept of the last three deflection readings is shown to be approximately 0.05, hence the depth to bedrock in this case would be estimated at being 4.5m.

8.3.3 Assessing the Answers from Back-Calculation

The most popular method at present to assess the accuracy of back-calculation results is to use the Root-Mean-Squared (RMS) of the error between the back-calculated results and that of the forward calculated. What a small RMS error (<2%) indicates is that there is a good match between the measured and calculated deflection bowl. However it does not insure the back-calculated modulus are correct. As indicated by Irwin (2005) *“The best way to overcome the problems and assess the validity of the back calculation results is to have a thorough understanding of the materials in the pavement.”* This is where the results for §8.2 become increasing important and the rules determined based on these fundamental material

properties. To ensure correct answers are achieved not just close matches to the deflection bowl.

8.3.4 Implications on Forward Calculations

Probably of greater importance in determining the true response of a pavement system to applied loading, than the set of rules developed in the previous sections for the determination of the pavement's response to loading, is ensuring that the assumptions made in the back-calculation phase match the assumptions made in the forward calculations. It is of no use going to all the effort to determine the non-linear pavement material responses if the forward calculation assumes all materials are linear elastic, as with the depth to bedrock. Therefore for practical implementation of any design procedure, there has to be a link established between the back-calculation procedure and the forward calculation procedure.

8.3.5 Pavement Model for Back-calculation

The model for the back calculation analysis used a 5 layer system with a varying depth to bedrock and is shown following.

- Asphalt thickness was determined from the combined asphalt layers thicknesses, from geotechnical investigation
- Base layer thickness was determined from the geotechnical investigation; thin base course layers (<150mm) were combined with lower layers.
- Sub-base, if any, was the combined sub-base layers from the geotechnical investigation. Where no sub-base existed, the upper subgrade (500mm) was modelled as a separate layer.
- Subgrade thickness was determined from intercept of inverse deflection plot or limited to a maximum 5000mm layer.
- A bedrock layer existed in all pavements with a stiffness of 5000MPa. The bedrock layer was infinite with depth.
- The approach used for back-calculation was based off a deflection basin fitting approach with the objective function of minimising RMS error.

The pavement model used for each site along with the back-calculated modulus is shown in Table 8-3, following for both the LLAP sites and the damaged non-LLAP pavement sites.

Table 8-3 Back-Calculated Results and Pavement Model

ID	Temp (°C)	Thickness (mm)				Modulus (MPa)					RMS
		L1	L2	L3	L4	E1	E2	E3	E4	E5	
LLAP Sites											
H-S22_1	31.9	200	200	300	2933	2288	206	112	125	5000	0%

H-S22_3	32.0	210	190	300	2978	2538	201	97	114	5000	0%
H-S22_9	31.5	200	220	300	2700	2410	223	94	109	5000	0%
H-S27_13	21.4	180	195	300	675	1312	345	66	55	5000	2%
H-S27_16	21.9	200	200	300	650	1030	292	70	35	5000	1%
H-S27_18	21.8	205	215	300	630	1124	344	49	99	5000	2%
H-S28_12*	25.8	265	205	150	730	862	147	864	33	5000	1%
H-S28_16*	26.1	285	240	300	525	1904	50	1016	54	5000	5%
H-S28_18*	25.6	265	235	300	550	1005	119	646	37	5000	1%
H-S29_1	26.5	160	190	70	930	3203	681	8139	84	5000	1%
H-S29_10	25.1	140	150	115	945	3643	351	5760	166	5000	4%
H-S29_9	25.5	150	130	120	950	2607	420	2582	165	5000	3%
H-S48_7	22.6	140	260	400	5000	3222	108	208	79	5000	0%
H-S48_8	22.5	130	345	425	5913	4602	175	82	86	5000	0%
H-S48_11	22.8	130	370	250	5000	3856	182	326	90	5000	1%
SOU-S035_3	21.3	280	300	700	5000	3200	150	80	150	5000	0%
SOU-S035_7	21.3	280	300	700	5000	2636	134	154	171	5000	0%
SOU-S035_14	20.4	215	300	700	5000	3092	199	218	202	5000	0%
SYD-S11_1	28.5	205	355	300	490	2492	2077	113	17	5000	1%
SYD-S13_4	30.6	260	170	400	1256	2450	1250	180	700	5000	1%
SYD-S13_7	30.8	270	170	400	5000	2250	1250	220	557	5000	1%
SYD-S15_18	30.8	210	165	400	4054	1686	228	460	292	5000	1%
SYD-S15_20	30.8	210	150	400	2232	2146	273	99	108	5000	0%
N4-150	16.1	180	220	330	287	1550	216	160	142	5000	0%
N7-70	17.5	225	220	330	5000	8333	263	252	180	5000	0%
Q5-90		345	200	450	5000	2172	105	164	394	5000	0%
Q6-0	19.4	345	200	450	5000	2664	164	210	248	5000	0%
V6-20	7.2	190	75	450	5000	7049	699	56	156	5000	0%
Non- LLAP Sites											
H-S23_1	32.5	220	230	400	1577	643	190	47	100	5000	2%
H-S23_8	31.9	200	300	400	1697	744	45	3268	79	5000	0%
H-S24_13	29.4	155	345	170	1638	840	68	71	56	5000	2%
H-S24_3	29.9	160	440	150	1772	828	92	10	49	5000	2%
H-S24_7	29.9	165	435	100	1854	1129	137	17	61	5000	1%
SYD-S24_2	24.1	190	310	260	5000	1460	315	22	76	5000	0%
SYD-S25_13	23.2	150	450	300	1385	1855	76	108	42	5000	0%

SYD-S25_2	23.4	150	520	480	1177	2004	50	95	36	5000	0%
SYD-S25_5	23.3	150	200	450	4472	1031	142	71	83	5000	0%
SYD-S16_3	20.4	130	190	380	2769	1297	130	90	88	5000	0%
SYD-S16_8	20.8	145	235	300	2658	1162	332	37	69	5000	0%
SYD-S46_12	26.1	160	210	130	1558	1029	95	87	74	5000	2%
SYD-S46_3	26.5	150	270	100	1790	984	163	32	53	5000	0%
SYD-S46_6	26.7	160	240	400	917	1126	57	122	60	5000	1%
H-S39_11	24.5	240	180	180	2839	2989	123	372	128	5000	0%
H-S39_6	24.8	240	330	300	5000	1554	204	481	167	5000	0%
H-S39_9	25.0	260	210	150	5000	2052	177	921	147	5000	0%
SYD-S26_1	24.5	130	250	520	2988	1900	162	47	46	5000	0%
SYD-S33_12	24.6	130	310	360	2663	3324	55	619	55	5000	0%
SYD-S33_2	25.0	140	310	130	5000	1408	138	376	53	5000	0%
SYD-S33_6	25.2	150	330	320	3702	1461	105	254	67	5000	0%
SYD-S44_18	26.1	130	290	360	2256	1700	54	1170	95	5000	0%
SYD-S44_20	26.6	150	300	450	1166	934	150	52	53	5000	0%
SOU-S089_14	22.9	240	120	300	2424	925	41	1345	154	5000	1%

**FWD results indicate damaged asphalt, therefore section H-S28 was excluded from being a LLAP.*

The results show the difference between the measured and calculated deflection bowls was typically less than 1% indicating a high confidence in the back-calculation results. These results are lower than what is typically achieved by back-calculation. This however is due to; the exact material profiles being known at the point of the back-calculation, the incorporation of the bedrock layer, and a higher degree of precession being used in the back-calculation process.

The results show that the subgrade support values found from the back-calculation are somewhat higher than what would be typical on new pavement design with values ranging from 60-150MPa found. However, these values are insitu, which are typically higher what would be expected from soaked ex-situ tests. Therefore, if the model is validated on insitu tests and ex-situ soaked test are used for the purpose of pavement design a degree of conservatism will be automatically built into the design.

Empirical LLAP design procedures such as that proposed by Nunn et al. (2001) place a high importance on determination of subgrade support for LLAP design. However the framework of both the AGPT002 (2012) and the APS-fL project is mechanistic-empirical procedure and as such places a higher emphasis on total support to the asphalt layer through the use of induced strain over subgrade support only. The approach has advantages in that it is not only a measure of the variation in subgrade support but the support additionally offered by

any base or sub-base layers. In this way subgrade support and variation in subgrade support is covered in the calculation of strain under the design vehicle. This was shown in the examination of the deflection bowls and confirmed by the NCAT test track results, which clearly showed that strain is directly related to asphalt performance.

8.4 Validation of Stiffness-FEL Relationship with Australian Data

To validate the NCAT findings to Australian conditions the APS-fL project examined the sites identified as LLAP and Non-LLAP from the RMS STEP database. The sections identified as LLAP, as shown in Table 8-1, were sites that were greater than 20 years old, had experienced in excess of 3×10^7 ESA loading and had no cracking. Additionally, to undertake the validation a number of thick (>140mm) Non-LLAP sites as shown in Table 8-2, which although had significant traffic loading, were experiencing some form of structural failure.

It was believed that by using both the sites which had undergone failure and the LLAP sites the stiffness-FEL relationship could be validated between real life Australian LLAP and fatigue susceptible pavements.

For each site in the RMS STEP database, FWD data, a full geo-tech investigation, maintenance history and condition assessment was available. The full details of the sites, material type, back calculated modulus and layer thickness can be found in Appendix B and E for the back calculation results.

For each of these sites the stiffness-strain relationship was established by:

- Determining the supporting layer modulus values from back-calculation of the deflection bowl as described previously and shown in Table 8-3.
- The mid-layer asphalt temperature was calculated for six seasons: summer, autumn, winter, and spring. Additionally, the mid layer temperature was calculated for the upper 10th percentile summer temperature and lower 10th percentile winter temperature using the calibrated Bells equation procedure developed by Roberts (2009).
- The vehicle speed for the heavy vehicle was taken as 10km lower than that of the posted speed limit.
- The design axle loading was taken as the upper 97.5th percentile axle loading in Australia of 9.0 tonnes.
- The effective modulus was calculated based on 40mm AC14C320 asphalt and the remaining asphalt being an AC20 C320 layer, typical of asphalt used to construct the pavements.
- For each season, the horizontal strain at the base of the combined asphalt layer was calculated using Layered Elastic analysis. (NB to be consistent with back-calculation all layers were isotropic)

Once the strains had been calculated, the relationship between stiffness and strain for each of the Australian validation sites was plotted as shown in Figure 8-18 following, which summarises the results of the analysis for the Australian validation sites. Detailed results can be found in Appendix F. To add to the data and the overall understanding of the performance of LLAP In addition to the Australian sites, the analysis included the results obtained from that of the structural sections on the NCAT test track and three sites from the UK Valmon data, which were the closest to the FEL and Australian LLAP. The results of the FWD analysis on the Colgreen, Brentwood and Thornbury Valmon LLAP can be found in Appendix E of this report. Figure 8-18 following shows the results obtained from the Australian LLAP and non-LLAP, the structural sections on the NCAT test track and the results obtained from the three Valmon sites, as well as the calibrated relationship obtained from analysis of the Phase II NCAT test track structural sections.

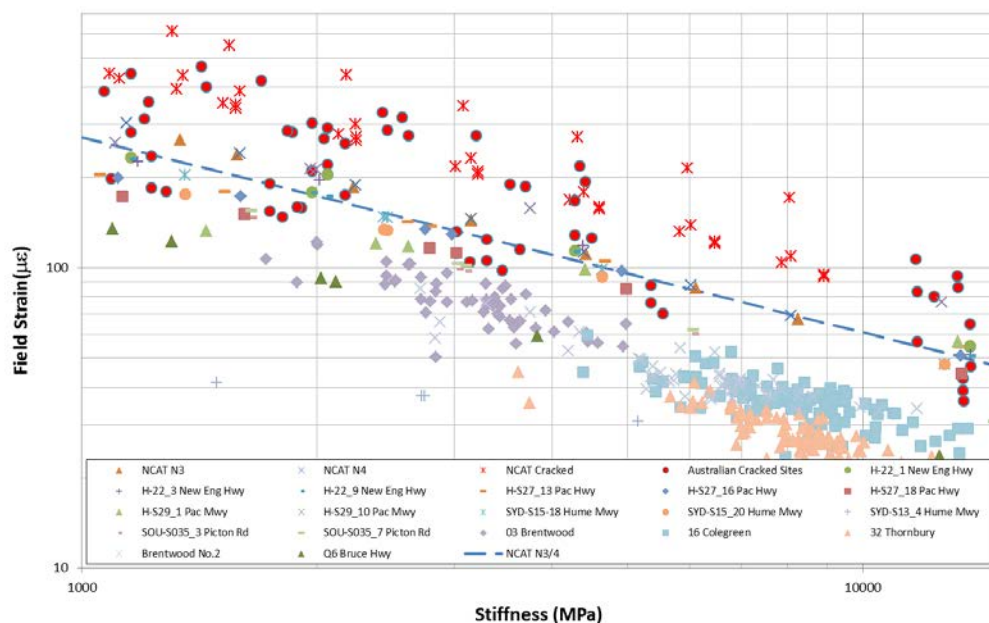


Figure 8-18 Modulus Strain Endurance Curve Australian Sites

As can be seen in the figure and as was found with the NCAT test sections, a clear differentiation exists in the stiffness-strain relationship between those sections which are; determinate, non-determinate and LLAP. As with the findings on the NCAT test track, the sections which showed signs of failure had strain levels across the whole range of stiffness values higher than the non-cracked sections, clearly showing structural failure again is a function of induced strains, which is a combination of both the subgrade and sub-base support.

The analysis shows that the FEL relationship determined from the NCAT test track appears to hold true for some but not all of the Australian sites. The NCAT level appears to be

around a 50% confidence level and while most pavements designed at this FEL will be LLAP, this will not always be the case and some pavement, which may have a long life but will be indeterminate in nature. The results show that a number of sites, which have signs of failure, particularly the Sydney Newcastle Freeway (H-S39) at Mooney-Mooney fall below the proposed NCAT endurance limit. The results also show that all of the UK Valmon LLAP sites fall below that of the NCAT limit.

The analysis shows that the modelling of the six seasons appears not to be required with 3 critical locations possible, summer, winter and a mid-point, if all these points fall below that of the FEL all points throughout the year will also. Given this, it is recommend that the design approach moving forward only use, the upper summer 95th percentile temperature, winter lower 95th percentile and the midpoint determined as the WMAPT.

The visual inspection of the results shows that a limit appears to exist between that Sydney Newcastle Freeway (H-S39) site and the Valmon and New England Highway site (H-S27_18). While the NCAT relationship may be practical to determine a pavement with a long and indeterminate life, it will not ensure that the pavement is a LLAP. Both the Australian and UK field validation data suggest a more conservative FEL is required.

This observation of the data thus suggests that the standard FEL curve needs to be shifted to the deviation between the Sydney Newcastle Freeway section (H-S39) and the Valmon and the New England Highway site (H-S27_18), as shown in Figure 8-19 following.

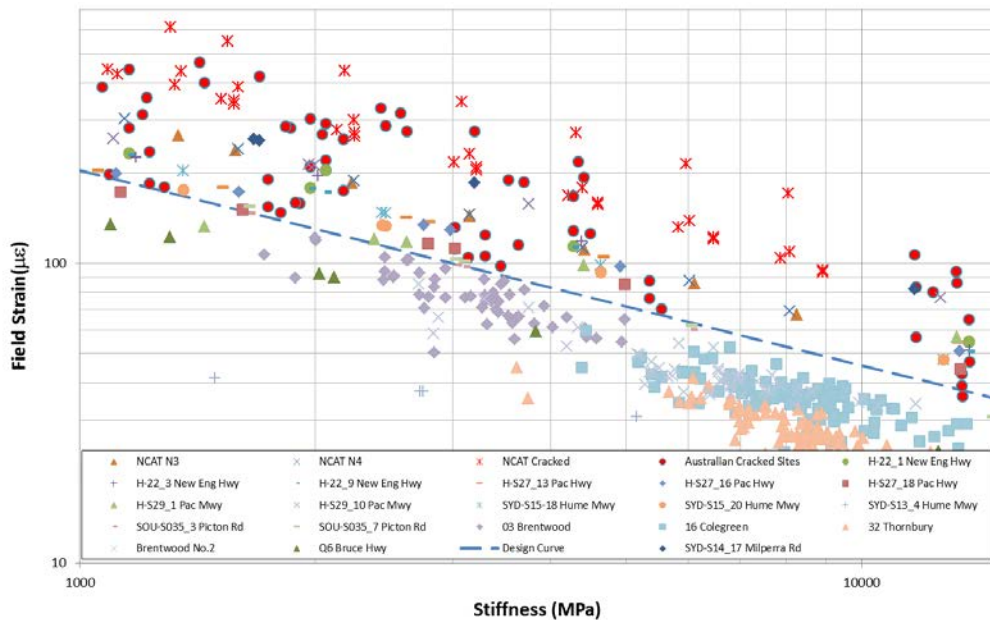


Figure 8-19 Validated Stiffness-Strain Endurance Curve Australian Sites

The results show that the confidence and rest factor, k_1 , needs an adjustment factor of 0.9 to move from the standard curve to the field observations.

Using the results of the Australian validation sites H22, S15 and H23 and the Valmon sections, a revised validated FEL-stiffness relationship was established from field validation data, as shown in Equation 8-2 following.

$$FEL = 0.9 \times 20200S_{mix}^{-0.65} \quad \text{Equation 8-2}$$

Where;

FEL is the Fatigue Endurance Limit at given modulus

S_{mix} is the equivalent stiffness of the combined asphalt layers

This relationship offers a practical stiffness-FEL, which can be used for LLAP pavement design. At levels below the stiffness-FEL relationship, Australian pavements have not experienced cracking with in excess 8×10^7 ESA loadings and 30 years of service. At strain levels above this relationship, pavements appear to be fatigue susceptible with a majority but not all pavements experiencing damage. As the FEL relationship was developed from Australian mixes and NCAT mixes, the relationship is:

- Valid for mixes with conventional bitumen and low levels of SBS modification.
- Valid over a full range of temperatures experienced by asphalt pavements 0-45°C.
- Valid for both freeway and high volume urban areas.
- Not valid for mixes with high RAP contents (>30%) and its use with higher RAP contents is not recommended.
- Only valid for dense graded mixes and cannot be used with mixes with design air voids of greater than 5%.

8.5 Establishing Confidence Levels

While the relationship found from visual observation of the stiffness-FEL curve shown in Figure 8-19 will for most cases result in a true LLAP, there is no statistical rational or confidence behind the recommended level. While it may be argued that a FEL design method does not require a statistical confidence level, statistical confidence can be easily inserted into the method by using the k_1 adjustment constants to move the design curve up or down to cover more points (or a higher or lower confidence), as shown in Equation 8-3.

$$FEL = k_1 20200S_{mix}^{-0.65} + k_2 \quad \text{Equation 8-3}$$

Where;

FEL is the Fatigue Endurance Limit

S_{mix} is the stiffness of the mix, and

k_1 is the adjustment constants for differences in rest periods, or confidence levels

k_2 is the mix adjustment factor

This approach moves the standard equation up or down to account for changes in potential of the healing of the mix to account for different binders and rest periods or in this case confidence levels incorporating all of these variables.

To establish confidence limits the predicted strain for each of the LLAP section which fell between fell the section with the lowest strain-stiffness relationship, which had shown signs of failure, (the Sydney Newcastle Freeway section H-S39) and the section with highest stiffness-strain relationship which showed no signs of failure (H-S29 and N4 as lines cross over) were analysed. The analysis fitted a power relationship to the stiffness strain curve for each of the 14 sections which fell in the indeterminate zone. These relationships were then used to predict the strain at stiffness values near the upper summer temperature (1,500MPa), the WMAPT (3,000MPa) and winter lower (6,500MPa). For each of the stiffness values the strains were then ranked in order of highest to lowest and the strains were then plotted against the inverse standard normal distribution (normal (z) score) as shown in Figure 8-20 following.

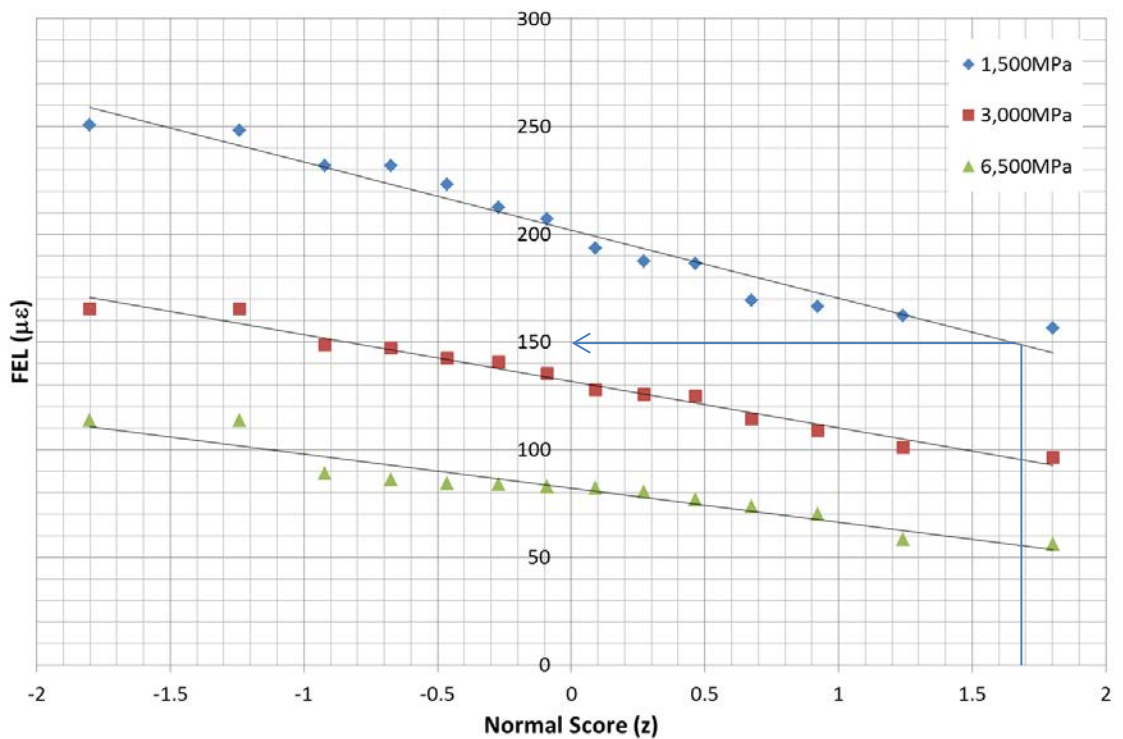


Figure 8-20 Normal Score (FEL)

As seen in the figure showing the resulting distributions for the three stiffness levels, the distribution can be seen to closely follow that of a normal distribution and for all practical purposes can be assumed to follow a normal distribution. Because the results follow that of a normal distribution, confidence levels can easily be developed by solving the line of best fit of the normal score against that of the predicted strain for the normal score(z) at a set confidence limit.

The AGPT002 (20120, uses 5 levels of project reliability 80, 85, 90, 95 and 97.5%. these reliability (probability) figures can be equated to a normal (z) score of the standard normal cumulative distribution (mean zero and standard deviation of 1) of 0.842, 1.036, 1.282, 1.644 and 1.960 respectively. This can be seen conceptually in Figure 8-20 where the 95th percentile value (1.64) can be seen to equate to a FEL of 150 $\mu\epsilon$ for a stiffness of 1500MPa.

Using these confidence levels the standard FEL equation can then be adjusted by changing the confidence coefficient, k_1 , to fit the predicted FEL level at the required confidence level. The resulting fitting parameters and the confidence based FEL are shown in Table 8-4 following. While the resulting confidence limits for 80 and 95 percentile can be seen on Figure 8-21 following.

Table 8-4 FEL and Confidence Limits

Confidence Limit	Normal Score (z)	FEL ($\mu\epsilon$)			k_2
		1500 MPa	3000 MPa	6500 MPa	
0.8	0.842	174	110	68	1
0.85	1.036	168	107	66	0.97
0.9	1.282	161	102	63	0.925
0.95	1.645	150	95	59	0.86
0.975	1.960	140	88	54	0.80

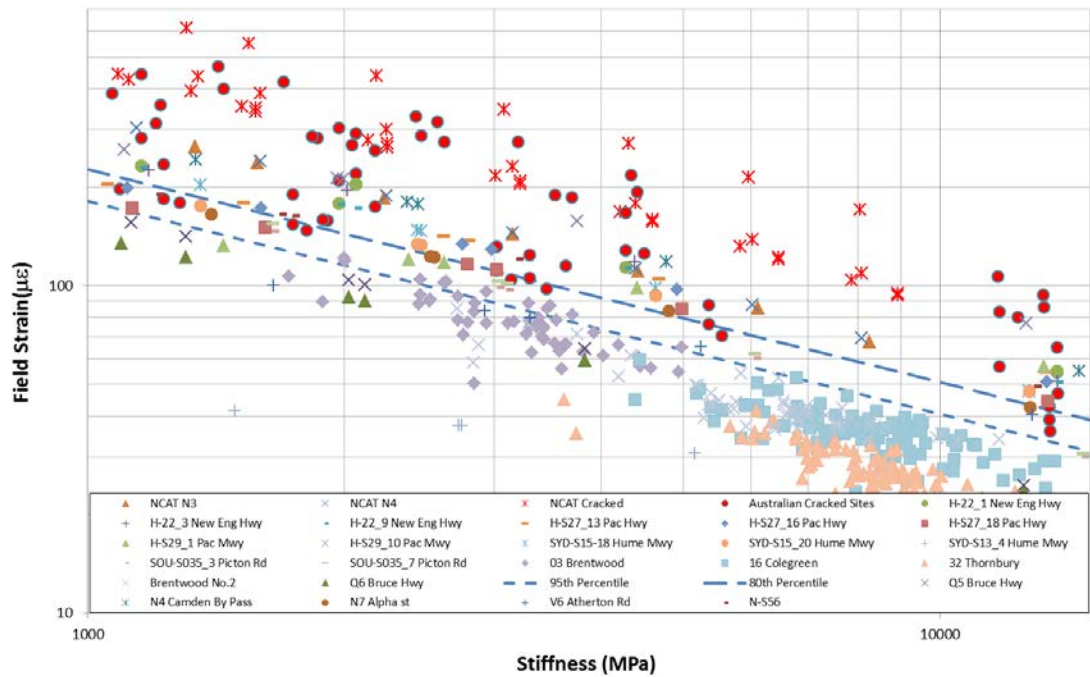


Figure 8-21 Confidence Limits and LLAP Sections

Using the recommended relationship, it can be found that on a subgrade of CBR 5 the 50% confidence level will give thicknesses in the range of 260-270mm and at the 95th percentile level thicknesses in the range of 330-340mm. these results compare very favourably with the recommendations of Rolt (2001) that a well-designed and constructed asphalt pavements with 270mm of thickness could provide a fatigue resistant pavement structure and Nunn (2001) that 280mm was sufficient to resist fatigue cracking. The additional thicknesses above these figures at higher confidence levels simply allow for increased confidence in design and possible deficiencies in materials and design.

8.6 Laboratory to Field Shift

Given that the confidence based shift factors are all a correction to the standard FEL relationship obtained from US and Australian mixes, the shift factor k_1 is simply a laboratory to field conversion. Given that this is a simple shift, confidence levels can easily be applied to mixes which do not fall on the standard FEL relationship, such as EME2 mix and A5E mixes. Simply the same confidence shift factors may be applied to the results of laboratory testing using the determined using the PV_L approach as found in this study.

8.7 Endurance limits for lower level traffic

While the stiffness-FEL establishes a simple tool for the design of LLAP, pavements which fall above this level can still be LLAP. However, in all cases the traffic loading would have to be less than the common freeway traffic loading experienced in Australia. Because of the

lower traffic levels, greater amounts of healing will be possible allowing for thinner pavement sections.

To do this, the database would have to be expanded to cover LLAP without any damage with traffic levels less than 4×10^7 ESA. The approach would again be to, simply move the confidence equation for the lower traffic levels.

8.8 Summary and Recommendations

This finding obtained from the analysis of LLAP on the NCAT test track was extended to actual LLAP in Australia and the UK. The analysis confirmed the same finding as on the NCAT test track that a direct relationship exists between the infield stiffness-strain curve of LLAP and the laboratory determined stiffness-FEL curve. This direct relationship allows the development of a phenomenological stiffness-FEL relationship which can be used for the purpose of pavement design.

Based upon both the calibrated relationship from the NCAT data and validated Australian LLAP, the use of a stiffness-FEL relationship is recommended for the design of long-life asphalt pavements in Australia. The relationship was validated to Australian data and only required a slight modification to the relationship developed from the NCAT, as shown previously in equation 8-3 and following.

$$FEL = k_1 20200 S_{mix}^{-0.65} + k_2 \quad \text{Equation 8-3}$$

Where;

FEL is the Fatigue Endurance Limit

S_{mix} is the stiffness of the mix, and

k_1 is the adjustment constant for differences in rest periods, or confidence levels

k_2 is the mix adjustment factor

It was found that confidence limits could be incorporated into the equation by the use of the k_1 adjustment factor and confidence limits could be determined from the Australian validation sites as shown following.

Table 8-5 FEL Confidence Limits

	Confidence Level				
	80 th	85 th	90 th	95 th	97.5 th
k_1	1	0.97	0.925	0.86	0.8

The analysis of the results showed that the design of LLAP can be supported by a fundamental test using the RDEC and the constant PV_L . However, a laboratory to field conversion is needed to use the test which is equivalent to the confidence values shown previously.

This procedure has been developed using the following assumptions:

- 9.0 design axle
- Model using 3 seasons; summer, median (WMAPT) and winter.
- Mid layer asphalt temperatures be taken from the ARRB modified Bells equation

Any deviation from these assumptions should result in a revalidation of the confidence level assumptions of Table 8-5.

9 Austroads Supplement Recommendations

9.1 Introduction

This chapter sets out the recommended format for a Supplement to the AGPT02 (2012) for LLAP design. The procedure is based on the recommendations found in this report and the design procedure used in the AGPT02. Where possible the procedure has attempted to follow the recommendation of the AGPT and incorporate the required additional steps for LLAP design.

The intent of the AAPA LLAP design procedure is to determine the maximum tensile strain(s) at which, whilst damage might occur, the asphalt will never develop macro-cracking requiring deep structural treatment. As the proposed procedure has been developed and validated for freeways, highways and urban arterial roads, this procedure is relevant to all those pavement types. The recommendation in this chapter should be read in conjunction with AGPT02 (Austroads, 2012).

9.2 (3) Construction and Maintenance Considerations

9.2.1 (3.2.5) Working Platforms

As compaction of asphalt layers on subgrades with stiffness of less than 100MPa (CBR 10%), is difficult, for a subgrade with a stiffness of less than a 100MPa, it is recommended that a working platform be established to achieve a supporting layer of sufficient quality to be assigned a design modulus of 100MPa (or greater) in CIRCLY should be placed directly below the bottom asphalt layer to support this bottom layer and assist with achieving compaction.

9.2.2 (3.7) Pavement Layering Considerations

The LLAP concept utilises a three layered asphalt system;

- 1) A wearing course and levelling course (surfacing layers), which should be durable and rut resistant
- 2) intermediate layer(s), which should be rut resistant and be the main structural layers
- 3) fatigue layer, which should be a fatigue resistant low air void mix

The high rut resistant durable surface layers may consist of dense grade asphalt, it is noted that many SRAs do not utilise DGA as a wearing course on freeways due to texture requirements or use a SMA, typically a maximum size of 14 mm. Where an OGA surfacing is proposed for noise and/or drainage considerations, an additional surface layer consisting of a 14mm DG asphalt should be provided immediately below the OGA surface. For durability and rut resistance, the asphalt in the surfacing layer(s) may incorporate a modified binder, if

so an A35P or Multigrade is recommended over elastomeric binders such as A10 or A15E as A35P offer more structural capacity to the pavement.

The intermediate asphalt layers(s) should consist of conventional (C320, 450 or 600) asphalt DG20 mix which is durable and rut resistant suitable for the climatic region.

It is recommended that the LLAP incorporate a low air void (<4%) asphalt fatigue layer, in the bottom 60mm of the pavement. The low void layer is usually achieved by the use of higher binder content in the bottom layer of the DG 20 asphalt mix. This lower level asphalt layer should consist of no more than 30% RAP, if more than 30% RAP it is recommended that the stiffness-FEL relationship of the mix be confirmed to fall on or above the standard stiffness-FEL mix curve.

9.2.3 (3.12) Maintenance Strategy

LLAP are designed to eliminate fatigue cracking therefore no full/partial depth repairs are expected due to structural failure of the pavement for an extended pavement life of greater than 40 years.

In LLAP all maintenance is expected to be top down resulting from oxidation and/or surface initiated cracking, or non-structural environmental cracking, therefore maintenance will be limited to periodic overlays or thin mill and re-sheets.

9.3 (4) Environment

9.3.1 (4.3) Temperature

The distribution of yearly and daily temperatures can have a significant effect on the performance of LLAP and should be taken into account in the design of LLAP. For example, traffic loading which occurs at night in the middle of winter will result in relatively brittle asphalt with a lower FEL. During the day in the middle of summer, the asphalt has a lower stiffness resulting in higher critical strains, but has a higher FEL.

For LLAP design, the temperature of asphalt should be characterised by use of the both Weighted Mean Annual Pavement Temperature (WMAPT) and the effective asphalt layer temperature at two extremes of temperature; midday in the hottest summer month and early morning in the coolest winter month.

The WMAPT is given in Appendix B of the AGPT02 the procedure for calculating the effective layer temperature for the combined asphalt layers is given in Section 9.3.2.

9.3.2 (4.3.1) Calculation of Effective Layer Temperature

The temperature at the midpoint of the combined asphalt layers can be calculated using the Bells equation, modified to Australian conditions (Roberts et al. (2010)).

$$T_2 = AAF \times \left[8.77 + 0.649 \times T_0 + (2.2 + 0.044 \times T_0) \times \sin \left(2\pi \times \frac{hr - 14}{24} \right) + \log_{10} \left(\frac{h_i}{100} \right) \times \left(-0.503 \times T_0 + 0.786 \times MMAT + 4.79 \right) \times \sin \left(2\pi \frac{hr - 18}{24} \right) \right] \quad \text{Equation 9-1}$$

Where;

- MMAT* = Mean Month Air Temperature, for the month of testing (°C)
T₀ = surface temperature at time of day (°C)
hr = time of test on 24 hour (decimal) clock. (e.g.: 14.33 = 2.20 pm)
h_i = Combined asphalt layer thicknesses (mm)
T₂ = temperature at mid-point in pavement layer (°C)
AAF = Australian Adjustment Factor, = 0.0175 x *MMAT* + 0.6773.

The advantage of this equation is that it uses readily available monthly statistical data from the Bureau of Meteorology, which is available at:

<http://www.bom.gov.au/climate/data/index.shtml?bookmark=200>

A Visual Basic (VBA) function which can be used in MS Excel can be found in Appendix G, to assist in determining *T₂*.

9.3.3 (4.3.1.1.) Surface Temperature (Summer)

The upper 95th percentile surface temperature (*T₀*) of the pavement can be estimated by using the average maximum temperature of the hottest summer month and the simplification of the radiation balance approach, shown in Equation 9-2 following.

$$T_0 = T_a + 25.5(\cos(Z)) - 2.5 \quad \text{Equation 9-2}$$

Where

- T_a* = Air Temperature (°C)
T₀ = Surface Temperature (°C)
z = Zenith angle

The Zenith angle is given by:

$z = \text{Latitude}^0 - 23.3^0$, below the tropic of Capricorn, and

$z = 0$ for locations above the tropic of Capricorn.

For calculation of upper the summer temperature (T_0) time should be taken as 1pm i.e. 13.0 in the modified Bells equation.

9.3.4 (4.3.1.1.) Lower Surface Temperature (Winter)

For the lower minimum surface temperature, which occurs in the early morning during winter, the radiation balance equation collapses to:

$$T_o = T_a$$

For calculation of the lower surface winter temperature (T_0) time should be taken as 6am i.e. 6.0 in the modified Bells equation.

9.3.5 (4.3.1.1.) Effective Pavement Temperature

The effective pavement temperature (T_{eff}) is then taken as the midpoint temperature (T_2) + 2°C.

9.4 (5) Subgrade Evaluation

The support provided to the asphalt layers in the LLAP is one of the most important factors in determining the required asphalt thickness.

9.4.1 (5.1) Measures of Subgrade Support

For LLAP design the subgrade support shall be characterised in terms of the stiffness (resilient modulus (M_r)). It is recommended that the stiffness of the subgrade be indirectly determined from CBR of the subgrade determined from;

- in-situ DCP Testing, converted to CBR in accordance with AGPT02,
- results of soaked CBR tests , or,
- Appreciation of the subgrade soil type

The CBR shall then be converted to stiffness in accordance with AGPT02 (10xCBR).

Alternatively subgrade support may be directly determined via tri-axial testing or determined from back calculation of FWD data.

For stiffness determined from FWD testing, it is essential to use the same analysis method in back and forward calculation. Therefore, if anisotropy is not considered in the back calculation it should not be used in the development of the LLAP design. It is recommended that the back calculated subgrade modulus be validated by comparing the back calculated results to insitu CBR determined indirectly from DCP testing in accordance with Section 5.5 of the AGPT02.

9.4.2 (5.9) Subgrade Failure Criteria

Research by Nunn et al. (2001) has shown that for asphalt pavements with asphalt thickness greater than 150mm, rutting is confined to the asphalt layer(s). However, to ensure adequate cover over the subgrade a minimum number of allowable repetitions of 1×10^8 shall be applied, or $650 \mu\epsilon$, for analysis conducted at the WMAPT.

9.5 (6.4) Asphalt

Because the APS-fL project requires the determination of the stiffness of the asphalt mix at the extremes of temperature, the use of section 6 of the AGPT02 is not recommended, as this procedure has only been developed for a limited range of WMAPT temperatures and one asphalt thickness. Additionally, the validation and calibration of the FEL is based on the inter-conversion found in this report and any deviation from this approach will lessen the accuracy of the approach.

9.5.1 (6.4.1.3) Characteristics for Design

Asphalt stiffness can be determined utilising any of the following test methods:

- Indirect Tension on Cylindrical (IT-CY) samples (AS2891.13.1)
- 4 Point Bending on Prismatic Beams (4PB-PB) samples (AG:PT/T233)
- Direct Compression on Cylindrical (DC-CY) samples (ASHTO TP62 or AASHTO TP79)

All of these test methods have a different definition of time and different stress states.

For the purposes of LLAP, the modulus results need to be converted to equivalent mix stiffness under a haversine load pulse resulting from a moving truck. Comparable stiffness is obtained from the three test methods by using a constant definition of time as shown following:

- The (IT-CY) should be considered a haversine pulse load with time equivalent to double the rise time.
- The (4PB-PR) Flexural modulus test should be considered a cyclic frequency load with a haversine load pulse of $\frac{1}{2}$ the full load pulse width.
- The (DC-CY) dynamic compressive modulus test should be considered as cyclic harmonic frequency with load pulse equal to the radial pulse time.

The mathematical conversion of these three time definitions is given in section 9.5.8.

At extreme temperatures and slow vehicle speeds there can be a difference between the modulus of asphalt in tension and compression due to the stress susceptibility of asphalt. Under normal Australian operating conditions this difference is negligible. However, under

extreme conditions ($>40^{\circ}\text{C}$) stress susceptibility can exhibit an influence on the stiffness of asphalt mixes. In LLAP design there is a net confining stress on the pavement.

Due to this confining effect it is not recommended that asphalt stiffness determined from tension or pure flexural tests be used for modelling at temperatures exceeding 40°C . For these extreme conditions, it is recommended that modulus be determined based on the results of the dynamic compressive modulus test undertaken at a confinement of 200kPa.

9.5.2 (6.4.2) *Factors Affecting Modulus and Poisson's Ratio*

While, it is known that Poisson's ratio varies as a function of asphalt mix type and temperature, the development and calibration of the design procedure used a constant Poisson's ratio for asphalt of 0.35. Therefore it is recommended that this value be used for all design calculations.

9.5.3 (6.4.2.1) *Binder Class and Content*

Australia has four major paving grades of binder C320, AR450, C600 and Multigrade binders. These grades of binders affect the stiffness and temperature susceptibility of the asphalt. At the time of design it is unlikely that the designer will know the exact properties of the binder which will be used in the design. It is therefore more relevant in Australia to use typical properties of binder classes in Australia over the measurement of binder properties. The use of typical properties has been found to be no less accurate than the use of actual binder properties in complicated modulus equations (Bari et al. 2006).

The range of bitumen contents used in Australia for typical mix design does not vary to a great extent. Again at the time of structural design it is unlikely that the final binder content of the asphalt mix will be known. Therefore it is more relevant, and as accurate, to use typical modulus values rather than use binder content to predict asphalt modulus.

9.5.4 (6.2.2.2) *Air Voids*

Design air void contents do not vary to a significant extent across Australia and have been found to have very low impact on modulus values. It is therefore relevant for Australian conditions that the effect of voids be ignored, provided the design air void range remains in the typical range of Australian mixes (3.5-5.5%).

9.5.5 (6.2.2.3) *Aggregates*

As all specifications in Australia control the shape and angularity of the aggregate, the effect of aggregate type is not measurable in Australian mixes. Provided the aggregates comply with the relevant specifications, type and grading need not be considered in design.

9.5.6 (6.2.2.4) Temperature

Temperature has a significant effect on the stiffness of Australian asphalt mixes. Under typical operating temperatures experienced in Australia modulus of Australian mixes can vary between 1,000MPa to 25,000MPa.

Therefore the effective temperature of the asphalt for the design season must be taken into account during pavement design.

Temperature shall be taken into account by using a polynomial temperature shift factor (a_T) at a 25°C reference temperature where the shift factor is given by:

$$a_T = 10^{a(T-25)^2 + b(T-25)} \quad \text{Equation 9-3}$$

Where:

T = pavement design or testing temperature (oC)

a and b = Fitting coefficients of the polynomial equation (refer Table 9-1)

9.5.7 (6.4.2.2) Rate of Loading (Time)

The effect of traffic speed on the stiffness of the asphalt is significant, especially between urban and freeway conditions. To determine the stiffness at a given loading speed the first step is to convert the loading speed to a time of loading.

The time of loading has been found to be directly related to the strain load pulse time resulting from vehicle loading. For design it should be assumed that the vehicle acts as a haversine pulse with a wave length of 1.8m, the 1.8m wave length should be used regardless of asphalt thickness. The equivalent haversine loading time may be estimated using the Equation 9-4 following.

$$t_{hp} = \frac{6.48}{(v)} \quad \text{Equation 9-4}$$

Where;

t_{hp} = load duration (seconds)

v = speed of traffic (km/hr.)

The equivalent loading time (reduced time) at the design temperature shall be determined using the time temperature superposition principle.

The reduced pulse time at the design temperature is then determined using the temperature shift factor (a_T) as shown following:

$$t_{hp(r)} = a_T t_{hp} \quad \text{Equation 9-5}$$

Where;

a_T = temperature shift factor

$t_{hp(r)}$ = the reduced load pulse time at the design temperature (seconds)

9.5.8 (6.4.3.2) Laboratory Measurement

The design procedure has been developed from the results of extensive dynamic modulus testing of typical Australian asphalt production mixes. The procedure makes use of dynamic modulus master curves which can be produced from temperature frequency sweep testing.

For consistency and to aid in interpretation it is recommended that master curves only be presented in the equivalent haversine pulse time (t_{hp}) space and be represented by a sigmoidal function as shown in Equation 9-6 following.

$$\log(|S_{mix}|) = \alpha + \frac{\beta}{1 + e^{(\gamma + \delta(t_{hp(r)})^2)}} \quad \text{Equation 9-6}$$

Where:

$t_{hp(r)}$ = reduced haversine pulse load at the reference temperature (seconds)

α = the minimum value of the mix stiffness

$\alpha + \beta$ = the maximum mix stiffness

γ, δ = shape fitting parameters, determined through numerical optimisation of experimental data

As part of the APS-fL project, it was found that there is no difference between the dynamic modulus determined from AASHTO TP62 or AASHTO TP79 and either method can be used to determine the dynamic modulus of the mix.

As the definition of time in other modulus test is different from that in the dynamic modulus tests, a frequency conversion will need to be undertaken if IT-CY, 4PB-PB, or DC-CY testing is proposed to determine the mix modulus.

It has been found that the following frequency conversions give comparable results to the results obtained from dynamic modulus testing (DC-CY).

Resilient Modulus, IT-CY

$$t_{hp} = 2R_t \quad \text{Equation 9-7}$$

Flexural Modulus, 4PB-PR (AG:PT/T233)

$$t_{hp} = \frac{1}{2f_{dm}} \quad \text{Equation 9-8}$$

Dynamic Compressive Modulus, DC-CY (AASHTO TP62 and TP 79)

$$t_{hp} = \frac{1}{2\pi f_{dm}} \quad \text{Equation 9-9}$$

Where;

f_{dm} is the equivalent dynamic modulus frequency (Hz)

R_t is the rise time (typically 0.04sec)

f_m is the flexural modulus frequency (typically 10Hz)

9.5.9 (6.4.3.3) Typical Charts

If the exact mix to be used in the pavement is not known at the time of design (which is typically the case) the typical master curves for Australian mixes (Figure 5-11 to Figure 5-16) should be used to estimate the dynamic modulus of the mix as a function of binder class and nominal aggregate size. The information required as an input for the master curves is:

- Vehicle speed, where speed is in km/hr.
- Effective temperature ($^{\circ}\text{C}$) of the asphalt

Alternatively, the stiffness can be determined using the standard temperature shift factors and master curve fitting parameters for the time temperature shift factors shown in Table 9-1 following and the sigmoidal master curve fitting parameters, shown in Table 9-2 following. The rate of loading is the equivalent haversine pulse loading time.

Table 9-1 Temperature Shift Factors

	a	b
Conventional Binders	-0.001	0.116

Table 9-2 Master Curve Fitting Parameters

Mix	α	β	γ	δ
DG14-C320	2.379	1.878	0.043	0.706
DG14-C450	2.357	1.860	-0.023	0.735
DG20-C320	2.569	1.715	0.157	0.818
DG20-C450	2.005	2.328	-0.454	0.647
DG20-C600	1.985	2.363	-0.465	0.658

9.5.10 (6.4.5) Suggested Fatigue Endurance Limit

The FEL developed from calibration on full scale test tracks and validated against actual LLAP in Australia is shown by the general relationship shown in Equation 9-10 following. This relationship determines the maximum tensile strain where damage may occur, but macro cracking will not form, and is given by:

$$FEL = k_1 20200 S_{mix}^{-0.65} + k_2 \quad \text{Equation 9-10}$$

Where;

FEL is the Fatigue Endurance Limit

S_{mix} is the stiffness of the mix, and

k_1 is the adjustment constants for differences in rest periods, or confidence levels, given in Table 9-3 following.

k_2 is the mix adjustment factor (0 for conventional mixes)

Table 9-3 Recommended Confidence Limits

	Confidence Level				
	80 th	85 th	90 th	95 th	97.5 th
k_1	1	0.97	0.925	0.86	0.8

9.6 (7) Design Traffic

The intent of this design procedure is to design a pavement where the healing potential of the asphalt mix becomes greater than the damage inflicted. Under this scenario the cumulative axle loading is immaterial, as the healing potential of the asphalt exceeds the damage caused by vehicle loading.

Research by Thompson et al. (2006) has shown that asphalt can withstand sporadic overloads and return to endurance limit performance. Therefore the critical vehicle used for LLAP design should be taken as the upper 97.5th percentile axle load. For the majority of Australian pavements this will equate to a standard axle loaded to 9 tonnes.

If the design axle is taken as the Standard Axle of Section 8 of the AGPT02 , then Equation 9-10 shall be scaled to account for the reduced loading applied in design, with the scaling shown in Equation 9-11 following.

$$FEL = \frac{8.2}{U_l} [k_1 20200 S_{mix}^{-0.65} + k_2] \quad \text{Equation 9-11}$$

Where U_l is the upper 97.5th percentile load, usually 9 tonnes

9.7 (8) Design of LLAP

9.7.1 (8.1) Mechanistic Procedure

In Summary the procedure consists of:

- 1) Granular materials are considered to be isotropic or cross-isotropic, depending on the characterisation method used.
- 2) Asphalt materials are considered to be isotropic.
- 3) The visco-elastic properties of asphalt are considered by using vehicle speed and effective layer temperature
- 4) Response to loading is calculated by linear elastic theory
- 5) Critical responses are assessed as
 - a. Tensile strain at the bottom of the asphalt layers
 - b. Vertical compressive strain on subgrade
- 6) Axle loading consisting of a single axle with dual tyres (SADT)
 - a. with a load of 9.0t, with the use of Equation 9-10.
 - b. with a load of 8.2t, with the use of Equation 9-11.
- 7) Tyre contact stress is assumed to be 750kPa
- 8) 3 Season are modelled
 - a. Morning loading in winter
 - b. WMAPT
 - c. Day time loading in summer

9.7.2 (8.2.3) Combined Asphalt Layer Modulus

It has been found that the use of a single equivalent layer of asphalt provides results as accurate as multiple asphalt layers. The equivalent modulus of multiple asphalt layers can be determined from the use of the conservation of the moment of inertia approach, as shown in Equation 9-12 following:

$$\left(\sum_{i=1}^n h_i \right) E_{eff}^{\frac{1}{3}} = \sum_{i=1}^n h_i E_i^{\frac{1}{3}} \quad \text{Equation 9-12}$$

Where:

E_{eff} = is the effective stiffness of the combined layers(MPa)

h_i = The thickness of the ith layer(mm)

E_i = The stiffness of the ith layer (MPa)

n = Number of asphalt layers

Where the asphalt surface courses or fatigue layer uses a different binder from that of the base course, it is recommended that the asphalt layer(s) be not combined into a single layer.

Table 9-4 (8.1) Mechanistic Design Procedure

Step	Activity	Reference
1	Select a trail pavement	Sec 3.7
2	Determine subgrade stiffness	Sec 5.1
3	Determine working platform stiffness (if relevant)	AGPT 6.2 & T6.4 & 8.2.3
4a	Determine WMAPT	AGPT AC
5	Obtain MMAT for January and July maximum daily temperature for January and minimum daily temperature for July.	
6a	Determine surface temperature (To) for summer maximum and winter minimum	Sec 4.3.1.1
7	Determine effective asphalt layer temperature (Teff)	Sec 4.3.1
8	Determine elastic parameters of asphalt layers for summer, WMAPT and winter	Sec 6.4.3
9	Determine effective modulus of combined asphalt layers	Sec 8.2.3
10	Determine FEL for summer, WMAPT, winter	6.4.5
11a	Approximate the axle load as two circular vertical loads with a total load of 45kN and centre to centre spacing of 330mm and uniform vertical stress of 750kPa	
11b	Determine the critical locations as: 1. Bottom of the asphalt layers (summer, WMAPT, winter) 2. Top of the Subgrade (WMAPT only)	
11c	Input the values into the layered elastic analysis and determine the maximum tensile strain at the base of the asphalt layers and top of the subgrade	
12	Compare calculated horizontal strain at bottom of the to the FEL for summer, WMAPT and winter to the FEL	
13	Compare calculated compressive strain to the allowable strain at the WMAPT	
14	If the calculated strain is less than the FEL than design is acceptable. If not; 1. Select a new pavement configuration and return to step 1, or, 2. Determine the life of the pavement as per AGPT-Part 2	

9.8 Example

Design Parameters:

a) Location Brisbane Metro

1) Trial Pavement

50mm DG 14 C320

xmm DG 20 C600, trail 215mm

60mm DG 20 C600 (low void)

150mm cement treated type 2.2

Subgrade 50MPa

a) Assume **215mm** DG 20 C600 Layer

2) 95th lower Percentile Subgrade stiffness 50MPa.

a. (Soaked CBR 5) (CHECK)

3) Working platform, 150mm cement treated type 2.3 material. Upper modulus 750MPa.

a. Design modulus 120MPa

4) Determine the WMAPT for Brisbane = 31.9 AGPT-Part 2 Appendix C

5) From all available climate statistics for BOM site 040214:

- Latitude 27.48
- MMAT January $= (29.4 + 20.7) / 2 = 25^{\circ}\text{C}$
- MMAT July $= (20.4 + 9.5) / 2 = 15^{\circ}\text{C}$
- Average maximum January = 29.4
- Average minimum July = 9.5°C

6) Calculate Surface temperature (T_0)

- a. 95th percentile upper temperature 52°C
b. Average minimum July 9.5°C

7) Calculate the effective pavement temperature using the VBA function in Appendix G

- a. Effective maximum temperature January 43°C
b. Effective minimum temperature July 16°C

8) From Figure 5-12 DG14 C320 modulus is:

- a. Summer 1279MPa
b. WMAPT 2570MPa
c. Winter 8070MPa

9) From Figure 5-16 DG20 C600 modulus is:

- a. Summer 1633MPa
b. WMAPT 3610MPa

- c. Winter 10832MPa
- 10) Calculate the effective layer modulus from Equation 9-12
 - a. Summer 1575MPa
 - b. WMAPT 3435MPa
 - c. Winter 10371MPa
- 11) Calculate the FEL at 95% confidence from Equation 9-10
 - a. Summer 1575MPa 145 $\mu\epsilon$
 - b. WMAPT 3435MPa 87 $\mu\epsilon$
 - c. Winter 10371MPa 43 $\mu\epsilon$
- 12) Using Linear Elastic Analysis (i.e. CIRCLY) calculate critical strain using a 9 tonne axle
 - a. Summer 143 $\mu\epsilon$
 - b. WMAPT 86 $\mu\epsilon$
 - c. Winter 37 $\mu\epsilon$
 - d. Subgrade 318 $\mu\epsilon$
- 13) Compare Calculated strain to FEL
 - a. Summer 143<145 $\mu\epsilon$ OK
 - b. WMAPT 86<87 $\mu\epsilon$ OK
 - c. Winter 37<43 $\mu\epsilon$ OK**

10 Conclusions and Recommendations

By reviewing the strategies for designing and maintaining long-life pavements in Australia, the UK, France, Netherlands and several states in the US, it was found LLAP could be achieved with a maximum thickness of 300-350mm and a minimum of 200mm was required for LLAP performance.

Examination of the gradation and volumetric properties of SRA Australian production mixes shows that despite the variability in the design methods (Marshall, gyratory and Superpave) and the differing compaction efforts, all mixes fit into a very small volumetric window. Additionally it was found the design gradation of all standard Australian production mixes closely follow the maximum density line, with nearly all mixes being slightly coarse graded, indicating that distinguishing between Australian mixes based on gradation and volumetric properties may be difficult.

The comparison of the results obtained by AAPA and NCAT on two un-aged samples showed that the difference in the compaction method between the AAPA study and US Superpave test method had no influence on the measured dynamic modulus results, with identical results obtained. Based on this finding, it was concluded that the APS-fL project could utilize the results of NCAT testing for modulus and performance data with confidence, to;

- correlate dynamic modulus estimates from back analysis of deflection data,
- validate measured strain and predicted strain using linear elastic analysis, and
- develop fatigue endurance limits.

Examination of the master curves of standard Australian production mixes suggested the minimum modulus value appeared to be the best at distinguishing between binders and nominal aggregate size. As there is little difference in the volumetrics of Australian mixes, no significance could be found in air void levels or binder contents within sub mix types. Unexpectedly, no correlation was found between the minimum modulus and RAP content, indicating that at current RAP levels, RAP has little effect on the minimum modulus value and therefore overall modulus values. The results showed that, most likely because of the small variance in aggregate gradation and volumetric properties, there was no change in the shape of the master curve within groups of the same binder types and nominal aggregate size.

Because of the consistency of the master curves for a given binder type and nominal mix size, it was found for practical implementation that it was not necessary to develop complex master curve equations for routine pavement designs. The results of grouping of Australian mixes showed that Australia can achieve a higher degree of accuracy by grouping common mixes, than from the use of complex model such as the Witczak or the Hirsch models.

It was found that because the variability in the prediction of modulus followed a normal distribution with the standard deviation equal to that of the standard error, confidence could be established from the grouped data by simply varying the minimum modulus data to move the dynamic modulus curve down the modulus scale. By doing this it was shown that confidence level master curves could be established for the nominal 14 and 20mm mixes and the three primary binder classes used in Australia, C320, AR450 and C600.

The analysis of dynamic modulus test results from NCAT, MnRoads and WesTrack, against field stiffness determined from FWD testing, found that frequency in the dynamic modulus test should be considered as an angular frequency and that a shift of $1/2\pi$ on the frequency axis will allow the use of dynamic modulus values to determine the modulus resulting from a pulse load in the field. Using this conversion it was found that dynamic modulus results at 5.3Hz ($1/(2\pi \cdot 0.03)$) could be used to accurately predict the modulus determined from FWD loading with a pulse width of approximately 0.03seconds over a wide range of temperatures. The results of the optimisation found that the use of the mid-layer depth resulted in a slight underestimation of the effective asphalt layer modulus for day time testing and that if mid-layer depth is used a correction of +2°C is required to correct for the average temperature within the asphalt layers. Therefore, if modulus calculations were to be undertaken at times of day other than typically mid-day, more work on modelling the full temperature with depth profile in the pavement structure would be needed to determine the effective temperature of the asphalt layers.

Using the pulse frequency conversion and temperature correction obtained from comparison with FWD testing, the multi-variable optimisation found that dynamic modulus could be used to accurately predict strain under a moving load using layer elastic analysis when time of load is corrected for the effective load length. It was found that when computing strain under a moving load, contrary to some published recommendations, the thickness of the asphalt layer was insignificant in determining strains. It was also found that the time of loading is more related to the length of the deflection response than the current approach of the use of a stress pulse.

The results of the optimisation on the thick asphalt sections of Phase II NCAT support the recommendation of Coffman (1968) that a vehicle acts as a cyclic load with a wave length of six feet, with the optimisation determining the wave length of 1.8m. Based on these findings the following frequencies in the dynamic modulus test are recommended for use in pavement design with an equivalent combined asphalt layer.

Speed (km/hr.)	50	60	70	80	90	100	110
Recommended Frequency Dynamic Modulus E* Test (Hz)	1.2	1.5	1.7	2.0	2.2	2.5	2.7

The analysis showed that multi layers were sensitive to the chosen sub layer thicknesses and more work would be required on determining both the appropriate sub layering of multilayer asphalts and the effect of temperature profiles in the sub layering, before a multilayer approach should be recommended over the use of the equivalent asphalt layer approach.

The analysis has shown that there is a direct link between laboratory modulus and strain under a moving vehicle and dynamic modulus can be used in the structural design of LLAP's. The use of the master curves will enable the determination of either threshold strains or cumulative distribution of asphalt strain in LLAP structures as a function of the climatic conditions and the traffic distribution spectrum. This calculated strain will provide the means to rationally evaluate the compliance of candidate LLAP structures with the limiting threshold strain or cumulative strain distribution empirically derived from the evaluation of international LLAP's.

The results of the modulus inter-conversion study found that 3 of the 4 common Australian test methods time has a different physical meaning and a frequency conversion is needed to shift between the time and frequency domain. It was found that shift factors could be established from single time/temperature testing and that the time shift factors found from the single time and temperature testing and are valid across the whole time frequency domain.

For the purposes of standardisation, the modulus results need to be converted to a reference stiffness value. Comparable stiffness is obtained, between any of the three test methods by using a constant definition of time (inter-conversion) as shown following.

Conversion From	Conversion To		
	IT-CY _(time)	4PB-PR _(frequency)	DC-CY _(frequency)
IT-CY _(time)		$\frac{1}{2t_{IT-CY}}$	$\frac{1}{2\pi t_{IT-CY}}$
4PB-PR _(frequency)	$\frac{1}{2f_{4PB-PR}}$		$\frac{f_{4PB-PR}}{\pi}$
DC-CY _(frequency)	$\frac{1}{2\pi f_{DC-CY}}$	πf_{DC-CY}	

It is evident from this study that frequency in the common Australian tests can have different physical meaning and the reporting of modulus at a frequency, without reference to the loading type is confusing. To remove this confusion, it is recommended that standard practice be established for the reporting of modulus values from different test methods and is referenced back to an equivalent design modulus. The study underlines the considerable challenges in comparing the modulus results from various test methods. It would be highly

recommendable to harmonise testing across Australia and implement a standard reporting method.

For both the low strain 4PB-PR results and the 2PB-TR only limited data has been used and the results should be confirmed over a wider range of mixes.

The examination of extensive overseas research showed that there is a clear and strong relationship between mix stiffness and the FEL of asphalt mix. The international research has found that as stiffness of the mix increases the FEL decreases asymptotically and most likely reaches a limiting value. The research work showed that the basic material property, stiffness, is directly related to the FEL of a mix and can be used to allow for changes in binder, temperature and healing.

The examination of the LLAP sites from the NCAT Phase II study confirmed, in field, the variable nature of the FEL relationship and that LLAP can withstand strains significantly higher than previously recommended (when the asphalt has low stiffness) without undergoing damage. The examination of the two LLAP on the NCAT test track showed a direct relationship exists between the infield stiffness-strain curve of the two undamaged sections and the stiffness-FEL developed by from Australian and US mixes. This finding was then extended to actual LLAP in Australia, which confirmed the same finding as on the NCAT test track that a direct relationship exists between the infield stiffness-strain curve of LLAP and the laboratory determined stiffness-FEL curve. This direct relationship allows the development of a phenomenological stiffness-FEL relationship which can be used for the purpose of pavement design.

Based upon both the calibrated relationship from the NCAT data and validated Australian and UK LLAP, the use of a stiffness-FEL relationship is recommended for the design of long-life asphalt pavements in Australia. The relationship was validated to Australian and UK data and only required a slight modification to the relationship developed from the NCAT, as shown following.

$$FEL = k_1 20200 S_{mix}^{-0.65} + k_2$$

Where;

FEL is the Fatigue Endurance Limit

S_{mix} is the stiffness of the mix, and

k_1 is the adjustment constant for differences in rest periods, or confidence levels

k_2 is the mix adjustment factor

It was found that confidence limits could be incorporated into the modelling approach by the use of the k_1 adjustment factor and confidence limits could be determined from the Australian validation sites as shown following.

	Confidence Level				
	80 th	85 th	90 th	95 th	97.5 th
k_1	1	0.97	0.925	0.86	0.8

The analysis of the results showed that the design of LLAP can be supported by a fundamental test using the Ratio of Dissipated Energy Change (RDEC) and the constant Plateau Value (PV_L). However, a laboratory to field conversion is needed to use the test which is equivalent to the confidence values shown previously.

It is recommended the stiffness-FEL design approach be incorporated into a multi-season design approach. The current design recommendation for Australia to use:

- 9.0t design axle (8.2t may be used with a shift in the equation)
- Model using 3 seasons; Summer, Mid temperature (WMAPT), Winter.
- Mid layer asphalt temperatures be taken from the ARRB modified Bells equation

By using this approach the limiting thickness of asphalt pavements can be obtained with confidence for the full spectrum of circumstances encountered on Australian projects.

10.1 Recommendations for Future Research

The procedure developed in this study is valid for conventional mixes only and While it is know that PMB mixes have higher fatigue endurance limits no recommendations have been made for the incorporation of adjustment factors for these mixes. It is recommended that further studies be undertaken utilizing the NCHRP9-38 approach and the standard FEL equation (Equation 9-10) on high performance mixes such as, EME2, A5E, high binder content and SBS modified mixes to obtain the shift factor for the FEL of these mixes.

While the use of modulus as a surrogate to fundamental material properties was found to be highly correlated to the FEL of an asphalt mix, it is not a fundamental parameter which relates to the FEL. Further research should be undertaken to determine the exact material property or properties which are directly related to the FEL of an asphalt mix.

The design approach recommended in the developed in this study only covered high traffic roads only. It is known that LLAP exist on lower traffic volume roads and further research should be undertaken into the incorporation of the FEL concept into pavements with lower traffic level and longer healing potentials.

The current recommended design approach recommends the use of three modelling temperatures to capture the potential for brittle, high strain high loading modes of failure. Further work should be undertaken on the need for the use of three modeling temperatures or if a single effective temperature can be used for the determination of the limiting thickness of long life to be achieved.

The fatigue endurance equation developed in Equation 9-10 covers all conventional mix designs, the addition of binder properties and/or volumes may result in a more precise model. If this is the case, the confidence intervals developed in Chapter 8 can be further refined allowing for more optimal design thicknesses to be obtained with higher confidence.

References

Every reasonable effort has been made to acknowledge the owners of copyright material. I would be pleased to hear from any copyright owner who has been omitted or incorrectly acknowledged.

- AASHTO 1997, *Segregation: "Causes and Cures for Hot Mix Asphalt"*, American Association of State Highway Transportation Officials, Washington, DC.
- AASHTO 2008, *"Mechanistic-Empirical Pavement Design Guide, Interim Edition": A Manual of Practice*, Washington, DC.
- Adhikari, S., You, Z., and Kutay, M. "Prediction of Dynamic Modulus of Asphalt Concrete Using Two-Dimensional and Three-Dimensional Discrete Element Modeling Approach." *GeoCongress* 2008: pp. 1020-1027
- Al-Qadi, IL, Wang, H, Yoo, PJ & Dessouky, SH 2008, "Dynamic analysis and in situ validation of perpetual pavement response to vehicular loading", 29-39.
- Anderson, D, Christen, D, Bahaia, H, "Binder Characterization and Evaluation, Volume 3: Physical Characterization," SHRP-A-369, Strategic Highway Research Program, National Research Council, Washington, DC 1994.
- Antes, P.W., van Dommelen, A.E., Houben, L.J.M., Molenaar, A.A.A., and Parajuli, U., "Stress dependent behaviour of asphalt mixtures at high temperatures". *Proceedings of the Association of Asphalt Paving Technologists*. 72 (2003) 1-25
- Appea, Flintsch, Al-Qadi "Backcalculation Through Field Instrumentation", 2002, <http://citeseerx.ist.psu.edu/viewdoc/download?rep=rep1&type=pdf&doi=10.1.1.123.8458>
- Asphalt Institute 1982, "Thickness design--asphalt pavements for highways and streets", Asphalt Institute.
- Asphalt Pavement Alliance 2002, "Perpetual Pavements: A Synthesis"
- Asphalt Pavement Environmental Council 2000, "Best Management Practices to Minimize Emissions
- Austrroads, "AP-T98/08 Technical Basis of the Austrroads Guide to Pavement Technology Part 2: Pavement Structural Design" Austrroads Ltd, Sydney, NSW, 2008.
- During HMA Construction*", Asphalt Pavement Environmental Council (APEC).
- Austrroads Guide to Pavement Technology, Part 2, "Structural Design of Pavements", Austrroads, AGPT02, 2012
- Bari, J, Witczak, M, "Development of a New Revised Version of the Witczak E* Predictive Model for Hot Mix Asphalt Mixes". *Journal of the Association of Asphalt Paving Professionals*, Savannah Georgia, 2006.
- Baker, MJ & Mahoney, JP 2000, "Identification and Assessment of Washington State Pavements with Superior and Inferior Performance" - Report No. WA-RD 437.1
- Barksdale R. 1971 "Compressive stress pulse times in flexible pavements for use in dynamic testing". *Highway Research Record*;(34):32-44
- Bayat A., Knight M "Investigation of Hot-Mix Asphalt Dynamic Modulus by Means of Field-Measured Pavement Response" 2005 ,http://pustaka.pu.go.id/files/pdf/BALITBANG-03-C000061-263310032011101757-investigation_of_HMA_dynamic.pdf
- Behbaharis, HA, Khaki, M & Amini, A 2009, 'Assessment of Perpetual Pavement Performance using Mechanistic-Empirical Pavement Design Guide (M-EPDG) and PerRoad Software Models,' *International Conference of Perpetual Pavements*
- Bejarano, MO & Thompson, MR 2001, "Subgrade Damage Approach for the Design of Airport Flexible Pavements," ASCE, 4-4.
- Bejarano, MO, Thompson, MR & Garg, N 1999, "Characterization of NAPTF Subgrades," *Federal Aviation Administration Technology Transfer Conference*.

- Bendana, J, Sargand, S & Hernandez, J 2009, "Comparison Between Perpetual and Standard Asphalt Concrete Pavement Sections on NY I-86", *International Conference of Perpetual Pavements*.
- Bennert, T & Williams, S 2009, "Precision of AASHTO TP62-07 for Use in Mechanistic—Empirical Pavement Design Guide for Flexible Pavements", *Transportation Research Record: Journal of the Transportation Research Board*, vol. 2127, no. -1, pp. 115-126.
- Bonnaure F., Gest G., Gravois A., Uge P., "A New Method of Predicting the Stiffness of Asphalt Paving Mixtures", *AAPT Proceedings*, Volume 46, 1977, pp. 64-104.
- Box, GEP & Muller, ME 1958, "A note on the generation of random normal deviates", *The Annals of Mathematical Statistics*, vol. 29, no. 2, pp. 610-611,
- Brown S,F. 1973 "Determination of young's modulus for bituminous materials in pavement design". *Highway Research Record*.(431):38–49
- Brown, E & Cooley Jr, L 1999, "NCHRP Report 425: Designing Stone Matrix Asphalt Mixtures for Rut Resistant Pavements", *Transportation Research Board, National Research Council, Washington, DC*
- Brown, E, Kandhal, PS & Zhang, J 2001, "Performance testing for hot mix asphalt - National Center for Asphalt Technology (NCAT) Report 01-05"
- Brown, E, Jr., LAC, Hanson, D, Lynn, C, Powell, B, Prowell, B & Watson, D 2002, "NCAT Test Track Design, Construction, and Performance"
- Brown, E, Hainin, M, Cooley, L & Hurley, G 2004, "NCHRP Report 531: Relationship of Air Voids, Lift Thickness, and Permeability in Hot Mix Asphalt Pavements"
- Brown, ER 2006, "Basics of Longitudinal Joint Construction", *Circular EC-105. Factors Affecting Compaction of Asphalt Pavements* Transportation Research Board. Washington, DC, pp. 86-95,
- Bushmeyer, B 2002, "The quest for long-life asphalt pavement", *Better Roads*, vol. 72, no. 2, p. 30,
- Carpenter S, Ghuzlan K, Shen S, 2003 "A Fatigue Endurance Limit for Highway and Airport Pavements", Paper submitted for possible presentation and publication by the Transportation Research Board at Annual Meeting.
- Carteret, R, Jameson, G 2009, "Asphalt Fatigue Endurance Limit" report AP-T131/09, Austroads, Sydney.
- Chenevière, P & Ramdas, V 2006, "Cost benefit analysis aspects related to long-life pavements", *International Journal of Pavement Engineering*, vol. 7, no. 2, pp. 145-152
- Clyne T., Chadbourn B., Engstrom B., Worel B. "Determination of HMA Modulus Values for Use In Mechanistic-Empirical Pavement Design". Minnesota Department of Transportation, 2004.
- Coffman B.S "Pavement Deflections from Laboratory Testing and Layer Theory" Second International Conference on the Structural Design of Asphalt Pavements, *Proceedings*, the University of Michigan, pp 819-862 1967
- Corte, JF 2001, "Development and uses of hard-grade asphalt and of high-modulus asphalt mixes in France", *Perpetual Bituminous Pavements*, 12.
- Cross, SA & Parsons, RL 2002, "Evaluation of Expenditures on Rural Interstate Pavements in Kansas: Executive Summary", *Kansas University Transportation Center*.
- D'Angelo, J, Bukowski, J, Harman, T & Lord, B 2004, 'The Federal Highway Administration's Long-Life Pavement Technology Program,' 103-118.
- Decker, D 2006, "Rubblization: Design and Construction Guidelines on Rubblizing and Overlaying PCC Pavements with Hot-Mix Asphalt (IS-132)", *National Asphalt Pavement Association, Lanham, MD*,
- Dehlen, G,L, "The Effect of Non-Linear Material in the Behavior of Pavements Subjected to Traffic Loads", *ARRB Group*, 1968

- Denneman, E, Austroads Project TT1826, *“Improved Design Procedures for Asphalt Pavements”*, Austroads, Sydney, 2013.
- Dickinson, EJ 1981, *“Pavement temperature regimes in Australia: their effect on the performance of bituminous constructions and their relationship with average climate indicators”*, special report 23, Australian Road Research Board, Vermont South, Vic
- Dongre, T., Myers, L., D’Angelo, J., Paugh, C., Gudimettla, J., *“Field evaluation of Witczak and Hirsch models for predicting dynamic modulus of hot-mix asphalt”*. Journal of the Association of Asphalt Paving Technologists. 73 (2005) 381-442
- Dongre, R., Myers, L., and D’Angelo, J., *“Conversion of testing frequency to loading time: Impact on performance predictions obtained from the M-E pavement design guide”* Proceedings of the Transportation Research Board. (2006) CD-ROM
- Driscoll, BS 2009, *“Cuyohoga County Constructs a Perpetual Pavement”* International Conference of Perpetual Pavements.
- El-Hakim, MY, Tighe, SL & Galal, KA 2009, *“M-E Performance Evaluation and LCCA of a Conventional Asphalt Pavement”*, International Conference on Perpetual Pavements
- Epps, J & Monismith, C 1972, *“Fatigue of Asphalt Concrete Mixtures-Summary of Existing Information”*, Fatigue of Compacted Bituminous Aggregate Mixtures, p. 19
- Estes, T 2005, *“Oregon Answers Perpetual Pavement Analysis with a Field Test”*, Better Roads, vol. 75, European Asphalt Pavement Association 2009, *High Modulus Asphalt*, EAPA. Brussels.
- Fee, F 2001, *“Extended-Life Asphalt Pavement: new approaches to increase durability”*, TR News - Transportation Research Board. Washington, DC, no. 215
- FEHRL 2004, *“A Guide to the Use of Long-Life Fully-Flexible Pavements- ELLPAG Phase 1”*
- FEHRL 2009, *“A Guide to the Use of Long-Life Fully-Flexible Pavements ELLPAG PHASE 2”*
- Ferry, J.D., *“Viscoelastic Properties of polymers”*, Wiley, 3rd edition (1980).
- Ferne, B 2006, *“Long-life pavements—a European study by ELLPAG”*, International Journal of Pavement Engineering, vol. 7, no. 2, pp. 91 - 100, viewed May 25, 2011.
- Ferne, B & Nunn, M, 2006, *“The European Approach to Long Lasting Asphalt Pavements—A State-of-the-Art Review by ELLPAG”* 87-101.
- Francken L. Partl, M, 1994, *“Complex Modulus Testing of Asphaltic Concrete: RILEM Inter laboratory Test Program”*, Transport Research Record 1545
- Foley G, 2008 *“Heavy Duty Asphalt Pavement Performance – Update Study”*. Australian Asphalt Pavement Association
- Gardiner, MS & Brown, E, 2000, *“Segregation in hot-mix asphalt pavements”* NCHRP Report 441
- Gedafa, DS, Hossain, M, Romanoschi, S & Gisi, AJ, 2010, *“Field verification of superpave dynamic modulus”*, Journal of Materials in Civil Engineering, vol. 22, no. 5, pp. 485-494,
- Ghuzlan, KA & Carpenter, SH, 2000, *“Energy-derived, damage-based failure criterion for fatigue testing”*, Transportation Research Record: Journal of the Transportation Research Board, vol. 1723, no. -1, pp. 141-149,
- Gibboney, WB 1995, *“Flexible and Rigid Pavement Costs on the Ohio Interstate Highway System”*
- Gierhart, D 2007, *“Analysis of Oklahoma Mix Designs for the National Center for Asphalt Technology Test Track using the Bailey Method”*, Practical Approaches to Hot-Mix Asphalt Mix Design and Production Quality Control Testing, p. 33,
- Hallenbeck, ME, Center, WST, Corporation, CS & Program, L-TPP 1997, *“Vehicle Volume distributions by Classification”*, Washington State Transportation Center.
- Harm, E 2001, *“Illinois extended-life hot-mix asphalt pavements”*, Perpetual Bituminous Pavements, pp. 108-113,
- Harman, T, Bukowski, J, Moutier, F Huber, G, 2002, *“The History and Future Challenges of Gyrotory Compaction”*, Annual Meeting of The Transportation Research Board

- Harvey, J, Monismith, C, Bejarano, M, Tsai, B & Kannekanti, V 2004, "Long-life AC pavements: a discussion of design and construction criteria based on California experience," International Symposium on Design and Construction of Long Lasting Asphalt Pavements, 285-334.
- Hornyak, NJ, Crovetti, JA, Newman, DE & Schabelski, JP 2007, "Perpetual Pavement Instrumentation for the Marquette Interchange Project- Phase 1"
- Huang, Y, "Pavement Analysis and Design", Pearson Education, Limited, 2004
- Huber, G 2000, "NCHRP Synthesis of Highway Practice 284: Performance Survey on Open-Graded Friction Course Mixes", Transportation Research Board, National Research Council, Washington, DC,
- Huber, G, Andrews, D & Gallivan, V 2009, "Design and Construction of Highways for Very Heavy Trucks" International Conference of Perpetual Pavements,
- Huddleston, J 2008, "Eugene Discovers More Miles in Its Roads", Oregon Roads Newsletter, no. 88
- Irwin L.H. "Practical Realities and Concerns Regarding Pavement Evaluation", Proceedings of the 4th International Conference on the Bearing Capacity of Roads and Airfields, Volume 1, pp 19.
- Jacobs, M.M.J. "Crack Growth in Asphaltic Mixes" PhD. Thesis, Delft University of Technology, Netherlands, 1995.
- Jackson, N, Chatti, K, Buch, N, Zollinger, D, K. Hall & Puccinelli, J 2009, "Using Existing Pavement in Place and Achieving Long Life"
- Kallas, B.F., "Dynamic modulus of asphalt concrete in tension and tension compression" Proceedings of the Association of Asphalt Paving Technologists. 39 (1970) 1-23.
- Kamal, MA, Hafeez, I & Muzaffarkhan, K 2006, "Feasibility of perpetual pavements in developing countries", International Conference on Perpetual Pavements
- Kandhal, PS & Mallick, RB 1999, "Design of new-generation open-graded friction courses – National Center of Asphalt Technology (NCAT)", Report No. 99-3
- Katicha S, "Analysis of Hot-Mix Asphalt (HMA) Linear Viscoelastic and Bimodular Properties Using Uniaxial Compression and Indirect Tension (IDT) Tests", PhD Dissertation, University of Virginia, 2007
- Khanal, P.P., and Mamlouk, M.S., "Tensile versus compressive moduli of asphalt concrete" Transportation Research Record. 1492 (1995) 144-150.
- Kim, Y.R., and Lee, Y.C., "Interrelationships among stiffnesses of asphalt-aggregate mixtures." Proceedings of the Association of Asphalt Paving Technologists. 64 (1995) 575-600.
- Kim, Y.R., Little, D. "One-dimensional constitutive modeling of asphalt concrete". J. Eng. Mech. 116, No. 4, 751-772 (1990).
- Jameson, G.W. and Hopman, P.C (2000). "Austroads Pavement Design Guide Chapter 6: development of Relationship between Laboratory Loading Rates and Traffic Speed". APRG Document 00/16(DA).
- Lande, KO, Lopez, HAG & Cook, E 2006, "Application of Perpetual Asphalt Pavement Principles for the Design and Construction of the Khandahar to Herat Highway in Afghanistan"
- Lane, B, Brown, AWS & Tighe, S 2006, "Perpetual Pavements - The Ontario Experiment" International Conference on Perpetual Pavements
- Lecsh, D & Nunn, M 1997, 'Deterioration mechanisms in flexible pavements,' 2nd European Conference on the Durability and Performance of Bituminous Materials,
- Liao, J & Sargand, SM 2009, "Controlled Load Vehicle Testing and Numerical Modeling of US 30 Perpetual Asphalt Concrete Test Section 664 (AC-390182)"
- Loizos, A 2006, "Assessment and Upgrading of In-service Heavy Duty Pavements to Long Life", International Journal of Pavement Engineering, vol. 7, no. 2, pp. 133 - 144, viewed May 30, 2011.

- Loulizi, A., G. W. Flintsch, I. L. Al-Qadi, and D. W. Mokarem. "Comparing Resilient Modulus and Dynamic Modulus of Hot-Mix Asphalt as Material Properties for Flexible Pavement Design". In Transportation Research Record: Journal of the Transportation Research Board, No. 1970, Transportation Research Board of the National Academies, Washington, D.C., 2006, pp. 161–170.
- Lytton R, "Dissipation of Crack Energy and Dynamic Mechanical Analysis", Peterson Conference, Cheyenne, Wyoming, June 24, 2005
- Mahoney, JP 2001, "Study of long-lasting pavements in Washington State. Perpetual bituminous pavements", Transportation Research Circular, vol. 503, pp. 88-95,
- Mahoney, JP, Monismith, CL, Coplantz, J, Harvey, JT, Kannekanti, V, Pierce, LM, Uhlmeyer, JS, Sivanewaran, N & Hoover, T 2007, "Pavement Lessons from the 50-Year-Old Interstate Highway System: California, Oregon, and Washington", E-Circular, vol. 118, pp. 88-113,
- Martin, JS, Harvey, JT, Long, F, Lee, E, Monismith, CL & Herritt, K 2001, "Long-life rehabilitation design and construction, I-710 Freeway, Long Beach, California", Transportation Research Board Circular No. 503, pp. 50-65,
- Merrill, D, Van Dommelen, A & Gáspár, L 2006, "A review of practical experience throughout Europe on deterioration in fully-flexible and semi-rigid long-life pavements", International Journal of Pavement Engineering, vol. 7, no. 2, pp. 101 - 109, viewed June 05, 2011.
- Mohammad, L, Bae, A, Elseifi, M, Button, J & Scherocman, J 2009, "Evaluation of Bond Strength of Tack Coat Materials in Field", Transportation Research Record: Journal of the Transportation Research Board, vol. 2126, no. -1, pp. 1-11,
- Monismith, C, Epps, J & Finn, F 1985, "Improved asphalt mix design", Technical Sessions of the Association of Asphalt Paving Technologists, 347-406.
- Monismith, C, Harvey, J, Bressette, T, Suszko, C & Martin, JS 2009, "The Phase One I-710 Rehabilitation Project: Initial Design (1999) to Performance After Five Years of Traffic (2008)", International Conference on Perpetual Pavements,
- Monismith, C & Long, F 1999, "Mix Design and Analysis and Structural Section Design for Full Depth Pavement for Interstate Route 710", Institute for Transportation Studies, University of California, Berkeley
- Monismith, C & Long, F 1999, "Overlay Design for Cracked and Sealed Portland Cement Concrete (PCC) Pavement—Interstate Route 710", Institute for Transportation Studies, University of California, Berkeley
- Monismith, CL 1992, "Analytically based asphalt pavement design and rehabilitation: Theory to practice, 1962-1992", Transportation Research Record, no. 1354
- Monismith, C. L. and D. B. McLean, "Technology of Thick Lift Construction: Structural Design Considerations", Proceedings, Association of Asphalt Paving Technologists, Vol 41, pp. 258-304 1972.
- Monismith, L, Epps, J, Kasianchuk, D & McLean, D 1970, "Asphalt Mixture Behavior in Repeated Flexure, Report No. 70-5", University of California, Berkeley
- Muench, S, White, G, Mahoney, J, Pierce, L & Sivanewaran, N 2004, "Long-Lasting Low-Volume Pavements in Washington State", 729-773.
- Muench, ST, Mahoney, JP, Wataru, W, Chong, L & Romanowski, J 2007, "Best Practices for Long-Lasting Low-Volume Pavements", Journal of Infrastructure Systems, vol. 13, no. 4, pp. 311-320,
- NAPA 2002, "Longitudinal Joints: Problems and Solutions", National Asphalt Pavement Association, Lanham, Maryland.
- NCHRP 2004, "Guide for Mechanistic-Empirical Design of New and Rehabilitated Pavement Structures", National Cooperative Highway Research Program (NCHRP), Washington, DC.
- NCHRP Report 646: "Validating the Fatigue Endurance Limit for Hot Mix Asphalt", National Cooperative Highway Research Program of Transport Research Board of The National

- Academies, 2012, Prowell, BD, Brown, E, Anderson, RM, Daniel, JS, Swamy, AK, Von Quintus, H, Shen, S, Carpenter, SH.
- NCHRP Report 9-44 A *“Validating an Endurance Limit for HMA Pavements: Laboratory Experiment and Algorithm Development Appendix A, Integrated Predictive Model for Healing and Fatigue Endurance Limit for Asphalt Concrete”* National Cooperative Highway Research Program of Transport Research Board of the National Academies, 2013.
- Newcomb, DE, Buncher, M & Huddleston, IJ 2001, *“Concepts of perpetual pavements”*, *Transportation Research Circular*, vol. 503, pp. 4-11,
- Newcomb, DE & Hansen, KR 2006, *“Mix Type Selection for Perpetual Pavements”*, International Conference on Perpetual Pavement
- Newcomb, DE, Willis, R & Timm, DH 2010, *“Perpetual Asphalt Pavements a Synthesis”*
- Nishizawa, T, Shimeno, S & Sekiguchi, M 1997, *“Fatigue analysis of asphalt pavements with thick asphalt mixture layer”*, Proceedings of the 8th International Conference on Asphalt Pavements
- Molenaar A, *“Structural performance and design of flexible road constructions and asphalt concrete overlays”*, TU Delft, 1983.
- Nunn, M. *“Long-life Flexible Roads.”* Proceedings of the 8th International Conference on Asphalt Pavements, Vol. 1, University of Washington, Seattle, WA, August 1997, pp. 3–16.
- Nunn, M, Brown, A & Weston, D 1997, *“Design of long-life flexible pavements for heavy traffic”*, TRL report 250
- Nunn, ME & Ferne, BW 2001, *“Design and assessment of long-life flexible pavements”*, *Transportation Research Circular*, vol. 503, pp. 32-49,
- Ovik, J, Birgisson, B & Newcomb, D 1999, *“Characterizing Seasonal Variations in Flexible Pavement Material Properties”*, *Transportation Research Record: Journal of the Transportation Research Board*, vol. 1684, no. -1, pp. 1-7,
- Packard, RG 1984, *“Thickness design for concrete highway and street pavements”*, Portland Cement Association.
- Papazianin, *“The Response of Linear Viscoelastic Materials in the Frequency Domain with Emphasis on Asphaltic Concrete”*, First International Conference on the Structural Design of Asphalt Pavements(1962).
- Pellinen, T *“Investigation of the Use of Dynamic Modulus as an Indicator of Hot-Mix Asphalt Performance”*, Ph.D dissertation Arizona State University, 2001.
- Peterson, R, Turner, P, Anderson, M & Buncher, M 2004, *“Determination of threshold strain level for fatigue endurance limit in asphalt mixtures”*, International symposium on design and construction of long lasting asphalt pavements, 385-410.
- Phillips, M.C. *“Multi-Step Models for Fatigue and Healing, and Binder Properties Involved in Healing”*, Proceedings, Eurobitumen Workshop on Performance Related Properties for Bituminous Binders, Luxembourg, Paper No. 115, 1998.
- PIARC Technical Committee 4.3 Road Pavements 2009, *“Long Life Pavements and Success Stories”*, Pierce, LM & Mahoney, JP 1996, 'Asphalt concrete overlay design case studies', *Transportation Research Record: Journal of the Transportation Research Board*, vol. 1543, no. -1, pp. 3-9,
- Prager S. and Tirrell M. *“The Healing Process at Polymer-Polymer Interfaces”*, *Journal of Chemical Physics*. pg 75, 5194-5198 (1981).
- Prowell, BD & Brown, ER 2006, *“Methods for Determining the Endurance Limit Using Beam Fatigue Tests”* International Conference on Perpetual Pavements
- Prowell, BD & Hurley, GC 2007, *“Warm-Mix Asphalt: Best Practices”*, National Asphalt Pavement Association, Lanham, Maryland.

- Qia, J, Xuan, D, Martin, F, Molenaar, A, 2009 “*Evaluation of the Shear Box Compactor as an Alternative Compactor for Asphalt Mixtures Beam Specimens*”, Third international Conference on Advances and Trends in Engineering Materials and their Applications, Montreal, Canada.
- Quints, V 2006, “*Application of the endurance limit premise in mechanistic-empirical based pavement design procedures*”, International Conference on Perpetual Pavement, 1-19.
- Renteria, R & Hunt, E 2008, “*Super Related: Oregon DOT uses Superpave mix designs for perpetual pavement project*”, Roads and Bridges, vol. 46, no. 6, p. 47,
- Rickards, I & Armstrong, P 2010, “*Long term full depth asphalt pavement performance in Australia*”, 24th ARRB Conference,
- Roberts, J. “*Modelling of Asphalt Temperature and Strength Variations with Time of Day and Depth in Pavement*”, Australian Road Research Board, Victoria, 2009.
- Rolt, J 2001, “*Long-life pavements*”, TRL Limited, United Kingdom, PA3736
- Romanoschi, SA, Gisi, A & Dumitru, C 2006, “*The Dynamic Response of Kansas Perpetual Pavements under Vehicle Loading*”, c 2008, 'First findings from the Kansas perpetual pavements experiment', pp. 41-48
- Romanoschi, SA, Lewis, P & Portillo, M 2009, “*The Stiffness and Fatigue Properties of the Asphalt Concrete Constructed at the Kansas Perpetual Pavements*”, International Conference on Perpetual Pavements
- Rosenberger, CE, Zurat, TJ & Cominsky, RJ 2006, “*A Practical Look at Pennsylvania’s Bradford Bypass— A Perpetual Pavement*”, International Conference on Perpetual Pavements
- Rowe, G, Sauber, R, Fee, F & Soliman, N 2001, “*Development of long-life overlays for existing pavement infrastructure projects with surface cracking in New Jersey*”, Transportation Research Board Circular No. 503, pp. 96-107,
- Rowe, GM & Bouldin, MG 2000, “*Improved techniques to evaluate the fatigue resistance of asphaltic mixes*”, Proc., 2nd Enrphalt and Eurobitume Congress, pp. 754-763,
- Sargand, SM, Khoury, IS, Romanello, MT & Figueroa, JL 2006, “*Seasonal and Load Response Instrumentation of the Way-30 Perpetual Pavements*”, International Conference on Perpetual Pavements
- Schapery, R. A., 1978, “*A Method for Predicting Crack Growth in Nonhomogeneous Viscoelastic Media*,” Int. J. Fract., 14, pp. 293–309.
- Schmorak, N & Dommelen, AV 1996, “*Analysis of the structural behaviour of asphalt concrete pavements in SHRP-NL test sections*”, Road Safety in Europe and Strategic Highway Research Program (SHRP), Swedish National Road and Transport Research Institute,
- Scholz, TV, Huddleston, J, Hunt, EA, Lundy, JR & Shippen, NC 2006, “*Instrumentation and Analysis of a Perpetual Pavement on an Interstate Freeway in Oregon*”, 2006 International Conference on Perpetual Pavement,
- Scullion, T 2006, “*Perpetual pavements in Texas: state of the practice*”,
- Sharp, K, Mangan, D, Armstrong, P & Tepper, S 2000, “*Performance of Heavy Duty Flexible Pavements*” AAPA 11th International Flexible Pavements Conference, Australian Asphalt Pavement Association
- Shell Laboratories, 1978, “*Shell Pavement Design Manual*”
- Shen, S & Carpenter, S 2005, “*Application of the Dissipated Energy Concept in Fatigue Endurance Limit Testing*”, Transportation Research Record: Journal of the Transportation Research Board, vol. 1929, no. -1, pp. 165-173,
- Shook, J, Finn, F, Witczak, M & Monismith, C 1982, “*Thickness Design of Asphalt Pavements—The Asphalt Institute Method*”, 17-44.
- Soe J, Kim, Y Jaeyeon, C and Jeong S, 2010, “*Estimation of in situ dynamic modulus by using MEPDG dynamic modulus and FWD data at different temperatures*”, International Journal of Pavement Engineering, Taylor and Francis.

- Sousa, J, Deacon, J, Weissman, S, Harvey, J, Monismith, C, Leahy, R, Paulsen, G & Coplantz, J 1994, *"Permanent Deformation Response of Asphalt-Aggregate Mixes"*, Strategic Highway Research Program, National Research Council, Washington, DC, Report No. SHRP-A-415
- Tarefoler, R & Bateman, D 2009, *"Determining the Optional Perpetual Pavement Structure"*, International Conference on Perpetual Pavements
- Tayebali, A. A., Rowe, G. M. and Sousa, J. B. 1992. *"Fatigue Response of Asphalt-Aggregate Mixtures"*, Journal of the Association of Asphalt Paving Technologists, 61: 333-360.
- Thomas, J, Newcomb, D & Siekmeier, J 2004, *"Foundation Requirements for Perpetual Pavements"*, International Symposium on Design and Construction of Long Lasting Asphalt Pavements, 263-283
- Thompson, MR & Carpenter, SH 2004, *"Design principles for long lasting HMA pavements"*, International Symposium on Design and Construction of Long Lasting Asphalt Pavements, 365-384.
- Thompson M.R., Carpenter S.H *"Considering Hot-Mix Asphalt Fatigue Endurance Limit in Full Depth Mechanistic Empirical Design"*, 2006 International Conference on Perpetual Pavements, Columbus Ohio, 2006
- Timm, DH 1997, *"Incorporation of reliability in mechanistic-empirical flexible pavement thickness design"*, thesis, University of Minnesota.
- Timm, D, West R, Priest A, *"Material Properties of the 2003 NCAT Test Track Structural Study"*, National Center for Asphalt Technology Auburn University, 2006.
- Timm, D, West R, Priest A, Powell B, Selvaraj I, Zhang, J, Brown, R, *"Phase II NCAT Test Track results"*, National Center for Asphalt Technology Auburn University, 2006.
- Timm, DH, Newcomb, DE & Selvaraj, I 2006, *"A Practical Guide to Low-Volume Road Perpetual Pavement Design"*, International Conference on Perpetual Pavements
- Timm, D, West R, Priest A, Powell B, Selvaraj I, Zhang, J, Brown, R, *"Phase II NCAT Test Track results"*, National Center for Asphalt Technology Auburn University, 2009
- Tipler, P, *"Physics for Scientist and Engineers"*, W. H. Freeman, Fourth Edition, 1992
- Tsai, B. W., J. T. Harvey, and C. L. Monismith. *"High Temperature Fatigue and Fatigue Damage Process of Aggregate-Asphalt Mixes"*, Journal of the Association of Asphalt Paving Technologists, Vol. 71, 2002, pp. 345–385.
- Tsoumbanos, B 2006, *"Top-Down Cracking in Melbourne Pavements"*, 22nd ARRB Conference, ARRB Group, Vermont South, Vic,
- Shen, S. and S. H. Carpenter, *"Application of Dissipated Energy Concept in Fatigue Endurance Limit Testing"* Transportation Research Record, Journal of Transportation Research Board, No. 1929, pp. 165 – 173, 2005
- Soe J, Kim, Y Jaeyeon, C and Jeong S, *"Estimation of in situ dynamic modulus by using MEPDG dynamic modulus and FWD data at different temperatures"*, International Journal of Pavement Engineering, Taylor and Francis, 2012
- Tayebali, A. A., Deacon, J. A., Coplantz, J. S., and Monismith, C.L., *"Modeling Fatigue Response of Asphalt Aggregate Mixtures"*, Proceedings of Association of Asphalt Paving Technologists, Vol. 62, 1993, pp. 385-421
- Vargas-Nordbeck, A, Timm, D, *"Physical and Structural Characterization of Sustainable Sections at the NCAT Test Track"*, National Center for Asphalt Technology Auburn University, 2013
- Ullditz, P. *"Pavement Analysis"*, Elsevier Science Publishers, New York, 1987.
- Ulditz P, *"Calibration of CALME models using Westrack Performance Data"*, UC Davis, 2006.
- Ursich, C 2005, *"Ohio takes perpetual pavement another step forward"*, Better Roads, vol. 75, no. 11, pp. 63-68,
- Uzan, J. *"Advanced Backcalculation Techniques"*, Nondestructive Testing of Pavements and Backcalculation of Moduli ASTM STP 1198, Philadelphia, PA, 1994.

- Vargas-Nordbeck, A, Timm, D *“Physical and Structural Characterization of Sustainable Sections at the NCAT Test Track”*, National Center for Asphalt Technology Auburn University, 2013
- Van Cauwelaert, FJ, Alexander, DR, White, TD & Barker, WR 1989, *“Multilayer elastic program for backcalculating layer moduli in pavement evaluation”*, Nondestructive testing of pavements and backcalculation of moduli, pp. 171-88,
- Van der Poel C, *“A general system describing the visco-elastic properties of bitumens and its relation to routine test data”*, Journal of Applied Chemistry, Volume 4, Issue 5, pages 221–236, May 1954 1954
- Vavrik, William, R, Harrell, MJ & Gillen, S 2009, *“Achieving Perpetual Pavement through Staged Construction – Illinois Tollways Case Study”*, International Conference of Perpetual Pavements
- VicRoads 2007, *“Top Down Cracking in Melbourne Pavements (Maintenance of Thick Asphalt Pavements)”* - Technical Note 82
- Von Quintus, H, Mallela, J, Jiang, J & Buncher, M 2007, *“Expected Service Life of Hot-Mix Asphalt Pavements in Long-Term Pavement Performance Program”*, Transportation Research Record: Journal of the Transportation Research Board, vol. 1990, no. -1, pp. 102-110,
- Von Quintus, HL 2001a, *“Hot-mix asphalt layer thickness design for longer-life bituminous pavements”*, Transportation Research Board Circular No. 503, pp. 66-78,
- Von Quintus, HL 2001, *“Pavement Structural Design Study: A Simplified Catalog of Solutions”*
- Von Quintus, HL & Tam, WO, 2001, *“HMA Overlay Design Study for Rubblization of PCC Slabs”*
- Walubita, LF, Liu, W, Scullion, T & Leidy, J 2008, *“Modeling Perpetual Pavements Using the Flexible Pavement System (FPS) Software”*, 87th Transportation Research Board Annual Meeting
- Walubita, LF, Scullion, S & Scullion, T 2007, *“Perpetual Pavements in Texas: The Fort Worth SH 114 Perpetual Pavement in Wise County”*, Technical Report FHWA/TX-05/0-4822-2
- Walubita, LF & Scullion, T 2010, *“Texas Perpetual Pavements: New Design Guidelines”*, Texas Transportation Institute, Texas A&M University System.
- Walubita, LF, Scullion, T, Leidy, J & Liu, W 2009, *“A Review of the Texas Structural Design Criteria for Perpetual Pavements”*, International Conference of Perpetual Pavements
- West, RC, Zhang, J & Moore, J 2005, *“Evaluation of bond strength between pavement layers”*
- Willis, JR 2008, *“A Synthesis of Practical and Appropriate Instrumentation Use for Accelerated Pavement Testing in the United States”*
- Willis, JR 2009, *“Field Based Strain Thresholds for Flexible Perpetual Pavement Design”*, thesis, Auburn University, Alabama
- Willis, JR & Timm, DH 2007, *“Forensic investigation of debonding in rich bottom pavement”*, Journal of the Transportation Research Board, no. 2040, pp. 107-114,
- Willis, JR & Timm, DH 2009a, *“A Comparison of Laboratory Thresholds to Measured Strains in Full-Scale Pavements”*, International Conference on Perpetual Pavements
- Willis, JR & Timm, DH 2009b, *“Field-based Strain Thresholds for Flexible Perpetual Pavement Designs”*
- Willis, R, Timm, D, West, R, Powell, B, Robbins, M, Taylor, A, Smit, A, Tran, N, Heitzman, M & Bianchini, A, 2009c, *“Phase III NCAT Test Track Findings”*
- Willoughby, KA, Mahoney, JP, Pierce, LM, Uhlmeier, JS & Anderson, KW 2002, *“Temperature and Density Differentials in Asphalt Concrete Pavements”*, 9th International Conference on Asphalt Pavements
- Witczak, MW, El-Badawy, S & El-Basyoury, M 2006, *“Incorporation of Fatigue Endurance Limit into the MEPDG Analysis”*
- Witczak, M, Kaloush K, Pellinen, T and Von Quintus, H, *“Simple Performance Test for Superpave Mix Design, National Cooperative Highway Research Program”*, NCHRP Report 465, National Academy Press, Washington, D.C. 2002

- Wu, Z & Hossain, M 2002, "*Lives of Mill-and-inlay Rehabilitation Strategies*", International Journal of Pavement Engineering, vol. 3, no. 3, pp. 173 - 183, viewed June 08, 2011.
- Yang, Y, Gao, X, Lin, W, Timm, DH, Priest, A, Huber, G & Andrewski, DA 2005, "*Perpetual Pavement Design in China*", International Conference on Perpetual Pavement
- Yut, I, Nener-Plante, D & Zofka, A 2010, "*Case Study on Perpetual Flexible Pavement in Connecticut*", First International Conference on Pavement Preservation
- Zeida W, 2012, "*Endurance Limit for HMA Based on Healing Phenomenon Using Viscoelastic Continuum Damage Analysis*" A Dissertation Presented in Partial Fulfilment of the Requirements for the Degree Doctor of Philosophy, Arizona State University

Appendices

Appendix A Mix Details and Dynamic Modulus Results

Appendix B STEP Sites

Appendix C Confidence Interval Calculations

Appendix D Laboratory to Field Conversions

1 FWD

2 Strain

Appendix E Backcalculation results

Appendix F FEL Validation

1 LLAP Sites

2 Non LLAP Sites



APS-fL Mix Properties and Dynamic Modulus Results

Report Number: RDM-12110

Page A1 of A95

Mix Details

AC/DG	20	Binder Content (%)	4.80
Aggregate Type:	Lattite/Igneous	VMA (%)	13.9
Binder Type	C600	Air Voids (%)	4.6
Mix Design Method	Marshall 50	VFB (%)	67
Filler Type		Effective Bit. Content (%)	4.1
		RAP (%)	15

Gradation Percent Passing (%)

26.5mm	100	2.36mm	36
19mm	99	1.18mm	27
13.2mm	80.00	0.6mm	20
9.5mm	65.000	0.3mm	13
6.7mm	57	0.15mm	8
4.75mm	49	0.075mm	5.5

Dynamic Modulus Results

Frequency (Hz)	Specimen	Modulus (MPa)	Phase Angle (deg)	Strain με	Temperature (oC)
-------------------	----------	------------------	----------------------	--------------	---------------------

Confinement (kPa): 0

Target Temperature (oC) 5

0.5	BKT2	16591	10.11	99	5.1
0.5	BKT1	16835	9.94	98	5.2
1	BKT1	18058	9.31	93	5.1
1	BKT2	17717	9.18	95	5.1
5	BKT2	20252	7.43	80	5.1
5	BKT1	20693	7.81	79	5.1
10	BKT1	21841	7.53	72	5.1
10	BKT2	21245	6.82	74	5.1
25	BKT1	23233	7	62	5.1
25	BKT2	22561	6.25	64	5.1

Target Temperature (oC) 20

0.5	BKT1	8873	20	99	19.7
0.5	BKT2	9316	19.41	99	20.3
1	BKT2	10570	17.86	97	20.3
1	BKT1	10076	18.34	98	19.9
5	BKT2	13604	14.3	96	20.2
5	BKT1	13112	14.48	96	20
10	BKT2	14947	13.03	93	20.2
10	BKT1	14451	13.17	96	20.1
25	BKT2	16748	11.68	84	20.2
25	BKT1	16253	11.76	92	20.1

Target Temperature (oC) 35

0.5	BKT2	2596	32.95	100	35.2
0.5	BKT1	2587	33.13	99	35.2
1	BKT1	3365	31.74	95	35.1

Report Date:

Monday, 21 September 2015



APS-fL Mix Properties and Dynamic Modulus Results

Report Number: RDM-12110

Page A2 of A95

1	BKT2	3392	31.57	95	35.1
5	BKT1	5654	27.18	91	35.1
5	BKT2	5740	27.15	90	35.1
10	BKT1	6783	25.51	98	35
10	BKT2	6873	25.4	90	35
25	BKT1	8375	23.55	92	35
25	BKT2	8457	23.18	91	35

Target Temperature (oC) 50

0.5	BKT1	490	38.28	101	50.4
0.5	BKT2	477	37.46	101	50.7
1	BKT2	672	38.26	104	50.7
1	BKT1	700	39.39	111	50.4
5	BKT2	1531	37.57	86	50.7
5	BKT1	1619	37.79	86	50.2
10	BKT2	2134	36.86	84	50.7
10	BKT1	2247	36.95	84	50.2
25	BKT1	3307	34.86	85	50.1
25	BKT2	3179	34.83	85	50.7

Confinement (kPa): 50

Target Temperature (oC) 35

0.5	BKT2	2644	32.29	99	35.1
0.5	BKT1	2678	32.77	100	35
1	BKT1	3470	31.25	95	35.1
1	BKT2	3424	31.2	95	35.2
5	BKT2	5737	27.04	91	35.3
5	BKT1	5752	26.54	91	35.2
10	BKT2	6864	25.34	91	35.4
10	BKT1	6812	25.01	92	35.3
25	BKT2	8495	23.18	91	35.4
25	BKT1	8391	22.82	93	35.3

Target Temperature (oC) 50

0.5	BKT1	619	34.48	100	50.1
0.5	BKT2	593	34.41	98	50.1
1	BKT1	828	35.96	100	50.3
1	BKT2	778	36.2	100	50.2
5	BKT2	1651	36.5	87	50.3
5	BKT1	1732	36.48	89	50.4
10	BKT1	2365	35.85	87	50.5
10	BKT2	2262	35.99	85	50.3
25	BKT1	3430	34.07	88	50.4
25	BKT2	3316	34.21	86	50.3

Confinement (kPa): 100

Target Temperature (oC) 35

0.5	BKT1	2760	32	99	34.6
0.5	BKT2	2683	32.23	99	34.6



APS-fL Mix Properties and Dynamic Modulus Results

Report Number: RDM-12110

Page A3 of A95

1	BKT1	3539	30.84	95	34.9
1	BKT2	3447	31.06	95	34.9
5	BKT2	5736	27.06	92	35.1
5	BKT1	5773	26.55	92	35.2
10	BKT1	6861	24.93	93	35.3
10	BKT2	6876	25.32	92	35.3
25	BKT2	8501	23.06	91	35.4
25	BKT1	8435	22.4	92	35.4

Target Temperature (oC) 50

0.5	BKT2	718	31.17	98	49.6
0.5	BKT1	777	31.49	102	49.3
1	BKT1	1021	32.72	99	49.9
1	BKT2	897	33.48	97	50
5	BKT2	1741	35.09	88	50.4
5	BKT1	1941	34.51	91	50.2
10	BKT2	2333	35.06	87	50.5
10	BKT1	2583	34.31	90	50.3
25	BKT2	3348	33.89	87	50.5
25	BKT1	3650	32.93	90	50.3

Confinement (kPa): 200

Target Temperature (oC) 35

0.5	BKT1	2875	31.86	99	33.7
0.5	BKT2	2839	31.02	99	34
1	BKT2	3537	30.31	95	34.5
1	BKT1	3607	30.87	95	34.3
5	BKT1	5759	26.52	93	34.8
5	BKT2	5672	26.36	93	34.9
10	BKT1	6859	24.84	94	35.1
10	BKT2	6788	24.63	94	35.1
25	BKT2	8447	22.21	92	35.3
25	BKT1	8434	22.28	94	35.3

Target Temperature (oC) 50

0.5	BKT2	1064	25.51	102	48.9
0.5	BKT1	995	29.28	104	48.3
1	BKT1	1301	30	99	49.2
1	BKT2	1305	27.24	99	49.5
5	BKT2	2137	30.42	93	49.9
5	BKT1	2268	32.06	93	49.8
10	BKT2	2712	31.09	93	50.2
10	BKT1	2916	32.25	93	50.1
25	BKT1	3989	31.19	93	50.3
25	BKT2	3693	30.68	93	50.4



APS-fL Mix Properties and Dynamic Modulus Results

Report Number: RDM-12100

Page A4 of A95

Mix Details

AC/DG	20	Binder Content (%)	4.80
Aggregate Type:	Basalt	VMA (%)	15.5
Binder Type	AR450	Air Voids (%)	4.8
Mix Design Method	Gryo 120	VFB (%)	69
Filler Type	Hydrated Lime	Effective Bit. Content (%)	4.6
		RAP (%)	15

Gradation Percent Passing (%)

26.5mm	100	2.36mm	32
19mm	98	1.18mm	26
13.2mm	86.00	0.6mm	20
9.5mm	72.000	0.3mm	12
6.7mm	56	0.15mm	6.6
4.75mm	45	0.075mm	4.6

Dynamic Modulus Results

Frequency (Hz)	Specimen	Modulus (MPa)	Phase Angle (deg)	Strain $\mu\epsilon$	Temperature (oC)
----------------	----------	---------------	-------------------	----------------------	------------------

Confinement (kPa): 0

Target Temperature (oC) 5

0.5	BKE2	18499	9.45	91	4.9
0.5	BKE1	18393	9.7	92	5.1
1	BKE1	19585	8.91	86	5.1
1	BKE2	19545	8.8	86	4.9
5	BKE2	21794	7.55	75	4.9
5	BKE1	22140	7.29	74	5.1
10	BKE1	23172	6.69	68	5.1
10	BKE2	22662	7.24	70	4.9
25	BKE1	24319	6.3	60	5
25	BKE2	23593	6.85	62	4.9

Target Temperature (oC) 20

0.5	BKE1	8244	21.9	99	20
0.5	BKE2	7775	22.18	99	20.1
1	BKE2	8985	20.23	96	20.1
1	BKE1	9510	19.88	98	20
5	BKE2	11916	15.56	95	20.1
5	BKE1	12672	15.57	96	20
10	BKE2	13122	13.87	94	20.1
10	BKE1	14098	14.08	95	20
25	BKE2	14721	12.07	87	20.1
25	BKE1	15995	12.55	89	20

Target Temperature (oC) 35

0.5	BKE2	1886	36.99	101	35.3
0.5	BKE1	1928	35.21	100	35.3
1	BKE1	2632	33.75	97	35.4

Report Date:

Monday, 21 September 2015



APS-fL Mix Properties and Dynamic Modulus Results

Report Number: RDM-12100

Page A5 of A95

1	BKE2	2590	35.16	97	35.3
5	BKE1	4840	29.25	91	35.5
5	BKE2	4800	30.19	91	35.2
10	BKE1	6003	27.43	97	35.5
10	BKE2	5948	28.26	91	35.2
25	BKE1	7574	25.71	89	35.4
25	BKE2	7582	26.21	91	35.2

Target Temperature (oC) 50

0.5	BKE1	307	39.69	103	50.3
0.5	BKE2	297	40.11	102	50.1
1	BKE2	435	41.26	106	50.1
1	BKE1	449	40.64	107	49.9
5	BKE2	1103	40.68	85	50.1
5	BKE1	1139	40.12	84	49.7
10	BKE2	1601	39.57	82	50.1
10	BKE1	1653	39.47	81	49.6
25	BKE1	2610	37.26	85	49.6
25	BKE2	2522	37.25	86	50.1

Confinement (kPa): 50

Target Temperature (oC) 35

0.5	BKE2	1987	36.29	100	34.9
0.5	BKE1	2010	35.22	99	35.1
1	BKE1	2697	33.99	96	35.2
1	BKE2	2680	34.83	97	35.1
5	BKE2	4840	29.99	91	35.3
5	BKE1	4885	29.35	91	35.3
10	BKE2	5953	27.98	92	35.4
10	BKE1	6013	27.49	91	35.4
25	BKE2	7517	25.34	92	35.4
25	BKE1	7605	25.35	90	35.4

Target Temperature (oC) 50

0.5	BKE1	343	38.96	102	49.9
0.5	BKE2	508	30.51	99	49.6
1	BKE1	484	39.96	105	50.1
1	BKE2	632	34.01	98	49.9
5	BKE2	1246	37.59	88	50.1
5	BKE1	1168	39.95	85	50.1
10	BKE1	1671	39.14	83	50.1
10	BKE2	1722	37.54	87	50.2
25	BKE1	2614	37.44	86	50.1
25	BKE2	2605	35.96	90	50.2

Confinement (kPa): 100

Target Temperature (oC) 35

0.5	BKE1	2047	35.1	100	34.6
0.5	BKE2	2103	35.1	99	34.6



APS-fL Mix Properties and Dynamic Modulus Results

Report Number: RDM-12100

Page A6 of A95

1	BKE1	2731	33.93	96	34.9
1	BKE2	2773	33.98	96	34.9
5	BKE2	4904	29.71	91	35.3
5	BKE1	4865	29.5	91	35.2
10	BKE1	5957	27.64	92	35.3
10	BKE2	5985	27.78	92	35.4
25	BKE2	7489	26.2	93	35.4
25	BKE1	7579	25.24	90	35.4

Target Temperature (oC) 50

0.5	BKE2	661	26.94	105	48.8
0.5	BKE1	381	37.82	103	49.3
1	BKE1	538	38.34	104	49.8
1	BKE2	810	29.58	98	49.7
5	BKE2	1424	34.44	90	50.1
5	BKE1	1231	38.88	87	50.1
10	BKE2	1885	35.3	90	50.3
10	BKE1	1744	38.37	86	50.2
25	BKE2	2725	34.84	91	50.4
25	BKE1	2673	36.9	88	50.3

Confinement (kPa): 200

Target Temperature (oC) 35

0.5	BKE1	2039	35.65	101	34.1
0.5	BKE2	2253	34.22	99	34.1
1	BKE2	2849	34.13	95	34.5
1	BKE1	2729	34.78	95	34.5
5	BKE1	4771	29.76	92	34.9
5	BKE2	4833	29.51	93	34.9
10	BKE1	5843	27.66	92	35.1
10	BKE2	5899	27.31	94	35.1
25	BKE2	7467	24.44	93	35.3
25	BKE1	7408	24.86	92	35.3

Target Temperature (oC) 50

0.5	BKE2	932	24.62	101	48.3
0.5	BKE1	474	34.48	110	48.2
1	BKE1	690	33.08	104	49.2
1	BKE2	1103	27.23	98	49.2
5	BKE2	1775	31.46	92	49.8
5	BKE1	1400	35.16	89	49.8
10	BKE2	2250	32.65	93	50
10	BKE1	1893	35.57	89	50.1
25	BKE1	2745	35.01	89	50.3
25	BKE2	3106	32.75	93	50.3



APS-fL Mix Properties and Dynamic Modulus Results

Report Number: RDM-12002

Page A7 of A95

Mix Details

AC/DG	14	Binder Content (%)	4.70
Aggregate Type:	Granite	VMA (%)	16.4
Binder Type	C320	Air Voids (%)	5.5
Mix Design Method	Marshall 75	VFB (%)	66
Filler Type	Hydrated Lime	Effective Bit. Content (%)	4.7
		RAP (%)	0

Gradation Percent Passing (%)

26.5mm	100	2.36mm	37.5
19mm	100	1.18mm	26.4
13.2mm	97.70	0.6mm	18.9
9.5mm	84.000	0.3mm	13
6.7mm	68	0.15mm	8.6
4.75mm	53.7	0.075mm	4.9

Dynamic Modulus Results

Frequency (Hz)	Specimen	Modulus (MPa)	Phase Angle (deg)	Strain με	Temperature (oC)
-------------------	----------	------------------	----------------------	--------------	---------------------

Confinement (kPa): 0

Target Temperature (oC) 5

0.5	BIS1	16720	12.18	97	5.1
1	BIS1	18056	11.15	92	5.2
2	BIS2	17074	10.77	97	5
5	BIS2	18408	9.82	91	5
5	BIS1	20959	9.09	76	5.1
10	BIS1	22127	8.22	70	5.2
10	BIS2	21284	8.05	76	5
20	BIS2	22448	7.45	70	5
25	BIS1	23628	7.32	59	5.2
25	BIS2	23843	6.48	61	5

Target Temperature (oC) 20

0.5	BIS1-R1	6826	25.13	98	20.1
0.5	BIS2	7410	24.59	98	20.1
1	BIS1-R1	7952	23.44	94	20.1
1	BIS2	8535	22.82	96	20.1
5	BIS2	11656	18.48	95	20.1
5	BIS1-R1	10937	18.94	94	20.1
10	BIS2	13050	16.81	94	20.1
10	BIS1-R1	12334	17.55	93	20.1
25	BIS2	14892	14.47	89	20.1
25	BIS1-R1	14192	15.57	92	20.1

Target Temperature (oC) 35

0.5	BIS1	1478	37.16	101	35.5
0.5	BIS2	1699	36	101	35.5
1	BIS1	2066	36	98	35.3

Report Date:

Monday, 21 September 2015

APS-fL Mix Properties and Dynamic Modulus Results



Report Number: **RDM-12002**

Page A8 of A95

1	BIS2	2344	34.72	97	35.6
5	BIS1	4058	31.83	89	35.2
5	BIS2	4436	30.3	89	35.6
10	BIS1	5138	30.16	88	35.2
10	BIS2	5548	28.63	89	35.6
25	BIS1	6700	28.18	86	35.2
25	BIS2	7104	26.48	88	35.6

Target Temperature (oC) 50

0.5	BIS2	260	41.1	104	50.1
0.5	BIS1	240	40.65	103	50
1	BIS1	349	41.89	106	49.9
1	BIS2	387	41.88	106	50.1
5	BIS1	894	42.45	82	50
5	BIS2	974	41.81	82	50
10	BIS2	1422	41.38	79	50
10	BIS1	1323	41.88	79	50
25	BIS2	2310	38.77	82	50
25	BIS1	2192	39.01	83	50

Confinement (kPa): 50

Target Temperature (oC) 35

0.5	BIS1	1695	34.43	100	35.6
0.5	BIS2	1829	34.7	100	35.4
1	BIS1	2279	34.94	103	35.5
1	BIS2	2480	33.67	97	35.5
5	BIS2	4593	29.75	90	35.5
5	BIS1	4254	30.7	90	35.3
10	BIS2	5697	28.16	89	35.5
10	BIS1	5354	29.18	89	35.3
25	BIS1	6913	27.02	87	35.3
25	BIS2	7256	26.07	89	35.6

Target Temperature (oC) 50

0.5	BIS2	575	28.35	99	49.9
0.5	BIS1	553	27.67	98	49.8
1	BIS2	690	31.53	97	49.9
1	BIS1	660	30.97	97	49.9
5	BIS1	1191	35.97	87	49.9
5	BIS2	1256	35.67	94	50
10	BIS2	1673	36.83	85	50
10	BIS1	1607	37.12	85	50
25	BIS2	2500	35.93	86	50
25	BIS1	2423	36.37	87	50

Confinement (kPa): 100

Target Temperature (oC) 35

0.5	BIS1	1895	32.37	98	35.3
0.5	BIS2	2028	33.22	99	35.3



APS-fL Mix Properties and Dynamic Modulus Results

Report Number: RDM-12002

Page A9 of A95

1	BIS2	2663	32.75	96	35.3
1	BIS1	2439	32.67	96	35.2
5	BIS1	4371	30.14	91	35.2
5	BIS2	4738	29.19	91	35.3
10	BIS1	5437	28.46	91	35.2
10	BIS2	5837	27.5	91	35.2
25	BIS1	6982	25.95	90	35.2
25	BIS2	7435	25.17	91	35.2

Target Temperature (oC) 50

0.5	BIS1	743	24.06	98	49.3
0.5	BIS2	754	25.17	98	49.1
1	BIS1	853	27.35	109	49.6
1	BIS2	860	27.99	96	49.5
5	BIS2	1394	33.15	88	49.8
5	BIS1	1402	32.79	91	49.8
10	BIS1	1812	34.38	88	49.9
10	BIS2	1787	34.58	86	49.9
25	BIS1	2582	34.68	88	50
25	BIS2	2535	35.06	85	50

Confinement (kPa): 200

Target Temperature (oC) 35

0.5	BIS2	2411	31.09	98	34.1
0.5	BIS1	2158	30.62	97	34.4
1	BIS1	2632	31.7	96	34.6
1	BIS2	2999	31.17	95	34
5	BIS1	4439	29.42	92	34.7
5	BIS2	4990	28.27	93	34
10	BIS1	5447	28.03	92	34.8
10	BIS2	6073	26.47	94	34
25	BIS1	6880	25.6	92	35
25	BIS2	7681	23.9	93	34

Target Temperature (oC) 50

0.5	BIS2	1062	21.84	101	48.4
0.5	BIS1	1050	20.69	100	48.4
1	BIS2	1201	24.12	100	49
1	BIS1	1191	23.23	100	49
5	BIS1	1724	28.63	85	49.5
5	BIS2	1754	28.51	92	49.5
10	BIS1	2145	29.98	93	49.7
10	BIS2	2130	30.48	92	49.7
25	BIS1	2861	31.25	89	49.9
25	BIS2	2823	31.62	87	49.9



APS-fL Mix Properties and Dynamic Modulus Results

Report Number: RDM-11123

Page A10 of A95

Mix Details

AC/DG	20	Binder Content (%)	4.90
Aggregate Type:	Latite	VMA (%)	14
Binder Type	AR450	Air Voids (%)	4.9
Mix Design Method	Gyro 120	VFB (%)	70
Filler Type		Effective Bit. Content (%)	3.9
		RAP (%)	20

Gradation Percent Passing (%)

26.5mm	100	2.36mm	32
19mm	91	1.18mm	24
13.2mm	80.00	0.6mm	17
9.5mm	72.000	0.3mm	11
6.7mm	55	0.15mm	7
4.75mm	42	0.075mm	4.5

Dynamic Modulus Results

Frequency (Hz)	Specimen	Modulus (MPa)	Phase Angle (deg)	Strain $\mu\epsilon$	Temperature (oC)
-------------------	----------	------------------	----------------------	-------------------------	---------------------

Confinement (kPa): 0

Target Temperature (oC) 5

0.5	BIT2	16620	9.63	97	5.1
0.5	BIT1	16342	9.22	97	5
1	BIT1	17387	8.34	96	5
1	BIT2	17732	8.68	94	5.1
5	BIT2	20118	6.97	80	5.1
5	BIT1	19688	6.97	81	5.1
10	BIT1	20626	6.43	75	5.1
10	BIT2	21052	6.36	75	5.1
25	BIT1	21922	5.75	64	5.1
25	BIT2	22141	5.7	65	5.1

Target Temperature (oC) 20

0.5	BIT1	7223	22.27	99	20.7
0.5	BIT2	7189	23.43	100	20
1	BIT2	8387	21.22	98	20
1	BIT1	8331	20.22	98	20.4
5	BIT2	11399	16.22	97	20
5	BIT1	11069	15.47	95	20.2
10	BIT2	12750	14.55	96	20
10	BIT1	12300	13.92	95	20.1
25	BIT2	14491	12.59	91	20
25	BIT1	13744	11.94	91	20

Target Temperature (oC) 35

0.5	BIT2	1558	38.17	102	35.2
0.5	BIT1	1942	37.02	100	34.8
1	BIT1	2669	35.14	97	34.9

Report Date:

Monday, 21 September 2015

APS-fL Mix Properties and Dynamic Modulus Results



Report Number: **RDM-11123**

Page A11 of A95

1	BIT2	2189	36.56	97	35.3
5	BIT1	4916	29.64	91	35
5	BIT2	4303	31.29	88	35.3
10	BIT1	6071	27.36	91	35
10	BIT2	5379	29.2	87	35.3
25	BIT1	7653	24.55	90	35
25	BIT2	6937	26.31	85	35.3

Target Temperature (oC) 50

0.5	BIT1	239	42.41	103	50.5
0.5	BIT2	256	47.84	103	50.3
1	BIT2	372	46.11	107	50.2
1	BIT1	352	43.71	108	50.5
5	BIT2	942	41.89	79	50.1
5	BIT1	956	42.09	93	50.4
10	BIT2	1389	41.02	76	50
10	BIT1	1422	41.06	90	50.3
25	BIT1	2292	38.68	83	50.3
25	BIT2	2287	38.26	80	50

Confinement (kPa): 50

Target Temperature (oC) 35

0.5	BIT2	1695	37.12	100	34.9
0.5	BIT1	2002	36.38	100	35
1	BIT1	2732	34.7	96	35
1	BIT2	2321	36.01	98	35.1
5	BIT2	4431	31.17	91	35.2
5	BIT1	4975	29.31	91	35
10	BIT2	5573	28.79	90	35.3
10	BIT1	6126	27.03	91	35
25	BIT2	7210	25.77	86	35.3
25	BIT1	7712	24.07	90	35

Target Temperature (oC) 50

0.5	BIT1	319	36.58	97	50.1
0.5	BIT2	457	30.92	98	49.8
1	BIT1	415	40.06	100	50.2
1	BIT2	566	34.47	96	49.9
5	BIT2	1136	39.05	86	50
5	BIT1	977	41.71	83	50.3
10	BIT1	1423	41.21	80	50.3
10	BIT2	1596	39.25	84	50
25	BIT1	2307	38.49	82	50.3
25	BIT2	2465	37.45	86	50

Confinement (kPa): 100

Target Temperature (oC) 35

0.5	BIT1	2059	35.84	100	34.8
0.5	BIT2	1876	35.38	99	34.7



APS-fL Mix Properties and Dynamic Modulus Results

Report Number: RDM-11123

Page A12 of A95

1	BIT1	2775	34.53	96	34.8
1	BIT2	2485	34.9	96	34.7
5	BIT2	4562	30.6	91	34.8
5	BIT1	4995	29.23	98	34.9
10	BIT1	6098	27.04	91	35
10	BIT2	5654	28.25	98	34.9
25	BIT2	7240	25.04	89	35.1
25	BIT1	7634	24.07	92	35

Target Temperature (oC) 50

0.5	BIT2	612	26.44	99	49.2
0.5	BIT1	402	32.64	101	49.4
1	BIT1	517	35.11	98	49.5
1	BIT2	727	29.99	97	49.7
5	BIT2	1283	36.04	89	50
5	BIT1	1056	38.62	86	49.7
10	BIT2	1720	37.16	87	50.1
10	BIT1	1486	38.82	84	49.8
25	BIT2	2538	36.6	87	50.1
25	BIT1	2310	37.15	86	49.9

Confinement (kPa): 200

Target Temperature (oC) 35

0.5	BIT1	2099	34.92	100	34.1
0.5	BIT2	2030	34.31	97	34.1
1	BIT2	2565	34.48	96	34.4
1	BIT1	2782	34.38	96	34.4
5	BIT1	4875	29.69	93	34.6
5	BIT2	4539	30.63	92	34.6
10	BIT1	5974	27.4	93	34.7
10	BIT2	5553	28.46	93	34.8
25	BIT2	7114	25.1	90	34.9
25	BIT1	7517	23.99	91	34.9

Target Temperature (oC) 50

0.5	BIT2	827	23.56	87	47.7
0.5	BIT1	643	29.64	103	48.6
1	BIT1	839	31.26	98	49.2
1	BIT2	972	25.82	99	48.9
5	BIT2	1529	31.68	90	49.4
5	BIT1	1566	35.01	90	49.5
10	BIT2	1929	33.57	91	49.6
10	BIT1	2100	35.45	90	49.7
25	BIT1	3053	34.31	90	49.9
25	BIT2	2696	34.37	89	49.9



APS-fL Mix Properties and Dynamic Modulus Results

Report Number: **RDM-12003**

Page A13 of A95

Mix Details

AC/DG	20	Binder Content (%)	4.50
Aggregate Type:	Granite	VMA (%)	14.2
Binder Type	C320	Air Voids (%)	3.8
Mix Design Method	Marshall 75	VFB (%)	73
Filler Type	Hydrated Lime	Effective Bit. Content (%)	4.4
		RAP (%)	0

Gradation Percent Passing (%)

26.5mm	100	2.36mm	32.9
19mm	98.9	1.18mm	23.4
13.2mm	79.40	0.6mm	16.8
9.5mm	61.200	0.3mm	11.6
6.7mm	51.6	0.15mm	7.6
4.75mm	44.4	0.075mm	4.3

Dynamic Modulus Results

Frequency (Hz)	Specimen	Modulus (MPa)	Phase Angle (deg)	Strain με	Temperature (oC)
-------------------	----------	------------------	----------------------	--------------	---------------------

Confinement (kPa): 0

Target Temperature (oC) 5

0.5	BIV1	16228	12.45	97	5
0.5	BIV2	17820	13.24	95	4.9
1	BIV1	17645	11.26	95	5.1
1	BIV2	19490	11.92	86	4.9
5	BIV1	20765	8.96	78	5.1
5	BIV2	23176	9.43	70	5
10	BIV2	24719	8.57	64	5
10	BIV1	21995	8.21	71	5.1
25	BIV1	23505	7.24	61	5.1
25	BIV2	26629	7.51	55	5

Target Temperature (oC) 20

0.5	BIV1	6308	27.92	98	20.1
0.5	BIV2	6266	28.43	99	20.1
1	BIV2	7559	26.23	95	20.1
1	BIV1	7422	25.87	93	20
5	BIV2	11077	20.61	95	20.1
5	BIV1	10426	20.54	94	20.1
10	BIV1	11852	18.68	94	20.1
10	BIV2	12767	18.64	94	20.1
25	BIV1	13821	16.39	90	20.1
25	BIV2	15044	16.13	88	20.1

Target Temperature (oC) 35

0.5	BIV2	1045	40.93	102	35.2
0.5	BIV1	1134	39.35	102	35.1
1	BIV2	1560	39.86	100	34.9

Report Date:

Monday, 21 September 2015

APS-fL Mix Properties and Dynamic Modulus Results



Report Number: **RDM-12003**

Page A14 of A95

1	BIV1	1644	38.64	99	35.2
5	BIV2	3543	35.23	87	34.8
5	BIV1	3554	34.65	88	35.3
10	BIV2	4725	33	86	34.8
10	BIV1	4687	32.64	87	35.4
25	BIV2	6422	30.25	86	34.7
25	BIV1	6328	30.25	85	35.4

Target Temperature (oC) 50

0.5	BIV1	148	41.06	105	50.7
0.5	BIV2	156	40.71	103	49.9
1	BIV1	221	42.4	110	50.6
1	BIV2	226	42.06	110	49.7
5	BIV1	607	43.34	78	50.5
5	BIV2	622	43.91	77	49.6
10	BIV1	941	43.52	74	50.4
10	BIV2	953	44.07	73	49.6
25	BIV1	1685	41.2	81	50.4
25	BIV2	1713	41.48	81	49.6

Confinement (kPa): 50

Target Temperature (oC) 35

0.5	BIV1	1218	37.86	101	35.7
0.5	BIV2	1120	38.9	101	35.1
1	BIV2	1610	38.6	100	35
1	BIV1	1739	37.53	99	35.6
5	BIV1	3677	34.07	87	35.6
5	BIV2	3560	34.76	88	35
10	BIV2	4736	32.67	88	35
10	BIV1	4787	32.12	87	35.6
25	BIV2	6461	29.93	87	35
25	BIV1	6411	29.64	85	35.6

Target Temperature (oC) 50

0.5	BIV2	378	27.28	99	49.9
0.5	BIV1	204	37.78	99	50.4
1	BIV2	449	30.93	97	49.9
1	BIV1	274	39.76	103	50.4
5	BIV1	666	41.95	79	50.3
5	BIV2	823	37.5	84	50.2
10	BIV1	995	42.5	75	50.3
10	BIV2	1136	39.41	80	50.3
25	BIV2	1832	39.25	83	50.4
25	BIV1	1731	40.56	81	50.2

Confinement (kPa): 100

Target Temperature (oC) 35

0.5	BIV1	1318	37.07	99	35
0.5	BIV2	1323	35.61	98	34.8

APS-fL Mix Properties and Dynamic Modulus Results



Report Number: **RDM-12003**

Page A15 of A95

1	BIV2	1771	36.78	97	34.6
1	BIV1	1792	37.29	98	35.1
5	BIV2	3653	34.37	88	34.8
5	BIV1	3718	33.92	97	35.2
10	BIV1	4808	32.15	87	35.3
10	BIV2	4787	32.73	88	34.9
25	BIV1	6386	30.07	86	35.4
25	BIV2	6410	30.2	89	35

Target Temperature (oC) 50

0.5	BIV1	274	34.03	97	50
0.5	BIV2	424	24.15	106	50.2
1	BIV2	516	27.2	99	50.2
1	BIV1	341	36.98	99	50.1
5	BIV2	883	34.38	86	50.3
5	BIV1	746	40.42	80	50.3
10	BIV2	1175	36.98	82	50.4
10	BIV1	1076	41.33	77	50.3
25	BIV2	1800	38.07	84	50.4
25	BIV1	1797	40.17	81	50.4

Confinement (kPa): 200

Target Temperature (oC) 35

0.5	BIV2	1720	31.64	97	34.2
0.5	BIV1	1585	34.57	99	34.5
1	BIV2	2132	33.42	94	34.6
1	BIV1	2061	35.38	95	34.7
5	BIV1	3851	33.55	91	35
5	BIV2	3857	33.08	91	34.9
10	BIV1	4904	31.85	89	35.1
10	BIV2	4942	31.82	92	35.1
25	BIV2	6587	29.16	92	35.2
25	BIV1	6427	29.69	92	35.3

Target Temperature (oC) 50

0.5	BIV2	882	19.1	101	49.2
0.5	BIV1	608	23.24	107	48.6
1	BIV1	762	24.87	103	49.3
1	BIV2	969	21.56	101	49.4
5	BIV2	1360	27.19	92	49.8
5	BIV1	1216	30.57	90	49.8
10	BIV2	1647	30.19	91	49.9
10	BIV1	1545	33.17	89	50.1
25	BIV1	2176	35.07	85	50.3
25	BIV2	2217	33.08	84	50.1



APS-fL Mix Properties and Dynamic Modulus Results

Report Number: RDM-11124

Page A16 of A95

Mix Details

AC/DG	14	Binder Content (%)	5.20
Aggregate Type:	Latite	VMA (%)	15
Binder Type	AR450	Air Voids (%)	5.0
Mix Design Method	Gryo 120	VFB (%)	72
Filler Type		Effective Bit. Content (%)	4.3
		RAP (%)	15

Gradation Percent Passing (%)

26.5mm	100	2.36mm	38
19mm	100	1.18mm	28
13.2mm	91.00	0.6mm	20
9.5mm	81.000	0.3mm	13
6.7mm	65	0.15mm	8
4.75mm	53	0.075mm	5.5

Dynamic Modulus Results

Frequency (Hz)	Specimen	Modulus (MPa)	Phase Angle (deg)	Strain με	Temperature (oC)
-------------------	----------	------------------	----------------------	--------------	---------------------

Confinement (kPa): 0

Target Temperature (oC) 5

0.5	BIW2	15747	9.24	98	5.2
0.5	BIW1	15692	11.4	99	5.4
1	BIW2	16757	8.34	96	5.2
1	BIW1	16798	10.33	97	5.3
5	BIW2	18937	6.64	85	5.2
5	BIW1	19305	8.28	84	5.3
10	BIW1	20225	7.61	77	5.3
10	BIW2	19797	6.08	79	5.2
25	BIW1	21438	7.11	66	5.3
25	BIW2	20916	5.41	68	5.2

Target Temperature (oC) 20

0.5	BIW2	7468	22.54	99	20.1
0.5	BIW1	7553	23.42	100	20.1
1	BIW1	8784	21.24	98	20.1
1	BIW2	8599	20.22	97	20.1
5	BIW1	11769	16.59	96	20.1
5	BIW2	11408	15.45	96	20
10	BIW1	13031	14.69	96	20.1
10	BIW2	12642	13.77	95	20
25	BIW1	14704	12.72	91	20.1
25	BIW2	14371	12.31	90	20

Target Temperature (oC) 35

0.5	BIW2	1645	39.71	109	35.6
0.5	BIW1	1909	36.46	100	35
1	BIW1	2603	34.59	97	34.9

Report Date:

Monday, 21 September 2015



APS-fL Mix Properties and Dynamic Modulus Results

Report Number: RDM-11124

Page A17 of A95

1	BIW2	2312	35.99	97	35.5
5	BIW1	4721	29.04	91	34.9
5	BIW2	4369	30.28	91	35.4
10	BIW1	5807	26.79	92	34.8
10	BIW2	5432	27.89	91	35.4
25	BIW1	7321	24	91	34.8
25	BIW2	6922	24.91	91	35.4

Target Temperature (oC) 50

0.5	BIW2	240	41.04	103	49.8
0.5	BIW1	262	42.41	102	50.4
1	BIW2	355	42.52	108	49.9
1	BIW1	386	43.17	106	50.8
5	BIW2	932	42.72	82	49.9
5	BIW1	992	42.39	83	50.9
10	BIW1	1450	41.19	81	50.8
10	BIW2	1378	41.82	79	49.9
25	BIW2	2232	38.91	82	49.9
25	BIW1	2315	38.07	83	50.8

Confinement (kPa): 50

Target Temperature (oC) 35

0.5	BIW2	1775	36.48	106	35.3
0.5	BIW1	2022	34.93	100	34.9
1	BIW2	2406	34.7	97	35.3
1	BIW1	2706	33.63	97	35
5	BIW2	4440	29.59	91	35.3
5	BIW1	4824	28.64	92	35
10	BIW2	5485	27.29	92	35.4
10	BIW1	5892	26.42	91	35
25	BIW2	6981	24.22	91	35.4
25	BIW1	7344	23.44	91	35

Target Temperature (oC) 50

0.5	BIW1	516	28.95	98	50.5
0.5	BIW2	502	27.7	98	50.1
1	BIW1	629	32.62	97	50.5
1	BIW2	605	31.69	96	50.3
5	BIW2	1127	37.47	87	50.4
5	BIW1	1204	37.26	88	50.5
10	BIW1	1652	37.67	86	50.5
10	BIW2	1535	38.46	85	50.5
25	BIW1	2494	36.09	86	50.5
25	BIW2	2309	37.51	84	50.5

Confinement (kPa): 100

Target Temperature (oC) 35

0.5	BIW1	2126	33.62	99	35.1
0.5	BIW2	1898	34.45	99	34.9



APS-fL Mix Properties and Dynamic Modulus Results

Report Number: RDM-11124

Page A18 of A95

1	BIW1	2768	32.79	96	35.1
1	BIW2	2491	33.87	96	35.2
5	BIW2	4472	29.31	92	35.4
5	BIW1	4816	28.24	93	35.2
10	BIW1	5894	26.05	93	35.3
10	BIW2	5495	27.18	93	35.5
25	BIW2	6973	24.18	92	35.5
25	BIW1	7420	23.07	91	35.3

Target Temperature (oC) 50

0.5	BIW2	691	23.46	99	50.3
0.5	BIW1	694	24.83	98	50.6
1	BIW1	809	28.39	97	50.4
1	BIW2	809	26.92	98	50.4
5	BIW2	1357	33.13	90	50.4
5	BIW1	1387	34.14	89	50.4
10	BIW2	1774	34.62	89	50.4
10	BIW1	1823	35.16	88	50.4
25	BIW2	2553	34.44	89	50.4
25	BIW1	2630	34.73	87	50.4

Confinement (kPa): 200

Target Temperature (oC) 35

0.5	BIW1	2293	33.66	97	34.4
0.5	BIW2	2039	34.34	99	34.4
1	BIW2	2611	34.15	95	34.5
1	BIW1	2858	33.36	95	34.7
5	BIW1	4795	28.73	94	35
5	BIW2	4484	29.94	93	34.8
10	BIW1	5836	26.48	94	35.2
10	BIW2	5469	27.43	94	35
25	BIW2	6923	23.98	93	35.2
25	BIW1	7329	23.12	92	35.4

Target Temperature (oC) 50

0.5	BIW2	888	22.42	99	49.5
0.5	BIW1	936	22.65	89	48.6
1	BIW1	1080	25.14	99	49.4
1	BIW2	1009	25.12	99	49.7
5	BIW2	1580	30.71	92	50
5	BIW1	1669	30.09	92	49.9
10	BIW2	1996	32.37	92	50.2
10	BIW1	2095	31.91	92	50.1
25	BIW1	2871	32.37	90	50.4
25	BIW2	2768	32.85	89	50.3



APS-fL Mix Properties and Dynamic Modulus Results

Report Number: RDM-11115

Page A19 of A95

Mix Details

AC/DG	20	Binder Content (%)	5.00
Aggregate Type:	Basalt	VMA (%)	15.2
Binder Type	C320	Air Voids (%)	5.3
Mix Design Method	Marsahl 50	VFB (%)	69
Filler Type		Effective Bit. Content (%)	4.1
		RAP (%)	

Gradation Percent Passing (%)

26.5mm	100	2.36mm	35
19mm	99	1.18mm	27
13.2mm	84.00	0.6mm	20
9.5mm	73.000	0.3mm	14
6.7mm	62	0.15mm	7.3
4.75mm	51	0.075mm	5.4

Dynamic Modulus Results

Frequency (Hz)	Specimen	Modulus (MPa)	Phase Angle (deg)	Strain με	Temperature (oC)
-------------------	----------	------------------	----------------------	--------------	---------------------

Confinement (kPa): 0

Target Temperature (oC) 5

0.5	BIX2	18703	10.67	90	5.2
0.5	BIX1	19424	10.42	87	5.3
1	BIX1	20880	8.94	80	5.3
1	BIX2	20133	9.47	83	5.2
5	BIX2	23033	7.63	70	5.2
5	BIX1	23864	7.27	68	5.3
10	BIX1	24987	6.57	63	5.3
10	BIX2	24228	7.13	64	5.2
25	BIX1	26412	5.69	54	5.3
25	BIX2	25550	6.21	56	5.2

Target Temperature (oC) 20

0.5	BIX1	8608	24.82	100	20.1
0.5	BIX2	7816	24.58	100	20.1
1	BIX2	9296	22.19	98	20.1
1	BIX1	10149	22.34	98	20.1
5	BIX2	12848	16.98	97	20.1
5	BIX1	13897	17.1	96	20.1
10	BIX2	14485	15.15	96	20.1
10	BIX1	15529	14.98	93	20.1
25	BIX2	16651	13.04	89	20.1
25	BIX1	17665	12.64	83	20.1

Target Temperature (oC) 35

0.5	BIX2	1565	39.27	101	35.2
0.5	BIX1	1458	40.2	101	35.4
1	BIX1	2110	38.68	98	35.4

Report Date:

Monday, 21 September 2015

APS-fL Mix Properties and Dynamic Modulus Results



Report Number: **RDM-11115**

Page A20 of A95

1	BIX2	2243	37.67	98	35.3
5	BIX1	4363	33.35	89	35.4
5	BIX2	4512	32.16	90	35.5
10	BIX1	5574	31.14	89	35.4
10	BIX2	5740	29.87	89	35.5
25	BIX1	7280	28.11	89	35.4
25	BIX2	7390	27.05	90	35.5

Target Temperature (oC) 50

0.5	BIX1	209	42.27	104	50.4
0.5	BIX2	232	40.46	104	50.4
1	BIX2	346	41.89	107	50.3
1	BIX1	313	43.58	108	50.2
5	BIX2	916	42.85	83	50.2
5	BIX1	859	44.01	80	50.2
10	BIX2	1379	42.27	80	50.1
10	BIX1	1293	43.41	78	50.2
25	BIX1	2173	40.42	81	50.2
25	BIX2	2301	39.35	84	50.1

Confinement (kPa): 50

Target Temperature (oC) 35

0.5	BIX2	1637	37.95	100	35.6
0.5	BIX1	1642	37.12	100	35.5
1	BIX1	2273	36.6	98	35.4
1	BIX2	2293	36.8	98	35.4
5	BIX2	4564	31.6	90	35.3
5	BIX1	4514	32.38	90	35.4
10	BIX2	5780	29.3	90	35.3
10	BIX1	5733	30.08	91	35.4
25	BIX2	7503	26.64	89	35.2
25	BIX1	7507	27.04	90	35.4

Target Temperature (oC) 50

0.5	BIX1	514	27.3	100	50.8
0.5	BIX2	541	26.29	99	50.2
1	BIX1	615	31.07	98	50.9
1	BIX2	641	30.25	97	50.2
5	BIX2	1162	36.83	88	50.1
5	BIX1	1127	37.35	87	50.8
10	BIX1	1545	38.55	85	50.8
10	BIX2	1585	38.12	86	50.1
25	BIX1	2395	37.81	86	50.8
25	BIX2	2441	37.32	88	50

Confinement (kPa): 100

Target Temperature (oC) 35

0.5	BIX1	1840	34.68	98	34.9
0.5	BIX2	1837	35.32	99	34.9



APS-fL Mix Properties and Dynamic Modulus Results

Report Number: RDM-11115

Page A21 of A95

1	BIX1	2414	35.1	96	34.8
1	BIX2	2454	35.22	97	35
5	BIX2	4654	31.23	91	35.2
5	BIX1	4566	31.98	91	35
10	BIX1	5774	30.06	91	35.1
10	BIX2	5841	28.98	92	35.3
25	BIX2	7544	26.2	90	35.4
25	BIX1	7469	27.35	91	35.1

Target Temperature (oC) 50

0.5	BIX2	762	22.85	92	49.9
0.5	BIX1	728	22.54	99	50
1	BIX1	833	26.01	99	49.8
1	BIX2	773	27.86	89	50.1
5	BIX2	1225	35.75	88	50.2
5	BIX1	1359	32.86	90	49.6
10	BIX2	1646	37.32	87	50.2
10	BIX1	1772	34.86	89	49.6
25	BIX2	2474	37.13	87	50.2
25	BIX1	2592	35.57	88	49.5

Confinement (kPa): 200

Target Temperature (oC) 35

0.5	BIX1	2124	32.8	97	34.4
0.5	BIX2	2126	33.02	97	34.4
1	BIX2	2677	33.73	95	34.7
1	BIX1	2656	33.82	95	34.4
5	BIX1	4701	31.48	92	34.5
5	BIX2	4700	30.89	92	35
10	BIX1	5850	29.55	93	34.5
10	BIX2	5835	28.9	93	35.1
25	BIX2	7456	25.82	92	35.3
25	BIX1	7598	26.32	93	34.6

Target Temperature (oC) 50

0.5	BIX2	995	20.15	101	49.1
0.5	BIX1	1056	18.79	99	49.1
1	BIX1	1166	21.61	99	49.7
1	BIX2	1131	22.95	100	49.4
5	BIX2	1681	28.88	92	49.9
5	BIX1	1685	27.84	93	50
10	BIX2	2089	31.28	93	50.1
10	BIX1	2073	30.46	93	50.2
25	BIX1	2824	32.43	89	50.4
25	BIX2	2861	32.87	89	50.3



APS-fL Mix Properties and Dynamic Modulus Results

Report Number: RDM-12039

Page A22 of A95

Mix Details

AC/DG	14	Binder Content (%)	5.20
Aggregate Type:	Basalt	VMA (%)	15.5
Binder Type	A15E	Air Voids (%)	5.4
Mix Design Method	Gyro 120	VFB (%)	65
Filler Type	Hydrated Lime	Effective Bit. Content (%)	4.4
		RAP (%)	0

Gradation Percent Passing (%)

26.5mm	100	2.36mm	37
19mm	100	1.18mm	28
13.2mm	97.00	0.6mm	23
9.5mm	82.000	0.3mm	15
6.7mm	68	0.15mm	7
4.75mm	52	0.075mm	5.3

Dynamic Modulus Results

Frequency (Hz)	Specimen	Modulus (MPa)	Phase Angle (deg)	Strain $\mu\epsilon$	Temperature (oC)
----------------	----------	---------------	-------------------	----------------------	------------------

Confinement (kPa): 0

Target Temperature (oC) 5

0.5	BIY2	7697	16	99	5.4
0.5	BIY1	8604	15.74	99	4.9
1	BIY1	9609	14.39	97	4.8
1	BIY2	8613	14.76	98	5.4
5	BIY2	10765	11.95	96	5.4
5	BIY1	11905	11.75	95	4.8
10	BIY1	12895	10.77	94	4.8
10	BIY2	11745	10.98	95	5.4
25	BIY1	14164	9.68	88	4.8
25	BIY2	12984	9.9	89	5.4

Target Temperature (oC) 20

0.5	BIY1	2533	29.61	99	20
0.5	BIY2	2720	27.74	98	20.2
1	BIY2	3265	26.54	95	20.2
1	BIY1	3116	28.51	96	20
5	BIY2	4910	22.76	94	20.2
5	BIY1	4810	24.45	93	20
10	BIY2	5737	21.28	94	20.2
10	BIY1	5653	22.76	94	20
25	BIY2	6980	19.27	92	20.2
25	BIY1	6903	20.49	92	20

Target Temperature (oC) 35

0.5	BIY2	690	32.28	100	35.2
0.5	BIY1	623	33.62	99	35.3
1	BIY1	818	34.22	99	35.4

Report Date:

Monday, 21 September 2015



APS-fL Mix Properties and Dynamic Modulus Results

Report Number: RDM-12039

Page A23 of A95

1	BIY2	900	32.75	100	35.3
5	BIY1	1574	32.94	85	35.4
5	BIY2	1697	31.43	86	35.4
10	BIY1	2022	32.25	84	35.4
10	BIY2	2170	30.75	84	35.4
25	BIY1	2763	30.56	82	35.4
25	BIY2	2953	29.05	83	35.4

Target Temperature (oC) 50

0.5	BIY1	158	33.37	99	50.4
0.5	BIY2	186	30.79	101	50.4
1	BIY2	234	32.61	103	50.5
1	BIY1	204	35.64	116	50.4
5	BIY2	460	35.54	75	50.6
5	BIY1	450	35.81	75	50.1
10	BIY2	626	36.51	69	50.6
10	BIY1	618	36.54	69	50
25	BIY1	982	34.65	72	50
25	BIY2	989	35.13	73	50.5

Confinement (kPa): 50

Target Temperature (oC) 35

0.5	BIY2	752	31.29	98	35.3
0.5	BIY1	677	32.78	99	35.2
1	BIY1	873	33.16	99	35.1
1	BIY2	949	32.04	98	35.5
5	BIY2	1729	31.24	87	35.5
5	BIY1	1633	32.33	86	35.1
10	BIY2	2191	30.64	86	35.5
10	BIY1	2101	31.74	85	35.2
25	BIY2	2962	29.09	83	35.5
25	BIY1	2847	30.09	83	35.2

Target Temperature (oC) 50

0.5	BIY1	324	24.33	101	50
0.5	BIY2	341	25.7	98	50.9
1	BIY1	380	26.6	99	50.2
1	BIY2	377	28.22	98	50.9
5	BIY2	592	32.32	83	50.9
5	BIY1	607	30.75	84	50.3
10	BIY1	763	32.41	79	50.4
10	BIY2	750	33.65	78	50.9
25	BIY1	1069	33.32	75	50.4
25	BIY2	1122	35.33	66	50.9

Confinement (kPa): 100

Target Temperature (oC) 35

0.5	BIY1	729	32.01	98	34.5
0.5	BIY2	860	29.43	97	34.8



APS-fL Mix Properties and Dynamic Modulus Results

Report Number: RDM-12039

Page A24 of A95

1	BIY1	917	32.87	98	34.8
1	BIY2	1039	30.76	96	34.9
5	BIY2	1781	30.79	88	35.1
5	BIY1	1665	32.08	87	35
10	BIY1	2122	31.63	86	35.1
10	BIY2	2235	30.46	87	35.1
25	BIY2	2973	29.23	84	35.1
25	BIY1	2855	30.23	84	35.2

Target Temperature (oC) 50

0.5	BIY2	474	21.76	99	49.6
0.5	BIY1	405	22.27	103	48.9
1	BIY1	479	24.3	118	49.2
1	BIY2	517	24.03	99	49.8
5	BIY2	739	28.44	88	49.9
5	BIY1	766	26.96	86	50.3
10	BIY2	889	30.45	84	50
10	BIY1	914	29.2	86	50.4
25	BIY2	1181	31.68	76	50
25	BIY1	1190	31.12	74	50.4

Confinement (kPa): 200

Target Temperature (oC) 35

0.5	BIY1	1030	27.27	98	34
0.5	BIY2	1128	26.75	99	34.2
1	BIY2	1300	28.06	97	34.6
1	BIY1	1195	28.67	97	34.4
5	BIY1	1858	29.38	91	34.8
5	BIY2	1991	28.83	92	35
10	BIY1	2259	29.37	92	35.1
10	BIY2	2420	28.82	92	35.1
25	BIY2	3122	27.75	86	35.3
25	BIY1	2947	28.35	87	35.3

Target Temperature (oC) 50

0.5	BIY2	781	17	100	49.2
0.5	BIY1	674	18.19	103	48.2
1	BIY1	758	19.94	102	49.2
1	BIY2	835	18.93	101	50
5	BIY2	1068	22.3	93	50.6
5	BIY1	1005	23.19	93	49.8
10	BIY2	1205	24.37	92	50.8
10	BIY1	1145	25.33	92	50.1
25	BIY1	1410	27.39	73	50.2
25	BIY2	1478	26.5	73	51



APS-fL Mix Properties and Dynamic Modulus Results

Report Number: RDM-12040

Page A25 of A95

Mix Details

AC/DG	14	Binder Content (%)	5.20
Aggregate Type:	Basalt	VMA (%)	15.5
Binder Type	AR450	Air Voids (%)	5.4
Mix Design Method	Gyro 120	VFB (%)	65
Filler Type	Hydrated Lime	Effective Bit. Content (%)	4.4
		RAP (%)	0

Gradation Percent Passing (%)

26.5mm	100	2.36mm	37
19mm	100	1.18mm	28
13.2mm	97.00	0.6mm	23
9.5mm	82.000	0.3mm	15
6.7mm	68	0.15mm	7
4.75mm	52	0.075mm	5.3

Dynamic Modulus Results

Frequency (Hz)	Specimen	Modulus (MPa)	Phase Angle (deg)	Strain με	Temperature (oC)
-------------------	----------	------------------	----------------------	--------------	---------------------

Confinement (kPa): 0

Target Temperature (oC) 5

0.5	BIZ2	11871	10.93	98	5.2
0.5	BIZ1	12726	11.39	99	5.1
1	BIZ1	13713	10.42	98	5.1
1	BIZ2	12710	10.03	98	5.3
5	BIZ2	14703	8.01	95	5.3
5	BIZ1	15855	8.51	95	5.1
10	BIZ1	16710	7.78	92	5.1
10	BIZ2	15455	7.33	93	5.3
25	BIZ1	17765	6.82	82	5.1
25	BIZ2	16415	6.62	84	5.3

Target Temperature (oC) 20

0.5	BIZ1	5152	24.58	101	20.2
0.5	BIZ2	4339	26.11	99	20
1	BIZ2	5101	24.26	96	20.1
1	BIZ1	6077	22.78	98	20.1
5	BIZ2	7212	19.78	95	20.1
5	BIZ1	8422	18.16	97	20.1
10	BIZ2	8198	17.88	96	20.1
10	BIZ1	9527	16.28	96	20.1
25	BIZ2	9545	15.9	94	20.1
25	BIZ1	11012	14.02	95	20.1

Target Temperature (oC) 35

0.5	BIZ2	1146	36.74	100	34.7
0.5	BIZ1	1360	35.1	100	35
1	BIZ1	1814	33.98	97	35

Report Date:

Monday, 21 September 2015



APS-fL Mix Properties and Dynamic Modulus Results

Report Number: RDM-12040

Page A26 of A95

1	BIZ2	1549	35.72	98	34.7
5	BIZ1	3276	30.09	90	34.9
5	BIZ2	2910	31.4	90	34.7
10	BIZ1	4043	28.33	90	34.9
10	BIZ2	3665	29.66	90	34.7
25	BIZ1	5178	26.01	90	34.8
25	BIZ2	4776	27.17	89	34.7

Target Temperature (oC) 50

0.5	BIZ1	273	37.47	102	50.5
0.5	BIZ2	224	38.49	102	50.1
1	BIZ2	313	39.78	104	50
1	BIZ1	384	39.08	114	50.4
5	BIZ2	731	40.42	82	49.9
5	BIZ1	890	38.34	83	50.2
10	BIZ2	1044	39.88	79	49.8
10	BIZ1	1244	38.09	80	50.1
25	BIZ1	1899	35.93	81	50
25	BIZ2	1644	37.21	82	49.8

Confinement (kPa): 50

Target Temperature (oC) 35

0.5	BIZ2	1177	36.7	100	34.6
0.5	BIZ1	1432	33	99	34.8
1	BIZ1	1856	32.66	97	34.9
1	BIZ2	1570	35.49	98	34.8
5	BIZ2	2935	31.36	90	34.9
5	BIZ1	3277	29.79	91	35
10	BIZ2	3684	29.62	89	34.9
10	BIZ1	4045	27.84	92	35
25	BIZ2	4776	27.21	89	34.9
25	BIZ1	5196	25.86	90	35

Target Temperature (oC) 50

0.5	BIZ1	539	26.59	98	50
0.5	BIZ2	473	27.08	98	49.8
1	BIZ1	631	29.76	97	50.1
1	BIZ2	546	30.36	95	50
5	BIZ2	923	35.09	87	50.2
5	BIZ1	1074	34.05	87	50.3
10	BIZ1	1396	35	85	50.3
10	BIZ2	1203	36.14	85	50.2
25	BIZ1	1988	34.64	84	50.4
25	BIZ2	1739	35.55	84	50.2

Confinement (kPa): 100

Target Temperature (oC) 35

0.5	BIZ1	1560	31.42	98	34.5
0.5	BIZ2	1226	35.49	100	34.5



APS-fL Mix Properties and Dynamic Modulus Results

Report Number: RDM-12040

Page A27 of A95

1	BIZ1	1954	31.61	97	34.9
1	BIZ2	1621	34.9	97	35
5	BIZ2	2967	31.22	89	35.3
5	BIZ1	3336	29.08	91	35.1
10	BIZ1	4093	27.57	92	35.2
10	BIZ2	3688	29.34	90	35.3
25	BIZ2	4779	26.83	90	35.4
25	BIZ1	5213	25.41	90	35.2

Target Temperature (oC) 50

0.5	BIZ2	460	27.44	99	49.4
0.5	BIZ1	712	23.25	98	49.3
1	BIZ1	805	26.14	97	49.8
1	BIZ2	547	30.4	97	49.8
5	BIZ2	932	34.97	87	50.1
5	BIZ1	1253	30.83	90	50.1
10	BIZ2	1208	36.1	85	50.2
10	BIZ1	1565	32.35	89	50.2
25	BIZ2	1724	35.87	83	50.2
25	BIZ1	2131	32.94	85	50.2

Confinement (kPa): 200

Target Temperature (oC) 35

0.5	BIZ1	1657	31.58	97	34.3
0.5	BIZ2	1373	33.01	100	34.3
1	BIZ2	1751	32.71	96	34.6
1	BIZ1	2012	32.03	96	34.6
5	BIZ1	3319	29.41	92	35
5	BIZ2	2999	29.96	92	34.9
10	BIZ1	4024	27.85	93	35.1
10	BIZ2	3706	28.51	94	35.1
25	BIZ2	4799	26.08	92	35.3
25	BIZ1	5126	25.24	92	35.3

Target Temperature (oC) 50

0.5	BIZ2	806	21.47	98	48.8
0.5	BIZ1	940	21.6	98	48.4
1	BIZ1	1033	23.91	98	49.3
1	BIZ2	881	24.04	98	49.4
5	BIZ2	1258	28.08	92	50
5	BIZ1	1478	27.72	92	49.9
10	BIZ2	1507	30.06	92	50.2
10	BIZ1	1766	29.4	92	50.1
25	BIZ1	2306	30.46	85	50.3
25	BIZ2	1970	31.38	84	50.4



APS-fL Mix Properties and Dynamic Modulus Results

Report Number: RDM-12045

Page A28 of A95

Mix Details

AC/DG	20	Binder Content (%)	4.50
Aggregate Type:	Honsfel & Granite	VMA (%)	15.2
Binder Type	C320	Air Voids (%)	5.0
Mix Design Method	Marshall	VFB (%)	67
Filler Type		Effective Bit. Content (%)	4.3
		RAP (%)	30

Gradation Percent Passing (%)

26.5mm	100	2.36mm	30
19mm	100	1.18mm	22
13.2mm	85.00	0.6mm	17
9.5mm	72.000	0.3mm	12
6.7mm	56	0.15mm	8
4.75mm	43	0.075mm	5.6

Dynamic Modulus Results

Frequency (Hz)	Specimen	Modulus (MPa)	Phase Angle (deg)	Strain $\mu\epsilon$	Temperature (oC)
Confinement (kPa): 0					
Target Temperature (oC) 5					
0.5	BJB3	17550	10.64	97	5
0.5	BJB1	17843	13.11	95	4.8
1	BJB1	19199	11.69	88	4.9
1	BJB3	18795	9.65	89	4.9
5	BJB3	21573	7.83	76	4.9
5	BJB1	22280	9.32	73	4.9
10	BJB1	23570	8.62	67	4.9
10	BJB3	22695	7.22	70	4.9
25	BJB1	25277	8.04	58	4.9
25	BJB3	24140	6.61	60	4.9
Target Temperature (oC) 20					
0.5	BJB1	7201	26.93	99	20.1
0.5	BJB3	7433	24.58	99	20.1
1	BJB3	8697	22.63	96	20.1
1	BJB1	8509	24.86	96	20.1
5	BJB3	11935	17.65	95	20.1
5	BJB1	11794	19.59	96	20.1
10	BJB3	13296	15.97	94	20.1
10	BJB1	13365	17.39	96	20.1
25	BJB3	15179	14.34	90	20.1
25	BJB1	15582	15.15	90	20.1
Target Temperature (oC) 35					
0.5	BJB3	1788	36.93	101	35.6
0.5	BJB1	1520	38.79	101	34.8
1	BJB1	2134	37.64	98	35.1

Report Date:

Monday, 21 September 2015

APS-fL Mix Properties and Dynamic Modulus Results



Report Number: **RDM-12045**

Page A29 of A95

1	BJB3	2463	35.65	97	35.6
5	BJB1	4171	33.4	89	35.2
5	BJB3	4599	31.23	90	35.5
10	BJB1	5287	31.13	90	35.3
10	BJB3	5721	29.26	91	35.5
25	BJB1	6904	28.72	91	35.4
25	BJB3	7576	27.05	80	35.5

Target Temperature (oC) 50

0.5	BJB1	246	40.33	103	50
0.5	BJB3	288	37.22	102	49.4
1	BJB3	407	38.86	104	49.4
1	BJB1	355	41.84	105	49.9
5	BJB3	992	39.89	82	49.5
5	BJB1	898	42.89	81	49.9
10	BJB3	1429	39.88	79	49.5
10	BJB1	1315	42.59	78	49.9
25	BJB1	2139	40.2	81	49.8
25	BJB3	2255	38.17	82	49.5

Confinement (kPa): 50

Target Temperature (oC) 35

0.5	BJB3	1945	35.11	100	35.1
0.5	BJB1	1639	38.13	100	35.2
1	BJB1	2241	37.07	97	35.1
1	BJB3	2606	34.64	96	35.1
5	BJB3	4734	30.71	90	35.1
5	BJB1	4283	32.85	90	35.1
10	BJB3	5829	28.93	91	35.1
10	BJB1	5374	30.95	91	35.1
25	BJB3	7383	26.97	92	35
25	BJB1	7020	28.64	91	35

Target Temperature (oC) 50

0.5	BJB1	483	30.96	98	49.8
0.5	BJB3	536	27.85	98	48.9
1	BJB1	572	34.38	95	49.9
1	BJB3	640	31.65	101	49.2
5	BJB3	1162	36.09	86	49.6
5	BJB1	1061	39.12	86	50
10	BJB1	1455	40.03	84	50
10	BJB3	1567	37.17	84	49.7
25	BJB1	2227	38.91	85	50
25	BJB3	2349	36.68	86	49.7

Confinement (kPa): 100

Target Temperature (oC) 35

0.5	BJB1	1796	37.06	99	34.9
0.5	BJB3	2103	34.15	99	34.7

APS-fL Mix Properties and Dynamic Modulus Results



Report Number: **RDM-12045**

Page A30 of A95

1	BJB1	2381	37.07	96	35
1	BJB3	2743	34.1	96	34.9
5	BJB3	4845	30.56	91	35.1
5	BJB1	4368	33.05	91	35.1
10	BJB1	5442	31.14	92	35.2
10	BJB3	5926	28.68	99	35.2
25	BJB3	7518	26.56	92	35.1
25	BJB1	7052	28.53	92	35.1

Target Temperature (oC) 50

0.5	BJB3	703	24.37	103	48.1
0.5	BJB1	660	26.92	98	49.1
1	BJB1	756	30.01	96	49.6
1	BJB3	814	27.05	97	49.3
5	BJB3	1324	32.62	89	49.7
5	BJB1	1246	35.38	88	50
10	BJB3	1706	34.42	88	49.8
10	BJB1	1614	36.85	87	50.1
25	BJB3	2425	35.13	87	49.9
25	BJB1	2334	36.98	85	50.1

Confinement (kPa): 200

Target Temperature (oC) 35

0.5	BJB1	2036	35.53	99	34.2
0.5	BJB3	2319	33.6	98	34
1	BJB3	2917	33.93	95	34.5
1	BJB1	2571	36.16	95	34.5
5	BJB1	4427	32.41	92	34.9
5	BJB3	4962	30.5	92	34.9
10	BJB1	5491	30.48	93	35.1
10	BJB3	6049	28.33	94	35.1
25	BJB3	7665	25.45	94	35.3
25	BJB1	7085	27.37	94	35.3

Target Temperature (oC) 50

0.5	BJB3	965	21.34	101	47.7
0.5	BJB1	848	22.69	100	48.3
1	BJB1	967	25.28	99	49.2
1	BJB3	1087	23.93	100	48.9
5	BJB3	1598	28.8	92	49.6
5	BJB1	1465	30.29	91	49.8
10	BJB3	1953	31.11	92	49.9
10	BJB1	1820	32.64	91	50.1
25	BJB1	2475	34.07	86	50.3
25	BJB3	2621	32.8	86	50.1



APS-fL Mix Properties and Dynamic Modulus Results

Report Number: RDM-12048

Page A31 of A95

Mix Details

AC/DG	14	Binder Content (%)	4.80
Aggregate Type:	Granite	VMA (%)	16
Binder Type	C320	Air Voids (%)	4.9
Mix Design Method	Marshall	VFB (%)	70
Filler Type	Hydrated Lime	Effective Bit. Content (%)	4.8
		RAP (%)	20

Gradation Percent Passing (%)

26.5mm	100	2.36mm	42
19mm	100	1.18mm	35
13.2mm	97.00	0.6mm	26
9.5mm	77.000	0.3mm	17
6.7mm	63	0.15mm	8
4.75mm	53	0.075mm	5.3

Dynamic Modulus Results

Frequency (Hz)	Specimen	Modulus (MPa)	Phase Angle (deg)	Strain $\mu\epsilon$	Temperature (oC)
----------------	----------	---------------	-------------------	----------------------	------------------

Confinement (kPa): 0

Target Temperature (oC) 5

0.5	BJC2	15243	12.45	98	5
0.5	BJC1	15723	11.3	98	4.9
1	BJC1	16986	10.18	96	4.9
1	BJC2	16457	11.35	97	5
5	BJC2	19180	9.4	85	5
5	BJC1	19744	8.16	82	4.9
10	BJC1	20839	7.46	75	4.9
10	BJC2	20309	8.85	78	5
25	BJC1	22218	6.72	64	5
25	BJC2	21772	8.4	67	5

Target Temperature (oC) 20

0.5	BJC1	5391	27.77	99	20.1
0.5	BJC2	5106	28.77	99	20.1
1	BJC2	6123	26.49	95	20.1
1	BJC1	6459	25.68	95	20.1
5	BJC2	8914	20.92	95	20.1
5	BJC1	9236	20.31	94	20.1
10	BJC2	10263	18.77	94	20.1
10	BJC1	10504	18.3	95	20.1
25	BJC2	11993	16.42	93	20.1
25	BJC1	12326	16.15	91	20.1

Target Temperature (oC) 35

0.5	BJC2	993	40	101	35.6
0.5	BJC1	1136	38.65	102	35.3
1	BJC1	1614	37.58	99	35.2

Report Date:

Monday, 21 September 2015



APS-fL Mix Properties and Dynamic Modulus Results

Report Number: RDM-12048

Page A32 of A95

1	BJC2	1434	38.89	100	35.6
5	BJC1	3288	33.42	89	35.1
5	BJC2	3006	34.7	88	35.5
10	BJC1	4223	31.67	88	35
10	BJC2	3877	32.93	88	35.5
25	BJC1	5603	29.14	88	35
25	BJC2	5205	30.62	87	35.5

Target Temperature (oC) 50

0.5	BJC1	177	38.61	103	50.2
0.5	BJC2	129	41.45	102	50
1	BJC2	188	43.06	107	50
1	BJC1	255	40.44	107	50.1
5	BJC2	514	44.34	75	50.1
5	BJC1	656	41.94	78	50.1
10	BJC2	776	44.61	71	50.1
10	BJC1	971	42.26	74	50
25	BJC1	1631	39.98	79	49.9
25	BJC2	1354	42.08	76	50.1

Confinement (kPa): 50

Target Temperature (oC) 35

0.5	BJC2	1070	38.78	100	35.2
0.5	BJC1	1272	36.2	99	35
1	BJC1	1713	36.35	97	35.1
1	BJC2	1488	38.59	98	35.2
5	BJC2	3018	35.08	89	35.2
5	BJC1	3335	33.23	89	35.2
10	BJC2	3889	33.33	89	35.2
10	BJC1	4219	31.58	89	35.3
25	BJC2	5188	30.65	90	35.2
25	BJC1	5542	29.03	95	35.3

Target Temperature (oC) 50

0.5	BJC1	428	26.11	99	50.1
0.5	BJC2	274	28.66	99	49.9
1	BJC1	502	29.67	97	50.3
1	BJC2	331	32.46	97	50.3
5	BJC2	634	38.75	82	50.4
5	BJC1	881	36.01	85	50.4
10	BJC1	1169	38.11	81	50.4
10	BJC2	881	40.83	78	50.5
25	BJC1	1763	38.26	81	50.5
25	BJC2	1405	40.51	79	50.5

Confinement (kPa): 100

Target Temperature (oC) 35

0.5	BJC1	1406	34.17	97	34.7
0.5	BJC2	1196	37.36	99	34.8



APS-fL Mix Properties and Dynamic Modulus Results

Report Number: RDM-12048

Page A33 of A95

1	BJC1	1803	35.24	95	35.1
1	BJC2	1608	37.65	97	35
5	BJC2	3158	34.7	89	35.2
5	BJC1	3338	32.94	89	35.4
10	BJC1	4181	31.47	90	35.5
10	BJC2	4012	32.96	90	35.3
25	BJC2	5341	30.5	89	35.3
25	BJC1	5490	28.96	90	35.5

Target Temperature (oC) 50

0.5	BJC2	420	25.41	99	49.6
0.5	BJC1	610	22.31	99	49.6
1	BJC1	691	25.39	99	49.9
1	BJC2	492	29.25	97	50.2
5	BJC2	863	35.67	86	50.5
5	BJC1	1082	31.72	89	50.2
10	BJC2	1148	37.9	83	50.6
10	BJC1	1372	34.24	86	50.3
25	BJC2	1715	38.64	81	50.5
25	BJC1	1940	35.76	83	50.4

Confinement (kPa): 200

Target Temperature (oC) 35

0.5	BJC1	1593	32.26	98	33.7
0.5	BJC2	1309	36.62	97	33.9
1	BJC2	1676	37.36	95	34.5
1	BJC1	1950	34.2	102	34.1
5	BJC1	3371	32.43	91	34.9
5	BJC2	3145	34.66	90	34.9
10	BJC1	4201	31.09	92	35.1
10	BJC2	3966	32.86	92	35.1
25	BJC2	5318	30.21	93	35.3
25	BJC1	5477	28.42	92	35.4

Target Temperature (oC) 50

0.5	BJC2	558	24.43	97	48.2
0.5	BJC1	866	20.38	99	48.7
1	BJC1	948	22.78	101	49.4
1	BJC2	624	27.68	97	49.3
5	BJC2	1020	33.53	87	49.9
5	BJC1	1359	27.81	92	49.9
10	BJC2	1310	35.81	86	50.1
10	BJC1	1648	30.38	91	50.1
25	BJC1	2202	32.34	82	50.3
25	BJC2	1881	36.87	82	50.3



APS-fL Mix Properties and Dynamic Modulus Results

Report Number: RDM-12013

Page A34 of A95

Mix Details

AC/DG	14	Binder Content (%)	4.65
Aggregate Type:	Hornsfel	VMA (%)	15.7
Binder Type	Multi	Air Voids (%)	5.7
Mix Design Method	Marshall	VFB (%)	64
Filler Type		Effective Bit. Content (%)	4.3
		RAP (%)	

Gradation Percent Passing (%)

26.5mm	100	2.36mm	36
19mm	100	1.18mm	26
13.2mm	96.00	0.6mm	20
9.5mm	85.000	0.3mm	14
6.7mm	69	0.15mm	7.3
4.75mm	57	0.075mm	5.6

Dynamic Modulus Results

Frequency (Hz)	Specimen	Modulus (MPa)	Phase Angle (deg)	Strain $\mu\epsilon$	Temperature (oC)
Confinement (kPa): 0					
Target Temperature (oC) 5					
0.5	BJD3	14746	10.48	98	4.9
0.5	BJD2	14597	12.64	99	5
1	BJD2	15738	11.92	97	5
1	BJD3	15828	9.77	98	4.9
5	BJD3	18401	8.5	88	4.9
5	BJD2	18294	10.06	89	5
10	BJD2	19331	9.08	82	5
10	BJD3	19546	8.01	80	4.9
25	BJD2	20793	8.69	69	5
25	BJD3	21024	7.7	68	4.9
Target Temperature (oC) 20					
0.5	BJD2	6913	20.62	100	20.1
0.5	BJD3	6671	19.33	99	20.1
1	BJD3	7564	18.22	97	20.1
1	BJD2	7851	19.58	97	20.1
5	BJD3	9880	15.66	99	20.1
5	BJD2	10275	16.94	96	20.1
10	BJD3	10999	14.67	99	20.1
10	BJD2	11435	15.56	96	20.1
25	BJD3	12563	13.45	93	20.1
25	BJD2	13038	14.27	94	20.1
Target Temperature (oC) 35					
0.5	BJD3	2607	26	99	35.1
0.5	BJD2	2614	26.19	98	34.9
1	BJD2	3116	25.81	95	34.9

Report Date:

Monday, 21 September 2015



APS-fL Mix Properties and Dynamic Modulus Results

Report Number: RDM-12013

Page A35 of A95

1	BJD3	3124	25.61	95	35.1
5	BJD2	4629	23.93	91	34.9
5	BJD3	4629	23.7	91	35
10	BJD2	5401	23.16	91	34.9
10	BJD3	5396	22.83	92	35
25	BJD2	6556	22.29	91	34.9
25	BJD3	6552	21.75	92	34.9

Target Temperature (oC) 50

0.5	BJD2	881	30.22	99	50
0.5	BJD3	887	29.68	98	50
1	BJD3	1099	30.36	97	50
1	BJD2	1102	30.55	97	50.1
5	BJD3	1886	29.85	87	50
5	BJD2	1891	29.82	86	50
10	BJD3	2324	29.77	85	50
10	BJD2	2320	29.77	85	50.1
25	BJD2	3027	28.86	87	50.1
25	BJD3	3033	28.96	86	50

Confinement (kPa): 50

Target Temperature (oC) 35

0.5	BJD3	2652	25.98	98	34.8
0.5	BJD2	2653	26.13	98	34.6
1	BJD2	3142	25.85	95	35
1	BJD3	3143	25.58	95	35
5	BJD3	4629	23.58	92	35.1
5	BJD2	4643	23.85	91	35.2
10	BJD3	5396	22.76	93	35.2
10	BJD2	5402	23.18	92	35.3
25	BJD3	6537	21.65	92	35.2
25	BJD2	6557	22.31	90	35.4

Target Temperature (oC) 50

0.5	BJD2	1007	28.9	97	49.6
0.5	BJD3	1016	28.46	97	49.6
1	BJD2	1204	29.79	96	50
1	BJD3	1215	29.56	96	49.8
5	BJD3	1985	29.37	88	50
5	BJD2	1982	29.39	87	50.1
10	BJD2	2419	29.24	87	50.2
10	BJD3	2419	29.26	87	50
25	BJD2	3120	28.51	88	50.2
25	BJD3	3125	28.4	87	50

Confinement (kPa): 100

Target Temperature (oC) 35

0.5	BJD2	2691	26.16	98	34.7
0.5	BJD3	2681	26.3	98	34.3

APS-fL Mix Properties and Dynamic Modulus Results



Report Number: **RDM-12013**

Page A36 of A95

1	BJD2	3167	25.87	94	34.8
1	BJD3	3160	25.84	95	34.6
5	BJD3	4636	23.79	92	35
5	BJD2	4647	24.03	91	35.1
10	BJD2	5398	23.4	92	35.2
10	BJD3	5384	22.94	92	35.2
25	BJD3	6511	21.73	92	35.3
25	BJD2	6554	22.28	91	35.2

Target Temperature (oC) 50

0.5	BJD3	1145	27.29	93	48.6
0.5	BJD2	1131	27.86	96	49.3
1	BJD2	1312	28.79	95	50
1	BJD3	1308	28.66	95	49.8
5	BJD3	2058	28.89	89	50.1
5	BJD2	2069	28.76	89	50.3
10	BJD3	2482	28.87	89	50.2
10	BJD2	2494	28.65	89	50.4
25	BJD3	3165	28.08	88	50.3
25	BJD2	3175	28.01	89	50.3

Confinement (kPa): 200

Target Temperature (oC) 35

0.5	BJD2	2691	26.74	97	34.1
0.5	BJD3	2716	25.82	97	34.1
1	BJD3	3146	25.56	95	34.5
1	BJD2	3137	26.59	95	34.5
5	BJD2	4618	24.37	92	35
5	BJD3	4555	23.4	93	34.9
10	BJD2	5390	23.09	92	35.3
10	BJD3	5298	22.38	95	35.1
25	BJD3	6460	20.96	94	35.3
25	BJD2	6505	21.6	91	35.5

Target Temperature (oC) 50

0.5	BJD3	1434	24.9	99	48.4
0.5	BJD2	1314	26.92	97	48.1
1	BJD2	1498	28.09	95	49.1
1	BJD3	1633	26.08	97	49.3
5	BJD3	2348	26.62	93	49.8
5	BJD2	2241	28.19	91	49.7
10	BJD3	2754	26.73	95	50.1
10	BJD2	2671	27.9	92	49.9
25	BJD2	3351	27.19	90	50
25	BJD3	3422	26.22	91	50.3



APS-fL Mix Properties and Dynamic Modulus Results

Report Number: RDM-12017

Page A37 of A95

Mix Details

AC/DG	20	Binder Content (%)	4.40
Aggregate Type:	Hornsfel	VMA (%)	14.6
Binder Type	Multi	Air Voids (%)	4.5
Mix Design Method	Marshall	VFB (%)	69
Filler Type		Effective Bit. Content (%)	4.3
		RAP (%)	15

Gradation Percent Passing (%)

26.5mm	100	2.36mm	40
19mm	100	1.18mm	28
13.2mm	94.00	0.6mm	21
9.5mm	80.000	0.3mm	13
6.7mm	63	0.15mm	7.1
4.75mm	55	0.075mm	5.1

Dynamic Modulus Results

Frequency (Hz)	Specimen	Modulus (MPa)	Phase Angle (deg)	Strain με	Temperature (oC)
-------------------	----------	------------------	----------------------	--------------	---------------------

Confinement (kPa): 0

Target Temperature (oC) 5

0.5	BJE2	15662	8.68	98	5
0.5	BJE1	14793	8.87	98	5
1	BJE1	15671	8.36	98	5
1	BJE2	16578	8.16	96	4.9
5	BJE2	18690	7.19	87	5
5	BJE1	17706	7.43	92	5
10	BJE1	18601	7.07	85	5
10	BJE2	19554	6.86	81	5
25	BJE1	19789	6.94	73	5
25	BJE2	20701	6.55	71	5

Target Temperature (oC) 20

0.5	BJE1	8233	15.11	100	20.2
0.5	BJE2	8096	16.37	99	20.1
1	BJE2	8998	15.31	98	20.2
1	BJE1	9129	14.11	99	20.2
5	BJE2	11200	13.05	97	20.2
5	BJE1	11252	12.07	97	20.1
10	BJE2	12246	12.2	96	20.2
10	BJE1	12234	11.36	96	20.2
25	BJE2	13675	11.39	94	20.2
25	BJE1	13543	10.67	92	20.2

Target Temperature (oC) 35

0.5	BJE2	3557	23.23	99	35
0.5	BJE1	3680	22.94	98	35
1	BJE1	4257	22.16	95	35.2

Report Date:

Monday, 21 September 2015

APS-fL Mix Properties and Dynamic Modulus Results



Report Number: **RDM-12017**

Page A38 of A95

1	BJE2	4147	22.43	95	34.9
5	BJE1	5865	19.79	93	35.3
5	BJE2	5795	20.11	93	34.8
10	BJE1	6638	19.03	93	35.4
10	BJE2	6605	19.23	94	34.8
25	BJE1	7764	18.02	92	35.4
25	BJE2	7790	18.13	93	34.7

Target Temperature (oC) 50

0.5	BJE1	1429	27.92	98	49.9
0.5	BJE2	1381	28.42	97	50.3
1	BJE2	1681	28.51	95	50.1
1	BJE1	1729	27.94	95	49.9
5	BJE2	2672	26.99	90	50.1
5	BJE1	2726	26.4	89	49.8
10	BJE2	3198	26.32	91	50.1
10	BJE1	3218	25.89	89	49.8
25	BJE1	4003	24.82	91	49.8
25	BJE2	4026	25.55	92	50.1

Confinement (kPa): 50

Target Temperature (oC) 35

0.5	BJE2	3553	23.63	98	34.8
0.5	BJE1	3745	22.74	99	35.3
1	BJE1	4321	21.94	95	35.2
1	BJE2	4100	22.88	95	35
5	BJE2	5701	20.38	93	35.1
5	BJE1	5940	19.57	93	35.1
10	BJE2	6473	19.4	94	35.1
10	BJE1	6716	18.73	93	35.2
25	BJE2	7630	18.19	94	35.2
25	BJE1	7974	17.58	82	35.2

Target Temperature (oC) 50

0.5	BJE1	1519	27.38	97	49.6
0.5	BJE2	1507	27.43	97	49.6
1	BJE1	1801	27.56	94	49.9
1	BJE2	1785	27.83	95	49.9
5	BJE2	2763	26.68	91	50.1
5	BJE1	2764	26.23	89	50.1
10	BJE1	3229	25.71	91	50.2
10	BJE2	3293	26.01	91	50.2
25	BJE1	3986	24.77	92	50.2
25	BJE2	4102	24.99	92	50.2

Confinement (kPa): 100

Target Temperature (oC) 35

0.5	BJE1	3709	22.94	98	34.9
0.5	BJE2	3565	23.52	98	34.5



APS-fL Mix Properties and Dynamic Modulus Results

Report Number: RDM-12017

Page A39 of A95

1	BJE1	4246	22.17	95	35.2
1	BJE2	4092	22.75	94	34.9
5	BJE2	5654	20.15	94	35.2
5	BJE1	5815	19.72	94	35.4
10	BJE1	6570	18.85	94	35.6
10	BJE2	6429	19.29	95	35.4
25	BJE2	7582	18.08	94	35.5
25	BJE1	7649	17.79	93	35.5

Target Temperature (oC) 50

0.5	BJE2	1579	26.75	98	49
0.5	BJE1	1636	26.62	96	49.2
1	BJE1	1893	27.01	94	49.8
1	BJE2	1848	26.87	96	49.6
5	BJE2	2817	26.01	93	50
5	BJE1	2809	26	92	50.2
10	BJE2	3332	25.64	91	50.1
10	BJE1	3293	25.51	92	50.4
25	BJE2	4062	23.43	91	50.3
25	BJE1	4031	24.7	93	50.3

Confinement (kPa): 200

Target Temperature (oC) 35

0.5	BJE1	3661	22.99	98	34
0.5	BJE2	3524	23.82	97	33.8
1	BJE2	4028	23.05	95	34.3
1	BJE1	4180	22.15	96	34.4
5	BJE1	5739	19.43	95	34.8
5	BJE2	5580	20.32	94	34.8
10	BJE1	6504	18.5	96	35.1
10	BJE2	6347	19.22	95	35
25	BJE2	7481	17.87	95	35.3
25	BJE1	7624	17.34	95	35.3

Target Temperature (oC) 50

0.5	BJE2	1786	26.17	96	48.2
0.5	BJE1	1828	25.84	97	48
1	BJE1	2079	26.23	95	49.1
1	BJE2	2017	26.63	95	49.2
5	BJE2	2913	25.5	93	49.8
5	BJE1	2981	25.03	94	49.8
10	BJE2	3399	25.03	94	50.1
10	BJE1	3471	24.52	96	50.1
25	BJE1	4246	23.64	95	50.3
25	BJE2	4144	24.01	94	50.3



APS-fL Mix Properties and Dynamic Modulus Results

Report Number: RDM-12061

Page A40 of A95

Mix Details

AC/DG	14	Binder Content (%)	5.40
Aggregate Type:	Dacite	VMA (%)	15.5
Binder Type	AR450	Air Voids (%)	4.3
Mix Design Method	Gyro 120	VFB (%)	73
Filler Type	Hydrated Lime	Effective Bit. Content (%)	4.8
		RAP (%)	0

Gradation Percent Passing (%)

26.5mm	100	2.36mm	39
19mm	100	1.18mm	27
13.2mm	96.00	0.6mm	16
9.5mm	83.000	0.3mm	12
6.7mm	62	0.15mm	9
4.75mm	54	0.075mm	6.5

Dynamic Modulus Results

Frequency (Hz)	Specimen	Modulus (MPa)	Phase Angle (deg)	Strain $\mu\epsilon$	Temperature (oC)
-------------------	----------	------------------	----------------------	-------------------------	---------------------

Confinement (kPa): 0

Target Temperature (oC) 5

0.5	BJF2	17342	10.69	97	5
0.5	BJF3	15695	11.01	97	5.1
1	BJF3	16862	9.9	95	5.1
1	BJF2	18699	9.6	90	5
5	BJF2	21597	7.66	76	5
5	BJF3	19385	8.09	83	5.1
10	BJF2	22774	6.99	70	5
10	BJF3	20326	7.61	77	5.1
25	BJF3	21352	6.09	67	5.1
25	BJF2	24233	6.32	61	5

Target Temperature (oC) 20

0.5	BJF3	6054	26.84	100	19.9
0.5	BJF2	6257	27.34	100	20.2
1	BJF2	7511	24.97	97	20.2
1	BJF3	7245	24.58	96	19.9
5	BJF2	10724	19.24	96	20.1
5	BJF3	10155	18.82	96	20
10	BJF3	11492	16.76	96	20
10	BJF2	12206	17.15	95	20.1
25	BJF2	14203	15.02	91	20.1
25	BJF3	13363	14.79	92	20

Target Temperature (oC) 35

0.5	BJF2	1193	39.69	102	35.4
0.5	BJF3	1200	39.9	101	35.3
1	BJF3	1713	38.77	99	35.3

Report Date:

Monday, 21 September 2015

APS-fL Mix Properties and Dynamic Modulus Results



Report Number: **RDM-12061**

Page A41 of A95

1	BJF2	1714	38.41	100	35.5
5	BJF3	3491	34.21	89	35.3
5	BJF2	3555	33.97	89	35.4
10	BJF3	4476	32.02	90	35.2
10	BJF2	4577	31.76	90	35.4
25	BJF2	6118	28.83	88	35.3
25	BJF3	5988	29.17	89	35.2

Target Temperature (oC) 50

0.5	BJF3	220	39.1	103	50.2
0.5	BJF2-R1	190	39.33	103	49.9
0.5	BJF2	187	39.37	105	50.5
1	BJF3	320	40.71	108	50
1	BJF2-R1	273	41.26	108	49.9
1	BJF2	271	41.05	107	50.2
5	BJF3	834	41.79	82	49.9
5	BJF2	704	43.11	80	50.1
5	BJF2-R1	720	42.81	79	49.9
10	BJF2	1050	43.24	76	50
10	BJF3	1259	40.96	88	49.9
10	BJF2-R1	1075	42.85	76	50
25	BJF3	2017	39.75	81	49.8
25	BJF2-R1	1796	40.56	80	50
25	BJF2	1764	41.07	80	49.9

Confinement (kPa): 50

Target Temperature (oC) 35

0.5	BJF3	1251	39.17	100	34.9
0.5	BJF2	1258	39.4	101	35.1
1	BJF3	1749	38.41	98	35.1
1	BJF2	1781	38.64	98	35.2
5	BJF2	3634	33.85	89	35.3
5	BJF3	3515	34.45	89	35.3
10	BJF2	4621	31.88	91	35.4
10	BJF3	4470	32.17	90	35.4
25	BJF3	5931	29.24	89	35.5
25	BJF2	6165	28.96	91	35.5

Target Temperature (oC) 50

0.5	BJF2-R1	453	26.28	95	49.2
0.5	BJF2	442	27.15	98	50
0.5	BJF3	503	27.52	101	49.5
1	BJF2-R1	512	30.5	98	49.6
1	BJF2	515	30.93	96	50.1
1	BJF3	588	31.14	97	49.9
5	BJF2-R1	922	37.09	85	49.9
5	BJF2	912	37.52	86	50.2
5	BJF3	1061	37.14	86	50.1



APS-fL Mix Properties and Dynamic Modulus Results

Report Number: RDM-12061

Page A42 of A95

10	BJF2	1229	39.34	83	50.2
10	BJF2-R1	1249	38.97	82	50.1
10	BJF3	1425	38.51	84	50.1
25	BJF2	1878	39.38	84	50.2
25	BJF3	2145	38.17	94	50
25	BJF2-R1	1896	38.69	85	50.1

Confinement (kPa): 100

Target Temperature (oC) 35

0.5	BJF2	1320	38.97	100	34.6
0.5	BJF3	1289	38.5	100	34.5
1	BJF2	1834	38.23	98	34.7
1	BJF3	1789	38.13	97	34.7
5	BJF3	3500	34.29	90	35
5	BJF2	3660	34.16	90	35
10	BJF3	4423	31.83	91	35.2
10	BJF2	4657	32.13	91	35.1
25	BJF3	5836	28.65	91	35.4
25	BJF2	6174	29.02	90	35.3

Target Temperature (oC) 50

0.5	BJF2-R1	650	22	98	48.6
0.5	BJF3	640	22.96	99	48.9
0.5	BJF2	575	23.86	99	49.1
1	BJF2-R1	721	25.23	98	49.4
1	BJF2	654	27.3	98	49.7
1	BJF3	722	26.43	98	49.6
5	BJF2	1066	34	88	50
5	BJF3	1144	33.06	88	50
5	BJF2-R1	1122	32.48	88	50
10	BJF3	1455	35.29	88	50.1
10	BJF2-R1	1418	34.97	87	50.2
10	BJF2	1383	36.31	86	50.1
25	BJF3	2076	36.65	84	50.2
25	BJF2-R1	2000	36.69	85	50.3
25	BJF2	2007	37.41	83	50.3

Confinement (kPa): 200

Target Temperature (oC) 35

0.5	BJF2	1572	35.86	98	33.8
0.5	BJF3	1306	38.15	99	33.9
1	BJF3	1774	38.23	97	34.3
1	BJF2	2027	36.39	95	34.3
5	BJF2	3698	33.58	91	34.7
5	BJF3	3425	34.22	91	34.7
10	BJF2	4643	31.66	92	35
10	BJF3	4334	32.28	92	35
25	BJF2	6102	28.51	93	35.2



APS-fL Mix Properties and Dynamic Modulus Results

Report Number: RDM-12061

Page A43 of A95

25	BJF3	5754	29.06	91	35.3
Target Temperature (oC) 50					
0.5	BJF2	696	22.11	110	46.3
0.5	BJF3	754	22.95	95	47.8
0.5	BJF2-R1	833	19.29	101	47.5
1	BJF3	792	25.07	99	49
1	BJF2	835	23.86	100	49
1	BJF2-R1	926	21.67	101	48.7
5	BJF2	1240	29.61	91	49.6
5	BJF3	1213	30.68	90	49.7
5	BJF2-R1	1320	27.65	93	49.6
10	BJF2	1527	32.38	90	49.9
10	BJF3	1515	33.09	89	50
10	BJF2-R1	1601	30.27	91	49.9
25	BJF2-R1	2140	32.85	84	50.3
25	BJF2	2089	34.6	82	50.3
25	BJF3	2093	34.82	83	50.3



APS-fL Mix Properties and Dynamic Modulus Results

Report Number: RDM-12058

Page A44 of A95

Mix Details

AC/DG	20	Binder Content (%)	5.00
Aggregate Type:	Dacite	VMA (%)	15.6
Binder Type	AR450	Air Voids (%)	5.2
Mix Design Method	Gyro 120	VFB (%)	67
Filler Type		Effective Bit. Content (%)	4.5
		RAP (%)	0

Gradation Percent Passing (%)

26.5mm	100	2.36mm	34
19mm	94	1.18mm	26
13.2mm	85.00	0.6mm	18
9.5mm	76.000	0.3mm	13
6.7mm	61	0.15mm	8.5
4.75mm	55	0.075mm	6.2

Dynamic Modulus Results

Frequency (Hz)	Specimen	Modulus (MPa)	Phase Angle (deg)	Strain με	Temperature (oC)
-------------------	----------	------------------	----------------------	--------------	---------------------

Confinement (kPa): 0

Target Temperature (oC) 5

0.5	BJG1	18585	10.1	91	5
0.5	BJG2-R1	16607	11.35	97	4.9
0.5	BJG2	20393	9.78	83	5
0.5	BJG1-R1	15252	10.91	96	5.1
1	BJG1	19904	9.2	84	5
1	BJG2-R1	17778	10.45	94	4.9
1	BJG2	21674	8.88	77	5.1
1	BJG1-R1	16069	10.19	95	5.1
5	BJG2	24444	7.28	66	5.1
5	BJG1	22758	7.57	71	5
5	BJG2-R1	20404	8.89	79	4.9
5	BJG1-R1	18395	8.51	89	5.1
10	BJG2-R1	21368	8	73	4.9
10	BJG2	25514	6.72	62	5.1
10	BJG1-R1	19271	8.01	82	5.1
10	BJG1	23937	7.03	66	5
25	BJG2-R1	22603	7.23	63	5
25	BJG1	25404	6.56	57	5
25	BJG1-R1	20324	7.34	71	5.1
25	BJG2	26887	6.32	53	5.1

Target Temperature (oC) 20

0.5	BJG1	8557	22.36	96	20.1
0.5	BJG2-R1	6580	24.52	99	20.2
0.5	BJG2	8514	22.57	99	20.1
0.5	BJG-R1	6346	23.58	98	20.2

Report Date:

Monday, 21 September 2015

APS-fL Mix Properties and Dynamic Modulus Results



Report Number: **RDM-12058**

Page A45 of A95

1	BJG-R1	7344	21.97	95	20.2
1	BJG1	9965	20.79	98	20.1
1	BJG2	9920	20.91	97	20.2
1	BJG2-R1	7672	22.63	96	20.1
5	BJG2	13372	16.51	95	20.2
5	BJG1	13305	16.62	96	20.1
5	BJG-R1	9949	17.36	94	20.2
5	BJG2-R1	10553	17.8	95	20.1
10	BJG2-R1	11783	15.92	94	20.1
10	BJG2	14889	14.93	95	20.1
10	BJG1	14888	15.32	95	20.1
10	BJG-R1	11033	15.63	93	20.2
25	BJG1	17089	13.97	87	20.1
25	BJG2	16905	12.89	86	20.1
25	BJG-R1	12487	13.63	91	20.2
25	BJG2-R1	13456	13.89	90	20.1
Target Temperature (oC) 35					
0.5	BJG1-R1	1631	35.67	101	35.4
0.5	BJG2	2172	35.54	101	35.5
0.5	BJG1-R1	1631	35.67	101	35.4
0.5	BJG1-R1	1639	36.41	101	35.3
0.5	BJG1	2120	34.69	100	35.3
0.5	BJG1-R1	1639	36.41	101	35.3
1	BJG1-R1	2245	35	97	35.1
1	BJG1-R1	2219	34.39	98	35.2
1	BJG1-R1	2245	35	97	35.1
1	BJG1	2858	33.47	97	35.3
1	BJG2	2900	34.27	97	35.5
1	BJG1-R1	2219	34.39	98	35.2
5	BJG1-R1	4188	30.27	91	35.1
5	BJG1-R1	4083	29.98	91	35.1
5	BJG1-R1	4188	30.27	91	35.1
5	BJG2	5143	29.68	92	35.4
5	BJG1-R1	4083	29.98	91	35.1
5	BJG1	5139	29.04	91	35.2
10	BJG2	6311	27.66	93	35.4
10	BJG1-R1	5081	27.98	91	35.1
10	BJG1-R1	5216	28.32	91	35
10	BJG1-R1	5081	27.98	91	35.1
10	BJG1-R1	5216	28.32	91	35
10	BJG1	6331	27.03	97	35.2
25	BJG2	8069	25.39	93	35.3
25	BJG1	7976	25.05	90	35.2
25	BJG1-R1	6684	25.77	92	35
25	BJG1-R1	6684	25.77	92	35

APS-fL Mix Properties and Dynamic Modulus Results



Report Number: **RDM-12058**

Page A46 of A95

25	BJG1-R1	6527	25.76	90	35
25	BJG1-R1	6527	25.76	90	35
Target Temperature (oC) 50					
0.5	BJG1	345	40.19	103	50.1
0.5	BJG2	402	37.35	102	50.1
0.5	BJG1-R1	276	39.6	103	50.2
0.5	BJG2-R1	282	38.75	103	50.2
1	BJG1-R1	403	40.6	105	50.2
1	BJG2	561	38.85	103	50.1
1	BJG2-R1	405	40.15	105	50.2
1	BJG1	503	40.93	107	50.1
5	BJG2	1300	39.25	85	50.1
5	BJG1-R1	992	40.54	83	50.2
5	BJG2-R1	987	40.57	83	50.2
5	BJG1	1249	40	85	50.2
10	BJG1-R1	1417	39.97	80	50.2
10	BJG2	1830	38.86	82	50
10	BJG1	1790	39.03	83	50.2
10	BJG2-R1	1415	40.14	80	50.1
25	BJG1-R1	2205	38.47	81	50.2
25	BJG2-R1	2215	38	82	50.1
25	BJG2	2757	36.77	83	50
25	BJG1	2750	36.85	86	50.2

Confinement (kPa): 50

Target Temperature (oC) 35

0.5	BJG1-R1	1717	35.44	100	34.9
0.5	BJG1	2218	34.4	100	34.9
0.5	BJG1-R1	1710	35.57	100	34.8
0.5	BJG2	2266	34.57	100	34.9
0.5	BJG1-R1	1717	35.44	100	34.9
0.5	BJG1-R1	1710	35.57	100	34.8
1	BJG1	2940	33.64	96	35
1	BJG1-R1	2298	34.72	97	35
1	BJG1-R1	2297	34.63	97	35.1
1	BJG1-R1	2297	34.63	97	35.1
1	BJG2	2978	33.79	96	35
1	BJG1-R1	2298	34.72	97	35
5	BJG2	5211	29.39	91	35.2
5	BJG1-R1	4192	30.43	91	35.3
5	BJG1-R1	4192	30.43	91	35.3
5	BJG1-R1	4141	30.65	91	35.1
5	BJG1-R1	4141	30.65	91	35.1
5	BJG1	5190	29.43	91	35.1
10	BJG1-R1	5093	28.75	91	35.2
10	BJG2	6319	27.48	93	35.3

Report Date:

Monday, 21 September 2015



APS-fL Mix Properties and Dynamic Modulus Results

Report Number: RDM-12058

Page A47 of A95

10	BJG1-R1	5093	28.75	91	35.2
10	BJG1-R1	5193	28.64	92	35.4
10	BJG1-R1	5193	28.64	92	35.4
10	BJG1	6320	27.49	92	35.2
25	BJG1	7970	25.1	92	35.2
25	BJG1-R1	6662	26.2	91	35.4
25	BJG1-R1	6458	25.86	91	35.3
25	BJG2	7964	25.09	94	35.3
25	BJG1-R1	6662	26.2	91	35.4
25	BJG1-R1	6458	25.86	91	35.3

Target Temperature (oC) 50

0.5	BJG1	492	35.41	100	49.6
0.5	BJG2	620	29.92	99	49.7
0.5	BJG1-R1	430	32.65	99	49.8
0.5	BJG2-R1	523	29.03	98	49.7
1	BJG2-R1	632	32.25	97	50
1	BJG1	646	37.35	100	49.9
1	BJG1-R1	550	35.18	98	50
1	BJG2	762	33.11	97	50
5	BJG1-R1	1125	37.99	86	50.2
5	BJG2-R1	1174	36.54	87	50.2
5	BJG2	1428	36.72	88	50.2
5	BJG1	1398	38.08	87	50.1
10	BJG1	1940	37.81	85	50.2
10	BJG2-R1	1584	37.19	85	50.3
10	BJG2	1929	36.93	87	50.3
10	BJG1-R1	1550	37.94	84	50.3
25	BJG2	2825	36.13	85	50.3
25	BJG1-R1	2325	36.29	85	50.3
25	BJG1	2893	36.01	88	50.2
25	BJG2-R1	2337	36.44	86	50.3

Confinement (kPa): 100

Target Temperature (oC) 35

0.5	BJG2	2360	33.56	98	34.6
0.5	BJG1-R1	1822	34.43	99	34.7
0.5	BJG1-R1	1824	35.89	105	34.3
0.5	BJG1-R1	1824	35.89	105	34.3
0.5	BJG1-R1	1822	34.43	99	34.7
0.5	BJG1	2335	34.4	99	34.6
1	BJG1	3043	33.64	96	34.8
1	BJG1-R1	2374	34.18	96	34.9
1	BJG1-R1	2374	34.18	96	34.9
1	BJG1-R1	2382	34.31	97	34.9
1	BJG2	3022	33.12	96	34.8
1	BJG1-R1	2382	34.31	97	34.9



APS-fL Mix Properties and Dynamic Modulus Results

Report Number: **RDM-12058**

Page A48 of A95

5	BJG1-R1	4243	30.17	92	35.1
5	BJG1-R1	4243	30.17	92	35.1
5	BJG1-R1	4238	30.33	92	35.1
5	BJG1	5277	29.55	92	35.1
5	BJG2	5189	29.12	93	35.1
5	BJG1-R1	4238	30.33	92	35.1
10	BJG1-R1	5244	28.11	92	35.2
10	BJG1-R1	5244	28.11	92	35.2
10	BJG1	6427	27.55	93	35.3
10	BJG1-R1	5225	28.28	92	35.3
10	BJG1-R1	5225	28.28	92	35.3
10	BJG2	6369	27.55	94	35.3
25	BJG1-R1	6652	25.65	93	35.4
25	BJG1-R1	6652	25.65	93	35.4
25	BJG2	8091	24.96	93	35.4
25	BJG1-R1	6687	25.38	90	35.4
25	BJG1-R1	6687	25.38	90	35.4
25	BJG1	8067	25.02	91	35.3

Target Temperature (oC) 50

0.5	BJG1-R1	586	28.6	99	49.3
0.5	BJG2-R1	704	25.1	99	49.1
0.5	BJG1	603	32.91	100	49
0.5	BJG2	782	26.33	99	49.1
1	BJG1	768	35	99	49.7
1	BJG2	924	29.31	97	49.8
1	BJG2-R1	824	28.17	97	49.8
1	BJG1-R1	711	31.6	97	49.9
5	BJG1	1539	36.68	88	50.1
5	BJG2	1569	34	89	50.2
5	BJG1-R1	1287	35.54	88	50.3
5	BJG2-R1	1370	33.34	90	50.2
10	BJG1-R1	1711	36.28	86	50.4
10	BJG2	2034	34.9	88	50.4
10	BJG2-R1	1767	34.79	88	50.3
10	BJG1	2084	36.59	87	50.3
25	BJG1	3020	35.29	88	50.4
25	BJG1-R1	2471	35.58	85	50.5
25	BJG2	2865	34.71	88	50.4
25	BJG2-R1	2492	35.06	87	50.4

Confinement (kPa): 200

Target Temperature (oC) 35

0.5	BJG2	2514	32.51	98	33.9
0.5	BJG1-R1	1924	33.51	98	34
0.5	BJG1-R1	1924	33.51	98	34
0.5	BJG1	2439	33.89	99	33.7



APS-fL Mix Properties and Dynamic Modulus Results

Report Number: **RDM-12058**

Page A49 of A95

0.5	BJG1-R1	1970	33.8	98	33.9
0.5	BJG1-R1	1970	33.8	98	33.9
1	BJG1-R1	2413	33.81	95	34.5
1	BJG1-R1	2471	33.84	96	34.4
1	BJG1-R1	2471	33.84	96	34.4
1	BJG2	3151	32.62	96	34.4
1	BJG1-R1	2413	33.81	95	34.5
1	BJG1	3109	33.79	95	34.3
5	BJG1	5250	29.64	93	34.8
5	BJG1-R1	4151	30.4	93	34.8
5	BJG1-R1	4151	30.4	93	34.8
5	BJG1-R1	4212	29.87	93	34.8
5	BJG2	5315	29.06	94	34.8
5	BJG1-R1	4212	29.87	93	34.8
10	BJG1-R1	5177	27.69	93	35.1
10	BJG1-R1	5103	28.5	94	35.1
10	BJG1-R1	5103	28.5	94	35.1
10	BJG1-R1	5177	27.69	93	35.1
10	BJG1	6373	27.45	94	35.1
10	BJG2	6525	27.21	94	35
25	BJG1	8035	24.47	93	35.3
25	BJG1-R1	6529	25.54	95	35.3
25	BJG1-R1	6565	24.77	93	35.3
25	BJG2	8244	24.35	94	35.3
25	BJG1-R1	6529	25.54	95	35.3
25	BJG1-R1	6565	24.77	93	35.3

Target Temperature (oC) 50

0.5	BJG2	1025	23.03	100	47.9
0.5	BJG1-R1	908	24.32	100	48.1
0.5	BJG1	828	28.74	100	48
0.5	BJG2-R1	956	22.68	99	48.1
1	BJG2-R1	1074	25.26	98	49.2
1	BJG1-R1	1051	26.58	98	49.2
1	BJG1	1008	30.8	98	49.1
1	BJG2	1174	25.44	98	49
5	BJG2-R1	1612	29.93	92	49.8
5	BJG2	1785	30.04	92	49.7
5	BJG1-R1	1624	30.64	92	49.8
5	BJG1	1784	33.32	90	49.8
10	BJG2-R1	1988	31.74	92	50.1
10	BJG2	2212	31.75	93	50
10	BJG1-R1	2016	32.17	92	50.1
10	BJG1	2319	33.86	90	50.1
25	BJG2-R1	2672	32.68	89	50.3
25	BJG1	3254	33.57	90	50.3



APS-fL Mix Properties and Dynamic Modulus Results

Report Number: **RDM-12058**

Page A50 of A95

25	BJG1-R1	2722	32.6	89	50.3
25	BJG2	2987	32.49	90	50.3



APS-fL Mix Properties and Dynamic Modulus Results

Report Number: RDM-12051

Page A51 of A95

Mix Details

AC/DG	14	Binder Content (%)	4.70
Aggregate Type:	Limeston over dolomit	VMA (%)	14.6
Binder Type	C320	Air Voids (%)	4.5
Mix Design Method	Gyro 80	VFB (%)	69
Filler Type	Bag House Dust	Effective Bit. Content (%)	4.3
		RAP (%)	0

Gradation Percent Passing (%)

26.5mm	100	2.36mm	35
19mm	100	1.18mm	27
13.2mm	91.00	0.6mm	20
9.5mm	73.000	0.3mm	13
6.7mm	62	0.15mm	6
4.75mm	48	0.075mm	4.3

Dynamic Modulus Results

Frequency (Hz)	Specimen	Modulus (MPa)	Phase Angle (deg)	Strain $\mu\epsilon$	Temperature (oC)
-------------------	----------	------------------	----------------------	-------------------------	---------------------

Confinement (kPa): 0

Target Temperature (oC) 5

0.5	BJH3	17284	10.37	97	5
0.5	BJH2	16600	10.85	98	4.9
0.5	BJH1	16817	10.48	97	5.2
1	BJH2	17785	9.77	95	4.9
1	BJH1	18060	9.39	93	5.1
1	BJH3	18521	9.38	90	5
5	BJH3	21082	7.71	77	5
5	BJH2	20352	7.74	80	4.9
5	BJH1	20594	7.55	78	5.2
10	BJH1	21651	7	72	5.2
10	BJH3	22106	7.11	71	5
10	BJH2	21349	7.04	74	4.9
25	BJH2	22630	6.33	65	4.9
25	BJH3	23353	6.64	62	5
25	BJH1	22998	6.51	62	5.2

Target Temperature (oC) 20

0.5	BJH1	7098	24.28	99	20.2
0.5	BJH3	7463	24.16	98	20.1
0.5	BJH2	7113	24.69	98	20.1
1	BJH1	8264	22.25	96	20.2
1	BJH2	8254	22.67	96	20.1
1	BJH3	8682	22.12	96	20
5	BJH2	11335	17.61	95	20.1
5	BJH3	11773	17.21	95	20
5	BJH1	11294	17.27	95	20.2

Report Date:

Monday, 21 September 2015



APS-fL Mix Properties and Dynamic Modulus Results

Report Number: **RDM-12051**

Page A52 of A95

10	BJH2	12646	15.57	93	20.1
10	BJH1	12618	15.46	95	20.2
10	BJH3	13135	15.27	97	20
25	BJH3	14979	13.32	88	20
25	BJH1	14477	13.47	90	20.2
25	BJH2	14368	13.47	89	20.1

Target Temperature (oC) 35

0.5	BJH3	1920	35.75	100	35.3
0.5	BJH2	1854	36.19	101	35.2
0.5	BJH1	1925	35.63	100	35.4
1	BJH1	2628	34.29	97	35.4
1	BJH3	2611	34.24	97	35.3
1	BJH2	2560	34.7	97	35.1
5	BJH2	4775	30.29	90	35
5	BJH1	4858	29.83	90	35.2
5	BJH3	4787	29.82	90	35.2
10	BJH3	5914	28.07	90	35.2
10	BJH2	5948	28.58	90	35
10	BJH1	6023	28.16	90	35.2
25	BJH3	7496	25.85	90	35.2
25	BJH2	7590	26.24	89	35
25	BJH1	7661	25.79	90	35.1

Target Temperature (oC) 50

0.5	BJH1	338	38.81	102	50.2
0.5	BJH3	325	38.83	102	50.2
0.5	BJH2	326	40.17	103	50.3
1	BJH3	472	39.91	105	50.2
1	BJH2	488	40.46	106	50.2
1	BJH1	493	39.63	105	50.2
5	BJH2	1244	39.91	84	50.2
5	BJH3	1174	39.7	84	50.1
5	BJH1	1216	39.57	84	50.2
10	BJH2	1788	39.39	81	50.1
10	BJH1	1743	39.14	82	50.2
10	BJH3	1686	39.42	81	50.1
25	BJH3	2620	37.5	83	50.1
25	BJH1	2713	37.15	83	50.2
25	BJH2	2768	37.56	83	50.1

Confinement (kPa): 50

Target Temperature (oC) 35

0.5	BJH2	2027	34.29	99	35
0.5	BJH1	2087	34.01	99	35.1
0.5	BJH3	2076	33.85	99	35
1	BJH2	2681	33.66	96	35.1
1	BJH1	2753	33.36	97	35.2

APS-fL Mix Properties and Dynamic Modulus Results



Report Number: **RDM-12051**

Page A53 of A95

1	BJH3	2726	33.36	96	35
5	BJH3	4870	29.8	91	35.1
5	BJH2	4847	30	90	35.2
5	BJH1	4944	29.62	91	35.3
10	BJH2	5955	28.42	90	35.2
10	BJH3	5986	28.41	91	35.2
10	BJH1	6078	28.13	91	35.3
25	BJH2	7531	26.2	91	35.3
25	BJH1	7710	25.87	91	35.3
25	BJH3	7578	26.44	90	35.2

Target Temperature (oC) 50

0.5	BJH1	690	28.6	98	49.7
0.5	BJH3	666	28.05	98	49.7
0.5	BJH2	691	28.92	98	49.7
1	BJH1	821	31.86	96	50
1	BJH2	828	32.31	95	50
1	BJH3	795	31.38	96	49.9
5	BJH1	1486	35.85	88	50.2
5	BJH3	1439	35.39	88	50.1
5	BJH2	1525	36.11	87	50.2
10	BJH3	1924	36.11	86	50.2
10	BJH2	2044	36.58	86	50.3
10	BJH1	1987	36.48	86	50.2
25	BJH3	2817	35.5	86	50.3
25	BJH1	2903	35.63	86	50.3
25	BJH2	2978	35.82	86	50.3

Confinement (kPa): 100

Target Temperature (oC) 35

0.5	BJH2	2198	32.56	98	34.6
0.5	BJH3	2252	32.94	97	34.6
0.5	BJH1	2275	32.71	98	34.7
1	BJH3	2840	33.11	94	34.8
1	BJH1	2885	32.9	95	35
1	BJH2	2784	32.98	95	34.9
5	BJH3	4897	29.97	91	35.2
5	BJH2	4857	30.04	91	35.2
5	BJH1	5000	29.7	91	35.2
10	BJH2	5938	28.56	91	35.3
10	BJH1	6098	28.2	92	35.3
10	BJH3	5915	28.42	92	35.4
25	BJH1	7683	25.84	90	35.3
25	BJH3	7458	26.07	91	35.4
25	BJH2	7450	26.24	92	35.4

Target Temperature (oC) 50

0.5	BJH3	908	24.14	99	49.3
-----	------	-----	-------	----	------



APS-fL Mix Properties and Dynamic Modulus Results

Report Number: **RDM-12051**

Page A54 of A95

0.5	BJH2	956	25.06	99	49.3
0.5	BJH1	933	24.67	102	48.7
1	BJH3	1044	27.29	97	49.8
1	BJH2	1103	28.25	96	49.9
1	BJH1	1073	27.35	96	49.7
5	BJH3	1690	32.16	90	50.2
5	BJH2	1804	33.08	90	50.3
5	BJH1	1718	32.55	90	50.1
10	BJH1	2177	33.9	90	50.2
10	BJH2	2310	34.3	89	50.4
10	BJH3	2163	33.73	98	50.3
25	BJH3	3014	33.92	87	50.4
25	BJH1	3023	34.2	87	50.4
25	BJH2	3214	34.44	88	50.5

Confinement (kPa): 200

Target Temperature (oC) 35

0.5	BJH3	2454	32.53	97	33.8
0.5	BJH2	2462	30.8	97	34
0.5	BJH1	2456	32.3	96	33.7
1	BJH1	2957	32.88	94	34.4
1	BJH3	2978	32.97	94	34.3
1	BJH2	2971	31.64	94	34.4
5	BJH1	4867	30.03	92	34.9
5	BJH2	4866	29.35	93	34.8
5	BJH3	4907	29.94	92	34.8
10	BJH1	5919	28.53	94	35.1
10	BJH2	5935	27.76	93	35.1
10	BJH3	5937	28.32	93	35
25	BJH1	7504	25.73	92	35.3
25	BJH2	7459	25.16	93	35.3
25	BJH3	7477	25.53	92	35.3

Target Temperature (oC) 50

0.5	BJH3	1249	21.18	99	48.2
0.5	BJH1	1274	21.16	99	48
0.5	BJH2	1346	22.05	99	48.5
1	BJH3	1392	23.8	99	49.2
1	BJH1	1414	23.61	99	49.1
1	BJH2	1511	24.5	99	49.3
5	BJH3	2034	28.25	93	49.8
5	BJH2	2238	28.82	93	49.9
5	BJH1	2039	28.01	93	49.8
10	BJH3	2472	30.16	93	50.1
10	BJH1	2456	30.11	94	50
10	BJH2	2733	30.58	93	50.1
25	BJH1	3231	31.46	89	50.3

Report Date:

Monday, 21 September 2015



APS-fL Mix Properties and Dynamic Modulus Results

Report Number: RDM-12051

Page A55 of A95

25	BJH3	3266	31.26	89	50.3
25	BJH2	3613	31.41	90	50.3



APS-fL Mix Properties and Dynamic Modulus Results

Report Number: RDM-12054

Page A56 of A95

Mix Details

AC/DG	20	Binder Content (%)	4.50
Aggregate Type:	Granite	VMA (%)	14.2
Binder Type	C320	Air Voids (%)	3.8
Mix Design Method	Marshall 75	VFB (%)	73
Filler Type		Effective Bit. Content (%)	4.4
		RAP (%)	0

Gradation Percent Passing (%)

26.5mm	100	2.36mm	33
19mm	99	1.18mm	23
13.2mm	79.00	0.6mm	17
9.5mm	61.000	0.3mm	12
6.7mm	52	0.15mm	8
4.75mm	44	0.075mm	4.3

Dynamic Modulus Results

Frequency (Hz)	Specimen	Modulus (MPa)	Phase Angle (deg)	Strain με	Temperature (oC)
-------------------	----------	------------------	----------------------	--------------	---------------------

Confinement (kPa): 0

Target Temperature (oC) 5

0.5	BJI3	14127	11.87	98	5
0.5	BJI2	14062	14.7	98	5.1
1	BJI2	15311	13.56	100	5.1
1	BJI3	15326	10.94	96	5
5	BJI3	18041	9.17	91	5
5	BJI2	18373	11.42	87	5.2
10	BJI2	19770	10.91	79	5.2
10	BJI3	19162	8.55	83	5
25	BJI2	21562	10.15	66	5.2
25	BJI3	20606	7.91	71	5

Target Temperature (oC) 20

0.5	BJI2	5792	24.69	98	20.3
0.5	BJI3	5770	24.11	98	20.1
1	BJI3	6659	22.69	95	20
1	BJI2	6752	23.55	96	20.2
5	BJI3	9143	18.79	94	20
5	BJI2	9399	19.53	94	20.2
10	BJI3	10298	17.15	94	20
10	BJI2	10660	18.07	95	20.1
25	BJI3	11876	15.47	93	20
25	BJI2	12459	16.29	92	20.1

Target Temperature (oC) 35

0.5	BJI3	1548	32.47	100	35.2
0.5	BJI2	1562	32.67	100	35
1	BJI2	2064	32.22	96	34.9

Report Date:

Monday, 21 September 2015

APS-fL Mix Properties and Dynamic Modulus Results



Report Number: **RDM-12054**

Page A57 of A95

1	BJI3	2050	31.85	97	35.2
5	BJI2	3671	29.85	88	34.9
5	BJI3	3667	29.25	88	35.2
10	BJI2	4505	28.89	88	35
10	BJI3	4521	28.14	87	35.2
25	BJI2	5743	27.66	88	35
25	BJI3	5763	26.45	87	35.1

Target Temperature (oC) 50

0.5	BJI2	323	33.41	102	50.2
0.5	BJI3	302	34.78	102	50
1	BJI3	422	35.49	103	50
1	BJI2	446	34.57	104	50.3
5	BJI3	939	36.08	81	50
5	BJI2	944	36.32	77	50.3
10	BJI3	1293	36.36	78	50
10	BJI2	1347	36.06	78	50.3
25	BJI2	2055	34.78	81	50.3
25	BJI3	1987	34.76	84	50

Confinement (kPa): 50

Target Temperature (oC) 35

0.5	BJI3	1667	30.94	98	34.8
0.5	BJI2	1685	32.06	91	34.5
1	BJI2	2149	31.8	96	34.8
1	BJI3	2115	31.33	96	34.9
5	BJI3	3666	29.5	89	35.1
5	BJI2	3731	29.36	89	35
10	BJI3	4467	28.6	88	35.2
10	BJI2	4549	28.51	89	35.1
25	BJI3	5613	26.95	88	35.2
25	BJI2	5764	27.03	89	35.1

Target Temperature (oC) 50

0.5	BJI2	647	25.13	98	49.8
0.5	BJI3	636	24.65	98	49.5
1	BJI2	746	27.8	96	50.1
1	BJI3	735	27.3	96	49.9
5	BJI3	1208	31.25	87	50.1
5	BJI2	1219	31.64	87	50.3
10	BJI2	1547	33.04	84	50.4
10	BJI3	1534	32.67	84	50.2
25	BJI2	2178	33.16	84	50.4
25	BJI3	2150	33.02	85	50.1

Confinement (kPa): 100

Target Temperature (oC) 35

0.5	BJI2	1851	29.99	98	34.3
0.5	BJI3	1886	29.03	98	34.4

APS-fL Mix Properties and Dynamic Modulus Results



Report Number: **RDM-12054**

Page A58 of A95

1	BJI2	2296	30.4	95	34.7
1	BJI3	2320	29.71	95	34.8
5	BJI3	3847	28.41	90	35
5	BJI2	3827	28.61	90	35.1
10	BJI2	4622	27.96	90	35.2
10	BJI3	4663	27.55	90	35.1
25	BJI3	5839	26.02	89	35.2
25	BJI2	5802	26.56	90	35.3

Target Temperature (oC) 50

0.5	BJI3	840	21.51	99	49.1
0.5	BJI2	864	22.04	98	49.4
1	BJI2	965	24.54	97	50.1
1	BJI3	957	23.84	98	49.8
5	BJI3	1434	27.98	90	50.2
5	BJI2	1429	28.7	90	50.5
10	BJI3	1750	29.77	88	50.4
10	BJI2	1742	30.48	88	50.6
25	BJI3	2313	31.08	85	50.4
25	BJI2	2299	31.82	84	50.6

Confinement (kPa): 200

Target Temperature (oC) 35

0.5	BJI2	2030	29.14	98	33.6
0.5	BJI3	2056	28.57	97	34.3
1	BJI3	2441	29.28	95	34.6
1	BJI2	2438	29.68	95	34.3
5	BJI2	3853	28.06	92	34.8
5	BJI3	3833	28.02	92	35
10	BJI2	4626	27.27	93	35
10	BJI3	4615	27.36	92	35.2
25	BJI3	5782	25.78	91	35.4
25	BJI2	5840	25.71	93	35.3

Target Temperature (oC) 50

0.5	BJI3	1135	18.79	100	47.8
0.5	BJI2	1148	20.46	98	48.1
1	BJI2	1229	22.49	100	49.1
1	BJI3	1267	20.69	99	49
5	BJI3	1749	24.24	93	49.7
5	BJI2	1740	25.84	93	49.8
10	BJI3	2054	26.15	94	50
10	BJI2	2070	27.47	93	50
25	BJI2	2646	28.64	87	50.3
25	BJI3	2591	27.62	88	50.3



APS-fL Mix Properties and Dynamic Modulus Results

Report Number: RDM-12062

Page A59 of A95

Mix Details

AC/DG	14	Binder Content (%)	5.10
Aggregate Type:	Basalt	VMA (%)	15.5
Binder Type	AR450	Air Voids (%)	4.2
Mix Design Method	Gryo 120	VFB (%)	73
Filler Type	Hydrated Lime	Effective Bit. Content (%)	4.9
		RAP (%)	15

Gradation Percent Passing (%)

26.5mm	100	2.36mm	39
19mm	100	1.18mm	31
13.2mm	98.00	0.6mm	24
9.5mm	88.000	0.3mm	14
6.7mm	72	0.15mm	7.6
4.75mm	59	0.075mm	5.1

Dynamic Modulus Results

Frequency (Hz)	Specimen	Modulus (MPa)	Phase Angle (deg)	Strain $\mu\epsilon$	Temperature (oC)
----------------	----------	---------------	-------------------	----------------------	------------------

Confinement (kPa): 0

Target Temperature (oC) 5

0.5	BJJ3	17964	8.41	94	5.1
0.5	BJJ2	16545	10.17	99	5.1
1	BJJ2	17313	9.39	97	5.1
1	BJJ3	18999	7.71	88	5
5	BJJ3	21276	6.43	76	5
5	BJJ2	20257	7.87	61	5.1
10	BJJ2	20588	7.11	77	5.1
10	BJJ3	22200	5.96	71	5
25	BJJ2	21797	6.58	66	5
25	BJJ3	23409	5.72	62	5

Target Temperature (oC) 20

0.5	BJJ2	7912	20.73	100	20.3
0.5	BJJ3	8447	19.89	100	20
1	BJJ3	9695	18.3	99	20.1
1	BJJ2	9068	18.93	98	20.2
5	BJJ3	12581	14.62	97	20.1
5	BJJ2	11788	15.01	96	20.1
10	BJJ3	13817	13.11	96	20.2
10	BJJ2	12948	13.58	96	20.1
25	BJJ3	15500	11.46	90	20.2
25	BJJ2	14572	12.08	92	20

Target Temperature (oC) 35

0.5	BJJ3	2366	34.28	100	35.1
0.5	BJJ2	2378	34.31	100	35.2
1	BJJ2	3097	32.93	96	35.2

Report Date:

Monday, 21 September 2015

APS-fL Mix Properties and Dynamic Modulus Results



Report Number: **RDM-12062**

Page A60 of A95

1	BJJ3	3091	32.63	96	35.1
5	BJJ2	5176	28.03	99	35.1
5	BJJ3	5206	27.5	92	35.1
10	BJJ2	6184	26.51	93	35.1
10	BJJ3	6233	25.77	94	35.1
25	BJJ2	7656	24.41	94	35.1
25	BJJ3	7772	23.72	95	35

Target Temperature (oC) 50

0.5	BJJ2	362	41.6	103	50.1
0.5	BJJ3	382	41.24	103	50.4
1	BJJ3	560	41.31	103	50.3
1	BJJ2	536	41.62	104	50
5	BJJ3	1334	39.61	86	50.3
5	BJJ2	1285	39.72	84	50.1
10	BJJ3	1868	38.47	84	50.3
10	BJJ2	1785	38.88	83	50.1
25	BJJ2	2652	36.72	85	50.1
25	BJJ3	2798	35.89	86	50.2

Confinement (kPa): 50

Target Temperature (oC) 35

0.5	BJJ3	2458	34.06	99	34.8
0.5	BJJ2	2482	34.51	99	35
1	BJJ2	3186	33.08	96	35.1
1	BJJ3	3159	32.57	96	34.9
5	BJJ3	5250	27.82	93	35
5	BJJ2	5244	28.24	92	35.3
10	BJJ3	6290	25.85	93	35.1
10	BJJ2	6222	26.25	94	35.4
25	BJJ3	7754	23.39	95	35.1
25	BJJ2	7725	23.82	94	35.3

Target Temperature (oC) 50

0.5	BJJ2	446	38.21	100	49.5
0.5	BJJ3	598	32.3	98	49.8
1	BJJ2	608	39.49	99	49.8
1	BJJ3	751	35.08	97	50
5	BJJ3	1482	37.04	88	50.2
5	BJJ2	1336	38.94	87	50.1
10	BJJ2	1841	38.28	86	50.1
10	BJJ3	2001	36.76	87	50.3
25	BJJ2	2714	36.22	87	50.2
25	BJJ3	2887	35.04	88	50.3

Confinement (kPa): 100

Target Temperature (oC) 35

0.5	BJJ2	2575	34.31	99	34.5
0.5	BJJ3	2517	33.68	98	34.3



APS-fL Mix Properties and Dynamic Modulus Results

Report Number: RDM-12062

Page A61 of A95

1	BJJ2	3283	32.71	96	34.9
1	BJJ3	3171	32.48	95	34.8
5	BJJ3	5188	27.67	93	35.1
5	BJJ2	5345	27.62	93	35.1
10	BJJ2	6366	25.7	94	35.2
10	BJJ3	6194	25.74	94	35.3
25	BJJ3	7638	22.97	95	35.3
25	BJJ2	7848	23.11	94	35.3

Target Temperature (oC) 50

0.5	BJJ3	767	28.25	98	49.4
0.5	BJJ2	536	35.53	102	49.2
1	BJJ2	723	36.99	87	49.8
1	BJJ3	920	31.26	96	50
5	BJJ3	1641	34.58	98	50.3
5	BJJ2	1456	38.04	74	50.2
10	BJJ3	2132	35.04	90	50.5
10	BJJ2	1965	37.48	71	50.3
25	BJJ3	2996	33.98	90	50.5
25	BJJ2	2866	35.55	59	50.4

Confinement (kPa): 200

Target Temperature (oC) 35

0.5	BJJ2	2660	33.42	99	33.8
0.5	BJJ3	2529	32.84	98	33.7
1	BJJ3	3136	31.99	95	34.3
1	BJJ2	3338	31.62	96	34.5
5	BJJ2	5367	26.44	94	34.9
5	BJJ3	5085	27.64	94	34.8
10	BJJ2	6355	24.35	95	35.1
10	BJJ3	6068	25.62	95	35
25	BJJ3	7553	22.45	95	35.3
25	BJJ2	7791	21.81	95	35.3

Target Temperature (oC) 50

0.5	BJJ3	980	25.53	100	48.4
0.5	BJJ2	863	27.96	102	48.2
1	BJJ2	1067	29.72	98	49.2
1	BJJ3	1152	28.18	98	49.3
5	BJJ3	1847	31.21	92	49.9
5	BJJ2	1761	32.47	92	49.8
10	BJJ3	2319	32.21	93	50.1
10	BJJ2	2226	33.07	92	50.1
25	BJJ2	3028	32.52	91	50.3
25	BJJ3	3156	31.65	92	50.3



APS-FL Mix Properties and Dynamic Modulus Results

Report Number: RDM-12072

Page A62 of A95

Mix Details

AC/DG	14	Binder Content (%)	4.80
Aggregate Type:	Dolmanite	VMA (%)	14.5
Binder Type	C320	Air Voids (%)	4.5
Mix Design Method	Gryo 80	VFB (%)	69
Filler Type	Bag House Dust	Effective Bit. Content (%)	4.3
		RAP (%)	15

Gradation Percent Passing (%)

26.5mm	100	2.36mm	36
19mm	100	1.18mm	27
13.2mm	88.00	0.6mm	19
9.5mm	74.000	0.3mm	11.3
6.7mm	64	0.15mm	6.4
4.75mm	51	0.075mm	4.8

Dynamic Modulus Results

Frequency (Hz)	Specimen	Modulus (MPa)	Phase Angle (deg)	Strain με	Temperature (oC)
-------------------	----------	------------------	----------------------	--------------	---------------------

Confinement (kPa): 0

Target Temperature (oC) 5

0.5	BJK1	19351	11.81	87	5.1
0.5	BJK2	17865	11.15	94	5
0.5	BJK3	17736	12.81	95	4.9
1	BJK1	20763	10.35	81	5.1
1	BJK2	19239	10.01	87	5.1
1	BJK3	19185	11.12	87	4.9
5	BJK2	22034	7.96	74	5.1
5	BJK1	23837	8.29	68	5.1
5	BJK3	22453	8.53	72	4.9
10	BJK1	25019	7.42	63	5.1
10	BJK2	23151	7.26	68	5.1
10	BJK3	23699	7.73	66	4.9
25	BJK2	24535	6.83	59	5.1
25	BJK1	26571	6.48	55	5.1
25	BJK3	25200	6.91	57	4.9

Target Temperature (oC) 20

0.5	BJK3	7414	26.8	98	20.1
0.5	BJK2	7161	26.42	99	20
1	BJK2	8498	24.16	97	19.9
1	BJK3	8812	24.52	97	20.1
5	BJK2	11924	18.44	95	19.9
5	BJK3	12603	18.99	96	20.1
10	BJK1	17162	13.46	46	20.1
10	BJK2	13395	16.67	94	19.9
10	BJK3	14308	17.01	94	20.1

Report Date:

Monday, 21 September 2015

APS-fL Mix Properties and Dynamic Modulus Results



Report Number: **RDM-12072**

Page A63 of A95

25	BJK2	15462	14.44	89	20
25	BJK1	17352	13.74	85	20.1
25	BJK3	16554	14.73	87	20.1

Target Temperature (oC) 35

0.5	BJK3	1373	40.1	101	35
0.5	BJK2	1319	39.82	101	35
0.5	BJK1	1512	38.97	102	35.1
1	BJK2	1898	38.86	98	35.1
1	BJK3	1994	38.88	99	34.9
1	BJK1	2186	37.65	98	35.1
5	BJK1	4500	32.86	90	35.2
5	BJK2	3948	34.37	89	35.2
5	BJK3	4203	34.27	89	34.9
10	BJK2	5093	32.26	89	35.2
10	BJK1	5773	30.92	90	35.1
10	BJK3	5418	32.1	89	34.9
25	BJK2	6793	29.94	88	35.2
25	BJK3	7159	29.59	89	34.9
25	BJK1	7607	28.39	89	35.1

Target Temperature (oC) 50

0.5	BJK2	206	38.37	103	50.3
0.5	BJK3	230	38.25	103	50.1
0.5	BJK1	238	38.19	103	50
1	BJK2	294	40.22	106	50.3
1	BJK1	345	40.26	108	50
1	BJK3	332	40.06	109	50.2
5	BJK2	762	42.23	81	50.3
5	BJK3	875	41.61	83	50.1
5	BJK1	909	41.75	82	50.1
10	BJK1	1361	41.65	79	50.1
10	BJK3	1311	41.83	79	50.1
10	BJK2	1146	42.6	77	50.3
25	BJK1	2274	39.66	83	50.1
25	BJK3	2194	40.03	83	50.1
25	BJK2	1943	40.78	80	50.3

Confinement (kPa): 50

Target Temperature (oC) 35

0.5	BJK1	1626	38.05	100	34.6
0.5	BJK3	1468	38.58	100	34.8
0.5	BJK2	1483	37.19	99	34.6
1	BJK2	2012	37.29	97	34.8
1	BJK3	2060	38.1	98	34.9
1	BJK1	2287	37.03	98	34.8
5	BJK1	4593	32.8	89	35
5	BJK2	4004	33.76	90	35



APS-fL Mix Properties and Dynamic Modulus Results

Report Number: RDM-12072

Page A64 of A95

5	BJK3	4221	34.03	90	35
10	BJK2	5131	31.9	89	35.1
10	BJK1	5806	30.81	90	35.1
10	BJK3	5442	32	90	35.1
25	BJK1	7611	28.33	89	35.2
25	BJK2	6769	29.55	88	35.2
25	BJK3	7182	29.2	90	35.1

Target Temperature (oC) 50

0.5	BJK3	528	27.41	100	49.6
0.5	BJK1	546	26.39	99	49.5
0.5	BJK2	537	25.14	99	49.9
1	BJK3	621	31.35	97	49.9
1	BJK1	638	30.44	97	49.9
1	BJK2	617	28.84	97	50.1
5	BJK1	1156	36.96	87	50.1
5	BJK3	1127	37.46	86	50.1
5	BJK2	1045	35.67	87	50.3
10	BJK3	1541	38.72	85	50.2
10	BJK1	1581	38.28	85	50.1
10	BJK2	1394	37.64	84	50.4
25	BJK2	2104	37.96	84	50.4
25	BJK1	2439	37.75	87	50.2
25	BJK3	2378	38.34	87	50.2

Confinement (kPa): 100

Target Temperature (oC) 35

0.5	BJK3	1617	36.58	98	34.4
0.5	BJK1	1768	36.5	99	34.5
0.5	BJK2	1642	35.03	97	34.5
1	BJK3	2173	36.9	96	34.8
1	BJK2	2118	36.19	95	34.6
1	BJK1	2404	36.26	97	35
5	BJK3	4294	33.67	90	35.2
5	BJK1	4667	32.6	91	35.3
5	BJK2	4028	33.79	90	34.9
10	BJK3	5483	31.79	90	35.4
10	BJK1	5930	30.74	90	35.5
10	BJK2	5112	32.05	91	35.1
25	BJK2	6735	29.49	89	35.2
25	BJK3	7213	28.93	90	35.4
25	BJK1	7663	28.05	91	35.5

Target Temperature (oC) 50

0.5	BJK3	702	23.93	100	49
0.5	BJK1	731	23.7	87	49.1
0.5	BJK2	749	21.4	99	49.3
1	BJK1	760	28.09	100	49.8

APS-fL Mix Properties and Dynamic Modulus Results



Report Number: **RDM-12072**

Page A65 of A95

1	BJK3	804	27.56	99	49.6
1	BJK2	831	24.63	98	49.9
5	BJK2	1268	31.41	90	50.2
5	BJK3	1320	34.04	89	50
5	BJK1	1321	34.16	89	50.1
10	BJK2	1604	33.99	88	50.4
10	BJK3	1717	36.16	88	50.2
10	BJK1	1748	35.84	87	50.2
25	BJK3	2503	37.1	87	50.3
25	BJK1	2575	36.05	87	50.3
25	BJK2	2259	35.82	85	50.4

Confinement (kPa): 200

Target Temperature (oC) 35

0.5	BJK1	1975	35.38	99	34.2
0.5	BJK2	2007	33.49	97	34.1
0.5	BJK3	1688	35.96	97	33.8
1	BJK2	2490	34.52	94	34.7
1	BJK1	2597	35.38	95	34.6
1	BJK3	2186	36.91	95	34.3
5	BJK3	4191	33.97	91	34.8
5	BJK2	4401	32.31	92	35
5	BJK1	4759	32.35	91	35
10	BJK1	5978	30.5	92	35.2
10	BJK3	5330	32.07	92	35.1
10	BJK2	5492	30.65	93	35.2
25	BJK2	7144	27.72	91	35.3
25	BJK1	7774	27.42	93	35.3
25	BJK3	7087	28.97	93	35.3

Target Temperature (oC) 50

0.5	BJK3	986	21	98	48.1
0.5	BJK1	819	24.14	102	47.5
0.5	BJK2	1039	18.53	98	48.4
1	BJK3	1058	23.89	98	49.1
1	BJK1	968	25.69	113	48.4
1	BJK2	1106	21.13	101	49.2
5	BJK2	1544	26.81	93	49.8
5	BJK3	1555	30.26	90	49.8
5	BJK1	1610	30.01	92	49.8
10	BJK3	1917	32.48	91	50
10	BJK1	2021	32.26	92	50.1
10	BJK2	1861	29.6	93	50.1
25	BJK3	2647	34.44	88	50.3
25	BJK2	2472	32.15	86	50.3
25	BJK1	2789	33.89	89	50.3

Report Date:

Monday, 21 September 2015



APS-fL Mix Properties and Dynamic Modulus Results

Report Number: RDM-12069

Page A66 of A95

Mix Details

AC/DG	20	Binder Content (%)	4.30
Aggregate Type:	Dolomitic Siltstone	VMA (%)	13.5
Binder Type	C320	Air Voids (%)	4.5
Mix Design Method	Gyro 80	VFB (%)	66
Filler Type	Bag House Dust	Effective Bit. Content (%)	3.8
		RAP (%)	15

Gradation Percent Passing (%)

26.5mm	100	2.36mm	29
19mm	89	1.18mm	23
13.2mm	69.00	0.6mm	17
9.5mm	60.000	0.3mm	10
6.7mm	52	0.15mm	5
4.75mm	41	0.075mm	3.6

Dynamic Modulus Results

Frequency (Hz)	Specimen	Modulus (MPa)	Phase Angle (deg)	Strain με	Temperature (oC)
-------------------	----------	------------------	----------------------	--------------	---------------------

Confinement (kPa): 0

Target Temperature (oC) 5

0.5	BJL2	19479	11.89	86	5
0.5	BJL1	18646	12.02	90	4.9
1	BJL1	20007	10.89	84	4.9
1	BJL2	20983	10.73	79	5
5	BJL2	24341	8.51	66	5.1
5	BJL1	22934	8.86	71	4.9
10	BJL1	24000	8.01	66	4.9
10	BJL2	25679	7.85	61	5.1
25	BJL1	25322	7.16	57	4.9
25	BJL2	27401	7.33	52	5.1

Target Temperature (oC) 20

0.5	BJL1	7023	27.9	98	20.1
0.5	BJL2	8208	25.82	99	20.1
1	BJL2	9793	23.4	98	20.1
1	BJL1	8372	25.66	101	20.1
5	BJL2	13701	17.94	96	20.1
5	BJL1	11898	19.65	95	20.1
10	BJL2	15488	15.6	94	20.1
10	BJL1	13441	17.7	94	20.1
25	BJL2	17841	13.4	84	20.1
25	BJL1	15460	15.08	91	20.1

Target Temperature (oC) 35

0.5	BJL2	1464	38.53	101	35.3
0.5	BJL1	1392	39.7	101	34.9
1	BJL1	2011	39.07	98	34.9

Report Date:

Monday, 21 September 2015

APS-fL Mix Properties and Dynamic Modulus Results



Report Number: **RDM-12069**

Page A67 of A95

1	BJL2	2099	37.97	98	35.3
5	BJL1	4201	34.57	89	34.9
5	BJL2	4322	33.87	89	35.2
10	BJL1	5406	32.18	89	34.9
10	BJL2	5571	31.78	89	35.2
25	BJL1	7163	29.07	89	34.9
25	BJL2	7339	29.13	89	35.2

Target Temperature (oC) 50

0.5	BJL1	234	39.56	110	50.3
0.5	BJL2	230	41.24	102	50.2
1	BJL2	334	41.99	109	50.3
1	BJL1	352	40.33	108	50.2
5	BJL2	905	42.42	80	50.3
5	BJL1	894	42.32	78	50.3
10	BJL2	1361	42.41	77	50.3
10	BJL1	1398	41.31	79	50.3
25	BJL1	2327	39.38	83	50.3
25	BJL2	2280	40.44	81	50.3

Confinement (kPa): 50

Target Temperature (oC) 35

0.5	BJL2	1558	37.46	100	34.7
0.5	BJL1	1525	37.93	100	34.8
1	BJL1	2114	37.41	98	34.9
1	BJL2	2170	37.42	97	34.9
5	BJL2	4380	33.8	89	35.1
5	BJL1	4300	33.48	90	35.1
10	BJL2	5565	31.7	90	35.2
10	BJL1	5515	31.41	90	35.2
25	BJL2	7289	28.78	91	35.2
25	BJL1	7298	28.91	90	35.3

Target Temperature (oC) 50

0.5	BJL1	511	28.13	99	49.5
0.5	BJL2	398	32.09	99	49.9
1	BJL1	608	32.13	96	49.6
1	BJL2	498	35.68	96	50.2
5	BJL2	1035	40.53	85	50.4
5	BJL1	1146	37.85	87	49.6
10	BJL1	1589	38.87	85	49.5
10	BJL2	1487	41.12	82	50.5
25	BJL1	2474	38.18	87	49.5
25	BJL2	2392	39.87	83	50.4

Confinement (kPa): 100

Target Temperature (oC) 35

0.5	BJL1	1701	35.65	98	34.6
0.5	BJL2	1703	35.15	98	34.5



APS-fL Mix Properties and Dynamic Modulus Results

Report Number: **RDM-12069**

Page A68 of A95

1	BJL1	2247	36.32	96	34.9
1	BJL2	2249	35.97	96	34.8
5	BJL2	4343	33.44	91	35.2
5	BJL1	4357	33.3	91	35.2
10	BJL1	5592	31.55	90	35.4
10	BJL2	5556	31.81	91	35.3
25	BJL2	7275	29.3	91	35.3
25	BJL1	7301	28.93	90	35.4

Target Temperature (oC) 50

0.5	BJL2	608	26.21	100	49.2
0.5	BJL1	697	24.5	99	49.5
1	BJL1	801	28.14	97	50.1
1	BJL2	724	29.82	96	49.9
5	BJL2	1268	36.31	96	50.3
5	BJL1	1352	34.72	89	50.4
10	BJL2	1698	38.24	86	50.4
10	BJL1	1781	36.51	88	50.5
25	BJL2	2557	38.5	85	50.3
25	BJL1	2610	37.14	87	50.4

Confinement (kPa): 200

Target Temperature (oC) 35

0.5	BJL1	1927	34.05	96	33.9
0.5	BJL2	2035	33.67	97	33.8
1	BJL2	2560	34.85	95	34.3
1	BJL1	2408	35.4	94	34.4
5	BJL1	4333	33.23	91	34.8
5	BJL2	4590	32.97	91	34.8
10	BJL1	5445	31.5	93	35
10	BJL2	5801	31.27	92	35
25	BJL2	7585	28.09	95	35.3
25	BJL1	7162	28.36	93	35.3

Target Temperature (oC) 50

0.5	BJL2	972	21.38	101	47.9
0.5	BJL1	778	25.48	103	48.4
1	BJL1	956	26.76	102	49.3
1	BJL2	1103	24.28	100	49
5	BJL2	1660	30.6	92	49.7
5	BJL1	1570	31.73	91	49.9
10	BJL2	2070	33.21	92	50
10	BJL1	2002	33.81	91	50.1
25	BJL1	2803	34.99	89	50.3
25	BJL2	2870	34.89	88	50.3



APS-fL Mix Properties and Dynamic Modulus Results

Report Number: RDM-12083

Page A69 of A95

Mix Details

AC/DG	20	Binder Content (%)	4.40
Aggregate Type:	Granite	VMA (%)	14
Binder Type	C320	Air Voids (%)	3.9
Mix Design Method	Gyro 120	VFB (%)	72
Filler Type	Hydrated Lime	Effective Bit. Content (%)	4.3
		RAP (%)	20

Gradation Percent Passing (%)

26.5mm	100	2.36mm	35
19mm	99	1.18mm	26
13.2mm	86.00	0.6mm	19
9.5mm	69.000	0.3mm	13
6.7mm	56	0.15mm	7.2
4.75mm	47	0.075mm	4.8

Dynamic Modulus Results

Frequency (Hz)	Specimen	Modulus (MPa)	Phase Angle (deg)	Strain με	Temperature (oC)
-------------------	----------	------------------	----------------------	--------------	---------------------

Confinement (kPa): 0

Target Temperature (oC) 5

0.5	BJM1	15702	12.83	97	5.1
0.5	BJM3	17677	10.92	95	5
1	BJM1	17122	11.64	97	5.1
1	BJM3	18946	9.84	88	4.9
5	BJM1	20212	9.35	81	5.1
5	BJM3	21810	7.94	74	4.9
10	BJM1	21478	8.65	74	5.1
10	BJM3	22900	7.52	68	5
25	BJM1	23065	7.96	63	5.1
25	BJM3	24285	6.94	58	5

Target Temperature (oC) 20

0.5	BJM3	5798	29.04	98	20
1	BJM3	6991	26.98	93	20
5	BJM3	10211	21.36	93	20.1
10	BJM3	11654	19.39	92	20.1
25	BJM3	13636	17.14	89	20.1

Target Temperature (oC) 35

0.5	BJM3	1117	41.2	103	35.4
0.5	BJM1	1067	40.44	101	35.3
1	BJM3	1656	40.1	100	35.3
1	BJM1	1550	40.11	99	35.3
5	BJM1	3391	36.24	87	35.3
5	BJM3	3679	35.52	88	35.2
10	BJM1	4476	33.89	88	35.2
10	BJM3	4880	33.28	88	35.1

Report Date:

Monday, 21 September 2015

APS-fL Mix Properties and Dynamic Modulus Results



Report Number: **RDM-12083**

Page A70 of A95

25	BJM3	6649	30.49	88	35.1
25	BJM1	6087	31.24	88	35.2

Target Temperature (oC) 50

0.5	BJM3	174	36.62	102	50.1
0.5	BJM1	170	36.89	102	50.1
1	BJM1	235	39.47	105	50.1
1	BJM3	241	39.44	107	50.1
5	BJM3	632	42.48	76	50.1
5	BJM1	597	42.82	78	50
10	BJM1	902	43.27	73	50
10	BJM3	962	42.95	72	50.1
25	BJM3	1708	40.47	81	50.1
25	BJM1	1578	41.16	80	50

Confinement (kPa): 50

Target Temperature (oC) 35

0.5	BJM1	1277	36.35	99	35
0.5	BJM3	1344	37.38	100	35
1	BJM1	1716	37.44	97	35.1
1	BJM3	1844	37.6	98	35.1
5	BJM1	3510	35.27	89	35.3
5	BJM3	3840	34.57	89	35.3
10	BJM3	5030	32.55	89	35.3
10	BJM1	4569	33.51	88	35.3
25	BJM1	6132	30.85	89	35.4
25	BJM3	6751	30.12	87	35.3

Target Temperature (oC) 50

0.5	BJM1	480	22.14	99	50
0.5	BJM3	478	23.01	99	49.8
1	BJM1	544	26.02	99	50.2
1	BJM3	547	26.95	97	50.1
5	BJM1	890	33.76	87	50.3
5	BJM3	918	34.6	86	50.2
10	BJM3	1220	37.5	82	50.3
10	BJM1	1168	36.72	83	50.4
25	BJM3	1869	38.58	86	50.3
25	BJM1	1761	38.23	83	50.4

Confinement (kPa): 100

Target Temperature (oC) 35

0.5	BJM1	1498	33.02	98	34.6
0.5	BJM3	1574	34.75	98	34.7
1	BJM1	1912	34.83	96	34.8
1	BJM3	2063	35.82	97	35
5	BJM3	4020	33.79	90	35.3
5	BJM1	3633	34.09	90	35
10	BJM3	5167	32.16	90	35.4

APS-fL Mix Properties and Dynamic Modulus Results



Report Number: RDM-12083

Page A71 of A95

10	BJM1	4685	32.51	90	35.2
25	BJM3	6823	29.75	90	35.5
25	BJM1	6256	30.09	90	35.3
Target Temperature (oC) 50					
0.5	BJM3	685	19.38	99	49.2
0.5	BJM1	686	18.85	99	49.4
1	BJM3	756	22.76	99	49.8
1	BJM1	755	22.27	99	49.9
5	BJM1	1119	29.48	97	50.2
5	BJM3	1138	30.12	89	50.2
10	BJM1	1403	32.65	88	50.3
10	BJM3	1432	33.31	87	50.3
25	BJM1	1966	35.4	83	50.4
25	BJM3	2020	35.95	85	50.4
Confinement (kPa): 200					
Target Temperature (oC) 35					
0.5	BJM3	1841	33.23	98	34.2
0.5	BJM1	1811	30.66	103	33.7
1	BJM1	2194	32.47	94	34.4
1	BJM3	2331	34.36	95	34.6
5	BJM3	4217	33.03	90	34.9
5	BJM1	3761	32.6	91	34.8
10	BJM1	4706	31.51	93	35.1
10	BJM3	5290	31.4	93	35.1
25	BJM1	6202	29.27	92	35.3
25	BJM3	6969	28.62	92	35.3
Target Temperature (oC) 50					
0.5	BJM1	1002	16.14	100	48.6
0.5	BJM3	1090	15.25	98	48.3
1	BJM3	1150	17.76	101	49.3
1	BJM1	1079	18.63	101	49.4
5	BJM3	1536	23.83	95	49.8
5	BJM1	1460	24.44	94	49.9
10	BJM3	1834	26.75	95	50.1
10	BJM1	1739	27.35	93	50.1
25	BJM3	2391	29.79	88	50.3
25	BJM1	2268	30.42	84	50.3



APS-fL Mix Properties and Dynamic Modulus Results

Report Number: RDM-12082

Page A72 of A95

Mix Details

AC/DG	14	Binder Content (%)	5.10
Aggregate Type:	Granite	VMA (%)	15
Binder Type	C320	Air Voids (%)	4.0
Mix Design Method	Gyro 120	VFB (%)	73
Filler Type	Hydrated Lime	Effective Bit. Content (%)	4.8
		RAP (%)	20

Gradation Percent Passing (%)

26.5mm	100	2.36mm	40
19mm	100	1.18mm	27
13.2mm	99.00	0.6mm	18
9.5mm	82.000	0.3mm	12
6.7mm	65	0.15mm	8
4.75mm	53	0.075mm	5.8

Dynamic Modulus Results

Frequency (Hz)	Specimen	Modulus (MPa)	Phase Angle (deg)	Strain με	Temperature (oC)
-------------------	----------	------------------	----------------------	--------------	---------------------

Confinement (kPa): 0

Target Temperature (oC) 5

0.5	BJO3	15853	11.08	98	5.3
0.5	BJO1	15644	12.12	108	5
1	BJO3	17121	10.09	97	5.3
1	BJO1	16963	10.79	97	5
5	BJO3	19925	7.82	82	5.3
5	BJO1	19884	8.55	82	5
10	BJO3	21050	7.15	76	5.3
10	BJO1	21079	7.86	76	5
25	BJO3	22419	6.48	65	5.3
25	BJO1	22634	6.99	65	5

Target Temperature (oC) 20

0.5	BJO1	6481	27.3	99	20.1
0.5	BJO3	5832	28.29	100	20.1
1	BJO1	7704	24.81	98	20.1
1	BJO3	7040	25.83	97	20
5	BJO1	10954	19.31	96	20.1
5	BJO3	10081	20.05	95	20
10	BJO3	11397	17.86	96	19.9
10	BJO1	12372	17.21	94	20.1
25	BJO1	14226	14.55	92	20.1
25	BJO3	13302	15.57	93	19.9

Target Temperature (oC) 35

0.5	BJO3	1019	43.81	102	35.3
0.5	BJO1	1062	41.84	102	35.4
1	BJO3	1493	42.19	99	35.3

Report Date:

Monday, 21 September 2015

APS-fL Mix Properties and Dynamic Modulus Results



Report Number: **RDM-12082**

Page A73 of A95

1	BJO1	1554	40.59	99	35.3
5	BJO1	3362	35.63	89	35.2
5	BJO3	3246	36.67	89	35.3
10	BJO1	4393	33.23	90	35.1
10	BJO3	4247	33.91	89	35.3
25	BJO3	5716	30.62	89	35.2
25	BJO1	5960	30.08	88	35.1

Target Temperature (oC) 50

0.5	BJO1	156	40.04	112	50.1
0.5	BJO3	138	42.29	103	50.1
1	BJO1	224	42.18	107	50.1
1	BJO3	201	44.41	105	50.1
5	BJO1	606	44.57	77	50.1
5	BJO3	553	46.73	74	50.1
10	BJO1	924	45.09	74	50.1
10	BJO3	843	46.74	72	50.1
25	BJO1	1597	42.62	79	50.1
25	BJO3	1471	43.58	79	50.1

Confinement (kPa): 50

Target Temperature (oC) 35

0.5	BJO1	1124	41.14	101	34.9
0.5	BJO3	1059	42.14	101	35
1	BJO3	1539	41.27	99	35.2
1	BJO1	1621	40.03	99	35.1
5	BJO3	3299	36.26	89	35.3
5	BJO1	3427	35.04	90	35.2
10	BJO3	4273	33.76	90	35.4
10	BJO1	4447	32.65	90	35.3
25	BJO3	5689	30.09	89	35.4
25	BJO1	5934	29.62	90	35.3

Target Temperature (oC) 50

0.5	BJO3	386	26.08	96	49.6
0.5	BJO1	417	25.04	102	49.5
1	BJO1	484	28.93	96	49.9
1	BJO3	433	30.5	92	49.9
5	BJO1	842	36.79	85	50.1
5	BJO3	738	38.97	81	50.1
10	BJO3	989	42.19	78	50.2
10	BJO1	1134	39.52	81	50.2
25	BJO1	1745	40.14	83	50.2
25	BJO3	1564	41.82	82	50.2

Confinement (kPa): 100

Target Temperature (oC) 35

0.5	BJO3	1110	41.38	100	34.6
0.5	BJO1	1179	39.92	101	34.7

APS-fL Mix Properties and Dynamic Modulus Results



Report Number: **RDM-12082**

Page A74 of A95

1	BJO3	1582	40.63	98	34.9
1	BJO1	1695	38.85	99	35
5	BJO1	3510	34.38	90	35.3
5	BJO3	3340	35.77	89	35.1
10	BJO3	4315	33.4	90	35.2
10	BJO1	4526	32.35	91	35.4
25	BJO3	5790	30.45	89	35.4
25	BJO1	6058	30.05	90	35.5

Target Temperature (oC) 50

0.5	BJO3	541	22.12	98	49.2
0.5	BJO1	607	20.89	99	49.2
1	BJO3	594	25.74	95	49.8
1	BJO1	680	24.71	98	49.8
5	BJO1	1059	32.92	88	50.2
5	BJO3	904	34.2	85	50.2
10	BJO3	1153	37.73	84	50.4
10	BJO1	1349	35.68	87	50.3
25	BJO1	1937	37.6	84	50.4
25	BJO3	1695	38.83	94	50.5

Confinement (kPa): 200

Target Temperature (oC) 35

0.5	BJO3	1343	37.46	101	34.1
0.5	BJO1	1310	37.64	101	33.9
1	BJO3	1830	37.69	96	34.5
1	BJO1	1811	37.39	98	34.4
5	BJO3	3449	35.14	91	34.9
5	BJO1	3543	34.3	91	34.8
10	BJO1	4526	32.25	91	35.1
10	BJO3	4380	32.83	93	35.1
25	BJO3	5807	29.97	93	35.3
25	BJO1	5959	28.81	92	35.3

Target Temperature (oC) 50

0.5	BJO3	578	20.94	100	48.1
0.5	BJO1	748	20.89	100	48.2
1	BJO3	669	23.13	105	49.2
1	BJO1	822	23.67	100	49.2
5	BJO3	1045	29.49	91	49.8
5	BJO1	1227	30.35	91	49.8
10	BJO3	1309	32.48	90	50
10	BJO1	1533	33.59	90	50.1
25	BJO1	2144	35.74	84	50.3
25	BJO3	1808	35.07	84	50.3



APS-FL Mix Properties and Dynamic Modulus Results

Report Number: RDM-12087

Page A75 of A95

Mix Details

AC/DG	20	Binder Content (%)	4.80
Aggregate Type:	Greywacke	VMA (%)	15.2
Binder Type	C600	Air Voids (%)	5.0
Mix Design Method	Marshall 50	VFB (%)	68
Filler Type		Effective Bit. Content (%)	4.4
		RAP (%)	0

Gradation Percent Passing (%)

26.5mm	100	2.36mm	34
19mm	98	1.18mm	25
13.2mm	78.00	0.6mm	20
9.5mm	68.000	0.3mm	12
6.7mm	61	0.15mm	8
4.75mm	49	0.075mm	6.5

Dynamic Modulus Results

Frequency (Hz)	Specimen	Modulus (MPa)	Phase Angle (deg)	Strain $\mu\epsilon$	Temperature (oC)
Confinement (kPa): 0					
Target Temperature (oC) 5					
0.5	BJP3	19749	10.35	85	5.1
0.5	BJP2	18311	12.02	92	5
1	BJP2	19696	10.55	85	5.1
1	BJP3	21389	9.41	78	5.1
5	BJP3	24869	7.69	65	5.1
5	BJP2	22788	8.83	71	5.1
10	BJP2	24073	8.39	65	5.1
10	BJP3	26333	7.26	60	5.1
25	BJP2	25827	8.06	55	5.1
25	BJP3	28301	7.09	51	5.1
Target Temperature (oC) 20					
0.5	BJP2	7356	25.13	98	19.9
0.5	BJP3	7784	23.65	99	20.1
1	BJP3	9084	21.96	97	20
1	BJP2	8598	23.6	94	20
5	BJP3	12492	17.75	96	20
5	BJP2	11820	19.1	94	20
10	BJP3	14095	16.11	95	20
10	BJP2	13231	17.31	92	20
25	BJP3	16334	14.16	90	20.1
25	BJP2	15176	15.18	87	20
Target Temperature (oC) 35					
0.5	BJP3	2042	33.68	100	35.3
0.5	BJP2	1806	33.9	100	35.2
1	BJP2	2438	33.36	97	35.2



APS-fL Mix Properties and Dynamic Modulus Results

Report Number: RDM-12087

Page A76 of A95

1	BJP3	2724	32.81	96	35.3
5	BJP2	4569	29.98	89	35.2
5	BJP3	4892	29.36	90	35.2
10	BJP2	5740	28.42	89	35.2
10	BJP3	6042	27.87	90	35.2
25	BJP2	7407	26.49	89	35.2
25	BJP3	7683	26.04	91	35.2

Target Temperature (oC) 50

0.5	BJP2	348	34.57	101	50.6
0.5	BJP3	401	35.57	101	50.2
1	BJP3	552	36.8	104	50.2
1	BJP2	476	36.19	105	50.5
5	BJP3	1250	37.24	85	50.1
5	BJP2	1082	37.34	84	50.3
10	BJP3	1755	37.3	82	50.1
10	BJP2	1524	37.47	81	50.2
25	BJP2	2362	36.42	84	50.2
25	BJP3	2690	35.73	84	50.1

Confinement (kPa): 50

Target Temperature (oC) 35

0.5	BJP3	2156	32.97	99	34.8
0.5	BJP2	1920	33.22	99	34.9
1	BJP2	2551	32.85	97	35.1
1	BJP3	2827	32.39	96	35
5	BJP3	4970	29	90	35.2
5	BJP2	4674	29.92	90	35.3
10	BJP3	6093	27.7	91	35.3
10	BJP2	5831	28.65	89	35.3
25	BJP3	7697	25.9	92	35.3
25	BJP2	7424	26.64	89	35.4

Target Temperature (oC) 50

0.5	BJP2	482	30.41	100	50.1
0.5	BJP3	630	29.54	98	49.6
1	BJP2	607	32.63	99	50.3
1	BJP3	769	32.13	97	49.9
5	BJP3	1429	34.9	88	50.1
5	BJP2	1181	35.73	87	50.4
10	BJP2	1611	36.33	84	50.4
10	BJP3	1923	35.45	87	50.1
25	BJP2	2431	35.75	85	50.4
25	BJP3	2831	34.75	87	50.2

Confinement (kPa): 100

Target Temperature (oC) 35

0.5	BJP2	2030	32.71	99	34.7
0.5	BJP3	2271	32.44	98	34.5

1	BJP2	2633	32.69	96	35
1	BJP3	2918	32.09	95	34.9
5	BJP3	5025	28.93	91	35.2
5	BJP2	4697	30.02	90	35.3
10	BJP2	5809	28.54	91	35.5
10	BJP3	6122	27.4	92	35.4
25	BJP3	7753	25.51	93	35.5
25	BJP2	7389	26.49	91	35.5

Target Temperature (oC) 50

0.5	BJP3	827	26.07	99	49.1
0.5	BJP2	618	27.24	102	49.5
1	BJP2	764	29.05	100	50
1	BJP3	977	28.74	97	49.7
5	BJP3	1641	32.85	90	50.1
5	BJP2	1324	33.33	90	50.3
10	BJP3	2119	33.9	90	50.3
10	BJP2	1737	34.35	88	50.4
25	BJP3	2978	33.78	88	50.3
25	BJP2	2495	34.72	87	50.5

Confinement (kPa): 200

Target Temperature (oC) 35

0.5	BJP2	2212	31.93	99	33.9
0.5	BJP3	2498	31.41	98	33.8
1	BJP3	3109	31.34	95	34.3
1	BJP2	2793	32.21	95	34.4
5	BJP2	4746	29.86	92	34.8
5	BJP3	5127	28.37	93	34.8
10	BJP2	5837	28.42	93	35.1
10	BJP3	6214	26.86	93	35
25	BJP3	7790	24.68	95	35.3
25	BJP2	7440	26.02	94	35.3

Target Temperature (oC) 50

0.5	BJP3	1124	23.17	100	48
0.5	BJP2	832	24.71	103	48.6
1	BJP2	998	26.12	102	49.4
1	BJP3	1293	25.46	98	49.1
5	BJP3	1956	29.47	93	49.8
5	BJP2	1567	29.94	92	49.9
10	BJP3	2406	31.03	94	50.1
10	BJP2	1956	31.38	93	50.1
25	BJP2	2661	32.56	89	50.4
25	BJP3	3216	31.72	91	50.3



APS-fL Mix Properties and Dynamic Modulus Results

Report Number: RDM-12098

Page A78 of A95

Mix Details

AC/DG	14	Binder Content (%)	4.40
Aggregate Type:	Granite	VMA (%)	15.17
Binder Type	C320	Air Voids (%)	5.0
Mix Design Method	Marshall 75	VFB (%)	67
Filler Type	Hydrated Lime	Effective Bit. Content (%)	4.3
		RAP (%)	7

Gradation Percent Passing (%)

26.5mm	100	2.36mm	39.24
19mm	100	1.18mm	32.12
13.2mm	98.33	0.6mm	26.04
9.5mm	86.640	0.3mm	15.64
6.7mm	70	0.15mm	6.86
4.75mm	54.78	0.075mm	4.3

Dynamic Modulus Results

Frequency (Hz)	Specimen	Modulus (MPa)	Phase Angle (deg)	Strain με	Temperature (oC)
-------------------	----------	------------------	----------------------	--------------	---------------------

Confinement (kPa): 0

Target Temperature (oC) 5

0.5	BJY3	12931	12.61	98	4.9
0.5	BJY1	11453	13.56	99	5
1	BJY1	12548	12.5	97	5
1	BJY3	14042	11.61	97	4.9
5	BJY3	16663	9.69	94	4.9
5	BJY1	15091	10.42	95	5
10	BJY1	16189	9.58	92	5
10	BJY3	17765	9.04	89	4.9
25	BJY1	17602	8.81	84	5.1
25	BJY3	19174	8.44	76	4.8

Target Temperature (oC) 20

0.5	BJY1	4322	25.89	98	20.2
0.5	BJY3	4800	25.23	98	20.2
1	BJY3	5650	23.72	95	20.1
1	BJY1	5046	24.54	95	20.2
5	BJY3	8028	19.6	93	20.1
5	BJY1	7217	20.47	95	20.1
10	BJY3	9081	18	92	20.2
10	BJY1	8264	18.91	96	20.1
25	BJY3	10500	16.02	91	20.2
25	BJY1	9788	16.99	94	20.1

Target Temperature (oC) 35

0.5	BJY3	1157	34.77	106	35.3
0.5	BJY1	1116	33.4	100	35.2
1	BJY1	1493	32.92	98	35.3

Report Date:

Monday, 21 September 2015



APS-fL Mix Properties and Dynamic Modulus Results

Report Number: RDM-12098

Page A79 of A95

1	BJY3	1572	33.41	99	35.3
5	BJY1	2758	30.85	88	35.2
5	BJY3	2922	31.4	87	35.2
10	BJY1	3466	29.94	87	35.2
10	BJY3	3656	30.43	87	35.2
25	BJY1	4547	28.97	86	35.2
25	BJY3	4778	28.81	86	35.2

Target Temperature (oC) 50

0.5	BJY1	204	35.25	100	50.3
0.5	BJY3	220	35.62	101	50.2
1	BJY3	305	36.52	104	50.2
1	BJY1	282	36.41	104	50.2
5	BJY3	700	37.73	78	50.3
5	BJY1	648	37.8	77	50.2
10	BJY3	983	38.12	74	50.3
10	BJY1	903	37.95	74	50.2
25	BJY1	1453	36.21	80	50.1
25	BJY3	1556	36.45	82	50.3

Confinement (kPa): 50

Target Temperature (oC) 35

0.5	BJY3	1356	31.05	98	34.9
0.5	BJY1	1251	32.32	99	35
1	BJY1	1609	32.6	96	35.2
1	BJY3	1708	31.68	96	35.2
5	BJY3	2995	30.65	89	35.4
5	BJY1	2861	30.99	88	35.3
10	BJY3	3716	29.92	87	35.5
10	BJY1	3536	30.36	87	35.4
25	BJY3	4772	28.62	85	35.5
25	BJY1	4559	29.09	86	35.4

Target Temperature (oC) 50

0.5	BJY1	506	23.7	98	49.5
0.5	BJY3	553	23.31	98	49.8
1	BJY1	582	26.49	97	49.8
1	BJY3	635	26	97	50.1
5	BJY3	1006	30.72	87	50.3
5	BJY1	929	31.02	86	50
10	BJY1	1166	33.14	83	50.1
10	BJY3	1265	32.59	84	50.3
25	BJY1	1637	33.74	83	50.1
25	BJY3	1761	33.38	84	50.3

Confinement (kPa): 100

Target Temperature (oC) 35

0.5	BJY1	1400	30.88	97	34.7
0.5	BJY3	1532	29.55	96	34.7



APS-fL Mix Properties and Dynamic Modulus Results

Report Number: RDM-12098

Page A80 of A95

1	BJY1	1717	31.74	95	35
1	BJY3	1825	30.76	94	34.9
5	BJY3	3025	30.03	89	35.2
5	BJY1	2892	30.76	90	35.3
10	BJY1	3534	30.19	90	35.4
10	BJY3	3664	29.72	89	35.4
25	BJY3	4693	28.48	88	35.3
25	BJY1	4560	28.81	88	35.5

Target Temperature (oC) 50

0.5	BJY3	772	19.86	99	49.3
0.5	BJY1	702	20.29	97	49.1
1	BJY1	762	22.86	99	49.7
1	BJY3	863	22.19	99	49.8
5	BJY3	1254	26.78	90	50.1
5	BJY1	1116	27.45	90	50.1
10	BJY3	1511	28.81	89	50.2
10	BJY1	1356	29.64	89	50.3
25	BJY3	1976	30.45	83	50.4
25	BJY1	1785	31.31	82	50.4

Confinement (kPa): 200

Target Temperature (oC) 35

0.5	BJY1	1691	29.05	97	33.8
0.5	BJY3	1821	27.83	97	34.1
1	BJY3	2109	29.08	95	34.5
1	BJY1	2000	30.07	95	34.3
5	BJY1	3164	29.13	91	34.8
5	BJY3	3270	28.7	91	34.9
10	BJY1	3797	28.49	92	35
10	BJY3	3918	28.36	92	35.1
25	BJY3	4963	27.33	90	35.3
25	BJY1	4807	26.94	92	35.3

Target Temperature (oC) 50

0.5	BJY3	1065	17.12	99	48.3
0.5	BJY1	879	19.05	103	48
1	BJY1	1010	19.87	103	49.2
1	BJY3	1155	19.17	101	49.2
5	BJY3	1564	22.94	94	49.8
5	BJY1	1401	23.64	94	49.8
10	BJY3	1823	24.89	94	50.1
10	BJY1	1639	25.75	94	50.1
25	BJY1	2060	27.64	81	50.3
25	BJY3	2275	26.62	84	50.3



APS-FL Mix Properties and Dynamic Modulus Results

Report Number: RDM-11119

Page A81 of A95

Mix Details

AC/DG	14	Binder Content (%)	5.00
Aggregate Type:	Basalt	VMA (%)	15.6
Binder Type	C320	Air Voids (%)	5.2
Mix Design Method	Marshall 50	VFB (%)	66
Filler Type		Effective Bit. Content (%)	4.4
		RAP (%)	0

Gradation Percent Passing (%)

26.5mm	100	2.36mm	37
19mm	100	1.18mm	29
13.2mm	99.00	0.6mm	22
9.5mm	83.000	0.3mm	15
6.7mm	71	0.15mm	8.4
4.75mm	57	0.075mm	5.4

Dynamic Modulus Results

Frequency (Hz)	Specimen	Modulus (MPa)	Phase Angle (deg)	Strain με	Temperature (oC)
-------------------	----------	------------------	----------------------	--------------	---------------------

Confinement (kPa): 0

Target Temperature (oC) 5

0.5	BIU1	16878	11.03	97	5
0.5	BIU3	17705	11.7	96	4.9
1	BIU1	18144	9.99	92	5
1	BIU3	18995	10.59	88	4.9
5	BIU1	20821	8.13	77	4.9
5	BIU3	21806	8.46	74	4.9
10	BIU1	21940	7.59	71	4.9
10	BIU3	22899	7.71	69	4.8
25	BIU1	23380	7.19	61	4.9
25	BIU3	24288	6.95	59	4.8

Target Temperature (oC) 20

0.5	BIU3	7642	26.72	99	19.9
1	BIU3	9032	24.4	96	19.9
5	BIU3	12542	19.05	95	19.9
10	BIU3	14115	16.94	93	19.9
25	BIU3	16043	14.17	86	19.9

Target Temperature (oC) 35

0.5	BIU3	1545	38.82	101	35.3
0.5	BIU1	1615	38.69	101	34.8
1	BIU3	2213	37.49	98	35.4
1	BIU1	2289	37.1	98	34.8
5	BIU1	4555	32.11	89	34.8
5	BIU3	4502	32.5	89	35.4
10	BIU1	5760	29.98	90	34.8
10	BIU3	5722	30.37	89	35.4

Report Date:

Monday, 21 September 2015

APS-fL Mix Properties and Dynamic Modulus Results



Report Number: **RDM-11119**

Page A82 of A95

25	BIU3	7531	27.72	88	35.4
25	BIU1	7527	27.27	88	34.8

Target Temperature (oC) 50

0.5	BIU3	245	40.24	104	50.4
0.5	BIU1	241	40.33	104	50.6
1	BIU1	358	41.6	108	50.6
1	BIU3	365	41.46	108	50.6
5	BIU3	962	42.17	83	50.6
5	BIU1	951	42.18	82	50.5
10	BIU1	1417	41.59	79	50.5
10	BIU3	1440	41.7	80	50.5
25	BIU3	2398	39.11	83	50.5
25	BIU1	2346	38.77	84	50.5

Confinement (kPa): 50

Target Temperature (oC) 35

0.5	BIU1	1771	36.09	100	34.9
0.5	BIU3	1709	36.6	99	34.8
1	BIU1	2409	35.54	97	35.1
1	BIU3	2332	36.15	97	34.9
5	BIU1	4648	31.48	90	35.1
5	BIU3	4568	32.03	90	35
10	BIU3	5810	30.07	90	35.1
10	BIU1	5887	29.37	90	35
25	BIU1	7616	26.55	89	35
25	BIU3	7594	27.26	89	35.2

Target Temperature (oC) 50

0.5	BIU1	568	27.07	99	50.5
0.5	BIU3	571	27.65	99	50.4
1	BIU1	675	30.69	97	50.3
1	BIU3	681	31.58	103	50.3
5	BIU1	1226	36.67	87	50.2
5	BIU3	1252	37.02	87	50.4
10	BIU3	1706	38.09	86	50.4
10	BIU1	1664	37.85	85	50.2
25	BIU3	2613	37.05	87	50.4
25	BIU1	2534	36.99	87	50.2

Confinement (kPa): 100

Target Temperature (oC) 35

0.5	BIU1	1937	34.17	98	34.7
0.5	BIU3	1925	34.5	98	35
1	BIU1	2525	34.49	96	34.9
1	BIU3	2523	34.9	96	35.1
5	BIU3	4726	31.62	91	35.2
5	BIU1	4663	31.42	91	35.1
10	BIU3	5953	29.75	91	35.2



APS-fL Mix Properties and Dynamic Modulus Results

Report Number: RDM-11119

Page A83 of A95

10	BIU1	5874	29.33	91	35.2
25	BIU3	7646	26.97	89	35.2
25	BIU1	7598	26.52	90	35.4
Target Temperature (oC) 50					
0.5	BIU3	814	23.25	99	50.2
0.5	BIU1	812	22.84	99	50.1
1	BIU3	934	26.83	98	50.2
1	BIU1	921	26.15	97	50.1
5	BIU1	1469	32.77	89	50.2
5	BIU3	1517	33.24	90	50.3
10	BIU1	1889	34.8	88	50.3
10	BIU3	1973	35.05	88	50.3
25	BIU1	2705	35.59	87	50.3
25	BIU3	2846	35.59	88	50.4
Confinement (kPa): 200					
Target Temperature (oC) 35					
0.5	BIU3	2146	33.01	97	34.1
0.5	BIU1	2148	33.08	97	33.7
1	BIU1	2677	33.94	94	34.2
1	BIU3	2680	33.98	95	34.4
5	BIU3	4725	31.35	93	34.6
5	BIU1	4635	31.34	92	34.5
10	BIU1	5727	29.45	93	34.7
10	BIU3	5901	29.55	93	34.8
25	BIU1	7343	26.24	92	34.9
25	BIU3	7572	26.41	93	34.9
Target Temperature (oC) 50					
0.5	BIU1	1159	20.52	99	48.4
0.5	BIU3	1128	21.09	100	48.6
1	BIU3	1263	23.95	99	49.1
1	BIU1	1263	23.27	97	49
5	BIU3	1868	29.76	92	49.7
5	BIU1	1807	28.89	92	49.6
10	BIU3	2312	32.03	92	49.9
10	BIU1	2213	31.45	93	49.9
25	BIU3	3149	33.48	88	50.2
25	BIU1	2995	32.87	89	50.2



APS-fL Mix Properties and Dynamic Modulus Results

Report Number: RDM-12105

Page A84 of A95

Mix Details

AC/DG	14	Binder Content (%)	5.30
Aggregate Type:	Greywacke	VMA (%)	14.7
Binder Type	A15E	Air Voids (%)	4.0
Mix Design Method	Marshall 50	VFB (%)	73
Filler Type		Effective Bit. Content (%)	4.7
		RAP (%)	0

Gradation Percent Passing (%)

26.5mm	100	2.36mm	40
19mm	100	1.18mm	29
13.2mm	98.00	0.6mm	22
9.5mm	80.000	0.3mm	15
6.7mm	67	0.15mm	9
4.75mm	54	0.075mm	6.5

Dynamic Modulus Results

Frequency (Hz)	Specimen	Modulus (MPa)	Phase Angle (deg)	Strain με	Temperature (oC)
-------------------	----------	------------------	----------------------	--------------	---------------------

Confinement (kPa): 0

Target Temperature (oC) 5

0.5	BKG2	12101	19.32	98	5.1
0.5	BKG1	11783	17.97	98	5
1	BKG1	13264	16.51	97	5.1
1	BKG2	13569	17.37	97	5.1
5	BKG2	17106	13.48	93	5.1
5	BKG1	16647	12.94	94	5.1
10	BKG1	18125	11.55	87	5.1
10	BKG2	18557	11.95	84	5.1
25	BKG1	19981	10.09	73	5.1
25	BKG2	20519	10.63	70	5.1

Target Temperature (oC) 20

0.5	BKG1	3280	33.03	98	20
0.5	BKG2	3245	32.95	98	20
1	BKG2	4141	31.51	95	19.9
1	BKG1	4145	31.92	94	20
5	BKG2	6864	26.76	92	20
5	BKG1	6803	27.19	91	20
10	BKG2	8191	24.7	93	20
10	BKG1	8067	25.37	93	20
25	BKG2	10128	22	93	20
25	BKG1	9928	22.54	93	20

Target Temperature (oC) 35

0.5	BKG2	670	32.81	104	35.2
0.5	BKG1	740	33.34	100	35.3
1	BKG1	975	34.55	100	35.3

Report Date:

Monday, 21 September 2015

APS-fL Mix Properties and Dynamic Modulus Results



Report Number: **RDM-12105**

Page A85 of A95

1	BKG2	862	35.15	101	35.2
5	BKG1	1983	35.24	86	35.2
5	BKG2	1800	36.51	86	35.3
10	BKG1	2662	35.04	85	35.2
10	BKG2	2450	36.26	84	35.3
25	BKG1	3848	33.58	85	35.2
25	BKG2	3613	34.58	83	35.3

Target Temperature (oC) 50

0.5	BKG1	226	27.91	100	50.2
0.5	BKG2	225	28.91	100	50.2
1	BKG2	269	31.05	101	50.2
1	BKG1	271	30.21	102	50.2
5	BKG2	496	35.45	78	50.2
5	BKG1	509	34.55	77	50.2
10	BKG2	674	37.68	72	50.2
10	BKG1	701	36.25	78	50.2
25	BKG1	1132	36.56	81	50.1
25	BKG2	1090	37.56	82	50.2

Confinement (kPa): 50

Target Temperature (oC) 35

0.5	BKG2	785	32.06	98	34.8
0.5	BKG1	833	32.07	98	34.9
1	BKG1	1047	33.91	98	35
1	BKG2	976	34.22	98	34.9
5	BKG2	1880	35.94	87	35
5	BKG1	2038	35.14	86	35.2
10	BKG2	2509	35.58	86	35
10	BKG1	2703	35.1	85	35.3
25	BKG2	3629	34.18	84	35
25	BKG1	3868	33.85	84	35.4

Target Temperature (oC) 50

0.5	BKG1	330	24.75	99	49.6
0.5	BKG2	350	24.74	100	49.7
1	BKG1	377	26.97	100	49.9
1	BKG2	401	26.74	101	50
5	BKG2	644	31.33	84	50.2
5	BKG1	623	31.23	83	50
10	BKG1	803	33.56	78	50.1
10	BKG2	822	33.75	79	50.3
25	BKG1	1200	35.05	83	50.1
25	BKG2	1203	35.63	83	50.3

Confinement (kPa): 100

Target Temperature (oC) 35

0.5	BKG1	929	30.77	96	34.6
0.5	BKG2	902	29.75	98	34.6

APS-fL Mix Properties and Dynamic Modulus Results



Report Number: **RDM-12105**

Page A86 of A95

1	BKG1	1125	33.11	96	35
1	BKG2	1095	31.81	97	35
5	BKG2	1974	34.38	89	35.4
5	BKG1	2085	34.8	86	35.4
10	BKG1	2724	35.03	86	35.5
10	BKG2	2589	34.72	88	35.5
25	BKG2	3693	34.06	86	35.5
25	BKG1	3850	34.02	85	35.6

Target Temperature (oC) 50

0.5	BKG2	457	22.78	100	49.1
0.5	BKG1	422	23.1	98	49.2
1	BKG1	477	25.03	102	49.7
1	BKG2	518	24.42	102	49.7
5	BKG2	782	28.48	88	50.1
5	BKG1	754	28.66	87	50
10	BKG2	964	30.86	85	50.2
10	BKG1	942	30.86	85	50.2
25	BKG2	1323	33.34	83	50.4
25	BKG1	1305	33.1	83	50.3

Confinement (kPa): 200

Target Temperature (oC) 35

0.5	BKG1	1260	26.18	99	33.9
0.5	BKG2	1085	27.4	99	34.1
1	BKG2	1280	28.9	98	34.4
1	BKG1	1476	27.94	96	34.5
5	BKG1	2336	31.09	91	34.9
5	BKG2	2123	32.05	91	34.8
10	BKG1	2906	31.94	92	35.1
10	BKG2	2709	32.92	91	35.1
25	BKG2	3755	32.81	88	35.3
25	BKG1	3934	31.79	90	35.3

Target Temperature (oC) 50

0.5	BKG2	660	20.75	103	48.3
0.5	BKG1	563	21.81	97	48.5
1	BKG1	616	23.47	102	49.3
1	BKG2	764	21.47	105	49.5
5	BKG2	1079	24.81	94	50.2
5	BKG1	914	26.44	89	49.8
10	BKG2	1273	27.14	94	50.5
10	BKG1	1105	28.4	87	50.1
25	BKG1	1456	30.85	79	50.3
25	BKG2	1632	29.97	81	50.6



APS-fL Mix Properties and Dynamic Modulus Results

Report Number: **RDM-12111**

Page A87 of A95

Mix Details

AC/DG	20	Binder Content (%)	4.70
Aggregate Type:	Metagraywacke	VMA (%)	14.8
Binder Type	C600	Air Voids (%)	4.8
Mix Design Method	Marshall 50	VFB (%)	68
Filler Type		Effective Bit. Content (%)	4.3
		RAP (%)	0

Gradation Percent Passing (%)

26.5mm	100	2.36mm	35
19mm	98	1.18mm	26
13.2mm	82.00	0.6mm	19
9.5mm	67.000	0.3mm	12
6.7mm	58	0.15mm	8
4.75mm	50	0.075mm	5.5

Dynamic Modulus Results

Frequency (Hz)	Specimen	Modulus (MPa)	Phase Angle (deg)	Strain μ ϵ	Temperature (oC)
-------------------	----------	------------------	----------------------	------------------------	---------------------

Confinement (kPa): 0

Target Temperature (oC) 5

0.5	BKL3	18722	11.55	90	4.9
0.5	BLD2	17301	10.35	96	5
0.5	BKL2	20693	9.53	82	5.1
0.5	BLD3	19020	10.77	89	4.9
1	BLD2	18262	9.56	91	4.9
1	BKL3	20151	10.6	83	5
1	BKL2	22084	8.61	76	5.1
1	BLD3	20343	9.87	83	5
5	BLD2	20655	8.04	78	4.9
5	BLD3	23347	8.36	70	5
5	BKL2	25097	7.05	65	5.2
5	BKL3	23282	8.83	70	5
10	BKL3	24531	8.27	65	5
10	BLD2	21629	7.67	72	4.9
10	BLD3	24614	7.94	65	5
10	BKL2	26312	6.63	60	5.2
25	BLD2	22993	7.39	62	4.9
25	BKL3	26449	8.36	55	5
25	BKL2	27914	6.2	52	5.2
25	BLD3	26248	7.75	56	5

Target Temperature (oC) 20

0.5	BLD2	7875	23.41	97	20
0.5	BKL3	7780	24.24	99	19.9
0.5	BKL2	8294	24.2	100	20.1
0.5	BLD3	8730	23.24	99	20.1

Report Date:

Monday, 21 September 2015



APS-fL Mix Properties and Dynamic Modulus Results

Report Number: RDM-12111

Page A88 of A95

1	BKL3	9099	22.6	97	20
1	BLD2	9045	21.51	93	20.1
1	BKL2	9772	22.31	99	20.2
1	BLD3	10178	21.46	97	20
5	BLD2	12049	16.91	93	20.1
5	BKL2	13516	17.48	95	20.2
5	BKL3	12552	17.63	97	20
5	BLD3	13706	17.02	95	20
10	BKL3	14245	16	96	20
10	BKL2	15034	15.8	95	20.1
10	BLD2	13164	15.2	92	20.1
10	BLD3	15290	15.57	93	20
25	BKL2	17555	13.53	86	20.1
25	BLD2	14755	13.22	87	20.1
25	BKL3	16624	14.24	90	20
25	BLD3	17443	13.74	86	20
Target Temperature (oC) 35					
0.5	BLD2	1866	36.82	107	35.3
0.5	BKL3	1884	35.33	100	35
0.5	BKL2	1773	37.06	100	35.3
0.5	BLD3	2025	34.78	100	35
1	BKL3	2562	34.32	97	35.2
1	BKL2	2435	36.15	97	35.2
1	BLD3	2738	33.73	97	35.1
1	BLD2	2563	35	97	35.3
5	BKL2	4626	32.03	90	35.1
5	BKL3	4746	30.3	90	35.1
5	BLD3	4997	29.73	90	35.2
5	BLD2	4783	30.86	90	35.2
10	BLD3	6191	27.91	91	35.2
10	BKL2	5803	29.89	99	35.1
10	BLD2	5968	28.94	90	35.1
10	BKL3	5896	28.58	90	35.1
25	BLD2	7635	26.43	92	35.1
25	BKL3	7558	26.54	91	35.1
25	BKL2	7513	27.65	92	35.1
25	BLD3	7877	25.68	92	35.1
Target Temperature (oC) 50					
0.5	BLD2	308	37.76	101	50.2
0.5	BKL3	294	37.23	102	50.6
0.5	BLD3	345	36.61	101	50.5
0.5	BKL2	282	37.13	102	50.4
1	BKL2	390	39.04	104	50.3
1	BLD3	483	38.18	104	50.3
1	BLD2	432	39.41	104	50.3



APS-fL Mix Properties and Dynamic Modulus Results

Report Number: RDM-12111

Page A89 of A95

1	BKL3	423	39.34	112	50.6
5	BKL2	935	40.17	84	50.3
5	BLD2	1046	40.08	83	50.2
5	BKL3	1030	39.57	84	50.3
5	BLD3	1152	39.04	84	50.2
10	BLD3	1657	38.95	82	50.2
10	BKL2	1363	40.13	82	50.2
10	BLD2	1514	39.82	81	50.2
10	BKL3	1490	39.48	81	50.2
25	BLD2	2404	38.03	83	50.2
25	BKL3	2368	37.87	83	50.2
25	BKL2	2213	38.29	87	50.2
25	BLD3	2592	37.28	84	50.2

Confinement (kPa): 50

Target Temperature (oC) 35

0.5	BLD2	1955	35.74	100	35
0.5	BKL2	1863	36.21	100	34.8
0.5	BLD3	2112	34.22	100	35
0.5	BKL3	1943	35.47	100	34.6
1	BLD2	2632	34.79	96	35.2
1	BKL3	2621	34.53	97	34.8
1	BLD3	2814	33.46	96	35.2
1	BKL2	2523	35.56	97	35.1
5	BLD3	5053	29.6	91	35.3
5	BLD2	4825	30.66	90	35.3
5	BKL3	4790	30.84	90	35
5	BKL2	4703	31.91	90	35.2
10	BKL3	5928	29.23	90	35.1
10	BLD3	6215	28.06	92	35.4
10	BKL2	5864	29.84	91	35.3
10	BLD2	5962	28.81	91	35.3
25	BKL2	7529	27.16	93	35.3
25	BKL3	7553	27.01	92	35.2
25	BLD2	7625	26.3	93	35.4
25	BLD3	7926	26.06	93	35.4

Target Temperature (oC) 50

0.5	BLD2	405	33.36	99	50
0.5	BKL2	358	34.03	99	49.9
0.5	BLD3	457	32.29	99	50
0.5	BKL3	382	34.75	97	50
1	BKL3	511	35.94	101	50.2
1	BLD3	585	35.08	99	50.2
1	BKL2	463	36.72	99	50.1
1	BLD2	524	35.97	99	50.3
5	BLD2	1106	38.77	86	50.4

Report Date:

Monday, 21 September 2015



APS-fL Mix Properties and Dynamic Modulus Results

Report Number: **RDM-12111**

Page A90 of A95

5	BLD3	1209	37.91	87	50.3
5	BKL3	1093	38.14	86	50.4
5	BKL2	998	39.23	85	50.2
10	BKL3	1533	38.63	83	50.4
10	BLD2	1563	38.88	84	50.5
10	BLD3	1699	37.99	85	50.4
10	BKL2	1449	38.83	93	50.3
25	BKL3	2382	37.58	85	50.4
25	BKL2	2256	38	86	50.3
25	BLD2	2433	37.64	86	50.5
25	BLD3	2626	36.67	87	50.4

Confinement (kPa): 100

Target Temperature (oC) 35

0.5	BLD2	2023	34.85	100	34.7
0.5	BKL3	2028	35.22	100	34.6
0.5	BKL2	1937	35.49	99	34.6
0.5	BLD3	2198	34.24	99	34.6
1	BKL3	2688	34.53	96	34.9
1	BLD3	2888	33.65	96	34.8
1	BLD2	2694	34.11	96	34.9
1	BKL2	2563	34.99	97	35
5	BLD3	5115	30.02	91	35.1
5	BKL3	4820	30.78	91	35.1
5	BKL2	4694	31.36	91	35.4
5	BLD2	4871	30.14	91	35.1
10	BLD3	6307	28.25	92	35.2
10	BKL2	5841	29.41	92	35.5
10	BLD2	6016	28.34	92	35.3
10	BKL3	5967	29.08	92	35.2
25	BKL2	7523	26.79	93	35.4
25	BLD2	7694	25.9	92	35.4
25	BLD3	7990	25.86	94	35.3
25	BKL3	7653	26.6	91	35.4

Target Temperature (oC) 50

0.5	BLD3	548	29.95	99	49.4
0.5	BKL3	488	30.7	101	49.5
0.5	BKL2	446	30.68	99	49.5
0.5	BLD2	482	31.12	99	49.3
1	BLD2	606	33.89	98	49.8
1	BKL3	625	32.61	100	49.9
1	BKL2	551	33.82	97	49.9
1	BLD3	679	32.78	97	49.8
5	BKL3	1204	36.09	88	50.2
5	BLD3	1311	36.49	88	50.1
5	BLD2	1192	37.28	88	50.1



APS-fL Mix Properties and Dynamic Modulus Results

Report Number: RDM-12111

Page A91 of A95

5	BKL2	1068	37.85	87	50.3
10	BLD2	1646	37.72	86	50.2
10	BLD3	1793	37	86	50.2
10	BKL2	1475	38.64	85	50.4
10	BKL3	1637	36.87	86	50.3
25	BLD2	2496	36.73	88	50.4
25	BLD3	2699	36.05	88	50.3
25	BKL2	2261	37.92	87	50.5
25	BKL3	2452	36.38	87	50.4

Confinement (kPa): 200

Target Temperature (oC) 35

0.5	BLD3	2259	33.64	99	34.1
0.5	BLD2	2071	34.2	99	34
0.5	BKL2	2073	33.49	98	34.1
0.5	BKL3	2156	34.56	99	34.1
1	BLD3	2900	33.46	95	34.4
1	BKL2	2636	33.8	96	34.5
1	BKL3	2774	34.16	95	34.5
1	BLD2	2695	33.66	96	34.5
5	BLD2	4772	30.01	91	34.9
5	BKL3	4810	30.71	92	34.9
5	BKL2	4639	31	100	34.9
5	BLD3	5030	29.83	92	34.6
10	BLD2	5846	28.18	93	35.1
10	BLD3	6187	28.1	93	34.8
10	BKL2	5767	29.02	94	35.1
10	BKL3	5946	29	93	35.2
25	BLD3	7896	25.32	94	35
25	BKL2	7471	26.25	95	35.3
25	BKL3	7632	26.31	92	35.4
25	BLD2	7505	25.11	92	35.3

Target Temperature (oC) 50

0.5	BLD2	592	29.11	107	47.9
0.5	BKL3	619	28.27	105	48.6
0.5	BKL2	717	24.15	102	48.7
0.5	BLD3	681	27.39	99	47.8
1	BKL3	802	29.5	100	49.4
1	BLD2	744	30.66	99	49.2
1	BLD3	808	30.28	102	48.4
1	BKL2	854	26.53	99	49.4
5	BLD2	1335	34.52	90	49.8
5	BLD3	1388	34.23	90	49.9
5	BKL2	1358	31.95	91	49.9
5	BKL3	1388	33.21	90	49.9
10	BLD3	1834	35.37	92	50.1



APS-fL Mix Properties and Dynamic Modulus Results

Report Number: RDM-12111

Page A92 of A95

10	BKL3	1802	34.54	90	50.1
10	BLD2	1776	35.47	89	50
10	BKL2	1740	33.94	91	50.1
25	BKL3	2566	34.91	88	50.3
25	BLD3	2668	35.47	100	50.4
25	BKL2	2455	35.01	90	50.3
25	BLD2	2576	35.38	89	50.3



APS-fL Mix Properties and Dynamic Modulus Results

Report Number: RDM-12106

Page A93 of A95

Mix Details

AC/DG	14	Binder Content (%)	4.80
Aggregate Type:	Granite	VMA (%)	14.2
Binder Type	C320	Air Voids (%)	3.8
Mix Design Method	Marshall 75	VFB (%)	73
Filler Type	Hydrated Lime	Effective Bit. Content (%)	4.4
		RAP (%)	20

Gradation Percent Passing (%)

26.5mm	100	2.36mm
19mm		1.18mm
13.2mm		0.6mm
9.5mm		0.3mm
6.7mm		0.15mm
4.75mm		0.075mm

Dynamic Modulus Results

Frequency (Hz)	Specimen	Modulus (MPa)	Phase Angle (deg)	Strain με	Temperature (oC)
-------------------	----------	------------------	----------------------	--------------	---------------------

Confinement (kPa): 0

Target Temperature (oC) 5

0.5	BKM2	16840	12.1	97	5.1
0.5	BKM1	16698	12.41	98	5.1
1	BKM1	18285	11.13	92	5.1
1	BKM2	18169	10.98	92	5.1
5	BKM2	21234	9	76	5.1
5	BKM1	21794	8.77	75	5.1
10	BKM1	23229	8.08	68	5.1
10	BKM2	22432	8.3	70	5.1
25	BKM1	25022	7.29	58	5.1
25	BKM2	24014	7.7	60	5.1

Target Temperature (oC) 20

0.5	BKM 1	6180	27.47	99	19.9
0.5	BKM2	6468	26.53	98	19.9
1	BKM2	7648	24.59	94	20
1	BKM 1	7441	25.43	96	20
5	BKM2	10849	19.72	94	20
5	BKM 1	10726	20.19	95	20
10	BKM2	12233	17.92	93	20
10	BKM 1	12298	18.23	95	20
25	BKM2	14188	15.58	88	20
25	BKM 1	14409	15.95	90	20

Target Temperature (oC) 35

0.5	BKM2	1195	38.39	102	35.2
0.5	BKM1	1214	40.21	102	35.2
1	BKM1	1736	39.59	99	35.2

Report Date:

Monday, 21 September 2015



APS-fL Mix Properties and Dynamic Modulus Results

Report Number: RDM-12106

Page A94 of A95

1	BKM2	1721	37.73	100	35.3
5	BKM1	3590	34.81	97	35.2
5	BKM2	3650	33.81	89	35.3
10	BKM1	4613	33.03	89	35.2
10	BKM2	4773	32.08	88	35.3
25	BKM1	6132	30.45	88	35.1
25	BKM2	6390	30.04	87	35.3

Target Temperature (oC) 50

0.5	BKM1	194	35.72	102	50.1
0.5	BKM2	201	36.71	103	50.2
1	BKM2	283	39.04	105	50.2
1	BKM1	264	38.27	107	50.1
5	BKM2	705	41.56	79	50.1
5	BKM1	649	41.76	78	50.1
10	BKM2	1050	41.91	76	50.1
10	BKM1	983	41.66	84	50.1
25	BKM1	1626	40.74	81	50.1
25	BKM2	1798	39.61	84	50.1

Confinement (kPa): 50

Target Temperature (oC) 35

0.5	BKM2	1335	36	100	35.2
0.5	BKM1	1311	37.38	100	35
1	BKM1	1801	37.31	98	35.1
1	BKM2	1834	36.32	98	35.2
5	BKM2	3723	33.64	89	35.3
5	BKM1	3626	33.89	89	35.3
10	BKM2	4804	31.89	89	35.3
10	BKM1	4666	32.15	98	35.3
25	BKM2	6405	29.95	87	35.3
25	BKM1	6132	29.8	91	35.4

Target Temperature (oC) 50

0.5	BKM1	406	25.21	100	49.9
0.5	BKM2	470	24.59	97	49.9
1	BKM1	477	28.72	98	50.2
1	BKM2	538	28.67	97	50.1
5	BKM2	941	35.62	86	50.3
5	BKM1	841	35.44	84	50.3
10	BKM1	1115	37.56	81	50.4
10	BKM2	1256	37.58	84	50.4
25	BKM1	1697	38.36	84	50.4
25	BKM2	1919	37.82	87	50.4

Confinement (kPa): 100

Target Temperature (oC) 35

0.5	BKM1	1448	35.55	99	34.5
0.5	BKM2	1517	33.38	99	34.5



APS-fL Mix Properties and Dynamic Modulus Results

Report Number: RDM-12106

Page A95 of A95

1	BKM1	1923	36.2	97	34.8
1	BKM2	1987	34.43	97	34.8
5	BKM2	3812	32.75	90	35.1
5	BKM1	3809	32.13	80	35.1
10	BKM1	4762	31.94	91	35.2
10	BKM2	4872	31.32	90	35.2
25	BKM2	6452	29	89	35.4
25	BKM1	6322	29.44	91	35.4

Target Temperature (oC) 50

0.5	BKM2	650	20.77	99	49.4
0.5	BKM1	524	23.35	91	49.5
1	BKM1	548	28.16	106	50.1
1	BKM2	739	24.17	99	50
5	BKM2	1158	31.15	90	50.3
5	BKM1	969	32.18	88	50.4
10	BKM2	1469	33.71	88	50.5
10	BKM1	1256	34.13	86	50.6
25	BKM2	2086	35.61	86	50.5
25	BKM1	1790	36.08	83	50.6

Confinement (kPa): 200

Target Temperature (oC) 35

0.5	BKM1	1589	34.77	98	33.9
0.5	BKM2	1789	30.74	98	34
1	BKM2	2223	32.46	95	34.4
1	BKM1	2067	35.3	97	34.4
5	BKM1	3841	33.24	91	34.9
5	BKM2	3890	31.91	91	34.8
10	BKM1	4870	31.76	92	35.1
10	BKM2	4888	30.93	92	35.1
25	BKM2	6461	28.66	91	35.3
25	BKM1	6438	29.23	92	35.3

Target Temperature (oC) 50

0.5	BKM2	907	17.81	101	48.2
0.5	BKM1	672	22.82	101	48.6
1	BKM1	787	25.49	101	49.4
1	BKM2	1016	20.24	102	49.2
5	BKM2	1449	26.01	94	49.8
5	BKM1	1255	30.08	91	49.9
10	BKM2	1756	28.59	93	50.1
10	BKM1	1598	31.9	90	50.1
25	BKM1	2212	33.7	86	50.4
25	BKM2	2415	31.62	85	50.3

Appendix B RMS STEP FDA and PDA sites

UniqueID	Lat	Long	Location	Year of Construction	Year of Surfacing	Surface Condition	Comments on AC	Asphalt Condition	Overall Surface Condition	Cracking		Cumulative Traffic	Material Type				Thickness (mm)				Maintenance
										Type	Intensity		L2	L3	L4	L1	L2	L3	L4		
H-509_11	-32.5214	152.2019		1970	2002/03	Poor		Good	Good			2.3E+07	Fine to Coarse Gravel	Clayey Gravel	Gravelly Clay	150	250	200	750		
H-509_7	-32.5214	152.2019		1970	2002/03	Poor		Good	Poor	Nil patched		2.1E+07	Fine to Coarse Gravel	Clayey Gravel	Clay of high Plasticity, Fat	150	270	280	650		
H-511_10	-33.0635	151.5359		1970	2003	Marginal		Fair	Marginal	Nil rubber seal		6.7E+05	Fine to Coarse Gravel	Silty Sand	Clay	190	190	220	750		
H-511_13	-33.0636	151.5356		1970	2003	Marginal		Fair	Marginal	Nil, rubber seal		6.7E+05	Fine to Coarse Gravel	Clay	Clay	150	200	400	600		
H-515_14	-32.831	151.7302		1991	2003/04				Good			4.7E+06	Fine to Coarse Gravel	Fine to Coarse Gravel	Poorly Graded Sand	130	50	220	950		
H-518_6	-32.3027	150.9321		1990	2007/2007	Marginal			Marginal	Nil Sealed last		1.2E+07	Poorly Graded Gravel	Silty Sand	Clay	150	400	350	450		
H-522_1	-32.8128	151.6622		1970	2002	Good		Sound	Good	Nil		8.9E+07	Fine to Coarse Gravel	Poorly Graded Sand	Poorly Graded Sand	200	200	300	650		
H-522_3	-32.8129	151.662		1970	2002	Good		Sound	Good	Nil		8.9E+07	Fine to Coarse Gravel	Poorly Graded Sand	Poorly Graded Sand	210	190	300	650		
H-522_9	-32.813	151.6613		1970	2002	Good		Sound	Good	Nil		8.9E+07	Fine to Coarse Gravel	Poorly Graded Sand	Poorly Graded Sand	200	220	300	630		
H-523_1	-32.8115	151.668		1970	1993	Marginal		Fair	Marginal	Crocodyle	High	8.9E+07	Fine to Coarse Gravel	Poorly Graded Sand	Clay	220	230	90	810		
H-523_3	-32.8115	151.6678		1970	1993	Marginal		Fair	Marginal	Crocodyle	High	8.9E+07	Fine to Coarse Gravel	Poorly Graded Sand	Clay	200	250	270	630		
H-523_8	-32.8116	151.6673		1970	1993	Poor		Fair	Poor	Crocodyle	High	8.9E+07	Fine to Coarse Gravel	Fine to Coarse Gravel	Clay of high Plasticity, Fat	200	300	400	450		
H-524_13	-100	1000		1970	2003	Poor		Fair	Poor	Crocodyle	High	8.9E+07	Fine to Coarse Gravel	Fine to Coarse Gravel	Clay	155	345	170	680		
H-524_3	-100	1000		1970	2003	Marginal		Fair	Marginal	Crocodyle	Medium	8.9E+07	Fine to Coarse Gravel	(C)Clay	Clay	160	440	150	600		
H-524_7	-100	1000		1970	2003	Marginal		Fair	Marginal	Crocodyle	Medium	8.9E+07	Fine to Coarse Gravel	Fine to Coarse Gravel	Clay	165	435	100	650		
H-525_11	-33.5203	151.1964		1999	1999		AC fair to good	Good	Good	Nil		2.4E+07	Fine to Coarse Gravel	Fine to Coarse Gravel	Fine to Coarse Gravel	225	155	300	670		
H-525_14	-33.5201	151.1965		1999	1999			Fair	Fair	Nil		2.4E+07	Fine to Coarse Gravel	Fine to Coarse Gravel	Fine to Coarse Gravel	200	200	300	650		
H-525_19	-33.5197	151.1964		1999	1999			Fair	Fair	Nil		2.4E+07	Fine to Coarse Gravel	Fine to Coarse Gravel	Fine to Coarse Gravel	200	190	300	660		
H-527_13	-33.5095	151.1903		1990	1998	Marginal		Fair	Marginal	Nil		4.6E+07	Fine to Coarse Gravel	Fine to Coarse Gravel	Fine to Coarse Gravel	180	195	300	675		
H-527_16	-33.5093	151.1903		1990	1998	Marginal		Good	Marginal	Nil		4.6E+07	Fine to Coarse Gravel	Fine to Coarse Gravel	Fine to Coarse Gravel	200	200	300	650		
H-527_18	-33.5091	151.1902		1990	1998	Marginal		Good	Marginal	Nil		4.6E+07	Fine to Coarse Gravel	Fine to Coarse Gravel	Fine to Coarse Gravel	205	215	300	630		
H-528_12	-33.5345	151.1998		1990	1990					cracking and Nil		4.6E+07	Fine to Coarse Gravel	Fine to Coarse Gravel	Fine to Coarse Gravel	265	205	150	730		
H-528_16	-33.5342	151.1999		1990	1990					Nil		4.6E+07	Fine to Coarse Gravel	Fine to Coarse Gravel	Fine to Coarse Gravel	285	240	300	525		
H-528_18	-33.534	151.1999		1990	1990					Nil		4.6E+07	Fine to Coarse Gravel	Fine to Coarse Gravel	Fine to Coarse Gravel	265	235	300	550		
H-529_1	-100	1000		1989	2002		New AC	Good	Good	Nil		4.6E+07	Fine to Coarse Gravel	Fine to Coarse Gravel	Silty Sand	160	190	70	930		
H-529_10	-100	1000		1989	2002		New AC	Good	Good	Nil		4.6E+07	Fine to Coarse Gravel	Cobbles Gravel	Silty Sand	140	150	115	945		
H-529_9	-100	1000		1989	2002		New AC	Good	Good	Nil		4.6E+07	Fine to Coarse Gravel	Cobbles Gravel	Silty Sand	150	130	120	950		
H-530_12	-33.4084	151.4628		1986	1998	Good		Good	Good	Nil		4.7E+06	Fine to Coarse Gravel	Fine to Coarse Gravel	Silty Clay	215	155	180	800		
H-530_3	-33.4089	151.4621		1986	1998	Good		Good	Good	Nil		4.7E+06	Fine to Coarse Gravel	Fine to Coarse Gravel	Standstone Boulders	130	155	195	870		
H-530_6	-33.4088	151.4623		1986	1998	Good		Good	Good	Nil		4.7E+06	Fine to Coarse Gravel	Fine to Coarse Gravel	Silty Clay	192	138	60	960		
H-531_10	-33.3858	151.3542		1970	2006	Good		New	Good	Nil		1.3E+07	Fine to Coarse Gravel	AC	Silty Sand	170	165	80	935	recently resurfaced	
H-531_13	-33.3856	151.3543		1970	2006	Good		New	Good	Nil		1.3E+07	Fine to Coarse Gravel	AC	Silty Sand	150	110	25	1065	recently resurfaced	
H-532_11	-33.3921	151.3528		1995	2006	Good	Coal tar in	New	Good	Nil		7.4E+06	Fine to Coarse Gravel	Fine to Coarse Gravel	Silty Sand	165	140	95	950	recently resurfaced	
H-532_14	-33.3923	151.3525		1995	2006	Good		New	Good	Nil		7.4E+06	Fine to Coarse Gravel	Fine to Coarse Gravel	Silty Sand	155	108	140	950	recently resurfaced	
H-532_19	-33.3924	151.352		1995	2006	Good		New	Good	Nil		7.4E+06	Fine to Coarse Gravel	Fine to Coarse Gravel	Silty Sand	145	95	160	950	recently resurfaced	
H-534_14	-33.3934	151.4738		2006	2006	Good	Adjacent to	Good	Good	Nil		7.1E+05	Steel/Stone	Fine to Coarse Gravel	Fine to Coarse Gravel	210	210	210	720		
H-535_19	-33.0046	151.6435		1970	1994	Marginal		Fair	Marginal	Longitudinal	Medium	6.5E+06	Fine to Coarse Gravel	Gravelly Clay	Gravelly Clay	175	275	300	600		
H-539_11	-33.5346	151.1998		1990	2005/06	Poor		Poor	Poor	Crocodyle	Low	1.5E+07	Fine to Coarse Gravel	Fine to Coarse Gravel	Fine to Coarse Gravel	240	180	180	750		
H-539_6	-33.535	151.1997		1990	2005/06	Poor		Poor	Poor	Crocodyle	Low	1.5E+07	Fine to Coarse Gravel	Fine to Coarse Gravel	Fine to Coarse Gravel	240	330	300	480		
H-539_9	-33.5348	151.1998		1990	2005/06	Poor		Poor	Poor	Crocodyle	Low	1.5E+07	Fine to Coarse Gravel	Fine to Coarse Gravel	Fine to Coarse Gravel	260	210	150	730		
H-540_10	-32.7862	151.5224		1970	2001/02	Poor		Fair	Poor	Crocodyle	Medium	6.1E+06	Fine to Coarse Gravel	Fine to Coarse Gravel	Sandy Clay	130	210	160	850		
H-543_6	-32.5541	151.1521		1994	2000/01	Marginal		Marginal	Marginal	Transverse	Medium	9.0E+06	Poorly Graded Gravel	Clay	Clay	150	300	300	600		
H-548_11	-32.8456	151.6932		1970	2006/07	Excellent		Fair	Excellent	Nil		5.5E+07	Fine to Coarse Gravel	Clayey Gravel	Clay	130	370	250	600		
H-548_7	-32.8459	151.6934		1970	2006/07	Excellent		Poor	Excellent	Nil		5.5E+07	Fine to Coarse Gravel	Clayey Gravel	Clay	140	260	400	550		
H-548_8	-32.8458	151.6933		1970	2006/07	Excellent		Poor	Excellent	Nil		5.5E+07	Fine to Coarse Gravel	Clayey Gravel	Clay	130	245	425	450		
H-549_18	-32.8514	151.6981		1970	1997	Marginal		Fair	Marginal	Longitudinal	Low	5.5E+07	Fine to Coarse Gravel	Fine to Coarse Gravel	Silty Sand	140	710	100	600		
H-553_11	-32.8455	151.693		1970	2005/06	Marginal		Fair	Marginal	Block	Medium	2.0E+07	Fine to Coarse Gravel	Clayey Gravel	Clay	180	370	225	575		
H-553_15	-32.8452	151.6927		1970	2005/06	Marginal		Fair	Marginal	Block	Medium	2.0E+07	Fine to Coarse Gravel	Clayey Gravel	Clay	150	350	250	600		
H-553_7	-32.8458	151.6932		1970	2005/06	Marginal		Fair	Marginal	Block	Medium	2.0E+07	Fine to Coarse Gravel	Clayey Gravel	Fine to Coarse Gravel	185	265	400	500		
H-555_15	-32.8344	151.687		1970	2007	Marginal	Fushed	Fair	Marginal	Block	Medium	2.0E+07	Fine to Coarse Gravel	Poorly Graded Sand	Poorly Graded Sand	130	270	300	650		
H-563_16	-32.2066	150.465		1970	1999/00	Very poor		Very poor	Very poor	Block	High	3.2E+06	Poorly Graded Gravel	Poorly Graded Gravel	Poorly Graded Gravel	200	180	300	850		
H-566_1	-32.579	152.1287		1970	2002	Marginal		Fair	Marginal	Nil		4.2E+06	Fine to Coarse Gravel	Fine to Coarse Gravel	Sandy Gravelly Clay	140	60	320	830		
H-566_6	-32.5794	152.1286		1970	2002	Marginal		Fair	Marginal	Nil		4.2E+06	Fine to Coarse Gravel	Fine to Coarse Gravel	Clay	170	50	170	960		
N-542_5	-29.2641	153.2288		1989	2004	Marginal		Fair	Marginal	Crocodyle	Medium	7.6E+06	Conglomerate	Silty Clay	Silty Clay	130	220	300	700		
N-556_17	-28.8292	153.5294		1988	2000	Good		Good	Good	N.A		1.2E+07	Argillite	Argillite	Silty Sand	200	100	200	850		
N-556_21	-28.829	153.5291		1988	2000	Marginal		Very poor	Very poor	Block	Medium	1.2E+07	Argillite	Argillite	Silty Sand	200	100	200	850		
N-578_17	-28.8575	153.2615		1992	2005	Very poor	Some cracking	Poor	Very poor	Longitudinal	High	2.8E+06	Basalt DGB	Basalt	Clayey Sand	140	160	250	800	Nil	
N-578_20	-28.8578	153.2615		1992	2005	Very poor	Severe	Poor	Very poor	Longitudinal	High	2.8E+06	Basalt DGB	Basalt	Clayey Sand	130	230	240	750	Nil	
SOU-5011_2	-36.3466	148.5645		1966	1995, 14	Poor	2m cut. 200m	Poor	Poor			5.8E+05	Well Graded Sand, Fine to	Clayey Gravel	Clayey Gravel	150	70	300	830	-,-	
SOU-5025_12	-34.9317	150.6032		1963	1999, 14	Good		Good	Good	Nil		1.1E+07	Unbound	Unbound	Unbound	140	200	300	710	-,-	
SOU-5034_11	-34.3632	150.8589		1980	2004, AC	Excellent		Excellent	Excellent	Low		3.2E+07	0	0							

SOU-5067_15	-35.1598	150.448	1963	1994, AC	Marginal		Poor	Marginal	Longitudinal	Low	5.6E+06	Ironstone gravel	Sandstone	Sandstone	180	120	300	750	-
SOU-5067_8	-35.1593	150.4483	1963	1994, AC	Good		Good	Good	Crocodile	Low	5.6E+06	Ironstone gravel	Silty/Clayey gravel	Silty/Clayey gravel	180	270	300	600	-
SOU-5085_12	-34.7858	150.676	1963	1995, AC	Excellent		Good	Excellent	Longitudinal	Low	1.1E+07	Unbound	Gravelly clay	Gravelly clay	220	100	300	730	1995, AC OVERLAY (> 50MM)
SOU-5085_18	-34.7863	150.6756	1963	1995, AC	Good		Good	Good	Longitudinal	Medium	1.1E+07	Unbound	Sandy/Silty clay	Sandy/Silty clay	225	75	300	750	1995, AC OVERLAY (> 50MM)
SOU-5085_8	-34.7855	150.6762	1963	1995, AC	Good		Good	Good	Longitudinal	Low	1.1E+07	Unbound	Gravelly clay	Gravelly clay	210	90	300	750	1995, AC OVERLAY (> 50MM)
SOU-5086_12	-34.7499	150.7796	1969	1997, AC	Very poor		Very poor	Very poor	Crocodile	High	9.1E+06	Unbound	Gravelly clay	Gravelly clay	185	165	300	700	-
SOU-5086_4	-34.7495	150.7789	1969	1997, AC	Poor		Poor	Poor	Crocodile	High	9.1E+06	Unbound	Gravelly clay	Gravelly clay	200	200	300	650	-
SOU-5086_9	-34.7498	150.7793	1969	1997, AC	Very poor		Very poor	Very poor	Crocodile	High	9.1E+06	Unbound	Gravelly clay	Gravelly clay	160	200	300	690	-
SOU-5087_10	-34.7496	150.7939	2000	1997, AC	Marginal		Good	Marginal	Block	Medium	1.8E+06	Domb base	Clayey Gravel	Clayey Gravel	200	185	300	665	-
SOU-5087_15	-34.7496	150.7934	2000	1997, AC	Poor		Poor	Poor	Crocodile	Medium	1.8E+06	DGB 20	Bound base	Sandy/ Silty clay	180	100	200	870	-
SOU-5087_8	-34.7496	150.7942	2000	1997, AC	Very poor		Fair	Very poor	Crocodile	High	1.8E+06	Bound base	Clayey Gravel	Clayey Gravel	140	140	300	770	-
SOU-5088_11	-35.0804	150.5243	1984	1993, AC	Excellent		Good	Excellent	Longitudinal	Nil	3.0E+06	Gravelly clay	Silty Gravelly clay	Silty Gravelly clay	290	110	300	650	1993, AC OVERLAY (> 50MM)
SOU-5088_18	-35.0804	150.5251	1984	1993, AC	Excellent		Good	Excellent	Longitudinal	Nil	3.0E+06	Gravelly clay	Crushed rock	Crushed rock	210	200	300	640	1993, AC OVERLAY (> 50MM)
SOU-5088_6	-35.0804	150.5238	1984	1993, AC	Excellent		Good	Excellent	Longitudinal	Nil	3.0E+06	Gravelly clay	Silty clayey gravel	Silty clay	295	105	150	800	1993, AC OVERLAY (> 50MM)
SOU-5089_12	-35.212	150.4362	1985	1997, AC	Marginal		Poor	Marginal	Transverse	Medium	2.9E+06	Gravelly clay	Silty Sandstone	Silty Sandstone	260	200	300	590	1997, AC M & R >50MM
SOU-5089_14	-35.2122	150.4361	1985	1997, AC	Poor		Poor	Poor	Crocodile	High	2.9E+06	Gravelly clay	Silty Sandstone	Silty Sandstone	240	120	300	690	1997, AC M & R >50MM
SOU-5089_19	-35.2126	150.4359	1985	1997, AC	Poor		Poor	Poor	Crocodile	High	2.9E+06	Gravelly clay	Silty Sandstone	Silty Sandstone	130	120	140	960	1997, AC M & R >50MM
SOU-5090_12	-35.2141	150.4353	1985	1997, AC	Marginal		Fair	Marginal	Transverse	High	2.9E+06	Sandstone gravel	Sandstone	Sandstone	235	235	300	580	1997, AC M & R >50MM
SOU-5090_6	-35.2136	150.4355	1985	1997, AC	Very poor		Very poor	Very poor	Block	Medium	2.9E+06	Sandstone gravel	Sandstone	Sandstone	140	190	300	720	1997, AC M & R >50MM
SOU-5090_8	-35.2138	150.4354	1985	1997, AC	Poor		Poor	Poor	Longitudinal	High	2.9E+06	Sandstone gravel	Sandy clay	Sandy clay	155	315	300	580	1997, AC M & R >50MM
SW-553_11	-34.7735	148.8188	2003	2003	Excellent		Excellent	Excellent	Nil	6.6E+06	Poorly Graded Gravel	Clayey Gravel	Clayey Gravel	150	380	270	550	0	
SW-553_15	-34.7735	148.8192	2003	2003	Excellent		Excellent	Excellent	Nil	6.6E+06	Poorly Graded Gravel	Clayey Gravel	Clayey Gravel	150	350	300	550	0	
SW-553_20	-34.7735	148.8197	2003	2003	Excellent		Excellent	Excellent	Nil	6.6E+06	Heavily bound silty sandy	Clayey Gravel	Clayey Gravel	150	400	250	550	0	
SW-555_18	-100	1000	1958	2003	Excellent		Excellent	Excellent	Nil	6.5E+06	Poorly Graded Gravel	AC	Poorly Graded Gravel	210	350	30	760	1991	
SW-555_4	-34.9042	148.1898	1958	2003	Excellent		Excellent	Excellent	Nil	6.5E+06	Poorly Graded Gravel	Primer seal	Poorly Graded Gravel	150	170	10	1020	1991	
SW-555_8	-34.9044	148.1894	1958	2003	Excellent		Excellent	Excellent	Nil	6.5E+06	Poorly Graded Gravel	Poorly Graded Gravel	Poorly Graded Gravel	240	200	300	610	1991	
SW-558_10	-35.2181	147.7888	1995	1995	Good		Good	Good	Crocodile	Medium	4.6E+06	Clayey Gravel	Clayey Gravel	180	200	300	670	0	
SW-558_3	-35.2181	147.7906	1995	1995	Good		Good	Good	Crocodile	Minor	4.6E+06	Clayey Gravel	Clayey Gravel	160	200	300	690	0	
SW-558_8	-35.2181	147.79	1995	1995	Good		Good	Good	Crocodile	Medium	4.6E+06	Clayey Gravel	Clayey Gravel	160	200	300	690	0	
SW-559_11	-100	1000	2003	2003	Excellent		Excellent	Excellent	Nil	2.3E+05	Sandstone	Sandstone	Sandstone	260	200	300	590	0	
SW-559_14	-100	1000	2003	2003	Excellent		Excellent	Excellent	Nil	2.3E+05	Sandstone	Sandstone	Sandstone	250	200	300	600	0	
SW-559_8	-34.7736	148.8184	2003	2003	Excellent		Excellent	Excellent	Nil	2.3E+05	Sandstone	Sandstone	Sandstone	240	200	300	610	0	
SYD-501_13	-33.6736	150.7495	1971	1971	Poor		Poor	Poor	Nil	1.3E+07	Silty Sand	Clay	Clay	230	340	130	650	1971	
SYD-501_2	-33.6728	150.7503	1971	1971	Marginal		Marginal	Marginal	Nil	1.3E+07	Poorly Graded Gravel	Clay	Clay	160	350	370	470	1971	
SYD-501_8	-33.6732	150.7498	1971	1971	Marginal		Marginal	Marginal	Nil	1.3E+07	Poorly Graded Sand	Clay	Clay	220	320	300	510	1971	
SYD-502_24	-33.6538	150.7728	1971	1971	Good		Good	Good	Nil	1.1E+07	Silty Sand	Silty Sand	Clay of high Plasticity, Fat	150	150	240	810	1971	
SYD-503_12	-33.6827	150.7395	1971	1971	Poor		Poor	Poor	Longitudinal	Low	1.1E+07	Silty Sand	Clay	Clay	200	410	170	570	1971
SYD-503_20	-33.6822	150.7401	1971	1971	Poor		Poor	Poor	Longitudinal	High	1.1E+07	Silty Sand	Clay	Clay	180	520	300	350	1971
SYD-503_23	-33.682	150.7403	1971	1971	Poor		Poor	Poor	Nil	1.1E+07	Well Graded Sand, Fine to	Silty Sand	Silty Sand	180	180	140	850	1971	
SYD-505_12	-33.7973	150.65	1996	1996	Poor		Poor	Poor	Nil	2.1E+06	Fine to Coarse Gravel	Clay	Clay	170	110	300	770	1996	
SYD-507_5	-33.6852	150.6736	1979	1979	Good		Good	Good	Nil	4.1E+06	Well Graded Sand, Fine to	Clay	Clay	130	130	170	920	1979	
SYD-507_7	-33.685	150.6736	1979	1979	Good		Good	Good	Nil	4.1E+06	Well Graded Sand, Fine to	Clay	Clay	130	150	380	690	1979	
SYD-510_11	-33.9643	151.2222	1977	1977	Good		Good	Good	Transverse	Low	1.7E+07	Fine to Coarse Gravel	Poorly Graded Sand	Poorly Graded Sand	240	340	320	450	1977
SYD-510_3	-33.9647	151.2229	1977	1977	Nil		Nil	Nil	Nil	1.7E+07	Fine to Coarse Gravel	Poorly Graded Sand	Poorly Graded Sand	230	300	370	450	1977	
SYD-510_7	-33.9645	151.2226	1977	1977	Nil		Nil	Nil	Nil	1.7E+07	Fine to Coarse Gravel	Poorly Graded Sand	Poorly Graded Sand	230	300	370	450	1977	
SYD-511_1	-33.9649	151.2231	1977	1977	Nil		Nil	Nil	Nil	3.4E+07	Fine to Coarse Gravel	Poorly Graded Sand	Poorly Graded Sand	205	355	300	490	1977	
SYD-511_12	-33.9643	151.2221	1977	1977	Marginal		Marginal	Marginal	Longitudinal	Medium	3.4E+07	Fine to Coarse Gravel	Poorly Graded Sand	Poorly Graded Sand	180	350	300	520	1977
SYD-511_6	-33.9646	151.2227	1977	1977	Marginal		Marginal	Marginal	Cannot see	3.4E+07	Fine to Coarse Gravel	Poorly Graded Sand	Poorly Graded Sand	190	340	420	400	1977	
SYD-512_16	-34.0201	151.0904	1988	1988	Good		Good	Good	Nil	4.3E+06	Poorly Graded Gravel	Fine to Coarse Gravel	Silty Gravel	220	80	120	930	1988	
SYD-512_6	-34.0192	151.0905	1988	1988	Marginal		Marginal	Marginal	Longitudinal	Medium	4.3E+06	Poorly Graded Gravel	Silty Sand	Clay	260	310	360	510	1988
SYD-512_9	-34.0195	151.0905	1988	1988	Marginal		Marginal	Marginal	Longitudinal	Medium	4.3E+06	Poorly Graded Gravel	Silty Sand	Clay	230	190	160	770	1988
SYD-513_4	-34.0233	150.8244	1973	1973	Good		Good	Good	Nil	1.1E+08	Fine to Coarse Gravel	Clay	Clay	260	160	180	750	1973	
SYD-513_7	-34.023	150.8244	1973	1973	Good		Good	Good	Nil	1.1E+08	Fine to Coarse Gravel	Clay	Clay	270	160	220	700	1973	
SYD-514_11	-33.9331	151.0025	1966	1966	Marginal		Marginal	Marginal	Transverse	High	3.6E+07	Fine to Coarse Gravel	Fine to Coarse Gravel	Clayey Sand	180	120	400	650	1966
SYD-514_17	-33.9328	151.0019	1966	1966	Good		Good	Good	Nil	3.6E+07	Fine to Coarse Gravel	Fine to Coarse Gravel	Clayey Sand	150	220	430	550	1966	
SYD-515_15	-34.0267	150.8243	1973	1973	Good		Good	Good	Nil	1.1E+08	Fine to Coarse Gravel	Clay	Clay	295	175	330	550	1973	
SYD-515_18	-34.0264	150.8243	1973	1973	Good		Good	Good	Nil	1.1E+08	Fine to Coarse Gravel	Clay	Clay	305	165	230	650	1973	
SYD-515_20	-34.0263	150.8243	1973	1973	Good		Good	Good	Nil	1.1E+08	Fine to Coarse Gravel	Clay	Clay	300	150	350	550	1973	
SYD-516_3	-33.9311	150.9969	1966	1966	Very poor		Very poor	Very poor	Crocodile	High	3.6E+07	Fine to Coarse Gravel	Poorly Graded Gravel	Poorly Graded Gravel	130	190	380	650	1966
SYD-516_8	-33.931	150.9963	1966	1966	Very poor		Very poor	Very poor	Crocodile	High	3.6E+07	Fine to Coarse Gravel	Poorly Graded Gravel	Poorly Graded Gravel	145	235	300	670	1966
SYD-517_12	55.66537	12.38582	1960	1960	Good		Good	Good	Transverse	Medium	2.8E+07	Poorly Graded Gravel	Poorly Graded Gravel	340	200	300	510	1960	
SYD-517_4	55.66537	12.38582	1960	1960	Marginal		Marginal	Marginal	Longitudinal	Medium	2.8E+07	Poorly Graded Gravel	Clay	Clay	360	140	300	550	1960
SYD-517_8	55.66537	12.38582	1960	1960	Good		Good	Good	Transverse	Medium	2.8E+07	Poorly Graded Gravel	Clay	Clay	350	200	300	500	1960
SYD-518_12	-33.7074	151.1828	1988	1988	Good		Good	Good	Nil	1.3E+07	Fine to Coarse Gravel	Clayey Sand	Poorly Graded Sand	155	125	420	650	1988	
SYD-518_15	-33.7074	151.1825	1988	1988	Good		Good	Good	Nil	1.3E+07	Fine to Coarse Gravel	Clayey Sand	Poorly Graded Sand	160	140	310	740	1988	
SYD-518_18	-33.7075	151.1822	1988	1988	Good		Good	Good	Nil	1.3E+07	Fine to Coarse Gravel	Clayey Sand	Clayey Sand	160	170	370	650	1988	
SYD-521_1	-33.972	151.1514	1979	1979	Good		Good	Good	Nil	1.5E+07	Poorly Graded Gravel	Poorly Graded Sand	Poorly Graded Sand	130	200	470	550	1979	
SYD-521_5	-33.9724	151.1513	1979	1979	Good		Good	Good	Nil	1.5E+07	Poorly Graded Gravel	Poorly Graded Sand	Poorly Graded Sand	150	200	450	550	1979	
SYD-521_9	-33.9728	151.1512	1979	1979	Good		Good	Good	Nil	1.5E+07	Poorly Graded Gravel	Poorly Graded Sand	Poorly Graded Sand	140	170	590	450	1979	
SYD-522_10	-33.8905	151.0389	1999	1999	Good		Good	Good	Nil	4.8E+06	Fine to Coarse Gravel	Poorly Graded Gravel	Poorly Graded Gravel	490	110	300	450	1999	
SYD-522_14	-33.8901	151.0389	1999	1999	Good		Good	Good	Nil	4.8E+06	Fine to Coarse Gravel	Poorly Graded Gravel	Poorly Graded						

SYD-530_3	-33.6859	151.3043	1985	1985	Poor			Poor	Crocodile		High	6.8E+06	Fine to Coarse Gravel	Clayey Sand	Clay	140	140	320	750	1985
SYD-530_9	-33.6864	151.3044	1985	1985	Poor			Poor	Crocodile		High	6.8E+06	Fine to Coarse Gravel	Clay	Clay	140	210	550	450	1985
SYD-531_13	-33.8902	151.0339	1999	1999	Good			Good		Nil		4.7E+06		Poorly Graded Gravel	Poorly Graded Gravel	450	200	300	400	1999
SYD-531_5	-33.8909	151.0388	1999	1999	Good			Good		Nil		4.7E+06		Poorly Graded Gravel	Poorly Graded Gravel	480	200	300	370	1999
SYD-531_9	-33.8906	151.0389	1999	1999	Good			Good		Nil		4.7E+06		Poorly Graded Gravel	Poorly Graded Gravel	450	200	300	400	1999
SYD-532_15	-33.9707	151.1519	1979	1979	Good			Good		Nil		8.8E+06		Poorly Graded Sand	Poorly Graded Sand	150	210	740	250	1979
SYD-532_19	-33.971	151.1517	1979	1979	Good			Good		Nil		8.8E+06	Cobblestone	Poorly Graded Sand	Poorly Graded Sand	140	240	620	350	1979
SYD-532_7	-33.97	151.1522	1979	1979	Good			Good		Nil		8.8E+06	Cobblestone	Poorly Graded Sand	Poorly Graded Sand	140	220	540	450	1979
SYD-533_12	-33.9645	151.2315	1960	1960	Poor			Poor	Crocodile			1.2E+07	Fine to Coarse Gravel	Clayey Sand	Poorly Graded Sand	130	310	360	550	1960
SYD-533_2	-33.9636	151.2317	1960	1960	Poor			Poor	Crocodile		High	1.2E+07	Fine to Coarse Gravel	Poorly Graded Sand	Poorly Graded Sand	140	310	130	770	1960
SYD-533_6	-33.9639	151.2317	1960	1960	Poor			Poor	Crocodile			1.2E+07	Fine to Coarse Gravel	Poorly Graded Sand	Poorly Graded Sand	150	330	320	550	1960
SYD-534_11	-34.0184	151.0906	1998	1998	Very poor		Very poor	Very poor	Crocodile		High	2.0E+06	Fine to Coarse Gravel	Poorly Graded Gravel	Clay	150	70	160	970	1998
SYD-534_3	-34.0191	151.0904	1998	1998	Poor			Poor	Crocodile		Medium	2.0E+06	Fine to Coarse Gravel	Silty Sand	Clay of high Plasticity, Fat	170	50	240	890	1998
SYD-534_9	-34.0186	151.0905	1998	1998	Poor			Poor	Crocodile		Medium	2.0E+06	Fine to Coarse Gravel	Poorly Graded Gravel	Clay	160	50	290	850	1998
SYD-536_2	-33.9298	151.1094	1999	1999	Poor			Poor	Crocodile		Medium	2.6E+06	Poorly Graded Gravel	Clay	Clay	170	150	150	880	1999
SYD-536_5	-33.9301	151.1095	1999	1999	Very poor		Very poor	Very poor	Crocodile		High	2.6E+06	Poorly Graded Gravel	Clay	Clay	200	70	70	1010	1999
SYD-536_7	-33.9302	151.1095	1999	1999	Marginal		Marginal	Marginal		Nil		2.6E+06	Fine to Coarse Gravel	Clay	Clay	130	230	380	610	1999
SYD-537_11	-33.6855	151.3041	1985	1985	Good			Good		Nil		2.5E+06	Fine to Coarse Gravel	Clay	Clay	300	300	300	450	1985
SYD-537_15	-33.6852	151.304	1985	1985	Good			Good		Nil		2.5E+06	Fine to Coarse Gravel	Clay	Clay	320	180	300	550	1985
SYD-537_3	-33.6862	151.3042	1985	1985	Good			Good		Nil		2.5E+06	Fine to Coarse Gravel	Clay	Clay	320	180	300	550	1985
SYD-538_11	-33.6731	151.3124	1985	1985	Nil			Nil		Nil		1.2E+06	Fine to Coarse Gravel	Clayey Sand	Clay	230	70	200	850	1985
SYD-538_2	-33.6736	151.3116	1985	1985	Nil			Nil		Nil		1.2E+06	Fine to Coarse Gravel	Clay	Clay	220	180	300	650	1985
SYD-538_7	-33.6733	151.3121	1985	1985	Nil			Nil		Nil		1.2E+06	Fine to Coarse Gravel	Clay	Clay	230	140	230	750	1985
SYD-539_16	-33.673	151.3123	1985	1985	Nil			Nil		Nil		5.3E+06	Fine to Coarse Gravel	Clay	Clay	190	110	200	850	1985
SYD-539_18	-33.6729	151.3124	1985	1985	Nil			Nil		Nil		5.3E+06	Fine to Coarse Gravel	Clay	Clay	205	95	300	750	1985
SYD-539_7	-33.6735	151.3116	1985	1985	Nil			Nil		Nil		5.3E+06	Fine to Coarse Gravel	Clayey Sand	Clay	210	90	200	850	1985
SYD-540_10	-33.7322	150.4652	1994	1994	Good			Good		Nil		9.7E+06		Fine to Coarse Gravel (GW)	Fine to Coarse Gravel	190	200	300	660	1994
SYD-540_2	-33.7316	150.4648	1994	1994	Good			Good		Nil		9.7E+06		Clayey Sand	Clayey Sand	190	710	300	150	1994
SYD-540_7	-33.7319	150.465	1994	1994	Good			Good		Nil		9.7E+06		Fine to Coarse Gravel	Fine to Coarse Gravel	210	200	300	640	1994
SYD-543_16	-33.9575	151.0731	1972	1972	Good			Good		Nil		1.1E+07	Poorly Graded Gravel	Silty clay CI /Clay of high	Clay	220	230	200	700	1972
SYD-543_4	-33.9577	151.0719	1972	1972	Good			Good		Nil		1.1E+07		0	0	210	200	300	640	1972
SYD-543_9	-33.9576	151.0724	1972	1972	Good			Good		Nil		1.1E+07	Poorly Graded Gravel	Clay	Clay of high Plasticity, Fat	220	100	230	800	1972
SYD-544_18	-33.9772	151.1366	1966	1966	Very poor		Very poor	Very poor	Crocodile		High	1.2E+07	Fine to Coarse Gravel	Poorly Graded Sand	Poorly Graded Sand	130	290	360	570	1966
SYD-544_20	-33.977	151.1366	1966	1966	Very poor		Very poor	Very poor	Crocodile			1.2E+07	Fine to Coarse Gravel	Poorly Graded Sand	Poorly Graded Sand	150	300	450	450	1966
SYD-545_14	-33.9575	151.0729	1972	1972	Good			Good		Nil		4.1E+06	Fine to Coarse Gravel	Poorly Graded Sand	Poorly Graded Sand	250	300	300	500	1972
SYD-545_5	-33.9577	151.072	1972	1972	Good			Good		Nil		4.1E+06	Fine to Coarse Gravel	Poorly Graded Sand	Poorly Graded Sand	190	390	300	470	1972
SYD-545_8	-33.9576	151.0723	1972	1972	Good			Good		Nil		4.1E+06	Fine to Coarse Gravel	Poorly Graded Sand	Poorly Graded Sand	250	300	300	500	1972
SYD-546_12	-33.9778	151.1366	1966	1966	Very poor		Very poor	Very poor	Crocodile		High	1.6E+07	Fine to Coarse Gravel	Poorly Graded Sand	Poorly Graded Sand	160	210	130	850	1966
SYD-546_3	-33.9769	151.1366	1966	1966	Very poor		Very poor	Very poor	Crocodile		High	1.6E+07	Poorly Graded Gravel	Poorly Graded Sand	Poorly Graded Sand	150	270	100	830	1966
SYD-546_6	-33.9772	151.1366	1966	1966	Very poor		Very poor	Very poor	Crocodile		High	1.6E+07	Poorly Graded Gravel	Poorly Graded Sand	Poorly Graded Sand	160	240	70	880	1966
W-563_10	-33.4129	149.5764	2002	2002					Crocodile				Clayey Sand	Clay	Clay	150	150	300	750	1995
W-563_6	-33.4127	149.5767	2002	2002						Nil			Clayey Sand	Clay	Clay	150	150	300	750	1995
W-564_5	-33.4122	149.5771	2002	2002					Crocodile				Clayey Sand	Clay	Clay	150	300	300	600	1995

Appendix C Confidence Interval Calculations

Temperature Shift Factors

a b
0.00067 -0.110002455

Se (log) 0.063

Master Curve Parameters

α β γ δ
0.977794 3.445824287 -0.8274485 -0.50166

R² Log 0.99

R² (Arith) 0.93

Se (Arith) 1468

Observations 80

Binder Type	Nominal Size (mm)	Confinement (KPa)	Frequency (Hz)	Modulus (MPa)	Test Temp (oC)	(Log) Modulus			Adjusted α for Confidence		
						Predicted	Measured	Error (log)	0.978	0.935	0.873
A15E	14	0	0.5	158	50.4	2.27	2.20	-0.07	187	170	147
A15E	14	0	0.5	186	50.4	2.27	2.27	0.00	187	170	147
A15E	14	0	0.5	225	50.2	2.28	2.35	0.07	190	172	149
A15E	14	0	0.5	226	50.2	2.28	2.35	0.08	190	172	149
A15E	14	0	1	234	50.5	2.39	2.37	-0.02	247	224	194
A15E	14	0	1	204	50.4	2.40	2.31	-0.09	249	226	196
A15E	14	0	1	269	50.2	2.40	2.43	0.03	253	229	198
A15E	14	0	1	271	50.2	2.40	2.43	0.03	253	229	198
A15E	14	0	5	460	50.6	2.69	2.66	-0.03	488	442	383
A15E	14	0	5	496	50.2	2.70	2.70	-0.01	503	456	395
A15E	14	0	5	509	50.2	2.70	2.71	0.01	503	456	395
A15E	14	0	5	450	50.1	2.70	2.65	-0.05	507	459	398
A15E	14	0	10	626	50.6	2.82	2.80	-0.02	658	597	517
A15E	14	0	0.5	623	35.3	2.82	2.79	-0.03	667	605	524
A15E	14	0	0.5	740	35.3	2.82	2.87	0.04	667	605	524
A15E	14	0	0.5	670	35.2	2.83	2.83	0.00	674	611	529
A15E	14	0	0.5	690	35.2	2.83	2.84	0.01	674	611	529
A15E	14	0	10	674	50.2	2.83	2.83	0.00	678	615	533
A15E	14	0	10	701	50.2	2.83	2.85	0.01	678	615	533
A15E	14	0	10	618	50	2.84	2.79	-0.05	689	624	541
A15E	14	0	1	818	35.4	2.95	2.91	-0.04	889	805	698
A15E	14	0	1	900	35.3	2.95	2.95	0.00	897	813	704
A15E	14	0	1	975	35.3	2.95	2.99	0.04	897	813	704
A15E	14	0	1	862	35.2	2.96	2.94	-0.02	905	821	711
A15E	14	0	25	989	50.5	2.99	3.00	0.00	979	888	769
A15E	14	0	25	1090	50.2	3.00	3.04	0.04	1001	907	786
A15E	14	0	25	1132	50.1	3.00	3.05	0.05	1009	914	792
A15E	14	0	25	982	50	3.01	2.99	-0.01	1016	921	798
A15E	14	0	5	1574	35.4	3.23	3.20	-0.04	1716	1555	1347
A15E	14	0	5	1697	35.4	3.23	3.23	0.00	1716	1555	1347
A15E	14	0	5	1800	35.3	3.24	3.26	0.02	1730	1568	1359
A15E	14	0	5	1983	35.2	3.24	3.30	0.06	1745	1582	1371
A15E	14	0	10	2022	35.4	3.35	3.31	-0.04	2234	2025	1754
A15E	14	0	10	2170	35.4	3.35	3.34	-0.01	2234	2025	1754
A15E	14	0	10	2450	35.3	3.35	3.39	0.04	2252	2041	1769
A15E	14	0	10	2662	35.2	3.36	3.43	0.07	2271	2058	1783
A15E	14	0	0.5	2720	20.2	3.46	3.43	-0.03	2897	2626	2275
A15E	14	0	0.5	2533	20	3.47	3.40	-0.07	2952	2675	2318
A15E	14	0	0.5	3245	20	3.47	3.51	0.04	2952	2675	2318
A15E	14	0	0.5	3280	20	3.47	3.52	0.05	2952	2675	2318
A15E	14	0	25	2763	35.4	3.49	3.44	-0.05	3097	2807	2432
A15E	14	0	25	2953	35.4	3.49	3.47	-0.02	3097	2807	2432
A15E	14	0	25	3613	35.3	3.49	3.56	0.06	3120	2828	2450
A15E	14	0	25	3848	35.2	3.50	3.59	0.09	3144	2849	2469
A15E	14	0	1	3265	20.2	3.56	3.51	-0.05	3657	3314	2872
A15E	14	0	1	3116	20	3.57	3.49	-0.08	3721	3372	2922

A15E	14	0	1	4145	20	3.57	3.62	0.05	3721	3372	2922
A15E	14	0	1	4141	19.9	3.57	3.62	0.04	3753	3401	2947
A15E	14	0	5	4910	20.2	3.77	3.69	-0.08	5879	5328	4616
A15E	14	0	5	4810	20	3.78	3.68	-0.09	5963	5404	4682
A15E	14	0	5	6803	20	3.78	3.83	0.06	5963	5404	4682
A15E	14	0	5	6864	20	3.78	3.84	0.06	5963	5404	4682
A15E	14	0	10	5737	20.2	3.85	3.76	-0.09	7008	6352	5503
A15E	14	0	10	5653	20	3.85	3.75	-0.10	7100	6434	5575
A15E	14	0	10	8067	20	3.85	3.91	0.06	7100	6434	5575
A15E	14	0	10	8191	20	3.85	3.91	0.06	7100	6434	5575
A15E	14	0	25	6980	20.2	3.94	3.84	-0.09	8618	7810	6767
A15E	14	0	25	6903	20	3.94	3.84	-0.10	8715	7899	6844
A15E	14	0	25	9928	20	3.94	4.00	0.06	8715	7899	6844
A15E	14	0	25	10128	20	3.94	4.01	0.07	8715	7899	6844
A15E	14	0	0.5	7697	5.4	3.97	3.89	-0.08	9339	8464	7333
A15E	14	0	0.5	12101	5.1	3.98	4.08	0.10	9513	8622	7470
A15E	14	0	0.5	11783	5	3.98	4.07	0.09	9571	8674	7516
A15E	14	0	0.5	8604	4.9	3.98	3.93	-0.05	9630	8727	7562
A15E	14	0	1	8613	5.4	4.03	3.94	-0.09	10629	9633	8347
A15E	14	0	1	13264	5.1	4.03	4.12	0.09	10806	9794	8485
A15E	14	0	1	13569	5.1	4.03	4.13	0.10	10806	9794	8485
A15E	14	0	1	9609	4.8	4.04	3.98	-0.06	10983	9954	8625
A15E	14	0	5	10765	5.4	4.13	4.03	-0.10	13617	12341	10693
A15E	14	0	5	16647	5.1	4.14	4.22	0.08	13788	12496	10827
A15E	14	0	5	17106	5.1	4.14	4.23	0.09	13788	12496	10827
A15E	14	0	5	11905	4.8	4.14	4.08	-0.07	13958	12650	10960
A15E	14	0	10	11745	5.4	4.17	4.07	-0.10	14849	13458	11660
A15E	14	0	10	18125	5.1	4.18	4.26	0.08	15013	13606	11789
A15E	14	0	10	18557	5.1	4.18	4.27	0.09	15013	13606	11789
A15E	14	0	10	12895	4.8	4.18	4.11	-0.07	15176	13754	11917
A15E	14	0	25	12984	5.4	4.21	4.11	-0.10	16388	14853	12869
A15E	14	0	25	19981	5.1	4.22	4.30	0.08	16540	14990	12988
A15E	14	0	25	20519	5.1	4.22	4.31	0.09	16540	14990	12988
A15E	14	0	25	14164	4.8	4.22	4.15	-0.07	16690	15127	13106

Appendix C Confidence Interval Calculations

Temperature Shift Factors

a b
0.000409 -0.106985082

Se (log) 0.117

Master Curve Parameters

α β γ δ
1.218 3.184 -1.287 -0.676

R² Log 0.98

R² (Arith) 0.97

Se (Arith) 4722

Observations 353

Binder Type	Nominal Size (mm)	Confinement (KPa)	Frequency (Hz)	Modulus (MPa)	Test Temp (oC)	(Log) Modulus			Adjusted α for Confidence		
						Predicted	Mesured	Error (log)	1.218	1.139	1.024
C320	14	0	0.5	241	50.6	2.36	2.38	0.03	227	189	145
C320	14	0	0.5	245	50.4	2.36	2.39	0.03	231	193	148
C320	14	0	0.5	204	50.3	2.37	2.31	-0.06	233	194	149
C320	14	0	0.5	206	50.3	2.37	2.31	-0.05	233	194	149
C320	14	0	0.5	326	50.3	2.37	2.51	0.15	233	194	149
C320	14	0	0.5	177	50.2	2.37	2.25	-0.12	236	196	151
C320	14	0	0.5	201	50.2	2.37	2.30	-0.07	236	196	151
C320	14	0	0.5	220	50.2	2.37	2.34	-0.03	236	196	151
C320	14	0	0.5	325	50.2	2.37	2.51	0.14	236	196	151
C320	14	0	0.5	338	50.2	2.37	2.53	0.16	236	196	151
C320	14	0	0.5	138	50.1	2.38	2.14	-0.24	238	198	152
C320	14	0	0.5	156	50.1	2.38	2.19	-0.18	238	198	152
C320	14	0	0.5	194	50.1	2.38	2.29	-0.09	238	198	152
C320	14	0	0.5	230	50.1	2.38	2.36	-0.01	238	198	152
C320	14	0	0.5	260	50.1	2.38	2.41	0.04	238	198	152
C320	14	0	0.5	129	50	2.38	2.11	-0.27	240	200	154
C320	14	0	0.5	238	50	2.38	2.38	0.00	240	200	154
C320	14	0	0.5	240	50	2.38	2.38	0.00	240	200	154
C320	14	0	1	358	50.6	2.51	2.55	0.05	322	268	206
C320	14	0	1	365	50.6	2.51	2.56	0.05	322	268	206
C320	14	0	1	294	50.3	2.52	2.47	-0.05	332	277	213
C320	14	0	1	282	50.2	2.53	2.45	-0.08	336	280	215
C320	14	0	1	283	50.2	2.53	2.45	-0.07	336	280	215
C320	14	0	1	305	50.2	2.53	2.48	-0.04	336	280	215
C320	14	0	1	332	50.2	2.53	2.52	0.00	336	280	215
C320	14	0	1	472	50.2	2.53	2.67	0.15	336	280	215
C320	14	0	1	488	50.2	2.53	2.69	0.16	336	280	215
C320	14	0	1	493	50.2	2.53	2.69	0.17	336	280	215
C320	14	0	1	201	50.1	2.53	2.30	-0.23	339	283	217
C320	14	0	1	224	50.1	2.53	2.35	-0.18	339	283	217
C320	14	0	1	255	50.1	2.53	2.41	-0.12	339	283	217
C320	14	0	1	264	50.1	2.53	2.42	-0.11	339	283	217
C320	14	0	1	387	50.1	2.53	2.59	0.06	339	283	217
C320	14	0	1	188	50	2.54	2.27	-0.26	343	286	219
C320	14	0	1	345	50	2.54	2.54	0.00	343	286	219
C320	14	0	1	349	49.9	2.54	2.54	0.00	346	289	222
C320	14	0	5	962	50.6	2.88	2.98	0.10	760	633	486
C320	14	0	5	951	50.5	2.89	2.98	0.09	768	640	492
C320	14	0	5	700	50.3	2.89	2.85	-0.05	785	654	502
C320	14	0	5	762	50.3	2.89	2.88	-0.01	785	654	502
C320	14	0	5	648	50.2	2.90	2.81	-0.09	793	661	508
C320	14	0	5	1216	50.2	2.90	3.08	0.19	793	661	508
C320	14	0	5	1244	50.2	2.90	3.09	0.20	793	661	508
C320	14	0	5	514	50.1	2.90	2.71	-0.19	801	668	513
C320	14	0	5	553	50.1	2.90	2.74	-0.16	801	668	513
C320	14	0	5	606	50.1	2.90	2.78	-0.12	801	668	513

C320	14	0	5	649	50.1	2.90	2.81	-0.09	801	668	513
C320	14	0	5	656	50.1	2.90	2.82	-0.09	801	668	513
C320	14	0	5	705	50.1	2.90	2.85	-0.06	801	668	513
C320	14	0	5	875	50.1	2.90	2.94	0.04	801	668	513
C320	14	0	5	909	50.1	2.90	2.96	0.05	801	668	513
C320	14	0	5	1174	50.1	2.90	3.07	0.17	801	668	513
C320	14	0	5	894	50	2.91	2.95	0.04	810	675	519
C320	14	0	5	974	50	2.91	2.99	0.08	810	675	519
C320	14	0	10	1417	50.5	3.05	3.15	0.11	1111	926	711
C320	14	0	10	1440	50.5	3.05	3.16	0.11	1111	926	711
C320	14	0	10	983	50.3	3.05	2.99	-0.06	1135	945	726
C320	14	0	10	1146	50.3	3.05	3.06	0.00	1135	945	726
C320	14	0	10	903	50.2	3.06	2.96	-0.10	1147	955	734
C320	14	0	10	1743	50.2	3.06	3.24	0.18	1147	955	734
C320	14	0	10	776	50.1	3.06	2.89	-0.17	1159	965	742
C320	14	0	10	843	50.1	3.06	2.93	-0.14	1159	965	742
C320	14	0	10	924	50.1	3.06	2.97	-0.10	1159	965	742
C320	14	0	10	983	50.1	3.06	2.99	-0.07	1159	965	742
C320	14	0	10	1050	50.1	3.06	3.02	-0.04	1159	965	742
C320	14	0	10	1311	50.1	3.06	3.12	0.05	1159	965	742
C320	14	0	10	1361	50.1	3.06	3.13	0.07	1159	965	742
C320	14	0	10	1686	50.1	3.06	3.23	0.16	1159	965	742
C320	14	0	10	1788	50.1	3.06	3.25	0.19	1159	965	742
C320	14	0	10	971	50	3.07	2.99	-0.08	1171	975	750
C320	14	0	10	1323	50	3.07	3.12	0.05	1171	975	750
C320	14	0	10	1422	50	3.07	3.15	0.08	1171	975	750
C320	14	0	0.5	993	35.6	3.08	3.00	-0.09	1214	1011	777
C320	14	0	0.5	1478	35.5	3.09	3.17	0.08	1228	1023	786
C320	14	0	0.5	1699	35.5	3.09	3.23	0.14	1228	1023	786
C320	14	0	0.5	1062	35.4	3.09	3.03	-0.07	1243	1036	796
C320	14	0	0.5	1925	35.4	3.09	3.28	0.19	1243	1036	796
C320	14	0	0.5	1019	35.3	3.10	3.01	-0.09	1258	1048	805
C320	14	0	0.5	1136	35.3	3.10	3.06	-0.04	1258	1048	805
C320	14	0	0.5	1157	35.3	3.10	3.06	-0.04	1258	1048	805
C320	14	0	0.5	1545	35.3	3.10	3.19	0.09	1258	1048	805
C320	14	0	0.5	1920	35.3	3.10	3.28	0.18	1258	1048	805
C320	14	0	0.5	1116	35.2	3.10	3.05	-0.06	1273	1060	815
C320	14	0	0.5	1195	35.2	3.10	3.08	-0.03	1273	1060	815
C320	14	0	0.5	1214	35.2	3.10	3.08	-0.02	1273	1060	815
C320	14	0	0.5	1854	35.2	3.10	3.27	0.16	1273	1060	815
C320	14	0	0.5	1512	35.1	3.11	3.18	0.07	1288	1073	824
C320	14	0	0.5	1319	35	3.11	3.12	0.01	1303	1086	834
C320	14	0	0.5	1373	35	3.11	3.14	0.02	1303	1086	834
C320	14	0	0.5	1615	34.8	3.13	3.21	0.08	1334	1112	854
C320	14	0	1	1434	35.6	3.24	3.16	-0.08	1731	1442	1108
C320	14	0	1	2344	35.6	3.24	3.37	0.13	1731	1442	1108
C320	14	0	25	2346	50.5	3.25	3.37	0.12	1779	1482	1139
C320	14	0	25	2398	50.5	3.25	3.38	0.13	1779	1482	1139
C320	14	0	1	2213	35.4	3.25	3.34	0.10	1771	1475	1133
C320	14	0	1	2628	35.4	3.25	3.42	0.17	1771	1475	1133
C320	14	0	25	1556	50.3	3.26	3.19	-0.07	1814	1511	1161
C320	14	0	25	1943	50.3	3.26	3.29	0.03	1814	1511	1161
C320	14	0	1	1493	35.3	3.25	3.17	-0.08	1791	1492	1146
C320	14	0	1	1493	35.3	3.25	3.17	-0.08	1791	1492	1146
C320	14	0	1	1554	35.3	3.25	3.19	-0.06	1791	1492	1146
C320	14	0	1	1572	35.3	3.25	3.20	-0.06	1791	1492	1146
C320	14	0	1	1721	35.3	3.25	3.24	-0.02	1791	1492	1146
C320	14	0	1	2066	35.3	3.25	3.32	0.06	1791	1492	1146
C320	14	0	1	2611	35.3	3.25	3.42	0.16	1791	1492	1146
C320	14	0	25	2713	50.2	3.26	3.43	0.17	1832	1526	1173
C320	14	0	1	1614	35.2	3.26	3.21	-0.05	1811	1509	1159

C320	14	0	1	1736	35.2	3.26	3.24	-0.02	1811	1509	1159
C320	14	0	25	1354	50.1	3.27	3.13	-0.14	1850	1541	1184
C320	14	0	25	1453	50.1	3.27	3.16	-0.10	1850	1541	1184
C320	14	0	25	1471	50.1	3.27	3.17	-0.10	1850	1541	1184
C320	14	0	25	1597	50.1	3.27	3.20	-0.06	1850	1541	1184
C320	14	0	25	1626	50.1	3.27	3.21	-0.06	1850	1541	1184
C320	14	0	25	1798	50.1	3.27	3.25	-0.01	1850	1541	1184
C320	14	0	25	2194	50.1	3.27	3.34	0.07	1850	1541	1184
C320	14	0	25	2274	50.1	3.27	3.36	0.09	1850	1541	1184
C320	14	0	25	2620	50.1	3.27	3.42	0.15	1850	1541	1184
C320	14	0	25	2768	50.1	3.27	3.44	0.17	1850	1541	1184
C320	14	0	1	1898	35.1	3.26	3.28	0.02	1831	1526	1172
C320	14	0	1	2186	35.1	3.26	3.34	0.08	1831	1526	1172
C320	14	0	1	2560	35.1	3.26	3.41	0.15	1831	1526	1172
C320	14	0	25	2192	50	3.27	3.34	0.07	1869	1557	1196
C320	14	0	25	2310	50	3.27	3.36	0.09	1869	1557	1196
C320	14	0	25	1631	49.9	3.28	3.21	-0.06	1887	1572	1208
C320	14	0	1	1994	34.9	3.27	3.30	0.03	1873	1560	1199
C320	14	0	1	2289	34.8	3.28	3.36	0.08	1894	1578	1213
C320	14	0	5	4436	35.6	3.56	3.65	0.09	3639	3032	2330
C320	14	0	5	3006	35.5	3.57	3.48	-0.09	3674	3061	2352
C320	14	0	5	4502	35.4	3.57	3.65	0.08	3709	3090	2374
C320	14	0	5	3246	35.3	3.57	3.51	-0.06	3744	3119	2397
C320	14	0	5	3650	35.3	3.57	3.56	-0.01	3744	3119	2397
C320	14	0	5	2758	35.2	3.58	3.44	-0.14	3779	3148	2419
C320	14	0	5	2922	35.2	3.58	3.47	-0.11	3779	3148	2419
C320	14	0	5	3362	35.2	3.58	3.53	-0.05	3779	3148	2419
C320	14	0	5	3590	35.2	3.58	3.56	-0.02	3779	3148	2419
C320	14	0	5	3948	35.2	3.58	3.60	0.02	3779	3148	2419
C320	14	0	5	4058	35.2	3.58	3.61	0.03	3779	3148	2419
C320	14	0	5	4500	35.2	3.58	3.65	0.08	3779	3148	2419
C320	14	0	5	4787	35.2	3.58	3.68	0.10	3779	3148	2419
C320	14	0	5	4858	35.2	3.58	3.69	0.11	3779	3148	2419
C320	14	0	5	3288	35.1	3.58	3.52	-0.06	3815	3178	2442
C320	14	0	5	4775	35	3.59	3.68	0.09	3851	3208	2465
C320	14	0	5	4203	34.9	3.59	3.62	0.03	3887	3238	2488
C320	14	0	5	4555	34.8	3.59	3.66	0.06	3923	3268	2512
C320	14	0	10	5548	35.6	3.68	3.74	0.06	4796	3996	3070
C320	14	0	10	3877	35.5	3.68	3.59	-0.10	4837	4030	3097
C320	14	0	10	5722	35.4	3.69	3.76	0.07	4879	4065	3123
C320	14	0	10	4247	35.3	3.69	3.63	-0.06	4920	4099	3150
C320	14	0	10	4773	35.3	3.69	3.68	-0.01	4920	4099	3150
C320	14	0	10	3466	35.2	3.70	3.54	-0.16	4962	4134	3177
C320	14	0	10	3656	35.2	3.70	3.56	-0.13	4962	4134	3177
C320	14	0	10	4613	35.2	3.70	3.66	-0.03	4962	4134	3177
C320	14	0	10	5093	35.2	3.70	3.71	0.01	4962	4134	3177
C320	14	0	10	5138	35.2	3.70	3.71	0.02	4962	4134	3177
C320	14	0	10	5914	35.2	3.70	3.77	0.08	4962	4134	3177
C320	14	0	10	6023	35.2	3.70	3.78	0.08	4962	4134	3177
C320	14	0	10	4393	35.1	3.70	3.64	-0.06	5004	4169	3204
C320	14	0	10	5773	35.1	3.70	3.76	0.06	5004	4169	3204
C320	14	0	10	4223	35	3.70	3.63	-0.08	5046	4204	3231
C320	14	0	10	5948	35	3.70	3.77	0.07	5046	4204	3231
C320	14	0	10	5418	34.9	3.71	3.73	0.03	5089	4240	3258
C320	14	0	10	5760	34.8	3.71	3.76	0.05	5132	4275	3285
C320	14	0	0.5	4322	20.2	3.79	3.64	-0.16	6183	5151	3958
C320	14	0	0.5	4800	20.2	3.79	3.68	-0.11	6183	5151	3958
C320	14	0	0.5	7098	20.2	3.79	3.85	0.06	6183	5151	3958
C320	14	0	0.5	5106	20.1	3.79	3.71	-0.09	6236	5195	3992
C320	14	0	0.5	5391	20.1	3.79	3.73	-0.06	6236	5195	3992
C320	14	0	0.5	5832	20.1	3.79	3.77	-0.03	6236	5195	3992

C320	14	0	0.5	6481	20.1	3.79	3.81	0.02	6236	5195	3992
C320	14	0	0.5	6826	20.1	3.79	3.83	0.04	6236	5195	3992
C320	14	0	0.5	7113	20.1	3.79	3.85	0.06	6236	5195	3992
C320	14	0	0.5	7410	20.1	3.79	3.87	0.07	6236	5195	3992
C320	14	0	0.5	7414	20.1	3.79	3.87	0.08	6236	5195	3992
C320	14	0	0.5	7463	20.1	3.79	3.87	0.08	6236	5195	3992
C320	14	0	0.5	7161	20	3.80	3.85	0.06	6289	5240	4026
C320	14	0	0.5	6180	19.9	3.80	3.79	-0.01	6343	5284	4060
C320	14	0	0.5	6468	19.9	3.80	3.81	0.01	6343	5284	4060
C320	14	0	0.5	7642	19.9	3.80	3.88	0.08	6343	5284	4060
C320	14	0	25	7104	35.6	3.82	3.85	0.03	6608	5505	4230
C320	14	0	25	5205	35.5	3.82	3.72	-0.11	6656	5545	4261
C320	14	0	25	7531	35.4	3.83	3.88	0.05	6704	5585	4292
C320	14	0	25	6390	35.3	3.83	3.81	-0.02	6753	5626	4323
C320	14	0	25	4547	35.2	3.83	3.66	-0.17	6802	5667	4354
C320	14	0	25	4778	35.2	3.83	3.68	-0.15	6802	5667	4354
C320	14	0	25	5716	35.2	3.83	3.76	-0.08	6802	5667	4354
C320	14	0	25	6700	35.2	3.83	3.83	-0.01	6802	5667	4354
C320	14	0	25	6793	35.2	3.83	3.83	0.00	6802	5667	4354
C320	14	0	25	7496	35.2	3.83	3.87	0.04	6802	5667	4354
C320	14	0	25	5960	35.1	3.84	3.78	-0.06	6851	5707	4386
C320	14	0	25	6132	35.1	3.84	3.79	-0.05	6851	5707	4386
C320	14	0	25	7607	35.1	3.84	3.88	0.05	6851	5707	4386
C320	14	0	25	7661	35.1	3.84	3.88	0.05	6851	5707	4386
C320	14	0	25	5603	35	3.84	3.75	-0.09	6900	5748	4417
C320	14	0	25	7590	35	3.84	3.88	0.04	6900	5748	4417
C320	14	0	25	7159	34.9	3.84	3.85	0.01	6949	5790	4449
C320	14	0	25	7527	34.8	3.85	3.88	0.03	6999	5831	4481
C320	14	0	1	5046	20.2	3.89	3.70	-0.18	7683	6401	4919
C320	14	0	1	8264	20.2	3.89	3.92	0.03	7683	6401	4919
C320	14	0	1	5650	20.1	3.89	3.75	-0.14	7741	6449	4956
C320	14	0	1	6123	20.1	3.89	3.79	-0.10	7741	6449	4956
C320	14	0	1	6459	20.1	3.89	3.81	-0.08	7741	6449	4956
C320	14	0	1	7704	20.1	3.89	3.89	0.00	7741	6449	4956
C320	14	0	1	7952	20.1	3.89	3.90	0.01	7741	6449	4956
C320	14	0	1	8254	20.1	3.89	3.92	0.03	7741	6449	4956
C320	14	0	1	8535	20.1	3.89	3.93	0.04	7741	6449	4956
C320	14	0	1	8812	20.1	3.89	3.95	0.06	7741	6449	4956
C320	14	0	1	7040	20	3.89	3.85	-0.04	7799	6497	4993
C320	14	0	1	7441	20	3.89	3.87	-0.02	7799	6497	4993
C320	14	0	1	7648	20	3.89	3.88	-0.01	7799	6497	4993
C320	14	0	1	8682	20	3.89	3.94	0.05	7799	6497	4993
C320	14	0	1	8498	19.9	3.90	3.93	0.03	7857	6545	5030
C320	14	0	1	9032	19.9	3.90	3.96	0.06	7857	6545	5030
C320	14	0	5	11294	20.2	4.06	4.05	-0.01	11463	9550	7339
C320	14	0	5	8065	20.1	4.06	3.91	-0.15	11524	9601	7377
C320	14	0	5	7217	20.1	4.06	3.86	-0.20	11524	9601	7377
C320	14	0	5	8028	20.1	4.06	3.90	-0.16	11524	9601	7377
C320	14	0	5	8914	20.1	4.06	3.95	-0.11	11524	9601	7377
C320	14	0	5	9236	20.1	4.06	3.97	-0.10	11524	9601	7377
C320	14	0	5	10937	20.1	4.06	4.04	-0.02	11524	9601	7377
C320	14	0	5	10954	20.1	4.06	4.04	-0.02	11524	9601	7377
C320	14	0	5	11335	20.1	4.06	4.05	-0.01	11524	9601	7377
C320	14	0	5	11656	20.1	4.06	4.07	0.00	11524	9601	7377
C320	14	0	5	12603	20.1	4.06	4.10	0.04	11524	9601	7377
C320	14	0	5	10081	20	4.06	4.00	-0.06	11585	9651	7416
C320	14	0	5	10726	20	4.06	4.03	-0.03	11585	9651	7416
C320	14	0	5	10849	20	4.06	4.04	-0.03	11585	9651	7416
C320	14	0	5	11773	20	4.06	4.07	0.01	11585	9651	7416
C320	14	0	5	11924	19.9	4.07	4.08	0.01	11645	9702	7455
C320	14	0	5	12542	19.9	4.07	4.10	0.03	11645	9702	7455

C320	14	0	10	9081	20.2	4.12	3.96	-0.16	13088	10903	8378
C320	14	0	10	12618	20.2	4.12	4.10	-0.02	13088	10903	8378
C320	14	0	10	8264	20.1	4.12	3.92	-0.20	13146	10952	8416
C320	14	0	10	10263	20.1	4.12	4.01	-0.11	13146	10952	8416
C320	14	0	10	10504	20.1	4.12	4.02	-0.10	13146	10952	8416
C320	14	0	10	12334	20.1	4.12	4.09	-0.03	13146	10952	8416
C320	14	0	10	12372	20.1	4.12	4.09	-0.03	13146	10952	8416
C320	14	0	10	12646	20.1	4.12	4.10	-0.02	13146	10952	8416
C320	14	0	10	13050	20.1	4.12	4.12	0.00	13146	10952	8416
C320	14	0	10	14308	20.1	4.12	4.16	0.04	13146	10952	8416
C320	14	0	10	17162	20.1	4.12	4.23	0.12	13146	10952	8416
C320	14	0	10	12233	20	4.12	4.09	-0.03	13205	11001	8454
C320	14	0	10	12298	20	4.12	4.09	-0.03	13205	11001	8454
C320	14	0	10	13135	20	4.12	4.12	0.00	13205	11001	8454
C320	14	0	10	11397	19.9	4.12	4.06	-0.07	13264	11050	8491
C320	14	0	10	13395	19.9	4.12	4.13	0.00	13264	11050	8491
C320	14	0	10	14115	19.9	4.12	4.15	0.03	13264	11050	8491
C320	14	0	0.5	15853	5.3	4.19	4.20	0.01	15335	12776	9817
C320	14	0	0.5	16817	5.2	4.19	4.23	0.04	15394	12825	9855
C320	14	0	0.5	16698	5.1	4.19	4.22	0.03	15453	12874	9893
C320	14	0	0.5	16720	5.1	4.19	4.22	0.03	15453	12874	9893
C320	14	0	0.5	16840	5.1	4.19	4.23	0.04	15453	12874	9893
C320	14	0	0.5	19351	5.1	4.19	4.29	0.10	15453	12874	9893
C320	14	0	0.5	11453	5	4.19	4.06	-0.13	15512	12923	9931
C320	14	0	0.5	15243	5	4.19	4.18	-0.01	15512	12923	9931
C320	14	0	0.5	15644	5	4.19	4.19	0.00	15512	12923	9931
C320	14	0	0.5	16878	5	4.19	4.23	0.04	15512	12923	9931
C320	14	0	0.5	17284	5	4.19	4.24	0.05	15512	12923	9931
C320	14	0	0.5	17865	5	4.19	4.25	0.06	15512	12923	9931
C320	14	0	25	10500	20.2	4.18	4.02	-0.16	15120	12596	9679
C320	14	0	25	14477	20.2	4.18	4.16	-0.02	15120	12596	9679
C320	14	0	0.5	12931	4.9	4.19	4.11	-0.08	15571	12972	9968
C320	14	0	0.5	15723	4.9	4.19	4.20	0.00	15571	12972	9968
C320	14	0	0.5	16600	4.9	4.19	4.22	0.03	15571	12972	9968
C320	14	0	0.5	17705	4.9	4.19	4.25	0.06	15571	12972	9968
C320	14	0	0.5	17736	4.9	4.19	4.25	0.06	15571	12972	9968
C320	14	0	25	9788	20.1	4.18	3.99	-0.19	15174	12641	9714
C320	14	0	25	11993	20.1	4.18	4.08	-0.10	15174	12641	9714
C320	14	0	25	12326	20.1	4.18	4.09	-0.09	15174	12641	9714
C320	14	0	25	14192	20.1	4.18	4.15	-0.03	15174	12641	9714
C320	14	0	25	14226	20.1	4.18	4.15	-0.03	15174	12641	9714
C320	14	0	25	14368	20.1	4.18	4.16	-0.02	15174	12641	9714
C320	14	0	25	14892	20.1	4.18	4.17	-0.01	15174	12641	9714
C320	14	0	25	16554	20.1	4.18	4.22	0.04	15174	12641	9714
C320	14	0	25	17352	20.1	4.18	4.24	0.06	15174	12641	9714
C320	14	0	25	14188	20	4.18	4.15	-0.03	15228	12686	9749
C320	14	0	25	14409	20	4.18	4.16	-0.02	15228	12686	9749
C320	14	0	25	14979	20	4.18	4.18	-0.01	15228	12686	9749
C320	14	0	25	15462	20	4.18	4.19	0.01	15228	12686	9749
C320	14	0	25	13302	19.9	4.18	4.12	-0.06	15282	12731	9783
C320	14	0	25	16043	19.9	4.18	4.21	0.02	15282	12731	9783
C320	14	0	1	17121	5.3	4.22	4.23	0.01	16725	13934	10707
C320	14	0	1	18056	5.2	4.22	4.26	0.03	16779	13979	10742
C320	14	0	1	18060	5.1	4.23	4.26	0.03	16833	14024	10776
C320	14	0	1	18169	5.1	4.23	4.26	0.03	16833	14024	10776
C320	14	0	1	18285	5.1	4.23	4.26	0.04	16833	14024	10776
C320	14	0	1	19239	5.1	4.23	4.28	0.06	16833	14024	10776
C320	14	0	1	20763	5.1	4.23	4.32	0.09	16833	14024	10776
C320	14	0	1	12548	5	4.23	4.10	-0.13	16887	14069	10811
C320	14	0	1	16457	5	4.23	4.22	-0.01	16887	14069	10811
C320	14	0	1	16963	5	4.23	4.23	0.00	16887	14069	10811

C320	14	0	1	18144	5	4.23	4.26	0.03	16887	14069	10811
C320	14	0	1	18521	5	4.23	4.27	0.04	16887	14069	10811
C320	14	0	1	14042	4.9	4.23	4.15	-0.08	16940	14113	10845
C320	14	0	1	16986	4.9	4.23	4.23	0.00	16940	14113	10845
C320	14	0	1	17785	4.9	4.23	4.25	0.02	16940	14113	10845
C320	14	0	1	18995	4.9	4.23	4.28	0.05	16940	14113	10845
C320	14	0	1	19185	4.9	4.23	4.28	0.05	16940	14113	10845
C320	14	0	2	17074	5	4.26	4.23	-0.03	18126	15101	11604
C320	14	0	5	19925	5.3	4.29	4.30	0.01	19428	16185	12437
C320	14	0	5	20594	5.2	4.29	4.31	0.02	19469	16219	12463
C320	14	0	5	20959	5.1	4.29	4.32	0.03	19509	16253	12489
C320	14	0	5	21234	5.1	4.29	4.33	0.04	19509	16253	12489
C320	14	0	5	21794	5.1	4.29	4.34	0.05	19509	16253	12489
C320	14	0	5	22034	5.1	4.29	4.34	0.05	19509	16253	12489
C320	14	0	5	23837	5.1	4.29	4.38	0.09	19509	16253	12489
C320	14	0	5	15091	5	4.29	4.18	-0.11	19550	16287	12515
C320	14	0	5	18408	5	4.29	4.27	-0.03	19550	16287	12515
C320	14	0	5	19180	5	4.29	4.28	-0.01	19550	16287	12515
C320	14	0	5	19884	5	4.29	4.30	0.01	19550	16287	12515
C320	14	0	5	21082	5	4.29	4.32	0.03	19550	16287	12515
C320	14	0	5	16663	4.9	4.29	4.22	-0.07	19590	16321	12541
C320	14	0	5	19744	4.9	4.29	4.30	0.00	19590	16321	12541
C320	14	0	5	20352	4.9	4.29	4.31	0.02	19590	16321	12541
C320	14	0	5	20821	4.9	4.29	4.32	0.03	19590	16321	12541
C320	14	0	5	21806	4.9	4.29	4.34	0.05	19590	16321	12541
C320	14	0	5	22453	4.9	4.29	4.35	0.06	19590	16321	12541
C320	14	0	10	21050	5.3	4.31	4.32	0.01	20362	16963	13035
C320	14	0	10	21651	5.2	4.31	4.34	0.03	20397	16993	13058
C320	14	0	10	22127	5.2	4.31	4.34	0.04	20397	16993	13058
C320	14	0	10	22432	5.1	4.31	4.35	0.04	20432	17022	13080
C320	14	0	10	23151	5.1	4.31	4.36	0.05	20432	17022	13080
C320	14	0	10	23229	5.1	4.31	4.37	0.06	20432	17022	13080
C320	14	0	10	25019	5.1	4.31	4.40	0.09	20432	17022	13080
C320	14	0	10	16189	5	4.31	4.21	-0.10	20467	17051	13103
C320	14	0	10	20309	5	4.31	4.31	0.00	20467	17051	13103
C320	14	0	10	21079	5	4.31	4.32	0.01	20467	17051	13103
C320	14	0	10	21284	5	4.31	4.33	0.02	20467	17051	13103
C320	14	0	10	22106	5	4.31	4.34	0.03	20467	17051	13103
C320	14	0	10	17765	4.9	4.31	4.25	-0.06	20502	17080	13125
C320	14	0	10	20839	4.9	4.31	4.32	0.01	20502	17080	13125
C320	14	0	10	21349	4.9	4.31	4.33	0.02	20502	17080	13125
C320	14	0	10	21940	4.9	4.31	4.34	0.03	20502	17080	13125
C320	14	0	10	23699	4.9	4.31	4.37	0.06	20502	17080	13125
C320	14	0	10	22899	4.8	4.31	4.36	0.05	20537	17109	13147
C320	14	0	20	22448	5	4.33	4.35	0.02	21257	17709	13608
C320	14	0	25	22419	5.3	4.33	4.35	0.02	21400	17828	13700
C320	14	0	25	22998	5.2	4.33	4.36	0.03	21429	17852	13718
C320	14	0	25	23628	5.2	4.33	4.37	0.04	21429	17852	13718
C320	14	0	25	17602	5.1	4.33	4.25	-0.09	21457	17876	13737
C320	14	0	25	24014	5.1	4.33	4.38	0.05	21457	17876	13737
C320	14	0	25	24535	5.1	4.33	4.39	0.06	21457	17876	13737
C320	14	0	25	25022	5.1	4.33	4.40	0.07	21457	17876	13737
C320	14	0	25	26571	5.1	4.33	4.42	0.09	21457	17876	13737
C320	14	0	25	21772	5	4.33	4.34	0.01	21486	17900	13755
C320	14	0	25	22218	5	4.33	4.35	0.01	21486	17900	13755
C320	14	0	25	22634	5	4.33	4.35	0.02	21486	17900	13755
C320	14	0	25	23353	5	4.33	4.37	0.04	21486	17900	13755
C320	14	0	25	23843	5	4.33	4.38	0.05	21486	17900	13755
C320	14	0	25	22630	4.9	4.33	4.35	0.02	21514	17923	13773
C320	14	0	25	23380	4.9	4.33	4.37	0.04	21514	17923	13773
C320	14	0	25	25200	4.9	4.33	4.40	0.07	21514	17923	13773

C320	14	0	25	19174	4.8	4.33	4.28	-0.05	21542	17947	13791
C320	14	0	25	24288	4.8	4.33	4.39	0.05	21542	17947	13791

Appendix C Confidence Interval Calculations

Temperature Shift Factors

a b
0.000463 -0.110658559

Se (log) 0.105

Master Curve Parameters

α β γ δ
1.269 3.080 -1.384 -0.670

R² Log 0.98

R² (Arith) 0.95

Se (Arith) 1551

Observations 165

Binder Type	Nominal Size (mm)	Confinement (KPa)	Frequency (Hz)	Modulus (MPa)	Test Temp (oC)	(Log) Modulus			Adjusted α for Confidence		
						Predicted	Mesured	Error (log)	1.269 50%	1.198 75%	1.093 95%
AR450	14	0	0.5	187	50.5	2.43	2.27	-0.15	267	227	178
AR450	14	0	0.5	273	50.5	2.43	2.44	0.01	267	227	178
AR450	14	0	0.5	262	50.4	2.43	2.42	-0.01	270	229	180
AR450	14	0	0.5	382	50.4	2.43	2.58	0.15	270	229	180
AR450	14	0	0.5	220	50.2	2.44	2.34	-0.10	275	233	183
AR450	14	0	0.5	224	50.1	2.44	2.35	-0.09	278	236	185
AR450	14	0	0.5	362	50.1	2.44	2.56	0.12	278	236	185
AR450	14	0	0.5	190	49.9	2.45	2.28	-0.17	283	240	189
AR450	14	0	0.5	240	49.8	2.46	2.38	-0.08	286	243	191
AR450	14	0	1	386	50.8	2.56	2.59	0.02	365	310	244
AR450	14	0	1	384	50.4	2.58	2.58	0.00	380	323	254
AR450	14	0	1	560	50.3	2.58	2.75	0.16	384	326	256
AR450	14	0	1	271	50.2	2.59	2.43	-0.16	388	329	259
AR450	14	0	1	313	50	2.60	2.50	-0.10	396	336	264
AR450	14	0	1	320	50	2.60	2.51	-0.09	396	336	264
AR450	14	0	1	536	50	2.60	2.73	0.13	396	336	264
AR450	14	0	1	273	49.9	2.60	2.44	-0.17	400	339	267
AR450	14	0	1	355	49.9	2.60	2.55	-0.05	400	339	267
AR450	14	0	5	992	50.9	2.92	3.00	0.08	825	700	551
AR450	14	0	5	1334	50.3	2.94	3.13	0.18	877	745	586
AR450	14	0	5	890	50.2	2.95	2.95	0.00	886	752	592
AR450	14	0	5	704	50.1	2.95	2.85	-0.10	896	760	598
AR450	14	0	5	1285	50.1	2.95	3.11	0.16	896	760	598
AR450	14	0	5	720	49.9	2.96	2.86	-0.10	914	776	610
AR450	14	0	5	731	49.9	2.96	2.86	-0.10	914	776	610
AR450	14	0	5	834	49.9	2.96	2.92	-0.04	914	776	610
AR450	14	0	5	932	49.9	2.96	2.97	0.01	914	776	610
AR450	14	0	10	1450	50.8	3.07	3.16	0.09	1185	1006	791
AR450	14	0	10	1868	50.3	3.10	3.27	0.18	1246	1058	832
AR450	14	0	10	1244	50.1	3.10	3.09	-0.01	1271	1079	848
AR450	14	0	10	1785	50.1	3.10	3.25	0.15	1271	1079	848
AR450	14	0	10	1050	50	3.11	3.02	-0.09	1284	1090	857
AR450	14	0	10	1075	50	3.11	3.03	-0.08	1284	1090	857
AR450	14	0	10	1259	49.9	3.11	3.10	-0.01	1297	1101	866
AR450	14	0	10	1378	49.9	3.11	3.14	0.03	1297	1101	866
AR450	14	0	10	1044	49.8	3.12	3.02	-0.10	1310	1112	874
AR450	14	0	0.5	1645	35.6	3.14	3.22	0.08	1367	1160	912
AR450	14	0	0.5	1193	35.4	3.15	3.08	-0.07	1399	1187	933
AR450	14	0	0.5	1200	35.3	3.15	3.08	-0.07	1415	1201	944
AR450	14	0	0.5	2378	35.2	3.16	3.38	0.22	1431	1214	955
AR450	14	0	0.5	2366	35.1	3.16	3.37	0.21	1447	1228	966
AR450	14	0	0.5	1360	35	3.17	3.13	-0.03	1464	1242	977
AR450	14	0	0.5	1909	35	3.17	3.28	0.12	1464	1242	977
AR450	14	0	0.5	1146	34.7	3.18	3.06	-0.12	1515	1286	1011
AR450	14	0	25	2315	50.8	3.27	3.36	0.10	1852	1572	1236
AR450	14	0	1	1714	35.5	3.29	3.23	-0.05	1929	1637	1287

AR450	14	0	1	2312	35.5	3.29	3.36	0.08	1929	1637	1287
AR450	14	0	25	2798	50.2	3.29	3.45	0.15	1959	1663	1308
AR450	14	0	1	1713	35.3	3.29	3.23	-0.06	1971	1673	1316
AR450	14	0	25	2652	50.1	3.30	3.42	0.13	1977	1678	1320
AR450	14	0	1	3097	35.2	3.30	3.49	0.19	1993	1691	1330
AR450	14	0	25	1796	50	3.30	3.25	-0.05	1996	1694	1332
AR450	14	0	25	1899	50	3.30	3.28	-0.02	1996	1694	1332
AR450	14	0	1	3091	35.1	3.30	3.49	0.19	2014	1709	1344
AR450	14	0	25	1764	49.9	3.30	3.25	-0.06	2015	1710	1345
AR450	14	0	25	2232	49.9	3.30	3.35	0.04	2015	1710	1345
AR450	14	0	25	1644	49.8	3.31	3.22	-0.09	2034	1726	1357
AR450	14	0	25	2017	49.8	3.31	3.30	0.00	2034	1726	1357
AR450	14	0	1	1814	35	3.31	3.26	-0.05	2036	1728	1359
AR450	14	0	1	2603	34.9	3.31	3.42	0.10	2058	1747	1374
AR450	14	0	1	1549	34.7	3.32	3.19	-0.13	2103	1785	1404
AR450	14	0	5	3555	35.4	3.59	3.55	-0.04	3876	3290	2587
AR450	14	0	5	4369	35.4	3.59	3.64	0.05	3876	3290	2587
AR450	14	0	5	3491	35.3	3.59	3.54	-0.05	3911	3319	2610
AR450	14	0	5	5176	35.1	3.60	3.71	0.11	3981	3379	2657
AR450	14	0	5	5206	35.1	3.60	3.72	0.12	3981	3379	2657
AR450	14	0	5	3276	34.9	3.61	3.52	-0.09	4052	3439	2705
AR450	14	0	5	4721	34.9	3.61	3.67	0.07	4052	3439	2705
AR450	14	0	5	2910	34.7	3.62	3.46	-0.15	4124	3500	2753
AR450	14	0	10	4577	35.4	3.70	3.66	-0.04	4990	4235	3330
AR450	14	0	10	5432	35.4	3.70	3.73	0.04	4990	4235	3330
AR450	14	0	10	4476	35.2	3.71	3.65	-0.05	5070	4303	3384
AR450	14	0	10	6184	35.1	3.71	3.79	0.08	5111	4337	3411
AR450	14	0	10	6233	35.1	3.71	3.79	0.09	5111	4337	3411
AR450	14	0	10	4043	34.9	3.72	3.61	-0.11	5192	4406	3465
AR450	14	0	10	5807	34.8	3.72	3.76	0.05	5233	4441	3493
AR450	14	0	10	3665	34.7	3.72	3.56	-0.16	5274	4476	3520
AR450	14	0	0.5	7912	20.3	3.80	3.90	0.09	6375	5410	4255
AR450	14	0	0.5	5152	20.2	3.81	3.71	-0.10	6426	5453	4289
AR450	14	0	0.5	6257	20.2	3.81	3.80	-0.01	6426	5453	4289
AR450	14	0	0.5	7468	20.1	3.81	3.87	0.06	6477	5496	4323
AR450	14	0	0.5	7553	20.1	3.81	3.88	0.07	6477	5496	4323
AR450	14	0	0.5	4339	20	3.81	3.64	-0.18	6528	5540	4357
AR450	14	0	0.5	8447	20	3.81	3.93	0.11	6528	5540	4357
AR450	14	0	0.5	6054	19.9	3.82	3.78	-0.04	6579	5584	4391
AR450	14	0	25	6922	35.4	3.82	3.84	0.02	6677	5667	4456
AR450	14	0	25	6118	35.3	3.83	3.79	-0.04	6722	5705	4487
AR450	14	0	25	5988	35.2	3.83	3.78	-0.05	6768	5744	4517
AR450	14	0	25	7656	35.1	3.83	3.88	0.05	6814	5782	4548
AR450	14	0	25	7772	35	3.84	3.89	0.05	6860	5821	4578
AR450	14	0	25	5178	34.8	3.84	3.71	-0.13	6952	5900	4640
AR450	14	0	25	7321	34.8	3.84	3.86	0.02	6952	5900	4640
AR450	14	0	25	4776	34.7	3.84	3.68	-0.17	6998	5939	4670
AR450	14	0	1	7511	20.2	3.89	3.88	-0.02	7801	6621	5207
AR450	14	0	1	9068	20.2	3.89	3.96	0.07	7801	6621	5207
AR450	14	0	1	5101	20.1	3.90	3.71	-0.19	7855	6666	5243
AR450	14	0	1	6077	20.1	3.90	3.78	-0.11	7855	6666	5243
AR450	14	0	1	8599	20.1	3.90	3.93	0.04	7855	6666	5243
AR450	14	0	1	8784	20.1	3.90	3.94	0.05	7855	6666	5243
AR450	14	0	1	9695	20.1	3.90	3.99	0.09	7855	6666	5243
AR450	14	0	1	7245	19.9	3.90	3.86	-0.04	7964	6758	5315
AR450	14	0	5	7212	20.1	4.05	3.86	-0.19	11180	9488	7462
AR450	14	0	5	8422	20.1	4.05	3.93	-0.12	11180	9488	7462
AR450	14	0	5	10724	20.1	4.05	4.03	-0.02	11180	9488	7462
AR450	14	0	5	11769	20.1	4.05	4.07	0.02	11180	9488	7462
AR450	14	0	5	11788	20.1	4.05	4.07	0.02	11180	9488	7462
AR450	14	0	5	12581	20.1	4.05	4.10	0.05	11180	9488	7462

AR450	14	0	5	10155	20	4.05	4.01	-0.04	11234	9534	7498
AR450	14	0	5	11408	20	4.05	4.06	0.01	11234	9534	7498
AR450	14	0	10	13817	20.2	4.10	4.14	0.04	12508	10615	8348
AR450	14	0	10	8198	20.1	4.10	3.91	-0.19	12559	10658	8382
AR450	14	0	10	9527	20.1	4.10	3.98	-0.12	12559	10658	8382
AR450	14	0	10	12206	20.1	4.10	4.09	-0.01	12559	10658	8382
AR450	14	0	10	12948	20.1	4.10	4.11	0.01	12559	10658	8382
AR450	14	0	10	13031	20.1	4.10	4.11	0.02	12559	10658	8382
AR450	14	0	10	11492	20	4.10	4.06	-0.04	12610	10702	8416
AR450	14	0	10	12642	20	4.10	4.10	0.00	12610	10702	8416
AR450	14	0	25	15500	20.2	4.15	4.19	0.04	14204	12055	9480
AR450	14	0	25	9545	20.1	4.15	3.98	-0.17	14251	12094	9511
AR450	14	0	25	11012	20.1	4.15	4.04	-0.11	14251	12094	9511
AR450	14	0	25	14203	20.1	4.15	4.15	0.00	14251	12094	9511
AR450	14	0	25	14704	20.1	4.15	4.17	0.01	14251	12094	9511
AR450	14	0	25	13363	20	4.16	4.13	-0.03	14297	12133	9542
AR450	14	0	25	14371	20	4.16	4.16	0.00	14297	12133	9542
AR450	14	0	25	14572	20	4.16	4.16	0.01	14297	12133	9542
AR450	14	0	0.5	15692	5.4	4.17	4.20	0.03	14626	12413	9762
AR450	14	0	0.5	11871	5.2	4.17	4.07	-0.09	14727	12498	9829
AR450	14	0	0.5	15747	5.2	4.17	4.20	0.03	14727	12498	9829
AR450	14	0	0.5	12726	5.1	4.17	4.10	-0.06	14776	12540	9862
AR450	14	0	0.5	15695	5.1	4.17	4.20	0.03	14776	12540	9862
AR450	14	0	0.5	16545	5.1	4.17	4.22	0.05	14776	12540	9862
AR450	14	0	0.5	17964	5.1	4.17	4.25	0.08	14776	12540	9862
AR450	14	0	0.5	17342	5	4.17	4.24	0.07	14826	12582	9895
AR450	14	0	1	12710	5.3	4.20	4.10	-0.09	15789	13399	10538
AR450	14	0	1	16798	5.3	4.20	4.23	0.03	15789	13399	10538
AR450	14	0	1	16757	5.2	4.20	4.22	0.02	15834	13438	10568
AR450	14	0	1	13713	5.1	4.20	4.14	-0.06	15879	13476	10598
AR450	14	0	1	16862	5.1	4.20	4.23	0.03	15879	13476	10598
AR450	14	0	1	17313	5.1	4.20	4.24	0.04	15879	13476	10598
AR450	14	0	1	18699	5	4.20	4.27	0.07	15924	13514	10628
AR450	14	0	1	18999	5	4.20	4.28	0.08	15924	13514	10628
AR450	14	0	5	14703	5.3	4.25	4.17	-0.09	17907	15197	11952
AR450	14	0	5	19305	5.3	4.25	4.29	0.03	17907	15197	11952
AR450	14	0	5	18937	5.2	4.25	4.28	0.02	17941	15225	11974
AR450	14	0	5	15855	5.1	4.25	4.20	-0.05	17974	15253	11996
AR450	14	0	5	19385	5.1	4.25	4.29	0.03	17974	15253	11996
AR450	14	0	5	20257	5.1	4.25	4.31	0.05	17974	15253	11996
AR450	14	0	5	21276	5	4.26	4.33	0.07	18006	15281	12018
AR450	14	0	5	21597	5	4.26	4.33	0.08	18006	15281	12018
AR450	14	0	10	15455	5.3	4.27	4.19	-0.08	18628	15808	12432
AR450	14	0	10	20225	5.3	4.27	4.31	0.04	18628	15808	12432
AR450	14	0	10	19797	5.2	4.27	4.30	0.03	18656	15833	12451
AR450	14	0	10	16710	5.1	4.27	4.22	-0.05	18685	15857	12470
AR450	14	0	10	20326	5.1	4.27	4.31	0.04	18685	15857	12470
AR450	14	0	10	20588	5.1	4.27	4.31	0.04	18685	15857	12470
AR450	14	0	10	22200	5	4.27	4.35	0.07	18713	15881	12489
AR450	14	0	10	22774	5	4.27	4.36	0.09	18713	15881	12489
AR450	14	0	25	16415	5.3	4.29	4.22	-0.07	19422	16483	12963
AR450	14	0	25	21438	5.3	4.29	4.33	0.04	19422	16483	12963
AR450	14	0	25	20916	5.2	4.29	4.32	0.03	19445	16502	12978
AR450	14	0	25	17765	5.1	4.29	4.25	-0.04	19468	16522	12993
AR450	14	0	25	21352	5.1	4.29	4.33	0.04	19468	16522	12993
AR450	14	0	25	21797	5	4.29	4.34	0.05	19491	16541	13009
AR450	14	0	25	23409	5	4.29	4.37	0.08	19491	16541	13009
AR450	14	0	25	24233	5	4.29	4.38	0.09	19491	16541	13009

Appendix C Confidence Interval Calculations

Temperature Shift Factors

a b
0.000452 -0.109181755

Se (log) 0.088

Master Curve Parameters

α β γ δ
1.289 3.132 -1.276 -0.694

R² Log 0.99

R² (Arith) 0.97

Se (Arith) 1393

Observations 235

Binder Type	Nominal Size (mm)	Confinement (KPa)	Frequency (Hz)	Modulus (MPa)	Test Temp (oC)	(Log) Modulus			Adjusted α for Confidence		
						Predicted	Mesured	Error (log)	1.289	1.229	1.142
C320	20	0	0.5	148	50.7	2.35	2.17	-0.18	223	194	159
C320	20	0	0.5	209	50.4	2.36	2.32	-0.04	229	200	163
C320	20	0	0.5	232	50.4	2.36	2.37	0.01	229	200	163
C320	20	0	0.5	234	50.3	2.36	2.37	0.00	231	202	165
C320	20	0	0.5	230	50.2	2.37	2.36	-0.01	234	204	166
C320	20	0	0.5	323	50.2	2.37	2.51	0.14	234	204	166
C320	20	0	0.5	170	50.1	2.37	2.23	-0.14	236	206	168
C320	20	0	0.5	174	50.1	2.37	2.24	-0.13	236	206	168
C320	20	0	0.5	246	50	2.38	2.39	0.01	238	208	170
C320	20	0	0.5	302	50	2.38	2.48	0.10	238	208	170
C320	20	0	0.5	156	49.9	2.38	2.19	-0.19	241	210	171
C320	20	0	0.5	288	49.4	2.40	2.46	0.06	253	220	180
C320	20	0	1	221	50.6	2.50	2.34	-0.16	318	277	227
C320	20	0	1	334	50.3	2.52	2.52	0.01	328	286	234
C320	20	0	1	346	50.3	2.52	2.54	0.02	328	286	234
C320	20	0	1	446	50.3	2.52	2.65	0.13	328	286	234
C320	20	0	1	313	50.2	2.52	2.50	-0.03	332	289	236
C320	20	0	1	352	50.2	2.52	2.55	0.03	332	289	236
C320	20	0	1	235	50.1	2.53	2.37	-0.15	335	292	239
C320	20	0	1	241	50.1	2.53	2.38	-0.14	335	292	239
C320	20	0	1	422	50	2.53	2.63	0.10	339	295	241
C320	20	0	1	355	49.9	2.53	2.55	0.02	342	298	244
C320	20	0	1	226	49.7	2.54	2.35	-0.19	349	305	249
C320	20	0	1	407	49.4	2.56	2.61	0.05	361	314	257
C320	20	0	5	607	50.5	2.88	2.78	-0.10	761	663	542
C320	20	0	5	894	50.3	2.89	2.95	0.06	777	677	554
C320	20	0	5	905	50.3	2.89	2.96	0.07	777	677	554
C320	20	0	5	944	50.3	2.89	2.97	0.08	777	677	554
C320	20	0	5	859	50.2	2.90	2.93	0.04	786	685	560
C320	20	0	5	916	50.2	2.90	2.96	0.07	786	685	560
C320	20	0	5	632	50.1	2.90	2.80	-0.10	794	692	566
C320	20	0	5	597	50	2.90	2.78	-0.13	803	700	572
C320	20	0	5	939	50	2.90	2.97	0.07	803	700	572
C320	20	0	5	898	49.9	2.91	2.95	0.04	812	707	578
C320	20	0	5	622	49.6	2.92	2.79	-0.13	839	731	597
C320	20	0	5	992	49.5	2.93	3.00	0.07	848	739	604
C320	20	0	10	941	50.4	3.05	2.97	-0.07	1118	974	796
C320	20	0	10	1347	50.3	3.05	3.13	0.08	1130	985	805
C320	20	0	10	1361	50.3	3.05	3.13	0.08	1130	985	805
C320	20	0	10	1398	50.3	3.05	3.15	0.09	1130	985	805
C320	20	0	10	1293	50.2	3.06	3.11	0.05	1142	995	813
C320	20	0	10	962	50.1	3.06	2.98	-0.08	1154	1006	822
C320	20	0	10	1379	50.1	3.06	3.14	0.08	1154	1006	822
C320	20	0	10	902	50	3.07	2.96	-0.11	1167	1017	831
C320	20	0	10	1293	50	3.07	3.11	0.04	1167	1017	831
C320	20	0	10	1315	49.9	3.07	3.12	0.05	1179	1027	840

C320	20	0	10	953	49.6	3.09	2.98	-0.11	1217	1061	867
C320	20	0	0.5	1788	35.6	3.09	3.25	0.16	1224	1067	872
C320	20	0	10	1429	49.5	3.09	3.16	0.07	1230	1072	876
C320	20	0	0.5	1117	35.4	3.10	3.05	-0.05	1254	1093	893
C320	20	0	0.5	1458	35.4	3.10	3.16	0.07	1254	1093	893
C320	20	0	0.5	1067	35.3	3.10	3.03	-0.08	1270	1106	904
C320	20	0	0.5	1464	35.3	3.10	3.17	0.06	1270	1106	904
C320	20	0	0.5	1045	35.2	3.11	3.02	-0.09	1285	1120	915
C320	20	0	0.5	1548	35.2	3.11	3.19	0.08	1285	1120	915
C320	20	0	0.5	1565	35.2	3.11	3.19	0.09	1285	1120	915
C320	20	0	0.5	1134	35.1	3.11	3.05	-0.06	1301	1134	927
C320	20	0	0.5	1562	35	3.12	3.19	0.07	1317	1148	938
C320	20	0	0.5	1392	34.9	3.12	3.14	0.02	1333	1162	949
C320	20	0	0.5	1520	34.8	3.13	3.18	0.05	1349	1176	961
C320	20	0	1	2463	35.6	3.24	3.39	0.15	1757	1531	1251
C320	20	0	1	2110	35.4	3.25	3.32	0.07	1798	1567	1281
C320	20	0	25	1685	50.4	3.26	3.23	-0.03	1805	1573	1286
C320	20	0	1	1550	35.3	3.26	3.19	-0.07	1819	1585	1296
C320	20	0	1	1656	35.3	3.26	3.22	-0.04	1819	1585	1296
C320	20	0	1	2099	35.3	3.26	3.32	0.06	1819	1585	1296
C320	20	0	1	2243	35.3	3.26	3.35	0.09	1819	1585	1296
C320	20	0	25	2055	50.3	3.26	3.31	0.05	1823	1589	1299
C320	20	0	25	2280	50.3	3.26	3.36	0.10	1823	1589	1299
C320	20	0	25	2327	50.3	3.26	3.37	0.11	1823	1589	1299
C320	20	0	1	1644	35.2	3.26	3.22	-0.05	1841	1604	1311
C320	20	0	1	2050	35.2	3.26	3.31	0.05	1841	1604	1311
C320	20	0	25	2173	50.2	3.27	3.34	0.07	1842	1605	1312
C320	20	0	25	1708	50.1	3.27	3.23	-0.04	1860	1621	1325
C320	20	0	25	2301	50.1	3.27	3.36	0.09	1860	1621	1325
C320	20	0	1	2134	35.1	3.27	3.33	0.06	1862	1623	1326
C320	20	0	25	1578	50	3.27	3.20	-0.08	1879	1637	1338
C320	20	0	25	1987	50	3.27	3.30	0.02	1879	1637	1338
C320	20	0	1	1560	34.9	3.28	3.19	-0.09	1906	1661	1358
C320	20	0	1	2011	34.9	3.28	3.30	0.02	1906	1661	1358
C320	20	0	1	2064	34.9	3.28	3.31	0.03	1906	1661	1358
C320	20	0	25	2139	49.8	3.28	3.33	0.05	1917	1671	1365
C320	20	0	25	1713	49.6	3.29	3.23	-0.06	1956	1705	1393
C320	20	0	25	2255	49.5	3.30	3.35	0.06	1976	1722	1407
C320	20	0	5	4512	35.5	3.58	3.65	0.08	3791	3304	2700
C320	20	0	5	4599	35.5	3.58	3.66	0.08	3791	3304	2700
C320	20	0	5	4363	35.4	3.58	3.64	0.06	3829	3336	2727
C320	20	0	5	3391	35.3	3.59	3.53	-0.06	3866	3369	2754
C320	20	0	5	3554	35.3	3.59	3.55	-0.04	3866	3369	2754
C320	20	0	5	3667	35.2	3.59	3.56	-0.03	3904	3402	2781
C320	20	0	5	3679	35.2	3.59	3.57	-0.03	3904	3402	2781
C320	20	0	5	4171	35.2	3.59	3.62	0.03	3904	3402	2781
C320	20	0	5	4322	35.2	3.59	3.64	0.04	3904	3402	2781
C320	20	0	5	3671	34.9	3.60	3.56	-0.04	4019	3502	2863
C320	20	0	5	4201	34.9	3.60	3.62	0.02	4019	3502	2863
C320	20	0	5	3543	34.8	3.61	3.55	-0.06	4058	3536	2890
C320	20	0	10	5721	35.5	3.70	3.76	0.06	5024	4378	3578
C320	20	0	10	5740	35.5	3.70	3.76	0.06	5024	4378	3578
C320	20	0	10	4687	35.4	3.70	3.67	-0.03	5068	4416	3610
C320	20	0	10	5574	35.4	3.70	3.75	0.04	5068	4416	3610
C320	20	0	10	5287	35.3	3.71	3.72	0.01	5113	4455	3641
C320	20	0	10	4476	35.2	3.71	3.65	-0.06	5158	4495	3674
C320	20	0	10	4521	35.2	3.71	3.66	-0.06	5158	4495	3674
C320	20	0	10	5571	35.2	3.71	3.75	0.03	5158	4495	3674
C320	20	0	10	4880	35.1	3.72	3.69	-0.03	5203	4534	3706
C320	20	0	10	4505	35	3.72	3.65	-0.07	5249	4574	3738
C320	20	0	10	5406	34.9	3.72	3.73	0.01	5294	4614	3771

C320	20	0	10	4725	34.8	3.73	3.67	-0.05	5340	4654	3804
C320	20	0	0.5	5792	20.3	3.82	3.76	-0.05	6550	5707	4665
C320	20	0	0.5	5770	20.1	3.82	3.76	-0.06	6666	5809	4748
C320	20	0	0.5	6266	20.1	3.82	3.80	-0.03	6666	5809	4748
C320	20	0	0.5	6308	20.1	3.82	3.80	-0.02	6666	5809	4748
C320	20	0	0.5	7023	20.1	3.82	3.85	0.02	6666	5809	4748
C320	20	0	0.5	7201	20.1	3.82	3.86	0.03	6666	5809	4748
C320	20	0	0.5	7433	20.1	3.82	3.87	0.05	6666	5809	4748
C320	20	0	0.5	7816	20.1	3.82	3.89	0.07	6666	5809	4748
C320	20	0	0.5	8208	20.1	3.82	3.91	0.09	6666	5809	4748
C320	20	0	0.5	8608	20.1	3.82	3.93	0.11	6666	5809	4748
C320	20	0	0.5	5798	20	3.83	3.76	-0.06	6725	5860	4789
C320	20	0	25	7390	35.5	3.84	3.87	0.03	6960	6065	4957
C320	20	0	25	7576	35.5	3.84	3.88	0.04	6960	6065	4957
C320	20	0	25	6328	35.4	3.85	3.80	-0.04	7012	6111	4994
C320	20	0	25	6904	35.4	3.85	3.84	-0.01	7012	6111	4994
C320	20	0	25	7280	35.4	3.85	3.86	0.02	7012	6111	4994
C320	20	0	25	6087	35.2	3.85	3.78	-0.07	7118	6202	5069
C320	20	0	25	7339	35.2	3.85	3.87	0.01	7118	6202	5069
C320	20	0	25	5763	35.1	3.86	3.76	-0.09	7170	6249	5107
C320	20	0	25	6649	35.1	3.86	3.82	-0.03	7170	6249	5107
C320	20	0	25	5743	35	3.86	3.76	-0.10	7224	6295	5145
C320	20	0	25	7163	34.9	3.86	3.86	-0.01	7277	6341	5183
C320	20	0	25	6422	34.7	3.87	3.81	-0.06	7384	6435	5259
C320	20	0	1	6752	20.2	3.91	3.83	-0.09	8222	7165	5856
C320	20	0	1	7559	20.1	3.92	3.88	-0.04	8285	7220	5901
C320	20	0	1	8372	20.1	3.92	3.92	0.00	8285	7220	5901
C320	20	0	1	8509	20.1	3.92	3.93	0.01	8285	7220	5901
C320	20	0	1	8697	20.1	3.92	3.94	0.02	8285	7220	5901
C320	20	0	1	9296	20.1	3.92	3.97	0.05	8285	7220	5901
C320	20	0	1	9793	20.1	3.92	3.99	0.07	8285	7220	5901
C320	20	0	1	10149	20.1	3.92	4.01	0.09	8285	7220	5901
C320	20	0	1	6659	20	3.92	3.82	-0.10	8349	7275	5946
C320	20	0	1	6991	20	3.92	3.84	-0.08	8349	7275	5946
C320	20	0	1	7422	20	3.92	3.87	-0.05	8349	7275	5946
C320	20	0	5	9399	20.2	4.09	3.97	-0.12	12267	10690	8737
C320	20	0	5	10211	20.1	4.09	4.01	-0.08	12333	10747	8784
C320	20	0	5	10426	20.1	4.09	4.02	-0.07	12333	10747	8784
C320	20	0	5	11077	20.1	4.09	4.04	-0.05	12333	10747	8784
C320	20	0	5	11794	20.1	4.09	4.07	-0.02	12333	10747	8784
C320	20	0	5	11898	20.1	4.09	4.08	-0.02	12333	10747	8784
C320	20	0	5	11935	20.1	4.09	4.08	-0.01	12333	10747	8784
C320	20	0	5	12848	20.1	4.09	4.11	0.02	12333	10747	8784
C320	20	0	5	13701	20.1	4.09	4.14	0.05	12333	10747	8784
C320	20	0	5	13897	20.1	4.09	4.14	0.05	12333	10747	8784
C320	20	0	5	9143	20	4.09	3.96	-0.13	12399	10805	8831
C320	20	0	10	10660	20.1	4.15	4.03	-0.12	14054	12247	10009
C320	20	0	10	11654	20.1	4.15	4.07	-0.08	14054	12247	10009
C320	20	0	10	11852	20.1	4.15	4.07	-0.07	14054	12247	10009
C320	20	0	10	12767	20.1	4.15	4.11	-0.04	14054	12247	10009
C320	20	0	10	13296	20.1	4.15	4.12	-0.02	14054	12247	10009
C320	20	0	10	13365	20.1	4.15	4.13	-0.02	14054	12247	10009
C320	20	0	10	13441	20.1	4.15	4.13	-0.02	14054	12247	10009
C320	20	0	10	14485	20.1	4.15	4.16	0.01	14054	12247	10009
C320	20	0	10	15488	20.1	4.15	4.19	0.04	14054	12247	10009
C320	20	0	10	15529	20.1	4.15	4.19	0.04	14054	12247	10009
C320	20	0	10	10298	20	4.15	4.01	-0.14	14117	12302	10055
C320	20	0	25	12459	20.1	4.21	4.10	-0.11	16188	14107	11530
C320	20	0	25	13636	20.1	4.21	4.13	-0.07	16188	14107	11530
C320	20	0	25	13821	20.1	4.21	4.14	-0.07	16188	14107	11530
C320	20	0	25	15044	20.1	4.21	4.18	-0.03	16188	14107	11530

C320	20	0	25	15179	20.1	4.21	4.18	-0.03	16188	14107	11530
C320	20	0	25	15460	20.1	4.21	4.19	-0.02	16188	14107	11530
C320	20	0	25	15582	20.1	4.21	4.19	-0.02	16188	14107	11530
C320	20	0	25	16651	20.1	4.21	4.22	0.01	16188	14107	11530
C320	20	0	25	17665	20.1	4.21	4.25	0.04	16188	14107	11530
C320	20	0	25	17841	20.1	4.21	4.25	0.04	16188	14107	11530
C320	20	0	25	11876	20	4.21	4.07	-0.14	16246	14157	11571
C320	20	0	0.5	19424	5.3	4.22	4.29	0.07	16600	14465	11823
C320	20	0	0.5	18703	5.2	4.22	4.27	0.05	16663	14520	11868
C320	20	0	0.5	14062	5.1	4.22	4.15	-0.08	16726	14575	11913
C320	20	0	0.5	15702	5.1	4.22	4.20	-0.03	16726	14575	11913
C320	20	0	0.5	14127	5	4.23	4.15	-0.07	16789	14630	11957
C320	20	0	0.5	16228	5	4.23	4.21	-0.01	16789	14630	11957
C320	20	0	0.5	17550	5	4.23	4.24	0.02	16789	14630	11957
C320	20	0	0.5	17677	5	4.23	4.25	0.02	16789	14630	11957
C320	20	0	0.5	19479	5	4.23	4.29	0.06	16789	14630	11957
C320	20	0	0.5	17820	4.9	4.23	4.25	0.02	16851	14684	12002
C320	20	0	0.5	18646	4.9	4.23	4.27	0.04	16851	14684	12002
C320	20	0	0.5	17843	4.8	4.23	4.25	0.02	16914	14739	12046
C320	20	0	1	20880	5.3	4.26	4.32	0.06	18027	15709	12840
C320	20	0	1	20133	5.2	4.26	4.30	0.05	18084	15759	12880
C320	20	0	1	15311	5.1	4.26	4.19	-0.07	18141	15809	12921
C320	20	0	1	17122	5.1	4.26	4.23	-0.03	18141	15809	12921
C320	20	0	1	17645	5.1	4.26	4.25	-0.01	18141	15809	12921
C320	20	0	1	15326	5	4.26	4.19	-0.07	18198	15858	12961
C320	20	0	1	20983	5	4.26	4.32	0.06	18198	15858	12961
C320	20	0	1	18795	4.9	4.26	4.27	0.01	18254	15907	13001
C320	20	0	1	18946	4.9	4.26	4.28	0.02	18254	15907	13001
C320	20	0	1	19199	4.9	4.26	4.28	0.02	18254	15907	13001
C320	20	0	1	19490	4.9	4.26	4.29	0.03	18254	15907	13001
C320	20	0	1	20007	4.9	4.26	4.30	0.04	18254	15907	13001
C320	20	0	5	23864	5.3	4.32	4.38	0.06	20758	18089	14784
C320	20	0	5	18373	5.2	4.32	4.26	-0.05	20800	18125	14814
C320	20	0	5	23033	5.2	4.32	4.36	0.04	20800	18125	14814
C320	20	0	5	20212	5.1	4.32	4.31	-0.01	20841	18162	14844
C320	20	0	5	20765	5.1	4.32	4.32	0.00	20841	18162	14844
C320	20	0	5	24341	5.1	4.32	4.39	0.07	20841	18162	14844
C320	20	0	5	18041	5	4.32	4.26	-0.06	20883	18198	14874
C320	20	0	5	23176	5	4.32	4.37	0.05	20883	18198	14874
C320	20	0	5	21573	4.9	4.32	4.33	0.01	20924	18234	14903
C320	20	0	5	21810	4.9	4.32	4.34	0.02	20924	18234	14903
C320	20	0	5	22280	4.9	4.32	4.35	0.03	20924	18234	14903
C320	20	0	5	22934	4.9	4.32	4.36	0.04	20924	18234	14903
C320	20	0	10	24987	5.3	4.34	4.40	0.06	21686	18897	15445
C320	20	0	10	19770	5.2	4.34	4.30	-0.04	21722	18929	15471
C320	20	0	10	24228	5.2	4.34	4.38	0.05	21722	18929	15471
C320	20	0	10	21478	5.1	4.34	4.33	-0.01	21758	18960	15496
C320	20	0	10	21995	5.1	4.34	4.34	0.00	21758	18960	15496
C320	20	0	10	25679	5.1	4.34	4.41	0.07	21758	18960	15496
C320	20	0	10	19162	5	4.34	4.28	-0.06	21793	18991	15522
C320	20	0	10	22900	5	4.34	4.36	0.02	21793	18991	15522
C320	20	0	10	24719	5	4.34	4.39	0.05	21793	18991	15522
C320	20	0	10	22695	4.9	4.34	4.36	0.02	21829	19022	15547
C320	20	0	10	23570	4.9	4.34	4.37	0.03	21829	19022	15547
C320	20	0	10	24000	4.9	4.34	4.38	0.04	21829	19022	15547
C320	20	0	25	26412	5.3	4.36	4.42	0.07	22707	19787	16173
C320	20	0	25	21562	5.2	4.36	4.33	-0.02	22736	19813	16193
C320	20	0	25	25550	5.2	4.36	4.41	0.05	22736	19813	16193
C320	20	0	25	23065	5.1	4.36	4.36	0.01	22765	19838	16214
C320	20	0	25	23505	5.1	4.36	4.37	0.01	22765	19838	16214
C320	20	0	25	27401	5.1	4.36	4.44	0.08	22765	19838	16214

C320	20	0	25	20606	5	4.36	4.31	-0.04	22794	19863	16234
C320	20	0	25	24285	5	4.36	4.39	0.03	22794	19863	16234
C320	20	0	25	26629	5	4.36	4.43	0.07	22794	19863	16234
C320	20	0	25	24140	4.9	4.36	4.38	0.02	22822	19888	16255
C320	20	0	25	25277	4.9	4.36	4.40	0.04	22822	19888	16255
C320	20	0	25	25322	4.9	4.36	4.40	0.05	22822	19888	16255

Appendix C Confidence Interval Calculations

Temperature Shift Factors

a b
0.000414 -0.110376947

Se (log) 0.054

Master Curve Parameters

α β γ δ
1.324 3.075 -1.417 -0.668

R² Log 0.99

R² (Arith) 0.97

Se (Arith) 1315

Observations 160

Binder Type	Nominal Size (mm)	Confinement (KPa)	Frequency (Hz)	Modulus (MPa)	Test Temp (oC)	(Log) Modulus			Adjusted α for Confidence		
						Predicted	Mesured	Error (log)	1.324	1.288	1.235
AR450	20	0	0.5	239	50.5	2.50	2.38	-0.12	314	289	256
AR450	20	0	0.5	256	50.3	2.51	2.41	-0.10	321	295	261
AR450	20	0	0.5	307	50.3	2.51	2.49	-0.02	321	295	261
AR450	20	0	0.5	276	50.2	2.51	2.44	-0.07	324	298	264
AR450	20	0	0.5	282	50.2	2.51	2.45	-0.06	324	298	264
AR450	20	0	0.5	297	50.1	2.51	2.47	-0.04	327	301	266
AR450	20	0	0.5	345	50.1	2.51	2.54	0.02	327	301	266
AR450	20	0	0.5	402	50.1	2.51	2.60	0.09	327	301	266
AR450	20	0	1	352	50.5	2.65	2.55	-0.10	443	407	360
AR450	20	0	1	372	50.2	2.66	2.57	-0.09	457	420	372
AR450	20	0	1	403	50.2	2.66	2.61	-0.05	457	420	372
AR450	20	0	1	405	50.2	2.66	2.61	-0.05	457	420	372
AR450	20	0	1	435	50.1	2.66	2.64	-0.03	462	425	376
AR450	20	0	1	503	50.1	2.66	2.70	0.04	462	425	376
AR450	20	0	1	561	50.1	2.66	2.75	0.08	462	425	376
AR450	20	0	1	449	49.9	2.67	2.65	-0.02	471	434	384
AR450	20	0	5	956	50.4	3.01	2.98	-0.03	1018	936	829
AR450	20	0	5	987	50.2	3.02	2.99	-0.02	1039	956	846
AR450	20	0	5	992	50.2	3.02	3.00	-0.02	1039	956	846
AR450	20	0	5	1249	50.2	3.02	3.10	0.08	1039	956	846
AR450	20	0	5	942	50.1	3.02	2.97	-0.05	1050	966	855
AR450	20	0	5	1103	50.1	3.02	3.04	0.02	1050	966	855
AR450	20	0	5	1300	50.1	3.02	3.11	0.09	1050	966	855
AR450	20	0	5	1139	49.7	3.04	3.06	0.02	1095	1008	892
AR450	20	0	10	1422	50.3	3.16	3.15	-0.01	1456	1340	1185
AR450	20	0	10	1417	50.2	3.17	3.15	-0.02	1471	1353	1198
AR450	20	0	10	1790	50.2	3.17	3.25	0.09	1471	1353	1198
AR450	20	0	10	1415	50.1	3.17	3.15	-0.02	1486	1367	1210
AR450	20	0	10	1601	50.1	3.17	3.20	0.03	1486	1367	1210
AR450	20	0	10	1389	50	3.18	3.14	-0.03	1501	1381	1222
AR450	20	0	10	1830	50	3.18	3.26	0.09	1501	1381	1222
AR450	20	0	10	1653	49.6	3.19	3.22	0.02	1563	1438	1273
AR450	20	0	0.5	2172	35.5	3.22	3.34	0.12	1654	1522	1346
AR450	20	0	0.5	1631	35.4	3.22	3.21	-0.01	1673	1539	1362
AR450	20	0	0.5	1639	35.3	3.23	3.21	-0.01	1692	1556	1377
AR450	20	0	0.5	1886	35.3	3.23	3.28	0.05	1692	1556	1377
AR450	20	0	0.5	1928	35.3	3.23	3.29	0.06	1692	1556	1377
AR450	20	0	0.5	2120	35.3	3.23	3.33	0.10	1692	1556	1377
AR450	20	0	0.5	1558	35.2	3.23	3.19	-0.04	1711	1574	1393
AR450	20	0	0.5	1942	34.8	3.25	3.29	0.04	1791	1647	1458
AR450	20	0	25	2292	50.3	3.35	3.36	0.01	2257	2076	1837
AR450	20	0	25	2205	50.2	3.36	3.34	-0.01	2279	2096	1855
AR450	20	0	25	2750	50.2	3.36	3.44	0.08	2279	2096	1855
AR450	20	0	1	2900	35.5	3.36	3.46	0.10	2296	2112	1869
AR450	20	0	25	2215	50.1	3.36	3.35	-0.02	2300	2116	1872
AR450	20	0	25	2522	50.1	3.36	3.40	0.04	2300	2116	1872

AR450	20	0	1	2632	35.4	3.37	3.42	0.05	2320	2135	1889
AR450	20	0	25	2287	50	3.37	3.36	-0.01	2322	2136	1890
AR450	20	0	25	2757	50	3.37	3.44	0.07	2322	2136	1890
AR450	20	0	1	2189	35.3	3.37	3.34	-0.03	2345	2158	1909
AR450	20	0	1	2590	35.3	3.37	3.41	0.04	2345	2158	1909
AR450	20	0	1	2858	35.3	3.37	3.46	0.09	2345	2158	1909
AR450	20	0	1	2219	35.2	3.37	3.35	-0.03	2371	2181	1930
AR450	20	0	1	2245	35.1	3.38	3.35	-0.03	2396	2204	1951
AR450	20	0	25	2610	49.6	3.38	3.42	0.03	2411	2218	1963
AR450	20	0	1	2669	34.9	3.39	3.43	0.04	2448	2252	1993
AR450	20	0	5	4840	35.5	3.65	3.68	0.03	4511	4149	3672
AR450	20	0	5	5143	35.4	3.66	3.71	0.05	4551	4186	3704
AR450	20	0	5	4303	35.3	3.66	3.63	-0.03	4591	4223	3737
AR450	20	0	5	4800	35.2	3.67	3.68	0.02	4631	4260	3770
AR450	20	0	5	5139	35.2	3.67	3.71	0.05	4631	4260	3770
AR450	20	0	5	4083	35.1	3.67	3.61	-0.06	4672	4298	3803
AR450	20	0	5	4188	35.1	3.67	3.62	-0.05	4672	4298	3803
AR450	20	0	5	4916	35	3.67	3.69	0.02	4713	4335	3836
AR450	20	0	10	6003	35.5	3.76	3.78	0.02	5777	5315	4703
AR450	20	0	10	6311	35.4	3.77	3.80	0.03	5823	5357	4740
AR450	20	0	10	5379	35.3	3.77	3.73	-0.04	5869	5399	4778
AR450	20	0	10	5948	35.2	3.77	3.77	0.00	5915	5441	4815
AR450	20	0	10	6331	35.2	3.77	3.80	0.03	5915	5441	4815
AR450	20	0	10	5081	35.1	3.78	3.71	-0.07	5962	5484	4853
AR450	20	0	10	5216	35	3.78	3.72	-0.06	6008	5527	4891
AR450	20	0	10	6071	35	3.78	3.78	0.00	6008	5527	4891
AR450	20	0	0.5	7223	20.7	3.86	3.86	0.00	7167	6593	5835
AR450	20	0	0.5	6346	20.2	3.87	3.80	-0.07	7451	6854	6065
AR450	20	0	0.5	6580	20.2	3.87	3.82	-0.05	7451	6854	6065
AR450	20	0	0.5	7775	20.1	3.88	3.89	0.02	7508	6907	6112
AR450	20	0	0.5	8514	20.1	3.88	3.93	0.05	7508	6907	6112
AR450	20	0	0.5	8557	20.1	3.88	3.93	0.06	7508	6907	6112
AR450	20	0	0.5	7189	20	3.88	3.86	-0.02	7566	6959	6159
AR450	20	0	0.5	8244	20	3.88	3.92	0.04	7566	6959	6159
AR450	20	0	25	7574	35.4	3.89	3.88	-0.01	7735	7116	6297
AR450	20	0	25	6937	35.3	3.89	3.84	-0.05	7787	7163	6339
AR450	20	0	25	8069	35.3	3.89	3.91	0.02	7787	7163	6339
AR450	20	0	25	7582	35.2	3.89	3.88	-0.01	7839	7211	6381
AR450	20	0	25	7976	35.2	3.89	3.90	0.01	7839	7211	6381
AR450	20	0	25	6527	35	3.90	3.81	-0.09	7942	7306	6466
AR450	20	0	25	6684	35	3.90	3.83	-0.07	7942	7306	6466
AR450	20	0	25	7653	35	3.90	3.88	-0.02	7942	7306	6466
AR450	20	0	1	8331	20.4	3.95	3.92	-0.03	8880	8168	7228
AR450	20	0	1	7344	20.2	3.95	3.87	-0.09	9000	8279	7326
AR450	20	0	1	9920	20.2	3.95	4.00	0.04	9000	8279	7326
AR450	20	0	1	7672	20.1	3.96	3.88	-0.07	9060	8334	7375
AR450	20	0	1	8985	20.1	3.96	3.95	0.00	9060	8334	7375
AR450	20	0	1	9965	20.1	3.96	4.00	0.04	9060	8334	7375
AR450	20	0	1	8387	20	3.96	3.92	-0.04	9120	8390	7424
AR450	20	0	1	9510	20	3.96	3.98	0.02	9120	8390	7424
AR450	20	0	5	9949	20.2	4.10	4.00	-0.11	12710	11692	10347
AR450	20	0	5	11069	20.2	4.10	4.04	-0.06	12710	11692	10347
AR450	20	0	5	13372	20.2	4.10	4.13	0.02	12710	11692	10347
AR450	20	0	5	10553	20.1	4.11	4.02	-0.08	12770	11747	10395
AR450	20	0	5	11916	20.1	4.11	4.08	-0.03	12770	11747	10395
AR450	20	0	5	13305	20.1	4.11	4.12	0.02	12770	11747	10395
AR450	20	0	5	11399	20	4.11	4.06	-0.05	12829	11801	10443
AR450	20	0	5	12672	20	4.11	4.10	-0.01	12829	11801	10443
AR450	20	0	10	11033	20.2	4.15	4.04	-0.11	14241	13100	11592
AR450	20	0	10	11783	20.1	4.16	4.07	-0.08	14297	13152	11638
AR450	20	0	10	12300	20.1	4.16	4.09	-0.07	14297	13152	11638

AR450	20	0	10	13122	20.1	4.16	4.12	-0.04	14297	13152	11638
AR450	20	0	10	14888	20.1	4.16	4.17	0.02	14297	13152	11638
AR450	20	0	10	14889	20.1	4.16	4.17	0.02	14297	13152	11638
AR450	20	0	10	12750	20	4.16	4.11	-0.05	14353	13204	11684
AR450	20	0	10	14098	20	4.16	4.15	-0.01	14353	13204	11684
AR450	20	0	25	12487	20.2	4.21	4.10	-0.11	16114	14823	13117
AR450	20	0	25	13456	20.1	4.21	4.13	-0.08	16165	14870	13159
AR450	20	0	25	14721	20.1	4.21	4.17	-0.04	16165	14870	13159
AR450	20	0	25	16905	20.1	4.21	4.23	0.02	16165	14870	13159
AR450	20	0	25	17089	20.1	4.21	4.23	0.02	16165	14870	13159
AR450	20	0	25	13744	20	4.21	4.14	-0.07	16215	14916	13200
AR450	20	0	25	14491	20	4.21	4.16	-0.05	16215	14916	13200
AR450	20	0	25	15995	20	4.21	4.20	-0.01	16215	14916	13200
AR450	20	0	0.5	15252	5.1	4.22	4.18	-0.04	16648	15314	13552
AR450	20	0	0.5	16620	5.1	4.22	4.22	0.00	16648	15314	13552
AR450	20	0	0.5	18393	5.1	4.22	4.26	0.04	16648	15314	13552
AR450	20	0	0.5	16342	5	4.22	4.21	-0.01	16702	15364	13596
AR450	20	0	0.5	18585	5	4.22	4.27	0.05	16702	15364	13596
AR450	20	0	0.5	20393	5	4.22	4.31	0.09	16702	15364	13596
AR450	20	0	0.5	16607	4.9	4.22	4.22	0.00	16756	15414	13640
AR450	20	0	0.5	18499	4.9	4.22	4.27	0.04	16756	15414	13640
AR450	20	0	1	16069	5.1	4.25	4.21	-0.05	17871	16439	14547
AR450	20	0	1	17732	5.1	4.25	4.25	0.00	17871	16439	14547
AR450	20	0	1	19585	5.1	4.25	4.29	0.04	17871	16439	14547
AR450	20	0	1	21674	5.1	4.25	4.34	0.08	17871	16439	14547
AR450	20	0	1	17387	5	4.25	4.24	-0.01	17919	16484	14587
AR450	20	0	1	19904	5	4.25	4.30	0.05	17919	16484	14587
AR450	20	0	1	17778	4.9	4.25	4.25	0.00	17967	16528	14626
AR450	20	0	1	19545	4.9	4.25	4.29	0.04	17967	16528	14626
AR450	20	0	5	18395	5.1	4.31	4.26	-0.04	20192	18575	16437
AR450	20	0	5	19688	5.1	4.31	4.29	-0.01	20192	18575	16437
AR450	20	0	5	20118	5.1	4.31	4.30	0.00	20192	18575	16437
AR450	20	0	5	22140	5.1	4.31	4.35	0.04	20192	18575	16437
AR450	20	0	5	24444	5.1	4.31	4.39	0.08	20192	18575	16437
AR450	20	0	5	22758	5	4.31	4.36	0.05	20228	18607	16466
AR450	20	0	5	20404	4.9	4.31	4.31	0.00	20263	18640	16495
AR450	20	0	5	21794	4.9	4.31	4.34	0.03	20263	18640	16495
AR450	20	0	10	19271	5.1	4.32	4.28	-0.04	20980	19299	17079
AR450	20	0	10	20626	5.1	4.32	4.31	-0.01	20980	19299	17079
AR450	20	0	10	21052	5.1	4.32	4.32	0.00	20980	19299	17079
AR450	20	0	10	23172	5.1	4.32	4.36	0.04	20980	19299	17079
AR450	20	0	10	25514	5.1	4.32	4.41	0.08	20980	19299	17079
AR450	20	0	10	23937	5	4.32	4.38	0.06	21011	19328	17104
AR450	20	0	10	21368	4.9	4.32	4.33	0.01	21041	19356	17129
AR450	20	0	10	22662	4.9	4.32	4.36	0.03	21041	19356	17129
AR450	20	0	25	20324	5.1	4.34	4.31	-0.03	21849	20099	17786
AR450	20	0	25	21922	5.1	4.34	4.34	0.00	21849	20099	17786
AR450	20	0	25	22141	5.1	4.34	4.35	0.01	21849	20099	17786
AR450	20	0	25	26887	5.1	4.34	4.43	0.09	21849	20099	17786
AR450	20	0	25	22603	5	4.34	4.35	0.01	21874	20122	17807
AR450	20	0	25	24319	5	4.34	4.39	0.05	21874	20122	17807
AR450	20	0	25	25404	5	4.34	4.40	0.06	21874	20122	17807
AR450	20	0	25	23593	4.9	4.34	4.37	0.03	21899	20144	17827

Appendix C Confidence Interval Calculations

Temperature Shift Factors

a b
0.000459 -0.112812107

Se (log) 0.068

Master Curve Parameters

α β γ δ
1.377 3.068 -1.381 -0.631

R² Log 0.99

R² (Arith) 0.98

Se (Arith) 1139

Observations 160

Binder Type	Nominal Size (mm)	Confinement (KPa)	Frequency (Hz)	Modulus (MPa)	Test Temp (oC)	(Log) Modulus			Adjusted α for Confidence		
						Predicted	Mesured	Error (log)	1.377	1.331	1.265
C600	20	0	0.5	477	50.7	2.57	2.68	0.11	374	337	289
C600	20	0	0.5	294	50.6	2.58	2.47	-0.11	378	340	292
C600	20	0	0.5	348	50.6	2.58	2.54	-0.04	378	340	292
C600	20	0	0.5	345	50.5	2.58	2.54	-0.04	382	343	295
C600	20	0	0.5	282	50.4	2.59	2.45	-0.14	385	347	298
C600	20	0	0.5	490	50.4	2.59	2.69	0.10	385	347	298
C600	20	0	0.5	308	50.2	2.59	2.49	-0.11	393	353	303
C600	20	0	0.5	401	50.2	2.59	2.60	0.01	393	353	303
C600	20	0	1	672	50.7	2.71	2.83	0.11	518	466	400
C600	20	0	1	423	50.6	2.72	2.63	-0.09	523	471	404
C600	20	0	1	476	50.5	2.72	2.68	-0.05	529	476	408
C600	20	0	1	700	50.4	2.73	2.85	0.12	534	480	412
C600	20	0	1	390	50.3	2.73	2.59	-0.14	539	485	416
C600	20	0	1	432	50.3	2.73	2.64	-0.10	539	485	416
C600	20	0	1	483	50.3	2.73	2.68	-0.05	539	485	416
C600	20	0	1	552	50.2	2.74	2.74	0.01	544	490	421
C600	20	0	5	1531	50.7	3.05	3.18	0.13	1126	1013	870
C600	20	0	5	935	50.3	3.07	2.97	-0.10	1171	1054	905
C600	20	0	5	1030	50.3	3.07	3.01	-0.06	1171	1054	905
C600	20	0	5	1082	50.3	3.07	3.03	-0.03	1171	1054	905
C600	20	0	5	1046	50.2	3.07	3.02	-0.05	1183	1064	914
C600	20	0	5	1152	50.2	3.07	3.06	-0.01	1183	1064	914
C600	20	0	5	1619	50.2	3.07	3.21	0.14	1183	1064	914
C600	20	0	5	1250	50.1	3.08	3.10	0.02	1194	1075	923
C600	20	0	10	2134	50.7	3.19	3.33	0.14	1564	1407	1208
C600	20	0	10	1363	50.2	3.22	3.13	-0.08	1641	1477	1268
C600	20	0	10	1490	50.2	3.22	3.17	-0.04	1641	1477	1268
C600	20	0	10	1514	50.2	3.22	3.18	-0.03	1641	1477	1268
C600	20	0	10	1524	50.2	3.22	3.18	-0.03	1641	1477	1268
C600	20	0	10	1657	50.2	3.22	3.22	0.00	1641	1477	1268
C600	20	0	10	2247	50.2	3.22	3.35	0.14	1641	1477	1268
C600	20	0	10	1755	50.1	3.22	3.24	0.03	1657	1491	1280
C600	20	0	0.5	1773	35.3	3.28	3.25	-0.03	1898	1708	1466
C600	20	0	0.5	1866	35.3	3.28	3.27	-0.01	1898	1708	1466
C600	20	0	0.5	2042	35.3	3.28	3.31	0.03	1898	1708	1466
C600	20	0	0.5	1806	35.2	3.28	3.26	-0.03	1918	1727	1482
C600	20	0	0.5	2587	35.2	3.28	3.41	0.13	1918	1727	1482
C600	20	0	0.5	2596	35.2	3.28	3.41	0.13	1918	1727	1482
C600	20	0	0.5	1884	35	3.29	3.28	-0.02	1960	1764	1515
C600	20	0	0.5	2025	35	3.29	3.31	0.01	1960	1764	1515
C600	20	0	25	3179	50.7	3.38	3.50	0.13	2372	2135	1833
C600	20	0	25	2213	50.2	3.39	3.34	-0.05	2481	2233	1917
C600	20	0	25	2362	50.2	3.39	3.37	-0.02	2481	2233	1917
C600	20	0	25	2368	50.2	3.39	3.37	-0.02	2481	2233	1917
C600	20	0	25	2404	50.2	3.39	3.38	-0.01	2481	2233	1917
C600	20	0	25	2592	50.2	3.39	3.41	0.02	2481	2233	1917

Appendix D1 Lab to Field Conversion FWD

Temperature Correction (Slope) 1
 Temperature Correction (+) 2
 Frequency 5.5

Cell	Temperature oC		FWD Modulus (MPa) a	Master Curve Parameters						Fr	E* _{pred}
	Mid	Corrected		b	α	β	γ	δ			
Mn33	-2	0	19500	0.000	-0.109	1.891	2.398	-0.592	-0.627	3.026	12740
	0	2	19000							2.788	11973
	0.5	3	18500							2.728	11775
	1	3	16000							2.669	11574
	2	4	12000							2.552	11168
	3	5	15000							2.434	10754
	4	6	10000							2.318	10334
	4	6	14000							2.318	10334
	7.5	10	10000							1.913	8838
	7.5	10	6500							1.913	8838
	8	10	11000							1.856	8623
	9	11	8500							1.742	8195
	11	13	5800							1.516	7352
	12	14	5100							1.403	6939
	13.5	16	7500							1.235	6334
	12.5	15	4800							1.347	6735
	13	15	4500							1.291	6534
	15	17	6000							1.069	5753
	15	17	9100							1.069	5753
	16	18	5000							0.958	5381
	17	19	4800							0.849	5021
	17.5	20	4000							0.794	4847
	18	20	6000							0.739	4676
	20	22	7100							0.522	4030
	20.5	23	2900							0.468	3879
	21	23	2900							0.414	3731
	22	24	3800							0.307	3448
	22.5	25	3000							0.254	3313
	25	27	4000							-0.011	2698
	26	28	3100							-0.116	2479
	27.5	30	2400							-0.273	2181
	28	30	2100							-0.325	2089
	30	32	2000							-0.531	1755
31	33	2300	-0.634	1608							
32	34	2100	-0.736	1473							
31	33	2900	-0.634	1608							
33	35	1400	-0.837	1350							
35	37	1300	-1.038	1134							
35	37	1700	-1.038	1134							
35	37	1150	-1.038	1134							
36	38	1300	-1.138	1040							
37	39	1200	-1.238	955							
36	38	1100	-1.138	1040							
38	40	900	-1.336	878							
40	42	900	-1.532	744							
	-1	1	9700							2.906	12889
	0	2	17000							2.788	12338
	0	2	11000							2.788	12338
	1	3	7000							2.669	11789
	2.5	5	9500							2.493	10970

Mn34	4	6	9500	0.001	-0.118	1.564	2.884	-0.500	-0.523	2.318	10164
	5	7	7500							2.201	9636
	6	8	9000							2.086	9117
	6.5	9	7200							2.028	8862
	9	11	6100							1.742	7631
	9	11	6500							1.742	7631
	9	11	6150							1.742	7631
	11	13	4600							1.516	6711
	10	12	4200							1.629	7163
	11.5	14	6100							1.459	6491
	12	14	4800							1.403	6275
	12	14	4300							1.403	6275
	14	16	6700							1.180	5457
	17	19	4100							0.849	4367
	18	20	4900							0.739	4041
	19	21	5500							0.630	3734
	19	21	4500							0.630	3734
	20	22	2000							0.522	3446
	22	24	2900							0.307	2923
	22	24	2300							0.307	2923
	24	26	2000							0.094	2469
	24	26	2400							0.094	2469
	24.5	27	1400							0.042	2365
	24.5	27	1600							0.042	2365
	25	27	1800							-0.011	2266
	25	27	2100							-0.011	2266
	29	31	1500							-0.428	1599
	29	31	2050							-0.428	1599
	29	31	1950							-0.428	1599
	32	34	1000							-0.736	1227
	31	33	2000							-0.634	1340
	33	35	1700							-0.837	1124
	35	37	1750							-1.038	944
	35.5	38	1200							-1.088	904
35.5	38	1100	-1.088	904							
36	38	1050	-1.138								
39	41	1100	-1.435								
45	47	900	-2.013								
45	47	1050	-2.013								
6	8	11376							2.073	11374	
9	11	11032							1.755	10317	
9	11	9653							1.692	10105	
10	12	11032							1.629	9894	
10	12	10342							1.629	9894	
11	13	11376							1.566	9683	
11	13	9653							1.503	9473	
12	14	9653							1.440	9264	
14	16	8963							1.192	8436	
15	17	7239							1.069	8031	
17	19	8618							0.824	7242	
18	20	6550							0.763	7050	
18	20	7067							0.703	6860	
19	21	7239							0.673	6766	
19	21	6895							0.642	6673	
20	22	6895							0.522	6307	
21	23	6033							0.462	6128	
22	24	6205							0.343	5778	
24	26	4482							0.136	5196	
24	26	5516							0.106	5116	

NCAT S9	24	26	5033	0.000	-0.115	1.935	2.413	-0.969	-0.489	0.047	4958
	25	27	3792							-0.011	4804
	26	28	3999							-0.070	4653
	26	28	3585							-0.128	4505
	27	29	4413							-0.186	4361
	28	30	3723							-0.273	4151
	28	30	3792							-0.302	4082
	29	31	3309							-0.417	3818
	29	31	3516							-0.474	3690
	32	34	2792							-0.758	3104
	33	35	2723							-0.871	2893
	34	36	2413							-0.927	2792
	34	36	2689							-0.983	2694
	35	37	2482							-1.038	2600
	36	38	2551							-1.122	2464
	36	38	2137							-1.122	2464
	36	38	2206							-1.149	2420
	36	38	2275							-1.149	2420
	37	39	2034							-1.260	2251
	38	40	1999							-1.314	2171
	38	40	2041							-1.342	2132
	39	41	1793							-1.424	2019
	39	41	1758							-1.451	1983
	39	41	1724							-1.478	1947
	41	43	1586							-1.586	1811
	41	43	1737							-1.586	1811
41	43	1586	-1.640	1746							
41	43	1724	-1.667	1715							
42	44	1655	-1.747	1624							
43	45	1517	-1.801	1566							
43	45	1517	-1.854	1511							
46	48	1344	-2.065	1309							
NCAT S11	9	11	10687	0.000	-0.115	2.014	2.316	-0.770	-0.506	1.692	8898
	11	13	9997							1.566	8484
	11	13	9308							1.503	8279
	12	14	7584							1.378	7873
	13	15	7239							1.254	7473
	16	18	6033							1.007	6700
	17	19	6757							0.855	6236
	17	19	6757							0.824	6145
	18	20	6205							0.703	5790
	19	21	5516							0.642	5617
	22	24	5171							0.283	4644
	22	24	5033							0.283	4644
	24	26	4275							0.077	4134
	27	29	3516							-0.186	3540
	27	29	3861							-0.244	3418
	29	31	2620							-0.474	2964
	34	36	2206							-0.983	2133
	37	39	1655							-1.205	1840
37	39	1586	-1.260	1773							
38	40	1724	-1.314	1709							
40	42	1655	-1.532	1475							
41	43	1448	-1.586	1423							
42	44	1344	-1.721	1299							
	9	11	9653							1.692	9301
	11	13	9997							1.566	8891
	11	13	9825							1.503	8687
	13	15	8274							1.316	8083

NCAT S10	14	16	7929	0.000	-0.115	1.704	2.638	-0.999	-0.475	1.130	7492
	15	17	7584							1.069	7299
	17	19	6895							0.824	6547
	18	20	6757							0.703	6185
	18	20	6205							0.703	6185
	19	21	5861							0.582	5834
	20	22	5861							0.522	5663
	23	25	5171							0.224	4850
	23	25	5102							0.165	4697
	24	26	4482							0.047	4400
	27	29	4137							-0.186	3846
	29	31	3620							-0.474	3229
	29	31	3103							-0.474	3229
	30	32	2758							-0.531	3115
	35	37	1999							-1.038	2235
	37	39	2344							-1.205	1995
	39	41	1655							-1.451	1680
	41	43	1655							-1.586	1527
	41	43	1586							-1.586	1527
	42	44	1517							-1.747	1361
	43	45	1551							-1.801	1310
43	45	1379	-1.854	1260							
44	46	1241	-1.960	1168							
48	50	1310	-2.274	931							
50	52	1172	-2.480	803							
NCAT N7	9	11	13100	0.000	-0.122	1.787	2.897	-0.649	-0.359	1.692	11000
	11	13	12411							1.566	10436
	11	13	9653							1.503	10161
	11	13	7584							1.503	10161
	13	15	11721							1.316	9365
	14	16	8274							1.192	8859
	16	18	7929							0.946	7905
	17	19	8274							0.885	7679
	17	19	7239							0.885	7679
	19	21	5516							0.642	6823
	19	21	6205							0.582	6621
	19	21	6550							0.582	6621
	19	21	4275							0.582	6621
	22	24	5516							0.283	5684
	27	29	4137							-0.244	4280
	27	29	3103							-0.244	4280
	31	33	3447							-0.588	3526
	32	34	2758							-0.758	3199
	32	34	2413							-0.758	3199
	32	34	3034							-0.758	3199
	33	35	3516							-0.871	2997
43	45	1310	-1.801	1727							
43	45	1172	-1.801	1727							
43	45	1517	-1.854	1673							
	4	6	20684	0.000	-0.117	1.781	2.808	-0.713	-0.358	2.266	12198
	4	6	15168							2.266	12198
	7	9	14479							2.009	11148
	10	12	12066							1.629	9664
	10	12	8274							1.629	9664
	12	14	11721							1.440	8967
	13	15	10342							1.316	8520
	16	18	7584							1.007	7467
	19	21	6895							0.582	6152
	21	23	7929							0.402	5645

NCAT N3 Phase IV	24	26	5171							0.047	4733
	24	26	5861							0.047	4733
	24	26	4137							0.106	4876
	26	28	4826							-0.070	4457
	28	30	3447							-0.302	3948
	29	31	4137							-0.417	3714
	29	31	4895							-0.474	3601
	32	34	3378							-0.702	3182
	33	35	3792							-0.871	2898
	35	37	2689							-1.038	2639
	38	40	2068							-1.314	2257
	38	40	3103							-1.369	2187
	39	41	1999							-1.424	2120
	41	43	1931							-1.640	1872
	46	48	1655							-2.118	1420
	47	49	1379							-2.170	1378
	47	49	1586							-2.170	1378
	49	51	1103							-2.429	1187
	49	51	1448							-2.429	1187
	52	54	896							-2.633	1056
52	54	1103							-2.633	1056	
NCAT N5	10	12	13100							1.629	9565
	11	13	8618							1.566	9337
	12	14	11032							1.440	8891
	12	14	9653							1.440	8891
	12	14	12411							1.378	8672
	13	15	6826							1.254	8246
	14	16	9653							1.192	8038
	15	17	6205							1.069	7633
	16	18	8274							1.007	7436
	17	19	6205							0.885	7052
	18	20	5171							0.703	6502
	19	21	6550							0.642	6326
	27	29	3792	0.000	-0.119	1.688	2.896	-0.770	-0.347	-0.244	4109
	27	29	3241							-0.244	4109
	29	31	2758							-0.417	3756
	29	31	3103							-0.474	3644
	29	31	3792							-0.474	3644
	29	31	2896							-0.474	3644
	30	32	2413							-0.531	3535
	31	33	3309							-0.588	3430
	31	33	2896							-0.645	3327
	32	34	2896							-0.758	3130
	43	45	1448							-1.854	1690
	46	48	1379							-2.118	1452

Appendix D2 Laboratory to Field Conversion (Strain)

Pulse Length (k1) 1800
 Pulse Slope (k2) 0.0

Dynamic Factor 1
 Frequency Conversion 6.283185

Tempertaure Correction (Slope) 1
 Tempertaure Correction (+) 2

Test Cell	Tempertaure Shift Factors		Master Curve Paratmenters				Temperature (oC)			Pulse		Reduced		Thickness (mm)		Modulus (MPa)		Predicted			NCAT Reported		
	a	b	α	β	γ	δ	Mid	Corrected	time (Sec)	Frequency	pulse	Th1	Th2	E1	E2	E3	Strain ($\mu\epsilon$)	$\beta 1$	$\beta 2$	$\mu\epsilon$			
N2 5"	0.000	-0.117	1.762	2.828	-0.713	-0.355	45	10	12.0	0.09	1.77	1.21	127	635	8,060	69	110	171	436			80	
							45	16	17.6	0.09	1.77	0.54	127	635	5,964	69	110	214				125	
							45	21	23.1	0.09	1.77	-0.11	127	635	4,316	69	110	272				175	
							45	27	28.7	0.09	1.77	-0.75	127	635	3,077	69	110	346				240	
							45	32	34.2	0.09	1.77	-1.36	127	635	2,180	69	110	439				375	
							45	38	39.8	0.09	1.77	-1.96	127	635	1,547	69	110	551				550	
							45	41	42.6	0.09	1.77	-2.25	127	635	1,308	69	110	614					
N3 9"	0.000	-0.116	1.810	2.775	-0.711	-0.363	45	10	12.0	0.09	1.77	1.20	229	533	8,234	90	214	67	5.50E-03	2.332		70	
							45	16	17.6	0.09	1.77	0.53	229	533	6,105	90	214	86				80	
							45	21	23.1	0.09	1.77	-0.11	229	533	4,429	90	214	111				110	
							45	27	28.7	0.09	1.77	-0.74	229	533	3,168	90	214	143				150	
							45	32	34.2	0.09	1.77	-1.34	229	533	2,254	90	214	186				195	
							45	38	39.8	0.09	1.77	-1.93	229	533	1,609	90	214	237				245	
							45	41	42.6	0.09	1.77	-2.21	229	533	1,364	90	214	266				260	
N4 9" Modified	0.001	-0.129	1.688	2.896	-0.770	-0.347	45	10	12.0	0.09	1.77	1.32	229	533	8,455	83	221	69	1.30E-03	2.632		60	
							45	16	17.6	0.09	1.77	0.57	229	533	6,109	83	221	88				75	
							45	21	23.1	0.09	1.77	-0.15	229	533	4,315	83	221	113				95	
							45	27	28.7	0.09	1.77	-0.83	229	533	3,010	83	221	146				130	
							45	32	34.2	0.09	1.77	-1.48	229	533	2,096	83	221	188				181	
							45	38	39.8	0.09	1.77	-2.09	229	533	1,473	83	221	241				240	
							45	43	45.3	0.09	1.77	-2.67	229	533	1,054	83	221	303				310	
N5 7" Modified	0.000	-0.119	1.688	2.896	-0.770	-0.347	45	10	12.0	0.09	1.77	1.23	178	584	8,164	48	193	109	1.09E-02	2.291		85	
							45	16	17.6	0.09	1.77	0.54	178	584	6,040	48	193	139				129	
							45	21	23.1	0.09	1.77	-0.12	178	584	4,379	48	193	179				184	
							45	27	28.7	0.09	1.77	-0.75	178	584	3,136	48	193	232				250	
							45	32	34.2	0.09	1.77	-1.36	178	584	2,238	48	193	301				327	
							45	38	39.8	0.09	1.77	-1.95	178	584	1,604	48	193	387				416	
							45	41	42.6	0.09	1.77	-2.23	178	584	1,363	48	193	436				466	
N6 7"	0.000	-0.118	1.715	2.882	-0.715	-0.348	45	10	12.0	0.09	1.77	1.21	178	584	7,894	76	221	104	1.89E-02	2.155		86	
							45	16	17.6	0.09	1.77	0.54	178	584	5,830	76	221	131				128	
							45	21	23.1	0.09	1.77	-0.12	178	584	4,209	76	221	169				178	
							45	27	28.7	0.09	1.77	-0.76	178	584	2,991	76	221	217				238	
							45	32	34.2	0.09	1.77	-1.38	178	584	2,109	76	221	278				307	
							45	38	39.8	0.09	1.77	-1.99	178	584	1,489	76	221	353				385	
							45	43	45.3	0.09	1.77	-2.58	178	584	1,060	76	221	442				473	
N7 SMA 7"	0.000	-0.122	1.787	2.897	-0.649	-0.359	45	10	12.0	0.09	1.77	1.25	178	584	9,095	79	221	93	8.31E-04	2.796		80	
							45	16	17.6	0.09	1.77	0.55	178	584	6,510	79	221	120				100	
							45	21	23.1	0.09	1.77	-0.13	178	584	4,561	79	221	156				125	
							45	27	28.7	0.09	1.77	-0.78	178	584	3,158	79	221	204				174	
							45	32	34.2	0.09	1.77	-1.41	178	584	2,184	79	221	265				242	
							45	38	39.8	0.09	1.77	-2.01	178	584	1,524	79	221	339				325	
							45	43	45.3	0.09	1.77	-2.59	178	584	1,082	79	221	427				424	
N8 7"	0.000	-0.122	1.787	2.897	-0.649	-0.359	45	10	12.0	0.09	1.77	1.25	178	584	9,095	72	207	95	1.17E-04	3.157		60	
							45	16	17.6	0.09	1.77	0.55	178	584	6,510	72	207	122				80	
							45	21	23.1	0.09	1.77	-0.13	178	584	4,561	72	207	160				90	
							45	27	28.7	0.09	1.77	-0.78	178	584	3,158	72	207	209				110	
							45	32	34.2	0.09	1.77	-1.41	178	584	2,184	72	207	272				190	
							45	38	39.8	0.09	1.77	-2.01	178	584	1,524	72	207	349				250	
							45	41	42.6	0.09	1.77	-2.30	178	584	1,281	72	207	393				300	

Appendix E Backcalculation Results

ID	Pres KPa	Temp	Measured (µm)										Thickness (mm)				Modulus (MPa)					Calculated (µm)										RMS
			0	200	300	450	600	750	900	1200	1500	L1	L2	L3	L4	E1	E2	E3	E4	E5	0	200	300	450	600	750	900	1200	1500			
LLAP Sections																																
H-S22_1	700	31.9	379	300	242	192	151	119	91	55	48	200	200	300	2933	2118	212	132	119	5000	380	293	248	193	150	118	93	59	39	0%		
H-S22_3	684	32.0	370	303	264	209	168	127	100	66	49	210	190	300	2978	2510	200	105	110	5000	374	299	259	208	165	132	105	67	44	0%		
H-S22_9	690	31.5	383	308	271	212	165	129	99	64	46	200	220	300	2700	2427	216	99	107	5000	386	306	263	209	165	131	104	66	42	0%		
H-S27_13	674	21.4	490	372	301	227	165	117	82	38	25	180	195	300	675	1312	345	66	55	5000	494	363	300	226	169	124	89	42	16	2%		
H-S27_16	699	21.9	560	434	361	266	203	143	106	60	36	200	200	300	650	1030	292	70	35	5000	568	417	348	270	209	159	119	63	29	1%		
H-S27_18	696	21.8	536	388	294	182	107	62	35	14	5	205	215	300	630	1124	344	49	99	5000	541	375	288	189	118	72	42	13	3	2%		
H-S28_12	707	25.8	482	346	281	202	156	119	92	62	45	265	205	150	730	862	147	864	33	5000	487	332	272	210	164	129	101	61	35	1%		
H-S28_16	687	26.1	329	235	192	153	118	92	75	51	41	285	240	300	525	1904	50	1016	54	5000	316	238	203	159	122	92	68	35	17	5%		
H-S28_18	698	25.6	398	294	222	152	107	83	64	41	33	265	235	300	550	1005	119	646	37	5000	407	271	217	161	120	91	69	41	24	1%		
H-S29_1	713	26.5	212	153	128	94	75	56	44	32	23	160	190	70	930	3203	681	8139	84	5000	208	152	126	98	78	63	50	31	19	1%		
H-S29_10	696	25.1	207	149	113	74	49	33	24	15	15	140	150	115	945	3643	351	5760	166	5000	209	143	109	75	54	39	28	14	7	4%		
H-S29_9	698	25.5	222	149	112	77	50	35	26	15	11	150	130	120	950	2607	420	2582	165	5000	221	147	113	79	57	41	30	15	7	3%		
H-S47_5	673	20.6	238	184	143	99	72	56	47	38	34	110	290	300	5000	6690	373	617	221	5000	239	176	138	99	75	60	50	37	28	1%		
H-S47_8	670	20.7	192	144	112	79	59	46	41	34	31	110	200	300	5000	7106	487	983	260	5000	193	139	109	79	62	51	43	32	24	1%		
H-S47_10	671	20.7	209	164	136	103	73	54	44	34	28	110	290	300	5000	8000	584	299	251	5000	211	160	130	97	74	59	48	34	25	0%		
H-S48_7	706	22.6	538	439	374	276	207	167	134	99	81	140	260	400	5000	3270	100	220	79	5000	543	435	364	277	214	170	139	100	76	0%		
H-S48_8	702	22.5	515	434	373	298	233	184	150	106	79	130	345	425	5913	4735	169	81	86	5000	517	429	369	292	233	187	153	106	78	0%		
H-S48_11	700	22.8	454	337	272	204	151	122	105	84	68	130	370	250	5000	2519	197	530	95	5000	454	335	268	198	154	126	107	82	63	0%		
SOU-S035_3	695	21.3	293	240	215	178	154	128	109	77	58	280	300	700	5000	3134	157	82	154	5000	286	238	214	183	156	131	110	77	54	0%		
SOU-S035_7	693	21.3	263	218	190	152	126	101	84	57	42	280	300	700	5000	2669	134	157	173	5000	267	212	186	154	127	104	85	58	40	0%		
SOU-S035_14	698	20.4	263	203	169	126	101	82	66	44	35	215	300	700	5000	2836	210	238	192	5000	263	201	169	132	103	81	65	44	32	0%		
SYD-S11_1	699	28.5	209	162	144	131	118	110	96	79	66	205	355	300	490	2492	2077	113	17	5000	210	162	146	131	118	106	95	74	56	0%		
SYD-S13_4	711	30.6	148	96	75	55	39	29	20	11	7	260	170	400	1256	2126	1438	202	561	5000	149	92	73	54	41	30	22	11	6	1%		
SYD-S13_7	694	30.8	155	92	74	56	45	38	27	23	15	270	170	400	5000	1791	2030	298	485	5000	155	91	73	57	46	37	30	20	14	0%		
SYD-S14_17	706	21.1	570	447	382	297	230	182	139	88	58	150	220	430	550	4556	2020	9322	32	5000	550	460	395	304	229	172	132	85	65	0%		
SYD-S15_18	731	30.8	253	172	131	83	61	51	32	30	21	210	165	400	4054	1727	209	518	296	5000	255	165	126	88	63	48	38	26	19	1%		
SYD-S15_20	698	30.8	382	299	256	206	159	123	93	61	39	210	150	400	2232	2104	278	103	108	5000	382	299	255	202	159	125	98	60	37	0%		
N4-150	698	16	381	284	208	145	98	51	18	18	18	180	220	330	5000	1550	216	160	142	5000	386	269	211	149	106	55	16	16	0%			
N7-70	696	18	144	134	121	108	93	69	38	38	38	225	220	330	5000	8333	263	252	180	5000	147	130	120	105	91	68	37	37	0%			
Q5-90	855		256	199	166	130	97	58	25	345	200	450	5000	5000	2172	105	164	394	5000	263	189	160	129	103	64	24	24	0%				
Q6-0	1020	19	276	212	183	150	120	80	41	345	200	450	5000	5000	2664	164	210	248	5000	278	207	180	150	124	85	41	41	0%				
V6-20	698	7	320	280	253	211	175	110	44	190	75	450	5000	5000	7049	699.8	56	156	5000	317	279	252	214	177	117	48	48	0%				
Non LLAP Sections																																
H-S23_1	696.0	32.4942	669	481	389	272	190	129	96	62	44	220	230	400	1577	643	190	47	100	5000	679	460	370	276	205	152	112	58.8	29.4	2%		
H-S23_3	691.0	32.0491	624	463	370	259	181	116	81	63	47	200	250	270	1712	906	144	52	103	5000	632	448	361	262	190	137	99	51	25.9	4%		
H-S23_8	693.0	31.8891	723	496	370	232	139	93	68	46	38	200	300	400	1697	744	45	3268	79	5000	729	486	364	233	148	97.3	69.3	46	35.8	0%		
H-S24_13	701.0	29.3833	1012	780	601	400	247	169	120	75	58	155	345	170	1638	840	68	71	56	5000	1033	744	583	402	279	197	142	77.1	42.7	2%		
H-S24_3	693.0	29.909	1083	869	714	516	371	254	186	121	94	160	440	150	1772	828	92	10	49	5000	1103	835	688	518	394	301	231	134	75.6	2%		
H-S24_7	701.0	29.8963	728	588	485	354	255	180	130	84	64	165	435	100	1854	1129	137	17	61	5000	744	559	460	348	267	206	160	96.5	57.2	1%		
SYD-S24_2	696.0	24.0754	569	477	411	349	282	234	185	133	93	190	310	260	5000	1460	315	22	76	5000	578	462	406	339	285	240	202	142	100	0%		
SYD-S25_13	702.0	23.2175	785	606	501	370	280	223	161	88	54	150	450	300	1385	1855	76	108	42	5000	777	612	507	376	279	209	158	94.6	58	0%		
SYD-S25_2	699.0	23.3771	860	761	614	466	301	238	164	93	65	150	520	480	1177	2004	50	95	36	5000	889	718	602	451	332	243	179	101	59.8	0%		
SYD-S25_5	700.0	23.3366	800	603	473	333	244	194	154	108	78	150	200	450	4472	1031	142	71	83	5000	806	588	471	343	256	195	152	98.6	68.5	0%		
SYD-S16_3	701.0	20.4486	766	565	422	300	191	148	111	74	55	130	190	380	2769	1297	130	90	88	5000	771	551	427	295	209	154	117	72.3	47.3	0%		
SYD-S16_8	698.0	20.8358	692	540	464	343	271	212	165	104	74	145	235	300	2658	1162	332	37	69	5000	696	530	447	353	280	221	175	108	67	0%		
SYD-S46_12	702.0	26.0931	773	553	458	295	186	128	92	48	37	160	210	130	1558	1029	95	87	74	5000	777	556	435	299	206	143	100	50.5	25.2	2%		
SYD-S46_3	698.0	26.535	841	629	516	379	281	213	154	90	55	150	270	100	1790	984	163	32	53	5000	844	624	509	379	285	216	163	92.6	51.2	0%		
SYD-S46_6	703	26.7207	799	594	477	292	186	114	78	41	24	160	240	400	917.7	1126	57	122	60	5000	810	585	453	302	199	131	88.1	41.3	19.2	1%		
H-S39_11	700	24.4717	293	233	200	166	132	103	82	53	35																					

SYD-S33_2	705.0	24.9679	764	584	477	368	296	254	206	154	116	140	310	130	5000	1408	138	376	53	5000	764	581	480	371	298	247	209	155	117	0%
SYD-S33_6	703.0	25.1727	687	486	393	294	238	180	142	101	74	150	330	320	3702	1461	105	254	67	5000	675	500	402	293	221	175	144	104	77.8	0%
SYD-S44_18	703.0	26.1475	731	515	387	240	142	111	74	50	44	130	290	360	2256	1700	54	1170	95	5000	730	515	382	237	150	102	77.4	54.2	39.5	0%
SYD-S44_20	699.0	26.6046	827	560	471	356	270	181	137	73	50	150	300	450	1166	934	150	52	53	5000	814	587	469	342	254	190	143	79.4	42.4	0%
SOU-S089_14	699.0	22.8863	456	328	247	149	100	80	56	35	30	240	120	300	2424	925	41	1345	154	5000	467	305	236	163	114	82.5	62	38.3	25	1%

Appendix F Threshold Strain Validation LLAP Sections

Site	Season	Temperature (°C)				Surface Temp (°C)	Thickness (mm)				AC Temp (°C)	Modulus					Strain (µε)		
		Upper	Lower	Speed	Lat		L1	L2	L3	L4		WC	BC	Eff	L2	L3		L4	L5
H-S27_13 Pac Hwy	Summer Ave	27	16.3	90	33.5	46	180	195	300	675	39.2	1377	1565	1522	345	66	55	5000	180
	Summer Upper 10%	34	19.6	90	33.5	53	180	195	300	675	43.7	951	1084	1054	345	66	55	5000	204
	Autumn	22	12	90	33.5	41	180	195	300	675	33.1	2323	2701	2614	345	66	55	5000	142
	Winter	15.8	6.1	90	33.5	36	180	195	300	675	26.6	4038	4865	4672	345	66	55	5000	105
	Winter Lower 10%	12.9	3	90	33.5	3	180	195	300	675	7.8	11557	13829	13301	345	66	55	5000	55
H-S27_16 Pac Hwy	Summer Ave	27	16.3	90	33.5	46	200	200	300	650	38.6	1440	1638	1597	292	70	35	5000	173
	Summer Upper 10%	34	19.6	90	33.5	53	200	200	300	650	43.1	1003	1142	1113	292	70	35	5000	199
	Autumn	22	12	90	33.5	41	200	200	300	650	32.6	2436	2840	2755	292	70	35	5000	134
	Winter	15.8	6.1	90	33.5	36	200	200	300	650	26.0	4220	5098	4914	292	70	35	5000	98
	Winter Lower 10%	12.9	3	90	33.5	3	200	200	300	650	7.8	11558	13830	13354	292	70	35	5000	51
H-S27_18 Pac Hwy	Summer Ave	27	16.3	90	33.5	46	205	215	300	630	38.5	1455	1656	1616	344	49	99	5000	151
	Summer Upper 10%	34	19.6	90	33.5	53	205	215	300	630	42.9	1016	1156	1128	344	49	99	5000	173
	Autumn	22	12	90	33.5	41	205	215	300	630	32.5	2463	2873	2790	344	49	99	5000	117
	Winter	15.8	6.1	90	33.5	36	205	215	300	630	25.9	4264	5154	4971	344	49	99	5000	85
	Winter Lower 10%	12.9	3	90	33.5	3	205	215	300	630	7.8	11558	13830	13365	344	49	99	5000	44
H-22_1 New Eng Hwy	Summer Ave	30.3	18.1	90	32.8	49	200	200	300	2933	42.6	1042	1185	1155	212	132	119	5000	233
	Summer Upper 10%	37	21.6	90	32.8	56	200	200	300	2933	46.8	762	880	855.6	212	132	119	5000	265
	Autumn	24.4	16	90	32.8	44	200	200	300	2933	36.3	1766	2024	1970	212	132	119	5000	179
	Winter	18	5.5	90	32.8	38	200	200	300	2933	27.7	3698	4432	4278	212	132	119	5000	114
	Winter Lower 10%	15.7	1	90	32.8	1	200	200	300	2933	6.8	11915	14200	13722	144	52	103	5000	55
H-22_3 New Eng Hwy	Summer Ave	30.3	18.1	90	32.8	49	210	190	300	2978	42.3	1062	1208	1179	200	105	110	5000	225
	Summer Upper 10%	37	21.6	90	32.8	56	210	190	300	2979	46.5	779	898	874.7	144	52	103	5000	306
	Autumn	24.4	16	90	32.8	44	210	190	300	2980	36.0	1804	2068	2016	144	52	103	5000	196
	Winter	18	5.5	90	32.8	38	210	190	300	2981	27.4	3781	4537	4386	144	52	103	5000	119
	Winter Lower 10%	15.7	1	90	32.8	1	210	190	300	2982	6.9	11907	14192	13736	144	52	103	5000	51
H-22_9 New Eng Hwy	Summer Ave	30.3	18.1	90	32.8	49	200	220	300	2700	42.6	1042	1185	1155	216	99	107	5000	230
	Summer Upper 10%	37	21.6	90	32.8	56	200	220	300	2700	46.8	762	880	855.6	216	99	107	5000	261
	Autumn	24.4	16	90	32.8	44	200	220	300	2700	36.3	1766	2024	1970	216	99	107	5000	177
	Winter	18	5.5	90	32.8	38	200	220	300	2700	27.7	3698	4432	4278	216	99	107	5000	113
	Winter Lower 10%	15.7	1	90	32.8	1	200	220	300	2700	6.8	11915	14200	13722	216	99	107	5000	51
H-S29_1 Pac Mwy	Summer Ave	27	16.3	90	33.2	46	160	190	70	930	39.8	1310	1488	1442	681	8139	84	5000	133
	Summer Upper 10%	34	19.6	90	33.2	53	160	190	70	930	44.5	897	1025	992.2	681	8139	84	5000	136
	Autumn	22	12	90	33.2	42	160	190	70	930	34.1	2134	2468	2382	681	8139	84	5000	121
	Winter	15.8	6.1	90	33.2	36	160	190	70	930	27.2	3841	4613	4411	681	8139	84	5000	98
	Winter Lower 10%	12.9	3	90	33.2	3	160	190	70	930	7.8	11556	13829	13235	681	8139	84	5000	57
H-S29_10 Pac Mwy	Summer Ave	29.1	17.5	90	34.0	48	140	150	115	945	43.0	1006	1145	1104	351	5760	166	5000	261
	Summer Upper 10%	35	20.7	90	34.0	54	140	150	115	945	50.1	616	727	693.8	351	5760	166	5000	292
	Autumn	23.5	12.1	90	34.0	43	140	150	115	945	36.0	1810	2076	1997	351	5760	166	5000	212
	Winter	17.3	4.9	90	34.0	37	140	150	115	945	29.0	3312	3940	3753	351	5760	166	5000	158
	Winter Lower 10%	17.3	4.9	90	34.0	5	140	150	115	945	9.2	11033	13275	12606	351	5760	166	5000	77
SYD-S15-18 Hume Mwy	Summer Ave	29.1	17.5	90	34.0	48	210	165	400	4054	40.6	1223	1388	1356	209	518	296	5000	203
	Summer Upper 10%	35	20.7	90	34.0	53	210	165	400	4054	47.6	720	835	811.8	209	518	296	5000	257
	Autumn	23.5	12.1	90	34.0	43	210	165	400	4054	33.8	2184	2530	2461	209	518	296	5000	147
	Winter	17.3	4.9	90	34.0	37	210	165	400	4054	26.8	3988	4801	4638	209	518	296	5000	98
	Winter Lower 10%	17.3	4.9	90	34.0	5	210	165	400	4054	9.4	10945	13180	12733	209	518	296	5000	48
SYD-S15_20 Hume Mwy	Summer Ave	29.1	17.5	90	34.0	48	210	150	400	2232	40.6	1223	1388	1356	278	103	108	5000	176
	Summer Upper 10%	35	20.7	90	34.0	53	210	150	400	2232	47.6	720	835	811.8	278	103	108	5000	214
	Autumn	23.5	12.1	90	34.0	43	210	150	400	2232	33.8	2184	2530	2461	278	103	108	5000	133
	Winter	17.3	4.9	90	34.0	37	210	150	400	2232	26.8	3988	4801	4638	278	103	108	5000	93
	Winter Lower 10%	17.3	4.9	90	34.0	5	210	150	400	2232	9.4	10945	13180	12733	278	103	108	5000	48
SYD-S14_17 Milperra Rd	Summer Ave	29.1	17.5	50	34.0	48	150	220	430	1385	42.3	900	1029	993.3	233	74	72	5000	322
	Summer Upper 10%	35	20.7	50	34.0	53	150	220	430	1385	49.3	567	676	646.1	233	74	72	5000	372
	Autumn	23.5	12.1	50	34.0	43	150	220	430	1385	35.6	1541	1756	1697	233	74	72	5000	257
	Winter	17.3	4.9	50	34.0	37	150	220	430	1385	28.6	2834	3337	3198	233	74	72	5000	185
	Winter Lower 10%	17.3	4.9	50	34.0	5	150	220	430	1385	9.2	10124	12282	11679	233	74	72	5000	82
SYD-S13_4 Hume Mwy	Summer Ave	29.1	17.5	90	34.0	48	260	170	400	1256	39.5	1335	1517	1488	1438	202	561	5000	41
	Summer Upper 10%	35	20.7	90	34.0	53	260	170	400	1256	46.6	773	891	872.3	1438	202	561	5000	43
	Autumn	23.5	12.1	90	34.0	43	260	170	400	1256	32.7	2411	2810	2746	1438	202	561	5000	37
	Winter	17.3	4.9	90	34.0	37	260	170	400	1256	25.6	4381	5303	5154	1438	202	561	5000	31
	Winter Lower 10%	17.3	4.9	90	34.0	5	260	170	400	1256	9.5	10898	13129	12768	1438	202	561	5000	20
SOU-S035_3 Picton Rd	Summer Ave	29.3	15.2	90	34.2	48	280	300	700	5000	38.4	1473	1677	1647	157	82	154	5000	147
	Summer Upper 10%	34.5	19	90	34.2	53	280	300	700	5000	45.0	868	994	975	157	82	154	5000	197
	Autumn	23.7	9.2	90	34.2	43	280	300	700	5000	31.4	2703	3173	3103	157	82	154	5000	97
	Winter	16.8	1.7	90	34.2	36	280	300	700	5000	23.5	5107	6229	6060	157	82	154	5000	60
	Winter Lower 10%	13.6	-3.3	90	34.2	-3	280	300	700	5000	4.4	12761	15051	14708	157	82	154	5000	30
SOU-S035_7 Picton Rd	Summer Ave	29.3	15.2	90	34.2	48	280	300	700	5000	31.7	2643	3097	3029	157	82	154	5000	99
	Summer Upper 10%	34.5	19	90	34.2	53	280	300	700	5000	45.0	868	994	975	134	157	173	5000	155
	Autumn	23.7	9.2	90	34.2	43	280	300	700	5000	31.4	2703	3173	3103	134	157	173	5000	112
	Winter	16.8	1.7	90	34.2	36	280	300	700	5000	23.5	5107	6229	6060	134	157	173	5000	62
	Winter Lower 10%	13.6	-3.3	90	34.2	-3	280	300	700	5000	4.4	12761	15051	14708	134	157	173	5000	31
SOU-S035_7 Picton Rd	Summer Ave	29	21.2	90	27.2	51	345	200	450	5000	41.2	1164	1322	1303	164	210	248	5000	122
	Summer Upper 10%	31.2	21.2	90	27.2	53	345	200	450	5000	43.4	976	1112	1095	164	210	248	5000	135
	Autumn	26	16.3	90	27.2	47	345	200	450	5000	36.1	1794	2057	2026	164	210	248	5000	

	Winter Lower 10%	18.7	5.4	90	27.2	5	345	200	450	5000	10.2	10609	12816	12546	164	210	248	5000	24
Q6 Bruce Hwy	Spring	25.4	15.7	90	27.2	47	345	200	450	5000	35.6	1871	2149	2116	164	210	248	5000	90
	Summer Ave	29	21.2	90	27.2	51	345	200	450	5000	41.2	1164	1322	1303	105	164	344	5000	141
	Summer Upper 10%	31.1	21.2	90	27.2	52	345	200	450	5000	43.0	1004	1142	1126	105	164	344	5000	156
	Autumn	26	16.3	90	27.2	47	345	200	450	5000	36.1	1794	2057	2026	105	164	344	5000	104
	Winter	20.8	9	90	27.2	43	345	200	450	5000	29.1	3287	3908	3832	105	164	344	5000	64
	Winter Lower 10%	18.7	5.4	90	27.2	5	345	200	450	5000	10.2	10609	12816	12546	105	164	344	5000	25
Q5 Bruce Hwy	Spring	25.4	15.7	90	27.2	47	345	200	450	5000	35.6	1871	2149	2116	105	164	344	5000	101
	Summer Ave	29.3	15.2	90	34.0	48	180	220	330	5000	40.7	1212	1376	1339	216	160	142	5000	243
	Summer Upper 10%	34.5	19	90	34.0	53	180	220	330	5000	47.2	740	856	829.1	216	160	142	5000	298
	Autumn	23.7	9.2	90	34.0	43	180	220	330	5000	33.9	2178	2522	2443	216	160	142	5000	178
	Winter	16.8	1.7	90	34.0	37	180	220	330	5000	26.3	4120	4970	4772	216	160	142	5000	118
N4 Camden	Winter Lower 10%	13.6	-3.3	90	34.0	-3	180	220	330	5000	4.3	12806	15094	14564	216	160	142	5000	55
By Pass	Spring	24	8.8	90	34.0	43	180	220	330	5000	34.2	2118	2448	2372	216	160	142	5000	181
	Summer Ave	29.1	17.5	90	34.0	48	225	220	330	5000	40.2	1258	1428	1397	263	252	180	5000	166
	Summer Upper 10%	35	20.7	90	34.0	53	225	220	330	5000	47.3	736	852	830.7	263	252	180	5000	203
	Autumn	23.5	12.1	90	34.0	43	225	220	330	5000	33.5	2255	2617	2550	263	252	180	5000	122
	Winter	17.3	4.9	90	34.0	37	225	220	330	5000	26.4	4112	4960	4801	263	252	180	5000	84
	Winter Lower 10%	17.3	4.9	90	34.0	5	225	220	330	5000	9.4	10930	13164	12746	263	252	180	5000	43
N7 Alpha st	Spring	24.1	10.8	90	34.0	43	225	220	330	5000	33.6	2234	2591	2525	263	252	180	5000	123
	Summer Ave	26.4	13.5	50	37.7	43	190	75	450	5000	36.0	1491	1698	1653	699	56	156	5000	100
	Summer Upper 10%	36	17.8	50	37.7	52	190	75	450	5000	46.7	664	777	752	699	56	156	5000	114
	Autumn	20.1	9.9	50	37.7	38	190	75	450	5000	29.7	2581	3020	2923	699	56	156	5000	84
	Winter	13	5.3	50	37.7	31	190	75	450	5000	23.0	4494	5448	5237	699	56	156	5000	65
V6 Atherton	Winter Lower 10%	10.5	1.6	50	37.7	2	190	75	450	5000	6.8	11087	13332	12836	699	56	156	5000	40
Rd	Spring	19.2	8.2	50	37.7	37	190	75	450	5000	28.4	2899	3419	3305	699	56	156	5000	80
	Summer Ave	28.2	19.7	90	28.8	49	200	100	200	850	42.0	1088	1237	1206	311	600	127	179	190
	Summer Upper 10%	31.1	19.7	90	28.8	52	200	100	200	850	44.9	869	995	968.9	311	600	127	179	205
	Autumn	24.9	15.3	90	28.8	46	200	100	200	850	37.6	1568	1788	1743	311	600	127	179	163
	Winter	19.9	8.6	90	28.8	41	200	100	200	850	31.0	2801	3295	3192	311	600	127	179	121
	Winter Lower 10%	17.5	4	90	28.8	4	200	100	200	850	8.8	11172	13423	12951	311	600	127	179	49
N-S56	Spring	24.9	16.5	90	28.8	46	200	100	200	850	38.0	1517	1728	1685	311	600	127	179	166
	Summer Ave	26.5	18.9	60	34.0	45	205	355	300	490	38.4	1285	1460	1425	2077	112	17	5000	32
	Summer Upper 10%	31.5	21.5	60	34.0	50	205	355	300	490	44.4	809	930	905.1	2077	112	17	5000	30
	Autumn	22.9	14.2	60	34.0	42	205	355	300	490	34.1	1870	2148	2092	2077	112	17	5000	32
	Winter	17	7.2	60	34.0	37	205	355	300	490	27.1	3414	4069	3935	2077	112	17	5000	31
Syd-S11	Winter Lower 10%	14.2	3.9	60	34.0	4	205	355	300	490	8.5	10707	12923	12469	2077	112	17	5000	22
Botany Road	Spring	22.6	13.2	60	34.0	42	205	355	300	490	33.4	1995	2299	2237	2077	112	17	5000	32

Appendix F2 Threshold Strain Validation Non LLAP Sections

Site	Season	Temperature (°C)				Surface Temp (°C)	Thickness (mm)				AC Temp (°C)	Modulus (MPa)					Strain (µε)		
		Upper	Lower	Speed	Lat		L1	L2	L3	L4		WC	BC	Eff	L2	L3		L4	L5
H-S39_6	Summer Ave	27	16.3	90	33.5	46	240	330	300	5000	37.7	1558	1776	1739	209	480	167	5000	154
	Summer Upper 10%	34	19.6	90	33.5	53	240	330	300	5000	41.9	1103	1253	1227	209	480	167	5000	185
	Autumn	22	12	90	33.5	41	240	330	300	5000	31.7	2642	3096	3017	209	480	167	5000	112
	Winter	15.8	6.1	90	33.5	36	240	330	300	5000	25.1	4548	5517	5347	209	480	167	5000	76
	Winter Lower 10%	12.9	3	90	33.5	3	240	330	300	5000	7.8	11559	13831	13434	209	480	167	5000	39
Spring	22.8	6.1	90	33.5	42	240	330	300	5000	30.7	2878	3391	3302	209	480	167	5000	105	
H-S39_11	Summer Ave	27	16.3	90	33.5	46	240	180	180	2839	37.7	1558	1776	1739	123	372	128	5000	191
	Summer Upper 10%	34	19.6	90	33.5	53	240	180	180	2839	41.9	1103	1253	1227	123	372	128	5000	235
	Autumn	22	12	90	33.5	41	240	180	180	2839	31.7	2642	3096	3017	123	372	128	5000	132
	Winter	15.8	6.1	90	33.5	36	240	180	180	2839	25.1	4548	5517	5347	123	372	128	5000	88
	Winter Lower 10%	12.9	3	90	33.5	3	240	180	180	2839	7.8	11559	13831	13434	123	372	128	5000	43
Spring	22.8	6.1	90	33.5	42	240	180	180	2839	30.7	2878	3391	3302	123	372	128	5000	124	
H-S39_9	Summer Ave	27	16.3	90	33.5	46	260	210	150	5000	37.3	1613	1841	1805	177	921	147	5000	148
	Summer Upper 10%	34	19.6	90	33.5	53	260	210	150	5001	41.3	1151	1307	1282	177	921	147	5000	179
	Autumn	22	12	90	33.5	41	260	210	150	5002	31.3	2737	3216	3139	177	921	147	5000	104
	Winter	15.8	6.1	90	33.5	36	260	210	150	5003	24.6	4697	5707	5543	177	921	147	5000	70
	Winter Lower 10%	12.9	3	90	33.5	3	260	210	150	5004	7.8	11560	13832	13465	177	921	147	5000	36
Spring	22.8	6.1	90	33.5	42	260	210	150	5005	30.2	2997	3541	3454	177	921	147	5000	98	
H-23_1	Summer Ave	30.3	18.1	90	32.8	49	220	230	810	1577	42.1	1083	1230	1202	82	99	72	5000	313
	Summer Upper 10%	37	21.6	90	32.8	56	220	230	810	1577	46.2	796	916	893.6	82	99	72	5000	375
	Autumn	24.4	16	90	32.8	44	220	230	810	1577	35.8	1840	2112	2061	82	99	72	5000	220
	Winter	18	5.5	90	32.8	38	220	230	810	1577	27.2	3861	4640	4491	82	99	72	5000	126
	Winter Lower 10%	15.7	1	90	32.8	1	220	230	810	1577	6.9	11900	14184	13749	144	52	103	5000	47
Spring	25.6	10.9	90	32.8	45	220	230	810	1577	35.2	1935	2227	2172	144	52	103	5000	175	
H-23_3	Summer Ave	30.3	18.1	90	32.8	49	200	250	270	1712	42.6	1042	1185	1155	144	52	103	5000	282
	Summer Upper 10%	37	21.6	90	32.8	56	200	250	270	1712	46.8	762	880	855.6	144	52	103	5000	328
	Autumn	24.4	16	90	32.8	44	200	250	270	1712	36.3	1766	2024	1970	144	52	103	5000	210
	Winter	18	5.5	90	32.8	38	200	250	270	1712	27.7	3698	4432	4278	144	52	103	5000	128
	Winter Lower 10%	15.7	1	90	32.8	1	200	250	270	1712	6.8	11915	14200	13722	144	52	103	5000	54
Spring	25.6	10.9	90	32.8	45	200	250	270	1712	35.8	1846	2119	2063	144	52	103	5000	204	
H-23_8	Summer Ave	30.3	18.1	90	32.8	49	200	300	400	1697	42.6	1042	1185	1155	45	3268	79	5000	442
	Summer Upper 10%	37	21.6	90	32.8	56	200	300	400	1697	46.8	762	880	855.6	45	3268	79	5000	540
	Autumn	24.4	16	90	32.8	44	200	300	400	1697	36.3	1766	2024	1970	45	3268	79	5000	302
	Winter	18	5.5	90	32.8	38	200	300	400	1697	27.7	3698	4432	4278	45	3268	79	5000	168
	Winter Lower 10%	15.7	1	90	32.8	1	200	300	400	1697	6.8	11915	14200	13722	45	3268	79	5000	65
Spring	25.6	10.9	90	32.8	45	200	300	400	1697	35.8	1846	2119	2063	45	3268	79	5000	292	
H-S24_13	Summer Ave	27	16.3	90	33.5	46	155	345	170	1638	39.9	1292	1468	1421	68	71	56	5000	468
	Summer Upper 10%	34	19.6	90	33.5	53	155	345	170	1638	44.7	883	1010	976.4	68	71	56	5000	588
	Autumn	22	12	90	33.5	41	155	345	170	1638	33.9	2172	2515	2423	68	71	56	5000	330
	Winter	15.8	6.1	90	33.5	36	155	345	170	1638	27.4	3789	4547	4342	68	71	56	5000	218
	Winter Lower 10%	12.9	3	90	33.5	3	155	345	170	1638	7.8	11556	13828	13216	68	71	56	5000	94
Spring	22.8	6.1	90	33.5	42	155	345	170	1638	33.3	2298	2669	2570	68	71	56	5000	317	
H-S24_3	Summer Ave	27	16.3	90	33.5	46	160	440	150	1772	39.8	1310	1488	1442	92	10	49	5000	400
	Summer Upper 10%	34	19.6	90	33.5	53	160	440	150	1772	47.9	709	823	793.6	92	10	49	5000	557
	Autumn	22	12	90	33.5	41	160	440	150	1772	33.7	2204	2553	2463	92	10	49	5000	287
	Winter	15.8	6.1	90	33.5	36	160	440	150	1772	27.2	3841	4613	4411	92	10	49	5000	193
	Winter Lower 10%	12.9	3	90	33.5	3	160	440	150	1772	7.8	11556	13829	13235	92	10	49	5000	86
Spring	22.8	6.1	90	33.5	42	160	440	150	1772	33.1	2336	2716	2618	92	10	49	5000	275	
H-S24_7	Summer Ave	27	16.3	50	33.5	46	165	435	100	1854	39.6	1105	1256	1218	137	17	61	5000	357
	Summer Upper 10%	34	19.6	50	33.5	53	165	435	100	1854	47.7	622	733	704.9	137	17	61	5000	462
	Autumn	22	12	50	33.5	41	165	435	100	1854	33.6	1839	2111	2043	137	17	61	5000	269
	Winter	15.8	6.1	50	33.5	36	165	435	100	1854	27.1	3242	3851	3697	137	17	61	5000	186
	Winter Lower 10%	12.9	3	50	33.5	3	165	435	100	1854	7.8	10694	12909	12346	137	17	61	5000	80
Spring	22.8	6.1	50	33.5	42	165	435	100	1854	32.9	1954	2249	2175	137	17	61	5000	259	
SYD-S24_2	Summer Ave	29.1	17.5	50	34.0	48	190	310	260	5000	41.1	984	1121	1091	315	22	76	5000	198
	Summer Upper 10%	35	20.7	50	34.0	53	190	310	260	5001	48.1	607	717	692.6	315	22	76	5000	226
	Autumn	23.5	12.1	50	34.0	43	190	310	260	5002	34.4	1717	1965	1911	315	22	76	5000	159
	Winter	17.3	4.9	50	34.0	37	190	310	260	5003	27.3	3173	3764	3634	315	22	76	5000	115
	Winter Lower 10%	17.3	4.9	50	34.0	5	190	310	260	5004	9.3	10070	12221	11745	315	22	76	5000	57
Spring	24.1	10.8	50	34.0	43	190	310	260	5005	34.5	1696	1940	1887	315	22	76	5000	160	
SYD-S24_8	Summer Ave	29.1	17.5	50	34.0	48	180	470	400	5000	41.3	964	1098	1067	104	40000	10	5000	386
	Summer Upper 10%	35	20.7	50	34.0	53	180	470	400	5001	48.4	597	707	681.6	104	40000	10	5000	482
	Autumn	23.5	12.1	50	34.0	43	180	470	400	5002	34.7	1675	1915	1859	104	40000	10	5000	283
	Winter	17.3	4.9	50	34.0	37	180	470	400	5003	27.6	3092	3662	3530	104	40000	10	5000	190
	Winter Lower 10%	17.3	4.9	50	34.0	5	180	470	400	5004	9.3	10082	12235	11733	104	40000	10	5000	83
Spring	24.1	10.8	50	34.0	43	180	470	400	5005	34.8	1653	1888	1834	104	40000	10	5000	285	
SYD-S25_13	Summer Ave	29.1	17.5	50	34.0	48	150	450	300	1385	42.3	900	1029	993.3	76	108	42	5000	577
	Summer Upper 10%	35	20.7	50	34.0	53	150	450	300	1385	49.3	567	676	646.1	76	108	42	5000	727
	Autumn	23.5	12.1	50	34.0	43	150	450	300	1385	35.6	1541	1756	1697	76	108	42	5000	419
	Winter	17.3	4.9	50	34.0	37	150	450	300	1385	28.6	2834	3337	3198	76	108	42	5000	276
	Winter Lower 10%	17.3	4.9	50	34.0	5	150	450	300	1385	9.2	10124	12282	11679	76	108	42	5000	107